FRIEDRICH-ALEXANDER
UNIVERSITÄT
ERLANGEN-NÜRNBERG

Synthesis of Buckybowls via Algorithm of C-F Bond Activations Executed on Alumina

---

Synthese von Buckybowls mittels eines Algorithmus zur Aktivierung von C-F-Bindungen an Aluminiumoxid

Der Naturwissenschaftlichen Fakultät der Frierdrich-Alexander-Universität Erlangen-Nürnberg

zur Erlangung des Doktorgrades Dr. rer. nat.

vorgelegt von

Vladimir Akhmetov

aus Moskau

Department
Chemie und Pharmazie

Als Dissertation genehmigt von der Naturwissenschaftlichen Fakultät der Friedrich-Alexander Universität Erlangen-Nürnberg

Tag der mündlichen Prüfung: 18 / 12 / 2019

Vorsitzender des Promotionsorgans: Prof. Dr. Georg Kreimer

Gutachter: Prof. Dr. Norbert Jux

Gutachter: Prof. Dr. Junji Ichikawa

This work has been carried out during the period from December 2017 to August 2019 at the department of Chemistry and Pharmacy in Friedrich-Alexander University located at Nikolaus-Fiebiger-Str. 10, 91058, Erlangen.

List of Abbreviations

HOMO – Highest Occupied Molecular Orbital

*i*Pr – Isopropyl Substituent

LDI – Laser Desorption Ionization

LUMO - Lowest Unoccupied Molecular Orbital

Me – Methyl Substituent

MS – Mass Spectrometry

NICS – Nucleus-Independent Chemical Shifts

o-DCB – *ortho*-Dichlorobenzene

PAH – Polycyclic Aromatic Hydrocarbon

POAV – π-Orbital Axis Vector

SWCNT – Single-Wall Carbon Nanotube

*t*Bu – *tert*-Butyl Substituent

THF – Tetrahydrofuran

TS – Transition State

Table of Contents

1 Introduction

With all its possible diversity the life on Earth occurred to be based almost solely on carbon and it comes as no surprise that this element is not only one of the most abundant in the observable universe but also by far is the most frequently studied by scientists. The unique idiosyncrasy making carbon such important element is its ability for catenation i.e. to form a great variety of stable compounds consisting of long chains of C-C bonds. Naturally, much attention is attached to the biological compounds, their synthesis, properties and applications. Nevertheless, carbon-rich materials such as fullerenes, graphene, single-wall carbon nanotubes (SWCNTs), graphene oxide, etc. also possess high priority on the scientific community's agenda. The discovery of fullerene C_{60} in 1985[1] and the mechanical exfoliation of graphene (single-atom-thick honeycomb lattice of carbon) from bulk graphite in 2004[2] serve as major milestones in the field. These discoveries open up an immense number of research directions for virtually any natural scientist, regardless of the field of studies. The growing at a rapid pace field faced and still faces the lack of synthetic approaches to the desired materials. Up to now this obstacle remains to be the major issue hampering further development in the field. The complexity of materials, oftentimes demanding peculiar subunits or functionalization, commonly does not complement the top-down approach, where the bulk materials are broken down to smaller parts of it. Meanwhile, large size and low solubility exacerbate the situation, making already laborious bottom-up approach (assembly of small molecules) even more sophisticated. Nevertheless, the later path still seems to be more appealing due to its precise control over the structure and functionalities. Moreover, modern synthetic advances and the development of novel highly efficient organic reactions gradually bring chemists closer to solution of this challenge. In order to achieve comprehensive results in the assembly of such complicated target molecules as fullerenes and nanotubes, one should definitely start with some simpler models. Eventually, this perspective leads to fusion of nanomaterial science and organic chemistry, and the issue becomes a matter of organic chemistry advances and capabilities. The synthesis of polycyclic aromatic hydrocarbons (PAHs), still remains rather obsolete and lacking techniques to obtain non-classical PAHs containing five-, seven- and eight-membered rings. The incorporation of these units not only drastically alters physical properties but also entails non-planarity of the resulting PAHs making them fascinating candidates for carbon nanomaterials assembly. Recently the stated problem became rather widespread attracting

scientists' attention, the majority of the anticipated results up to now belong to the synthesis of pentagon-imbedded PAHs. The incorporation of the pentagon increases electron affinity and allows considering the molecule as an electron acceptor in multiple applications, but even more intriguing consequence is the deviation of sp^2-carbon bonds valence angles forcing PAH to bend into a geodesic-like structure. The similarity of a bowl to these structures, which might be considered as Buckminsterfullerene's fragments, accounts for the widely accepted name: "Buckybowls", otherwise known as open geodesic polyarenes.[3] Along with non-planarity, buckybowls also acquire considerable strain energy, which must be overcome in order to obtain such kind of PAHs. This fact alters the applicability of some well-established synthetic methods and forces scientist to develop novel approaches. This work is aimed to contribute to the organic chemistry methodologies and push forward the current state of synthesis of non-planar PAHs and further assembly of complex carbon-rich nanomaterials. Prior to diving into the synthetic aspects, the general definition, properties and promising applications of buckybowls shall be considered.

1.1 Buckybowls

1.1.1 Definition and POAV concept

Aromaticity, defined on a quantum mechanical basis, was generally formulated by Hückel in 1931[4] and later succinctly expressed by Doering as a simple and famous "4n+2" electron rule. Thus, aromatic compounds are defined as hydrocarbons, which are (i) cyclic, (ii) contain a fully conjugated planar π-system, and (iii) contain 4n+2 electrons. Strictly speaking, this definition is only applicable for monocyclic conjugated systems i.e. [n]annulenes. Meanwhile, all-benzoid PAHs usually display local aromaticity with π-electrons predominantly localized at certain benzene rings according to Clar's aromatic sextet rule.[5] These rules, easily applicable for benzene, become somewhat cumbersome in case of less trivial examples such as fullerenes[6] and non-planar PAHs. Nevertheless, such compounds oftentimes clearly possess aromaticity, which can be confirmed based on various criteria of aromaticity.[7] Nucleus-Independent Chemical Shifts (NICS) is one of the most popular and reliable aromaticity indexes used for quantitative estimation.[8] In general, the loss of planarity is quite ubiquitous situation one may come across with studying PAHs and this phenomenon might be caused by three major reasons.[9] One of them is atom crowding, when two or several function groups repel each other and this repulsion entails the deviation from planarity, as for example in case of helicenes (Figure 1d). Another type of geometrical constraint might be induced by macrocyclic nature of the compound e.g. nanotubes. On the other hand incorporation of the five-, seven-, eight-membered rings into a honey-comb like PAHs structure leads to the alteration of the valence angles and, thus, to appearance of non-planar surface as a mean to minimize energy of the system. The latter case is particularly interesting, since several interesting consequences appear together with the pentagons, which will be mainly considered in this work. Among them is the specific shape that resembles a bowl, thus, this kind of PAHs is oftentimes referred to as buckybowls (alike buckyballs standing for fullerenes). Besides two unequal (i.e. concave and convex) surfaces, buckybowls, as any other distorted PAH, possess peculiar double bonds, which are not coplanar with their four substituents. Such kind of deformation is known as pyramidalization and its value can be quantified via broad variety of indexes.[10–12] For example, angle of pyramidalization i.e. angle between the extension of C=C and the bisectrix of X-C-X (where Xs are two neighboring substituents) describes pyramidalized double bonds having C_{2v} symmetry (Figure 1b). More generally, π-orbital axis vector (POAV)

analysis is used for description of the pyramidalization.[13,14] Here, angle between POAV and any of three σ-bonds is depicted as θ, and θ-90 °C is frequently used to characterize deviation from planarity. This angle represents not only the structural features, but it is also a valuable parameter to estimate the reactivity and stability of the conjugated system with non-planar structure. [15,16]

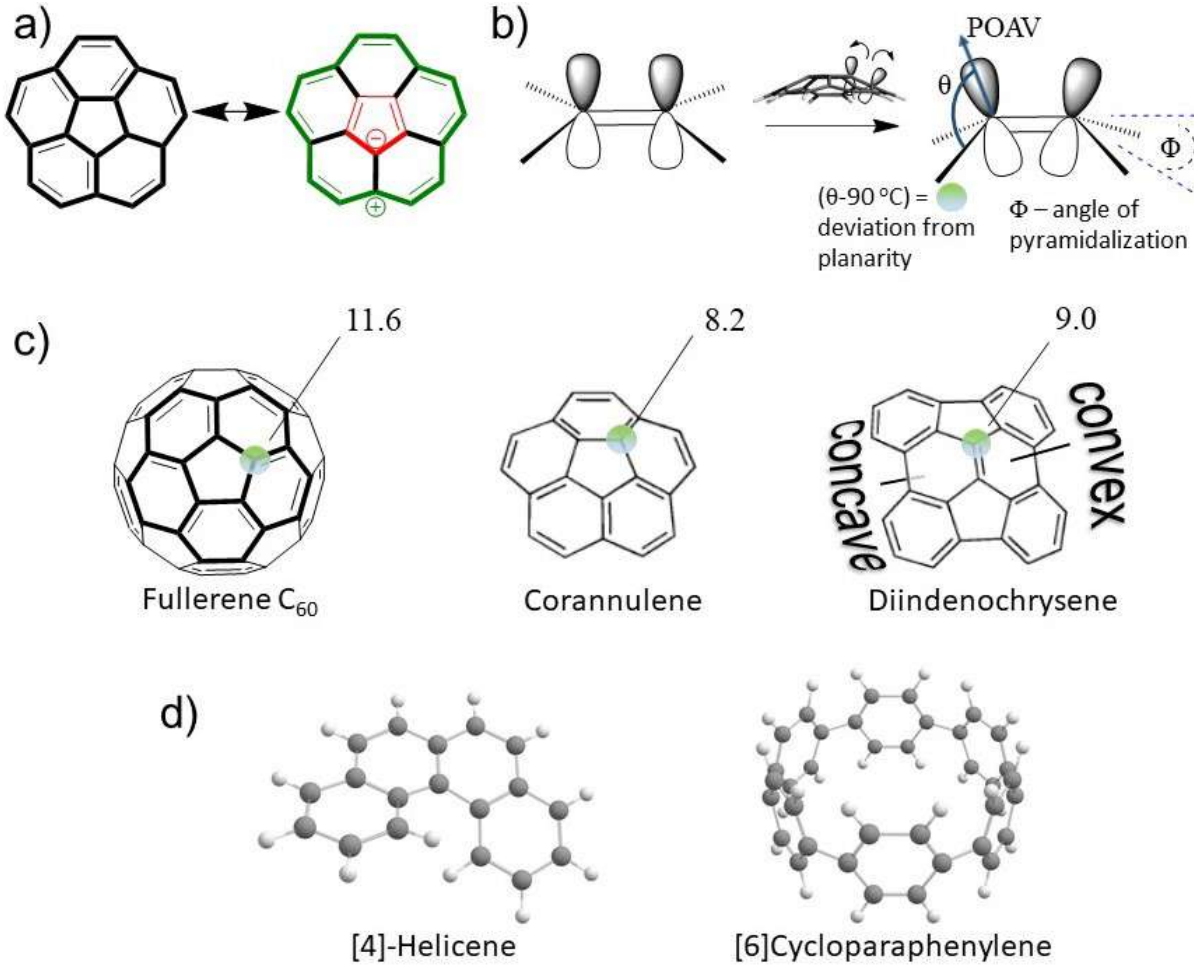

Figure 1. a) Archetypal buckybowl, corannulene, and its resonance form. b) Schematic representation of pyramidalization and its possible descriptors c) POAV angles of some fundamental bowl-shaped PAHs and fullerene C_{60}. d) Other types of distorted PAHs, atom crowding in [4]-helicene and macrocyclic [6]cycloparaphenylene.

Among buckybowls, several representatives deserve special attention, e.g. corannulene, the simplest non-planar fragment of fullerene C_{60} was synthesized for the first time in 1966,[17,18] long before the discovery of fullerene. At that time the unusual shape of the molecule hardly induced fundamental interest not to mention questions of its properties and applications. The major reason for that was non-trivial 17-step synthesis, which required immense efforts to obtain the compound

in milligram scale. This is why corannulene remained in oblivion till the explosion of interest to fullerene and its fragments, when aspiration to the synthesis of non-planar PAHs was reinvigorated. It was not until 1997, when the three-step synthesis of corannulene was developed by Scott et al.[19] Procedure enabling kilogram scale synthesis of the buckybowls was published only in 2012 by Siegel et al.[20] As a matter of fact, some other fundamental buckybowls such as diindenochrysene and sumanene were also obtained,[21–23] however the complexity and peculiarities of the synthesis did not allow broad studies of these compounds. Thus, corannulene and its derivatives remain virtually the only buckybowls that have been intensively studied for their chemical and physical properties. Nevertheless, the scope of these properties, both already observed and potential, strongly encourage synthetic chemists to face the challenge and develop the novel approaches to buckybowls. That is why the properties of buckybowls, as motivation for synthetic endeavors, shall be considered.

1.1.2 Properties and Applications

1.1.2.1 Fullerene-like Chemistry

Despite the absence of the peripheral hydrogens typical for PAHs, C_{60} has quite rich chemistry, which has been vigorously studied over the past two decades. As a part of its chemical properties, fullerene readily undergoes typical for olephines addition reactions. This becomes possible due to already discussed pyramidalized double bonds inherent in fullerene. Multiple examples such as Prato reaction[24,25], Bingel-Hirsch reaction,[26] addition of carbenes [27] and many others[28] demonstrate the broad spectrum of opportunities to modify buckyballs. Interestingly, buckybowls possess not only curved geometry, but also peripheral hydrogens. Such combination gives rise to a duality in chemical properties of buckybowls, indeed, they can react like a regular PAHs undergoing S_EAr[29] and additionally they may interact with carbenes and some other particles in a fullerene-like manner, which was demonstrated on example of corannulene, circumtriindene and diindenochrysene, where non-peripheral double bonds are exposed to attack.[3,30]

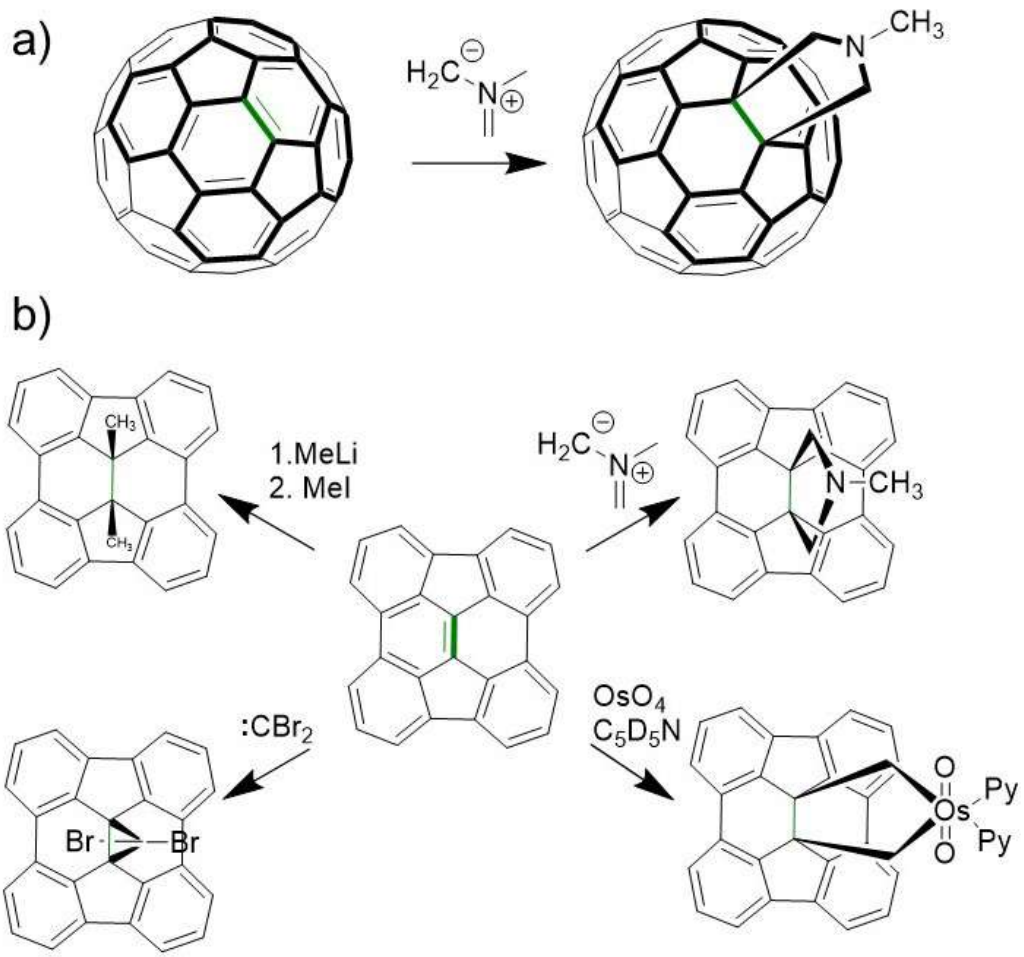

Figure 2. Reactivity of pyramidalized double bond: a) [6,6]-addition to fullerene; b) fullerene-like chemistry demonstrated on diindenochrysene.

Thus, buckybowls are extremely interesting molecules from a fundamental standpoint, since the studies on their behavior may shed some light on the chemical nature of large carbon-based materials,[31] such as graphene and especially fullerenes and nanotubes. Nevertheless, the chemical properties of open geodesic polyarenes remain poorly studied, due to the lack and complexity of the approaches towards pristine buckybowls.

1.1.2.2 Buckybowls as Electron Acceptors

Since buckybowls combine non-planar geometry and aromaticity, the studies on this class of compound and interplay of these phenomena could shed light on fundamental aspects of aromaticity. Moreover, stepwise electrochemical reduction would drastically alter electronic properties and structure of initial buckybowl, generating multiple peculiar anion species. Besides

the loss of planarity, the incorporation of pentagons into a PAH's structure also leads to enhanced electron-accepting properties, which are induced by formation of the stabilized cyclopentadienyl anion moiety upon addition of electrons. Thus, buckybowls are undoubtedly interesting objects for electrochemical studies and applications. For example, it has been shown that reduction may serve as a tool to govern magnetic properties alternating their magnetic behavior from paramagnetic in odd-number reduction states to diamagnetic with even numbers of electrons.[32] Considering a specific example, corannulene, as an archetypal buckybowl having doubly-degenerate LUMO, which accounts for the possibility to accept up to four electrons,[33] it has been shown that first three reductions are reversible.[34] Speaking of magnetic properties of corannulene and its anions, the electronic structure of pristine molecule will be considered first. Twenty π-electrons do not allow considering corannulene as an aromatic species, since this quantity does not correspond to "4n+2" rule, on the other hand, consideration of two distinct annulenes (Figure 1a) within corannulene's moiety resolves the apparent issue. ^{1}H NMR clearly confirms the presence of diatropic ring current revealing a singlet at 7.93 ppm in THF-d_8.[35] Meanwhile, dianion has paratropic current shifting the proton signal to -5.6 ppm.[36] The formation of tetraanion has been also shown, however, the formation of such species was found to be irreversible in a lithium reduction, due to the emergence of a thermodynamically favorable supramolecular dimer.[34]

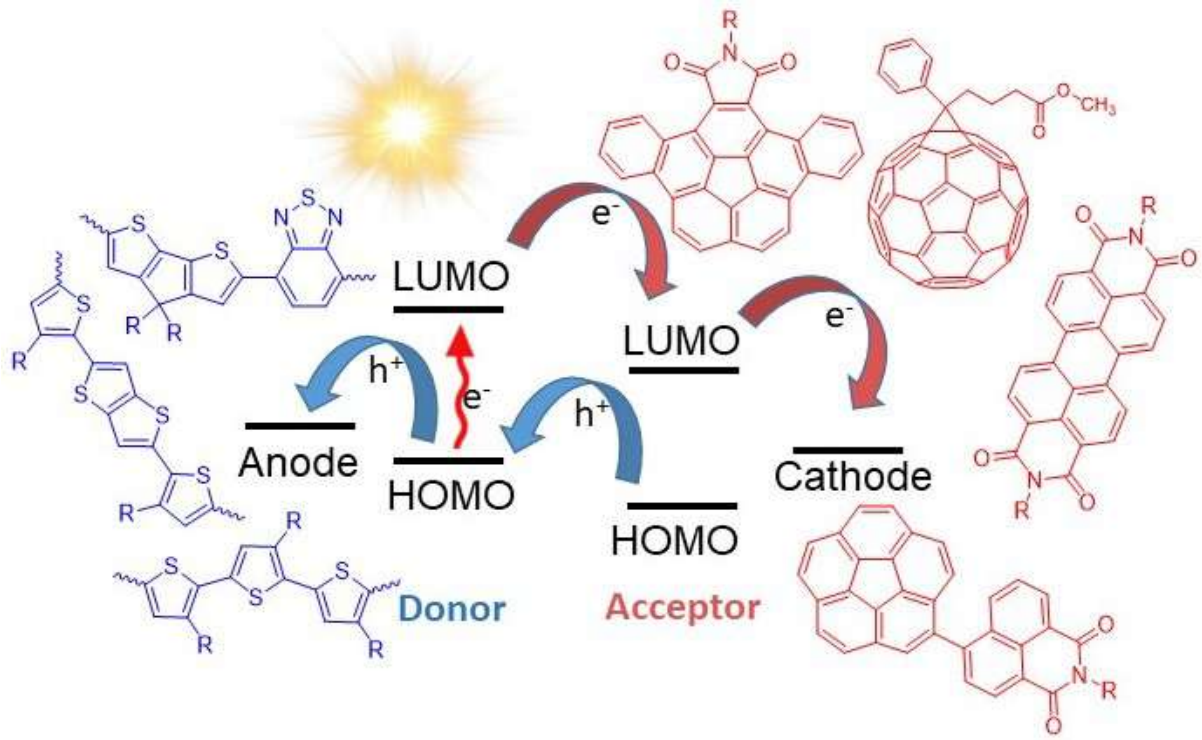

Figure 3. Schematic representation of donor-acceptor relations in photovoltaic cell. Sunlight excites one of the electrons on the donor's HOMO, subsequently, charge separation occurs as electron moves to LUMO of the acceptor.

Among immense number of fascinating properties based on high electron affinity, one may list electrogenerated chemiluminescence[37,38] and supercharging (characteristic for symmetrical PAHs), which might be exploited in charge storage.[32] Moreover, buckybowls have high potential in the field of organic electronics, where they exhibit promising values characterizing energy/electron transfer.[39] Special attention deserves rapidly rising field studying buckybowls as electron acceptors in photovoltaic cells,[40] where thiophene based polymer-donors are normally exploited in tandem with fullerene derivatives.[41] One of the issues in the field is the necessity of fine-tuning of HOMO and LUMO levels of donors and acceptors. This becomes oftentimes problematic in case of fullerenes, since functionalization of available C_{60} (C_{70}) is virtually the only mean to tune its HOMO and LUMO (Figure 3).[42] Buckybowls, on the other hand, offer not only a huge variety of derivatives but also different backbones, i.e. corannulene, diindenochrysene etc.

1.1.2.3 Specific π-π Stacking Interactions

Another emerging field attracting synthetic chemists is supramolecular chemistry, which in contrast to traditional chemistry relies on weak and reversible interactions instead of covalent bonding.[43,44] Among the most essential interactions considered in supramolecular chemistry are π-π interactions, which might be exploited to implement the key concept of supramolecular chemistry, host-guest complexation, where one molecule or a group of molecules serves as a specific receptor for another one.[45,46] In general, there is no driving force for π-π stacking to have any recognition pattern, unless the surface of PAH is non-planar e.g. has concave-convex surfaces, which interact significantly stronger with PAHs having a complementary shape.[47] Particular interest arises around buckybowls-fullerene recognition.[48–51] Thus, buckybowls represent extremely interesting systems for the studies on specific π-π interactions and construction of host-guest systems. For example, some corannulene based molecular tweezers[52,53] show selective binding to C_{70} over C_{60}.[54]

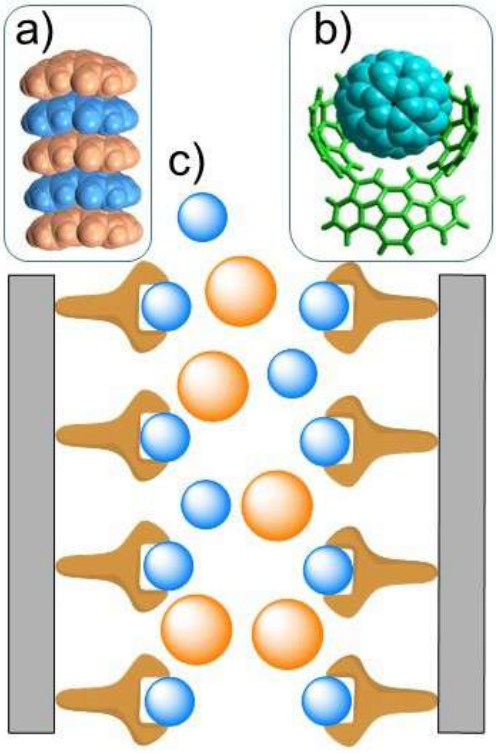

Figure 4. Examples of π-π interactions. a) Crystal packing of 1,7-dimethyldiindenochrysene, indirectly indicating effective complementary interactions. b) Host-Guest system with fullerene. c) Illustration of chromatographic separation of two different fullerenes; buckycatcher is immobilized on the stationary phase.

These complexation processes might be used for example in liquid chromatography (Figure 4c), where stationary phase modified with buckybowls would be capable of extremely effective separation of complex carbon-based materials such as higher fullerenes.[55] Moreover, the perspective to employ buckybowls in molecular electronics appears to be an immense field, as fullerene-buckybowls complexes show promising characteristics, e.g. hole transfer rates between fullerenes can be increased by three orders of magnitude if mediated by corannulene based tweezer.[56]

1.1.2.4 Chirality and Inversion

Another noteworthy difference between buckybowls and planar PAHs is the absence of a symmetry plane along the aromatic rings. Thus, buckybowls become less symmetrical in comparison to planar PAHs and specific type of chirality oftentimes referred to as "bowl chirality". Moreover, it is possible to break all chiral bowls into three categories based on the origin of their chirality.[57] The chirality may be contained in the conjugated system itself, (e.g. hemifullerene), on the other hand the introduction of substituents (trimethylsumanene)[58] or heteroatoms (triazasumanene)[59] may also account for the appearance of chirality.

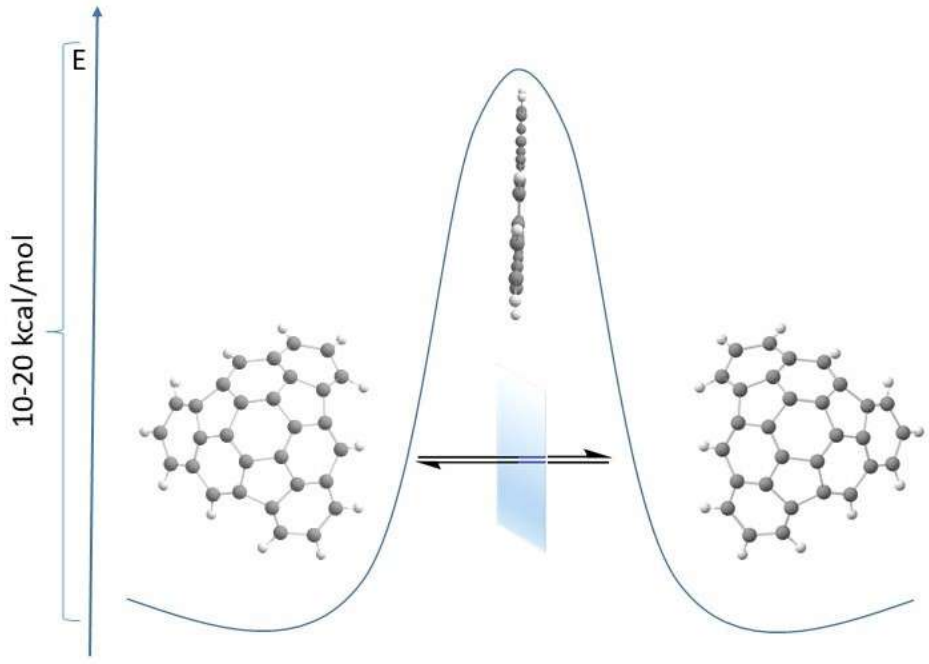

Figure 5. Inversion of two enantiomeric forms of hemifullerene via flat TS.

There are two independent stereodescriptors applied to assign bowl chirality, since buckybowls share many common features with fullerenes and CNTs it comes as no surprise that *C* and *A* nomenclature, generally used to describe fullerenes, fits buckybowls as well.[58,60] Another stereodescriptor system *P* and *M* relies on conventional Cahn-Ingold-Prelog sequence rule[61] modified for buckybowls.[62]

Naturally, asymmetric synthesis of such buckybowls comes at a price of immense effort, where the problem is not only the synthesis itself but also in the avoiding of the racemization. Thus, the synthesis of trimethylsumanene requires fast work up at low temperatures in order to detect optical activity, which gradually disappears already at 10 °C.[58] The vast majority of the obtained and studied buckybowls possess rather low inversion barriers of 10-20 kcal/mol, which depend not only on the depth of the bowl but also on the substituent. This phenomenon was demonstrated on corannulene and its derivatives.[63] The corresponding barrier for pristine corannulene is estimated to be 10-11 kcal/mol, which corresponds to more than 200 000 inversions per second at room temperature.[64]

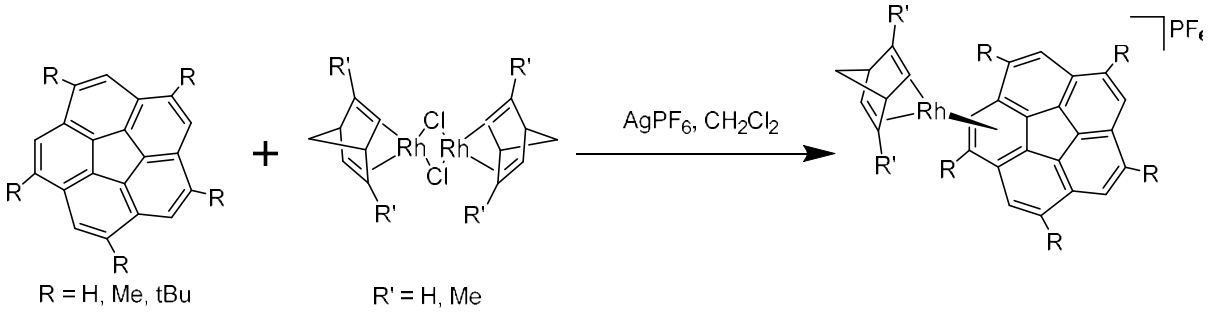

Figure 6. π-coordination of Rh with corannulene and its derivatives.[65]

Nevertheless, buckybowls and their unique type of chirality excite significant interest in multiple areas such as supramolecular chemistry, where chiral molecules capable of weak intermolecular interactions are a matter of particular interest.[61,66,67] Moreover, specific π-coordination with various transition metals[68–77] allows considering buckybowls as promising ligands for enantioselective catalysis.[65,74,78] The complexation with metals or assembly of buckybowls into a cluster-like particle may drastically increase the inversion barrier, making thus buckybowls even more interesting systems in terms of their chirality.

1.1.2.5 Preparation of Carbon Nanomaterials with Predefined Structure and Chirality

One of the major longstanding problem in the field of the rational synthesis of fullerenes and SWCNTs is the possibility to carry out directed synthesis toward material with a strictly defined structure. The bottom-up approach offers possible pathways to implement such idea, although it still remains to be not implemented in a full manner. In order to build fullerene cage, exploiting this approach, one would need corresponding building blocks, buckybowls in their turn are nothing else but fragments of fullerenes and caps of nanotubes. There are several works demonstrating the proof of concept,[79] e.g. assembly of C_{60} under laser-desorption ionization (LDI) conditions from the rationally synthesized precursor.[80] Moreover, it has been shown that buckybowls might be used as a seed for the growth of nanotube and the construction of other carbon materials.[81–87]

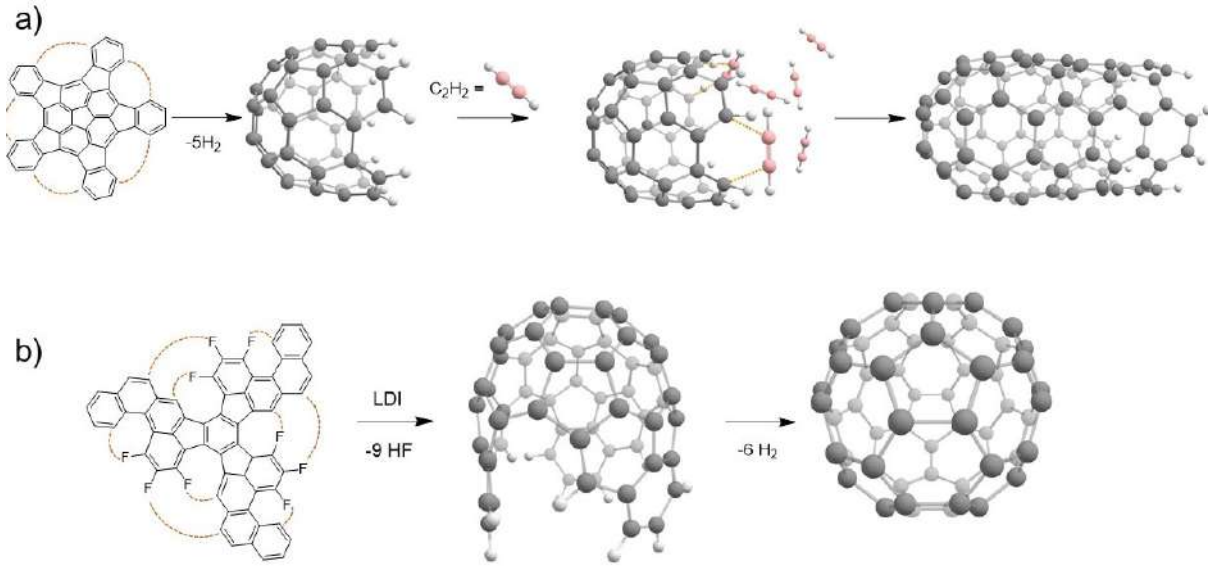

Figure 7. a) Directed synthesis and growth of [5,5]-SWCNT from tetraindenocorannulene, suggested by L. Scott et al. b) Assembly of C_{60} from the rationally fluorinated precursor, suggested and implemented by K. Amsharov et al.

Even though these works, indeed, show that the issue might be solved exploiting bottom-up approach, this area has been virtually unexplored due since it is nearly impossible to operate with molecules having such high molecular weights and low solubility, not to mention the lack of chemical reactions allowing effective assembly or elongation of such molecules.

1.2 Synthesis of Buckybowls

Considering all the prospective fields of applications that might be implemented in the nearest future, the reasonable question of the synthetic approaches towards such structures arises. Naturally, there are already quite a few structures both synthesized and thoroughly studied, nevertheless, it does not mean the better pathways should not be developed. The effective formation of C-C bond is obviously the key step during the construction of buckybowls, less obvious is that the most common and conventional techniques tend to fail if faced with strain energies needed to overcome. Thus, Friedel-Crafts acylation does not allow synthesis of corannulene's core,[88–91] photocyclization as well as Scholl reaction also generally fail to give buckybowls.[89,92,93]

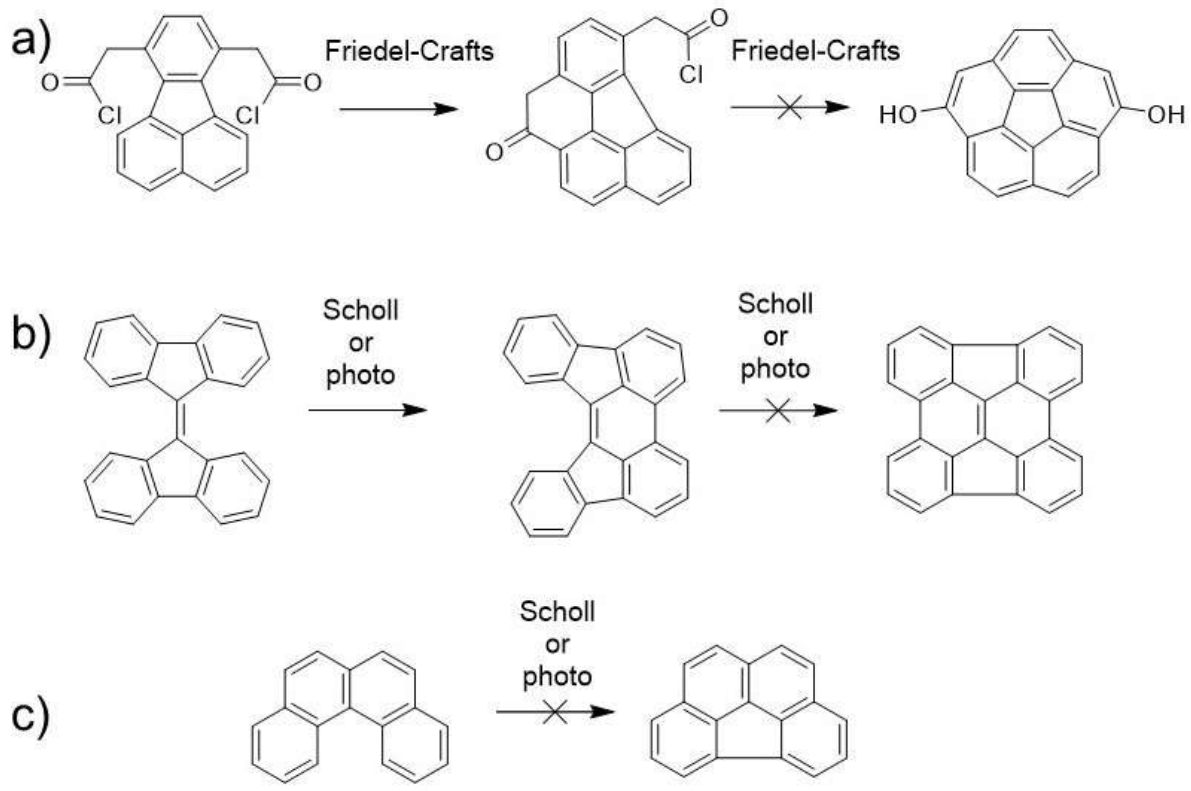

Scheme 1. Selected exaples showing that majority of conventional methods usually fails to yield buckybowls.

The apparent variety of available buckybowls comes from the functionalization of available blocks, where corannulene is virtually the only available block. Thus, the multitude of studied samples is generally reduced to corannulene based materials.[88,94,95] This brings synthetic chemists to a choice either to develop a synthetic approach to each distinct buckybowl or to develop some general chemical approaches which would allow the synthesis of any desirable non-planar PAH. Historically, the first option occurred at first, in 1966 Barth and Lawton synthesized dibenzofluoranthene (later named corannulene) implementing the synthetic route with more than 17 steps.[96,97]

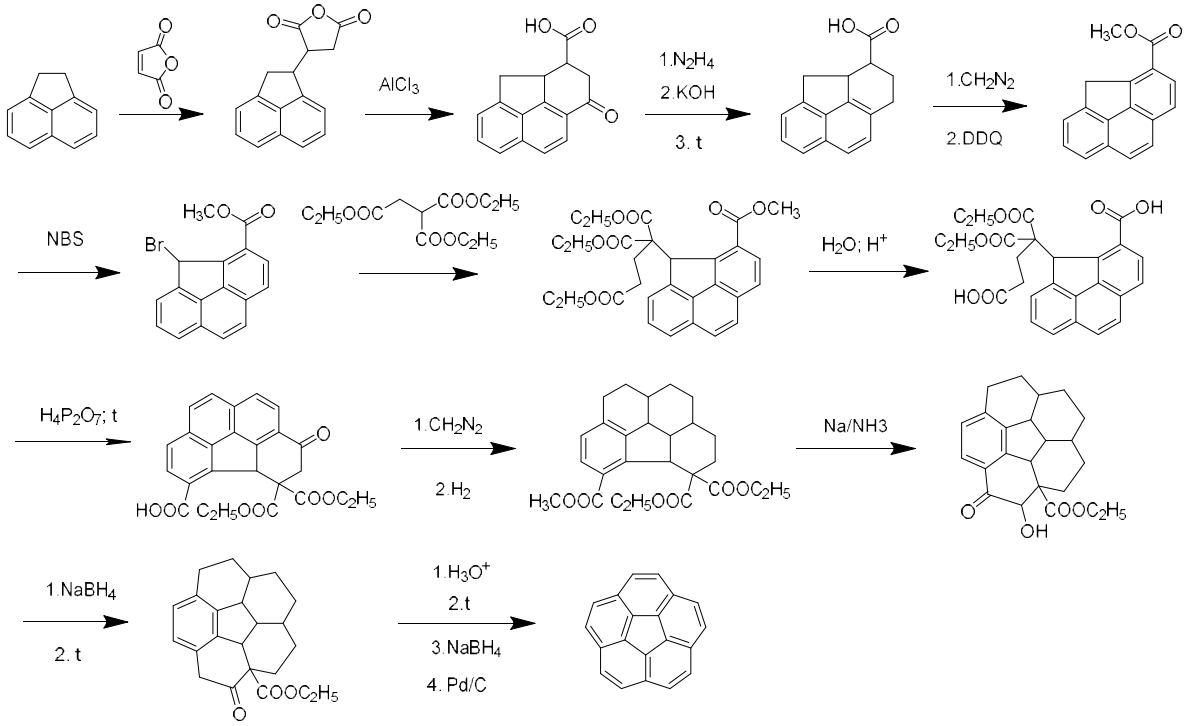

Scheme 2. The first synthesis of corannulene published by Barth and Lawton in 1966.

As already mentioned, the major issue in the synthesis of buckybowls is the bending of the aromatic fragment in order to create the remaining C-C bonds. For this purpose, significant energies are required to be overcome and there are several possibilities to tackle the issue. One of those is to carry out reactions at elevated temperatures, which are believed to be the reason why flash-vacuum pyrolysis (discussed in chapter 1.2.1) turned out to be so successful in the fabrication of buckybowls. Another possibility is to introduce the strain as late as possible i.e. introduce aromaticity after all C-C bonds have been constructed. This solution appears reasonable due to

enhanced flexibility and bond lengths in case of sp^3-hybridized carbons. This was exactly the approach of Barth and Lawton used for the first synthesis of corannulene.

Modern science tends to require the development of the most general chemical reaction with a large scope of applicability. Thus, some general approaches to buckybowls are required and despite significant efforts, there are only a few methods enabling the synthesis of buckybowls from regular PAHs precursors. In the following chapters the main reactions shall be considered, compared and discussed.

1.2.1 Flash-Vacuum Pyrolysis

Heating up the precursor molecules in the gas phase at 500-1100 °C was proven to be an extremely effective method allowing the synthesis of a wide range of buckybowls including Buckminster fullerene C_{60} in a fully rational manner.[80] This technique is well known under the name of flash-vacuum pyrolysis or FVP. This method enables the transformation of planar or quasi planar PAHs into buckybowls via intramolecular cyclodehydrogenation or cyclodehydrohalogenation (Figure 8a).[64,98–100] The scope of the bowl-shaped molecules obtained via FVP is impressive (Figure 9). The approach was mainly developed in the group of Lawrence Scott, where it has been shown that the method is capable of producing marvelous at that time buckybowls.[101–106]

During this procedure molecules are heated up to a very high temperature within a very short period of time. Such treatment stimulates out of plane deformations required for the synthesis of buckybowls with an extremely bent surface. The short heating times of about 10^{-6} seconds prevent molecule from undesirable decomposition and/or possible skeletal rearrengements.[107,108] As an illustrative example of FVP's utility, L. Scott et al. demonstrated an effective three-step synthesis of corannulene.[19] With all decent advantages that allowed FVP to push the synthesis of buckybowls to a new level, there are several inherent drawbacks. First of all, the precursor should be robust enough to survive severe temperature regime. Moreover, due to radical nature of the reaction the process is frequently accompanied by various side precesess and has extremely poor tolerance to virtually any functionalities on the rim of PAHs.

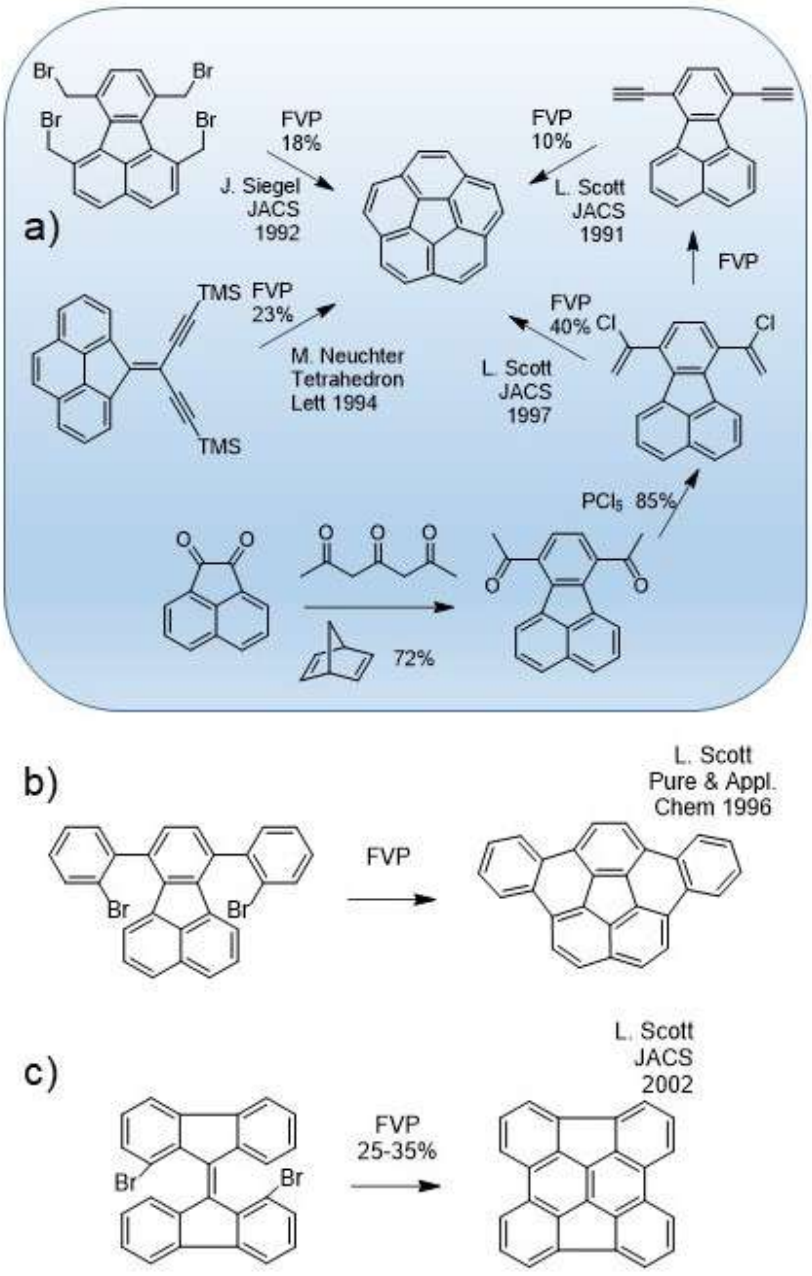

Figure 8. Synthesis of buckybowls by FVP approach. a) Applicability of several functional groups to generate C-C bonds under FVP conditions. Alternative syntheses of corannulene, including three-step synthesis suggested by L. Scott. b) Synthesis of dibenzocorannulene. c) The first synthesis of diindenochrysene.

This complicates further modification and building of functionalized carbon materials. Moreover, yields generally do not exceed 20-30%, regularly showing even way lower values (1-5%), which drastically exacerbate the whole approach since the precursor oftentimes require rather complicated multi-step synthesis. From the technical standpoint, it is also not trivial to scale the synthetic procedure up, in order to avoid intramolecular side reactions the concentration of the molecules in the gas phase should stay low.

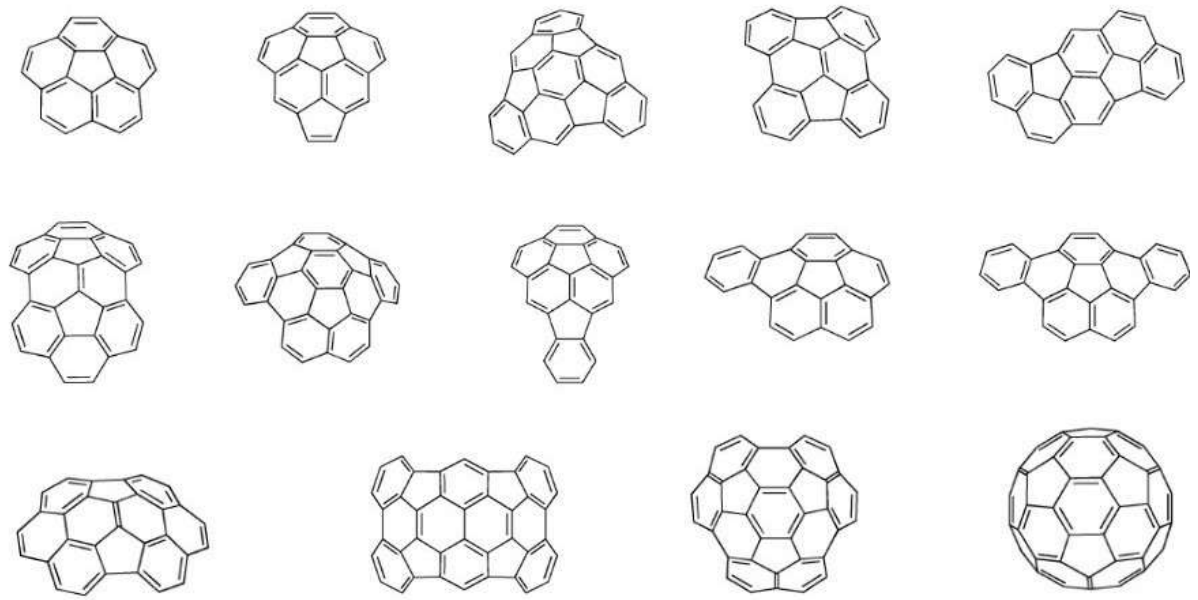

Figure 9. Some representatives of buckybowls obtained via FVP.

Summing up this superficial review on FVP, the main conclusion is that despite all the advantages, softer approaches are desired. The perfect approach would be still able to climb up significant energy barriers under milder conditions, which would tolerate various functionalities. Due to this urge, several non-pyrolytic methods have been developed,[109] and the next chapters cover the most important representatives of these reactions.

1.2.2 Solution-Phase Synthesis of Buckybowls

First of all, it is worth to underline again that the majority of conventional ways to create C-C bond failed to overcome strain energies. For example, neither Friedel-Crafts acylation of fluoranthene derivatives nor oxidation of cyclophanes did not lead even to trace amounts of the target, corannulene.[90,91] These facts were described in a rather precise manner by J. Siegel et al.: "*In the*

glory of hindsight and physical organic chemical analysis, both these unsuccessful approaches underestimated the strain needed to reach the transition state route to the final closure, and overestimated the aromatic stabilization benefit one might obtain from creating the corannulene unit. Indeed, higher-energy reaction conditions or higher-energy synthetic precursors would be needed to bring a new synthesis to fruition.".[20] Among high temperatures, another approach to counter strain energies is to accumulate twisting energy within the precursor molecule. Atom crowding, generally, leads to distortion of the molecule, e.g. helicenes or 1,6,7,10-tetrasubstituted fluoranthenes, which were shown to undergo C-C bond formation giving 2,5-dimethylcorannulene in modest yield via low-valent titanium coupling followed by dehydrogenation (Scheme 3a).[110–112] The exploitation of distorted fluoranthene derivatives proved to be effective, thus, more strained octabrominated derivative turned out to be even more effective precursor for corannulene (Scheme 3b).[113,114]

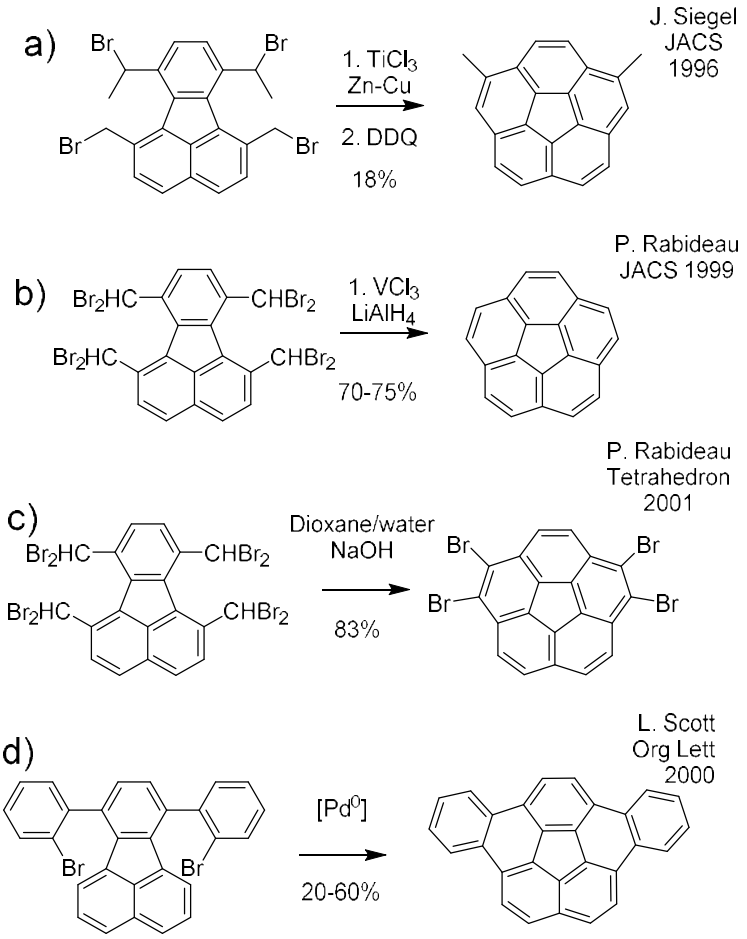

Scheme 3. Some of the first non-pyrolytic approaches to corannulene's core.

Another pathway, serendipitously discovered by P. Rabiadeau er al., is based on the hydrolysis of already mentioned octabromide. Initially, it was intended to carry out intramolecular McMurry coupling of 1,6,7,10-tetraaldehyde fluoranthene. However, after hydrolysis of corresponding octabromide, instead of the desired precursor, a mixture of brominated corannulene's derivatives was obtained. The brominated corannulenes were finally reduced to pristine buckybowl according to Scheme 3c.[93,115] This unexpected discovery was used later on as a key transformation by J. Siegel et al. to obtain corannulene in kilogram scale.[20]

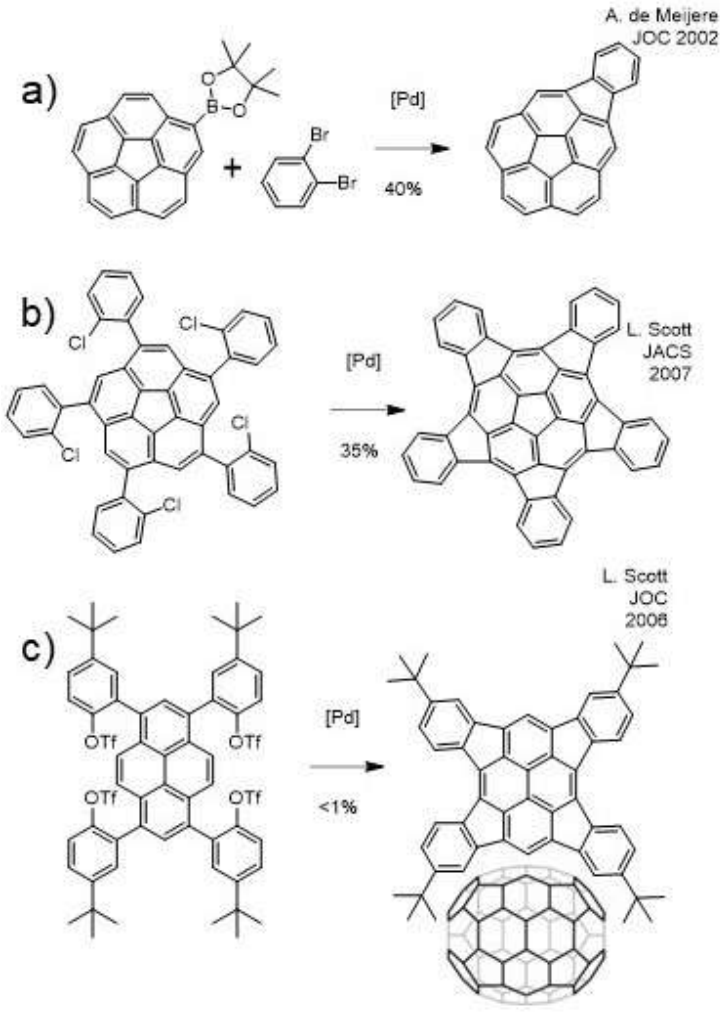

Scheme 4. Pd-catalyzed indenoannulation. a) One-step synthesis of indenocorannulene. b) Synthesis of pentaindenocorannulene. c) Synthesis of tetraindenopyrene – a fragment of C_{70} fullerene.

As of more general non-pyrolytic approaches, Pd-catalyzed C-C coupling was found to be both effective and broadly applicable. One of the first works demonstrating the synthesis of buckybowl

from brominated precursor was a report of L. Scott et al., who showed the possibility to exploit Pd-catalysts to obtain dibenzocorannulene (Scheme 3d).[103] This report entailed a huge number of works, where Br-,[116] Cl- and triflates (TfO-)[117] functionalities were used in the synthesis of strained PAHs and buckybowls.[118–120] Incorporation of pentagons goes hand by hand with the synthesis of buckybowls, and one of the most straightforward approaches to introduce pentagon is indenoannulation, which was developed in several groups.[121] This reaction enables incorporation of several pentagons in one synthetic step, providing buckybowls, such as tetraindenopyrene[122] and various indenocorannulenes, in a facile manner.[123–126]

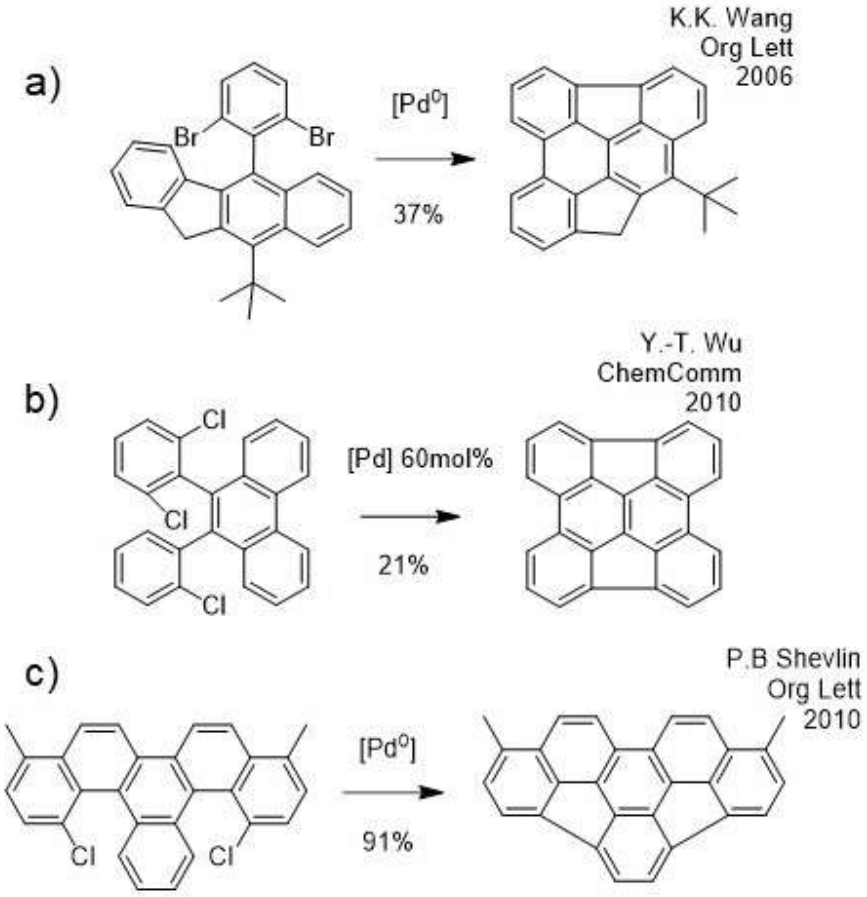

Scheme 5. Implementation of Pd-catalysis to synthesize some important buckybowls.

The synthesis of indacenopicene[127] (Scheme 5c), diindenochrysene and its fragment (Scheme 5a and b) also demonstrates the power of Pd-catalyzed approach,[128,129] since only FVP managed to generate diindenochrysene prior to report of Y.-T. Wu et al, despite numerous attempts.[89,92,130]

Even though Pd-catalysis is, indeed a powerful technique enabling the synthesis of strained buckybowls, it has a couple of serious downsides. Naturally, the most important restriction is the price of catalyst, especially considering the high loadings of 20-60 mol%, which are oftentimes required. Eventually, in some cases, mass of catalyst may exceed the mass of the substrate. Nevertheless, this is not the most fundamental downside of the approach. The major obstacle in using of Pd-catalyst is a very low tolerance towards the C-Br bond, thus it is not possible to generate brominated buckybowls, which are very promising building blocks. Moreover, the efficiency of C-C coupling drastically drops, if more than two bonds are introduced. This was clearly shown on the synthesis of oligoindenopyrenes, where the desired tetraindenopyrene was obtained in less than 1% yield.[122] Thus, in order to develop a more advanced approach, one should address the following issues: low costs, tolerance to functionalities and preservation of efficient for multiple C-C coupling. As it turns out C-F functionality allows to cope with all described problems of Pd-catalysis.

In the context of this work C-F bond activation and its utility for the synthesis of buckybowls and C-C coupling in general plays a crucial role. For this reason, key methods exploiting C(sp^2)-F bond as a functional group for C-C bond formation will be covered in the next chapter.

1.2.3 C-F activation

Even though aromatic C-Hal bond is widely used in all spheres of chemistry, C-F bond (especially C_{aryl}-F) remain significantly underestimated. For such injustice C-F owes to its high bond energy, due to which the bond is, allegedly, inert and hard-to-cleave.[131] Activation of aromatic C–F bonds has been conventionally achieved via nucleophilic substitution (S_NAr)[132] or recently via transition-metal-catalyzed oxidative addition.[133–136] However, the former methods are typically limited to electron-deficient fluoroarene substrates, while the latter often requires special ligands, directing groups and/or harsh conditions. Among modern approaches, several deserve special attention. One of interesting and valuable in terms of buckybowls' synthesis transformation is studied in the research group of J. Ichikawa, where they exploit CF_2 vinyl activation to generate various distorted PAHs, which may serve as excellent precursors to give buckybowls.[75,137–144]

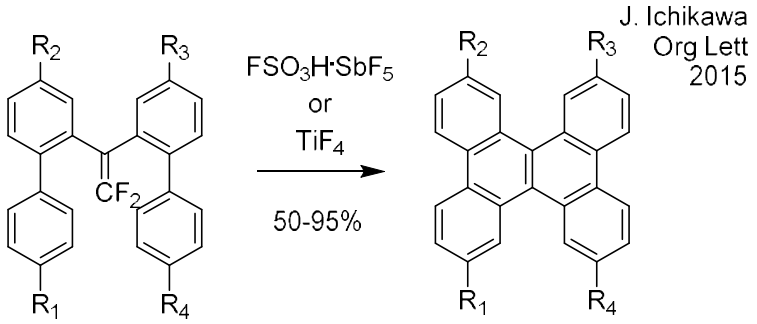

Scheme 6. Friedel-Crafts-type cyclization of difluoroethenes.

Another method allowing to generate strained PAHs, including buckybowls, is C-F bond polarization technique developed in the research group of J. Siegel. Thus, it has been shown that silylium carboranes can effectively polarize C-F bond.[145] Moreover, the possibility to use this activation to induce effective C-C coupling has been also demonstrated.[146] Silylium-mediated indenoannulation deserves particular attention since it allows facile synthesis of such strained systems as indenocorannulene under mild conditions (Scheme 7b).[147] Unfortunately, the price of catalyst and a remarkable drop of efficacy in case of highly curved PAHs serves as a major obstacle to the wide application of this strategy.

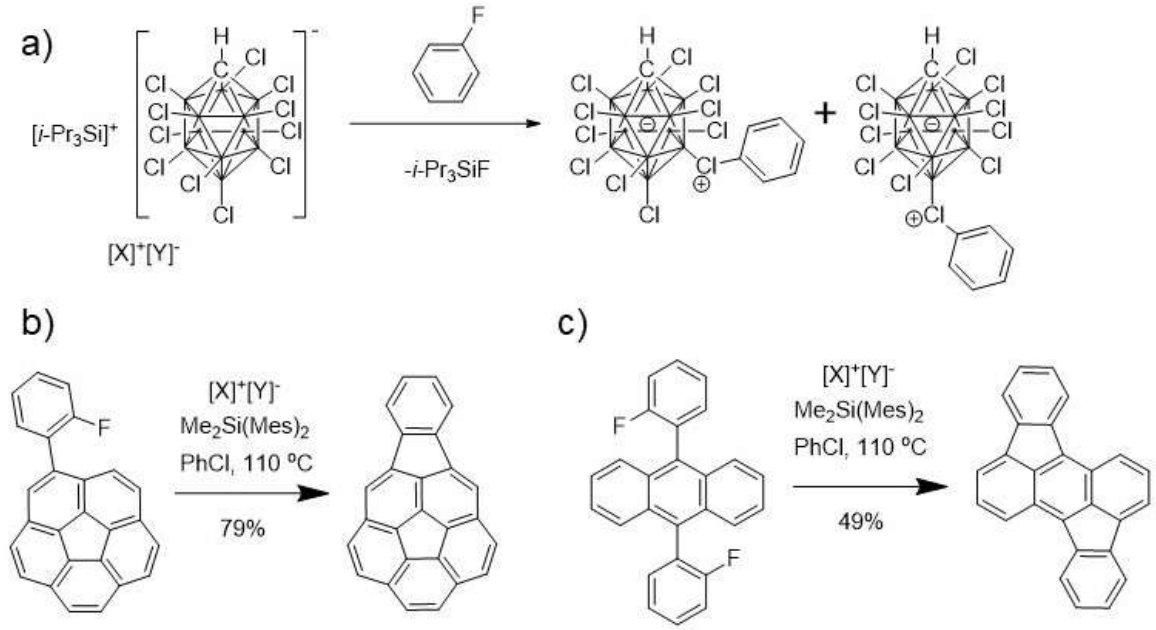

Scheme 7. Proton catalyzed, silane-fueled Friedel-Crafts coupling of fluoroarenes and its application for synthesis of strained PAHs.

Another opportunity to exploit C-F bond is to expose fluorinated PAHs to high temperatures in the gas phase (FVP conditions).[148] . Although this chemistry is undoubtedly interesting by itself, this approach leads back to all *pros* and *cons* of FVP. Nevertheless, some interesting works have been carried out by M. Jansen et al. who demonstrated how rationally fluorinated PAHs can be assembled yielding fullerene C_{60}.[86,149] As a matter of fact, HF elimination can be also photo-induced.[150] This was shown on example of some fluorinated stilbenes and closely related molecules, where HF elimination occurs in a competition with Mallory cyclization.[151,152]

1.2.3.1 Alumina-mediated C-F Bond Activation

Special attention should be paid to solid-state HF elimination on activated alumina.[153,154] This method has been recently explored in our group, where effective C-C coupling in various fluorinated PAHs has been demonstrated. Surprisingly, the technique turned out to be tolerant towards C-Br and C-Cl bonds showing regioselective C-F activation.[155] While the importance of the first phenomenon was already mentioned, the second observation indicates that alumina can distinguish active and dormant C-F bonds. This enabled synthetic chemists in our group to obtain large PAHs via zipping approach, where several C-C bonds created one by one.[156] Thus, various readily available fluorinated precursors may be used to generate large PAHs in one synthetic step.

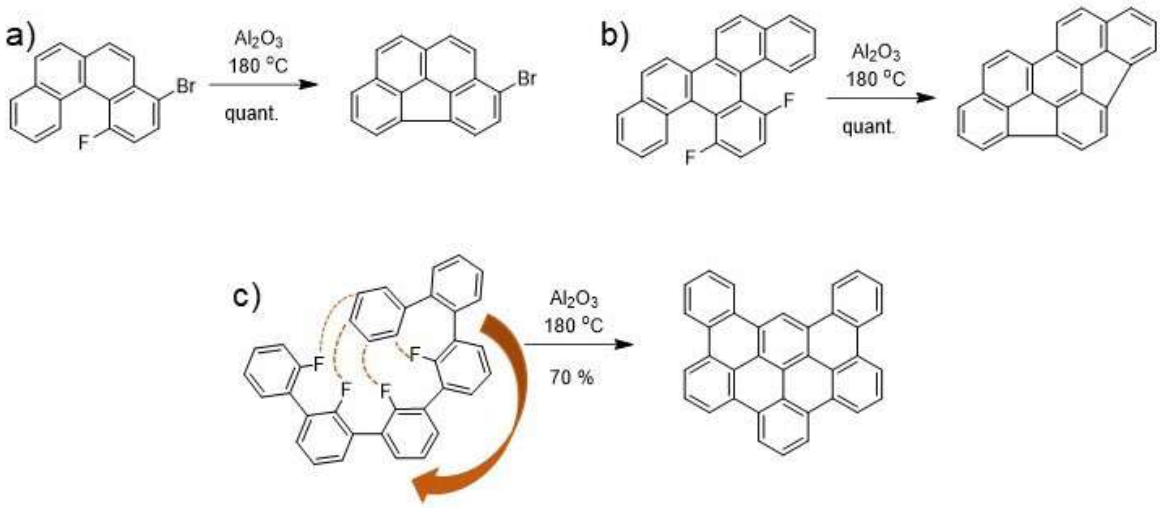

Scheme 8. Alumina-mediated C-F activation. a) Tolerance of the method towards C-Br bond. b) Synthesis of indacenopicene. c) HF-zipping approach to large PAHs.

Additionally to these impressive features, alumina-mediated C-F bond activation can also be exploited for the synthesis of buckybowls, which were obtained in nearly quantitative yields.[157]

Thus, the method seems to combine the majority of possible advantages synthetic method could have. This large potential triggered the current thesis, which mainly aimed to understand the mechanism of this peculiar transformation and to fulfill its synthetic capabilities.

2 Proposal

This work is oriented on the development of alumina-mediated HF elimination as a new general approach to buckybowls. While still in its infancy, this method has a large potential to be fulfilled. Previously it has been shown that C-F functionality exposed to activated alumina allows effective C(aryl)-C(aryl) coupling. Moreover, the method demonstrates selective C-F activation, tolerance to C-Br functionality and nearly quantitative cove-region closures yielding highly strained buckybowls. These mentioned idiosyncrasies open up a new horizon for this technique to be broadly exploited as a tool to generate highly strained, functionalized, non-planar PAHs. Firstly, C-Br bond can be fairly claimed to be the most demanded functionality for PAHs, since it undergoes the whole spectrum of transition metal-catalyzed reactions, such as Suzuki-, Sonogashira-, Yamamoto- coupling, etc. Thus, facile access to brominated buckybowls appears crucial for the future applications of these molecules. For this reason, we endeavor to show the feasibility of the idea and generate several functionalized buckybowls via alumina-mediated C-F activation (Publication 1). In general, we aim not only to synthesize some archetypal buckybowls, but we also care about synthetic simplicity of the procedures, trying to shrink the synthesis to the smallest possible number of stages. Selective C-F activation may serve as a valuable ally to achieve this goal since alumina distinguishes between “active” and “dormant” fluorine atoms, it becomes possible to program fluorinated precursor to undergo consequent C-C couplings and generate several C-C bonds in one synthetic step.

We study several different approaches to implement this idea i.e. zipping-like manner or multi-assemblies, where several C-F bonds are activated one after another and create all ‘missing’ C-C bonds to generate buckybowl from its fluorinated precursor. Apart from studying the most appropriate and effective precursor we also strive to find an optimal approach to the desired precursor (Publications 2 and 3). Thus, we reduce the number of required steps during the final procedure i.e. HF-elimination, as well as during the synthesis of precursors via a combination of available fluorinated blocks. Naturally, we aim to gain some mechanistic insights and unravel the peculiar nature of the reaction, moreover, the scope and limitations of alumina-mediated C-F activation appear as a matter of great importance. Our observations and conclusions on this issue might be found in corresponding works (Publications 4 and 5).

3 Index of Publications

Publication 1.

O. Papaianina, V. Akhmetov, A. A. Goryunkov, F. Hampel, F. W. Heinemann, K. Y. Amsharov.

Synthesis of Rationally Halogenated Buckybowls by Chemoselective Aromatic C−F Bond Activation.

Angew. Chemie - Int. Ed. **2017**, 56, 4834–4838.

V.Akhmetov developed the approach to rationally brominated buckybowls and carried out synthetic procedures confirming the tolerance to C-Br functionality. O.Papaianina carried out synthesis and optimized conditions for alumina activation and consequent HF elimination, she also prepared supporting information. F.Hampel and F.Heinemann obtained and analyzed X-Ray data. K.Amsharov wrote the manuscript and supervised the project. A.Goryunkov carried out DFT calculations and also supervised the project.

Publication 2.

V. Akhmetov, M. Feofanov, V. Ioutsi, F. Hampel, K. Amsharov.

Unusual Fusion of α-Fluorinated Benzophenones under McMurry Reaction Conditions.

Chem. - A Eur. J. **2019**, 25, 1910-1913

V.Akhmetov and M. Feofanov discovered unusual side-product and explored the scope of the reaction by carrying out several synthetic experiments. V.Akhmetov also carried out DFT calculations and wrote the manuscript. M.Feofanov prepared supporting information. V.Ioutsy suggested a possible mechanism. F.Hampel obtained and analyzed X-Ray data. K.Amsharov supervised the project.

Publication 3.

V. Akhmetov, M. Feofanov, S. Troyanov, K. Y. Amsharov.

Tailoring Diindenochrysene through Intramolecular Multi-Assemblies by C-F Bond Activation on Aluminum Oxide.

Chem. – A Eur. J. **2019**, 25, 7607-7612.

V.Akhmetov wrote the manuscript, suggested and carried out the major part of synthesis along with DFT-calculations and interpretation of the observed/calculated data. M.Feofanov implemented a part of synthetic procedures and prepared supporting information. S.Troyanov obtained and analyzed X-Ray data. K.Amsharov supervised the project.

Publication 4.

V. Akhmetov, K. Y. Amsharov.

Effect of the Cove Region Geometry in PAHs on Alumina Assisted Cyclodehydrofluorination.

Phys. Status Solidi B DOI:10.1002/pssb.201900254. First published online on 11th of July, **2019**.

V.Akhmetov and K.Amsharov carried out alumina-mediated HF elimination and analyzed the outcome of the reaction. V.Akhmetov wrote the manuscript and prepared supporting information.

Publication 5.

V. Akhmetov, M. Feofanov, O. Papaianina, S. Troyanov, K. Y. Amsharov.

Towards Non-alternant Nanographenes by Self-Promoted Intramolecular Indenoannulation Cascade via C-F Bond Activation.

Chem. – A Eur. J. DOI: 10.1002/chem.201902586. First published online on 13th of July, **2019**.

V.Akhmetov, O.Papaianina and M.Feofanov carried out synthesis, where V.Akhmetov took the major part of synthesis and interpretation of the results and wrote the manuscript. M.Feofanov and O.Papaianina prepared supporting information. S.Troyanov obtained and analyzed X-Ray data. K.Amsharov supervised the project.

4 Results and Discussions

This chapter will cover our successful attempts to obtain brominated buckybowls; synthesize archetypal buckybowl, diindenochrysene, in two-step synthesis, where five C-C bonds are generated at the last stage. Moreover, mechanistic details of the reaction and utility of some features will be shown and discussed, namely, the crucial role of electronic effects and the importance of structural preorganization of fluorinated precursors.

4.1 Functionalized Buckybowls.

Importance of C-Br bond in chemistry of PAHs is hard to overestimate since it can be exploited in a great variety of chemical reactions. Among the most important are Suzuki and Yamamoto couplings, which are widely used to generate required C-C bonds. The respective halogenated buckybowls play a crucial role in building of large and complex molecules. Such molecules might be used as caps for directed nanotubes' growth. Moreover, oligomerized or interconnected buckybowls may serve as potential recognition systems for fullerenes and related materials, as it has been discussed in chapter 1.1.2.

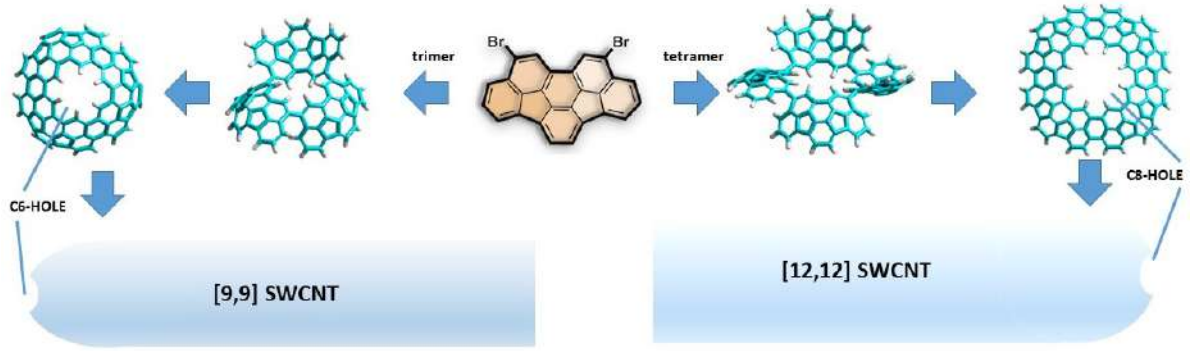

Figure 10. The potential application of brominated buckybowls as precursors for SWCNT-seeds.

Thus, brominated PAHs are precious building blocks for the bottom-up approach towards carbon-rich nanomaterials. While the lack and complexity of synthetic procedures yielding curved PAHs serve as major obstacles to generate sufficient quantities of pristine buckybowls, rationally brominated buckybowls are even less available molecules. Nevertheless, their intriguing properties and outstanding potential as useful synthetic building blocks stirs up the interest of synthetic

chemists. Considering tolerance to C-Br bond, alumina-mediated HF elimination becomes a very suitable technique to tackle this issue. In our work, we exploit bromine atoms both as an orienting group and as a substituent for the further functionalization of buckybowls (Publication 1). The demonstrated strategy allows facile gram-scale synthesis of functionalized buckybowls and enables to examine properties and applications of these attractive molecules.

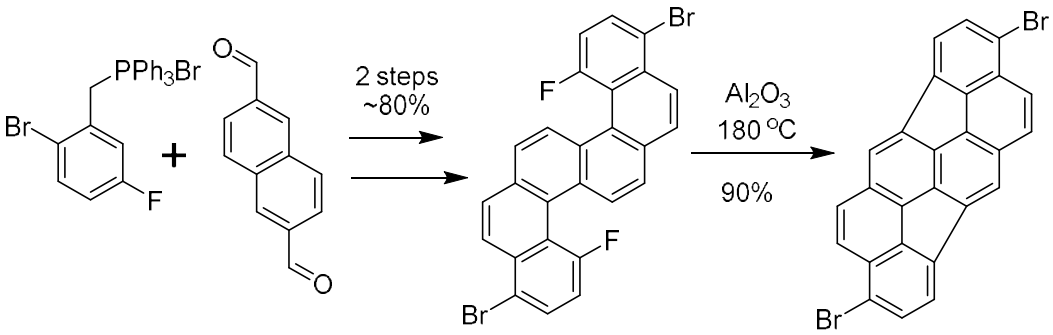

Scheme 9. Developed synthesis of brominated buckybowl.

In this work, we develop two alternative technical implementations of the reaction. The first option is to carry out the reaction in solid-state under vacuum at 160-200 °C, where the fluorinated precursor is simply mixed with activated alumina in a sealed glass vial. Another way is to mix activated alumina and precursor in *o*-DCB, which helps homogenous distribution of fluorinated PAHs over solid catalyst. In this case, reaction is carried out under inert atmosphere in a microwave oven. The described techniques do not show any crucial differences and can be used equally, depending on convenience and available equipment.

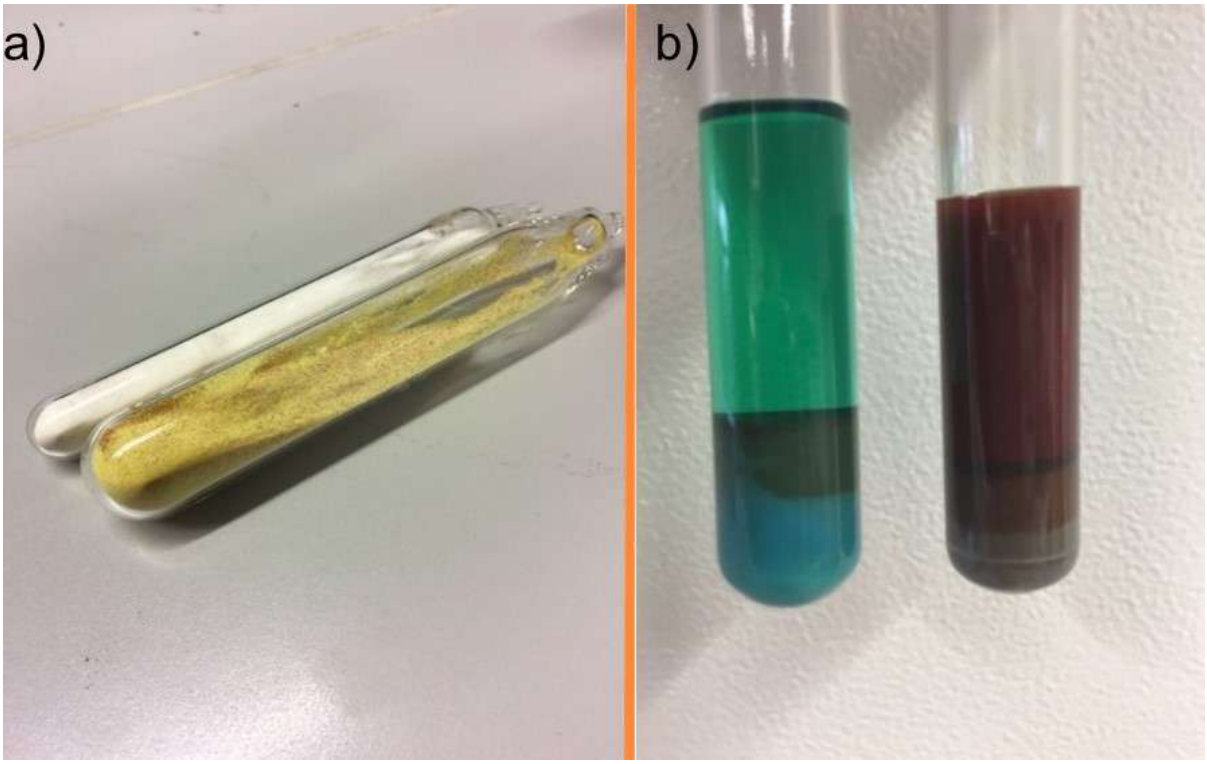

Figure 11. Two modifications of alumina-mediated HF elimination. a) Solid-state reaction under vacuum in a sealed tube. b) Reaction in *o*-DCB in a microwave vial.

4.2 Synthesis of Buckybowls via Programmed C-F activation.

The possibility to activate C-F bond selectively makes alumina-mediated C-F activation especially attractive. Since the catalytic centers can distinguish «active» and «dormant» fluorine atoms, it is possible to implement consequent C-C coupling, where the strict algorithm of C-F activations is dictated by the structure of fluorinated PAHs.

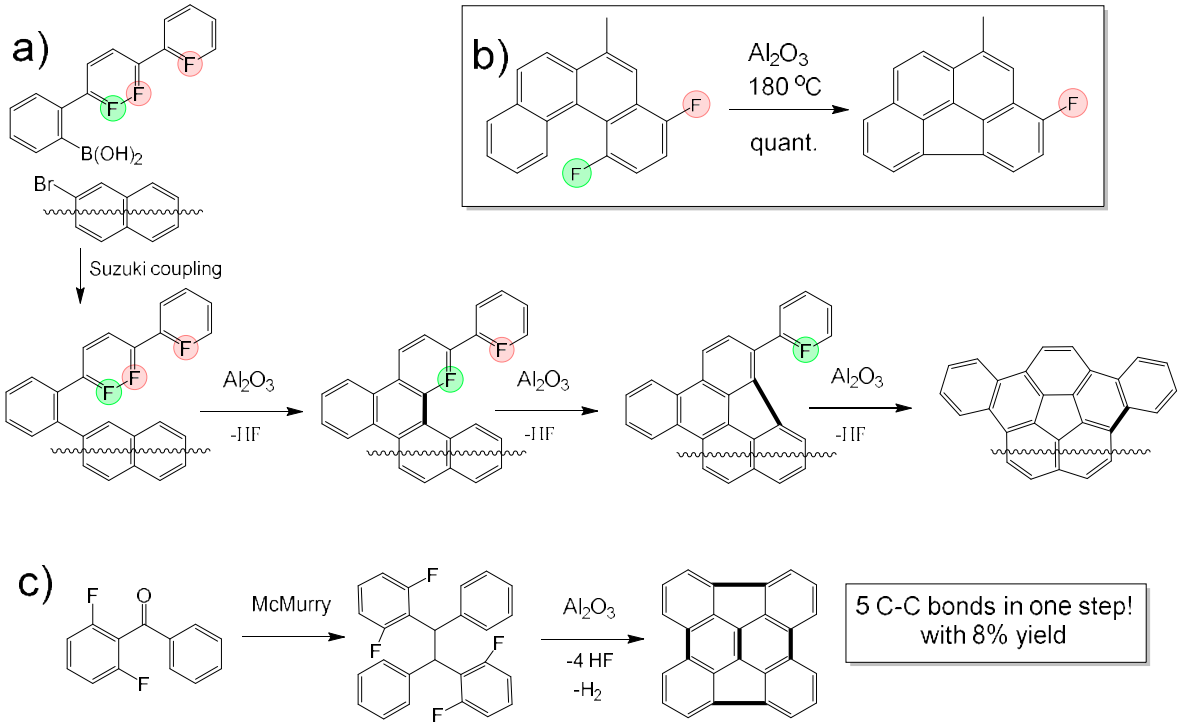

Scheme 10. Synthesis of buckybowls via C-F activation. a) Concept of the HF-zipping approach, where dormant fluorine atoms (labeled pink) become active (labeled green) after previous C-C coupling. c) Multi-assembly yielding diindenochrysene.

This concept is a very promising approach to buckybowls, as well as any other large PAHs since it requires rather simple convergent synthesis (Scheme 10a). Once fluorinated blocks are obtained, they are attached to brominated PAH core and these two subunits are zipped on alumina via consequent HF elimination. The flexibility of the technique is yet another advantage, several different building blocks can be used to attain the very same buckybowl. Moreover, positions of fluorine atoms play a crucial role and it is easy to interchange the position of this key element in the precursor structure. The described methodology opens a vast number of synthetic pathways to

valuable buckybowls and resembles some sort of programming language with its elements (structure of the precursor, positions of fluorines, etc), input-fluorinated PAH, output-buckybowl and implementing machine-activated alumina. We have studied the key aspects of such an approach on the example of archetypal buckybowl - diindenochysene. We have proved the applicability of the HF-zipping approach to gain diindenochrysene in moderate 6% yield. Additionally we have successfully examined another attractive way to assemble diindenochrysene. This approach requires only two-step synthesis and yields diindenochrysene at the last step with 8% yield. This number becomes impressive if five C-C bonds created during the last step are considered. All the details on our investigation and development of algorithm-like synthesis and its implementation on activated alumina are collected in corresponding work (Publication 2).

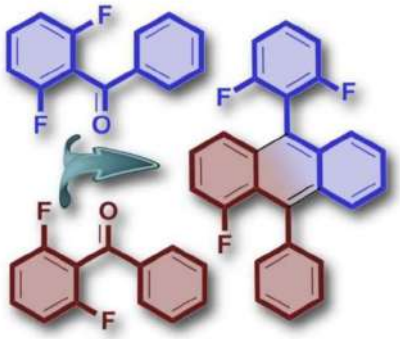

Figure 12. A fusion of two molecules of 2,6-difluorobenzophenones to give fluorinated 9,10-dihenylanthracene.

In the course of the synthesis of some fluorinated precursors for diindenochrysene, serendipitously we discovered a rather unusual reaction that fluorinated benzophenones undergo simultaneously with McMurry coupling, which was believed to be the only process under applied conditions. The mechanistic details and scope of this unexpected benzophenone transformation are presented and discussed in our recent investigation (Publication 3). This work supports the statement that C-F chemistry still remains extremely underestimated and unexplored.

4.3 Mechanistic insights into alumina-mediated HF elimination.

Since alumina-mediated C-F bond activation holds heterogeneous nature, it becomes extremely sophisticated to strictly determine the mechanism of the reaction. First of all, exploited alumina possesses amorphous structure, which complicates studies on possible appearance of the catalytic centers. Thus, activated alumina and particularly the course of the discussed reaction remain to be a black box. Nevertheless, some observation on the outcomes of some reactions leads to certain conclusions that the process is likely to bear cation-like nature. While it is clear that extremely reactive phenyl cations do not form during the reaction, some sort of concerted transformation with formation of partially charged species should take place. A quantum chemical investigation on DFT level was carried out previously in our group, where it has been shown how the process might occur.[158] The cove-region closure clearly indicates that eliminated hydrogen plays a crucial role in stabilization of transition state, reducing activation barriers. Moreover, this study, indeed, confirms cation-like nature of the reaction. Even though this particular DFT study does not directly relate to the current thesis, it is crucial for the following chapter.

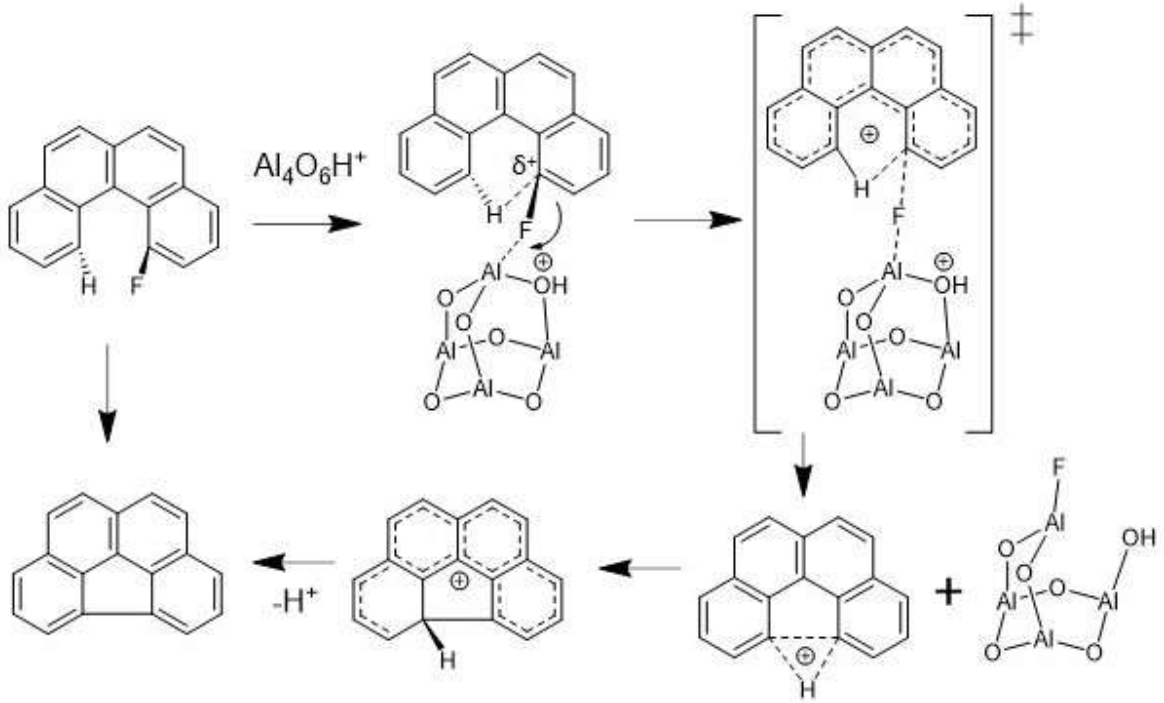

Scheme 11. The suggested mechanism of alumina-mediated cyclodehydrofluorination.

4.3.1 Effect of cove region geometry on C-C coupling during Alumina-Mediated C-F Bond Activation

It has been shown in several different examples that cove-region closure proceeds extremely effective, frequently giving a desired product in quantitative yields. Actually, it comes as a rather intuitive outcome, since [4]-helicene is already a highly strained moiety. Its twisted geometry caused by atom crowding, makes it is less problematic to overcome barriers to generate curved buckybowls due to accumulated in the molecule energy. Thus, this transformation can be considered as a transfer of twisted energy to curved analog. Meanwhile, molecular systems bearing several helical motives could undergo gradual extension of the remaining cove-regions after the closure of the previous ones, thus releasing the accumulated strain energy. It has been shown that four cove-regions can be closed in an effective manner.[157] Nevertheless, it is a matter of fundamental interest to estimate whether this extension has a limit, after which C-C coupling will not occur. In order to address this important issue, we have obtained an interesting molecular system with four fluorinated cove-regions, where each previous HF-elimination drastically increases strain and flattens the remaining helicene-moieties. We found out that the helical structure is, indeed, crucial for effective coupling and that after a certain point alumina cannot induce C-C coupling in the fluorinated PAHs. All the details of this insightful study may be found in the corresponding work (Publication 4).

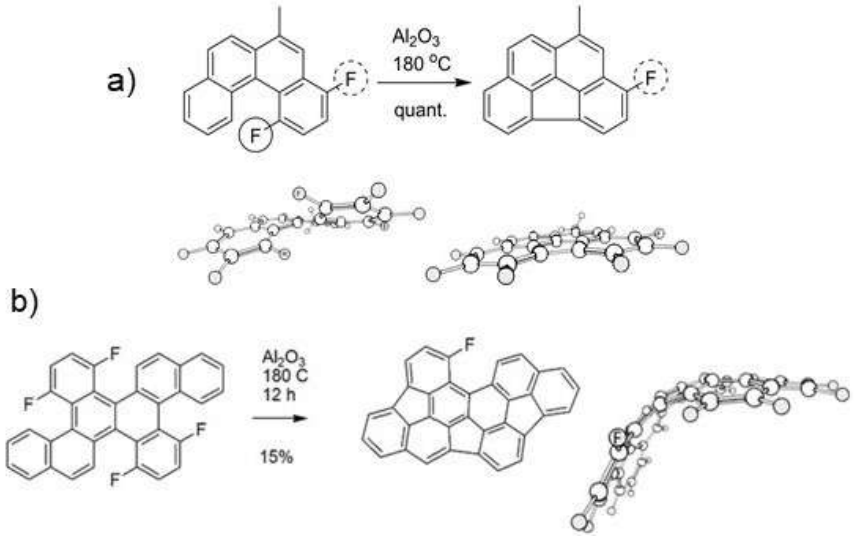

Figure 13. Investigated molecules containing multiple fluorinated [4]-helicene motives.

4.3.2 Role of electronic effects in Self-Promoted Intramolecular Indenoannulation Cascade via Alumina-Mediated C-F Bond Activation

Despite a large number of attractive features, non-alternant nanographenes (NGs) bearing pentagons in their structure still remain hard-to-reach materials. Incorporation of five-membered rings into PAHs being already sophisticated task by itself, the synthetic availability of such compounds becomes even lower, provided poor solubility of the desired molecules and their precursors. While other conventional synthetic approaches stumble upon this problem, alumina-mediated C-F bond activation turns the size of the molecules into an ally. Among several approaches, the indenoannulation appears to be optimal for these purposes, since it generally requires only two-step procedure and enables a great variety of extended PAHs. Using this strategy along with the unique nature of alumina-assisted HF elimination, we show the capability of this tandem to create several C-C bonds in one step (Publication 5). Moreover, the efficiency of coupling has been shown to increase with the number of C-C bonds being created. Thus, rolling-up of NGs on activated alumina resembles a snowball rolling down the slope. As the snowball accelerates and becomes bigger after each turn, PAH becomes more and more prone to undergo indenoannulation after each previous cyclization.

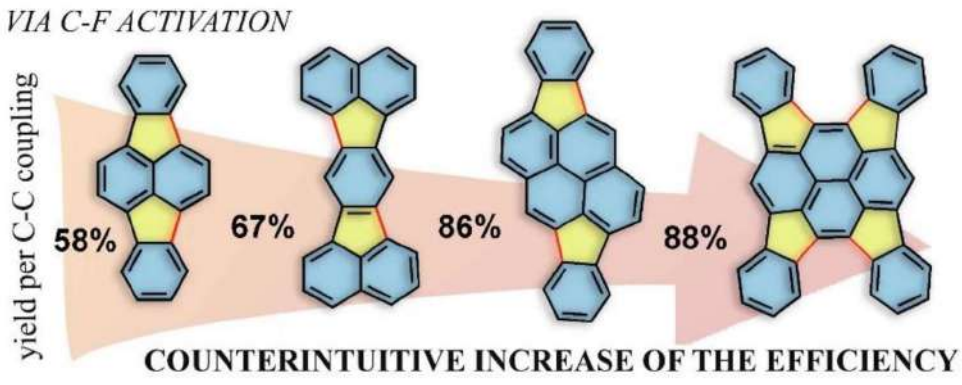

Figure 14. Correlation between size of involved π-sytem and efficiency of C-C coupling.

Comparing several indenoannulations of naphthalene and pyrene cores we confirm this concept and show that C-C coupling efficiency depends on the readiness of π-system to undergo electrophilic attack. In contrast to the vast majority of reactions dealing with overcoming strain energies inherent to the synthesis of non-alternant PAHs, alumina-mediated C-F bond activation

turns out to be more sensitive to electronic effects rather than steric. In this manner, the technique stands out from the rest of synthetic methods yielding non-alternant PAHs and opens up new venues to unavailable, yet intriguing extra large nonalternant PAHs.

4.4 Publications

Publication 1.

Synthesis of Rationally Halogenated Buckybowls by Chemoselective Aromatic C−F Bond Activation.

O. Papaianina, V. Akhmetov, A. A. Goryunkov, F. Hampel, F. W. Heinemann, K. Y. Amsharov.

Angew. Chemie - Int. Ed. **2017**, 56, 4834–4838. DOI: 10.1002/anie.201700814.

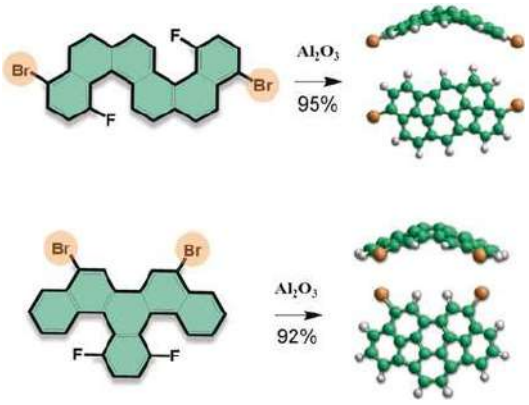

ABSTRACT:

Halogenated buckybowls or bowl-shaped polycyclic aromatic hydrocarbons (BS-PAHs) are key building blocks for the “bottom-up” synthesis of various carbon-based nanomaterials with outstanding potential in different fields of technology. The current state of the art provides quite a limited number of synthetic pathways to BS-PAHs; moreover, none of these approaches show high selectivity and tolerance of functional groups. Herein we demonstrate an effective route to BS-PAHs that includes directed intramolecular aryl–aryl coupling through C−F bond activation. The coupling conditions were found to be completely tolerant toward aromatic C−Br and C−Cl bonds, thus allowing the facile synthesis of rationally halogenated buckybowls with an unprecedented level of selectivity. This finding opens the way to functionalized BS-PAH systems that cannot be obtained by alternative methods.

Bowl-Shaped Aromatic Systems

International Edition: DOI: 10.1002/anie.201700814
German Edition: DOI: 10.1002/ange.201700814

Synthesis of Rationally Halogenated Buckybowls by Chemoselective Aromatic C–F Bond Activation

*Olena Papaianina, Vladimir A. Akhmetov, Alexey A. Goryunkov, Frank Hampel, Frank W. Heinemann, and Konstantin Y. Amsharov**

Abstract: *Halogenated buckybowls or bowl-shaped polycyclic aromatic hydrocarbons (BS-PAHs) are key building blocks for the "bottom-up" synthesis of various carbon-based nanomaterials with outstanding potential in different fields of technology. The current state of the art provides quite a limited number of synthetic pathways to BS-PAHs; moreover, none of these approaches show high selectivity and tolerance of functional groups. Herein we demonstrate an effective route to BS-PAHs that includes directed intramolecular aryl–aryl coupling through C–F bond activation. The coupling conditions were found to be completely tolerant toward aromatic C–Br and C–Cl bonds, thus allowing the facile synthesis of rationally halogenated buckybowls with an unprecedented level of selectivity. This finding opens the way to functionalized BS-PAH systems that cannot be obtained by alternative methods.*

The amount of research in the field of bowl-shaped polycyclic aromatic hydrocarbons (BS-PAHs) has been expanding rapidly in recent years. The widespread interest in BS-PAHs is induced by their unique properties originating from the curved π system.[1–3] Because of the tremendous strain inherent to the geodesic structure, the fabrication of buckybowls frequently requires harsh reaction conditions that do not tolerate functional groups. As a result, the controllable functionalization of the buckybowl system still remains a challenge, thus hampering further development in this field. Appropriate functionalized buckybowls are important starting materials for further derivatization[4–16] and key building blocks for the rational synthesis of fullerenes, nanotubes, and other related carbon-based nanostructures by a bottom-up strategy.[17–26] In this respect, halogenated, and in particular brominated, bowls appear to be the most important derivatives.[4–16] The most often studied approaches to buckybowls are based on the intramolecular aryl–aryl coupling of appropriate precursor molecules by means of flash vacuum pyrolysis (FVP),[2,27] surface-assisted cyclodehydrogenation,[28–31] and palladium-catalyzed direct arylation methods.[32–36] Unfortunately, none of these methods can be applied to the synthesis of halogenated BS-PAHs. Although the postsynthetic halogenation of corannulene, the smallest buckybowl, has proven to be effective,[37,38] this approach is not effective in the case of large and less symmetrical molecules. Thus, the development of new methods that enable the facile synthesis of halogenated BS-PAHs in a fully controllable way is a matter of great interest and importance.

Previously, Siegel and co-workers,[39] Ichikawa and co-workers,[40–42] and Amsharov and co-workers[43,44] demonstrated the efficiency of the C–F bond activation strategy for the synthesis of PAH systems through intramolecular aryl–aryl coupling. After thorough research, we discovered that aluminum oxide mediated cyclodehydrofluorination is an effective method for the synthesis of BS-PAHs.[45] Herein we demonstrate that aryl–aryl coupling by γ-aluminum oxide mediated C–F bond activation occurs under mild conditions with an unprecedented level of chemoselectivity. We also found that the C–F bond can be effectively activated in the presence of more labile aromatic C–Br and C–Cl bonds, thus allowing the facile synthesis of halogenated BS-PAHs in a fully controllable manner. The described technique is not only straightforward and highly reproducible but opens access to halogenated bowl-shaped systems which are not accessible by other methods. Variously brominated indacenopicenes and several halogenated diindenochrysenes were synthesized by this approach with unprecedented levels of efficiency and conversion.

In the course of our studies on alumina-promoted aromatic C–F bond activation, we have found that the solvent plays a crucial role. Namely, it was found that the solvent does not only help to distribute the precursor homogeneously over alumina but fundamentally influences the efficiency of the cyclodehydrofluorination. The promoting effect of the solvent was investigated on the basis of the model conversion of 1-fluoro-4-bromobenzo[*c*]phenanthrene (**1**) into 3-bromobenzo[*ghi*]fluoranthene (**2**; Figure 1). To evaluate the solvent effect, we carried out the cyclodehydrofluorination for 30 min at the relatively low temperature of 120°C. Under these conditions, only 0.5% conversion of **1** into **2** was observed when a solid-state strategy was applied (no solvent).

The screening of various solvents revealed that *o*-dichlorobenzene (*o*-DCB) was superior in accelerating the reaction. In the presence of *o*-DCB, the cyclodehydrofluori-

[*] O. Papaianina, Dr. F. Hampel, Dr. K. Y. Amsharov
Department of Organic Chemistry
Friedrich Alexander University Erlangen-Nuremberg
Henkestrasse 42, 91054 Erlangen (Germany)
E-mail: konstantin.amsharov@fau.de
Dr. F. W. Heinemann
Department of Inorganic Chemistry
Friedrich Alexander University Erlangen-Nuremberg
Egerlandstrasse 1, 91058 Erlangen (Germany)
V. A. Akhmetov, Dr. A. A. Goryunkov
Department of Chemistry, Lomonosov Moscow State University
Leninskie Gory, 1–3, 119991 Moscow (Russia)
Supporting information and the ORCID identification number(s) for the author(s) of this article can be found under: http://dx.doi.org/10.1002/anie.201700814.

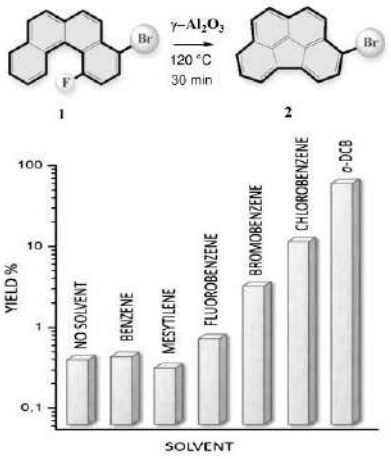

Figure 1. Top: Model transformation of **1** into **2**, used for optimization of the condensation conditions. Bottom: Diagram showing the effect of the solvent on the conversion efficiency. All reactions were carried out at 120 °C for 30 min. A logarithmic scale has been used to show the yields.

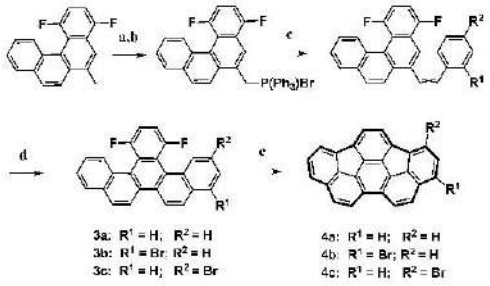

Scheme 1. Synthetic route to the brominated indacenopicenes. a) NBS, DBPO, CCl_4, reflux 4 h, 85 %; b) PPh_3, toluene, reflux 16 h, 98 %; c) ArCHO, *t*BuOK, EtOH, reflux 10 h, 80 %; d) *hν*, I_2, propylene oxide, cyclohexane (**3a**: 84 %; **3b**: 50 %; **3c**: 55 %); e) γ-Al_2O_3, *o*-DCB, microwave irradiation (**4a**: 150 °C, 30 min, 99 %; **4b**: 150 °C, 1.5 h, 96 %; **4c**: 240 °C, 1.5 h 80 %). DBPO = dibenzoyl peroxide, NBS = *N*-bromosuccinimide.

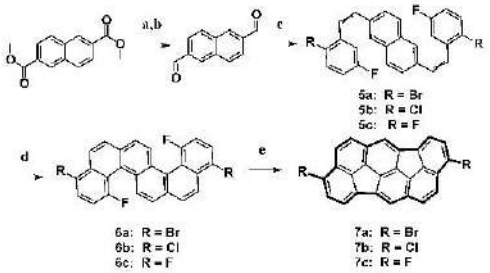

Scheme 2. Synthetic route to the halogenated diindenochrysenes. a) $LiAlH_4$, THF, 3 h; b) PCC, CH_2Cl_2, 0 °C, 4 h, 65 %; c) $ArCH_2PPh_3Br$, *t*BuOK, EtOH, reflux, 10 h, 70 %; d) *hν*, I_2, propylene oxide, cyclohexane (**6a**: 50 %; **6b**: 42 %; **6c**: 47 %); e) γ-Al_2O_3, *o*-DCB, microwave irradiation (**7a**: 240 °C, 1 h, 95 %; **7b**: 220 °C, 0.5 h, 98 %; **7c**: 230 °C, 1 h, 63 %). PCC = pyridinium chlorochromate.

nation was found to be about 200 times faster than without a solvent, thus resulting in the formation of **2** in more than 60 % yield after 30 min. Chlorobenzene and bromobenzene showed acceptable acceleration, yielding the target product in 14 and 5 % yield, respectively. Almost no effect was observed for fluorobenzene (0.8 %) and nonpolar solvents, such as benzene (0.5 %) and mesytilene (0.3 %). Polar aprotic solvents, such as DMSO, DMF, and DMA, completely inhibited the reaction because of the deactivation of active centers at the alumina interface. When *o*-DCB was used as the solvent, full conversion of **1** into **2** could be achieved by increasing either the reaction time or the reaction temperature. Thus, a reaction at 150 °C was already complete after 30 min and yielded pure **2** in nearly quantitative yield. HPLC analysis revealed clean conversion into the target compound without any sign of side-product formation. The condensation in *o*-DCB could be conducted with the same efficiency either by conventional heating in sealed glass ampoules or by microwave-assisted heating. Although no remarkable microwave effect was detected, all further experiments were carried out in a microwave reactor.

The efficiency of the method was examined by the synthesis of several halogenated bowl-shaped PAHs with an indacenopicene or diindenochrysene core. The respective precursor molecules were obtained by multistep organic synthesis in accordance with the synthetic routes depicted in Schemes 1 and 2. Because of the strain imposed by the bowl-shaped indacenopicene structure, the corresponding cyclodehydrofluorination proceeded more slowly than the model reaction. Thus, when the solid-state strategy was applied, the nonbrominated precursor **3a** required about 60 h at 150 °C to be fully converted into the target **4a**. The introduction of additional bromine functionalities complicated the cyclization to a remarkable extent, probably because of mass-transfer problems caused by a high melting point. All attempts to generate the brominated indacenopicene **4b** by using the solid-state strategy showed a disappointedly low conversion level even after 100 h at 150 °C. An increase in the temperature up to 200–250 °C affected the selectivity without a remarkable improvement in the yield. According to HPLC analysis, in the high-temperature reactions, partial debromination and the formation of several unidentified side products occurred.

In contrast, in the presence of *o*-DCB, the reaction proceeded very smoothly and rapidly. Thus, **3b** was converted into the brominated product **4b** in nearly quantitative yield in just 1.5 h at 150 °C. Interestingly, a further increase in the temperature to 250 °C did not affect the selectivity of the process. In contrast to the solid-state strategy, no significant debromination occurred, and no other side products were detected. In the case of **3c**, in which the bromine functionality

is in close proximity to the cove region, the cyclodehydrofluorination proceeds less readily because of steric hindrance around one C–F bond. Thus, the cyclization of **3c** at 150 °C gave monocyclized product as a major component. Acceptable conversion of **3c** into **4c** was observed only at high temperature (240 °C for 1.5 h), although the monocyclized intermediate was still present in the reaction mixture. Finally, we examined the cyclization of the dibrominated precursor **3d**, which was obtained by the direct bromination of precursor **3a**. In this case, the cyclodehydrofluorination proceeded smoothly to yield the desired dibrominated bowl **4d** exclusively. The bromine positions after cyclization were unambiguously confirmed by single-crystal X-ray analysis (Figure 2). The single crystals of **4d** were obtained by the slow evaporation of a solution in toluene.

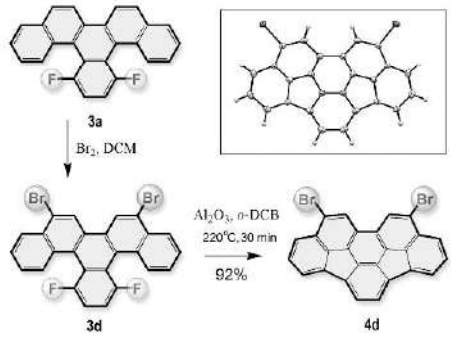

Figure 2. Synthesis of dibrominated indacenopicene **4d** by twofold C–F bond activation. The molecular structure of the target bowl **4d** as determined by X-ray diffraction analysis is shown in the inset. Thermal ellipsoids are set at the 50% probability level.

Importantly, the desired BS-PAHs were formed as the sole product and required no further purification procedure (except for **4c**), which makes the method highly attractive for preparative synthesis. The pure product can be obtained typically in 95–98% yield by simple precipitation with methanol directly from the reaction mixture. All indacenopicenes **4** were obtained as air-stable deep-orange crystalline solids. Compounds showed moderate to low solubility in typical PAH solvents, such as toluene, dichloromethane, and chlorobenzene, and exhibited rich UV/Vis spectra with an absorption tail in the visible region extending beyond 500 nm (see the Supporting Information).

The strategy was also applied to the generation of novel, more curved diindenochrysenes bearing Cl, Br, and F functionalities. Because of the enhanced strain (in comparison with indacenopicenes), the cyclodehydrofluorination in this case required higher temperatures. Effective HF elimination was observed upon heating at 200–240 °C after several hours. Both dibrominated and dichlorinated bowls **7a** and **7b** were obtained in high yield in pure form without any additional purification steps by cyclization in *o*-DCB at 240 °C for 1 h. In contrast, the cyclization of fluorinated precursor **7c** occurred with the formation of several side products. MS analysis revealed that the main side reaction was a cross-coupling reaction of the target **7c**.

These results indicate that at high temperatures (above 200 °C), not only the C–F bond in the cove regions, but also the C–F bond on the periphery undergoes partial activation, thus leading to coupling products. Interestingly, such a transformation has never been observed for the solid-state approach. In other words, the high-temperature C–F activation of fluoroarenes by alumina in *o*-DCB also seems to be suitable for intermolecular, transition-metal-free aryl–aryl cross-coupling. A decreased in the condensation temperature to 180 °C completely prevented dimerization, but the condensation virtually stopped after the first ring closure to yield the monocyclized product as the major component. The best results were obtained by heating **6c** at 220 °C for 2 h. In this case, the desired difluorinated bowl was obtained in pure form by means of preparative HPLC in 63% yield.

Considerable difficulties were encountered with the growing of crystals of diindenochrisenes. Regardless of the method used, the chlorinated and fluorinated bowls **7b** and **7c** formed long and extremely thin needles, which were not suitable for X-ray crystallographic analysis. In the case of dibrominated **7a**, it was possible to grow thin needles that showed only weak diffraction. Fortunately, after replacing the bromine substituents with phenyl groups by a double Suzuki coupling reaction with phenylboronic acid, the resulting compound **8** crystallized as orange blocks, thus allowing us to observe the bowl-shaped character of the diindenochrysene core experimentally for the first time (Figure 3).

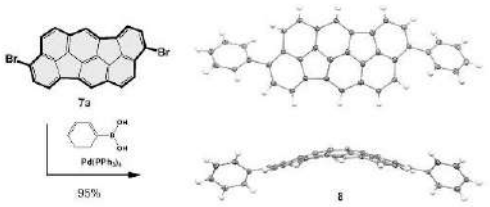

Figure 3. Synthesis of bowl **8** and top and side views of the molecular structure as determined by X-ray diffraction analysis. Thermal ellipsoids are shown at the 50% probability level.

The molecular structures and electronic properties of the two series of halogenated bowls with diindenochrysene and indacenopicene carbon frameworks were considered at the DFT level of the theory. It was found that halogenation had no notable effect on the C–C bond lengths and the bond orders with respect to the pristine bowls (see the Supporting Information). Notably, the diindenochrysene bowl is more curved than indacenopicene (bowl depths are 1.78 and 1.62 Å, respectively), thus showing the larger steric strain of the former molecule (Figure 4). This result is consistent with the large relative formation energies of pristine and dibrominated diindenochrysene **7a** with respect to isomeric pristine and

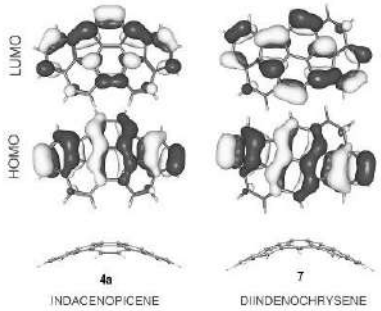

Figure 4. Top: Frontier molecular orbital distributions in pristine diindenochrysene and pristine indacenopicene (contour levels are given for value of 0.03 e Å^{-3}). Bottom: Side view of the DFT-optimized structures showing the bowl-shaped geometries of the diindenochrysene and indacenopicene cores.

dibrominated indacenopicene **4d** (17 and 13 kJ mol^{-1}, respectively). The HOMO and LUMO density distributions determined by DFT calculations for diindenochrysene and indacenopicene are shown in Figure 4. The orbitals show the same spatial structure associated with the pyracylene moiety embedded in the buckybowls. The electronic structural data obtained from DFT calculations and UV/Vis measurements are summarized in Table 1.

Table 1: Electronic properties of pristine and halogenated diindenochrysenes and indacenopicenes.

Compound	DFT data [eV][a]					E_G^{opt} [eV][b]
	E_{HOMO}	E_{LUMO}	E_G	λ_i	EA	
Indacenopicene derivatives						
4a	−5.30	−3.20	2.10	0.15	1.56	2.43
4b	−5.38	−3.34	2.04	0.15	1.73	2.40
4c	−5.43	−3.33	2.10	0.16	1.72	2.43
4d	−5.56	−3.48	2.08	0.16	1.90	2.42
Diindenochrysene derivatives						
7	−5.32	−3.16	2.15	0.17	1.52	–
7a	−5.47	−3.44	2.03	0.17	1.87	2.56
7b	−5.47	−3.43	2.04	0.17	1.84	2.58
7c	−5.39	−3.31	2.08	0.19	1.67	–

[a] PBE/TZ2P; values of the HOMO–LUMO gap (E_G), the internal reorganization energy of electron transfer (λ_i), and the adiabatic electron affinity (EA) are given. [b] Optical gap, $E_G^{opt} = 1240/\lambda_{onset}$.

Notably, pristine diindenochrysene and indacenopicene have virtually the same frontier molecular orbital levels and are characterized by similar relatively high electron affinity values. Halogenation of the bowls results in lowering of the HOMO and LUMO levels by 0.1–0.3 eV, depending on the number and nature of the halogen atoms, and the stepwise growth of electron affinity by approximately 0.1–0.2 eV per halogen atom. The optical HOMO–LUMO energy gaps were estimated from the absorption-edge wavelength during UV/Vis spectral analysis of the compounds dissolved in a mixture of toluene and methanol. Our calculations and measured optical E_G values indicate that both bowls can be regarded as wide-band-gap semiconductors. As shown recently, pristine indacenopicene is a soft one-electron acceptor and has suitable HOMO and LUMO energy levels to function as a π-acceptor material for organic electronic applications.[16] The small internal reorganization energy (λ_i) for electron transport and enhanced electron affinity of indacenopicene and diindenochrysene cores make them suitable building blocks for novel n-channel semiconductive materials in organic thin-film transistors.

In summary, we have demonstrated a facile method for the synthesis of halogenated bowl-shaped PAHs through selective C–F activation. The unprecedented high efficiency of the approach has been demonstrated by the transformation of appropriate precursors into the desired halogenated buckybowls in nearly quantitative yield. Besides its simplicity and scalability, the presented strategy enables the introduction of halogen functionalities at virtually any desired position, which makes the approach superior to all alternative methods for buckybowl synthesis. The obtained halogenated diindenochrysenes and indacenopicenes are electron acceptors with frontier molecular orbitals delocalized over the whole molecule and are characterized by band-gap values typical for wide-band-gap semiconductors. The presence of the peripheral halogen atoms makes possible further functionalization and the fine tuning of physical–chemical properties. Thus, these compounds can be considered as highly promising building blocks for novel acceptor materials with electronic-type conductivity for organoelectronic applications, including solar cells, thin-film transistors, and blue-light-emitting diodes.

Experimental Section

General procedure: γ-Al_2O_3 (neutral, 50–200 μm, 1 g) was activated in a glass ampoule at 250 °C in air for 10 min and then activated at 550 °C for 15 min in a vacuum (10^{-3} mbar). Activated aluminum oxide was added to a microwave vial containing the fluoroarene (20 mg) dissolved in anhydrous *o*-dichlorobenzene (3 mL). For a 100 mg scale, 3–5 g of alumina and 10–15 mL of *o*-dichlorobenzene were used. The glass vial was closed with the cap and placed in the microwave oven. All preparation steps were performed under an argon atmosphere. Condensation was carried out typically at 150–240 °C for 0.5–3 h. After cooling to room temperature, products were extracted with toluene. Pure products were typically obtained in 95–98 % yield by direct precipitation with MeOH from the corresponding toluene extract.

Acknowledgements

K.Yu.A. and O.P. are grateful to the Deutsche Forschungsgemeinschaft for financial support (AM 407). A.A.G. and V.A.A. are grateful to the Russian Foundation for Basic Research (grant no. 15-33-21083 mol_a_ved) for financial support.

Conflict of interest

The authors declare no conflict of interest.

Keywords: aryl–aryl coupling · buckybowls · C–F activation · halogenation · polycyclic aromatic hydrocarbons

How to cite: *Angew. Chem. Int. Ed.* **2017**, *56*, 4834–4838
Angew. Chem. **2017**, *129*, 4912–4916

[1] Y. T. Wu, J. S. Siegel, *Chem. Rev.* **2006**, *106*, 4843–4867.
[2] *Fragments of Fullerenes and Carbon Nanotubes: Designed Synthesis, Unusual Reactions, and Coordination Chemistry* (Eds.: M. A. Petrukhina, L. T. Scott), Wiley, Hoboken, **2012**.
[3] Y. T. Wu, T. C. Wu, M. K. Chen, H. J. Hsin, *Pure Appl. Chem.* **2014**, *86*, 539–544.
[4] A. K. Dutta, A. Linden, L. Zoppi, K. K. Baldridge, J. S. Siegel, *Angew. Chem. Int. Ed.* **2015**, *54*, 10792–10796; *Angew. Chem.* **2015**, *127*, 10942–10946.
[5] K. Kawasumi, Q. Zhang, Y. Segawa, L. T. Scott, K. Itami, *Nat. Chem.* **2013**, *5*, 739–744.
[6] E. A. Jackson, B. D. Steinberg, M. Bancu, A. Wakamiya, L. T. Scott, *J. Am. Chem. Soc.* **2007**, *129*, 484–485.
[7] T. Amaya, T. Nakata, T. Hirao, *J. Am. Chem. Soc.* **2009**, *131*, 10810–10811.
[8] L. Meng, T. Fujikawa, M. Kuwayama, Y. Segawa, K. Itami, *J. Am. Chem. Soc.* **2016**, *138*, 10351–10355.
[9] L. T. Scott, E. A. Jackson, Q. Zhang, B. D. Steinberg, M. Bancu, B. Li, *J. Am. Chem. Soc.* **2012**, *134*, 107–110.
[10] C. M. Álvarez, H. Barbero, S. Ferrero, D. Miguel, *J. Org. Chem.* **2016**, *81*, 6081–6086.
[11] C. W. Lee, E. C. Liu, Y. T. Wu, *J. Org. Chem.* **2015**, *80*, 10446–10456.
[12] E. C. Liu, M. K. Chen, J. Y. Li, Y. T. Wu, *Chem. Eur. J.* **2015**, *21*, 4755–4761.
[13] F. Furrer, A. Linden, M. C. Stuparu, *Chem. Eur. J.* **2013**, *19*, 13199–13206.
[14] A. Sygula, R. Sygula, P. W. Rabideau, *Org. Lett.* **2005**, *7*, 4999–5001.
[15] R.-Q. Lu, Y.-N. Zhou, X.-Y. Yan, K. Shi, Y.-Q. Zheng, M. Luo, X.-C. Wang, J. Pei, H. Xia, L. Zoppi, K. K. Baldridge, J. S. Siegel, X.-Y. Cao, *Chem. Commun.* **2015**, *51*, 1681–1684.
[16] A. Sygula, G. Xu, Z. Marcinow, P. W. Rabideau, *Tetrahedron* **2001**, *57*, 3637–3644.
[17] A. Mueller, K. Y. Amsharov, M. Jansen, *Fullerenes, Nanotubes, Carbon Nanostruct.* **2012**, *20*, 401–404.
[18] A. Mueller, K. Y. Amsharov, M. Jansen, *Tetrahedron Lett.* **2010**, *51*, 3221–3225.
[19] A. Mueller, K. Y. Amsharov, *Eur. J. Org. Chem.* **2012**, 6155–6164.
[20] B. Liu, J. Liu, H. B. Li, R. Bhola, E. A. Jackson, L. T. Scott, A. Page, S. Irle, K. Morokuma, C. Zhou, *Nano Lett.* **2015**, *15*, 586–595.
[21] K. Y. Amsharov, *Phys. Status Solidi B* **2015**, *252*, 2466–2471.
[22] J. R. Sanchez-Valencia, T. Dienel, O. Gröning, I. Shorubalko, A. Mueller, M. Jansen, K. Amsharov, P. Ruffieux, R. Fasel, *Nature* **2014**, *512*, 61–64.
[23] X. Yu, J. Zhang, W. Choi, J. Y. Choi, J. M. Kim, L. Gan, Z. Liu, *Nano Lett.* **2010**, *10*, 3343–3349.
[24] E. H. Fort, P. M. Donovan, L. T. Scott, *J. Am. Chem. Soc.* **2009**, *131*, 16006–16007.
[25] T. J. Hill, R. K. Hughes, L. T. Scott, *Tetrahedron* **2008**, *64*, 11360–11369.
[26] A. Mueller, K. Y. Amsharov, *Eur. J. Org. Chem.* **2015**, 3053–3056.
[27] V. M. Tsefrikas, L. T. Scott, *Chem. Rev.* **2006**, *106*, 4868–4884.
[28] K. T. Rim, M. Siaj, S. Xiao, M. Myers, V. D. Carpentier, L. Liu, C. Su, M. L. Steigerwald, M. S. Hybertsen, P. H. McBreen, G. W. Flynn, C. Nuckolls, *Angew. Chem. Int. Ed.* **2007**, *46*, 7891–7895; *Angew. Chem.* **2007**, *119*, 8037–8041.
[29] N. Abdurakhmanova, A. Mueller, S. Stepanow, S. Rauschenbach, M. Jansen, K. Kern, K. Y. Amsharov, *Carbon* **2015**, *84*, 444–447.
[30] K. Amsharov, N. Abdurakhmanova, S. Stepanow, S. Rauschenbach, M. Jansen, K. Kern, *Angew. Chem. Int. Ed.* **2010**, *49*, 9392–9396; *Angew. Chem.* **2010**, *122*, 9582–9586.
[31] G. Otero, G. Biddau, C. Sánchez-Sánchez, R. Caillard, M. F. López, C. Rogero, F. J. Palomares, N. Cabello, M. A. Basanta, J. Ortega, J. Méndez, A. M. Echavarren, R. Pérez, B. Gómez-Lor, J. A. Martín-Gago, *Nature* **2008**, *454*, 865–868.
[32] A. M. Echavarren, B. Gómez-Lor, J. J. González, Ó. de Frutos, *Synlett* **2003**, 0585–0597.
[33] D. Alberico, M. E. Scott, M. Lautens, *Chem. Rev.* **2007**, *107*, 174–238.
[34] S. Pascual, P. de Mendoza, A. M. Echavarren, *Org. Biomol. Chem.* **2007**, *5*, 2727–2734.
[35] J. Liu, S. Osella, J. Ma, R. Berger, D. Beljonne, D. Schollmeyer, X. Feng, K. Müllen, *J. Am. Chem. Soc.* **2016**, *138*, 8364–8367.
[36] T. C. Wu, M. K. Chen, Y. W. Lee, M. Y. Kuo, Y. T. Wu, *Angew. Chem. Int. Ed.* **2013**, *52*, 1289–1293; *Angew. Chem.* **2013**, *125*, 1327–1331.
[37] T. J. Seiders, K. K. Baldridge, E. L. Elliott, G. H. Grube, J. S. Siegel, *J. Am. Chem. Soc.* **1999**, *121*, 7439–7440.
[38] B. M. Schmidt, B. Topolinski, M. Yamada, S. Higashibayashi, M. Shionoya, H. Sakurai, D. Lentz, *Chem. Eur. J.* **2013**, *19*, 13872–13880.
[39] O. Allemann, S. Duttwyler, P. Romanato, K. K. Baldridge, J. S. Siegel, *Science* **2011**, *332*, 574–577.
[40] K. Fuchibe, Y. Mayumi, N. Zhao, S. Watanabe, M. Yokota, J. Ichikawa, *Angew. Chem. Int. Ed.* **2013**, *52*, 7825–7828; *Angew. Chem.* **2013**, *125*, 7979–7982.
[41] N. Suzuki, T. Fujita, J. Ichikawa, *Org. Lett.* **2015**, *17*, 4984–4987.
[42] N. Suzuki, T. Fujita, K. Yu. Amsharov, J. Ichikawa, *Chem. Commun.* **2016**, *52*, 12948–12951.
[43] K. Y. Amsharov, M. A. Kabdulov, M. Jansen, *Chem. Eur. J.* **2010**, *16*, 5868–5871.
[44] K. Y. Amsharov, P. Merz, *J. Org. Chem.* **2012**, *77*, 5445–5448.
[45] K. Y. Amsharov, M. A. Kabdulov, M. Jansen, *Angew. Chem. Int. Ed.* **2012**, *51*, 4594–4597; *Angew. Chem.* **2012**, *124*, 4672–4675.
[46] S. N. Spisak, J. Li, A. Y. Rogachev, Z. Wei, O. Papaianina, K. Amsharov, A. V. Rybalchenko, A. A. Goryunkov, M. A. Petrukhina, *Organometallics* **2016**, *35*, 3105–3111.

Manuscript received: January 23, 2017
Final Article published: March 24, 2017

Angewandte Chemie
Eine Zeitschrift der Gesellschaft Deutscher Chemiker

Supporting Information

Synthesis of Rationally Halogenated Buckybowls by Chemoselective Aromatic C–F Bond Activation

*Olena Papaianina, Vladimir A. Akhmetov, Alexey A. Goryunkov, Frank Hampel, Frank W. Heinemann, and Konstantin Y. Amsharov**

anie_201700814_sm_miscellaneous_information.pdf

Supporting Information

General aspects.

Synthesis. Reagents and solvents were used as received at highest commercial quality. All reaction mixtures were stirred magnetically. Microwave assisted experiments were carried out using Discover SP Microwave Synthesizer, CEM. Flash chromatography purifications were carried out with flash grade silica gel Kiesegel 60 (0.06-0.2 mm). Thin layer chromatography (TLC) was performed on silica-backed silica plates with fluorescent indicator 254 nm (layer thickness 0.25 mm, medium pore diameter 60 Å, Fluka). HPLC analyses were carried out using analytical Cosmosil 5-PYE (4.6 x 250 mm) column and purification using semi-preparative PBB-R (10 x 250 mm) column (UV-Vis detection). ^{1}H NMR: Spectra were recorded on Bruker Avance 400 and Jeol EX400 spectrometers. Chemical shifts are quoted in ppm and referenced to the appropriated solvent peaks. ^{13}C NMR: Spectra were recorded on Bruker Avance 400 MHz and Oxford 400 spectrometers. Chemical shifts are quoted in ppm and referenced to the appropriated solvent peaks. ^{19}F NMR: Spectra were recorded on Bruker Avance 300 MHz spectrometer. m/z: LDI-TOF mass spectra were recorded on the Axima Confidence Spectrometer, Shimadzu Deutschland, GmbH. HRMS: High resolution mass spectra data were obtained on maXis 4G Spectrometer, Bruker Daltonic GmbH and are reported as (m/z).

Quantum chemical calculations. The molecular geometry of each structure in question was optimized at the DFT level of theory by means of the PRIRODA v. 6 software that implements efficient RI approximation [1], PBE exchange-correlation functional [2] and a built-in basis set of triple zeta quality with (11s6p2d)/[6s3p2d] contraction scheme for first row atoms and (5s1p)/[3s1p] for hydrogen atoms were used. Further refinement of the electron structure was performed using the Firefly 8.1 software [3] (partly based on the GAMESS (US) source code [4]) and the ORCA program v. 3.0.3 [5] employing the hybrid functionals B3LYP [6,7] and TPSSh [8] as well as Def2-TZVP basis set [9]. The internal (bond) reorganization energy of electron transfer was estimated as a sum of the two differences between the formation energies of (1) neutral molecules with molecular configurations optimized for monoanionic and neutral states as well as (2) monoanionic molecules with molecular configurations optimized for neutral and monoanionic states, correspondingly.

2. Synthetic Procedures and Spectroscopic Data

General procedures:

Synthesis of arylethenes. Halogenated arylethenes were obtained by Wittig reactions following general procedure as described in [10].

General procedure A.

Synthesis of 13,16-difluoro-benzo[*s*]picenes. 13,16-difluoro-benzo[*s*]picenes were obtained by double photoclyzation of the respective arylethenes according procedure described in [10]. All arylethenes were used in the form of a *cis/trans* isomer mixture since the isomers interconvert under photocyclization conditions. 13,16-difluoro-benzo[*s*]picene (**4a**), 4-bromo-13,16-difluorobenzo[*s*]picene (**4b**) and 2-bromo-13,16-difluorobenzo[*s*]picene (**4c**) were synthesized utilizing benzaldehyde, 2-bromobenzaldehyde and 4-bromobenzaldehyde respectively.

General procedure B.

Synthesis 4,12-difluorodibenzo[*c,l*]chrysenes. 4,12-difluorodibenzo[*c,l*]chrysenes (1,9-dibromo-4,12-difluorodibenzo[*c,l*]chrysene (**6a**), 1,9-dichloro-4,12-difluorodibenzo[*c,l*]chrysene (**6b**) and 1,4,9,12-tetrafluorodibenzo[c,l]chrysene (**6c**)) were obtained by double photoclyzation of the respective arylethenes according general procedure described in [10]. The respective arylethenes were synthesised by double Wittig coupling according general procedure using naphthalene-2,6-dicarbaldehyde (1.0 mmol) and respective triphenylphosphonium bromides (2-bromo-5-fluorobenzyl, 2-chloro-5-fluorobenzyl and 2,5-difluorobenzyl) (2.4 mmol). Naphthalene-2,6-dicarbaldehyde was synthesized according previously described procedure [11].

General procedure for Aryl-Aryl coupling via C-F activation. 1 g of γ-Al_2O_3 (neutral, 50-200 micron) were preactivated in glass ampule at 250 °C under air conditions for 10 minutes and then activated at 550 °C for 15 minutes in vacuum (10^{-3} mbar). Activated aluminium oxide was added to the microwave glass vial containing 20 mg of fluoroarene dissolved in 3 mL of anhydrous *o*-dichlorobenzene. For 100 mg scale 3-5 g of alumina and 10-15 mL of *o*-dichlorobenzene were used. The glass vial was closed with the cap and placed into microwave oven. All preparation steps were performed under argon atmosphere. Condensation was carried out typically at 150-240 °C for 0.5-3 h. After cooling to room temperature, products were extracted with toluene. Pure products with typical yield of 95-98% were obtained by direct precipitation with MeOH from the respective toluene extract.

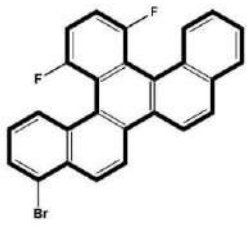

4-bromo-13,16-difluorobenzo[*s*]picene (3b). 3b was synthesised according general procedure B (yield 50%). **^{1}H NMR** [400 MHz, $CDCl_3$, 293K] 8.59 (1H, d, *J*=9.28 Hz), 8.51 (1H, d, *J*=8.80 Hz), 8.50 (1H, d, *J*=8.88 Hz), 8.24-8.12 (2H, m), 8.10 (1H, d, *J*=8.64 Hz), 7.98-7.93 (1H, m), 7.84 (1H, dd, *J*=0.64, J=7.40 Hz), 7.62-7.55 (2H, m), 7.43-7.31 (3H, m). **^{13}C NMR** [100 MHz, $CDCl_3$, 293K] 156.36, 156.21, 153.90, 153.84, 153.74, 132.49, 131.68, 131.63, 130.74, 130.41, 130.13, 130.08, 129.73, 129.66, 129.58, 129.45, 128.11, 127.19, 126.36, 125.45, 125.43, 125.37 125.35, 123.77, 123.75, 123.73, 123.36, 123.34, 123.31, 122.04, 122.02, 121.21, 120.33, 120.30, 120.19, 120.16, 119.99, 119.96, 119.86, 119.82, 119.62, 114.87, 114.77, 114.64, 114.59, 114.54, 114.49, 114.36, 114.26. **^{19}F NMR** [282 MHz, $CDCl_3$, 293K] -103.50- -103.74 (m), -103.87 - -104.10 (m). **HRMS** (APPI): Chemical Formula: $C_{26}H_{13}BrF_2$ calc. 442.0163, found 442.0163.

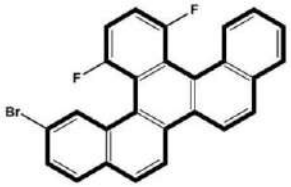

2-bromo-13,16-difluorobenzo[*s*]picene (3c). 3c was synthesised according general procedure B (55 yield %). **^{1}H NMR** [400 MHz, $CDCl_3$, 293K] 8.53 (1H, d, *J*=8.80 Hz), 8.50 (1H, d, *J*=8.84 Hz), 8.34 (1H, dd, *J*=1.94, 13.62 Hz), 8,23-8,14 (1H, m), 8.11 (1H, d, *J*=8.80 Hz), 8.05 (1H, d, *J*=8.76 Hz), 7.98-7.93 (1H, m), 7.81 (1H, d, *J*=8.72 Hz), 7.64 (1H, dd, *J*=1.84, 8.60 Hz), 7.62-7.55 (2H, m), 7.45-7.33 (2H, m). **^{13}C NMR** [100 MHz, $CDCl_3$, 293K] 153.90, 153.73, 132.44, 131.97, 131.81, 131.38, 130.68, 130.08, 129.75, 129.71, 129.60, 129.48, 129.30, 128.92, 128.63, 127.13, 126.34, 125.36, 120.23, 119.66, 119.59, 114.72, 114.89-114.40. **^{19}F NMR** [282 MHz, $CDCl_3$, 293K] -103.55- -103.76 (m), -104.23 - -104.47 (m). **HRMS** (APPI): Chemical Formula: $C_{26}H_{13}BrF_2$ calc. 442.0186, found 442.0166.

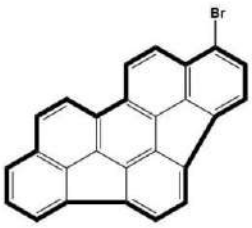

1-bromo-*as*-indaceno[*3,2,1,8,7,6-pqrstuv*]picene (4b). 4b was obtained from **3b** according general procedure for Aryl-Aryl coupling via C-F bond activation (yield 96%, determined by HPLC). **^{1}H NMR** [400 MHz, CD_2Cl_2, 293K] 8.13 (1H, d, *J*=8.85 Hz), 8.09 (1H, d, *J*=8.76 Hz), 7.86 (1H, d, *J*=8.85 Hz), 7.79 (1H, d, J=8.76 Hz), 7.70 (1H, d, *J*=6.96 Hz), 7.64 (1H, d, *J*=8.13 Hz), 7.59 (2H, ABq, *J*=7.32 Hz), 7.55 (1H, d, *J*=7.38 Hz), 7.48 (1H, d, *J*=7.38 Hz), 7.40 (1H, dd, *J*=8.18, 6.98 Hz). **^{13}C NMR** [100 MHz, CD_2Cl_2, 293K] 139.44, 139.25, 138.96, 138.76, 138.37, 138.33, 138.29, 138.05, 138.03, 136.94, 131.90, 130.67, 129.87, 129.65, 129.44, 129.15, 127.44, 127.23, 126.25,

126.22, 126.10, 125.55, 124.75, 124.31, 124.08, 122.16. **HRMS** (APPI): Chemical Formula: $C_{26}H_{11}Br$ calc. 402.0039, found 402.0040.

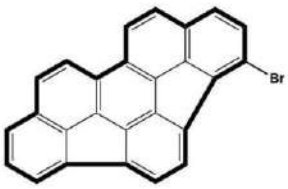

3-bromo-*as*-indaceno[*3,2,1,8,7,6-pqrstuv*]picene (4c). **4c** was obtained from **3c** according general procedure for Aryl-Aryl coupling via C-F bond activation (small amount was collected by analytical HPLC for NMR measurement). **^{1}H NMR** [300 MHz, $CDCl_3$, 293K] 8.10 (1H, dd, *J*=0.78, 8.76 Hz), 7.98 (1H, d, *J*=7.38 Hz), 7.80 (1H, d, *J*=8.79 Hz), 7.77-7.69 (3H, m), 7.65 (1H, d, *J*=8.16 Hz), 7.51-7.37 (3H, m). ^{13}C NMR spectrum could not be recorded due to the low solubility. **HRMS** (APPI): Chemical Formula: $C_{26}H_{11}Br$ calc. 402.0039, found 402.0039.

1,9-dibromo-4,12-difluorodibenzo[*c,l*]chrysene (6a). Compound **6a** was obtained according general procedure B (yield 50 %). **^{1}H NMR** [400 MHz, $C_2D_2Cl_4$, 353K] 8.40-8.31 (4H, m), 7.96-7.89 (4H, m), 7.83 (2H, d, *J*=9.47 Hz), 7.27 (2H, dd, *J*=11.96, 8.36 Hz). ^{13}C NMR spectrum could not be recorded due to the low solubility. **^{19}F NMR** [282 MHz, $CDCl_3$, 293K] -101.26 - -101.70 (m), -125.76 - -125.97 (m) **HRMS** (APPI): Chemical Formula: $C_{26}H_{12}Br_2F_2$ calc. 519.9277, found 519.9268.

1,9-dichloro-4,12-difluorodibenzo[*c,l*]chrysene (6b). Compound **6b** was obtained according general procedure B (yield 42 %). **^{1}H NMR** [400 MHz, $C_2D_2Cl_4$, 353K] 8.41-8.33 (4H, m), 7.96 (2H, d, *J*=8.92 Hz), 7.83 (2H, d, *J*=9.20 Hz), 7.72 (1H, d, *J*=8.36 Hz), 7.71 (1H, d, *J*=8.36 Hz), 6.77 (2H, dd, *J*=11.87, 8.34). ^{13}C NMR spectrum could not be recorded due to the low solubility. **HRMS** (APPI): Chemical Formula: $C_{26}H_{12}Cl_2F_2$ calc. 436.0592, found 436.0599.

1,4,9,12-tetrafluorodibenzo[*c,l*]chrysene (6c). **6c** was obtained according general procedure B (yield 47 %). **^{1}H NMR** [400 MHz, $C_2D_2Cl_4$, 353K] 8.35 (2H, dd, *J*=8.72, 14.05 Hz), 8.14 (2H, dd, *J*=1.64, 8.68 Hz), 7.90 (2H, d, *J*=8.84 Hz), 7.82 (2H, d, *J*=8.88 Hz), 7.31 (4H, m). ^{13}C NMR spectrum could not be recorded due to the low solubility. **^{19}F NMR** [282 MHz, $CDCl_3$, 293K] -105.41 - -105.70 (m), -125.76 - -125.97 (m). **MS** (LDI): Chemical Formula: $C_{26}H_{12}F_4$ calc. 400.09, found 399.99.

3,9-dibromodiindeno[*4,3,2,1-cdef:4',3',2',1'-lmno*]chrysene (7a). 7a was obtained from **6a**

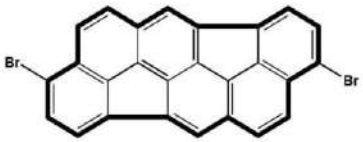

according general procedure for Aryl-Aryl coupling via C-F bond activation Reaction according to procedure C (yield 95%). **^{1}H NMR** [400 MHz, $C_2D_2Cl_4$, 353K] 7.85 (2H, s), 7.53 (2H, d, *J*=7.44 Hz), 7.57 (2H, d, *J*=7.44 Hz), 7.72 (2H, d, *J*=8.88 Hz), 7.79 (2H, d, J=8.92 Hz). ^{13}C NMR spectrum could not be recorded due to the low solubility. **HRMS** (APPI): Chemical Formula: $C_{26}H_{10}Br_2$ calc. 479.9144, found 479.9146.

3,9-dichlorodiindeno[*4,3,2,1-cdef:4',3',2',1'-lmno*]chrysene (7b). 7b was obtained from **6b**

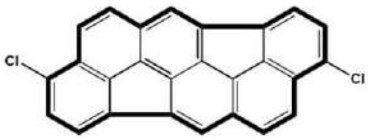

according general procedure for Aryl-Aryl coupling via C-F bond activation (yield 98%, defined by HPLC). **^{1}H NMR** [400 MHz, $C_2D_2Cl_4$, 353K] 7.86(2H, s), 7.81 (4H, s), 7.61 (2H, d, *J*=7.52 Hz), 7.37 (2H, d, *J*=7.52 Hz). ^{13}C NMR spectrum could not be recorded due to the low solubility. **HRMS** (APPI): Chemical Formula: $C_{26}H_{10}Cl_2$ calc. 392.0154, found 392.0155.

3,9-difluorodiindeno[*4,3,2,1-cdef:4',3',2',1'-lmno*]chrysene (7c). 7c was obtained from **6c**

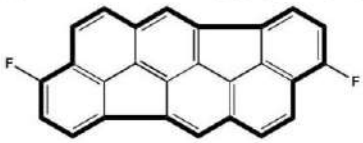

according general procedure for Aryl-Aryl coupling via C-F bond activation (yield 63%, defined by HPLC). **^{1}H NMR** [400 MHz, CD_2Cl_2, 293 K] 7.90 (2H, s), 7.83 (2H, d, *J*=8.91Hz), 7.76 (2H, d, *J*=8.91 Hz), 7.71 (2H, dd, *J*=3.44, 7.68 Hz), 7.01 (2H, dd, *J*=11.33, 7.69 Hz). ^{13}C NMR spectrum could not be recorded due to the low solubility. **^{19}F NMR** [282 MHz, CD_2Cl_2, 293 K] -121.05 - -121.09 (d, J=3.41 Hz), -121.10 - -121.15 (d, J=3.41 Hz). **MS** (LDI): Chemical Formula: $C_{26}H_{10}F_2$ calc. 360.07, found 359.97.

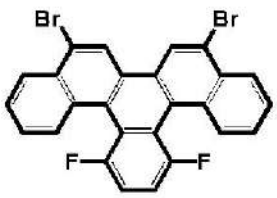

5,8-dibromo-13,16-difluorobenzo[*s*]picene (3d). 13,16-difluoro-benzo[*s*]picene (1.0 mmol) was dissolved in 50 mL of $CHCl_3$. Bromine (2.2 mmol) in 20 mL of chloroform was added dropwise to the mixture under stirring at room temperature. The reaction was monitored by TLC. After 2 hours the reaction was stopped and organic phase was washed with aq. $NaHSO_3$ solution, dried over Na_2SO_4 and filtrated through silica plague. Solvent was removed under reduced pressure. Purification of product was made on HPLC (5PYE column, toluene:methanol mixture as eluent). Yield 60%. **^{1}H**

NMR [400 MHz, $CDCl_3$, 293K] 8.73 (2H, s), 8.38 (2H, d, *J*=7.93Hz), 8.22-8.12 (2H, m), 7.72-7.61 (4H, m), 7.41-7.36 (2H, m). ^{13}C NMR spectrum could not be recorded due to the low solubility. **^{19}F NMR** [282 MHz, $CDCl_3$, 293K] -99.75 - -99.93 (m), -11.80 - - 112.96 (m). **HRMS** (APPI): Chemical Formula: $C_{26}H_{12}Br_2F_2$ calc. 519.9268, found 519.9273.

9,12-dibromo-*as*-indaceno[*3,2,1,8,7,6-pqrstuv*]picene (4d). 4d was obtained from **3d** according

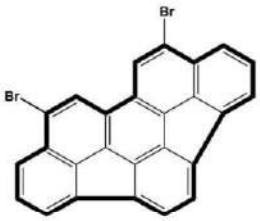

general procedure for Aryl-Aryl coupling via C-F bond activation (yield 92%, defined by HPLC). **^1H NMR** [400 MHz, $C_2D_2Cl_4$, 353K] 8.29 (2H, s), 7.78 (2H, d, *J*=8.32 Hz), 7.72 (2H, d, 6.96 Hz), 7.83 (2H, dd, *J*=0.96, 8.80 Hz), 7.65 (2H, s), 7.46 (2H, dd, *J*=7.04, 8.32 Hz). ^{13}C NMR spectrum could not be recorded due to the low solubility. **HRMS** (APPI): Chemical Formula: $C_{26}H_{10}Br_2$ calc. 479.9144, found 479.9149.

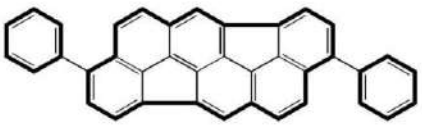

3,9-diphenyldiindeno[*4,3,2,1-cdef:4',3',2',1'-lmno*]chrysene (8). 3,9-dibromodiindeno[*4,3,2,1-cdef:4',3',2',1'-lmno*]chrysene **(7a)** (1 mmol) and phenylboronic acid (2.4 mmol) were dissolved in toluene:methanol (2:1) mixture containing potassium carbonate (2.4 mmol) and 5% mol of tetrakis(triphenylphosphine)palladium(0) as catalyst. The reaction mixture was stirred under reflux in nitrogen atmosphere during 15 hours. After reaction mixture was washed with water, organic layer dried over Na_2SO_4, filtrated through silica plague. Solvent was removed under reduced pressure. Flash chromatography purification of product was made with hexane:dichloromethane (2.5:1) as eluent. Yield 95%. **^1H NMR** [400 MHz, CD_2Cl_2, 293K] 7.98 (2H, s), 7.85 (2H, d, *J*=7.20 Hz), 7.81 (2H, d, *J*=9.00 Hz), 7.78 (2H, d, *J*=9.00 Hz), 7.69-7.65 (4H, m), 7.56-7.50 (4H, m), 7.49-7.43 (4H, m, *J*=7.20 Hz). ^{13}C NMR spectrum could not be recorded due to the low solubility.

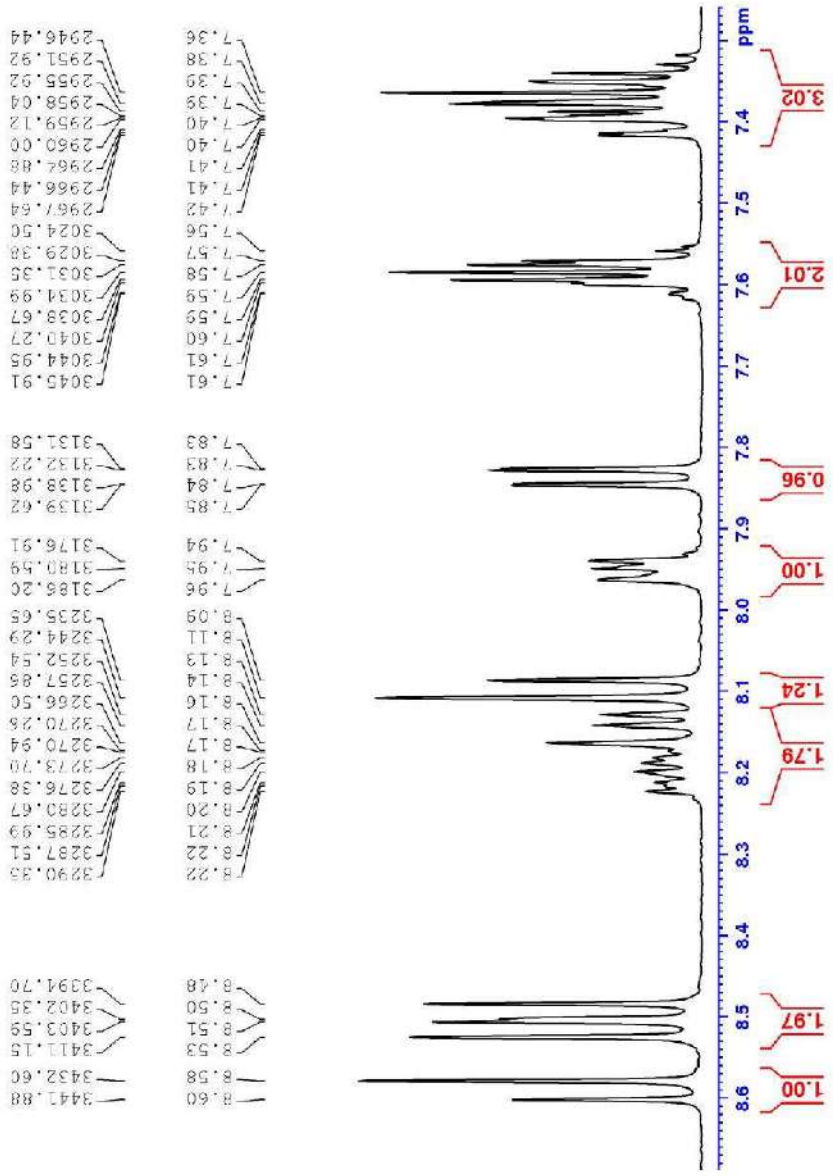

Figure S1. ^{1}H NMR (400 MHz, $CDCl_3$, 293K) spectrum of 4-bromo-13,16-difluorobenzo[*s*]picene (**3b**).

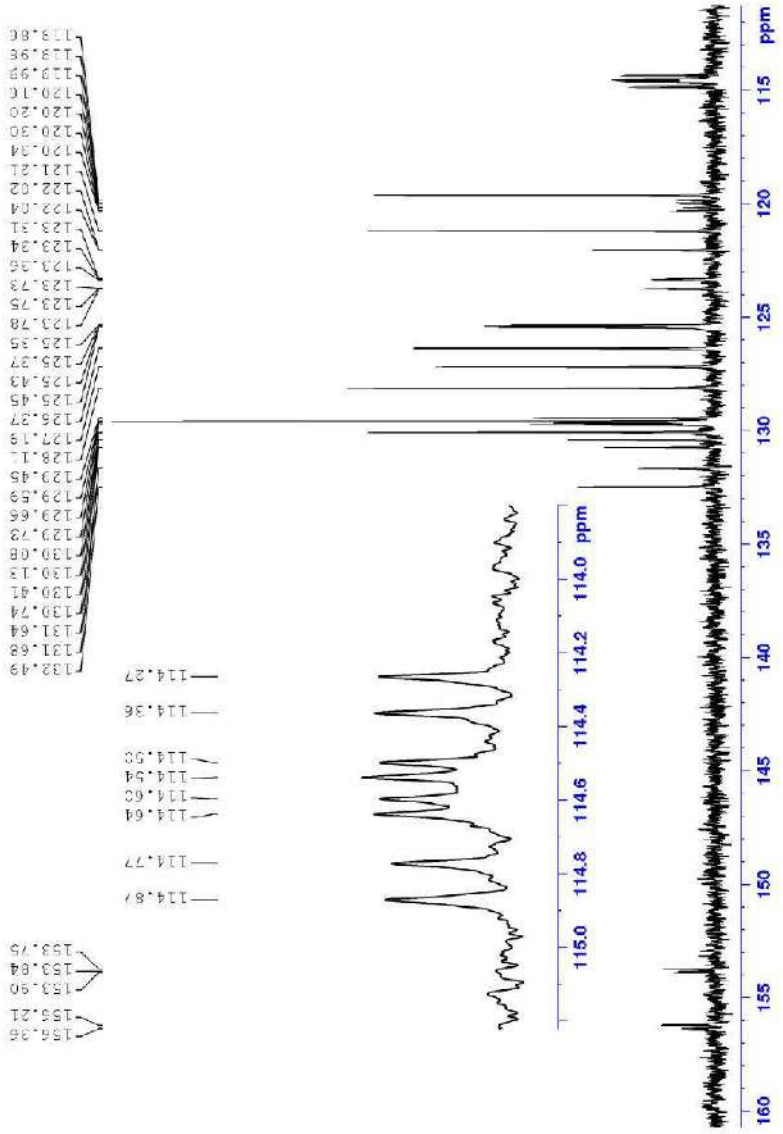

Figure S2. ^{13}C NMR (100 MHz, $CDCl_3$, 293K) spectrum of 4-bromo-13,16-difluorobenzo[*s*]picene (**3b**).

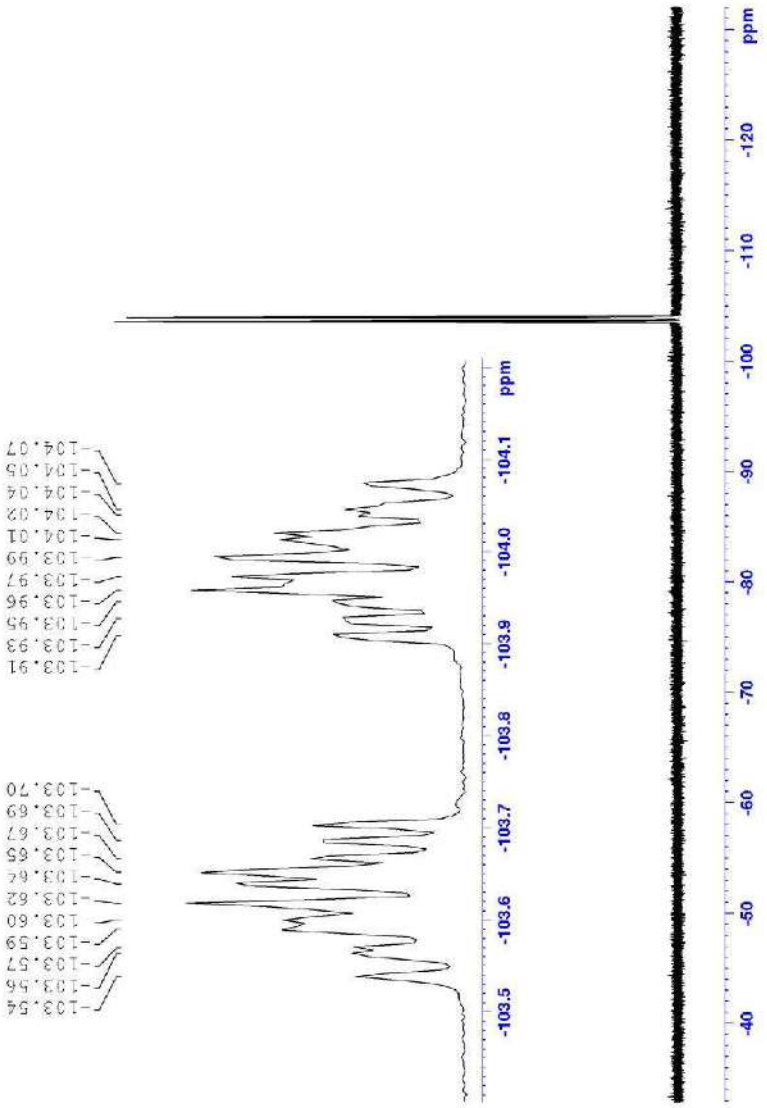

Figure S3. ^{19}F NMR (282 MHz, $CDCl_3$, 293K) spectrum of 4-bromo-13,16-difluorobenzo[*s*]picene (**3b**).

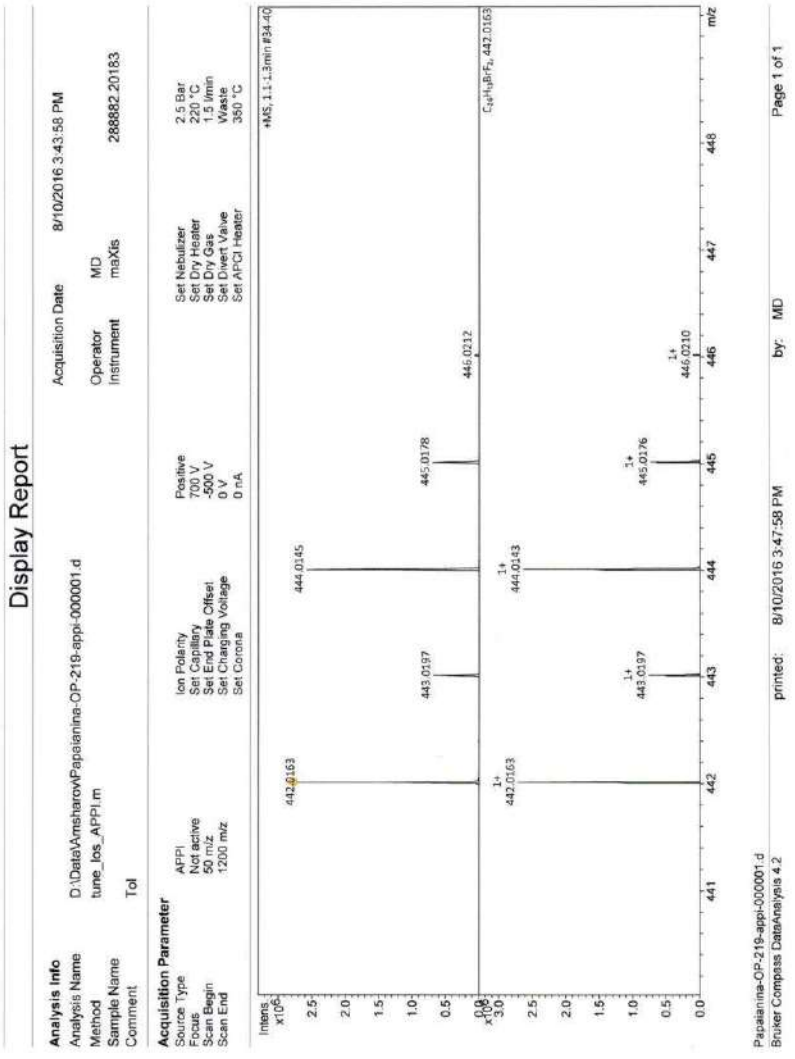

Figure S4. APPI-MS spectrum of 4-bromo-13,16-difluorobenzo[*s*]picene (**3b**).

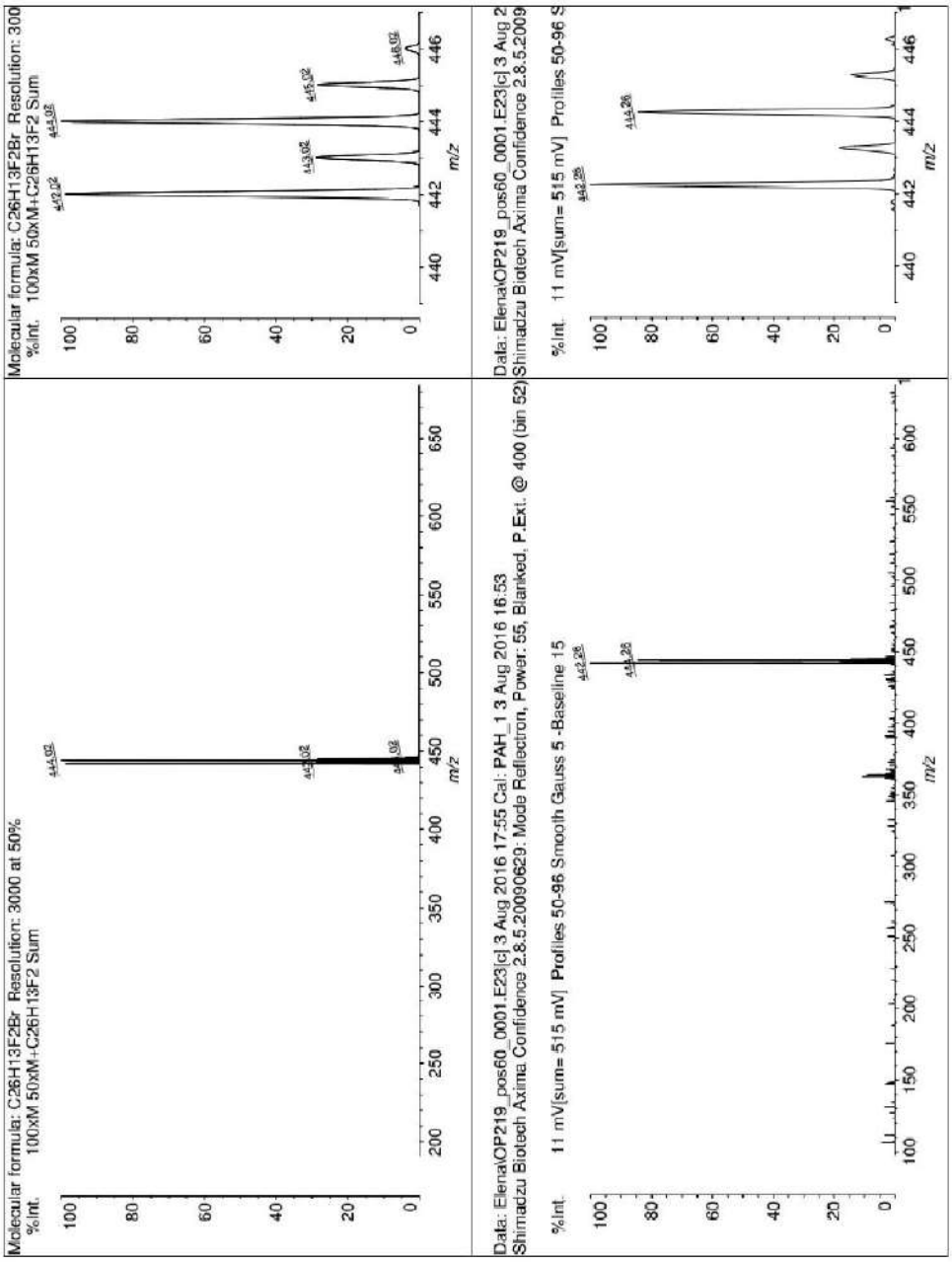

Figure S5. LDI-MS spectrum of 4-bromo-13,16-difluorobenzo[*s*]picene (**3b**) in positive mode.

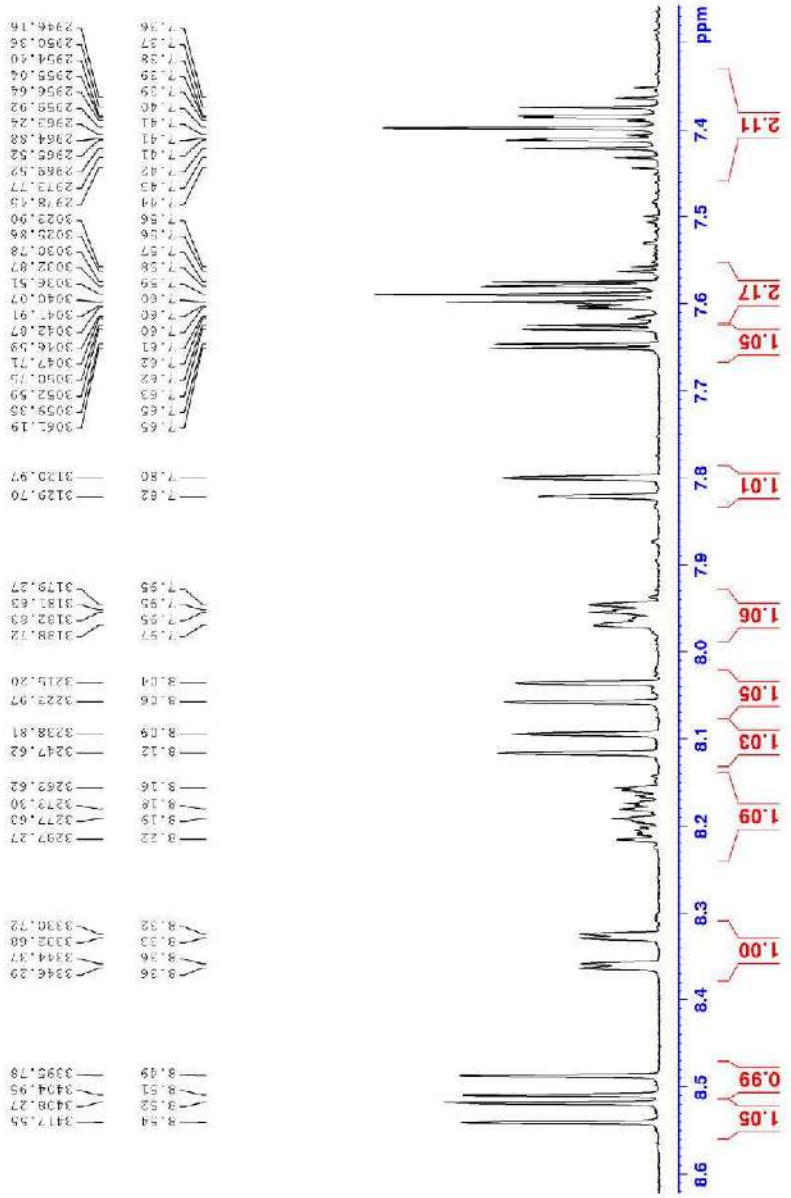

Figure S6. ^{1}H NMR (400 MHz, $CDCl_3$, 293K) spectrum of 2-bromo-13,16-difluorobenzo[*s*]picene (**3c**).

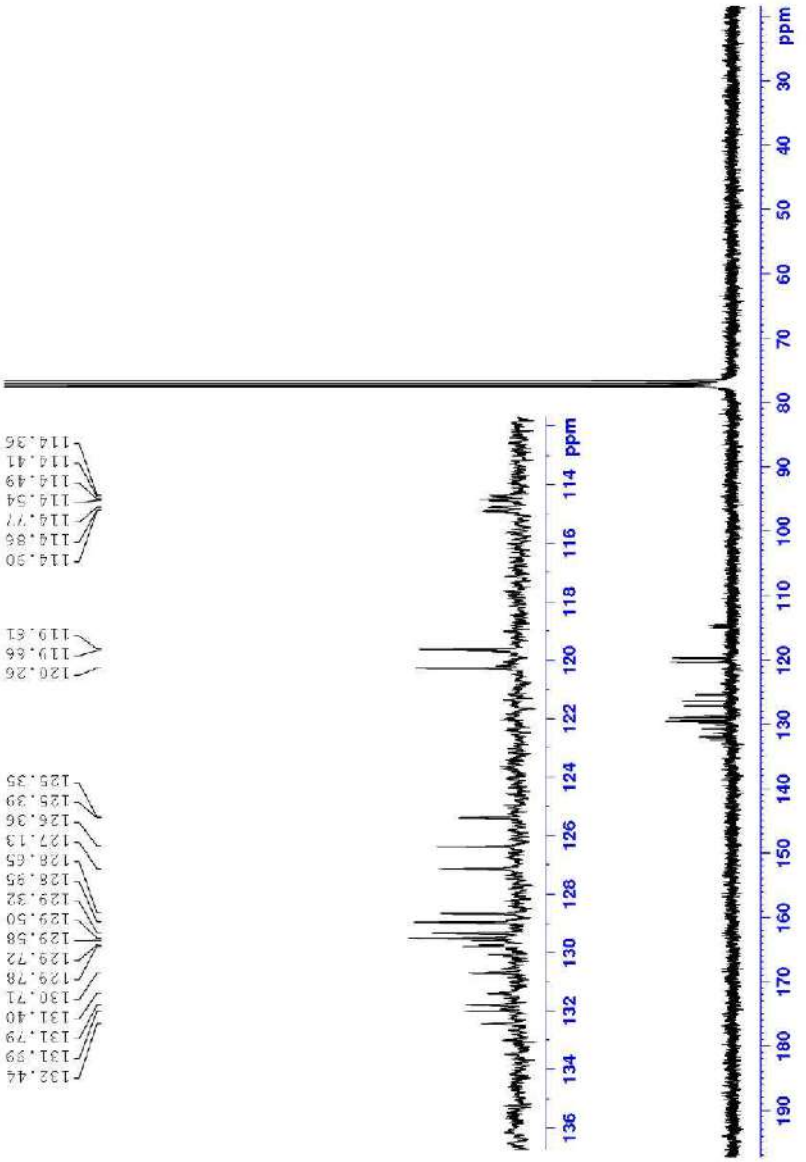

Figure S7. ^{13}C NMR (100 MHz, $CDCl_3$, 293K) spectrum of 4-bromo-13,16-difluorobenzo[*s*]picene (**3c**).

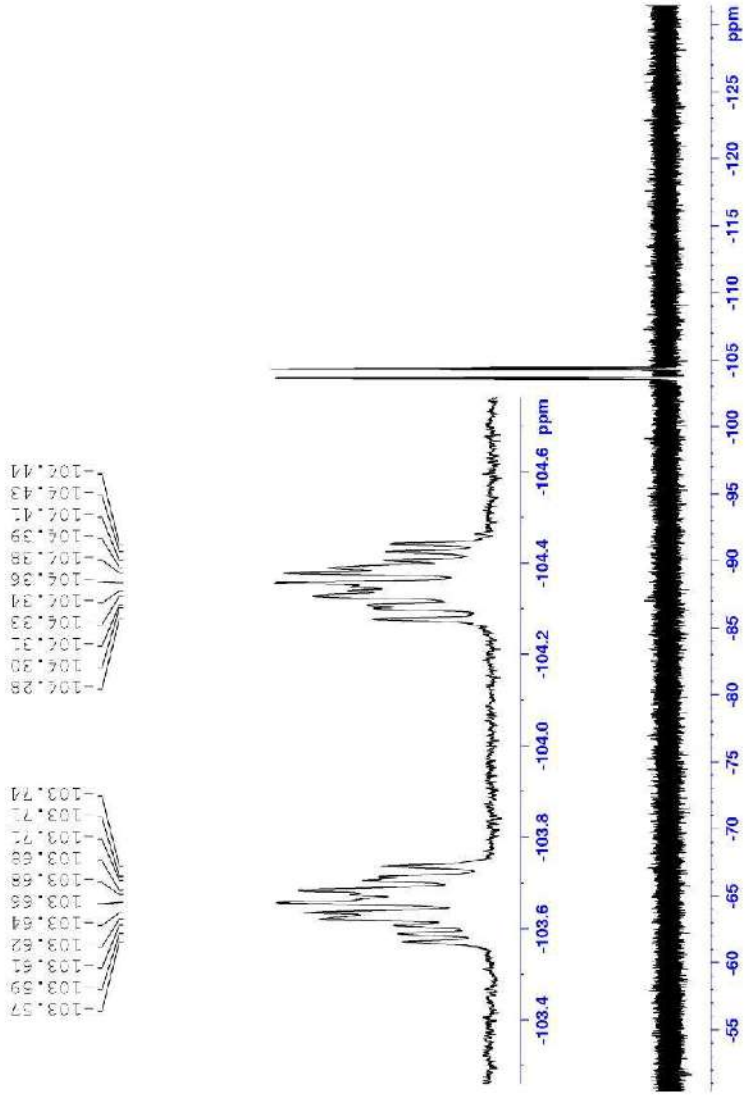

Figure S8. ^{19}F NMR (282 MHz, $CDCl_3$, 293K) spectrum of 2-bromo-13,16-difluorobenzo[*s*]picene (**3c**).

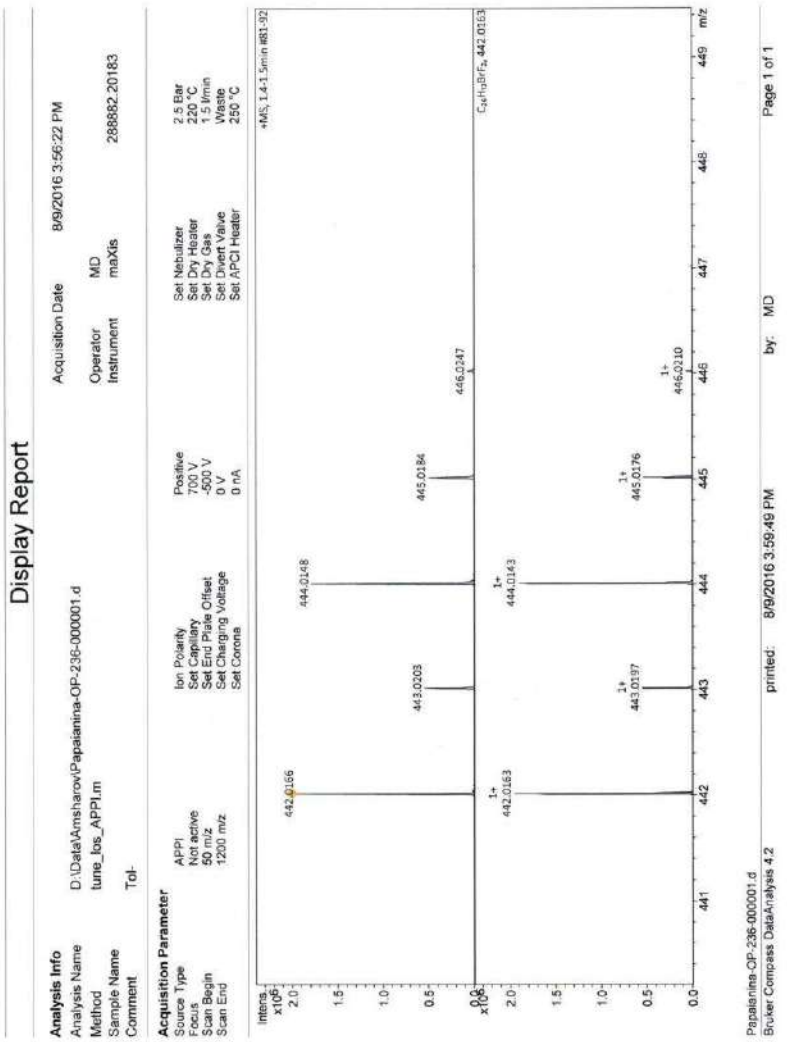

Figure S9. APPI-MS spectrum of 2-bromo-13,16-difluorobenzo[*s*]picene (**3c**).

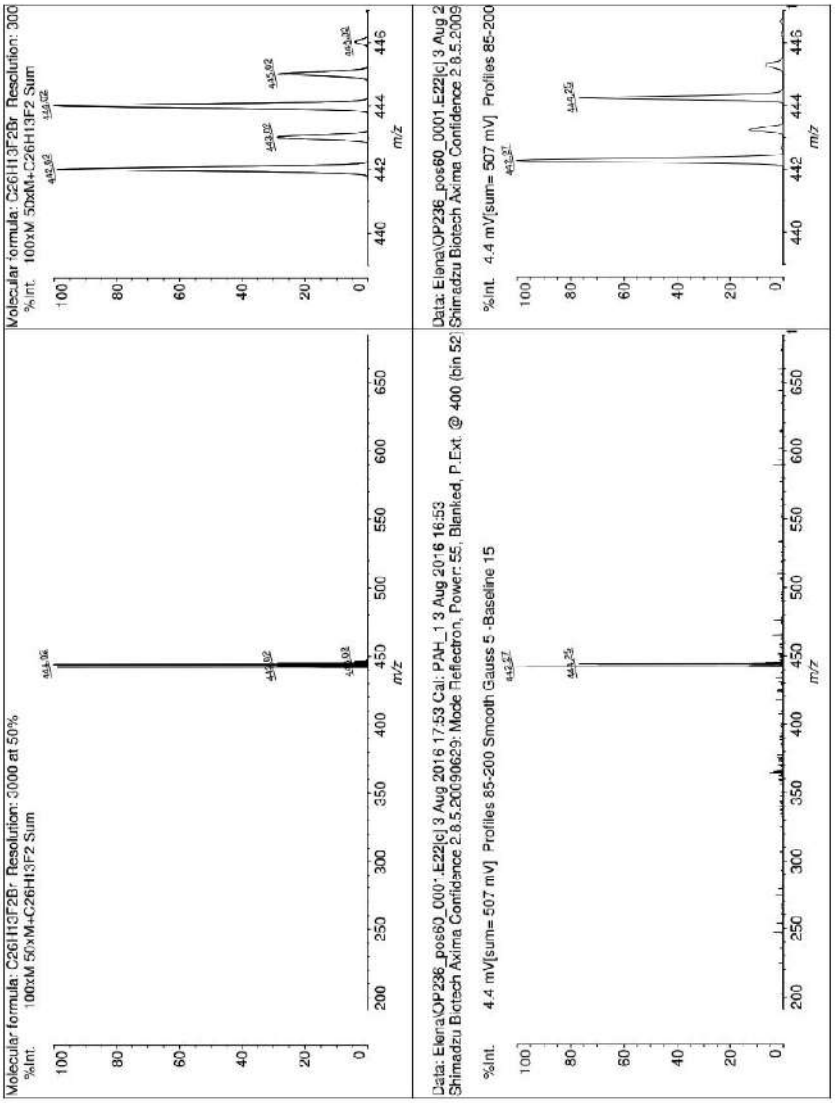

Figure S10. LDI-MS spectrum of 2-bromo-13,16-difluorobenzo[*s*]picene (**3c**) in positive mode.

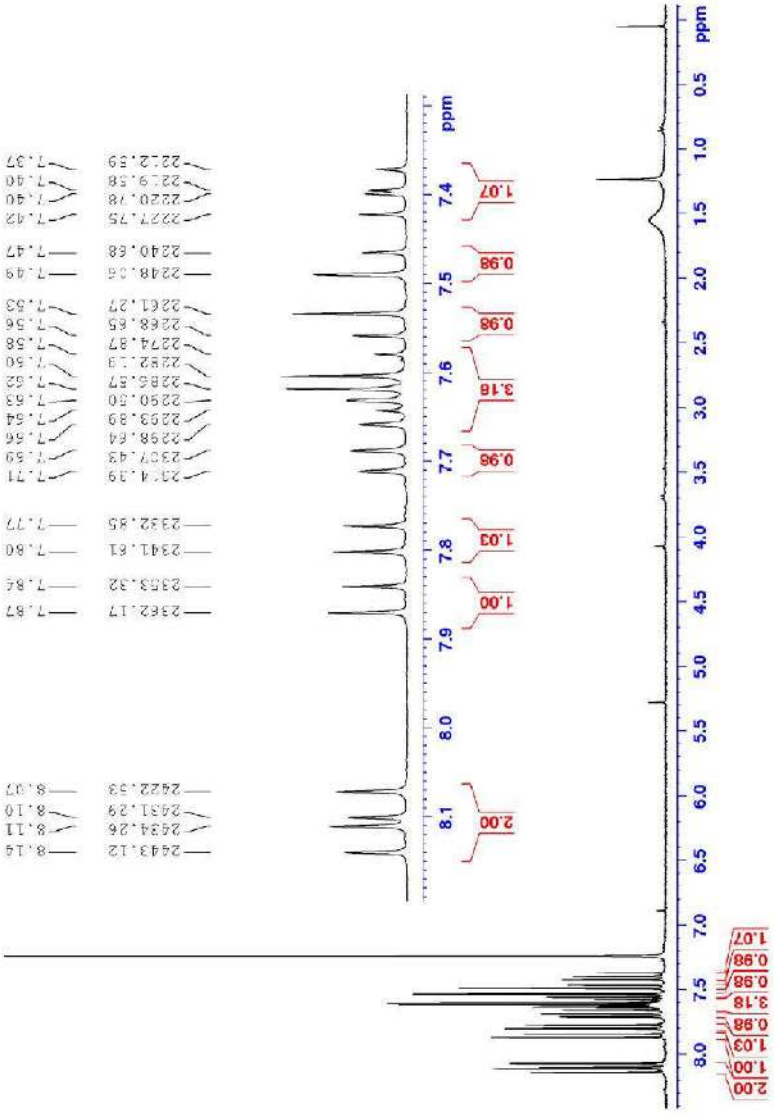

Figure S11. ^{1}H NMR (400 MHz, $CDCl_3$, 293 K) spectrum of 1-bromo-*as*-indaceno[*3,2,1,8,7,6-pqrstuv*]picene (**4b**).

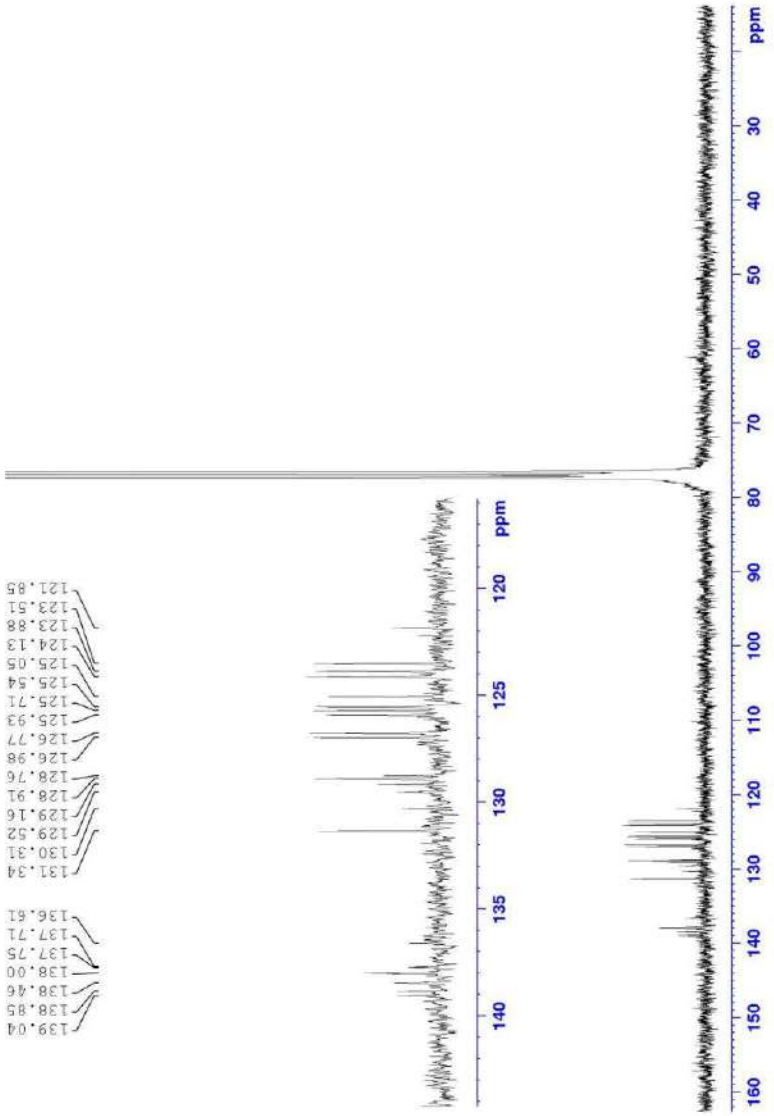

Figure S12. ^{13}C NMR (100 MHz, $CDCl_3$, 293K) spectrum of 1-bromo-*as*-indaceno[*3,2,1,8,7,6-pqrstuv*]picene (**4b**).

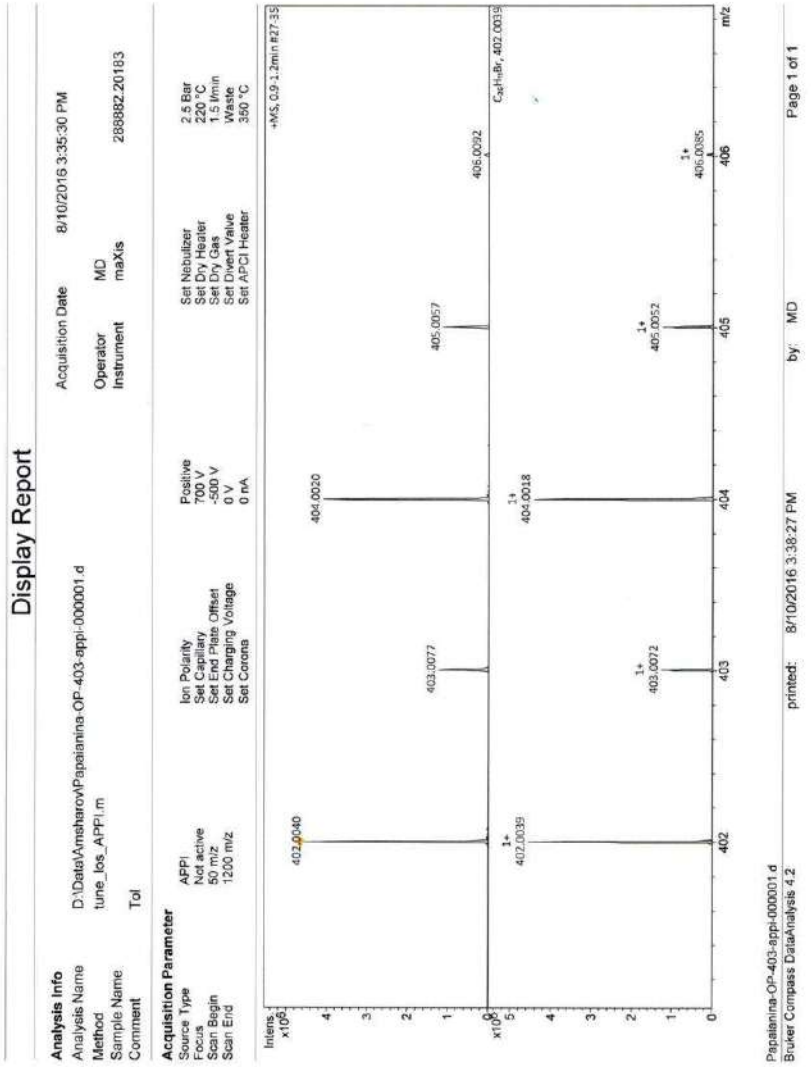

Figure S13. APPI-MS spectrum of 1-bromo-*as*-indaceno[*3,2,1,8,7,6-pqrstuv*]picene (**4b**).

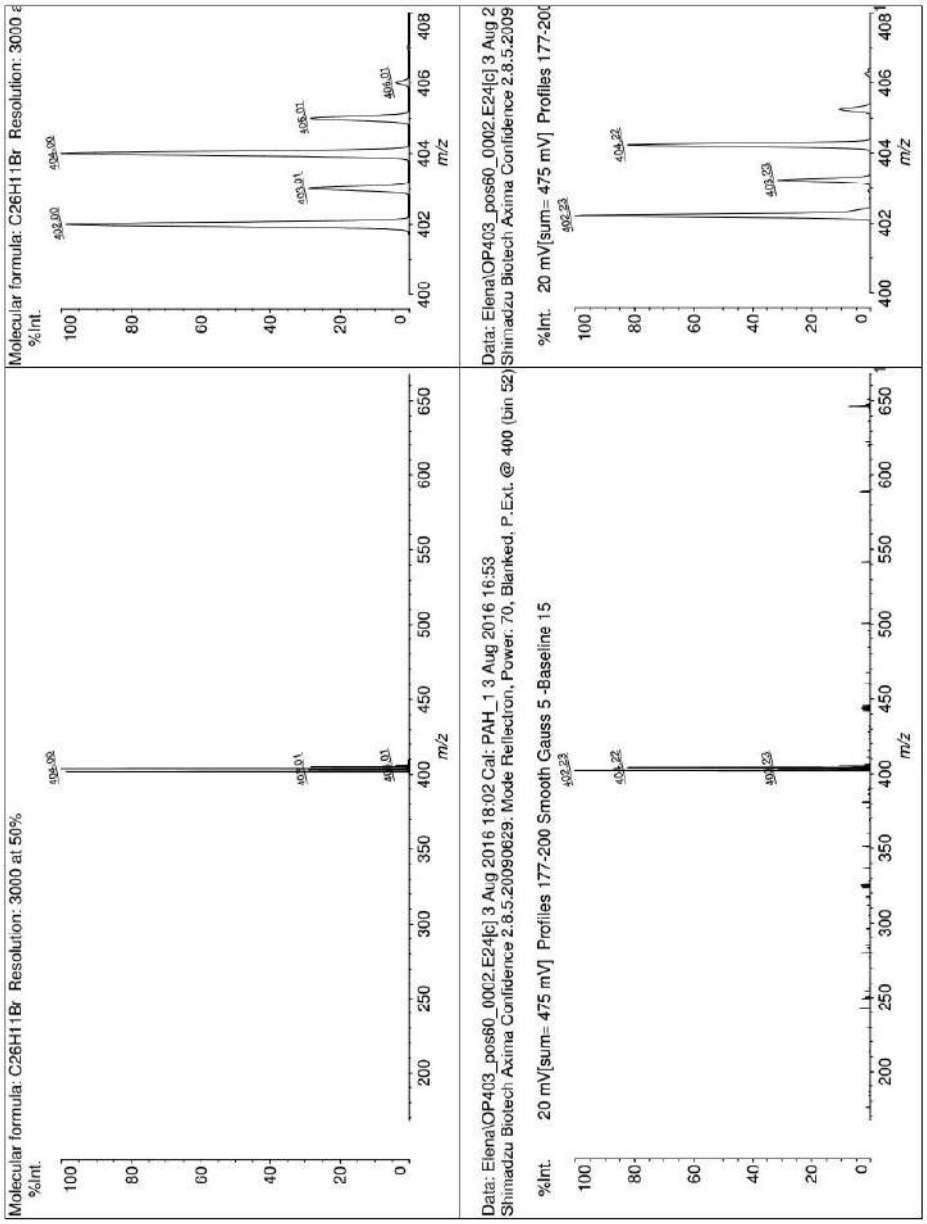

Figure S14. LDI-MS spectrum of 1-bromo-*as*-indaceno[*3,2,1,8,7,6-pqrstuv*]picene (**4b**) in positive mode.

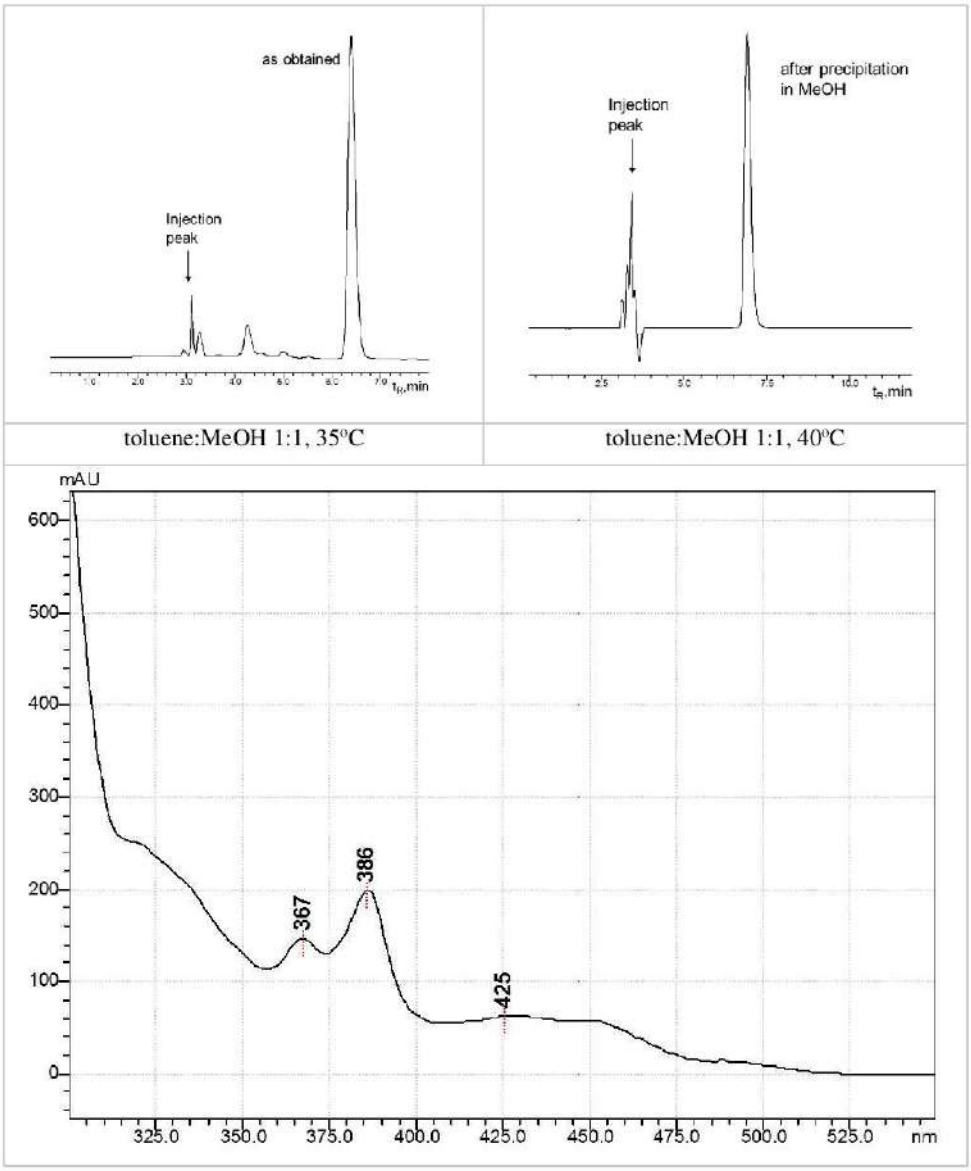

Figure S15. HPLC profile of 1-bromo-as-indaceno[*3,2,1,8,7,6-pqrstuv*]picene (**4b**) as obtained after reaction (150°C, 1.5h, *o*-DCB) and after precipitation in MeOH, detected at 320 nm (5PYE column, toluene:MeOH as eluent, 1.0 ml/min). UV-Vis spectrum of 1-bromo-as-indaceno[*3,2,1,8,7,6-pqrstuv*]picene in toluene:MeOH 1:1.

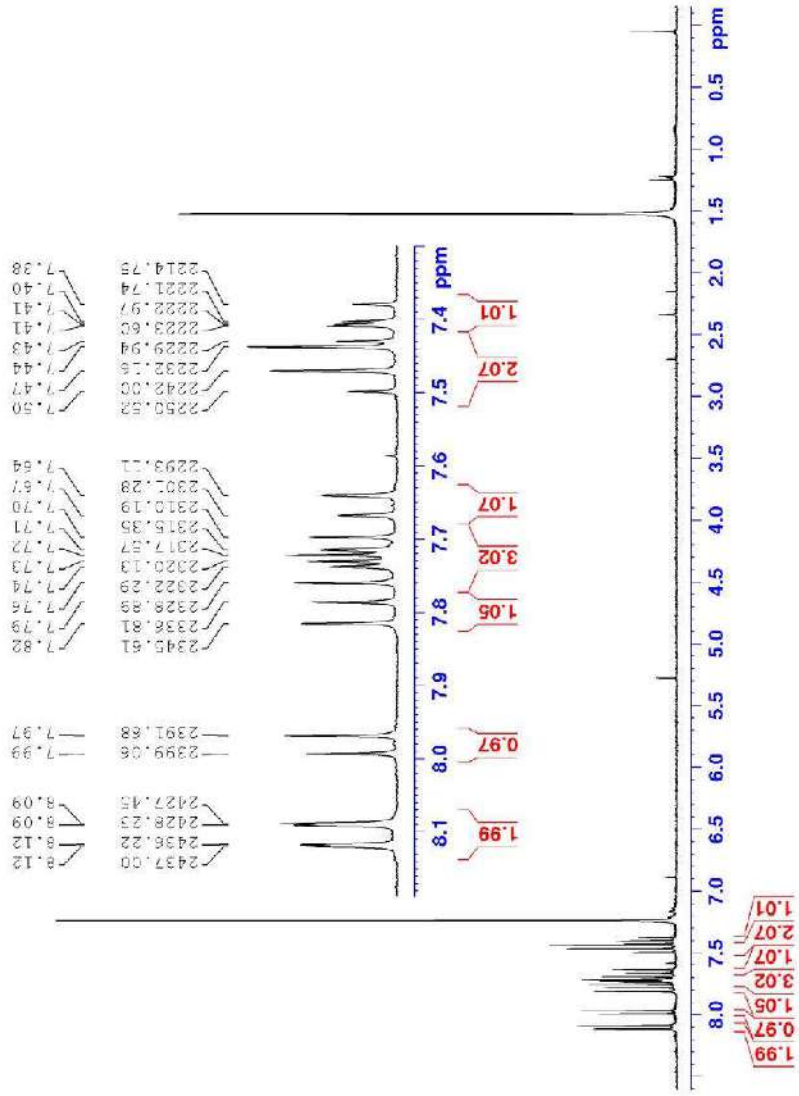

Figure S16. ^{1}H NMR (300 MHz, $CDCl_3$, 293 K) spectrum of 3-bromo-*as*-indaceno[*3,2,1,8,7,6-pqrstuv*]picene (**4c**).

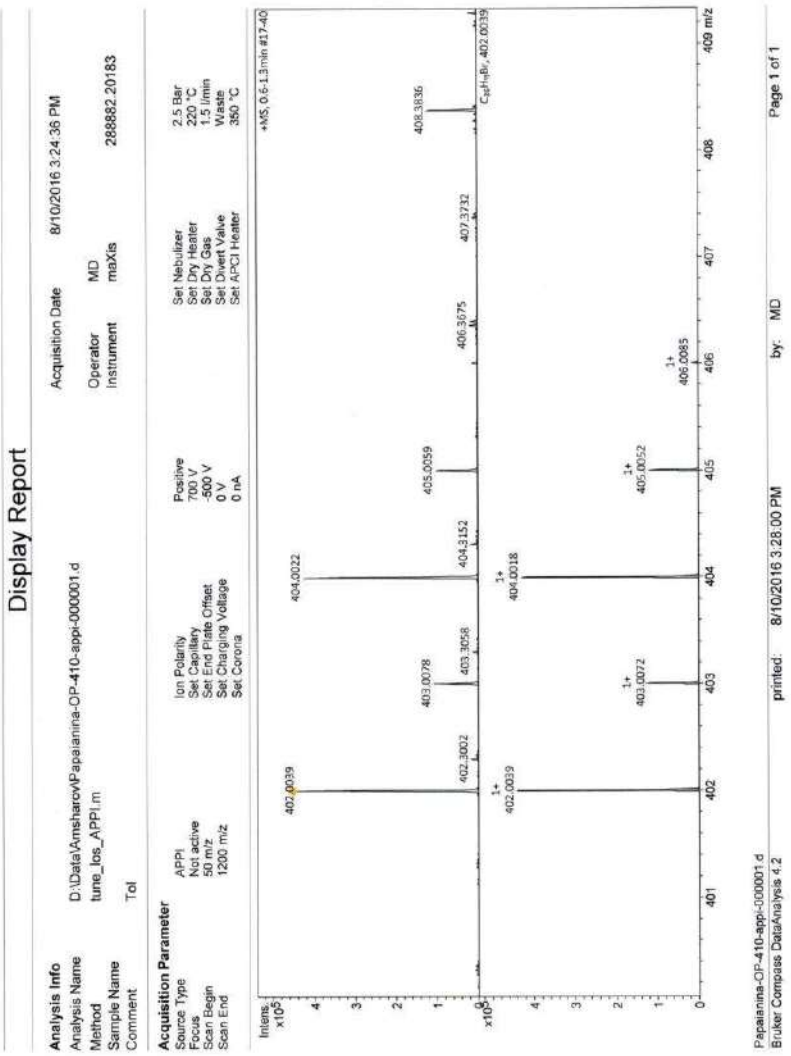

Figure S17. APPI-MS spectrum of 3-bromo-*as*-indaceno[*3,2,1,8,7,6-pqrstuv*]picene (**4c**).

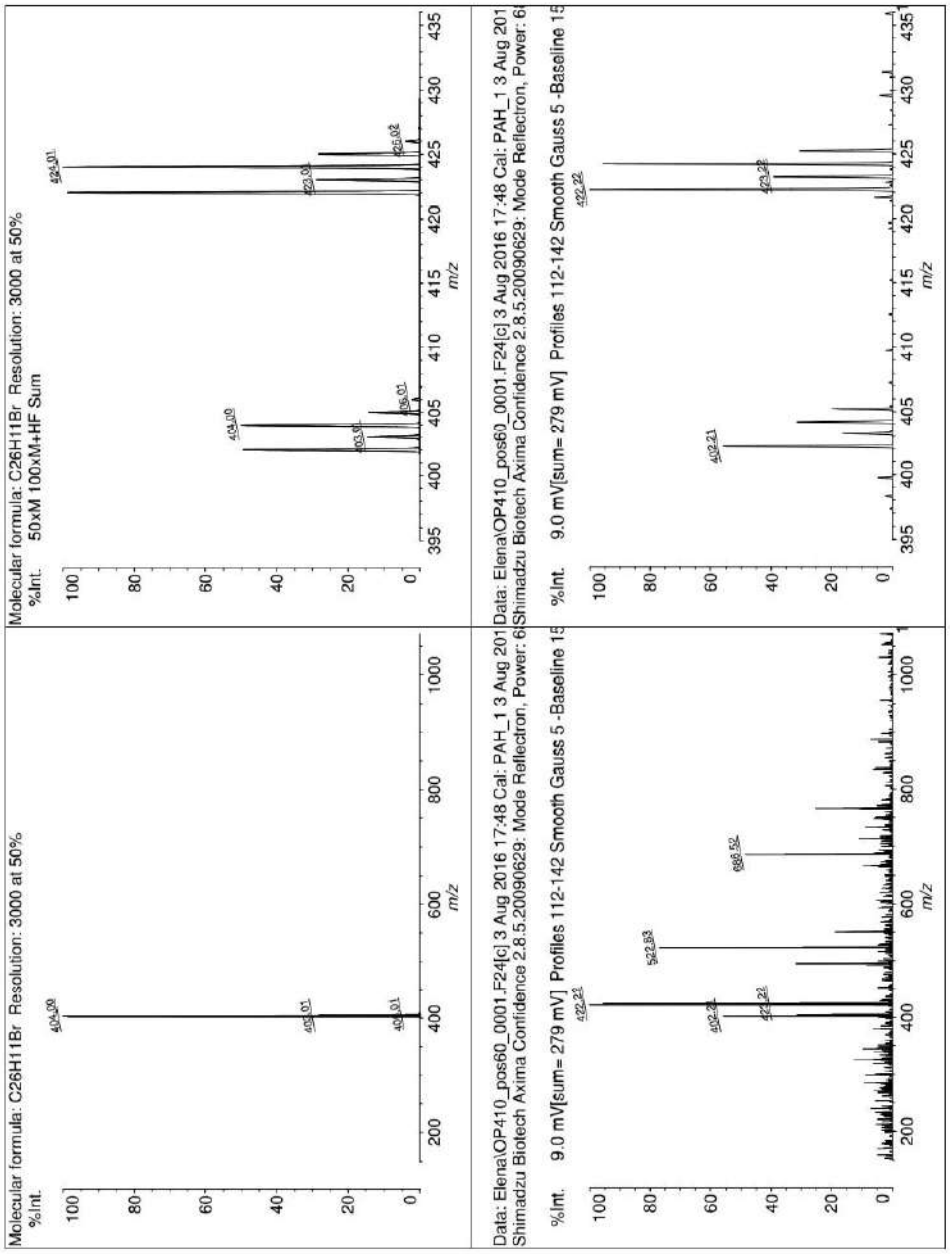

Figure S18. LDI-MS spectrum of 3-bromo-*as*-indaceno[*3,2,1,8,7,6-pqrstuv*]picene (**4c**) in positive mode.

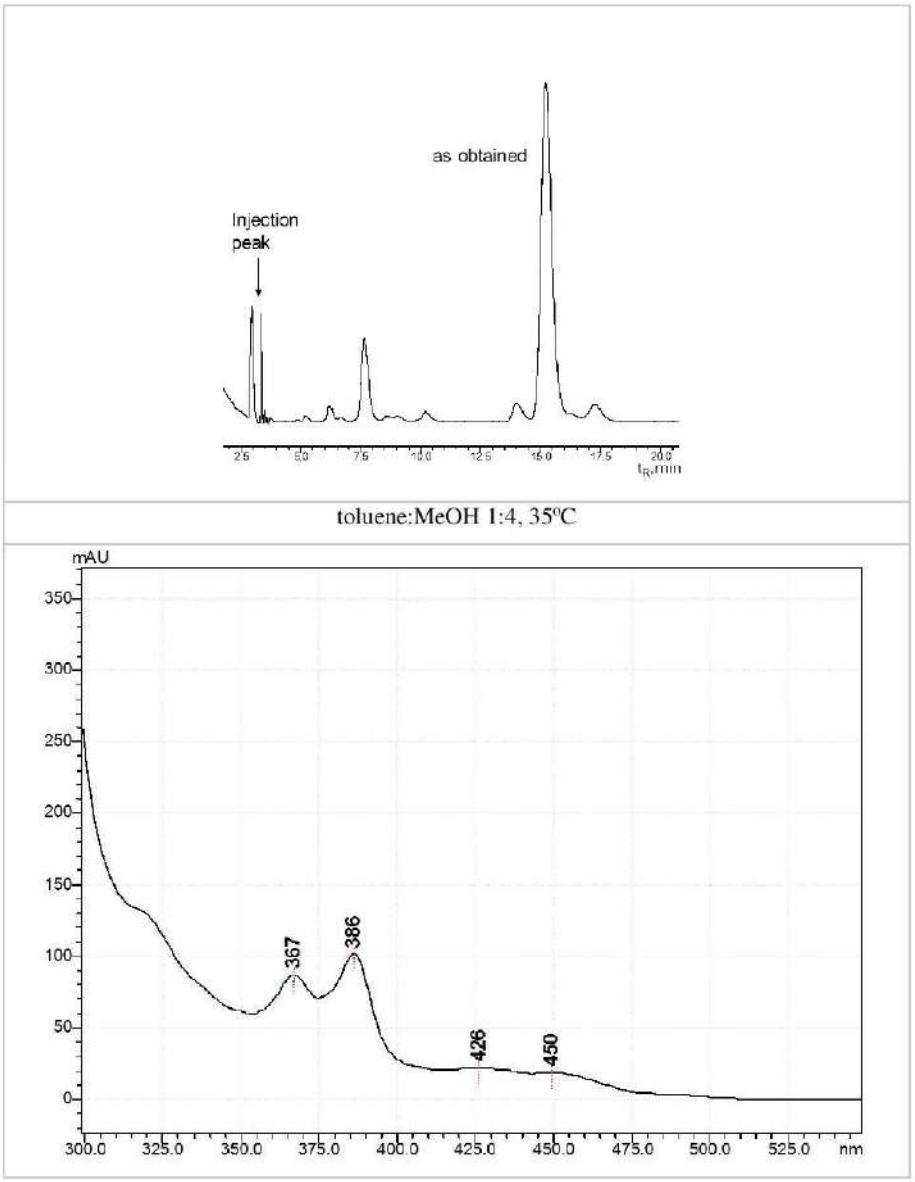

Figure S19. HPLC profile 3-bromo-as-indaceno[*3,2,1,8,7,6-pqrstuv*]picene (**4c**) as obtained after reaction (240ºC, 1.5h, *o*-DCB), detected at 320 nm (5PYE column, toluene:MeOH as eluent, 1.0 ml/min). UV-Vis spectrum of 3-bromo-*as*-indaceno[*3,2,1,8,7,6-pqrstuv*]picene in toluene:MeOH 1:1.

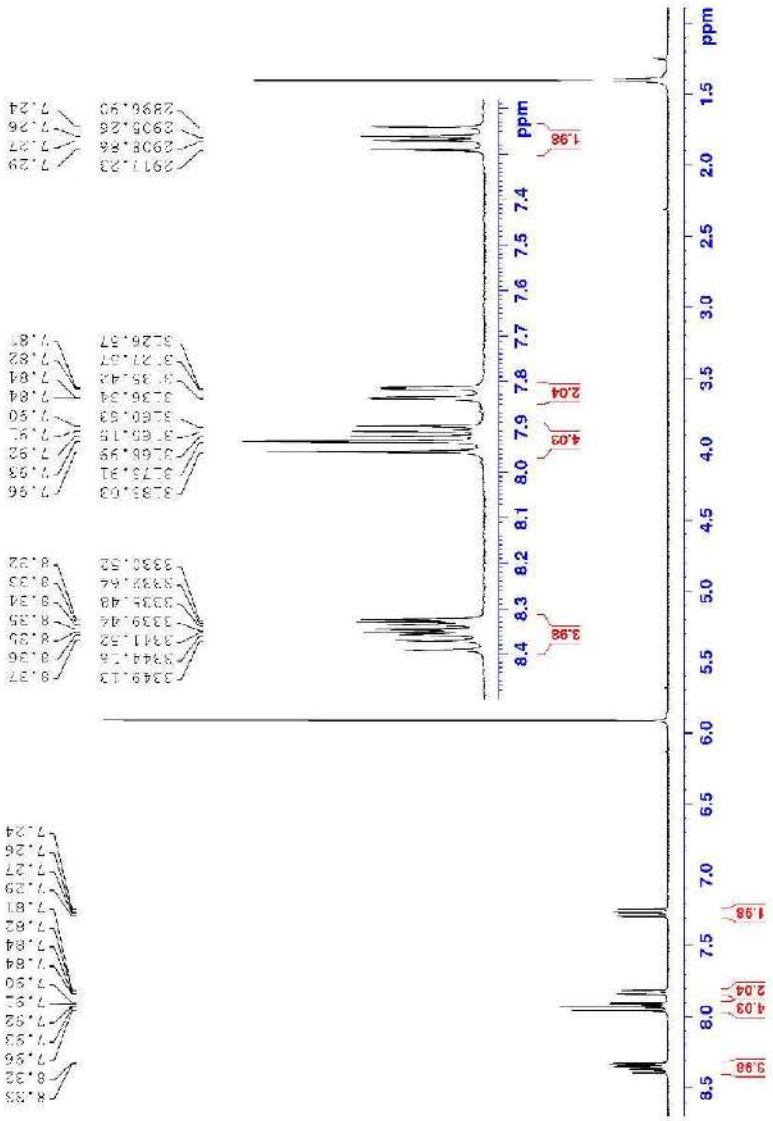

Figure S20. ^{1}H NMR (400 MHz, $C_2D_2Cl_4$, 353K) spectrum of 1,9-dibromo-4,12-difluorodibenzo[*c,l*]chrysene (**6a**).

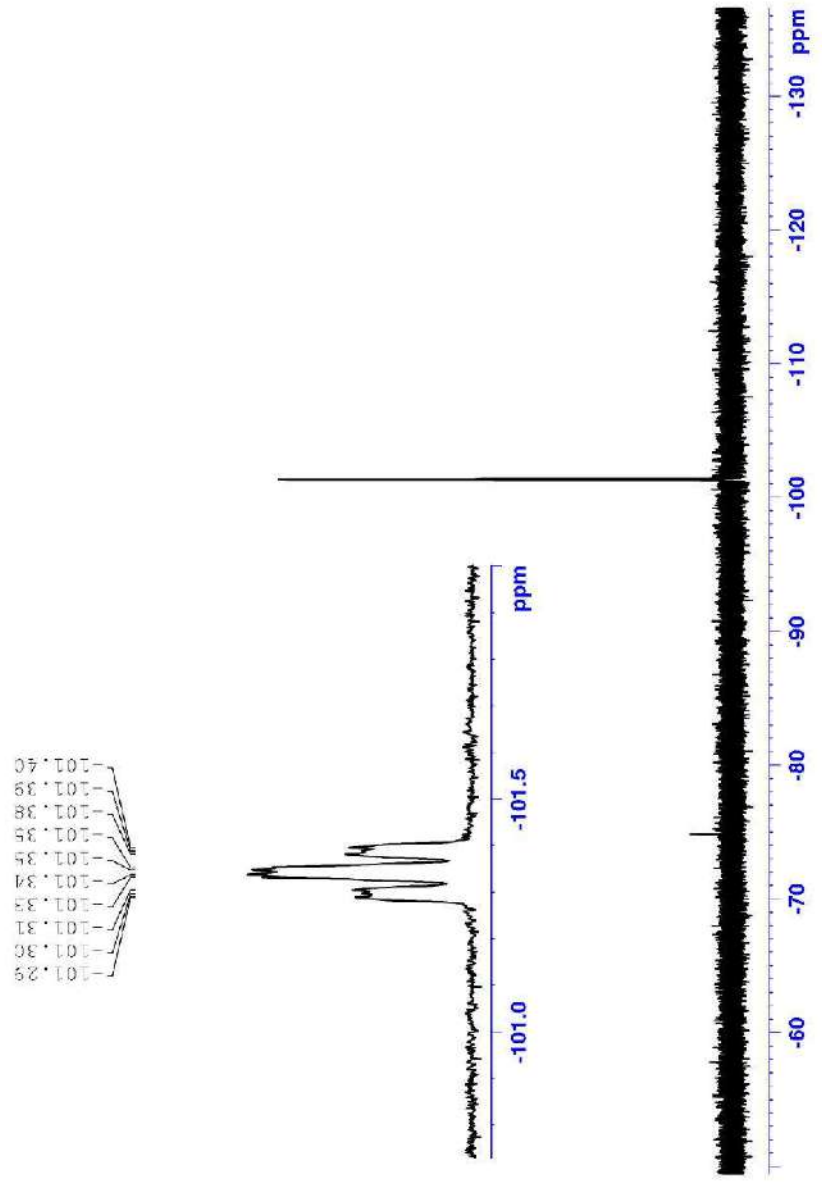

Figure S21. ^{19}F NMR (282 MHz, $C_2D_2Cl_4$, 293K) spectrum of 1,9-dibromo-4,12-difluorodibenzo[*c,l*]chrysene (**6a**).

Figure S22. APPI-MS spectrum of 1,9-dibromo-4,12-difluorodibenzo[*c,l*]chrysene (**6a**).

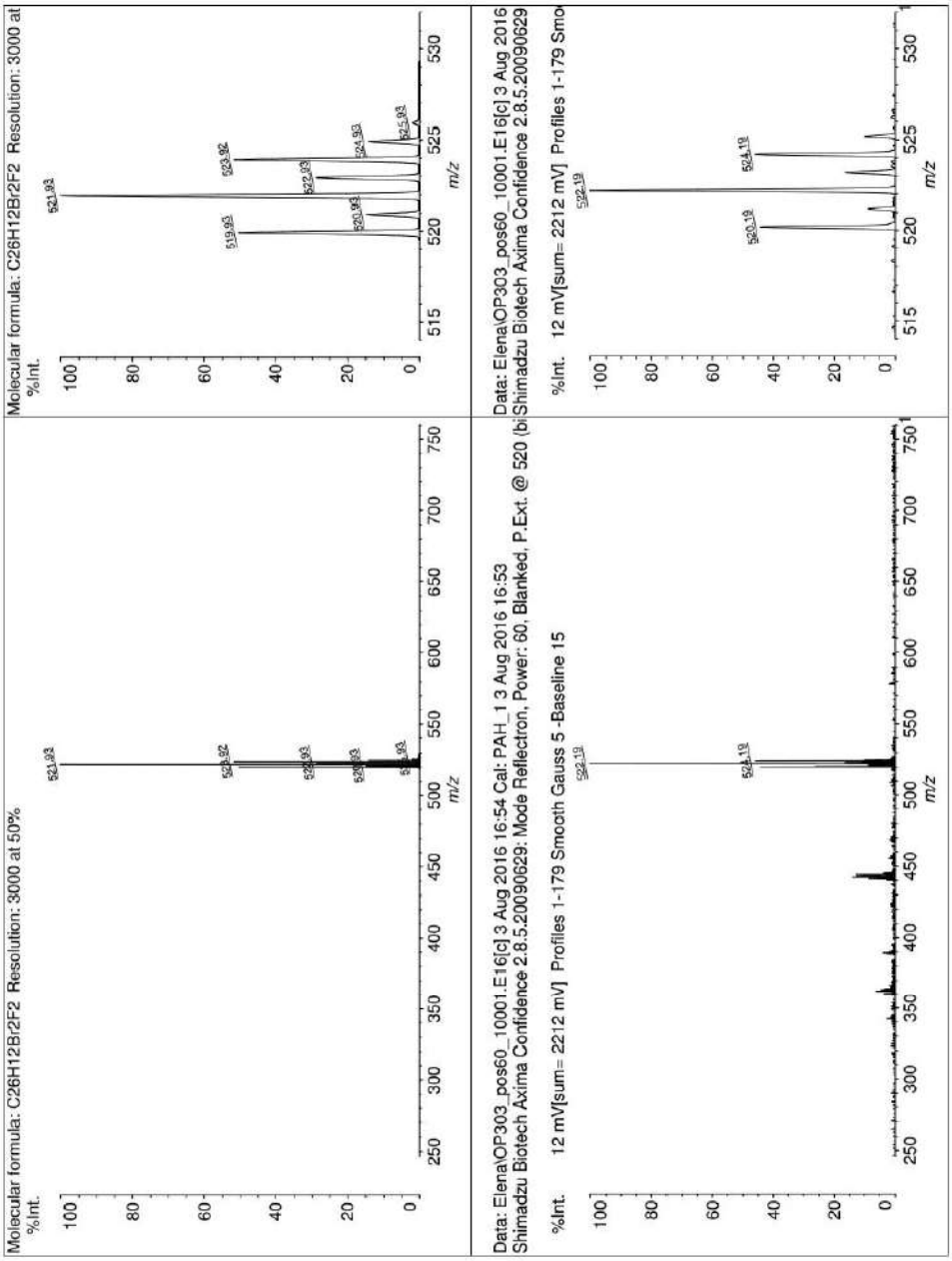

Figure S23. LDI-MS spectrum of 1,9-dibromo-4,12-difluorodibenzo[*c,l*]chrysene (**6a**) in positive mode.

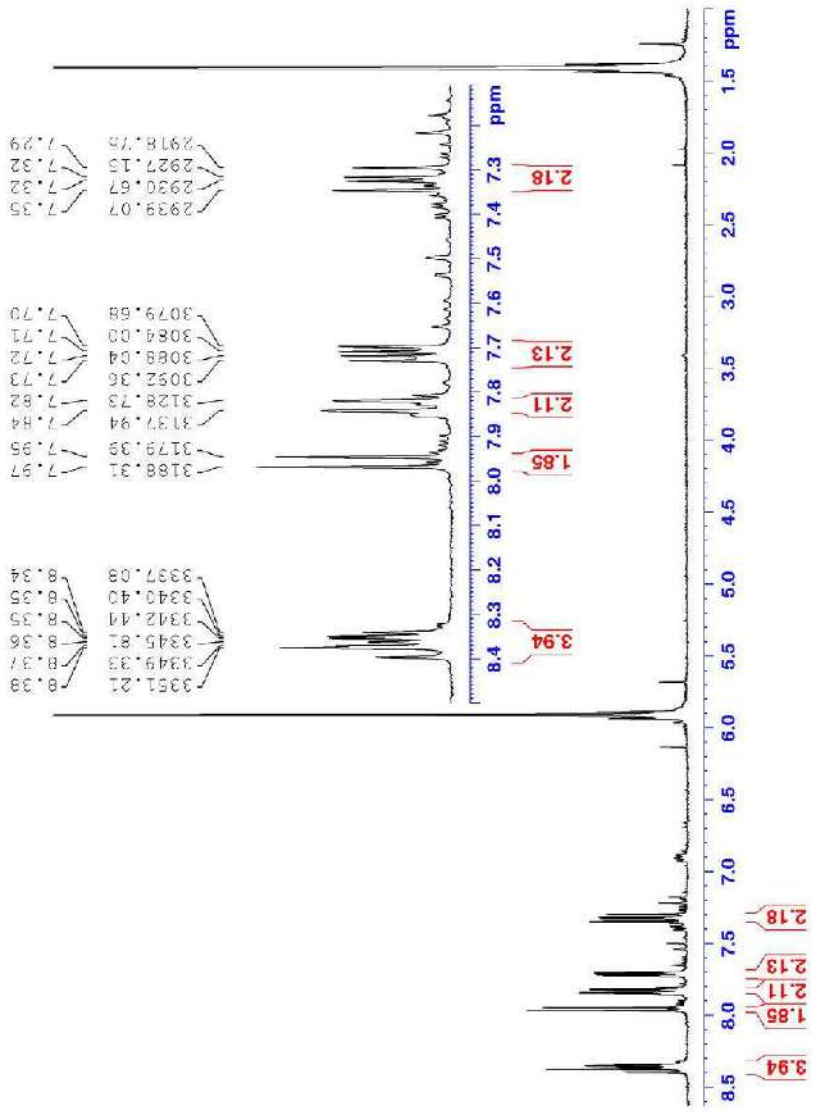

Figure S24. ^{1}H NMR (400 MHz, $C_2D_2Cl_4$, 353K) spectrum of 1,9-dichloro-4,12-difluorodibenzo[*c,l*]chrysene (**6b**).

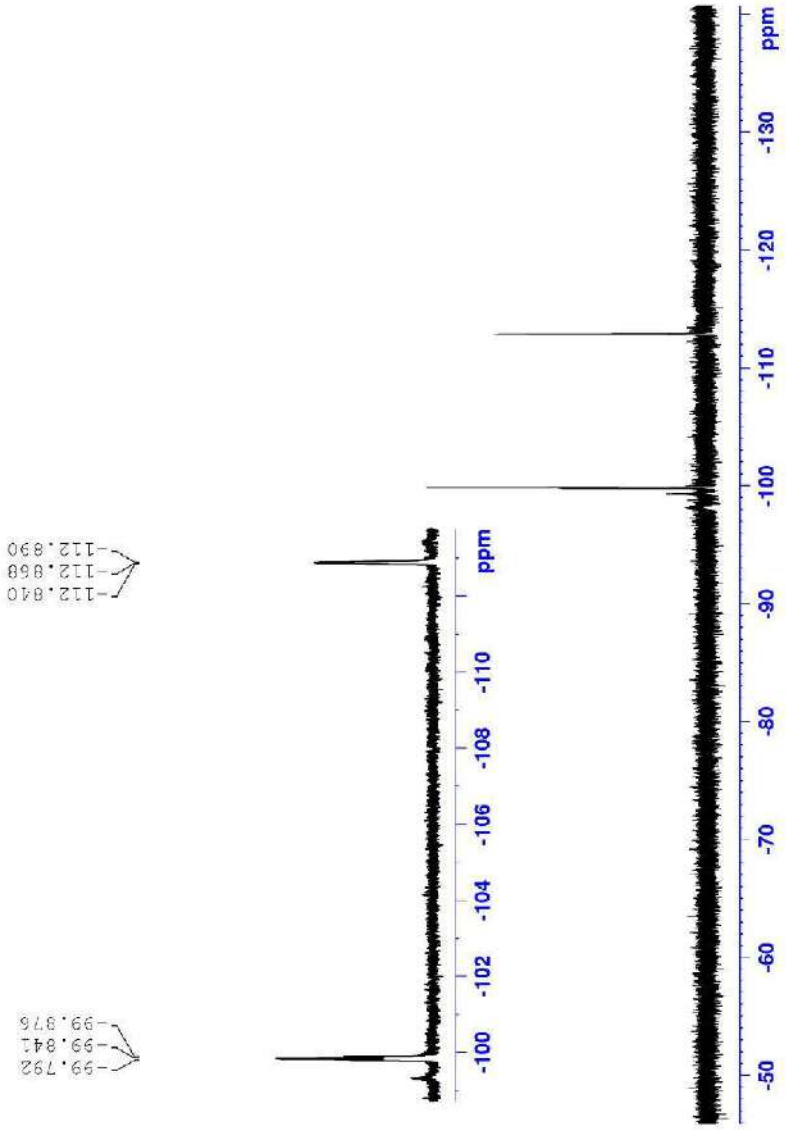

Figure S25. ^{19}F NMR (282 MHz, $C_2D_2Cl_4$, 293K) spectrum of 1,9-dichloro-4,12-difluorodibenzo[*c,l*]chrysene (**6b**).

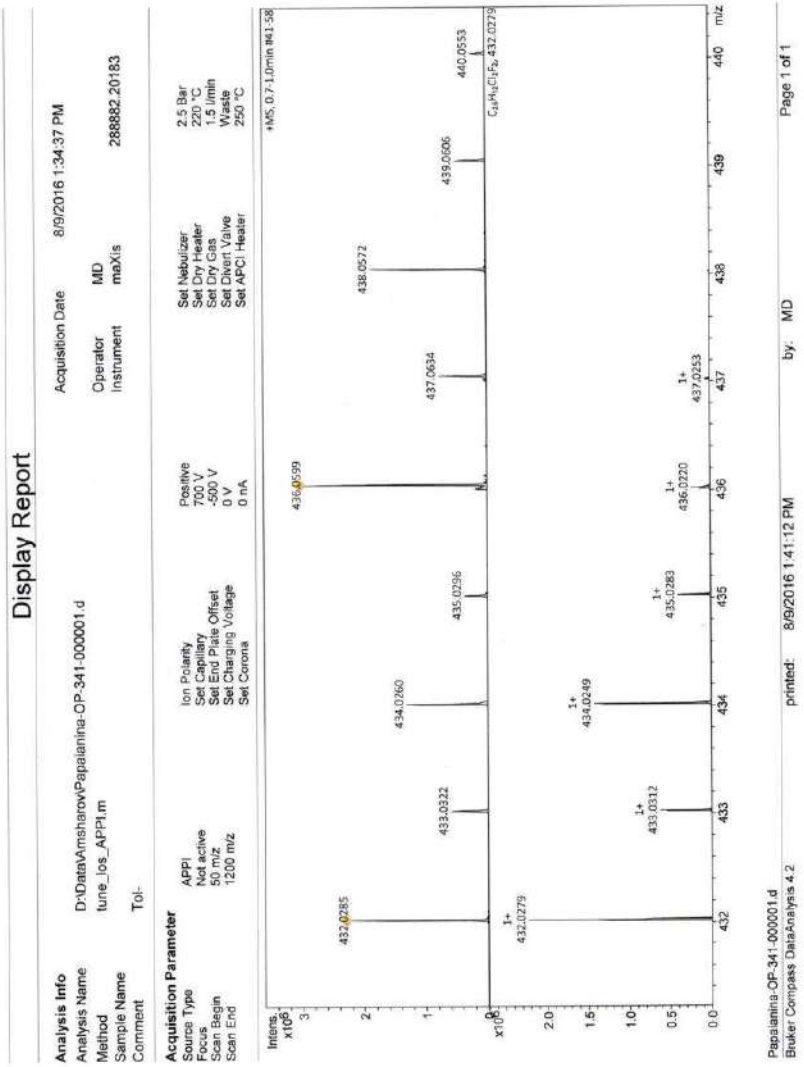

Figure S26. APPI-MS spectrum of 1,9-dichloro-4,12-difluorodibenzo[*c*,*l*]chrysene (**6b**).

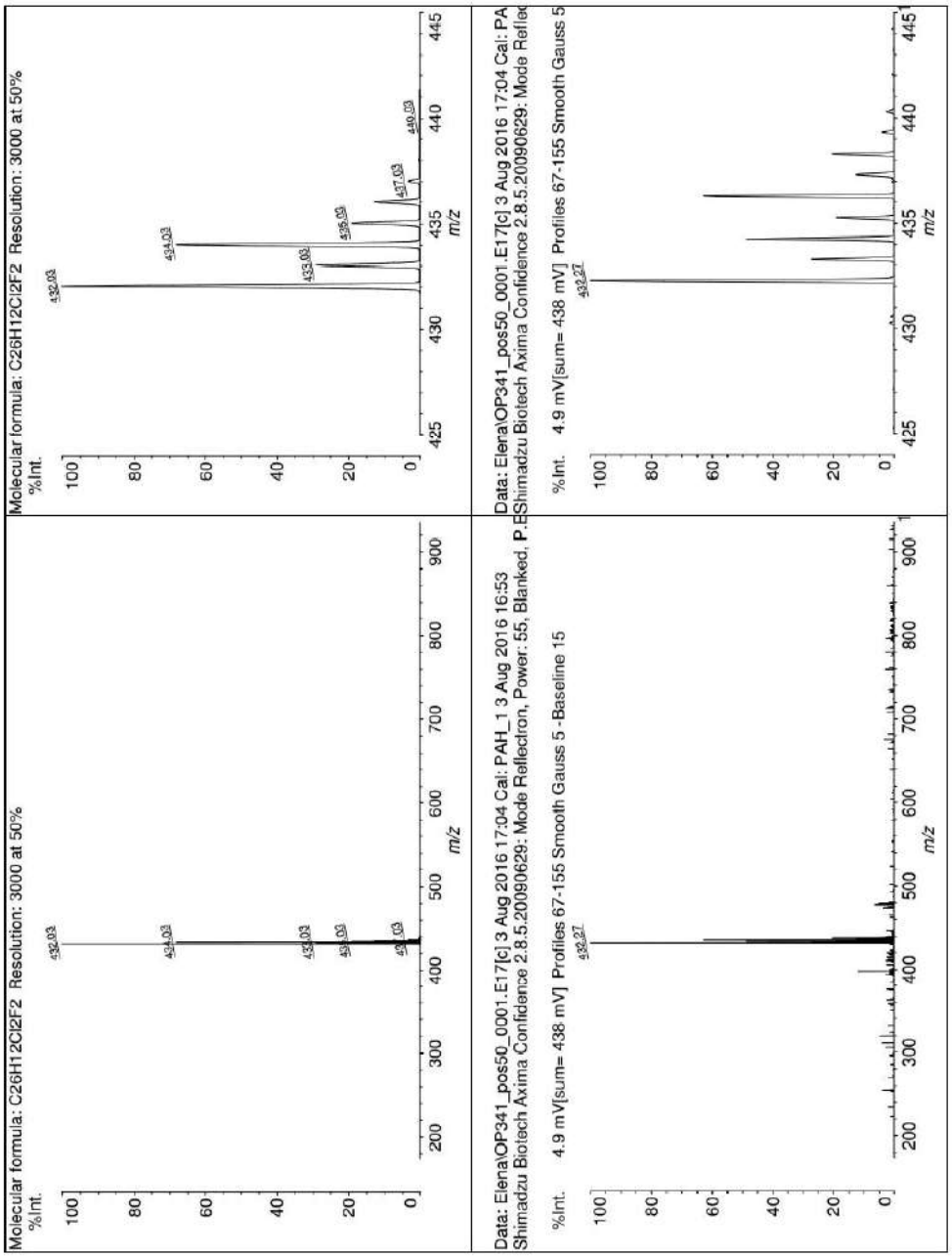

Figure S27. LDI-MS spectrum of 1,9-dichloro-4,12-difluorodibenzo[*c*,*l*]chrysene (**6b**) in positive mode.

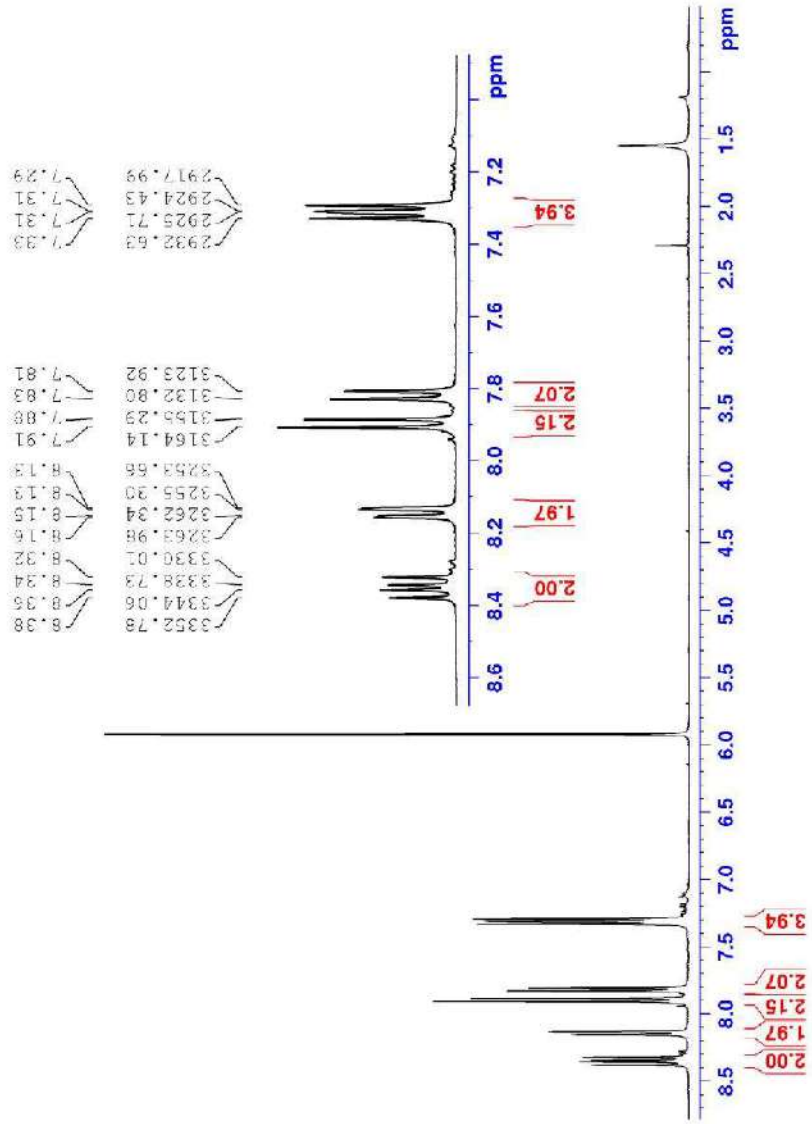

Figure S28. ^{1}H NMR (400 MHz, $C_2D_2Cl_4$, 293K) spectrum of 1,4,9,12-tetrafluorodibenzo[*c,l*]chrysene (**6c**).

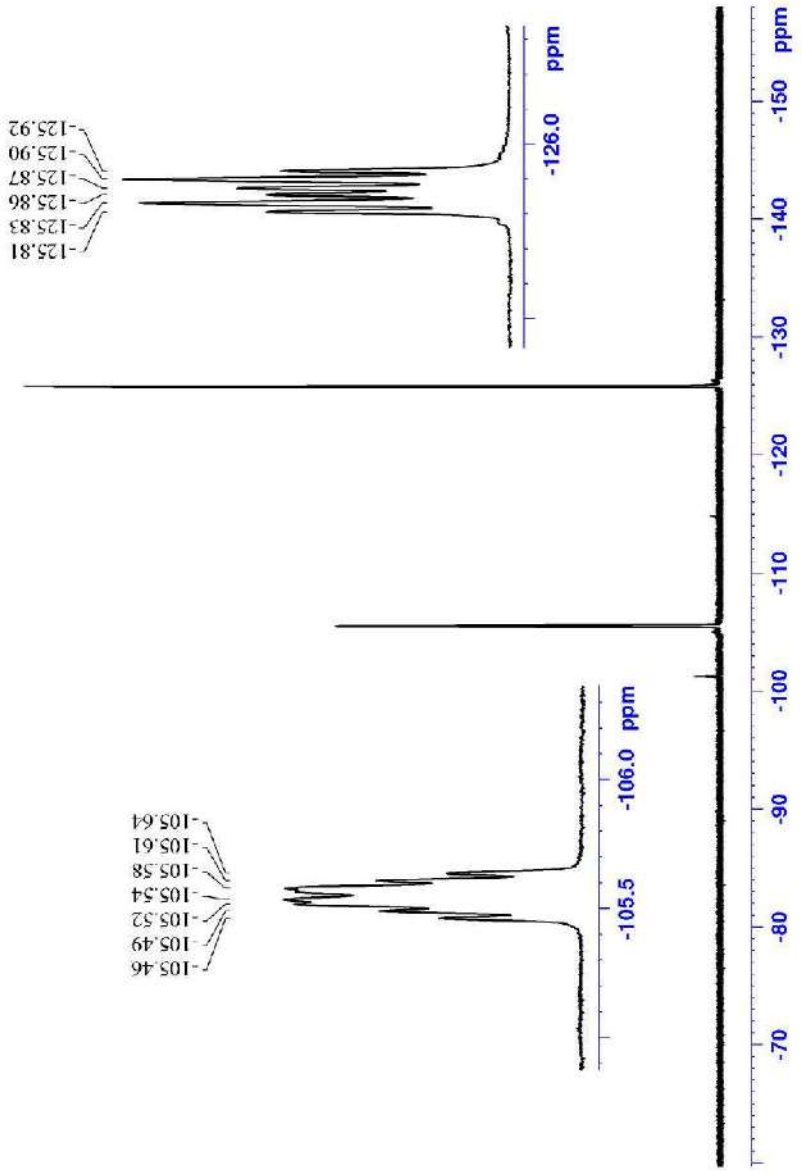

Figure S29. ^{19}F NMR (282 MHz, $C_2D_2Cl_4$, 293K) spectrum of 1,4,9,12-tetrafluorodibenzo[*c,l*]chrysene (**6c**).

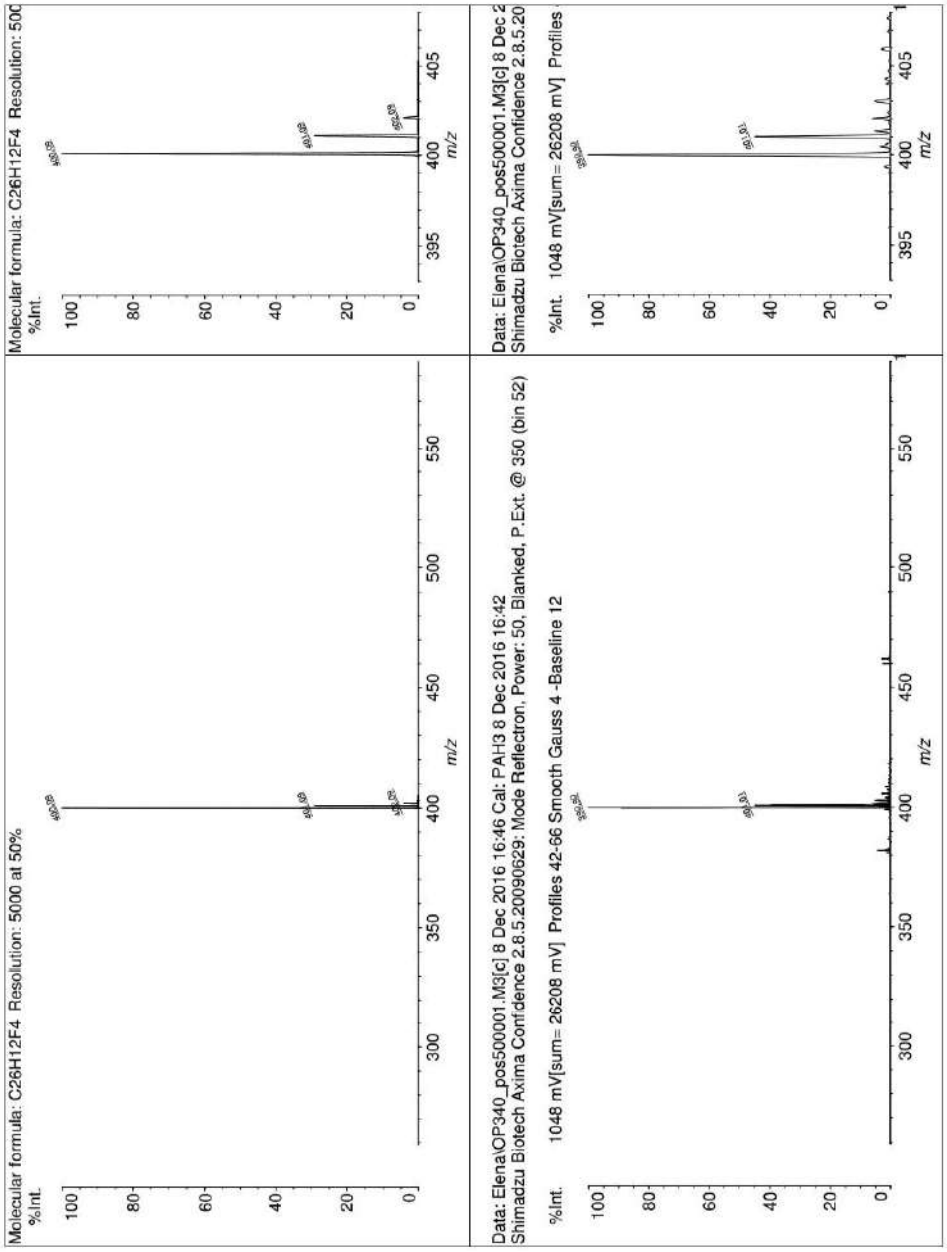

Figure S30. LDI-MS spectrum of 1,4,9,12-tetrafluorodibenzo[*c,l*]chrysene (**6c**) in positive mode.

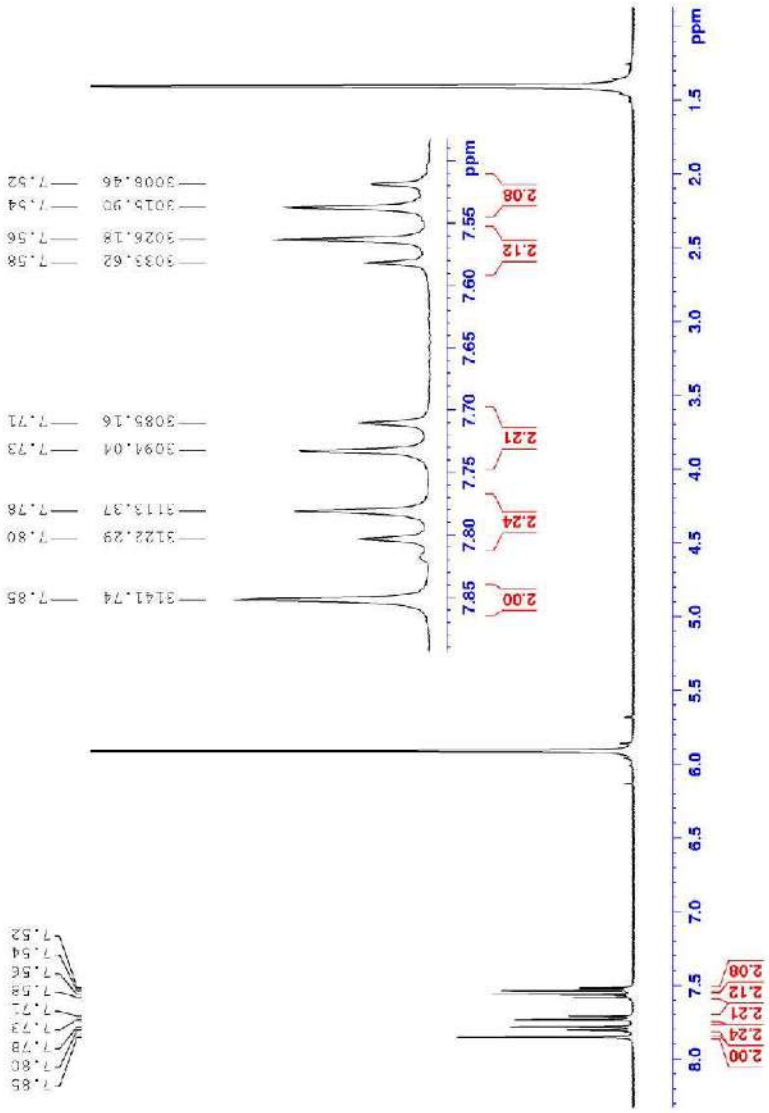

Figure S31. ^{1}H NMR (400 MHz, $C_2D_2Cl_4$, 353K) spectrum of 3,9-dibromodiindeno[*4,3,2,1-cdef:4',3',2',1'-lmno*]chrysene (**7a**).

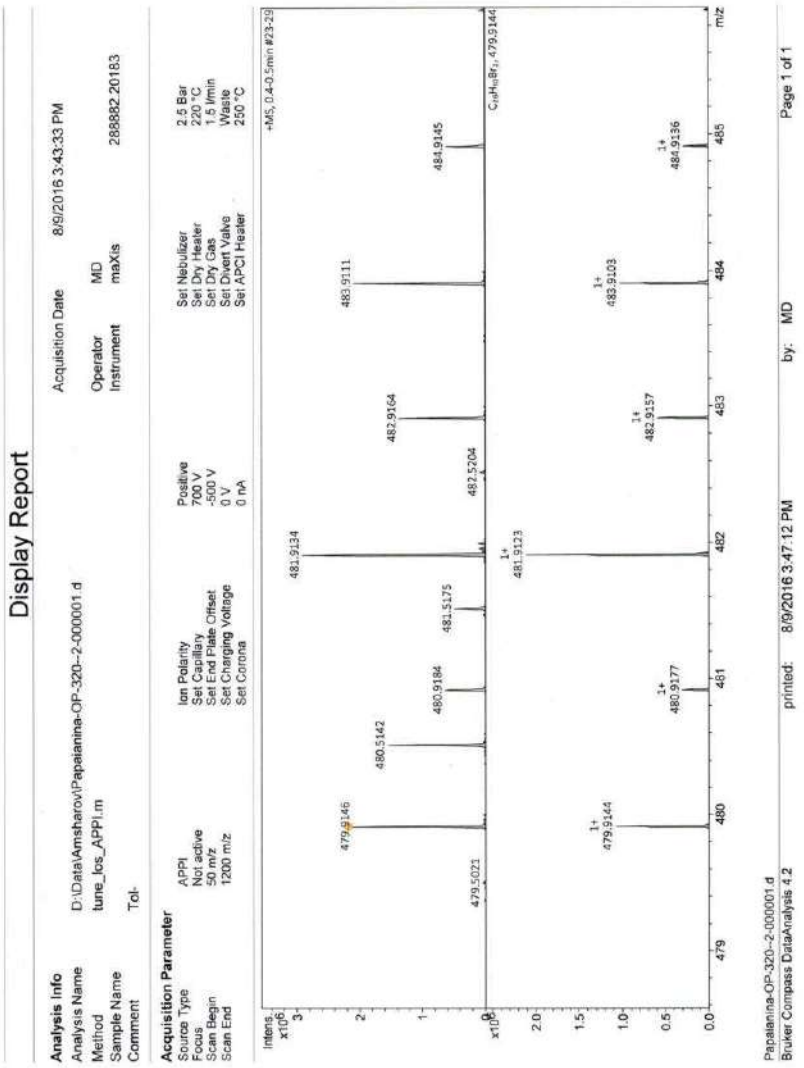

Figure S32. APPI-MS spectrum of 3,9-dibromodiindeno[*4,3,2,1-cdef:4',3',2',1'-lmno*]chrysene (**7a**).

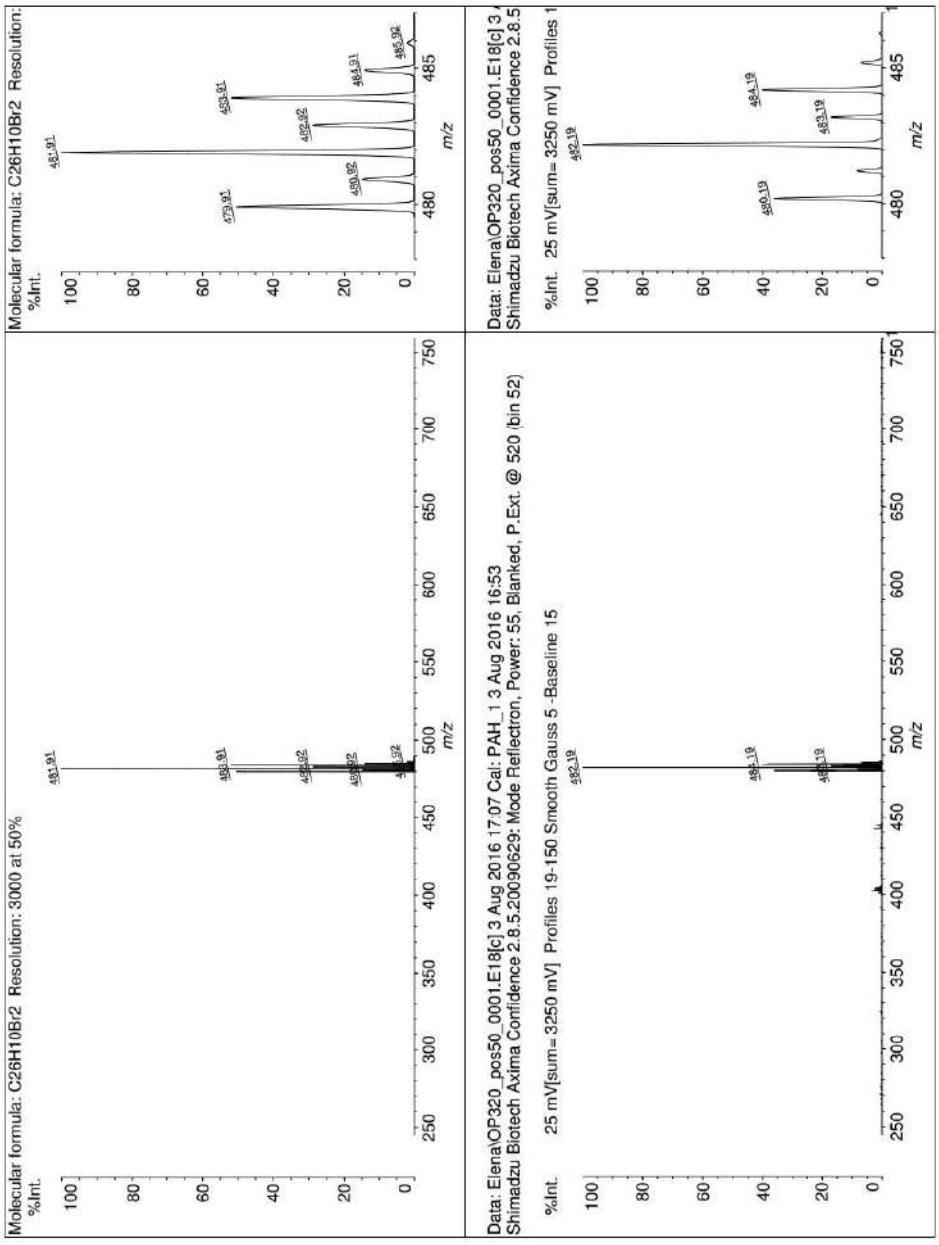

Figure S33. LDI-MS spectrum of 3,9-dibromodiindeno[*4,3,2,1-cdef:4',3',2',1'-lmno*]chrysene (**7a**) in positive mode.

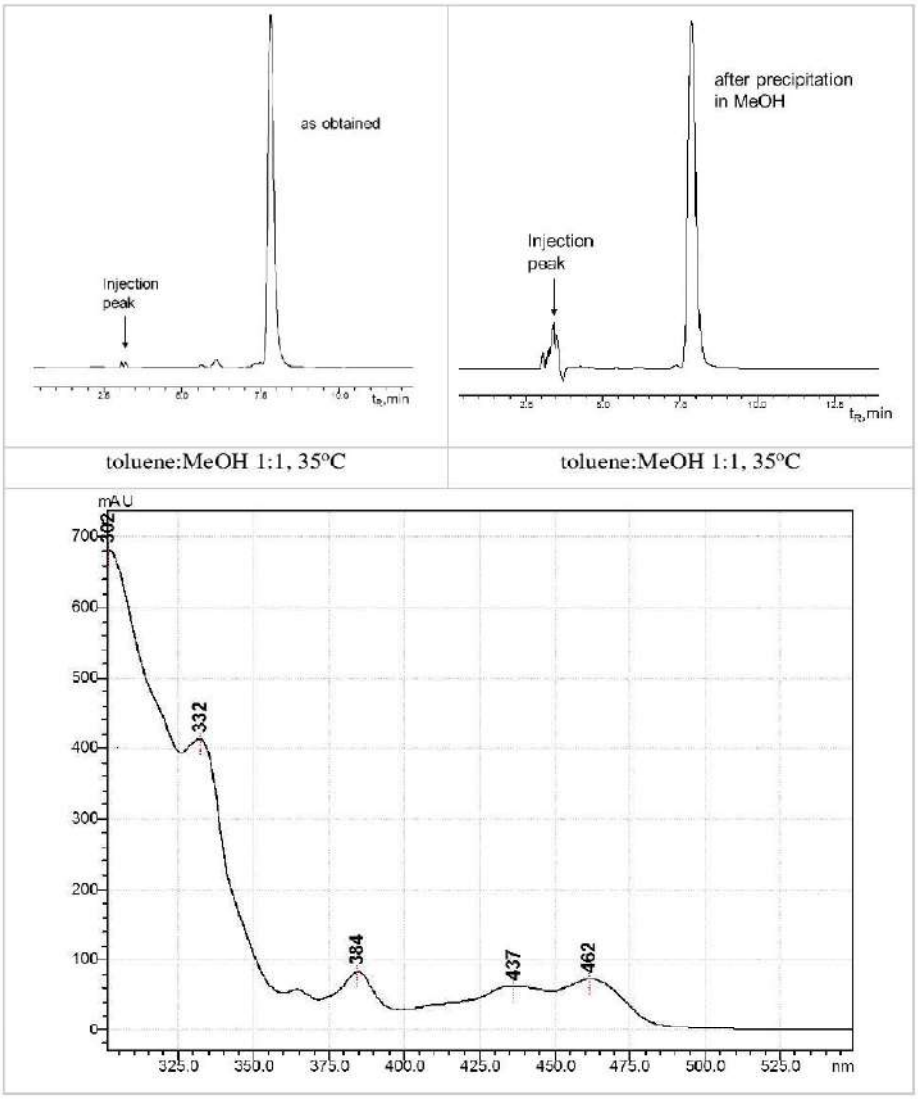

Figure S34. HPLC profile 3,9-dibromodiindeno[*4,3,2,1-cdef:4',3',2',1'-lmno*]chrysene (7a) as obtained after reaction (240°C, 1h, *o*-DCB) and precipitated in MeOH, detected at 320 nm (5PYE column, toluene:MeOH as eluent, 1.0 ml/min). UV-Vis spectrum of 3,9-dibromodiindeno[*4,3,2,1-cdef:4',3',2',1'-lmno*]chrysene (**7a**) in toluene:MeOH 1:1.

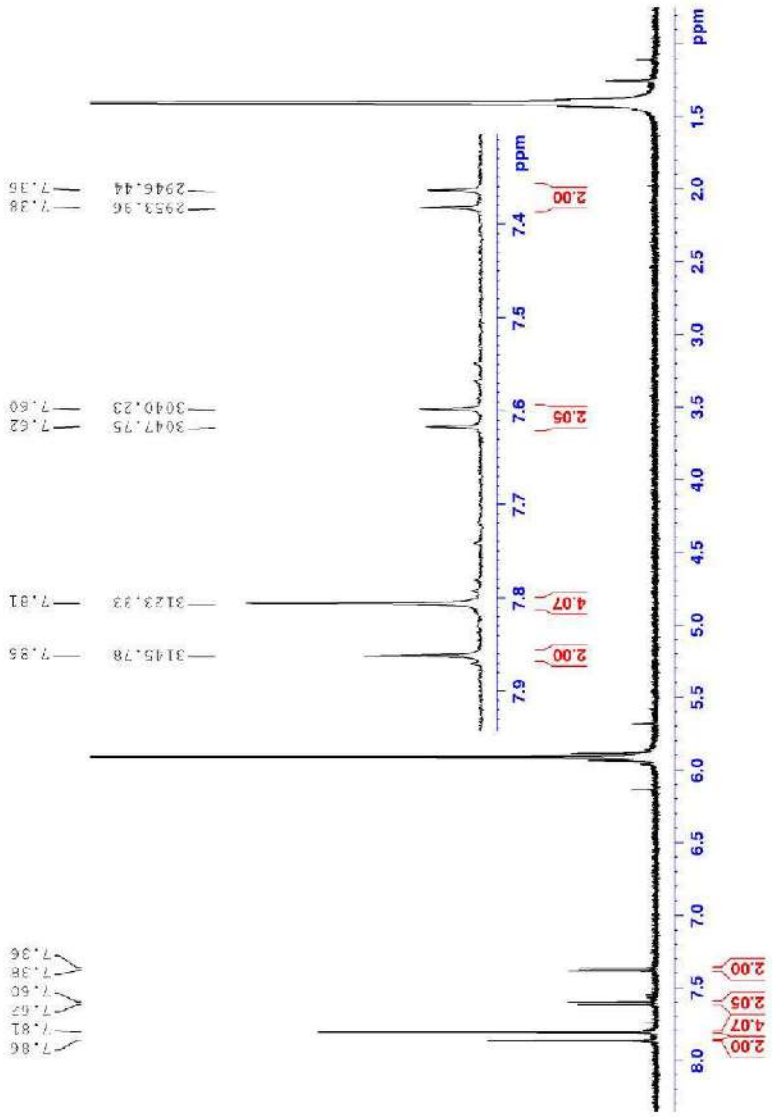

Figure S35. ^{1}H NMR (400 MHz, $C_2D_2Cl_4$, 353K) spectrum of 3,9-dichlorodiindeno[*4,3,2,1-cdef:4',3',2',1'-lmno*]chrysene (**7b**).

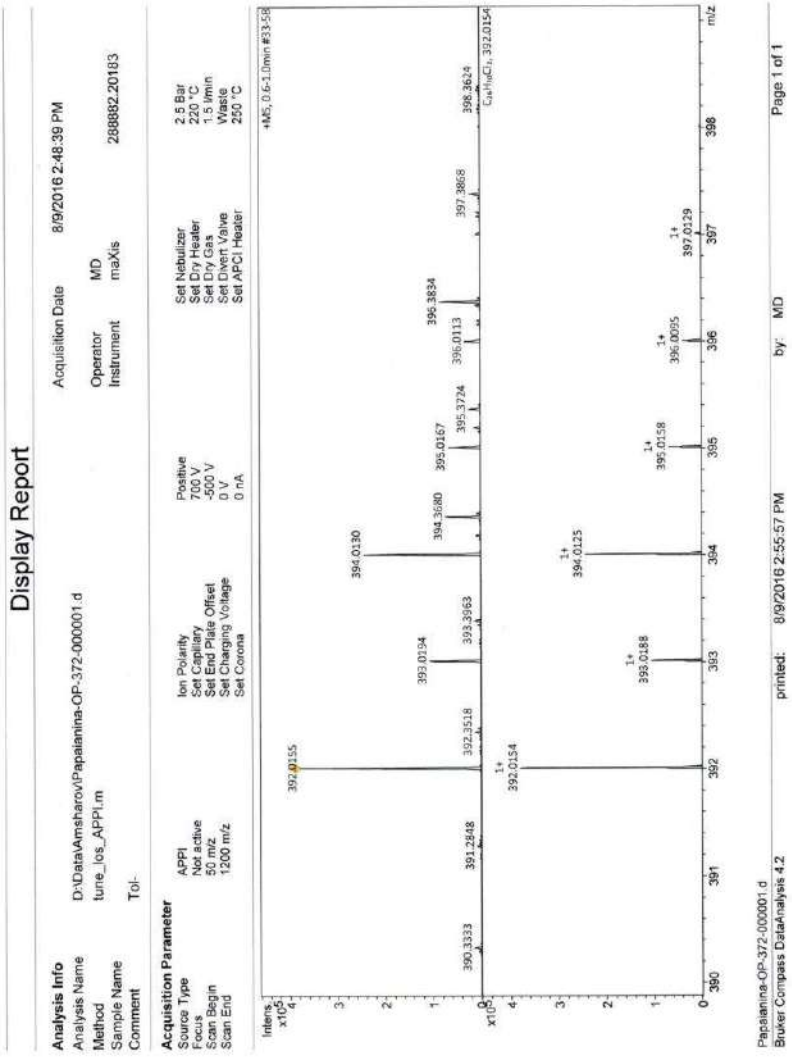

Figure S36. APPI-MS spectrum of 3,9-dichlorodiindeno[*4,3,2,1-cdef:4',3',2',1'-lmno*]chrysene (**7b**).

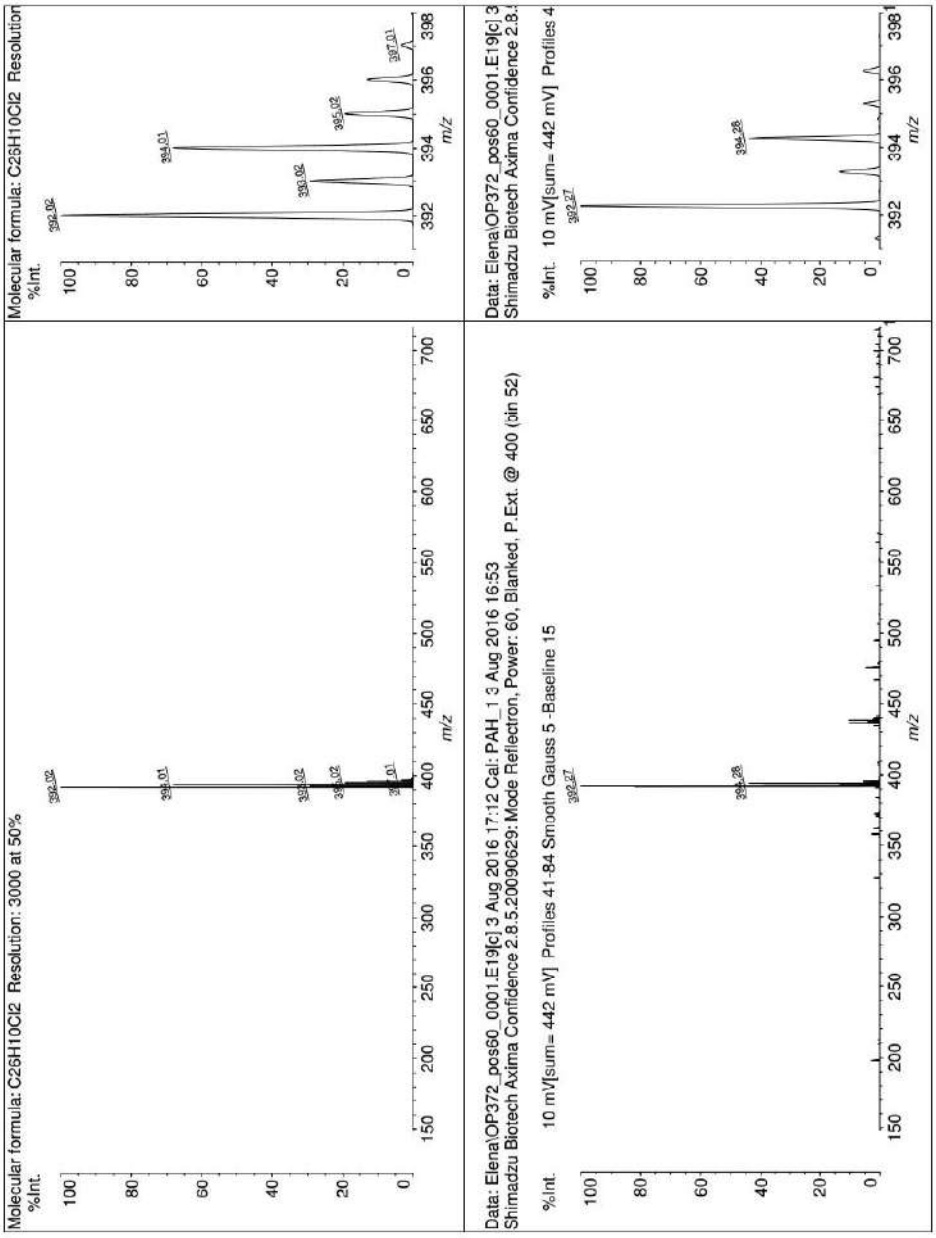

Figure S37. LDI-MS spectrum of 3,9-dichlorodiindeno[*4,3,2,1-cdef:4',3',2',1'-lmno*]chrysene (**7b**) in positive mode.

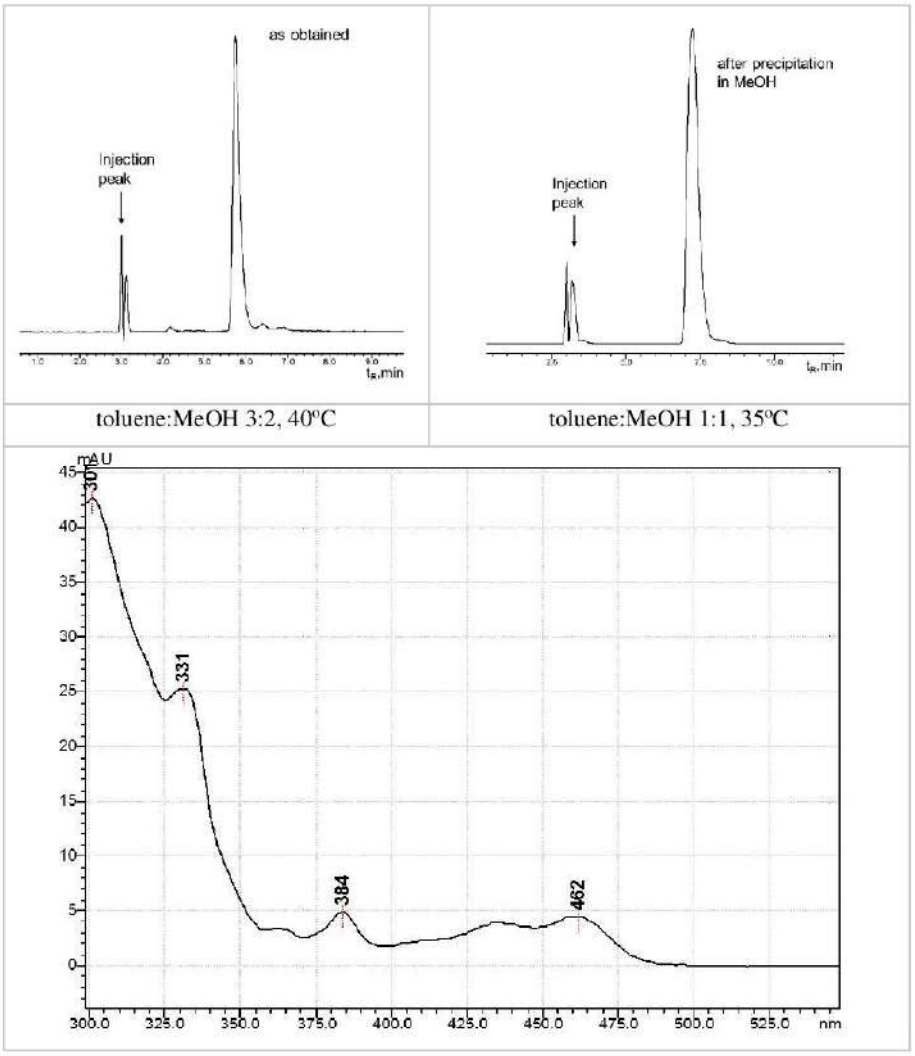

Figure S38. HPLC profile 3,9-dichlorodiindeno[*4,3,2,1-cdef:4',3',2',1'-lmno*]chrysene (**7b**) as obtained after reaction (220°C, 0.5h, *o*-DCB) and precipitated in MeOH, detected at 320 nm (5PYE column, toluene:MeOH as eluent, 1.0 ml/min). UV-Vis spectrum of 3,9-dichlorodiindeno[*4,3,2,1-cdef:4',3',2',1'-lmno*]chrysene (**7b**) in toluene:MeOH 1:1.

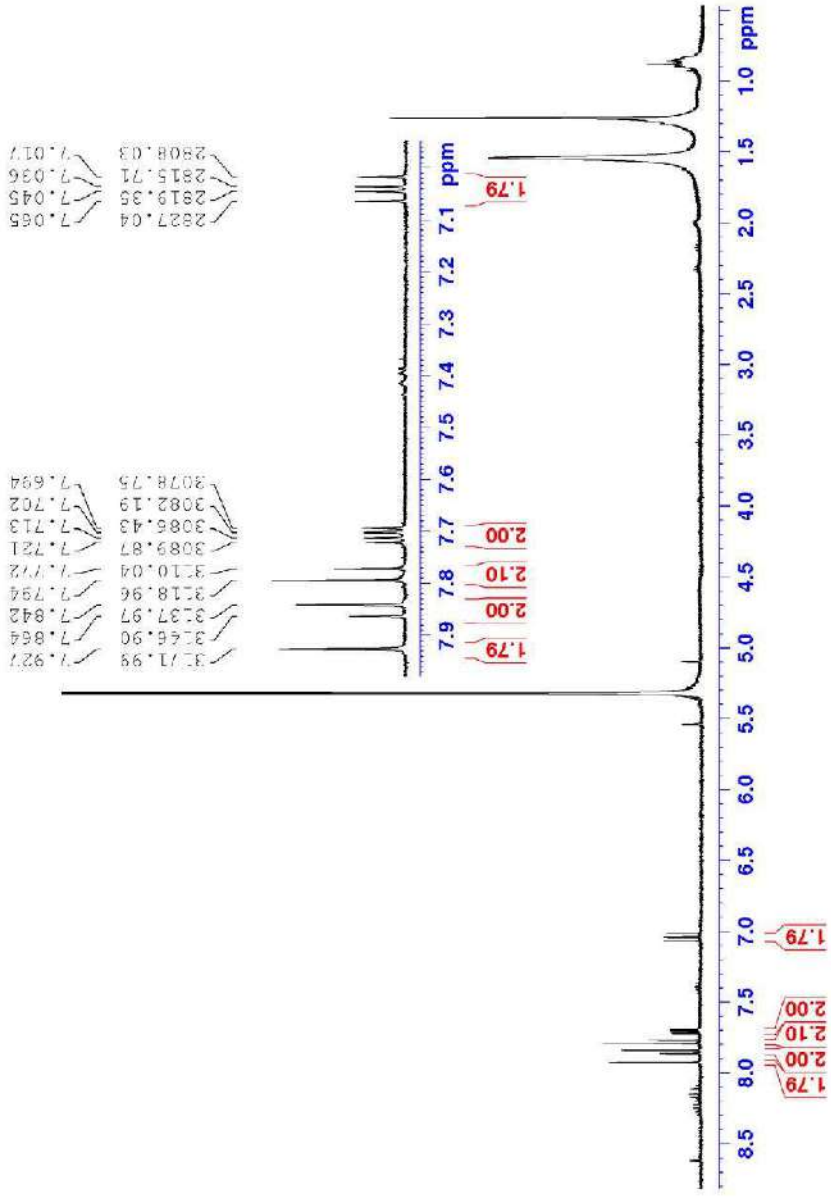

Figure S39. ^{1}H NMR (400 MHz, $C_2D_2Cl_4$, 293K) spectrum of 3,9-difluorodiindeno[*4,3,2,1-cdef:4',3',2',1'-lm*no]chrysene (**7c**).

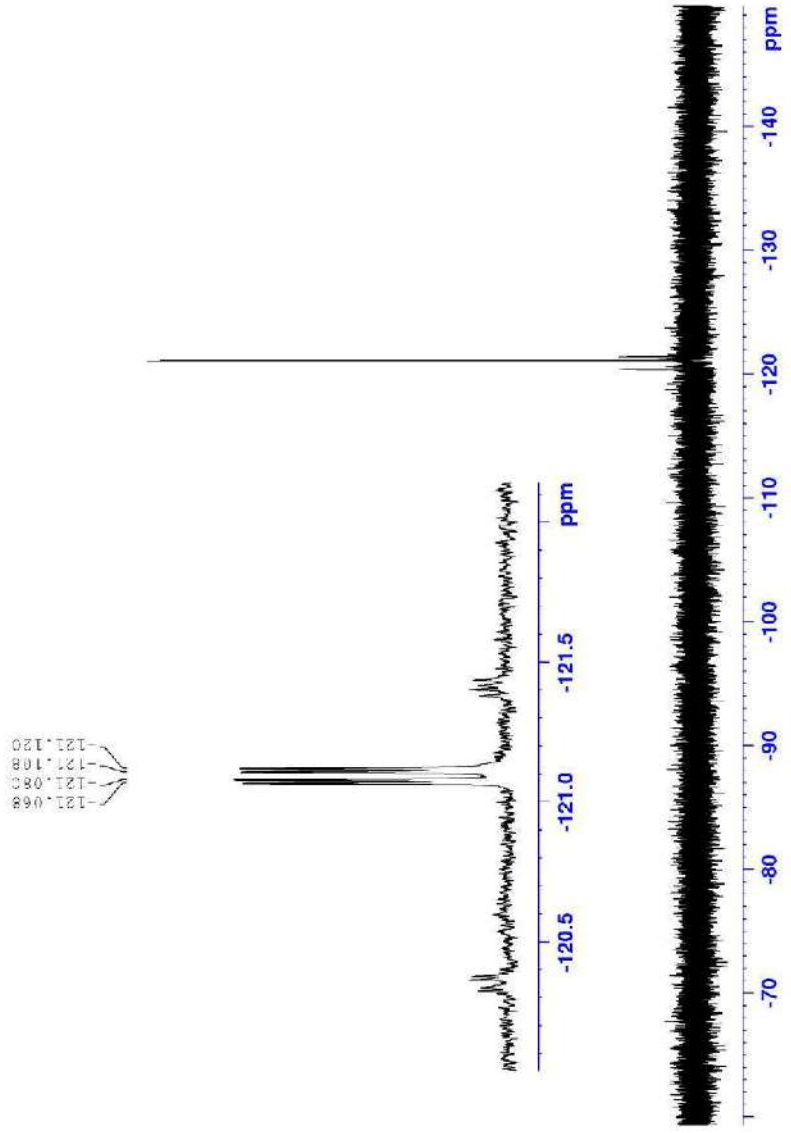

Figure S40. ^{19}F NMR (282 MHz, $C_2D_2Cl_4$, 293K) spectrum 3,9-difluorodiindeno[*4,3,2,1-cdef:4',3',2',1'-lm*no]chrysene (**7c**).

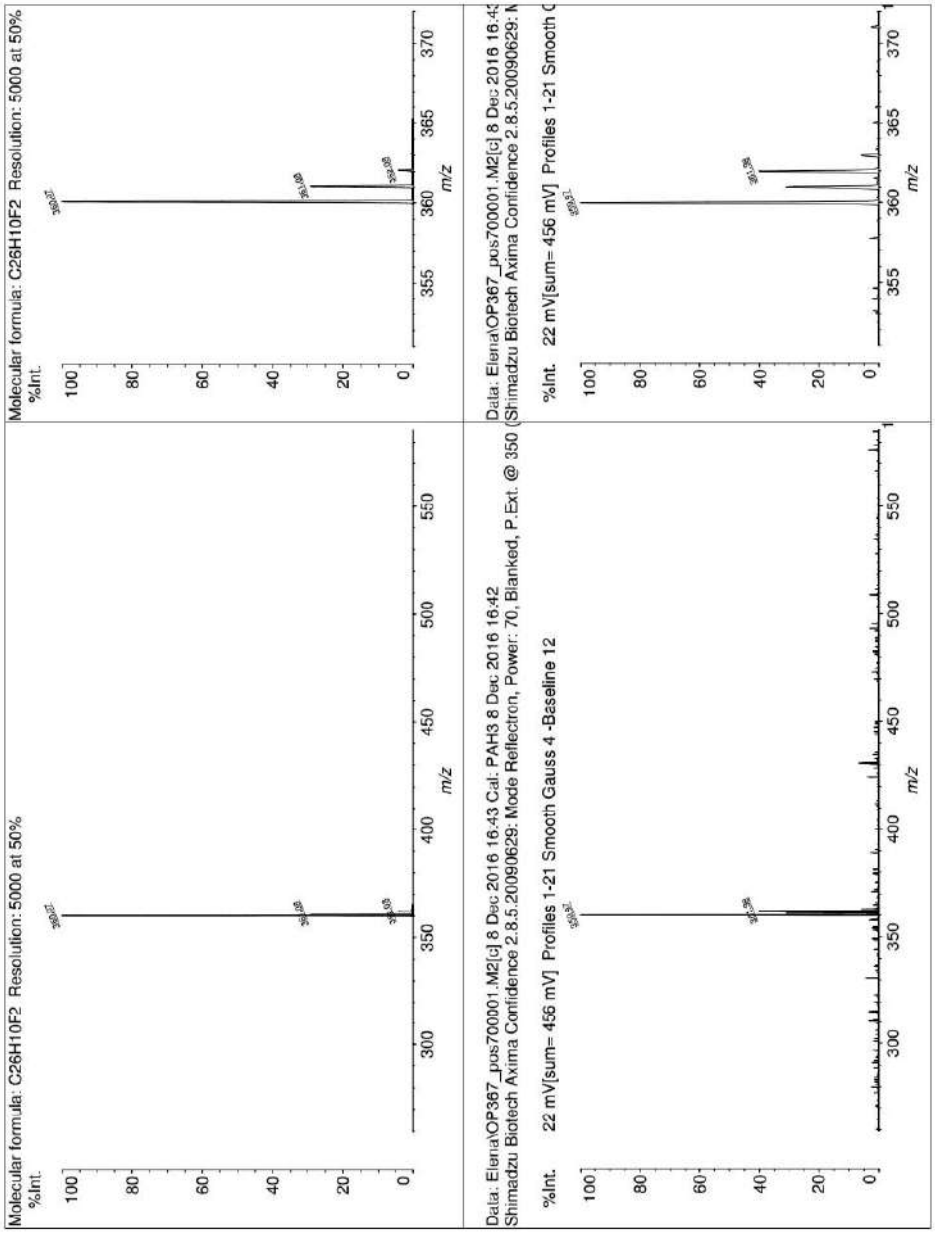

Figure S41. LDI-MS spectrum of 3,9-difluorodiindeno[*4,3,2,1-cdef:4',3',2',1'-lmno*]chrysene (**7c**) in positive mode.

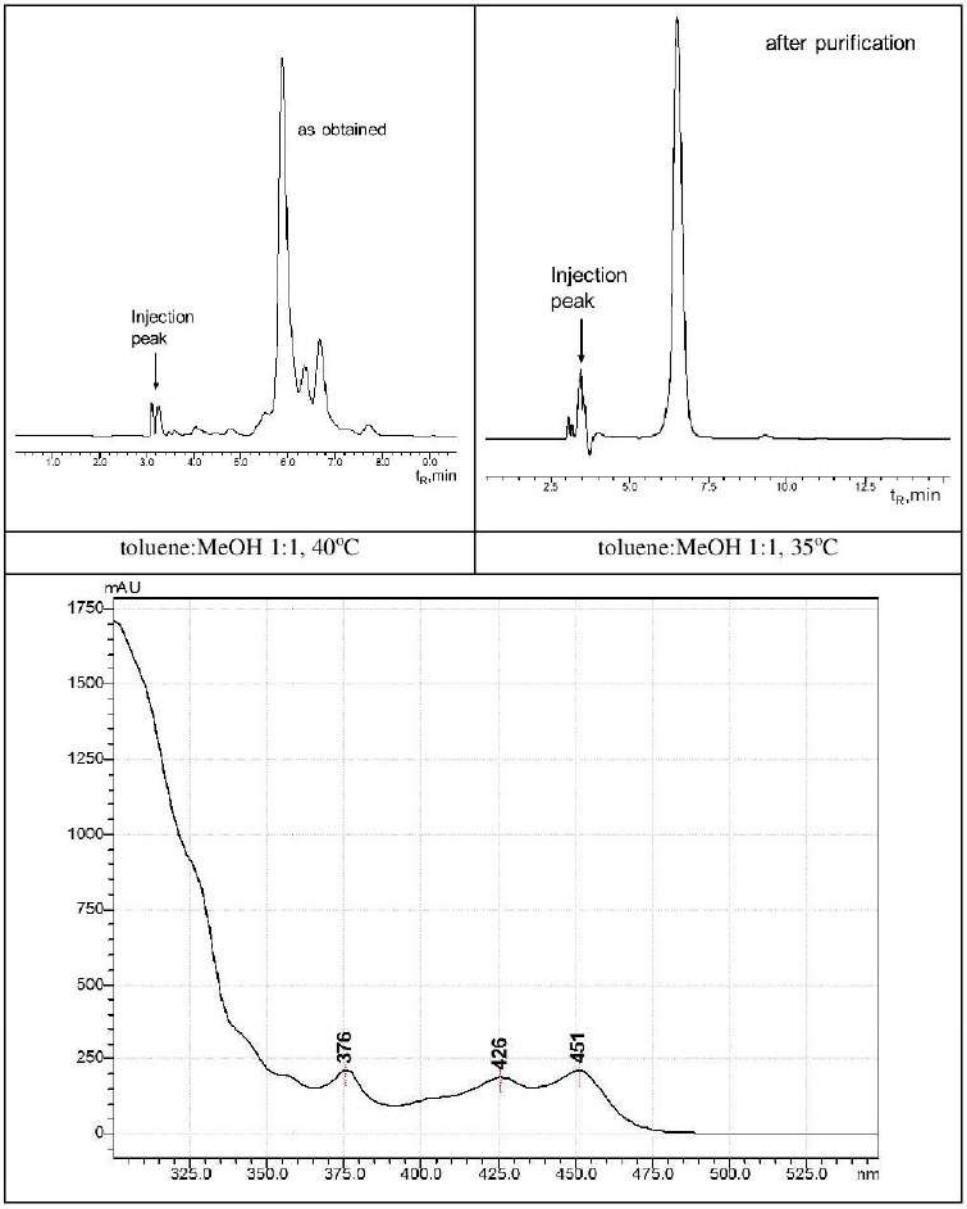

Figure S42. HPLC profile 3,9-difluorodiindeno[*4,3,2,1-cdef:4',3',2',1'-lmno*]chrysene (**7c**) as obtained after reaction (230ºC, 1h, *o*-DCB) and purified by HPLC, detected at 320 nm (5PYE column, toluene:MeOH as eluent, 1.0 ml/min). UV-Vis spectrum of 3,9-difluorodiindeno[*4,3,2,1-cdef:4',3',2',1'-lmno*]chrysene (**7c**) in toluene:MeOH 1:1.

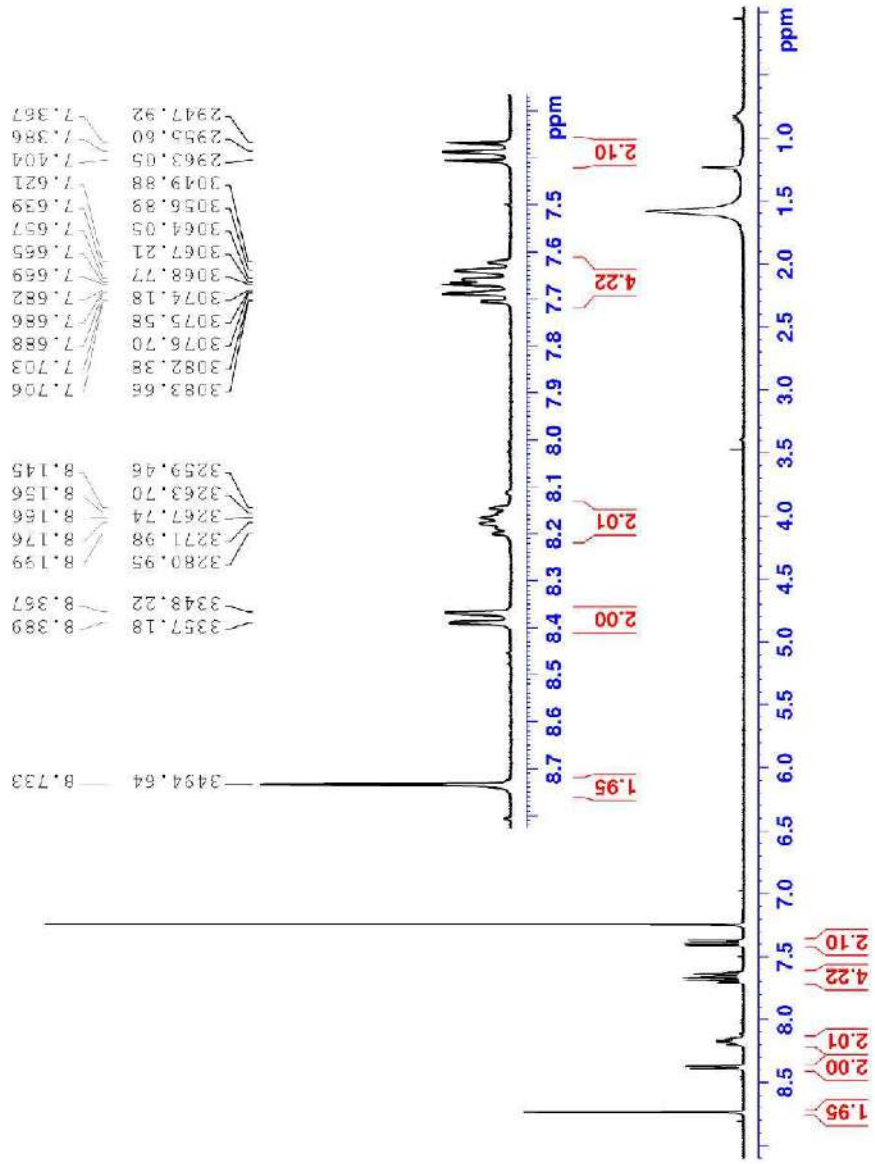

Figure S43. ^{1}H NMR (400 MHz, $CDCl_3$, 293K) spectrum 5,8-dibromo-13,16-difluorobenzo[*s*]picene (**3d**).

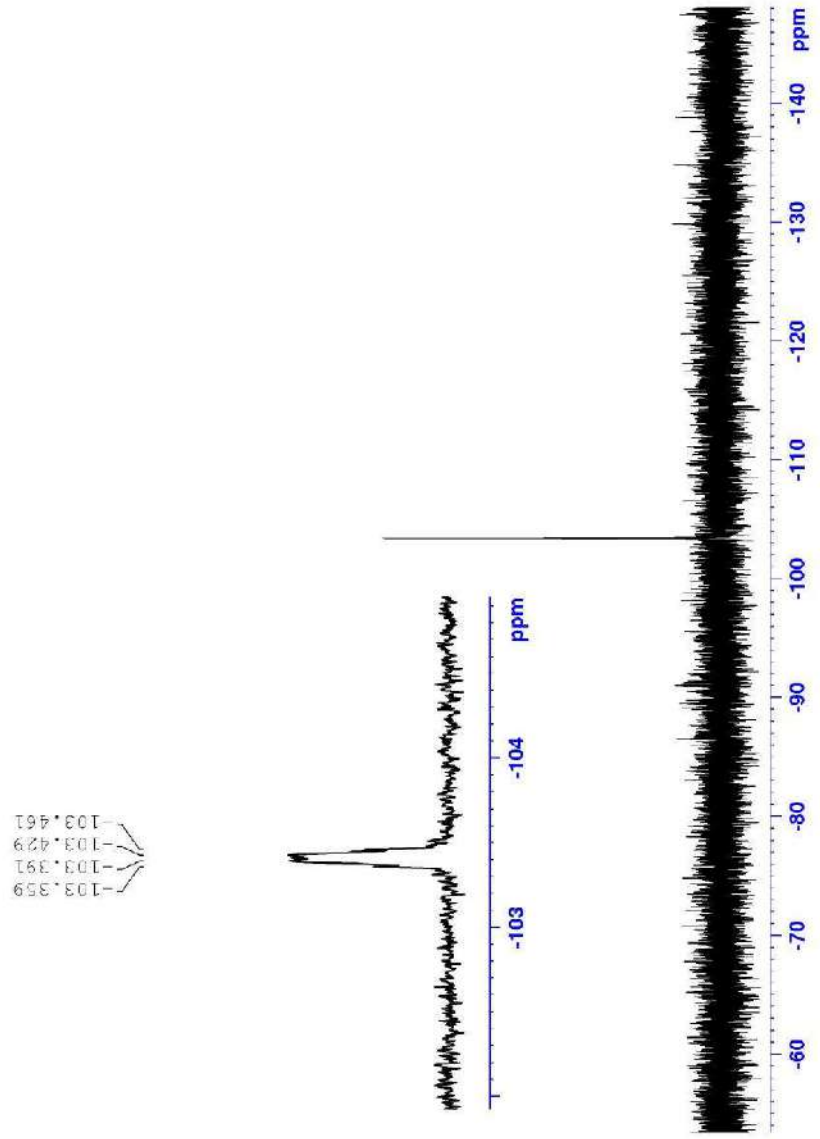

Figure S44. ^{19}F NMR (282 MHz, $CDCl_3$, 293K) spectrum 5,8-dibromo-13,16-difluorobenzo[*s*]picene (**3d**).

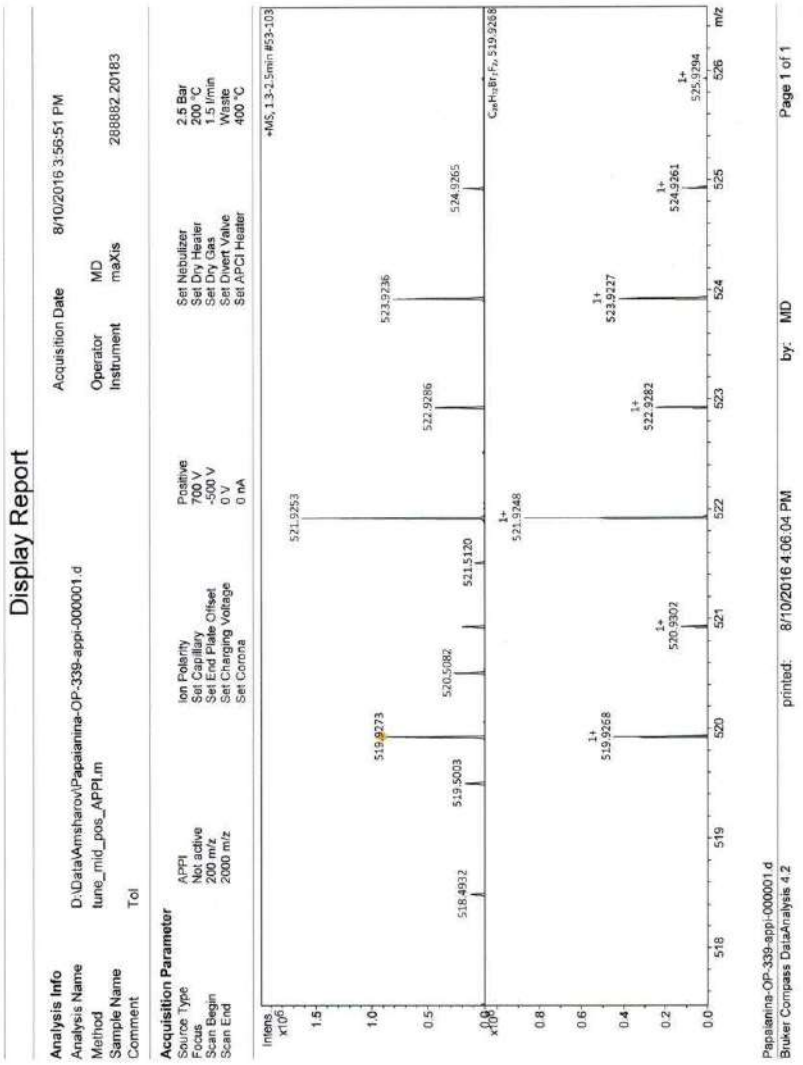

Figure S45. APPI-MS spectrum of 5,8-dibromo-13,16-difluorobenzo[*s*]picene (**3d**).

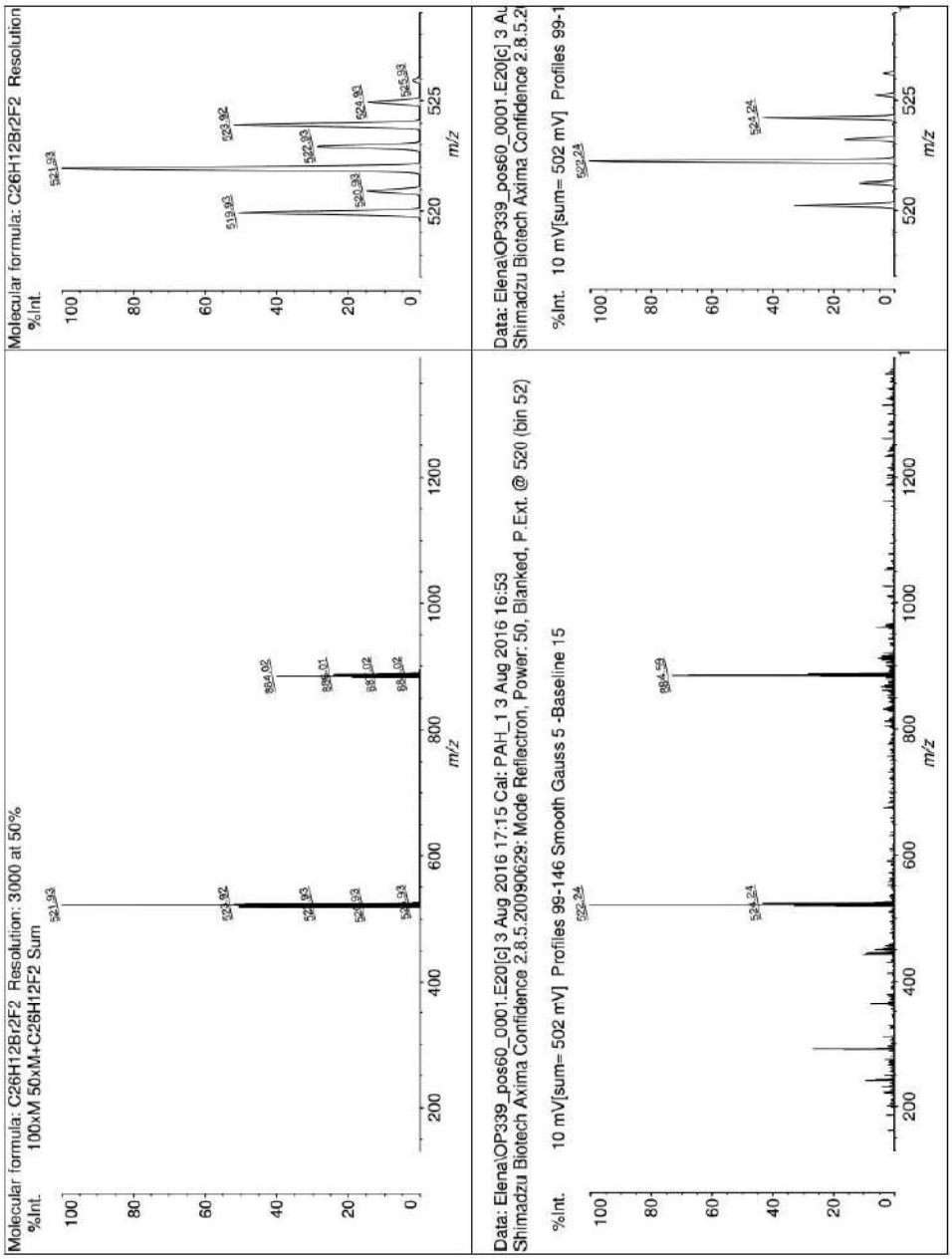

Figure S46. LDI-MS spectrum of 5,8-dibromo-13,16-difluorobenzo[*s*]picene (**3d**) in positive mode.

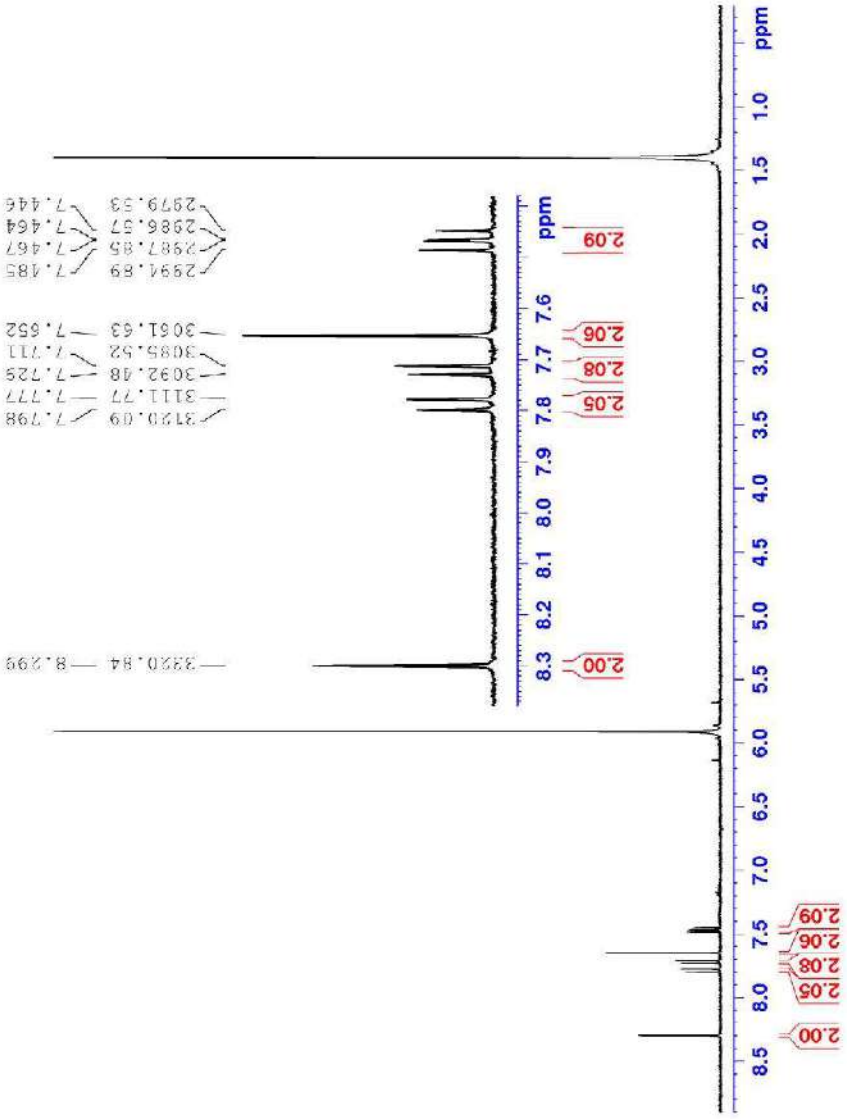

Figure S47. ^{1}H NMR (400 MHz, C2D2Cl$_4$, 353K) spectrum of 9,12-dibromo-*as*-indaceno[*3,2,1,8,7,6-pqrstuv*]picene (**4d**).

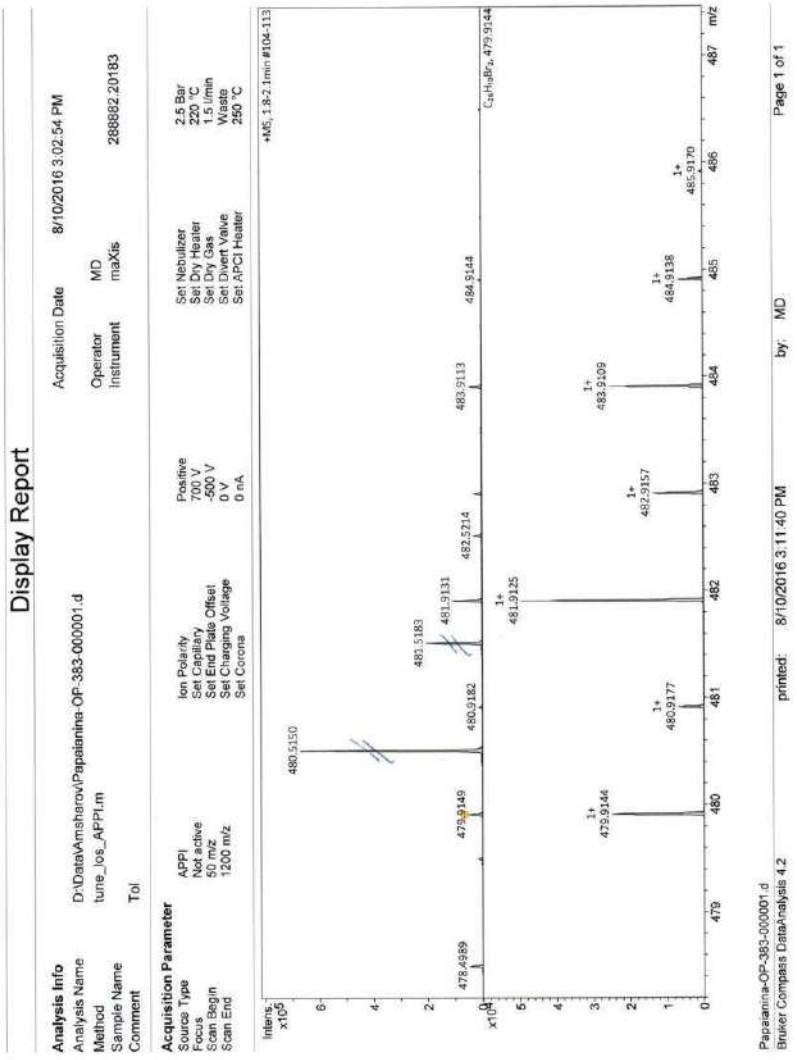

Figure S48. APPI-MS spectrum of 9,12-dibromo-*as*-indaceno[*3,2,1,8,7,6-pqrstuv*]picene (**4d**).

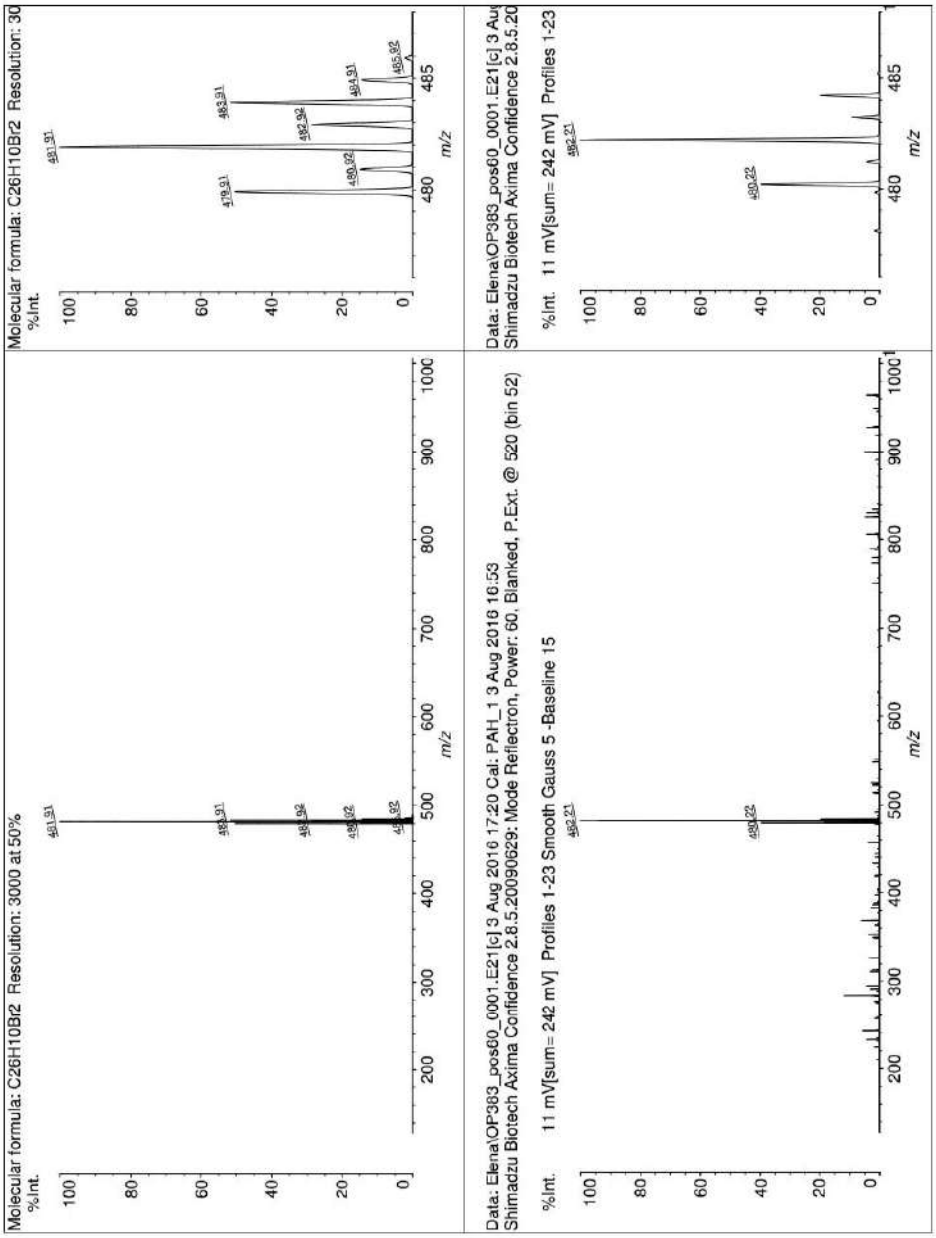

Figure S49. LDI-MS spectrum of 9,12-dibromo-*as*-indaceno[*3,2,1,8,7,6-pqrstuv*]picene (**4d**) in positive mode.

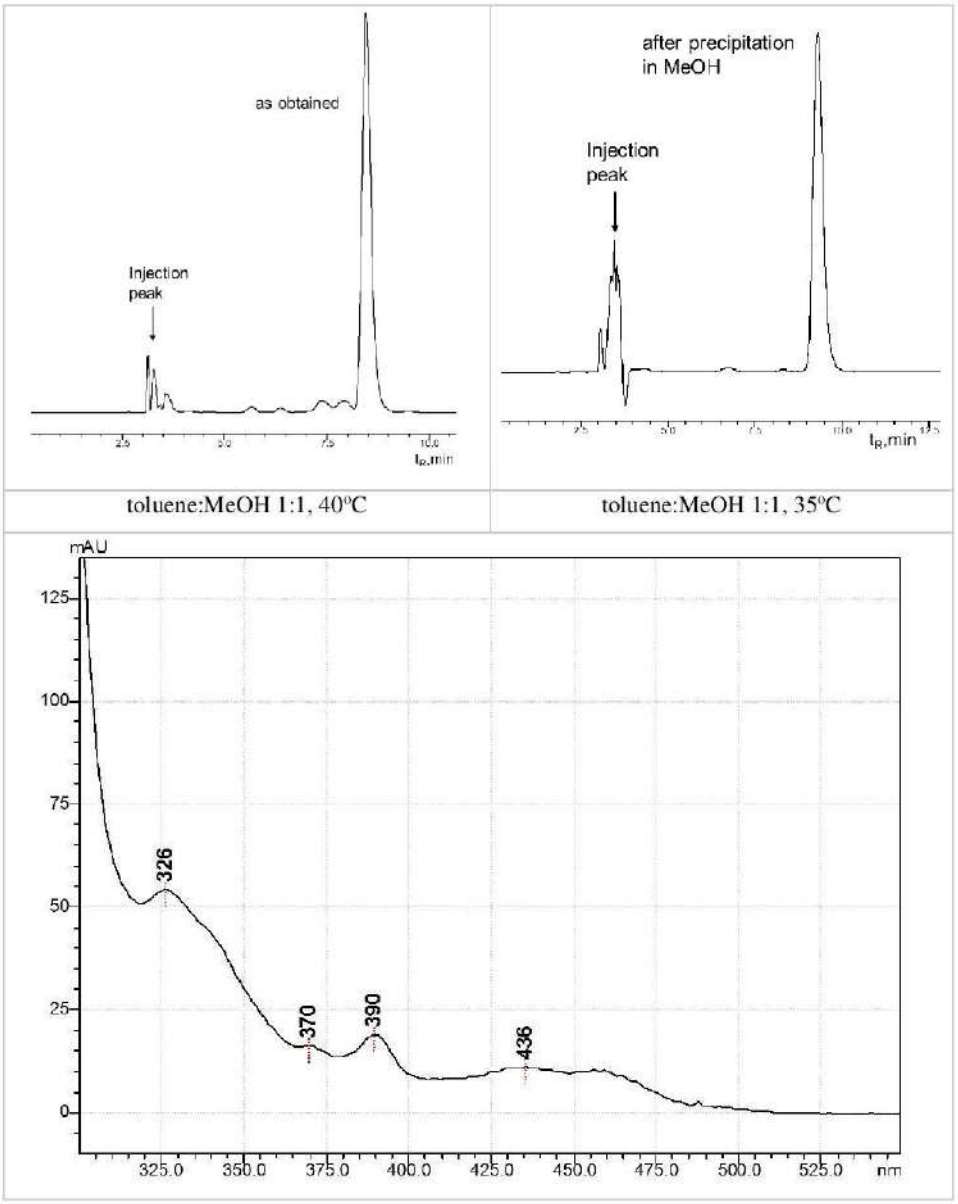

Figure S50. HPLC profile 9,12-dibromo-*as*-indaceno[*3,2,1,8,7,6-pqrstuv*]picene (**4d**) as obtained after reaction (220°C, 0.5h, *o*-DCB) and precipitated in MeOH, detected at 320 nm (5PYE column, toluene:MeOH as eluent, 1.0 ml/min). UV-Vis spectrum of 9,12-dibromo-*as*-indaceno[*3,2,1,8,7,6-pqrstuv*]picene (**4d**) in toluene:MeOH 1:1.

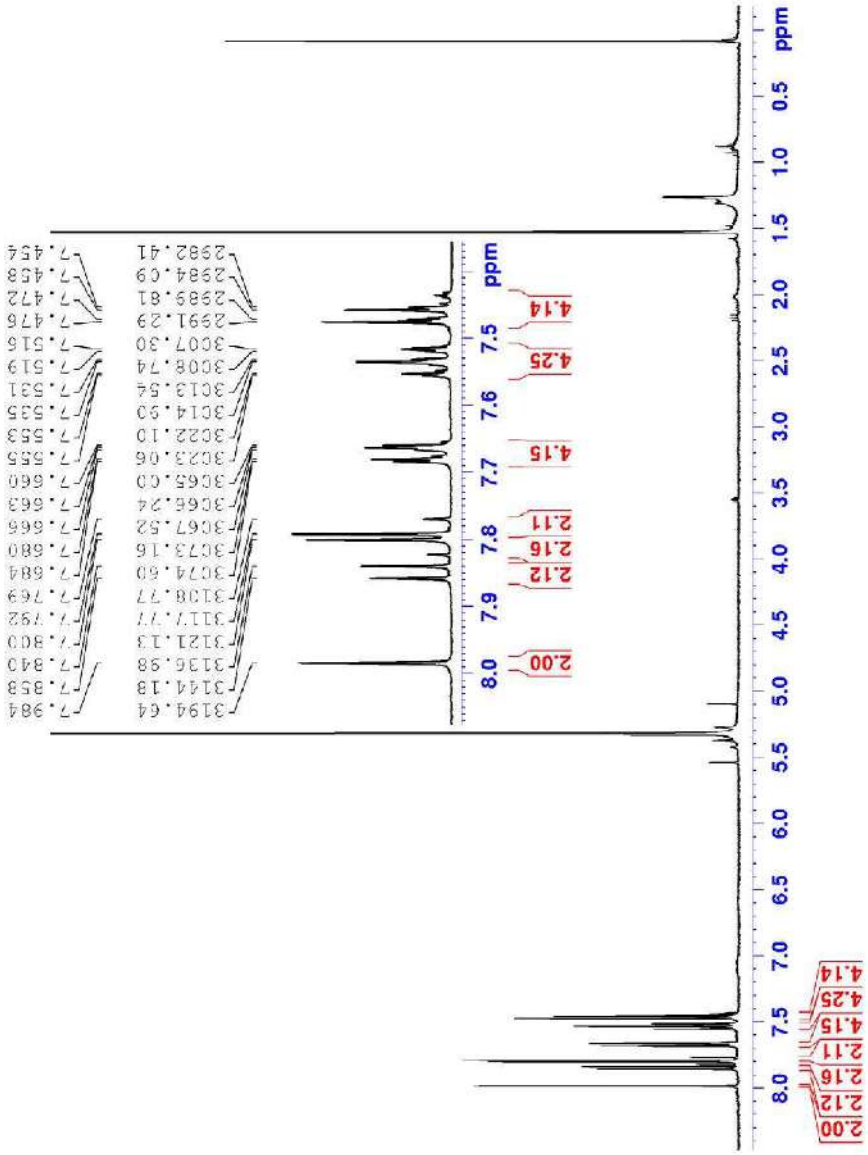

Figure S51. ^{1}H NMR (400 MHz, CD_2Cl_2, 293K) spectrum of 3,9-diphenyldiindeno[*4,3,2,1-cdef:4',3',2',1'-lmno*]chrysene (**8**).

3. X-Ray Crystallographic Data

Compound	**4d**	**8**
Empirical formula	$C_{26}H_{10}Br_2$	$C_{38}H_{20}$
Formula weight	482.16	476.54
Temperature (K)	153	100
Crystal system	orthorhombic	orthorhombic
Space group	*Pnma*	$P2_12_12_1$
a (Å)	16.9127(5)	7.4347(4)
b (Å)	25.0146(9)	14.0208(7)
c (Å)	3.90987(16)	21.5954(10)
α (°)	90	90
β (°)	90	90
γ (°)	90	90
Volume (Å^3)	1654.1(1)	2251.1(2)
Z	4	4
D_{ber} (g·cm^{-3})	1.936	1.406
μ (mm)	-1 6.274	0.080
F(000)	944.0	992
Crystal size (mm)	0.316 × 0.06 × 0.033	0.41×0.21×0.07
Radiation	CuK_a (λ = 1.54184 Å)	MoK_a (λ = 0.71073 Å)
2Θ (°)	$5.5 \leq 2\Theta \leq 61.5$	$3.4 \leq 2\Theta \leq 57.4$
Index ranges	$-18 \leq h \leq 18$,	$-10 \leq h \leq 10$,
	$-26 \leq k \leq 27$,	$-18 \leq k \leq 18$,
	$-4 \leq l \leq 3$	$-29 \leq l \leq 29$
Reflections collected	3178	100207
Independent reflections	1297	5800
Data/restraints/parameters	1297/0/127	5800/0/343
Goodness-of-fit on F2	1.044	1.044
Final R indexes	$R_1 = 0.0445$, $wR_2 = 0.1163$	$R_1 = 0.0423$, $wR_2 = 0.1018$
Largest peak/hole (e Å^{-3})	0.76/-0.52	0.48/-0.23
Measurement:	SuperNova, Dual, Atlas	APEX 3 (Bruker AXS, 2016)
Data reduction		SAINT (Bruker AXS, 2009)
Absorption correction:	SADABS 2014	SADABS 2014/5 (Bruker AXS, 2014)
Structure solution:	SHELXS-2014	SHELXTL NT 6.12 (Bruker AXS, 2002)
Refinement	SHELXS-2014	SHELXTL 2014/6 (Sheldrick, 2008)

Table S1. Crystal data and structure refinement details for compounds **4d** and **8**.

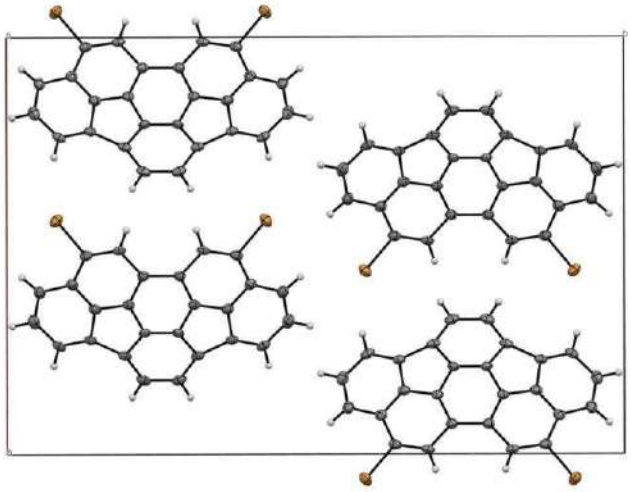

Figure S52. ORTEP projection of the crystal structure of dibromoindacenopicene **4d** onto the [001] plane. Thermal ellipsoids are set at the 50% probability level.

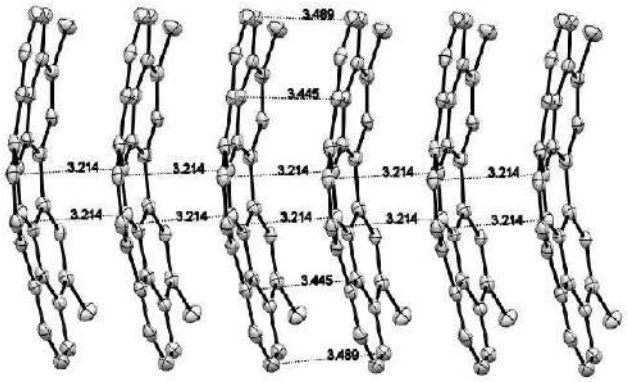

Figure S53. ORTEP projection of the crystal structure of **4d** showing extended π- π columnar staking along *a* axis with short intermolecular C···C contacts. Thermal ellipsoids are set at the 50% probability level. Hydrogen atoms are omitted for clarity.

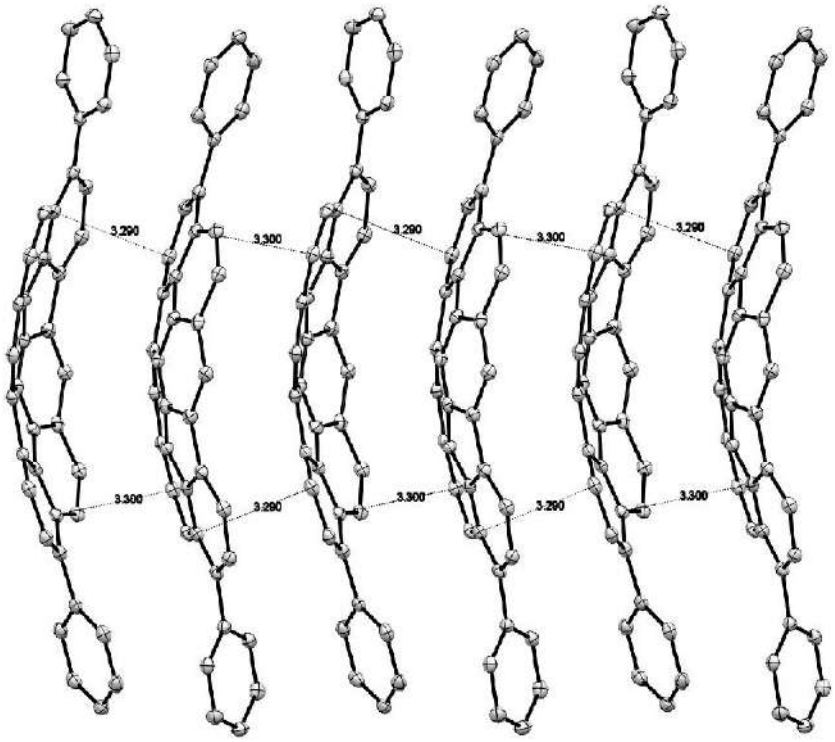

Figure S54. ORTEP projection of the crystal structure of **8** showing extended π- π columnar staking along a axis with short intermolecular C···C contacts. Thermal ellipsoids are set at the 50% probability level. Hydrogen atoms are omitted for clarity.

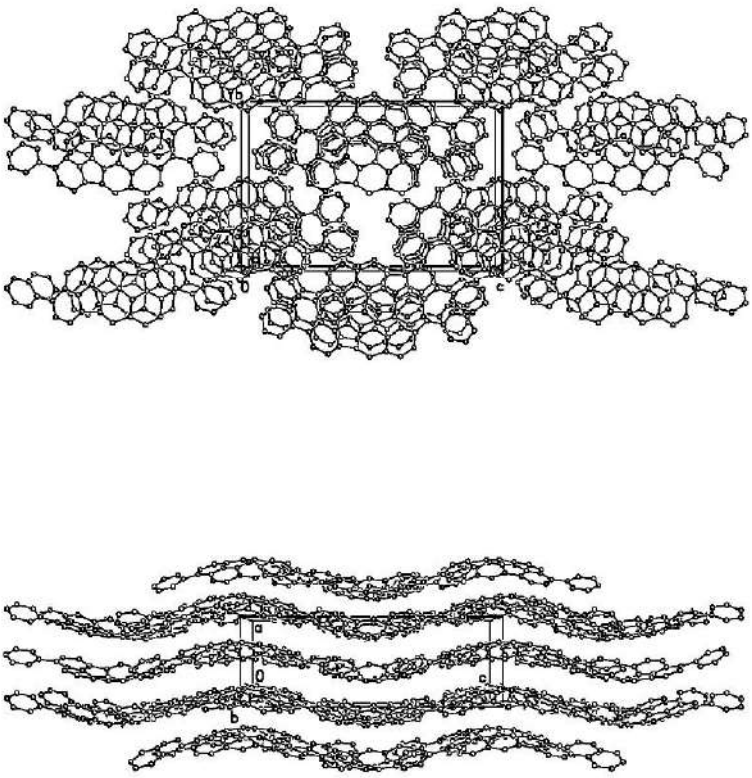

Figure S55. Projections of crystal structure of compound **8** along *a* axis (top) and *b* axis (bottom). Hydrogen atoms are omitted for clarity.

4. Quantum Chemical calculations

The calculated bond lengths and bond orders for pristine diindenochrysene and indacenopicene (**4a**) are summarized in Table S2. Interpentagonal C–C bond **3–3'** and pentagon bond **2–6** were found the most shorter double bond (1.36 Å, bond order of 1.36–1.37) and the most longer single bonds (1.50–1.51 Å, bond order of 1.03–1.04) in both bowls, respectively. The bond alternation is observed for peripheral and inner C–C bonds; C–C bonds having double-character are characterized by typical bond lengths of 1.36–1.41 Å and bond orders of 1.29–1.60, whereas single-character C–C bonds are lengthen to 1.40–1.52 Å and have bond orders of 1.03–1.32. Notably, that diindenochrysene bowl is larger curved in comparison with indacenopicene (bowls depths are 1.78 Å and 1.62 Å, correspondingly), evidencing larger steric strain of the former molecule. It is consistent with large relative formation energies of pristine and dibrominated diindenochrysene with respect to isomeric pristine and dibrominated indacenopicene (17 and 13 kJ mol^{-1}, respectively).

Table S2. Bond lengths and bond orders of diindeno[4,3,2,1-*cdef*:4',3',2',1'-*lmno*]chrysene (*a*) and *as*-indaceno[3,2,1,8,7,6-*pqrstuv*]picene (*b*).

Diindenochrysene			Indacenopicene			Indexation scheme
Bonds	**r(C–C)[a] / Å**	**Bond orders[b]**	**Bonds**	**r(C–C)[a] / Å**	**Bond orders[b]**	
pentagon-hexagon bonds						
2–3	1.440	1.15	2–3	1.414	1.23	
2–6	1.515	1.03	2–6	1.510	1.04	
3–4	1.396	1.17	3–4	1.415	1.13	
4–5	1.406	1.16	4–5	1.407	1.19	
5–6	1.435	1.21	5–6	1.439	1.04	
hexagon-hexagon bonds						
1–13'	1.459	1.17	1'–1	1.441	1.32	
1–2	1.399	1.51	1–2	1.407	1.42	
3–3'	1.361	1.37	3–3'	1.360	1.36	
4–13	1.401	1.32	4–13	1.403	1.38	
5–10	1.397	1.29	5–10	1.398	1.29	
6–7	1.387	1.46	6–7	1.386	1.47	
7–8	1.427	1.30	7–8	1.428	1.29	
8–9	1.394	1.52	8–9	1.392	1.53	
9–10	1.424	1.24	9–10	1.426	1.23	
10–11	1.448	1.16	10–11	1.442	1.18	
11–12	1.390	1.60	11–12	1.393	1.58	
12–13	1.447	1.16	12–13	1.440	1.21	
			13–13'	1.484	1.10	

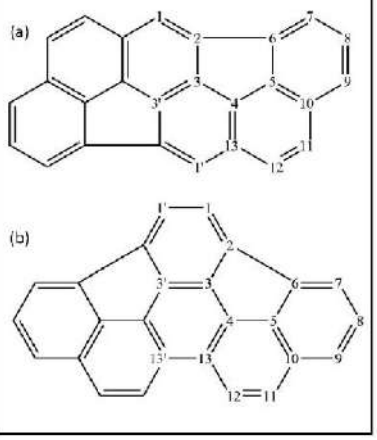

[a] PBE/TZ2P. [b] B3LYP5/Def2-TZVP//PBE/TZ2P

Electronic structural data obtained from DFT calculations as well as from electrochemical investigation and UV/Vis measurements are summarized in Table S2. One can see, halogenation of the bowls results in lowering of the HOMO and LUMO levels for 0.1–0.3 eV depending on number and nature halogen atoms. It is notable that pristine diindenochrysene and indacenopicene have same frontier MO levels which are intermediate between the corresponding levels of pyracylene and benzo[*ghi*]fluoranthene composing these molecules. Estimated adiabatic electron affinities (EA) values demonstrate same tendency. Large conjugated systems of diindenochrysene and indacenopicene derivatives favors in effective electron delocalization yielding slightly superior EA values than in case of pyracylene (1.5–1.6 eV), whereas EA value for benzo[*ghi*]fluoranthene is notable lower (ca 1.0 eV). Halogenation resulted in the stepwise growth of the EA values of the compounds by ca 0.1–0.2 eV per halogen atom.

The optical HOMO–LUMO energy gaps (E_G^{opt}) were estimated from the absorption edge of the UV-Vis spectra of the compounds (see Table 2). The E_G^{opt} values were ca. 2.6 eV and 2.4 eV for diindenochrysene and indacenopicene derivatives, respectively, demonstrating intermediating values between that for benzo[*ghi*]fluoranthene (2.9 eV and pyracylene (1.9 eV and, therefore, can be regarded as wide band gap semiconductors. The DFT calculation of the E_G values using PBE exchange-correlation functional [2] resulted in systematically underestimated values of 2.0–2.1 eV. This underestimation is known issue of the generalized gradient approximation (GGA) functionals including PBE, and often better estimation is achieved by using hybrid functionals, which mix some exact exchange with a GGA0 [12]. Application of hybrid functionals B3LYP [6,7] and TPSSh [8] for E_G estimation resulted in 3.3 and 2.8 eV for diindenochrysene as well as 3.2 and 2.7 eV (3.7 eV in case of PBE0 [13]) for indacenopicene, respectively. Evidently, tested hybrid functionals overestimated E_G values, but more reliable values were found in the case of TPSSh functional.

Table S3. Electronic properties of diindenochrysenes, indacenopicenes, and related polyenes.

Compound	DFT data[a] / eV					Experimental data[c] / eV			
	E_{HOMO}	E_{LUMO}	E_G	λ_i[b]	EA	E_{HOMO}^{EC}	E_{LUMO}^{EC}	E_G^{opt}	Ref[d]
pyracylene	–4.99	–3.50	1.49	0.25	1.47	–5.7	–3.4	1.9	[14,15,16]
benzo[*ghi*]fluoranthene	–5.56	–2.85	2.71	0.16	0.97	–5.9	–2.7	2.9	[10,16]
Indacenopicene derivatives									
indacenopicene **4a**	–5.30 [–5.77] {–5.53}	–3.20 [–2.53] {–2.79}	2.10 [3.24] {2.74}	0.15	1.56	–5.8	–3.0	2.43	[10,13]
4b	–5.38	–3.34	2.04	0.15	1.73	–	–	2.40	t.w.
4c	–5.43	–3.33	2.10	0.16	1.72	–	–	2.43	t.w.
4d	–5.56	–3.48	2.08	0.16	1.90	–	–	2.42	t.w.
Diindenochrysene derivatives									
diindenochrysene	–5.32 [–5.78] {–5.54}	–3.16 [–2.48] {–2.74}	2.16 [3.30] {2.80}	0.17	1.52	–	–	–	–
7a	–5.47	–3.44	2.03	0.17	1.87	–5.9	–3.1	2.56	t.w.
7b	–5.47	–3.43	2.04	0.17	1.84	–	–	2.58	t.w.
7c	–5.39	–3.31	2.08	0.19	1.67	–	–	–	–

[a]PBE/TZ2P; B3LYP/Def2-TZVP//PBE/TZ2P values are given in square brackets, TPSSh/Def2-TZVP//PBE/TZ2P values are given in curly braces. Adiabatic electron affinities values are given. [c]The internal reorganization energy of the electron transfer. [c]The electrochemical (EC) HOMO and LUMO energies were calculated using the following equations: $E_{HOMO}^{EC} = -e(E_{ox}^{onset} + 4.8)$ eV and $E_{LUMO}^{EC} = -e(E_{red}^{onset} + 4.8)$ eV, where the reference potential of the $Fc^{+/0}$ couple with respect to vacuum level is –4.8 eV [17,18]; the optical gap, $E_G^{opt} = 1240/\lambda_{onset}$ eV. [d]t.w – this work.

The HOMO and LUMO levels of the **7a** were estimated from onsets of the reduction and oxidation potentials (see Table S2). The measured levels shown same tendency with theoretically predicted ones. One can see, that the levels of the frontier molecular orbitals are dipper for 0.1 eV in comparison with that for indacenopicene. Evidently, the presence of the two bromine atoms in the compound **7a** is the main reason of this slight growth of the electron acceptor properties of the molecule.

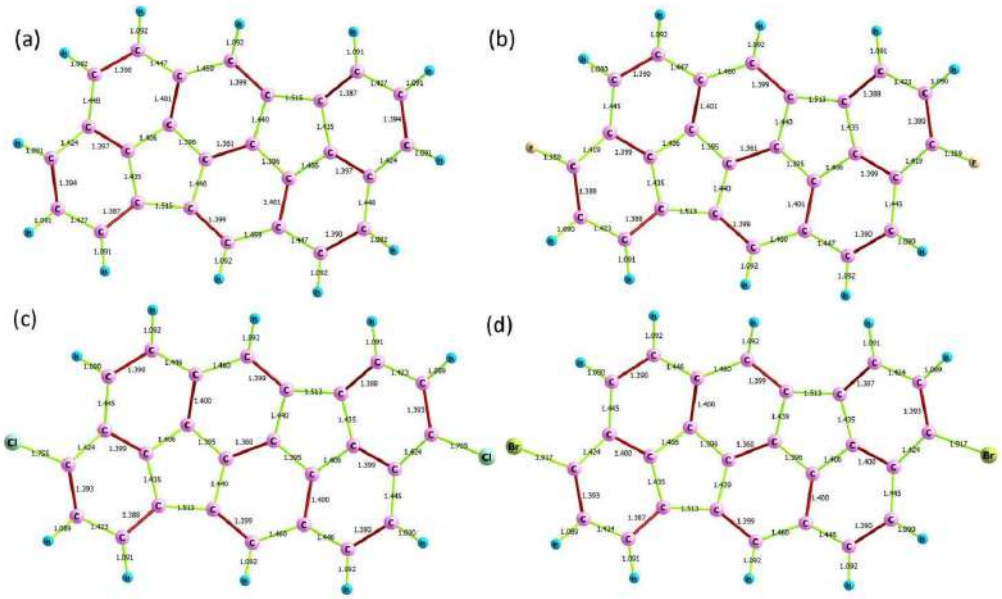

Figure S56. DFT calculated molecular geometries and bond lengths of pristine diindenochrysene (*a*) and its halogenated derivatrives **7c**, **7b**, and **7a** (*b–c*)

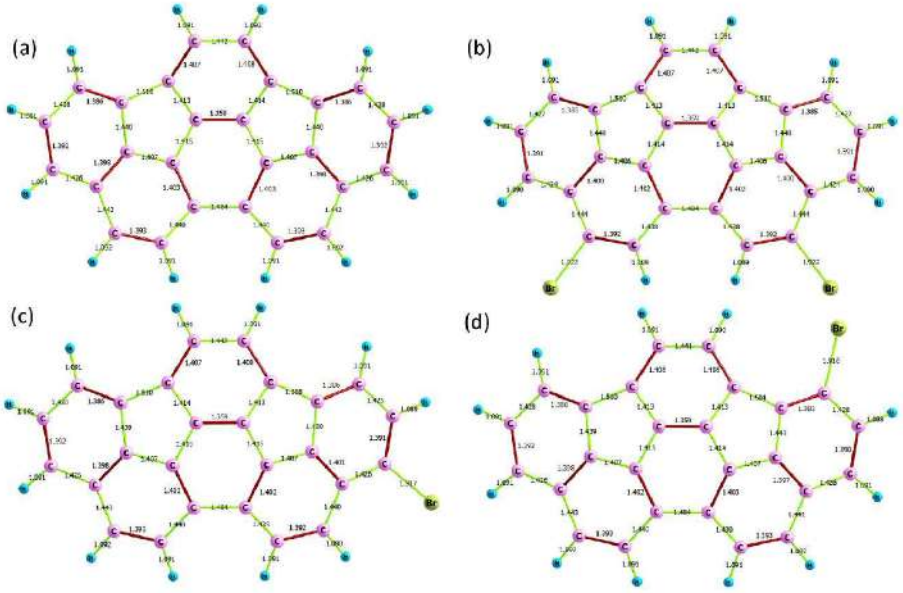

Figure S57. DFT calculated molecular geometries and bond lengths of pristine indacenopicene **4a** (*a*) and its halogenated derivatives **4d, 4c**, and **4b** (*b–c*)

Table S4. Bond lengths and bond orders of diindeno[4,3,2,1-*cdef*:4',3',2',1'-*lmno*]chrysene

Bonds	r(C–C)[a] / Å	Bond orders[b]		
		PBE	B3LYP	TPSSh
1–13'	1.459	0.95	1.17	1.13
1–2	1.399	1.24	1.51	1.47
2–3	1.440	1.31	1.15	1.18
2–6	1.515	0.77	1.03	1.04
3–3'	1.361	1.20	1.37	1.32
3–4	1.396	1.20	1.17	1.16
4–5	1.406	1.15	1.16	1.14
4–13	1.401	1.53	1.32	1.29
5–6	1.435	1.42	1.21	1.20
5–10	1.397	1.57	1.29	1.28
6–7	1.387	1.38	1.46	1.44
7–8	1.427	1.19	1.30	1.33
8–9	1.394	1.37	1.52	1.53
9–10	1.424	1.08	1.24	1.20
10–11	1.448	1.06	1.16	1.14
11–12	1.390	1.38	1.60	1.62
12–13	1.447	0.98	1.16	1.13

[a] PBE/TZ2P. [b] PBE/TZ2P as well as B3LYP5/Def2-TZVP and TPSSh/Def2-TZVP data for the molecular geometry optimized at the PBE/TZ2P level.

Table S5. Bond lengths and bond orders of *as*-indaceno[3,2,1,8,7,6-*pqrstuv*]picene

Bonds	r(C–C)[a] / Å	Bond orders[b]		
		PBE	B3LYP	TPSSh
1'–1	1.441	1.18	1.32	1.32
1–2	1.407	1.32	1.42	1.39
2–3	1.414	1.46	1.23	1.25
2–6	1.510	0.66	1.04	1.02
3–3'	1.360	1.03	1.36	1.32
3–4	1.415	1.20	1.13	1.13
4–5	1.407	1.19	1.19	1.17
4–13	1.403	1.43	1.38	1.40
5–6	1.439	1.41	1.04	1.20
5–10	1.398	1.60	1.29	1.23
6–7	1.386	1.37	1.47	1.42
7–8	1.428	1.17	1.29	1.28
8–9	1.392	1.37	1.53	1.55
9–10	1.426	1.05	1.23	1.25
10–11	1.442	1.06	1.18	1.16
11–12	1.393	1.34	1.58	1.58
12–13	1.440	1.05	1.21	1.18
13–13'	1.484	0.71	1.10	1.07

[a] PBE/TZ2P. [b] PBE/TZ2P as well as B3LYP5/Def2-TZVP and TPSSh/Def2-TZVP data for the molecular geometry optimized at the PBE/TZ2P level.

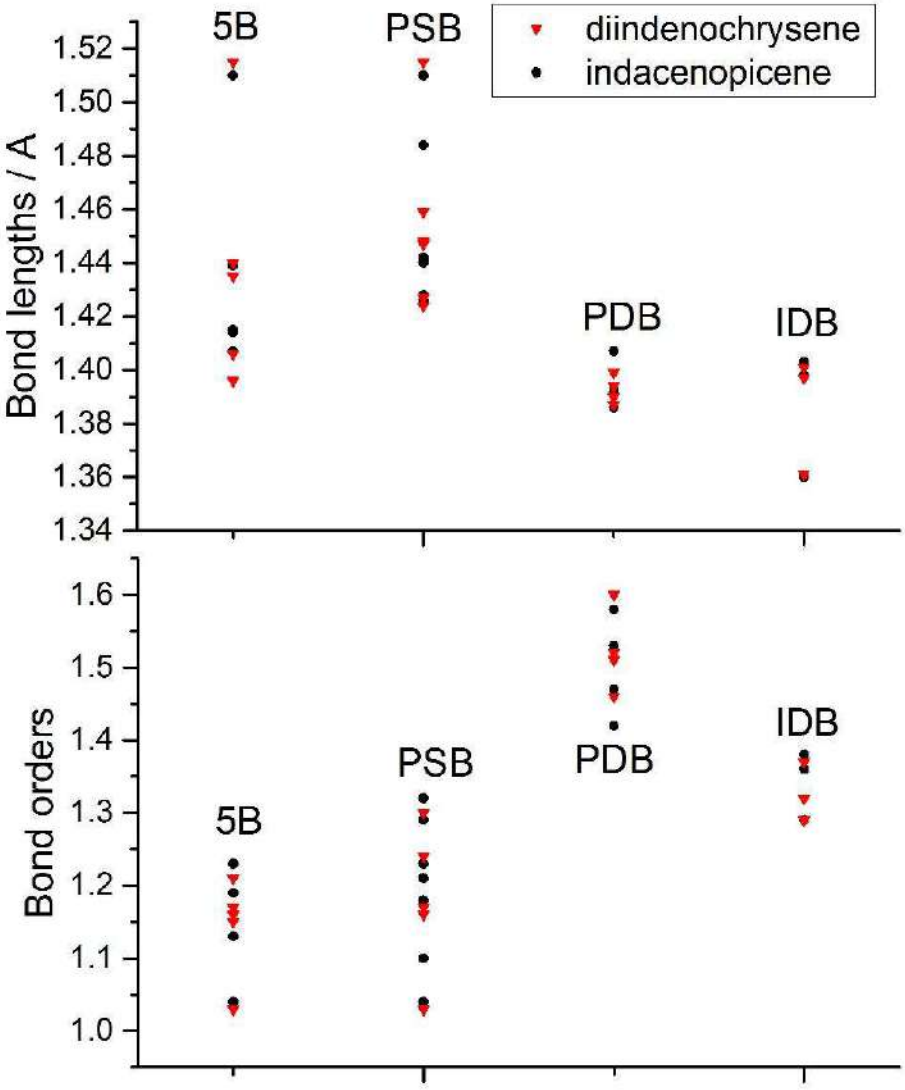

Figure S58. C–C Bond lengths (top) and bond orders (bottom) distributions for diindeno[4,3,2,1-*cdef*:4',3',2',1'-*lmno*]chrysene and *as*-indaceno[3,2,1,8,7,6-*pqrstuv*]picene. Abbreviations: 5B - pentagon bonds, PSB – peripheral single bonds, PDB – peripheral double bonds, IDB - inner double bonds.

5. References

1. Laikov, D.N. Fast evaluation of density functional exchange-correlation terms using the expansion of the electron density in auxiliary basis sets. *Chem. Phys. Lett.* **281**, 151–156 (1997).
2. Perdew, J.P., Burke, K. & Ernzerhof, M. Generalized Gradient Approximation Made Simple. *Phys Rev Lett.* **77**, 3865–3868(1996).
3. Granovsky, A.A. Firefly v. 8.1.1 (Formerly PC GAMESS), 2015. http://classic.chem.msu.su/gran/gamess/index.html.
4. Schmidt, M.W. et al. General atomic and molecular electronic structure system. *J. Comput. Chem.* **14**, 1347–1363 (1993).
5. Neese, F. The ORCA program system. WIRes Comput. Mol. Sci. **2**, 73–78 (2012).
6. Becke, A.D. Density-functional thermochemistry. III. The role of exact exchange. *J. Chem. Phys.* **98**, 5648–5652 (1993).
7. Stephens, P.J., Devlin, F.J., Chabalowski, C.F. & M.J. Frisch. Ab Initio Calculation of Vibrational Absorption and Circular Dichroism Spectra Using Density Functional Force Fields. *J. Phys. Chem.* **98**, 11623–11627 (1994).
8. Staroverov, V.N., Scuseria, G.E., Tao, J. & Perdew, J.P. Comparative assessment of a new nonempirical density functional: Molecules and hydrogen-bonded complexes. *J. Chem. Phys.* **119**, 12129-12137 (2003).
9. Weigend, F. & Ahlrichs, R. Balanced basis sets of split valence, triple zeta valence and quadruple zeta valence quality for H to Rn: Design and assessment of accuracy. *Phys. Chem. Chem. Phys.* **7**, 3297–3305 (2005).
10. Amsharov, K. Y., Kabdulov, M. A. & Jansen, M. Facile Bucky-Bowl Synthesis by Regiospecific Cove-Region Closure by HF Elimination. *Angew. Chem. Int. Ed.* **51**, 4594-4597 (2012).
11. Xie, G.-Y., Jiang L. & Lu, T.-B. Discrimination of *cis-trans* isomers by dinuclear metal cryptates at physiological pH: selectivity for fumarate vs. maleate. *Dalton Trans.* **42**, 14092-14099 (2013).
12. Rappoport, D., Crawford, N.R.M., Furche, F. & Burke, K. *Approximate Density Functionals: Which Should I Choose?* Encycl. Inorg. Chem. (Wiley, Chichester, 2009).
13. Spisak, S.N. et al. From Corannulene to Indacenopicene: Effect of Carbon Framework Topology on Aromaticity and Reduction Limits. *Organometallics* **35**, 3105-3111 (2016).

14 Zilber, G. et al. Reduction of pyracylene by alkali metals: Mechanism and formation of aggregates. *Res. Chem. Intermed.* **22**, 839–854 (1996).

15. Freiermuth, B., Gerber, S., Riesen, A., Wirz, J. & Zehnder, M. Molecular and electronic structure of pyracylene. *J. Am. Chem. Soc.* **112**, 738–744 (1990). doi:10.1021/ja00158a037.

16. Koper, C., Sarobe, M. & Jenneskens, L.W. Redox properties of non-alternant cyclopenta-fused polycyclic aromatic hydrocarbons: The effect of peripheral pentagon annelation. *Phys. Chem. Chem. Phys.* **6**, 319–327 (2004).

17. Trasatti S. The absolute electrode potential: an explanatory note (Recommendations 1986). Pure Appl. Chem. **58**, 955–966 (1988).

18. Pommerehne, J. et al. Efficient two layer leds on a polymer blend basis. *Adv. Mater.* **7**, 551–554 (1995).

Publication 2.

Unusual Fusion of α-Fluorinated Benzophenones under McMurry Reaction Conditions.

V. Akhmetov, M. Feofanov, V.Ioutsy, F. Hampel, K. Y. Amsharov.

Chem. - A Eur. J. **2019**, 25, 1910-1913. DOI:10.1002/chem.201805290.

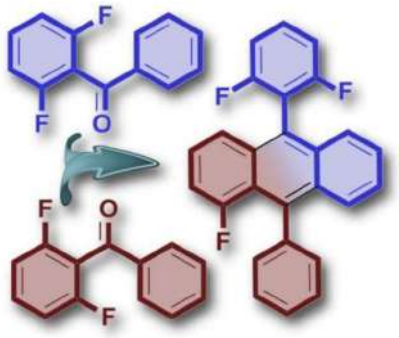

ABSTRACT:

By exposure of α-fluorinated benzophenones to McMurry reaction conditions, we have observed the remarkable formation of 9,10-diphenylanthracenederivatives. This unexpected transformation necessitates the cleavage of the exceptionally stable aromatic C-F bond under mild McMurry conditions. In this work, the condensation of several related fluorinated benzo-and acetophenones has been investigated, which allow us to propose a domino-like fusion mechanism for this unusual transformation. The scope and limitations of the fluorine-promoted benzophenone fusion are subsequently discussed.

ChemPubSoc Europe

DOI: 10.1002/chem.201805290

CHEMISTRY A European Journal Communication

Organic Chemistry

Unusual Fusion of α-Fluorinated Benzophenones under McMurry Reaction Conditions

Vladimir Akhmetov,[a] Mikhail Feofanov,[a] Vitaliy Ioutsi,[b] Frank Hampel,[a] and Konstantin Amsharov*[a]

Abstract: By exposure of α-fluorinated benzophenones to McMurry reaction conditions, we have observed the remarkable formation of 9,10-diphenylanthracene derivatives. This unexpected transformation necessitates the cleavage of the exceptionally stable aromatic C–F bond under mild McMurry conditions. In this work, the condensation of several related fluorinated benzo- and acetophenones has been investigated, which allow us to propose a domino-like fusion mechanism for this unusual transformation. The scope and limitations of the fluorine-promoted benzophenone fusion are subsequently discussed.

Fluoroorganic chemistry remains a poorly investigated field due to the often misleading assumption of bond stability and thus its inertness. Nevertheless, there is some pioneering work in the field showing the applicability of the C–F bond for organic synthesis,[1] for example, for aryl–aryl coupling.[2] Moreover, some methods allow the synthesis of highly interesting strained polycyclic aromatic hydrocarbons (PAHs) with a curved surface, known as geodesic polyarenes,[3–5] which remain scarce since there are only a few synthetic approaches enabling their preparative synthesis.[6]

Addressing the issue, we have suggested a possible pathway enabling facile three-step synthesis of diindeno[1,2,3,4-defg:1′,2′,3′,4′-mnop]chrysene (**4**) (Scheme 1) which may serve as an example of important representative of geodesic polyarenes.[7] Leaving aside the final outcome of our efforts to synthesize **4** here, we describe rather the unexpected reaction observed during the implementation of the first step corresponding to the transformation of **1** to **2**. The required precursor **2** can be obtained by standard McMurry coupling of the respective fluorinated benzophenone **1**. The McMurry reaction is well known for its high functional-group tolerance and appears as a well-established synthetic approach to various alkenes by using carbonyl compounds as reactants.[8] The reaction is also suitable for the preparation of highly substituted phenylethanes.[9] Surprisingly, beside the expected product, we observed the formation of nonsymmetrical fluorinated 9,10-diphenylanthracene **5**. Due to the idiosyncrasy of the structure it is virtually impossible to synthesize such a derivative by known conventional methods.[10] Even though the obtained molecule is interesting itself as a precursor to non-IPR fullerenes' fragments,[11] it is even more important to consider this side product as a harbinger of the great potential of the C–F bond and its exploitation under various conditions.

The 2,6-difluoro-benzophenone **1** was chosen for the synthesis of target diindenochrysene **4** in accordance with Scheme 1. As a first step, fluorinated benzophenone was subjected to standard McMurry conditions. Analysis of the reactionary mixture revealed the formation of the two diastereomers of the desired product **2** with 50% yield and the presence of an unexpected side product, which turned out to have a UV/Vis spectrum corresponding to anthracene's core. The product was isolated and investigated by means of NMR and X-ray diffraction analysis, which revealed that the molecular structure of the isolated substance corresponds to 10-(2,6-difluorophenyl)-1-fluoro-9-phenylanthracene **5** (Figure 1).

The yield of anthracene **5** was found to be 35%. Among major **2** and **5**, only trace amounts of several unidentified byproducts were detected according HPLC analysis. To investigate whether this reaction is applicable for different related substrates, a set of reactions with various α-fluorinated aceto- and benzophenone derivatives were carried out (Scheme 2). As a matter of fact, only in the case of α-fluorinated benzophenone was the formation of the 9,10-diphenylanthracene core **7** observed along with the formation of the expected tetraphenylethane **6**. However, exposing 2,2′-difluorobenzophenone to the reaction conditions led to the isolation of **8** as a single major product with the moderate yields.

In the case of 2-fluoroacetophenone and 2-fluorobezaldehyde, no anthracene formation was detected and only the expected McMurry products were isolated: two isomers of **10** and only the *E*-isomer **12**. Additionally, we attempted to investigate whether perfluoroaromatic compounds show the formation of the corresponding anthracene derivatives. For this purpose, we subjected 2,3,4,5,6-tetrafluorobezophenone to McMurry conditions and obtained a complicated mixture that did not contain any major product that could be isolated.

[a] V. Akhmetov, M. Feofanov, F. Hampel, K. Amsharov
Department of Chemistry and Pharmacy, Organic Chemistry II
Friedrich-Alexander University Erlangen-Nuernberg
Nikolaus-Fiebiger Str. 10, 91058 Erlangen (Germany)
E-mail: konstantin.amsharov@fau.de

[b] V. Ioutsi
Endocrinology Research Centre, 117036 Moscow
Dmitriya Ul'yanova str. 11 (Russia)

Supporting information and the ORCID identification number(s) for the author(s) of this article can be found under: https://doi.org/10.1002/chem.201805290. It contains experimental procedures and compound characterization data (NMR; UV/Vis; X-ray diffraction data).

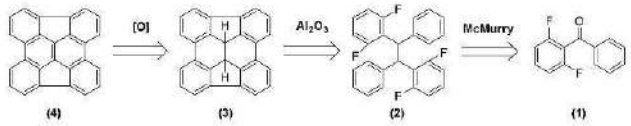

Scheme 1. Three-step synthetic approach to **4** from commercially available 2,6-difluoro-benzophenone.

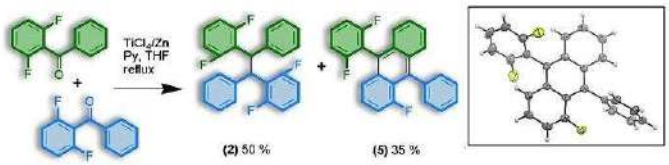

Figure 1. The implementation of the first step of the synthesis. The benzophenone molecules participating in the fusion are highlighted by different colors. Inset: ORTEP plot of **5** in the crystal. Thermal ellipsoids are drawn at the 50% probability level (only one orientation of **5** in the crystal is shown for clarity).

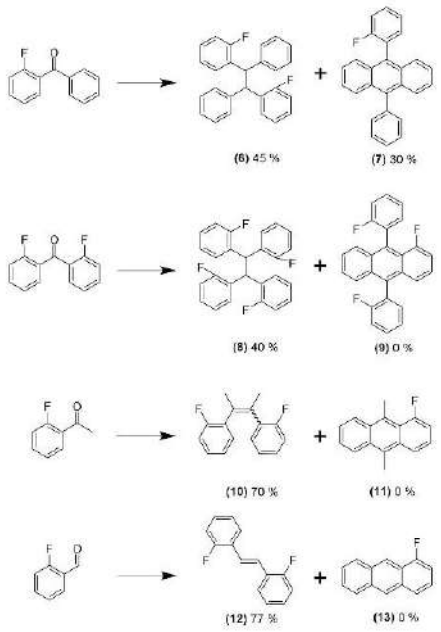

Scheme 2. Transformations of various α-fluorinated phenylcarbonyl compounds under McMurry reaction conditions.

Moreover, we did not observe any products that would have the UV/Vis spectrum corresponding to an anthracene derivative. This evidence shows that the activation of C–F bonds in such a case is not selective and leads to a huge number of possible reaction pathways.

Due to the heterogeneous nature of the McMurry reaction, the investigation of the reaction mechanism appears to be difficult. However, on the basis of common knowledge, the following mechanism can be proposed (Scheme 3). As a first step, a set of single-electron transfers from reduced titanium particles to the carbonyl group of the reactant takes place. The generated anion then attacked the activated π-system of the fluoroarene leading to the aromatic nucleophilic substitution of fluoride. The substitution is facilitated by the presence of the electron-withdrawing groups. The next step according to our experimental observation most probably includes electrophilic aromatic substitution, since the presence of the electron-withdrawing groups in the attacked phenyl ring tends to prevent further formation of anthracene's cores as was observed in the cases of **9**, **11**, and **13**. This step can be induced by po-

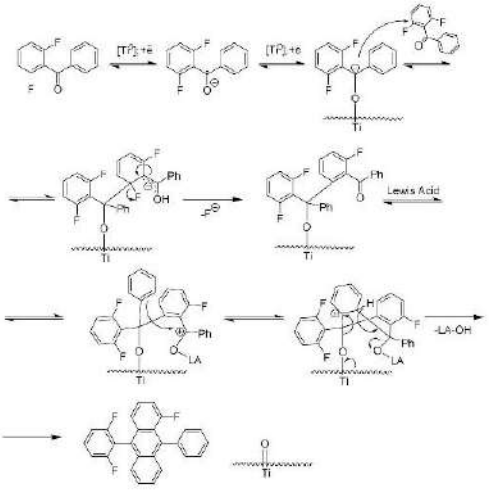

Scheme 3. Suggested mechanism for the transformation of 2,6-difluorobenzophenone under McMurry reaction conditions.

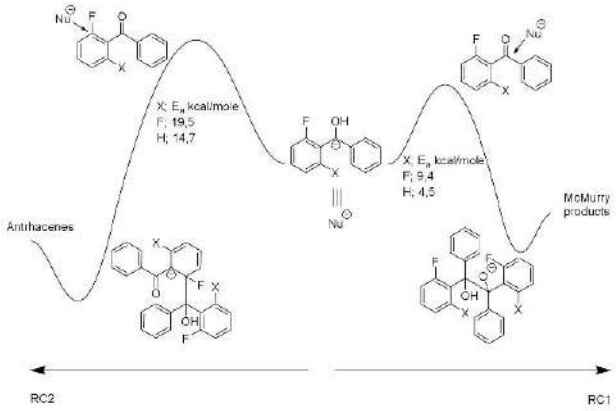

Figure 2. Schematic representation of the DFT data on the competition between two nucleophilic attacks.

larization of the carbonyl group by Lewis acids, such as Ti^{3+}- and Zn^{2+}-containing species. Another strong piece of evidence for the cationic nature of the last step is the formation of **7** without the second possible isomer containing the fluorine atom within the anthracene fragment, which was confirmed by means of X-ray diffraction analysis (see the Supporting Information).

Considering the proposed mechanism, it is reasonable to assume that the yields and selectivity of the reaction might be increased by the introduction of additional electron-withdrawing groups to the fluorinated rings of benzophenone and electron-donating groups to opposite one, thus facilitating both steps, initial nucleophilic attack of the C–F bond and consequent electrophilic substitution.

To estimate and compare kinetic barriers of the nucleophilic attacks by the carbonyl anion leading to either McMurry products or anthracene-based compounds we carried out model DFT calculations at the PBE/TZ2p level. In the model, the titanium particle was replaced by a hydrogen atom for simplicity reasons.[12]

The obtained energies (Figure 2) are in line with the observed experimental data showing lower barriers for nucleophilic attack of the carbonyl group and two-to -three times higher, although still reasonable values for the attack of fluorinated carbon.

Since the C–F bond is considered to be one of the most stable bonds in organic chemistry, it is commonly assumed that it difficult to be exploited in organic synthesis due to its inert nature. However, there are quite a few evidences revealed during recent years that refute this fallacy. The discovered reaction proves that fluoroorganic chemistry still remains an undeveloped and extremely promising field. Moreover, the transformation seems to be quite an attractive tool enabling synthesis of fluorinated 9,10-diphenylanthracenes that are not otherwise available.

Experimental Section

See the Supporting Information for full details. CCDC 1867159 and 1867160 contain the supplementary crystallographic data for this paper. These data are provided free of charge by The Cambridge Crystallographic Data Centre.

Acknowledgements

The authors thank the Deutsche Forschungsgemeinschaft (DFG-SFB 953 "Synthetic Carbon Allotropes"–Projects A6, AM-407). We also thank Olga Mazaleva for the help with carrying out DFT calculations.

Conflict of interest

The authors declare no conflict of interest.

Keywords: anthracene · arenes · C–F chemistry · McMurry reaction · organic chemistry

[1] a) S. Duttwyler, C. Douvris, N. L. P. Fackler, F. S. Tham, C. Reed, K. K. Baldridge, J. S. Siegel, *Angew. Chem. Int. Ed.* **2010**, *49*, 7519–7522; *Angew. Chem.* **2010**, *122*, 7681–7684; b) T. Fujita, M. Takazawa, K. Sugiyama, N. Suzuki, J. Ichikawa, *Org. Lett.* **2017**, *19*, 588–591; c) T. Fujita, K. Fuchibe, J. Ichikawa, *Angew. Chem. Int. Ed.* **2019**, DOI: https://doi.org/10.1002/anie.201805292.

[2] a) A.-K. Steiner, K. Y. Amsharov, *Angew. Chem. Int. Ed.* **2017**, *56*, 14732–14736; *Angew. Chem.* **2017**, *129*, 14926–14931; b) A. K. Dutta, A. Linden, L. Zoppi, K. K. Baldridge, J. S. Siegel, *Angew. Chem. Int. Ed.* **2015**, *54*, 10792–10796; *Angew. Chem.* **2015**, *127*, 10942–10946; c) O. Allemann, S. Duttwyler, P. Romanato, K. K. Baldridge, J. S. Siegel, *Science* **2011**, *332*, 574–577.

[3] a) K. Yu. Amsharov, M. A. Kabdulov, M. Jansen *Angew. Chem. Int. Ed.* **2012**, *51*, 4594–4597; *Angew. Chem.* **2012**, *124*, 4672–4675; b) O. Papaianina, V. A. Akhmetov, A. A. Goryunkov, F. Hampel, F. W. Heinemann, K. Y. Amsharov, *Angew. Chem. Int. Ed.* **2017**, *56*, 4834–4838; *Angew. Chem.* **2017**, *129*, 4912–4916.

[4] M. A. Petrukhina, in *Fragments of Fullerenes and Carbon Nanotubes* (Ed.: L. T. Scott), Wiley, **2012**.
[5] a) L. T. Scott, *Pure Appl. Chem.* **1996**, *68*, 291; b) P. W. Rabideau, A. Sygula, *Acc. Chem. Res.* **1996**, *29*, 235; c) L. T. Scott, *Angew. Chem. Int. Ed.* **2004**, *43*, 4994; *Angew. Chem.* **2004**, *116*, 5102; d) L. T. Scott, E. A. Jackson, Q. Zhang, B. D. Steinberg, M. Bancu, B. Li, *J. Am. Chem. Soc.* **2012**, *134*, 107–110.
[6] a) A. M. Butterfield, B. Gilomen, J. S. Siegel, *Org. Process Res. Dev.* **2012**, *16*, 664–676; b) V. M. Tsefrikas, L. T. Scott, *Chem. Rev.* **2006**, *106*, 4868–4884; c) D. Alberico, M. E. Scott, M. Lautens, *Chem. Rev.* **2007**, *107*, 174–238; d) N. Suzuki, T. Fujita, K. Y. Amsharov, J. Ichikawa, *Chem. Commun.* **2016**, *52*, 12948–12951.
[7] a) L. T. Scott, H. E. Bronstein, D. V. Preda, R. B. M. Ansems, M. S. Bratcher, S. Hagen, *Pure Appl. Chem.* **1999**, *71*, 209–219; b) H. I. Chang, H. T. Huang, C. H. Huang, M. Y. Kuo, Y. T. Wu, *Chem. Commun.* **2010**, *46*, 7241–7243; c) L. T. Scott, H. E. Bronstein, N. Choi, *J. Am. Chem. Soc.* **2002**, *124*, 2951.
[8] X. Duan, J. Zeng, J. Lu*, Z. Zhang, *J. Org. Chem.* **2006**, *71*, 9873–9876.
[9] a) R. Willem, H. Pepermans, K. Hallenga, M. Gielen, R. Dams, H. J. Giese, *J. Org. Chem.* **1983**, *48*, 1890–1898; b) F. A. Bottino, P. Finocchiaro, E. Libertini, A. Reale, A. Recca, *J. Chem. Soc. Perkin Trans. 2* **1982**, 77–81; c) F.-A. von Itter, F. Vögtle, *Chem. Ber.* **1985**, *118*, 2300–2313.
[10] a) W. Fudickar, T. Linker, *Chem. Commun.* **2008**, *0*, 1771–1773; b) W. Cui, Y. Wu, H. Tian, Y. Geng, F. Wang, *Chem. Commun.* **2008**, *0*, 1017–1019; c) C. Shu, C.-B. Chen, W.-X. Chen, L.-W. Ye, *Org. Lett.* **2013**, *15*, 5542–5545.
[11] K. Amsharov, *Phys. Status Solidi B* **2017**, *254*, 1700170.
[12] a) D. N. Laikov, *Chem. Phys. Lett.* **1997**, *281*, 151–156; b) J. P. Perdew, K. Burke, M. Ernzerhof, *Phys. Rev. Lett.* **1996**, *77*, 3865–3868.

Manuscript received: October 22, 2018
Revised manuscript received: November 24, 2018
Accepted manuscript online: November 26, 2018
Version of record online: January 9, 2019

CHEMISTRY
A European Journal

Supporting Information

Unusual Fusion of α-Fluorinated Benzophenones under McMurry Reaction Conditions

Vladimir Akhmetov,[a] Mikhail Feofanov,[a] Vitaliy Ioutsi,[b] Frank Hampel,[a] and Konstantin Amsharov*[a]

chem_201805290_sm_miscellaneous_information.pdf

Supporting Information

Contents

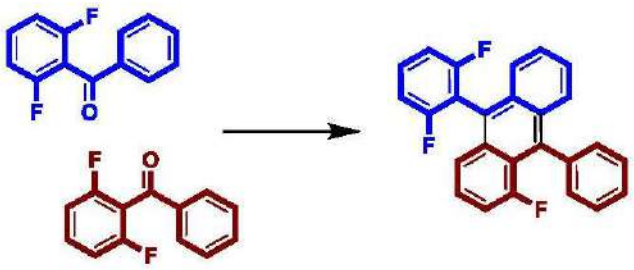

1. General Information

All chemicals and solvents were purchased in reagent grade from commercial suppliers (Acros®, SigmaAldrich® or Fluka®, Fluorochem®, Merck®, chemPur®) and used as received unless otherwise specified. Solvents in HPLC grade were purchased from VWR® and SigmaAldrich®. Flash column chromatography was performed on Interchim PuriFlash 430 using flash grade silica gel from MacheryNagel 60 M (40-63 mm, deactivated). NMR spectra were recorded on Bruker Avance 400 operating at 400 MHz (^{1}H NMR) and 100 MHz (^{13}C NMR) at room temperature. The signals were referenced to residual solvent peaks (in parts per million (ppm) ^{1}H: $CDCl_3$, 7.27 ppm; CD_2Cl_2, 5.32 ppm; ^{13}C: $CDCl_3$, 77.0 ppm; CD_2Cl_2, 53.84 ppm). Coupling constants were assigned as observed. The obtained spectra were evaluated with the program MestReNova. High resolution APPI MS spectra were recorded on a Bruker ESI TOF maXis4G instrument. The data was evaluated with the program Bruker Compass DataAnalysis 4.2. HPLC measurements were performed on a Shimadzu Prominence Liquid Chromatograph LC-20AT with communication bus

module CBM-20A, diode array detector SPDM20A, the degassing unit DGU-20A5 R, column oven CTO-20AC or CTO-20A, respectively and with auto sampler SIL-20A HT. For separation a Cosmosil 5-PYE column (4.6 mm x 250mm) from Nacalai Tesque was used. As eluent a DCM/MeOH or toluene/MeOH mixture was used (UV-vis detection). The data was evaluated with the programs Shimadzu LCsolution and Shimadzu LabSolutions. TLC analyses were carried out with TLC sheets coated with silica gel with fluorescent indicator254 nm from Machery-Nagel (ALUGRAM® SIL G/UV254) and visualized via UV-light of 254nm or 366 nm.

2. Experimental Procedures

2,2'-difluorobenzophenone

A two-neck flask equipped with a magnetic stirrer was charged with 60 mL of anhydrous THF, cooled down to -78 °C, degassed and filled with argon. 2,2,6,6-tetramethylpiperidine (3.2 mL, 1.6 eq.) was added dropwise before adding n-BuLi (7.0 mL, 1.5 eq., 2.5M solution in hexane). Mixture was stirred at -78 °C for 30 min, then fluorobenzene (1.2 g, 1 eq.) was added and the mixture was stirred for another 45 min. 2-fluorobenzaldehyde (1.5 g, 1 eq.) was added and the mixture was stirred for 2 h before warming it up to r.t. overnight. The obtained mixture was washed with saturated NH_4Cl solution and extracted with diethyl ether. Organic layer was dried over Na_2SO_4 and filtered through silica plug. After evaporation of the solvent obtained alcohol was used for the next step. Alcohol was dissolved in 125 mL of dichloromethane and pyridinium chlorochromate (6.4 g, 5 eq) was added. The obtained mixture was stirred at r.t. overnight, filtered through short silica plug and washed with dichloromethane (300 mL). The product was purified by flash chromatography (Hexane:Ethylacetate=95:5) yielding 1,1 g of yellowish oil. Yield 63%. ^{1}H NMR (400 MHz, CD_2Cl_2) δ 7.73 (td, J = 7.5, 1.8 Hz, 2H), 7.67 – 7.56 (m, 2H), 7.33 (td, J = 7.6, 1.0 Hz, 2H), 7.18 (ddd, J = 10.7, 8.4, 0.9 Hz, 2H). ^{19}F NMR (377 MHz, CD_2Cl_2) δ -113.13 (d, J = 10.4 Hz). ^{13}C NMR (101 MHz, CD_2Cl_2) δ 189.4, 162.1 (d, J = 254.3 Hz), 134.2 (d, J = 9.4 Hz), 130.8, 127.5 (d, J = 13.1 Hz), 124.3, 116.2 (d, J = 22.5 Hz).

General procedure for McMurry coupling

A two-necked flask equipped with a magnetic stirrer was charged with zinc powder (1.6 g, 24 mmol) and 35 mL of THF. Afterwards the flask was filled with argon and the mixture was cooled to 0 °C. Then $TiCl_4$ (1.3 mL, 12 mmol) was added dropwise by a syringe, keeping the temperature of the reactionary mixture below 10 °C. The obtained suspension was warmed up to room temperature and stirred for 30 min. Then the mixture was refluxed for 2 hours, cooled down again to 0 °C, charged with pyridine (0.5 mL, 6 mmol) and stirred for 15 min. The solution of carbonyl compound (2.4 mmol) in 15 mL of THF was added and the mixture was heated at reflux until the full consumption of the carbonyl compound (monitored by TLC). The reaction was quenched with 10% K_2CO_3 aqueous solution and extracted with dichloromethane. The organic layer was dried over Na_2SO_4. The products were purified by flash chromatography (Hexane:Dichloromethane).

1,2-bis(2,6-difluorophenyl)-1,2-diphenylethane (2)

Yield 243 mg (50%). Mixture of two diastereomers (molar ratio 5:2). ^{1}H NMR (400 MHz, CD_2Cl_2) δ 7.50 (d, J = 7.6 Hz, 4H), 7.41 (d, J = 7.5 Hz, 10H), 7.20 (t, J = 7.4 Hz, 14H), 7.06 (m, 14H), 6.87 – 6.62 (m, 14H), 5.80 (s, 2H), 5.70 (s, 5H). ^{19}F NMR (377 MHz, CD_2Cl_2) δ -110.29, -110.75, -114.56, -115.24. ^{13}C NMR (101 MHz, CD_2Cl_2) δ 162.3, 159.8, 141.2, 141.2, 128.5, 128.4, 128.3, 128.1, 126.8, 126.7, 119.5, 119.3, 119.2, 119.1, 119.1, 111.5, 43.6, 42.6. APPI HRMS calculated for $C_{26}H_{18}F_4$ [M$^+$] m/z 406.1339, found 406.1341.

10-(2,6-difluorophenyl)-1-fluoro-9-phenylanthracene (5)

Yield 162 mg (35%). ^{1}H NMR (300 MHz, CD_2Cl_2) δ 7.68 – 7.51 (m, 6H), 7.46-7.30 (m, 6H), 7.23 (dd, J = 8.4, 7.1 Hz, 2H), 7.04 (ddd, J = 13.4, 7.3, 1.1 Hz, 1H). ^{19}F NMR (282 MHz, CD_2Cl_2) δ -105.22 (dd, J = 13.4, 4.9 Hz), -111.21 (t, J = 6.5 Hz). ^{13}C NMR (101 MHz,) δ 161.4 (dd, J=249.2, 29.6 Hz), 160.3 (d, J=257.2 Hz), 141.4, 136.4, 132.4, 131.7, 131.4, 131.1, 130.2, 128.1, 127.6, 127.2, 126.3, 125.8, 124.6, 122.5, 121.4, 115.5, 112.5, 112.2, 110.4, 110.1. UV/vis (DCM/Methanol) λ_{max} 255, 342, 355, 363, 374, 384, 394 nm. Crystal Data for $C_{26}H_{15}F_3$ (M =384.38 g/mol): monoclinic, space group $P2_1/c$ (no. 14), a = 7.6532(2) Å, b = 20.5853(7) Å, c = 11.8776(4) Å, β = 91.659(3)°, V = 1870.45(10) Å^3, Z = 4, T = 153(1) K, μ(CuKα) = 0.821 mm^{-1}, $Dcalc$ = 1.365 g/cm^3, 6205 reflections measured (8.598° ≤ 2Θ ≤ 145.998°), 3595 unique (R_{int} = 0.0300, R_{sigma} = 0.0488) which were used in all calculations. The final R_1 was 0.0463 (I > 2σ(I)) and wR_2 was 0.1226. APPI HRMS calculated for $C_{26}H_{15}F_3$ [M$^+$] m/z 384.1120, found 384.1127.

1,2-bis(2-fluorophenyl)-1,2-diphenylethane (6)

Yield 197 mg (45%). Mixture of two diastereomers (molar ratio 1:1). ^{1}H NMR (400 MHz, CD_2Cl_2) δ 7.53 (m, 2H), 7.41 (d, J = 7.5 Hz, 2H), 7.37 (d, J = 7.5 Hz, 2H), 7.25 – 6.88 (m, 18H), 5.42 (s, 1H), 5.38 (s, 1H). ^{19}F NMR (377 MHz, CD_2Cl_2) δ -117.78, -118.02. ^{13}C NMR (101 MHz, CD_2Cl_2) δ 160.8 (d, J = 244.1 Hz), 160.8 (d, J = 244.1 Hz), 142.5, 142.5, 137.7, 133.6, 133.2, 132.5, 132.3, 131.5, 130.9, 130.8, 130.0, 129.5, 129.0, 128.7, 128.7, 128.3, 128.2, 128.1, 126.8, 126.8, 124.6, 115.9, 115.6, 47.4, 47.2. APPI HRMS calculated for $C_{26}H_{20}F_2$ [M$^+$] m/z 370.1528, found 370.1530.

9-(2-fluorophenyl)-10-phenylanthracene (7)

Yield 120 mg (30 %). ^{1}H NMR (400 MHz, CD_2Cl_2) δ 7.72 – 7.68 (m, 2H), 7.66 – 7.59 (m, 6H), 7.53 – 7.32 (m, 11H). ^{19}F NMR (377 MHz, CD_2Cl_2) δ -114.46. ^{13}C NMR (101 MHz, CD_2Cl_2) δ

160.9 (d, J = 244.9 Hz), 139.2, 138.4, 133.9, 131.7, 131.6, 130.51, 130.4, 130.3, 128.9, 128.8, 128.0, 127.5, 126.5, 125.9, 125.5, 124.8, 124.8, 116.4, 116.1. UV/vis (DCM/Methanol) λ_{max} 251, 341, 353, 361, 371, 382, 392 nm. Crystal Data for $C_{26}H_{15}F$ (M =346.38 g/mol): monoclinic, space group $C2/c$ (no. 15), a = 10.6999(4) Å, b = 13.4035(6) Å, c = 12.3046(6) Å, β = 90.969(4)°, V = 1764.43(13) Å^3, Z = 4, T = 153.00(10) K, μ(CuKα) = 0.645 mm^{-1}, $Dcalc$ = 1.304 g/cm^3, 2367 reflections measured (10.58° ≤ 2Θ ≤ 128.954°), 1419 unique (R_{int} = 0.0281, R_{sigma} = 0.0310) which were used in all calculations. The final R_1 was 0.0454 ($I > 2\sigma(I)$) and wR_2 was 0.1246. APPI HRMS calculated for $C_{26}H_{17}F$ [M$^+$] m/z 348.1309, found 348.1306.

1,1,2,2-tetrakis(2-fluorophenyl)ethane (8)

Yield 195 mg (40%). ^{1}H NMR (400 MHz, CD_2Cl_2) δ 7.48 (t, J = 7.2 Hz, 4H), 7.12 – 7.05 (m, 4H), 7.00 (td, J = 7.6, 1.3 Hz, 4H), 6.87 (ddd, J = 10.4, 8.1, 1.2 Hz, 4H), 5.68 (s, 2H). ^{19}F NMR (377 MHz, CD_2Cl_2) δ -117.39. ^{13}C NMR (101 MHz, CD_2Cl_2) δ 160.9 (d, J = 245.6 Hz), 129.7, 129.0 (d, J = 14.5 Hz), 128.6 (d, J = 8.7 Hz), 124.45, 115.4 (d, J = 23.2 Hz), 39.4. APPI HRMS calculated for $C_{26}H_{18}F_4$ [M$^+$] m/z 406.1339, found 406.1343.

(Z/E)-2,2'-(but-2-ene-2,3-diyl)bis(fluorobenzene) (10)

Yield 210 mg (70 %). Mixture of two isomers (molar ratio 4:1). ^{1}H NMR (400 MHz, DMSO) δ 7.41 – 7.31 (m, 1H), 7.29 – 7.22 (m, J = 8.6, 4.8 Hz, 1H), 7.14 – 7.07 (m, 2H), 6.97 (dd, J = 10.2, 8.0 Hz, 2H), 6.93 – 6.87 (m, J = 10.2, 5.1 Hz, 3H), 2.09 (s, 6H). ^{19}F NMR (377 MHz, DMSO) δ -115.23, -115.67. ^{13}C NMR (101 MHz, CD_2Cl_2) δ 159.64 (d, J = 244.6 Hz), 159.43 (d, J = 244.5 Hz), 131.80, 131.64, 130.80, 130.58, 130.26, 129.45, 128.46, 127.97, 127.91, 124.04, 123.37, 115.70, 115.45, 115.01, 114.81, 22.69, 21.22. APPI HRMS calculated for $C_{16}H_{14}F_2$ [M$^+$] m/z 244.1058, found 244.1059.

(E)-1,2-bis(2-fluorophenyl)ethene (12)

Yield 200 mg (77 %). ^{1}H NMR (400 MHz, CD_2Cl_2) δ 7.67 (td, J = 7.7, 1.7 Hz, 1H), 7.36 (s, 1H), 7.31 – 7.24 (m, 1H), 7.18 (td, J = 7.6, 1.2 Hz, 1H), 7.10 (ddd, J = 10.9, 8.2, 1.2 Hz, 1H). ^{19}F NMR (377 MHz, CD_2Cl_2) δ -118.56 (d, J = 10.2 Hz). The NMR spectral data were consistent with that reported. [1]

3. Spectroscopic Analysis and Characterization

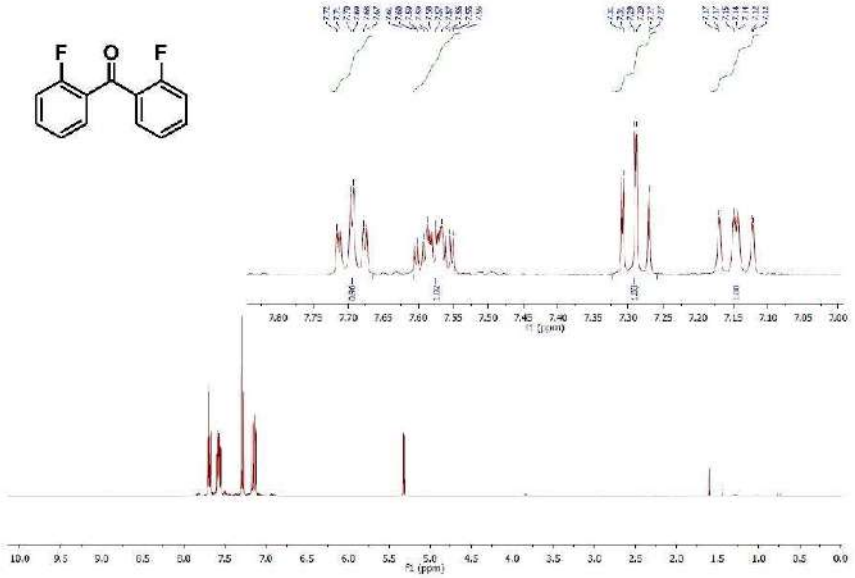

Figure S1. ^{1}H NMR spectrum of 2,2'-difluorobenzophenone (400 MHz, CD_2Cl_2).

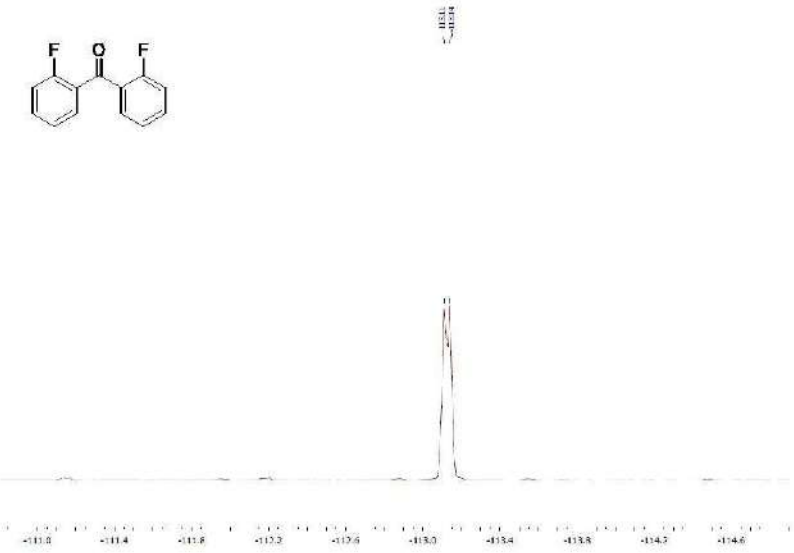

Figure S2. ^{19}F NMR spectrum of 2,2'-difluorobenzophenone (377 MHz, CD_2Cl_2).

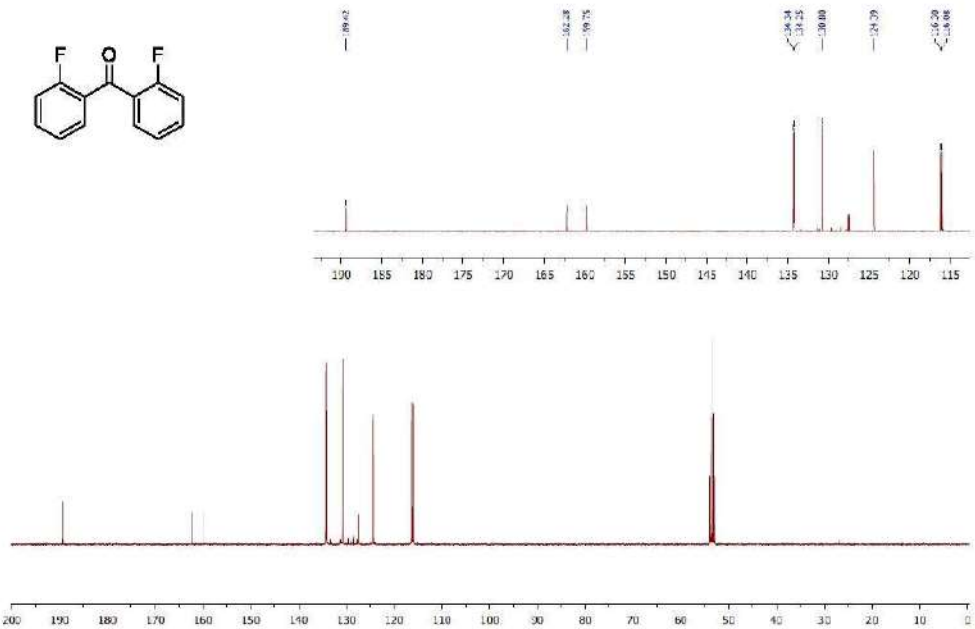

Figure S3. ^{13}C NMR spectrum of 2,2'-difluorobenzophenone (101 MHz, CD_2Cl_2).

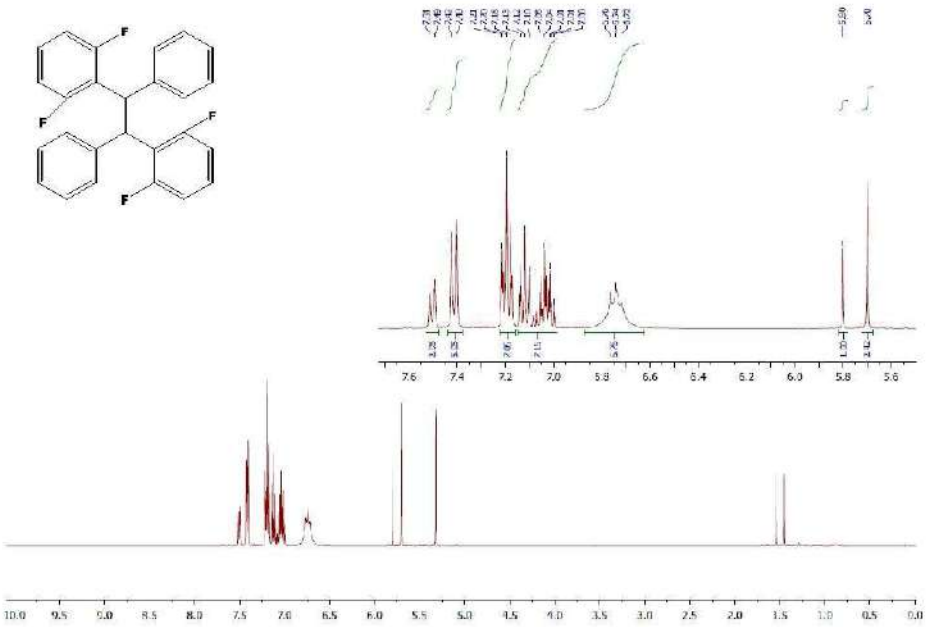

Figure S4. ^{1}H NMR spectrum of (8) (400 MHz, CD_2Cl_2).

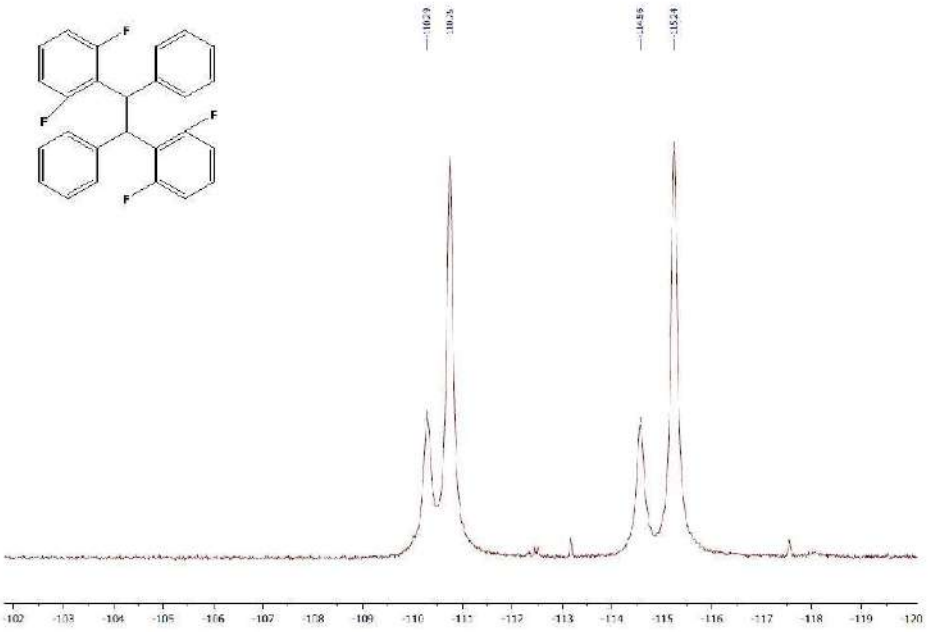

Figure S5. ^{19}F NMR spectrum of (8) (377 MHz, CD_2Cl_2).

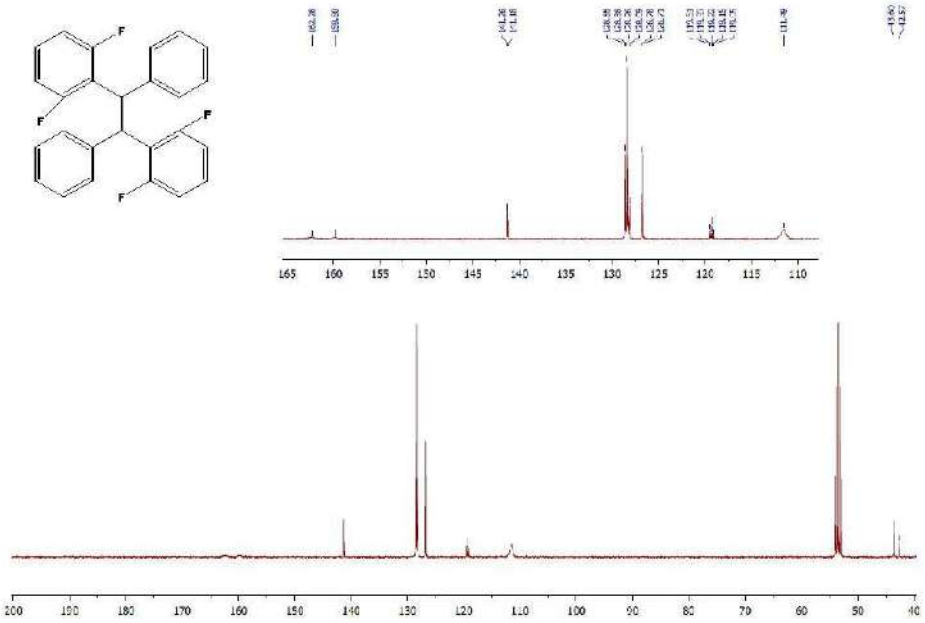

Figure S6. ^{13}C NMR spectrum of (8) (101 MHz, CD_2Cl_2).

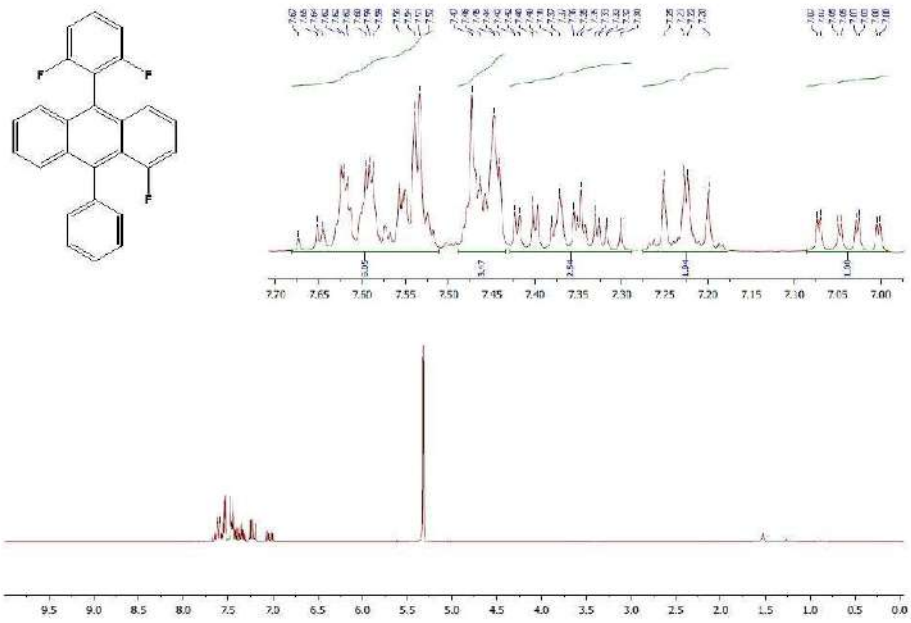

Figure S7. ^{1}H NMR spectrum of (5) (400 MHz, CD_2Cl_2).

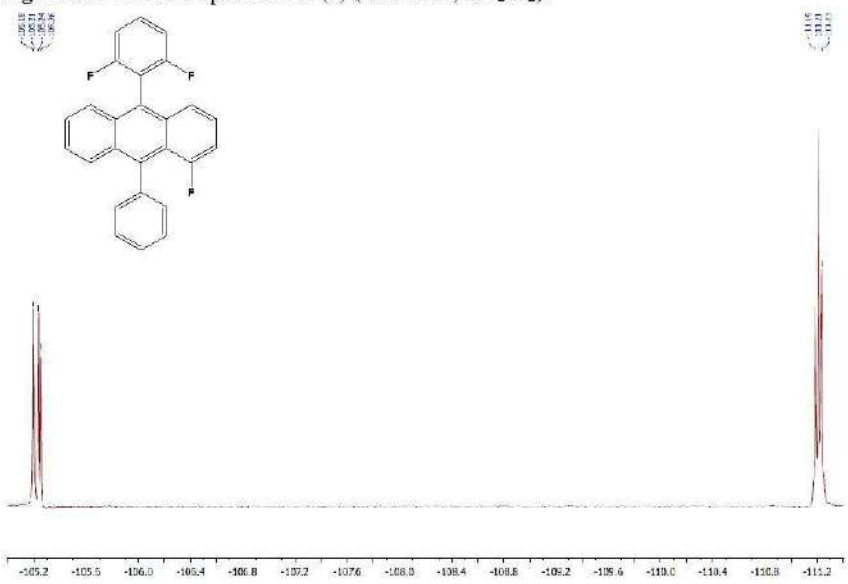

Figure S8. ^{19}F NMR spectrum of (5) (377 MHz, CD_2Cl_2).

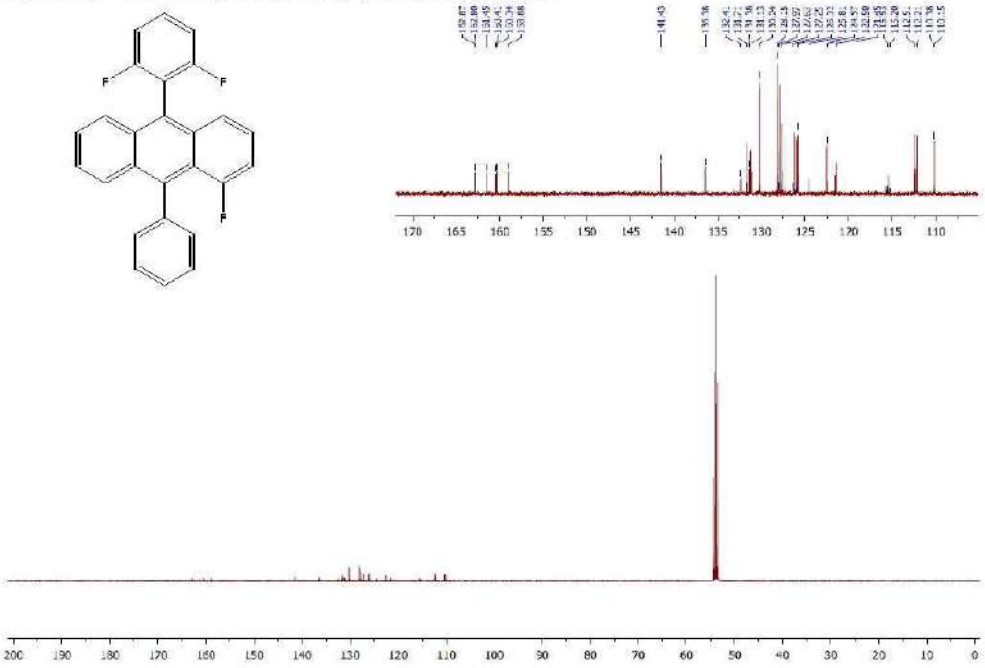

Figure S9. ^{13}C NMR spectrum of (5) (101 MHz, CD_2Cl_2).

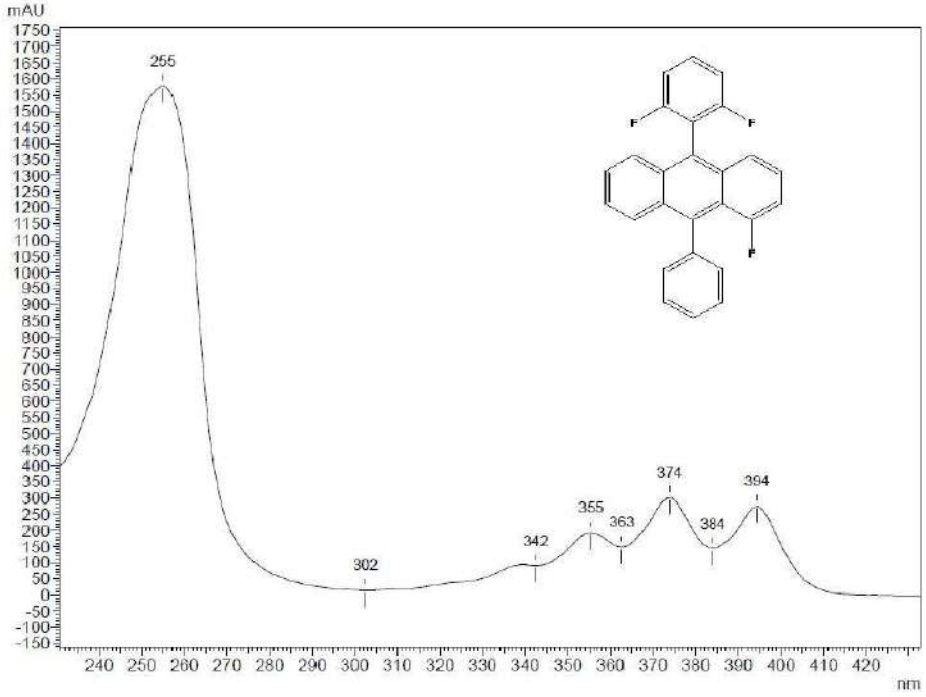

Figure S10. UV-vis spectrum of (5) (CD_2Cl_2/MeOH).

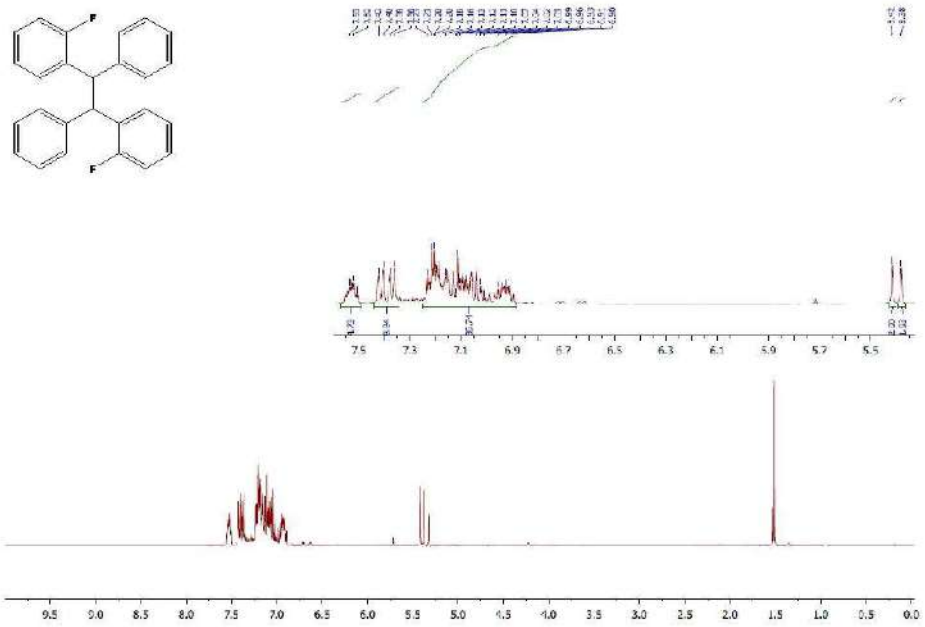

Figure S11. ^{1}H NMR spectrum of (6) (400 MHz, CD_2Cl_2).

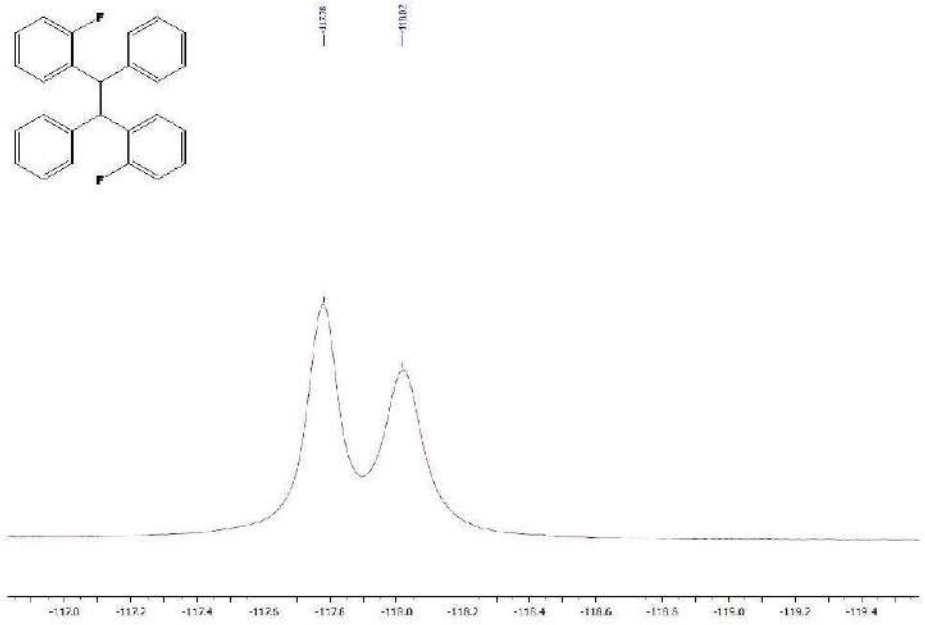

Figure S12. ^{19}F NMR spectrum of (6) (377 MHz, CD_2Cl_2).

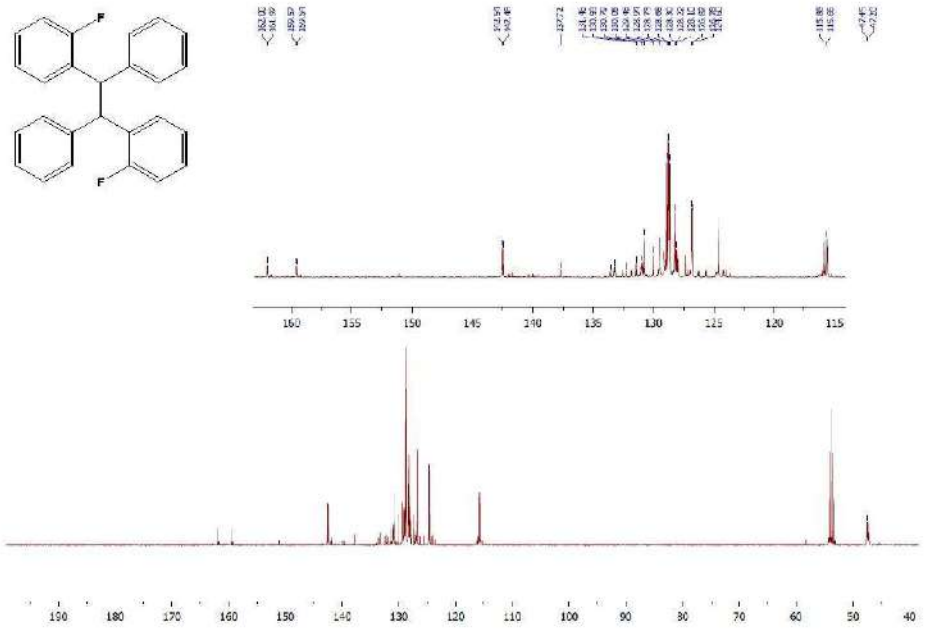

Figure S13. ^{13}C NMR spectrum of (6) (101 MHz, CD_2Cl_2).

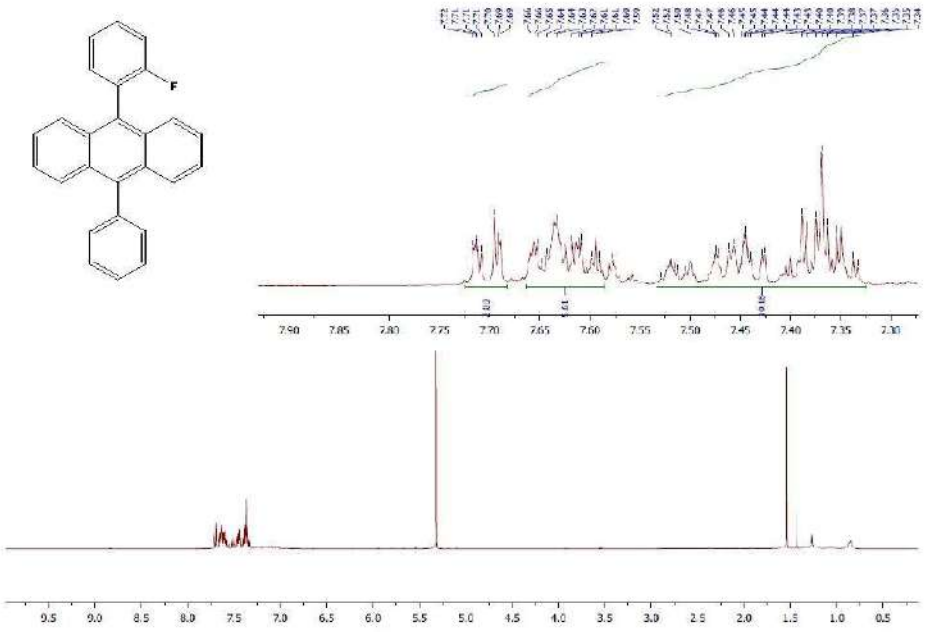

Figure S14. ^{1}H NMR spectrum of (7) (400 MHz, CD_2Cl_2).

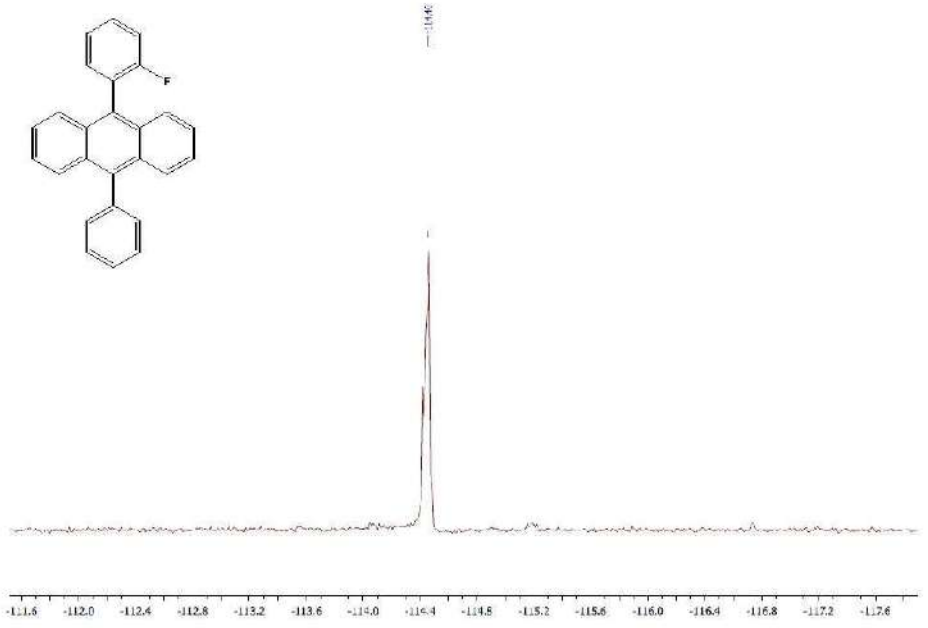

Figure S15. ^{19}F NMR spectrum of (7) (377 MHz, CD_2Cl_2).

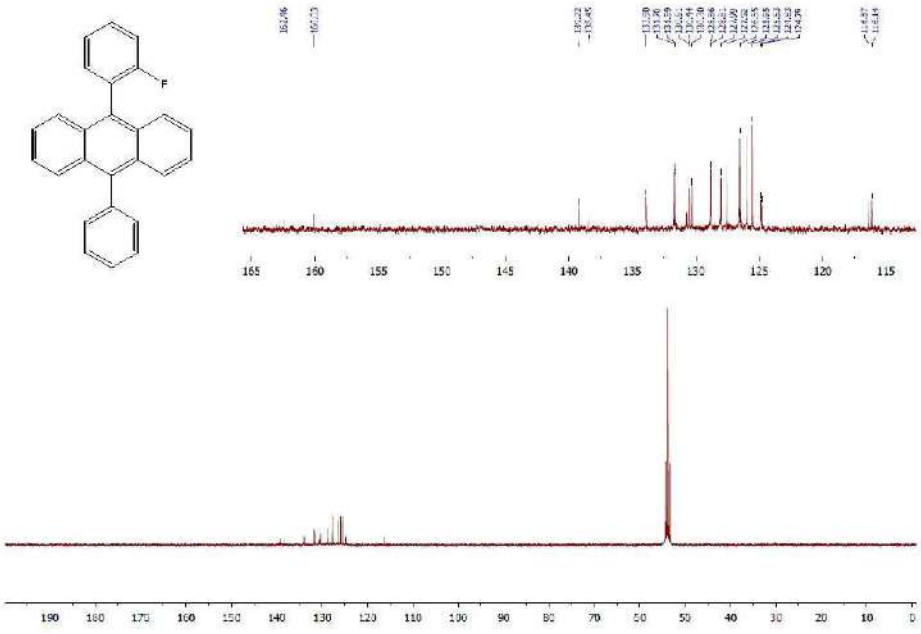

Figure S16. ^{13}C NMR spectrum of (7) (101 MHz, CD_2Cl_2).

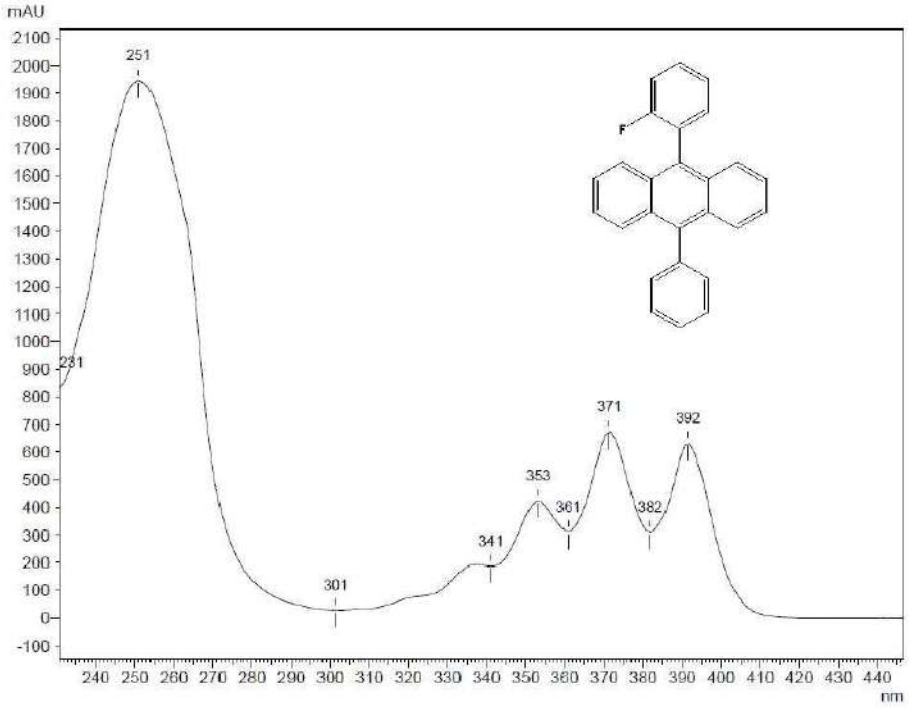

Figure S17. UV-vis spectrum of (7) (CD_2Cl_2/MeOH).

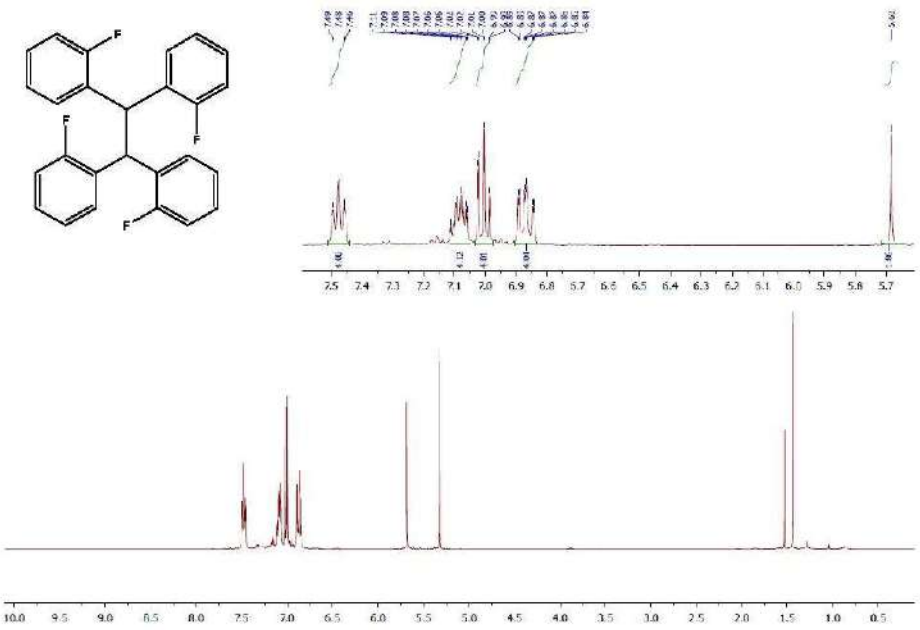

Figure S18. ^{1}H NMR spectrum of (8) (400 MHz, CD_2Cl_2).

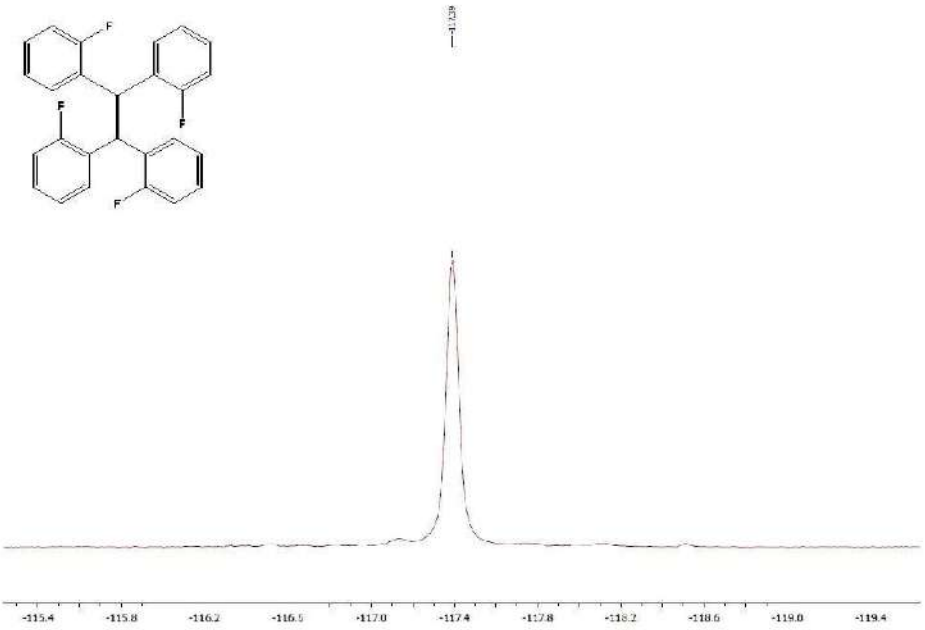

Figure S19. ^{1}H NMR spectrum of (8) (377 MHz, CD_2Cl_2).

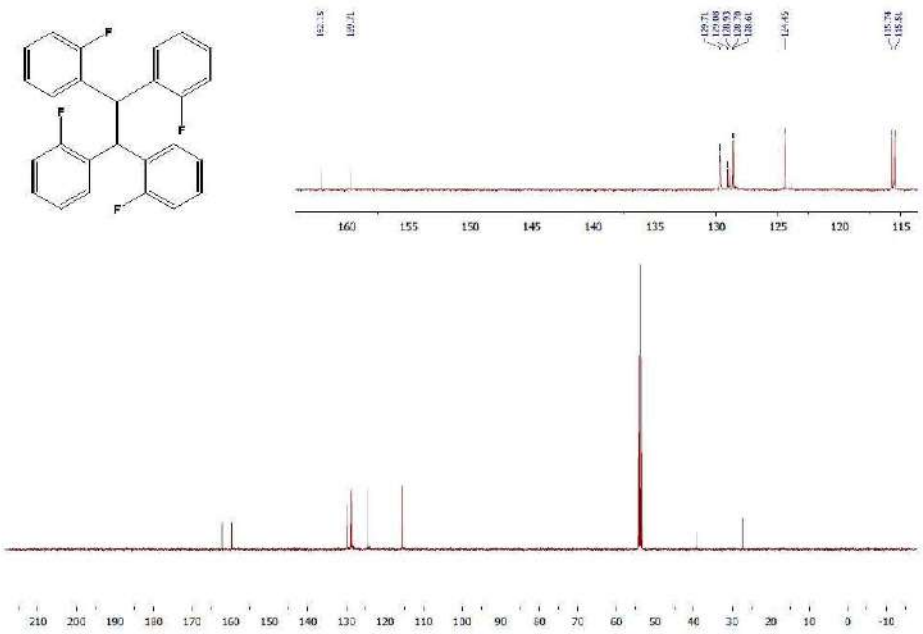

Figure S20. ^{13}C NMR spectrum of (8) (101 MHz, CD_2Cl_2).

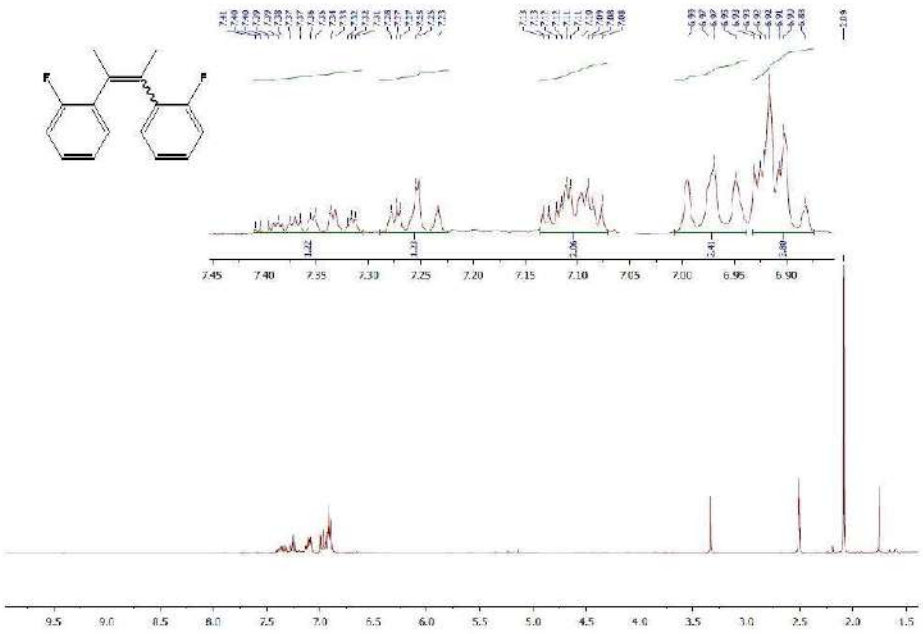

Figure S21. ^{1}H NMR spectrum of (10) (400 MHz, CD_2Cl_2).

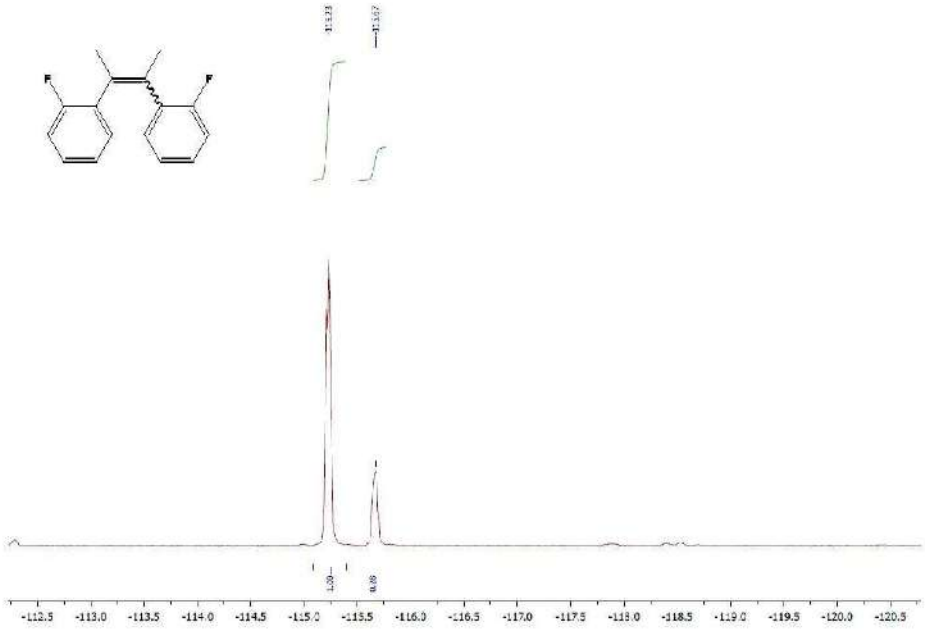

Figure S22. ^{13}F NMR spectrum of (10) (400 MHz, CD_2Cl_2).

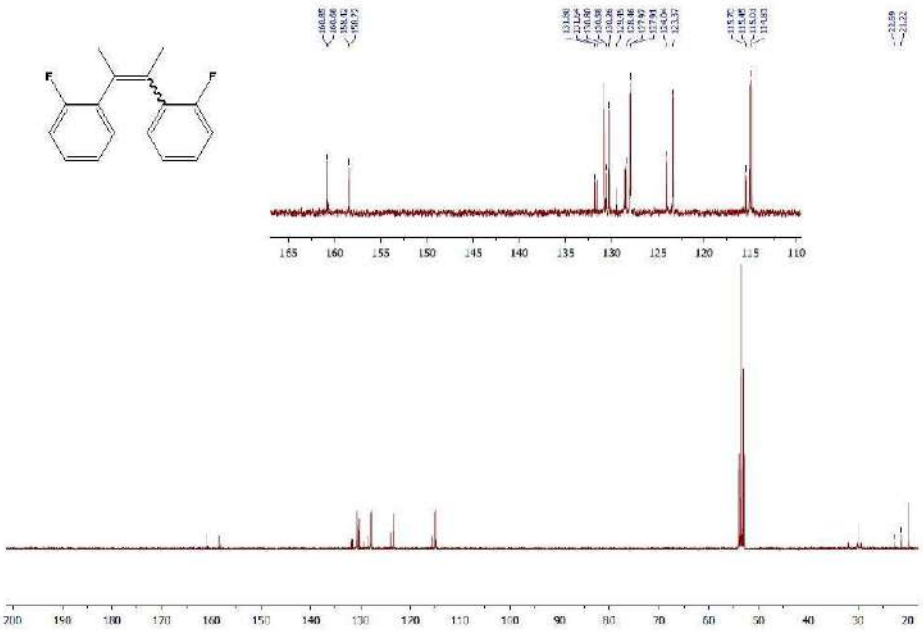

Figure S23. ^{13}C NMR spectrum of (10) (101 MHz, CD_2Cl_2).

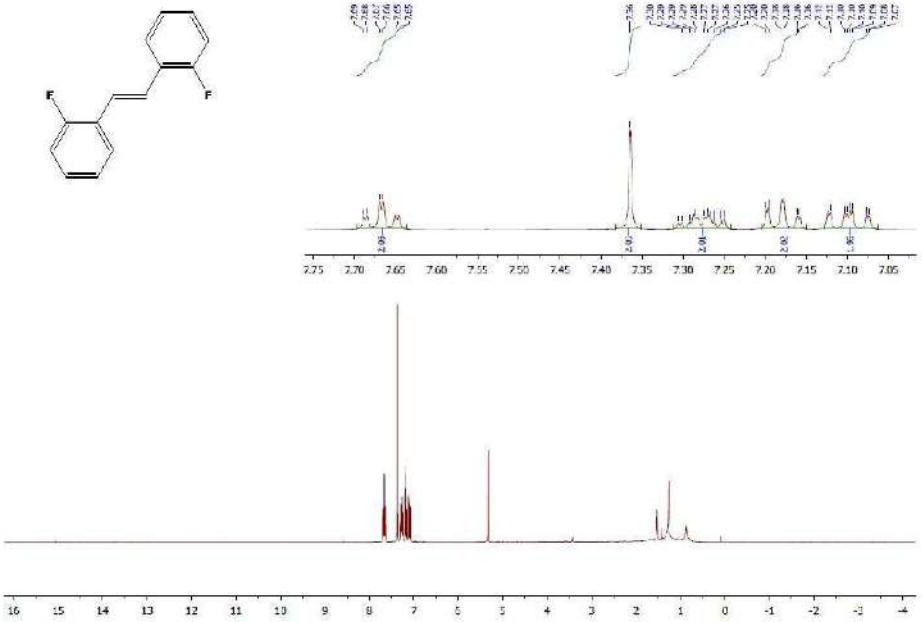

Figure S24. ^{1}H NMR spectrum of (12) (400 MHz, CD_2Cl_2).

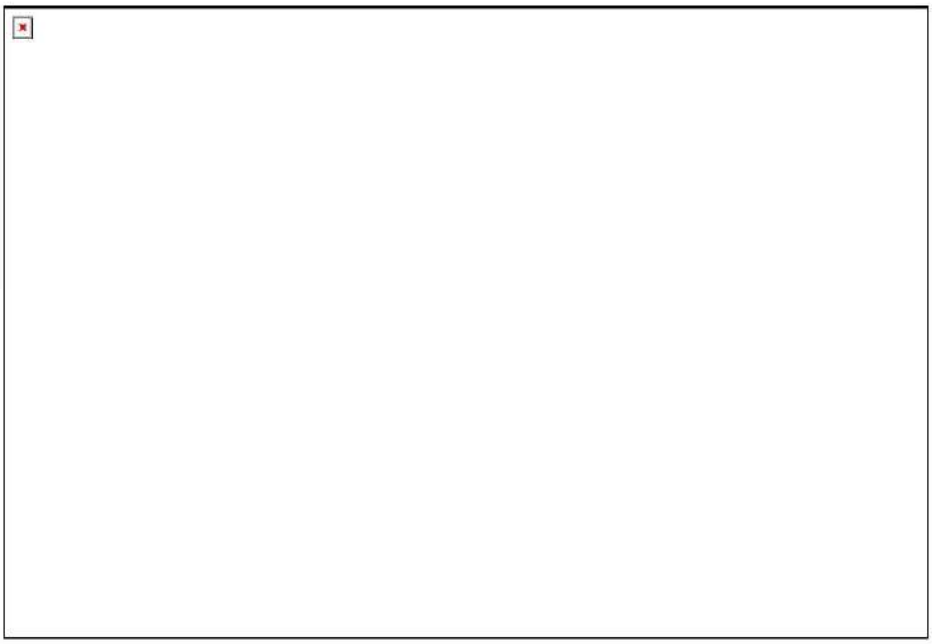

Figure S25. ^{19}F NMR spectrum of (12) (377 MHz, CD_2Cl_2).

4. X-Ray Crystal Data

4.1. 10-(2,6-difluorophenyl)-1-fluoro-9-phenylanthracene (5)

Table S1: Crystal data and structure refinement for (5).

Identification code	17Ams_VA01
Empirical formula	$C_{26}H_{15}F_3$
Formula weight	384.38
Temperature/K	153(1)
Crystal system	monoclinic
Space group	$P2_1/c$
a/Å	7.6532(2)
b/Å	20.5853(7)
c/Å	11.8776(4)
α/°	90
β/°	91.659(3)
γ/°	90
Volume/Å^3	1870.45(10)
Z	4
ρ_{calc}g/cm^3	1.365
μ/mm^{-1}	0.821
F(000)	792.0
Crystal size/mm^3	0.278 × 0.121 × 0.084
Radiation	CuKα (λ = 1.54184)
2Θ range for data collection/°	8.598 to 145.998
Index ranges	$-9 \leq h \leq 8$, $-18 \leq k \leq 24$, $-14 \leq l \leq 13$
Reflections collected	6205
Independent reflections	3595 [R_{int} = 0.0300, R_{sigma} = 0.0488]
Data/restraints/parameters	3595/1/266
Goodness-of-fit on F^2	0.988
Final R indexes [I>=2σ (I)]	R_1 = 0.0463, wR_2 = 0.1069
Final R indexes [all data]	R_1 = 0.0746, wR_2 = 0.1226
Largest diff. peak/hole / e Å^{-3}	0.19/-0.21

Table S2. Fractional Atomic Coordinates ($\times 10^4$) and Equivalent Isotropic Displacement Parameters ($Å^2 \times 10^3$) for (5). U_{eq} is defined as 1/3 of of the trace of the orthogonalised U_{IJ} tensor.

Atom	*x*	*y*	*z*	U(eq)
F12	3046.9(16)	3675.8(7)	8229.2(12)	53.5(4)
F16	-1538.6(18)	4820.0(7)	6453.8(12)	58.8(4)
F26	-5195.5(19)	3143.1(7)	10235.7(12)	40.2(4)
F26'	-2310(7)	1484(3)	7475(5)	40.2(4)
C11	703(2)	4224.5(10)	7354.0(16)	31.5(4)
C12	2476(3)	4196.3(11)	7630.9(18)	38.1(5)
C13	3666(3)	4662.7(12)	7341(2)	48.3(6)
C14	3055(4)	5191.8(13)	6730(2)	57.0(7)
C15	1305(4)	5249.5(12)	6421(2)	55.9(7)
C16	187(3)	4766.2(11)	6743.1(18)	41.9(5)
C21	-532(2)	3714.8(9)	7737.4(15)	27.2(4)
C22	-1691(2)	3859.7(9)	8594.7(15)	27.9(4)
C23	-1689(3)	4484.7(10)	9131.3(17)	33.6(4)
C24	-2792(3)	4622.6(10)	9966.2(17)	37.7(5)
C25	-3994(3)	4153.6(11)	10332.4(17)	36.8(5)
C26	-4022(2)	3561.6(10)	9849.0(16)	32.3(4)
C27	-2885(2)	3370.1(10)	8970.5(15)	28.1(4)
C28	-2857(2)	2743.7(9)	8493.4(15)	28.1(4)
C29	-1649(2)	2598.4(9)	7654.7(15)	27.4(4)
C30	-1504(3)	1965.5(10)	7170.5(16)	33.5(4)
C31	-356(3)	1829.4(10)	6355.4(18)	38.0(5)
C32	752(3)	2319.8(11)	5954.4(17)	38.7(5)
C33	694(2)	2928.2(10)	6392.4(16)	33.2(4)
C34	-482(2)	3090.0(9)	7263.9(15)	27.4(4)
C41	-4061(2)	2218.1(9)	8878.7(15)	28.7(4)
C42	-5593(3)	2073.0(11)	8281.2(18)	37.5(5)
C43	-6677(3)	1581.5(11)	8652(2)	42.9(5)
C44	-6247(3)	1232.7(10)	9610.1(19)	39.5(5)
C45	-4721(3)	1377.2(11)	10209.4(18)	40.4(5)
C46	-3634(3)	1865.8(10)	9844.8(16)	35.8(5)

Table S3. Anisotropic Displacement Parameters ($Å^2 \times 10^3$) for (5). The Anisotropic displacement factor exponent takes the form: $-2\pi^2[h^2a^{*2}U_{11}+2hka^*b^*U_{12}+\ldots]$.

Atom	U_{11}	U_{22}	U_{33}	U_{23}	U_{13}	U_{12}
F12	35.5(7)	56.1(9)	68.1(9)	-1.2(7)	-11.4(6)	1.3(6)
F16	55.8(8)	53.3(9)	66.6(9)	18.9(7)	-11.2(7)	2.9(7)
F26	38.6(8)	41.2(8)	41.7(8)	-1.7(7)	15.1(6)	-4.6(6)
F26'	38.6(8)	41.2(8)	41.7(8)	-1.7(7)	15.1(6)	-4.6(6)
C11	33.7(10)	32.2(10)	28.9(9)	-3.0(8)	4.9(8)	-6.4(8)
C12	33.7(10)	42.7(12)	38.2(11)	-8.2(9)	4.2(9)	-3.4(9)
C13	38.8(12)	55.5(15)	51.6(13)	-21.8(12)	17.4(10)	-17.8(11)
C14	68.9(17)	53.2(16)	50.4(14)	-11.7(12)	27.4(12)	-33.4(13)
C15	80.5(19)	41.0(14)	46.7(13)	7.0(11)	11.2(13)	-15.1(13)
C16	45.9(12)	39.9(12)	40.0(11)	3.6(10)	3.4(9)	-6(1)
C21	24.2(9)	29.4(10)	27.9(9)	2.0(8)	-0.4(7)	-0.9(7)
C22	26.6(9)	29.7(10)	27.2(9)	-0.1(8)	-0.9(7)	2.3(7)
C23	33.7(10)	28.9(10)	38.2(11)	-1.2(9)	0.0(8)	1.0(8)
C24	40.0(11)	33.9(11)	39.4(11)	-9.9(9)	0.5(9)	7.3(9)
C25	33.2(10)	44.7(13)	32.7(10)	-5.8(9)	4.2(8)	5.5(9)
C26	26.3(9)	40.2(11)	30.6(10)	2.7(8)	3.3(8)	-0.2(8)
C27	25.9(9)	30.7(10)	27.7(9)	-0.8(8)	-0.4(7)	1.8(7)
C28	26.0(9)	32.6(10)	25.7(9)	2.4(8)	0.0(7)	-0.9(8)
C29	25.8(9)	29.7(10)	26.5(9)	-0.5(8)	-1.6(7)	-0.1(7)
C30	35.1(10)	31.2(11)	34(1)	-1.2(8)	-3.2(8)	0.9(8)
C31	38.5(11)	34.3(11)	40.8(11)	-10.1(9)	-3.2(9)	5.9(9)
C32	30.4(10)	48.6(13)	37.1(11)	-13.1(10)	3.1(8)	5.9(9)
C33	26.0(9)	40.4(11)	33.3(10)	-1.7(9)	3.6(8)	-1.5(8)
C34	23.9(9)	31.4(10)	27.0(9)	-0.6(8)	-0.5(7)	2.3(7)
C41	27.7(9)	29.5(10)	29.3(9)	-2.3(8)	4.8(7)	0.1(8)
C42	32.5(10)	41.7(12)	37.9(11)	3.4(9)	-2.6(8)	-4.3(9)
C43	28.3(10)	47.0(13)	53.4(13)	-3.9(11)	-1.0(9)	-8.6(9)
C44	35.0(11)	35.3(11)	49.0(13)	-1.5(10)	16.6(9)	-4.4(9)
C45	43.0(12)	42.4(12)	36.3(11)	7.1(9)	8.9(9)	-3.2(10)
C46	33.3(10)	42.1(12)	31.8(10)	3.3(9)	0.5(8)	-5.7(9)

Table S4. Bond Lengths for (5).

Atom	Atom	Length/Å	Atom	Atom	Length/Å
F12	C12	1.351(3)	C25	C26	1.347(3)
F16	C16	1.359(3)	C26	C27	1.433(3)
F26	C26	1.336(2)	C27	C28	1.409(3)
F26'	C30	1.228(5)	C28	C29	1.411(3)
C11	C12	1.388(3)	C28	C41	1.501(3)
C11	C16	1.382(3)	C29	C30	1.430(3)
C11	C21	1.492(2)	C29	C34	1.435(3)
C12	C13	1.374(3)	C30	C31	1.355(3)
C13	C14	1.383(4)	C31	C32	1.410(3)
C14	C15	1.383(4)	C32	C33	1.357(3)
C15	C16	1.374(3)	C33	C34	1.430(3)
C21	C22	1.402(2)	C41	C42	1.385(3)
C21	C34	1.405(3)	C41	C46	1.388(3)
C22	C23	1.436(3)	C42	C43	1.388(3)
C22	C27	1.440(3)	C43	C44	1.377(3)
C23	C24	1.351(3)	C44	C45	1.382(3)
C24	C25	1.411(3)	C45	C46	1.383(3)

Table S5. Bond Angles for (5).

Atom	Atom	Atom	Angle/°	Atom	Atom	Atom	Angle/°
C12	C11	C21	121.45(18)	C28	C27	C22	119.91(16)
C16	C11	C12	114.89(19)	C28	C27	C26	124.15(18)
C16	C11	C21	123.62(18)	C27	C28	C29	119.74(17)
F12	C12	C11	117.18(18)	C27	C28	C41	121.35(16)
F12	C12	C13	118.6(2)	C29	C28	C41	118.89(17)
C13	C12	C11	124.2(2)	C28	C29	C30	122.50(18)
C12	C13	C14	117.7(2)	C28	C29	C34	120.35(17)
C13	C14	C15	121.1(2)	C30	C29	C34	117.14(16)
C16	C15	C14	118.0(2)	F26'	C30	C29	124.9(3)
F16	C16	C11	117.35(18)	F26'	C30	C31	112.6(3)
F16	C16	C15	118.6(2)	C31	C30	C29	122.37(19)
C15	C16	C11	124.0(2)	C30	C31	C32	120.11(19)
C22	C21	C11	119.47(17)	C33	C32	C31	120.28(18)
C22	C21	C34	120.72(17)	C32	C33	C34	121.37(19)
C34	C21	C11	119.78(16)	C21	C34	C29	119.45(16)
C21	C22	C23	121.36(17)	C21	C34	C33	121.87(17)
C21	C22	C27	119.79(17)	C33	C34	C29	118.68(17)
C23	C22	C27	118.83(17)	C42	C41	C28	121.14(17)

C24	C23	C22	121.42(19)	C42	C41	C46	119.06(18)
C23	C24	C25	120.63(19)	C46	C41	C28	119.80(17)
C26	C25	C24	119.34(18)	C41	C42	C43	120.0(2)
F26	C26	C25	116.08(17)	C44	C43	C42	120.8(2)
F26	C26	C27	120.09(18)	C43	C44	C45	119.42(19)
C25	C26	C27	123.83(18)	C44	C45	C46	120.1(2)
C26	C27	C22	115.92(17)	C45	C46	C41	120.65(19)

Table S6. Hydrogen Atom Coordinates ($Å \times 10^4$) and Isotropic Displacement Parameters ($Å^2 \times 10^3$) for (5).

Atom	*x*	*y*	*z*	U(eq)
H13	4842	4624	7549	58
H14	3833	5514	6523	68
H15	897	5605	6008	67
H23	-911	4801	8899	40
H24	-2759	5030	10303	45
H25	-4759	4252	10902	44
H26	-4826	3260	10100	39
H30	-2223	1635	7424	40
H31	-300	1412	6060	46
H32	1527	2226	5388	46
H33	1433	3246	6120	40
H42	-5894	2305	7632	45
H43	-7705	1487	8249	52
H44	-6977	903	9852	47
H45	-4425	1145	10859	48
H46	-2608	1959	10251	43

Table S7. Atomic Occupancy for (5).

Atom	*Occupancy*	Atom	*Occupancy*	Atom	*Occupancy*
F26	0.786(2)	F26'	0.214(2)	H26	0.214(2)
H30	0.786(2)				

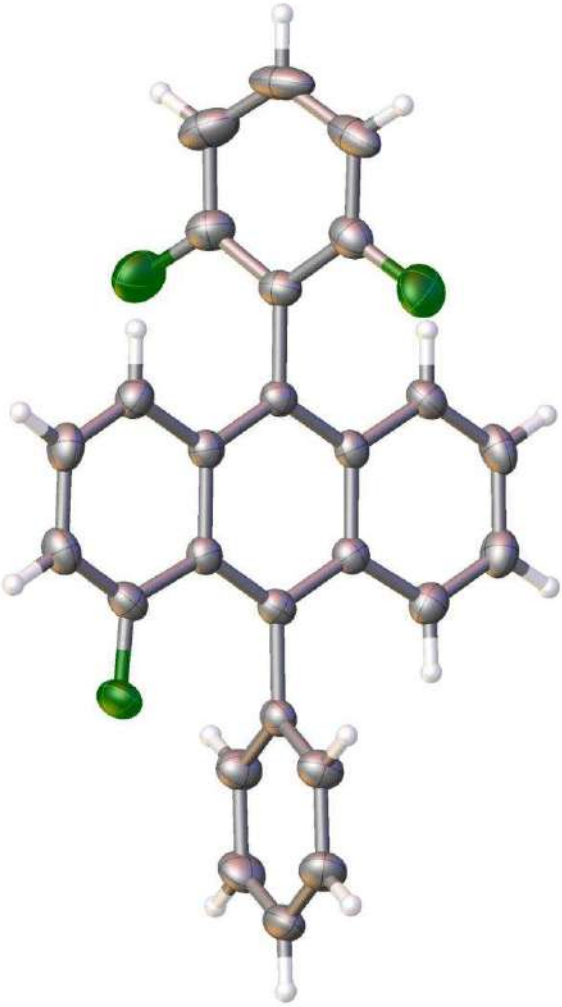

Figure S26. ORTEP plot of (5) in the crystal. Thermal ellipsoids are given at 50% probability level.

4.2. 9-(2-fluorophenyl)-10-phenylanthracene (7)

Table S8. Crystal data and structure refinement for (7).

Identification code	(7)
Empirical formula	$C_{26}H_{15}F$
Formula weight	346.38
Temperature/K	153.00(10)
Crystal system	monoclinic
Space group	C2/c
a/Å	10.6999(4)
b/Å	13.4035(6)
c/Å	12.3046(6)
α/°	90
β/°	90.969(4)
γ/°	90
Volume/Å^3	1764.43(13)
Z	4
ρ_{calc}g/cm^3	1.304
μ/mm^{-1}	0.645
F(000)	720.0
Crystal size/mm^3	0.375 × 0.037 × 0.036
Radiation	CuKα (λ = 1.54184)
2Θ range for data collection/°	10.58 to 128.954
Index ranges	$-10 \leq h \leq 12$, $-9 \leq k \leq 15$, $-14 \leq l \leq 14$
Reflections collected	2367
Independent reflections	1419 [R_{int} = 0.0281, R_{sigma} = 0.0310]
Data/restraints/parameters	1419/1/130
Goodness-of-fit on F^2	1.048
Final R indexes [I>=2σ (I)]	R_1 = 0.0454, wR_2 = 0.1138
Final R indexes [all data]	R_1 = 0.0581, wR_2 = 0.1246
Largest diff. peak/hole / e Å^{-3}	0.33/-0.23

Table S9. Fractional Atomic Coordinates ($\times 10^4$) and Equivalent Isotropic Displacement Parameters ($Å^2 \times 10^3$) for (7). U_{eq} is defined as 1/3 of of the trace of the orthogonalised U_{IJ} tensor.

Atom	*x*	*y*	*z*	U(eq)
F1	8477(3)	3618(2)	2332(2)	45.8(7)
F1'	6071(9)	5053(7)	4850(7)	45.8(7)
C26	4237.5(16)	1555.7(15)	4854.5(15)	37.7(5)
C15	6414.6(16)	5934.5(14)	3345.9(16)	37.3(5)
C14	7009.4(18)	5987.0(15)	2362.4(16)	41.9(5)
C13	7733.6(18)	5203.7(15)	2020.7(15)	42.3(5)
C22	7398.4(15)	3369.9(12)	4342.2(12)	26.7(4)
C23	6334.0(14)	2774.1(12)	4519.9(13)	26.8(4)
C21	8559.2(14)	3102.0(12)	4811.5(13)	26.5(4)
C11	7272.4(14)	4285.8(13)	3658.6(13)	29.2(4)
C24	5147.2(15)	2996.4(14)	4026.5(14)	32.3(4)
C27	5343.0(15)	1305.8(14)	5333.4(14)	32.6(4)
C16	6553.6(15)	5090.9(14)	3989.9(14)	32.2(4)
C25	4136.6(16)	2410.9(15)	4188.5(15)	37.3(5)
C12	7854.8(17)	4360.1(14)	2658.6(14)	36.8(5)

Table S10. Anisotropic Displacement Parameters ($Å^2 \times 10^3$) for (7). The Anisotropic displacement factor exponent takes the form: $-2\pi^2[h^2a^{*2}U_{11}+2hka^*b^*U_{12}+\ldots]$.

Atom	U_{11}	U_{22}	U_{33}	U_{23}	U_{13}	U_{12}
F1	59.7(16)	44.9(17)	33.5(14)	3.7(12)	17.6(12)	7.0(14)
F1'	59.7(16)	44.9(17)	33.5(14)	3.7(12)	17.6(12)	7.0(14)
C26	31.9(9)	34.7(11)	46.4(11)	1.0(8)	-0.5(8)	-8.5(7)
C15	34.6(9)	31.1(11)	46.0(11)	2.7(8)	-6.3(8)	0.3(7)
C14	48.0(11)	37.0(12)	40.6(11)	11.0(8)	-7.7(9)	-4.9(9)
C13	55.1(11)	40.5(12)	31.6(10)	9.5(8)	5.9(8)	-4.0(9)
C22	33.2(9)	25.0(9)	22.0(8)	-2.9(7)	2.6(7)	-2.7(7)
C23	31.5(8)	25.8(9)	23.1(8)	-3.4(7)	1.2(6)	-2.9(7)
C21	31.0(8)	24.1(9)	24.4(8)	-3.8(7)	3.0(6)	-2.2(7)
C11	29.1(8)	28.7(9)	29.8(9)	1.2(7)	-3.0(7)	-5.0(7)
C24	36.6(9)	29.5(10)	30.8(9)	0.9(7)	-2.0(7)	-1.7(7)
C27	36.4(9)	27.4(10)	34.0(9)	0.9(7)	2.8(7)	-4.6(7)
C16	30.2(8)	31.9(10)	34.5(10)	0.9(8)	-2.2(7)	-3.3(7)
C25	32.1(9)	36.4(11)	43.1(10)	0.0(8)	-6.1(8)	-3.6(8)
C12	44.7(10)	32.3(11)	33.6(9)	3.0(8)	4.3(8)	-2.4(8)

Table S11. Bond Lengths for (7).

Atom	Atom	Length/Å	Atom	Atom	Length/Å
F1	C12	1.266(3)	C22	C11	1.493(2)
F1'	C16	1.186(8)	C23	C21[1]	1.437(2)
C26	C27	1.355(3)	C23	C24	1.430(2)
C26	C25	1.412(3)	C21	C23[1]	1.437(2)
C15	C14	1.379(3)	C21	C27[1]	1.431(2)
C15	C16	1.387(3)	C11	C16	1.390(3)
C14	C13	1.375(3)	C11	C12	1.392(2)
C13	C12	1.381(3)	C24	C25	1.354(2)
C22	C23	1.411(2)	C27	C21[1]	1.431(2)
C22	C21	1.407(2)			

[1]3/2-X,1/2-Y,1-Z

Table S12. Bond Angles for (7).

Atom	Atom	Atom	Angle/°	Atom	Atom	Atom	Angle/°
C27	C26	C25	120.71(16)	C16	C11	C22	121.21(15)
C14	C15	C16	119.76(17)	C16	C11	C12	117.50(16)
C13	C14	C15	120.02(17)	C12	C11	C22	121.29(16)
C14	C13	C12	119.96(17)	C25	C24	C23	121.52(17)
C23	C22	C11	119.16(14)	C26	C27	C21[1]	121.42(17)
C21	C22	C23	120.07(15)	F1'	C16	C15	120.0(5)
C21	C22	C11	120.76(14)	F1'	C16	C11	118.7(5)
C22	C23	C21[1]	119.64(15)	C15	C16	C11	121.31(16)
C22	C23	C24	121.99(16)	C24	C25	C26	120.17(16)
C24	C23	C21[1]	118.34(15)	F1	C12	C13	120.53(19)
C22	C21	C23[1]	120.28(15)	F1	C12	C11	118.0(2)
C22	C21	C27[1]	121.87(16)	C13	C12	C11	121.44(18)
C27[1]	C21	C23[1]	117.83(15)				

[1]3/2-X,1/2-Y,1-Z

Table S13. Hydrogen Atom Coordinates (Å×10^4) and Isotropic Displacement Parameters (Å^2×10^3) for (7).

Atom	*x*	*y*	*z*	U(eq)
H26	3537	1160	4966	45
H15	5922	6463	3577	45
H14	6921	6552	1930	50
H13	8142	5242	1361	51
H24	5068	3556	3584	39
H27	5390	737	5766	39
H16	6158	5063	4657	39
H25	3374	2572	3860	45
H12	8336	3830	2415	44

Table S14. Atomic Occupancy for (7).

Atom	*Occupancy*	Atom	*Occupancy*	Atom	*Occupancy*
F1	0.38	F1'	0.12	H16	0.38
H12	0.12				

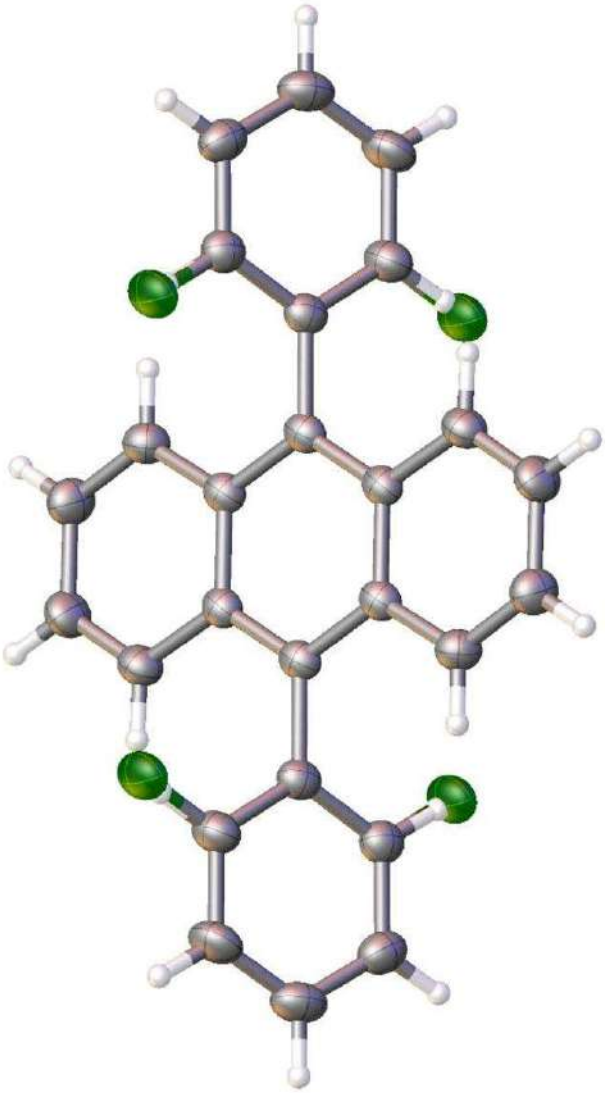

Figure S27. ORTEP plot of (7) in the crystal. Thermal ellipsoids are given at 50% probability level.

5. DFT Calculations

All DFT calculations were performed in Priroda package, [2] with PBE funcional[3] and tz2p basis. Reaction paths were controlled by IRC procedure[4].

TS1 (Nucleophilic attack C-F; diflourobenzophenone).

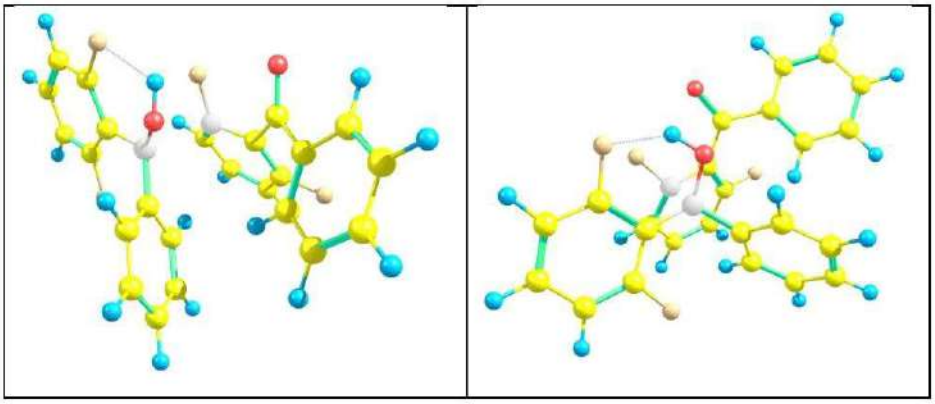

6	-5.649087220	-3.011622200	0.498695590
6	-7.022945230	-3.178656970	0.599387850
6	-7.786395240	-2.283181000	1.353378980
6	-7.119824930	-1.240100780	2.003038890
6	-5.746426010	-1.110600750	1.875579610
6	-4.896848010	-1.963030410	1.107454420
6	-3.473427160	-1.714999060	0.870495270
8	-2.820855770	-0.816596430	1.740681680
6	-2.514910780	-2.846215430	0.632297150
6	-2.316548710	-3.457945610	-0.617009120
6	-1.348435010	-4.449798770	-0.786781840
6	-0.546997410	-4.857699610	0.284370860
6	-0.724459500	-4.250738820	1.531655390
6	-1.687405570	-3.254615320	1.699401050
9	-4.991373290	-3.965599710	-0.229364650
9	-5.195392310	-0.055277010	2.575949100
1	-3.402699520	-0.041872650	1.843727190
1	-7.472532240	-4.026946290	0.083336900
1	-8.866182250	-2.396669310	1.436411030
1	-7.647934780	-0.510845630	2.616952190
1	-2.911048340	-3.139023730	-1.469858490
1	-1.207021610	-4.894063900	-1.774096230
1	0.213700190	-5.628286870	0.145290630
1	-0.102383120	-4.547114440	2.379200030
1	-1.800114820	-2.762008190	2.664282580
6	-3.604690130	-0.369701850	-0.915911670
6	-4.431185400	-0.959233770	-1.923089670

6	-3.890922020	-1.388758950	-3.116802720
6	-2.522807240	-1.193996390	-3.406330850
6	-1.752024850	-0.527177130	-2.464315600
6	-2.226137080	-0.036958340	-1.235400850
6	-1.417197620	0.875453580	-0.384137970
6	0.035572960	0.558425340	-0.116048040
8	-1.892668060	1.912571600	0.105990480
6	0.551918610	-0.745981080	-0.146705300
6	0.879295790	1.613806040	0.269629540
6	2.213874270	1.376062270	0.596299550
6	2.721857690	0.071774800	0.561031210
6	1.884682960	-0.986641570	0.193805700
9	-4.284215800	0.563529270	-0.124379110
1	-5.492868650	-1.072360570	-1.705965020
1	-4.531603840	-1.875938270	-3.854528450
1	-2.078818070	-1.485924820	-4.355905890
9	-0.457450980	-0.243515410	-2.833006310
1	-0.100443010	-1.576749950	-0.414345330
1	2.266331510	-2.009164160	0.180693860
1	3.764020770	-0.118986350	0.825497190
1	2.861259790	2.207072450	0.884743030
1	0.451237050	2.615882170	0.314706200

TS2 (Nucleophilic attack C=O; diflourobenzophenone).

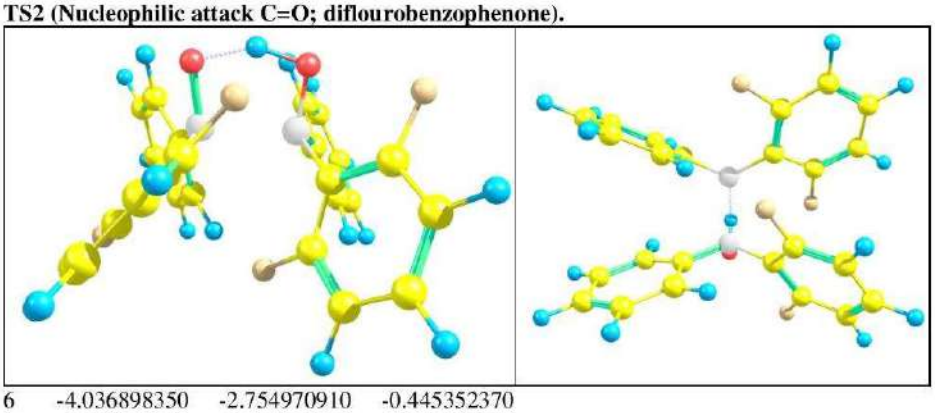

6	-4.036898350	-2.754970910	-0.445352370
6	-5.328840520	-3.074975070	-0.853386040
6	-6.390561600	-2.805994380	0.007359690
6	-6.122558170	-2.245784390	1.255099730
6	-4.808103190	-1.948667010	1.617435280
6	-3.689204850	-2.151843930	0.776242700
6	-2.261557400	-1.766945780	1.180582070
8	-2.225114170	-0.861931410	2.199899810
6	-1.408712220	-2.983360890	1.509049000
6	-0.243660770	-2.774375840	2.273795750
6	0.581065750	-3.833549780	2.645378480
6	0.261024480	-5.146780160	2.280000960
6	-0.902080860	-5.375171920	1.542469310
6	-1.724811660	-4.309008200	1.164048610
9	-3.042815960	-3.086331610	-1.326234360
9	-4.654453340	-1.470128790	2.875465660
1	-1.771924340	0.000434100	1.680118390
1	-5.474202750	-3.524031290	-1.834876980
1	-7.413959680	-3.040063020	-0.286211830
1	-6.913452240	-2.040540270	1.975914040
1	-0.011923920	-1.754945960	2.578116800
1	1.483199070	-3.634137320	3.227932510
1	0.904935170	-5.978138390	2.573520640
1	-1.180558900	-6.393288930	1.260486410
1	-2.631180240	-4.526004640	0.601008880
6	-3.554322680	0.449167060	-1.023896300
6	-4.450223970	0.917700190	-1.981304120
6	-4.183578470	0.709743930	-3.333726850
6	-3.016387280	0.039908950	-3.690141080
6	-2.149789420	-0.412084780	-2.694147990
6	-2.361001310	-0.258505920	-1.308902700
6	-1.386368720	-0.597262810	-0.163723070
6	-0.060795090	-1.268065270	-0.547944850
8	-1.210700770	0.491018230	0.589339230
6	0.073388110	-2.529625750	-1.152355030
6	1.117293590	-0.584186370	-0.206249730

6	2.378690660	-1.128456180	-0.463621720
6	2.495046910	-2.384572820	-1.063280490
6	1.330155040	-3.080480950	-1.403781230
9	-3.891552910	0.711800140	0.262274210
1	-5.343013390	1.440253820	-1.640021620
1	-4.872828490	1.069901610	-4.097703720
1	-2.743836330	-0.136661920	-4.730286980
9	-1.023721780	-1.027872310	-3.158200850
1	-0.813158320	-3.092332500	-1.430702230
1	1.400240480	-4.069366530	-1.862192730
1	3.477203350	-2.820193530	-1.258477010
1	3.275263870	-0.567361960	-0.188644650
1	1.004607650	0.385088830	0.278651790

TS2 (Nucleophilic attack C-F; flourobenzophenone).

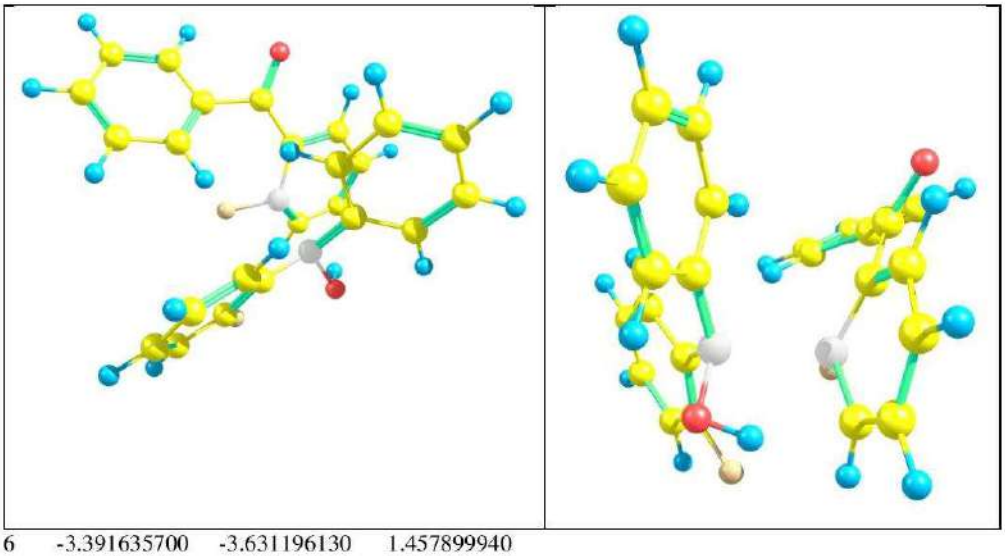

6	-3.391635700	-3.631196130	1.457899940
6	-2.479131870	-4.572625230	1.935774660
6	-1.743979500	-4.318278600	3.096233310
6	-1.951041320	-3.109392700	3.766650550
6	-2.860084200	-2.183021150	3.268517600
6	-3.614393080	-2.384724530	2.088232680
6	-4.600231790	-1.375270940	1.599137790
8	-5.393817310	-0.934656190	2.680105150
6	-5.433578170	-1.743016680	0.413514310
6	-6.839924860	-1.676561350	0.496799270
6	-7.649413490	-1.964016040	-0.601412500
6	-7.081165060	-2.318158570	-1.830910000
6	-5.690318200	-2.386714270	-1.935535700
6	-4.879667370	-2.103764290	-0.833439370
1	-3.969125920	-3.862152170	0.564295080
9	-2.991878230	-1.032983180	3.988529060
1	-5.333181010	0.058077050	2.659428450
1	-2.352418770	-5.514341530	1.398678900
1	-1.023795300	-5.042612060	3.478607140
1	-1.405387300	-2.858080800	4.676603100
1	-7.279952770	-1.392319830	1.451366860
1	-8.735612120	-1.907370540	-0.497908170
1	-7.712975370	-2.532079560	-2.694913570
1	-5.223875300	-2.643388440	-2.888275760
1	-3.800418180	-2.163695000	-0.955529520
6	-3.556987290	0.366977200	1.073130150
6	-4.150984840	1.339569630	1.987502170
6	-5.167258460	2.174230490	1.570730060
6	-5.563670460	2.192959040	0.212163050

6	-4.784458170	1.511338850	-0.710280780
6	-3.680550070	0.701008660	-0.351135960
6	-2.762065800	0.389087740	-1.457896360
6	-1.421899210	-0.314750190	-1.306439710
8	-3.009011180	0.777320900	-2.623574990
6	-1.185617210	-1.477540460	-0.558868610
6	-0.372692740	0.188611670	-2.099081950
6	0.876515000	-0.430631770	-2.120562770
6	1.095173130	-1.597169140	-1.378364030
6	0.054890640	-2.120877790	-0.607168200
9	-2.257764980	0.038395180	1.490095930
1	-3.744813450	1.380894230	2.998800760
1	-5.634264990	2.852897040	2.289516490
1	-6.392433580	2.820482230	-0.116415870
1	-4.945077200	1.644171050	-1.780727510
1	-1.962406280	-1.892096000	0.077745010
1	0.203530190	-3.033078240	-0.026132510
1	2.067670000	-2.093041170	-1.402697940
1	1.680918180	-0.008312700	-2.726832440
1	-0.571855890	1.069367480	-2.709403650

TS4 (Nucleophilic attack C=O; flourobenzophenone).

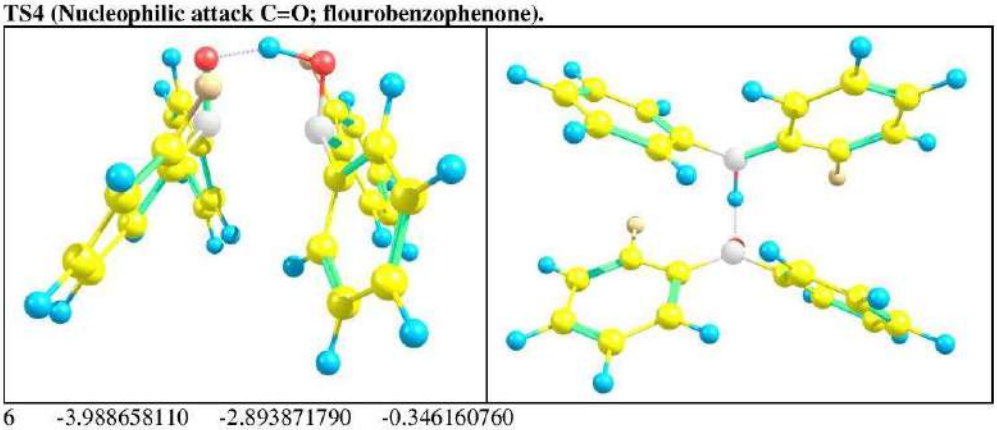

6	-3.988658110	-2.893871790	-0.346160760
6	-5.290849460	-3.154181380	-0.776909080
6	-6.387088520	-2.713604990	-0.028077040
6	-6.154219630	-2.000721860	1.153698220
6	-4.852209960	-1.739372040	1.580700410
6	-3.734321050	-2.194979280	0.852862080
6	-2.360116280	-1.881922430	1.369021780
8	-2.321923030	-0.929385950	2.324830010
6	-1.448028990	-3.041778240	1.609418350
6	-0.199570180	-2.898530210	2.264888330
6	0.652287090	-3.965344990	2.532929550
6	0.305635290	-5.260712380	2.141384290
6	-0.922277660	-5.456288690	1.505485530
6	-1.764929800	-4.373761210	1.249466560
1	-1.854562050	-0.064629810	1.789366640
1	-5.449781580	-3.686302630	-1.717366530
1	-7.405609470	-2.914093750	-0.365776080
1	-6.997805070	-1.636350780	1.744947000
1	1.597862620	-3.751646480	3.032287640
1	0.972577660	-6.097510110	2.353377930
1	-1.230182170	-6.457537470	1.197432680
6	-3.550193330	0.516107250	-1.030846070
6	-4.445141760	0.827256600	-2.050468970
6	-4.164444710	0.457046100	-3.367319220
6	-2.975627670	-0.226119840	-3.631539770
6	-2.091237590	-0.526452870	-2.593530300
6	-2.344073650	-0.190323830	-1.245004980
6	-1.356378180	-0.428369520	-0.131749010
6	-0.061795820	-1.100418920	-0.509873450
8	-1.276611630	0.522171990	0.773055680
6	0.029743130	-2.320872970	-1.208192050
6	1.142749320	-0.478461540	-0.130620170
6	2.380360340	-1.035199690	-0.455377280
6	2.453467080	-2.240279060	-1.162741110
6	1.266341010	-2.881409950	-1.532577810

9	-3.905307110	0.924127140	0.213913320
1	-5.357670320	1.362866910	-1.787371900
1	-4.869396600	0.691878320	-4.166132260
1	-2.719458380	-0.511675660	-4.653653280
1	-1.160314210	-1.039143340	-2.829105300
1	-0.881411540	-2.854153890	-1.480096850
1	1.302955880	-3.836588230	-2.060667990
1	3.420732730	-2.679464010	-1.414136160
1	3.297649370	-0.527533860	-0.147701900
1	1.066935680	0.447163370	0.439613420
1	-4.658561810	-1.168349400	2.488126900
1	-3.152242690	-3.217596910	-0.965975430
1	-2.728447520	-4.561884270	0.779499300
9	0.236015900	-1.678825040	2.677771710

6. References

[1] Z. Li, R. J. Twieg. *Chem. Eur. J.* **2015**, 21, 15534 –15539.

[2] Laikov D.N. *Chem. Phys. Lett.* **1997**, vol. 281, pp. 151-156.

[3] J. P. Perdew, K. Burke, M. Ernzerhof, *Phys. Rev. Lett.* **1996**, *77*, 3865; J. P. Perdew, K. Burke, M. Ernzerhof, *Phys. Rev. Lett.* **1997**, *78*, 1396

[4] K. Fukui, *Acc. Chem. Res.* **1981**, 14, 363.

Publication 3.

Tailoring Diindenochrysene through Intramolecular Multi-Assemblies by C-F Bond Activation on Aluminum Oxide.

V. Akhmetov, M. Feofanov, S. Troyanov, K. Y. Amsharov.

Chem. - A Eur. J. **2019**, 25, 7607-7612. DOI:10.1002/chem.201901450.

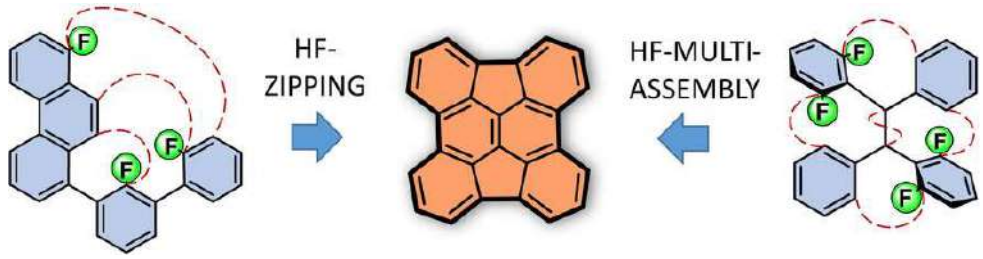

ABSTRACT:

The unique nature of the alumina-mediated cyclodehydrofluorination gives the opportunity to execute the preprogrammed algorithm of the C−C couplings rationally built into a precursor. Such multi-assemblies facilitate the construction of the carbon-skeleton, superseding the conventional step-by-step by the one-pot intramolecular assembly. In this work, the feasibility of the alumina-mediated C−F bond activation approach for multi-assembly is demonstrated on the example of a fundamental bowl-shaped polycyclic aromatic hydrocarbon (diindenochrysene) through the formation of all “missing” C−C bonds at the last step. Among valuable insights into the reaction mechanism and the design of the precursors, a facile pathway enabling the two-step synthesis of diindenochrysene was elaborated, in which five C−C bonds form in a single synthetic step. It is shown that the relative positions of fluorine atoms play a crucial role in the outcome of the assembly and that governing the substituent positions enables the design of effective precursor molecules “programmed” for the consecutive C−C bond formations. In general, these findings push the state of the field towards the facile synthesis of sophisticated bowl-shaped carbon-based nanostructures through multi-assembly of fluoroarenes.

CHEMISTRY
A European Journal

A Journal of

ChemPubSoc Europe

www.chemeurj.org

2019-25/32

Cover Feature:
K. Amsharov et al.
Tailoring Diindenochrysene through Intramolecular Multi-Assemblies by C–F Bond Activation on Aluminum Oxide

Supported by

ACES Asian Chemical Editorial Society

WILEY-VCH

ChemPubSoc Europe
DOI: 10.1002/chem.201901450
CHEMISTRY A European Journal Communication

Aryl–Aryl Coupling

Tailoring Diindenochrysene through Intramolecular Multi-Assemblies by C–F Bond Activation on Aluminum Oxide

Vladimir Akhmetov,[a] Mikhail Feofanov,[a] Sergey Troyanov,[b] and Konstantin Amsharov*[a]

Abstract: The unique nature of the alumina-mediated cyclodehydrofluorination gives the opportunity to execute the preprogrammed algorithm of the C–C couplings rationally built into a precursor. Such multi-assemblies facilitate the construction of the carbon-skeleton, superseding the conventional step-by-step by the one-pot intramolecular assembly. In this work, the feasibility of the alumina-mediated C–F bond activation approach for multi-assembly is demonstrated on the example of a fundamental bowl-shaped polycyclic aromatic hydrocarbon (diindenochrysene) through the formation of all "missing" C–C bonds at the last step. Beside valuable insights into the reaction mechanism and the design of the precursors, a facile pathway enabling the two-step synthesis of diindenochrysene was elaborated, in which five C–C bonds form in a single synthetic step. It is shown that the relative positions of fluorine atoms play a crucial role in the outcome of the assembly and that governing the substituent positions enables the design of effective precursor molecules "programmed" for the consecutive C–C bond formations. In general, these findings push the state of the field towards the facile synthesis of sophisticated bowl-shaped carbon-based nanostructures through multi-assembly of fluoroarenes.

Geodesic polyarenes constitute a unique group of polycyclic aromatic hydrocarbons (PAHs) that contain pentagons and possess a concave surface,[1–3] which formally can be considered as fragments of the fullerene cages. Although the synthesis of the smallest representative, corannulene, has been known for more than fifty years,[4,5] organic chemistry still faces a lack of approaches that allow for a facile synthesis of this class of molecules. Among the main reasons for this are the substantial strain energies, which need to be overcome to create bowl-shaped geometry. The following existing approaches, such as flash-vacuum pyrolysis (FVP),[6] Pd-catalyzed arylation,[7–9] and coupling through C–F bond activation,[10–14] must be mentioned. Although the first two methods face both low group tolerance and moderate yields, the last one often possess high selectivity and frequently leads to nearly quantitative yields showing tolerance to various functional groups.[15,16] Diindeno[1,2,3,4-*defg*:1′,2′,3′,4′-*mnop*]chrysene (**1**) is one of the simplest representative of geodesic polyarenes containing two pentagons. It possesses intriguing both physical and chemical properties. For example, **1** may react with electrophiles at the periphery as a conventional PAHs to give a product of S_EAr; alternatively, it also reacts in fullerene-like (olefin) fashion with both nucleophiles and electrophiles through addition to the central double bond.[1,17] Although **1** appears as an easy target molecule, there are only two currently published approaches allowing for its synthesis (Figure 1).[18–22] The first has been reported by Scott and co-workers, in which the flash vacuum pyrolysis approach was employed. Another known pathway is based on intramolecular Pd-catalyzed aryl-aryl coupling. Both methods have some severe limitations, including low overall yields and moderate yields at the last step. In this regard, alumina-mediated HF elimination appears to be an attractive alternative allowing for an effective and selective aryl–aryl coupling. Here, we report facile synthesis of 1 and its derivatives through C–F bond activation on alumina, exploiting various multiple-bond assemblies.

Figure 1. Known and implemented in this work approaches to the synthesis of diindenochrysene.

[a] V. Akhmetov, M. Feofanov, Dr. K. Amsharov
Department of Chemistry and Pharmacy, Organic Chemistry II
Friedrich-Alexander University Erlangen-Nürnberg
Nikolaus-Fiebiger Str. 10, 91058 Erlangen (Germany)
E-mail: konstantin.amsharov@fau.de

[b] Prof. Dr. S. Troyanov
Institut für Chemie, Humboldt-Universität zu Berlin
Brook-Taylor-Str. 2, 12489 Berlin-Adlershof (Germany)

Supporting information and the ORCID identification number(s) for the author(s) of this article can be found under: https://doi.org/10.1002/chem.201901450.

In accordance with our experience in the field, the cove region serves as a very attractive fragment to create five-membered rings through intramolecular aryl–aryl coupling (cove-region closure),[10,12] hence, our first approach included simultaneous closure of two cove regions (Figure 2). The required dibenzochrysene core can be obtained by using several known procedures,[23–27] however, not all of them are suitable for the synthesis of derivatives with fluorine atoms in cove regions. We have proposed a simple synthetic route to **4** and **5** with two substituents on the periphery. However, during the synthesis of **4**, formation of traces of several regioisomers (see the Supporting Information) makes it barely possible to isolate the desired precursor in pure form. Nevertheless, using the mixture of the regioisomers of **4** for the next step permits to obtain the desired diindenochrysene derivative **6** in substantial yields of 60%.

To avoid the formation of the mixture of isomers along with **4**, we have modified our approach by replacing the methyl groups with fluorine atoms. As a result of this modification, we were able to synthesize **5** as a single product and to confirm its structure by means of X-ray crystallography (see the Supporting Information). The synthesis of **7** was implemented in five steps with the overall yield of 26%, which is comparable or even exceeds the yields of the last stages implemented in the previously known approaches. Furthermore, the HPLC monitoring of the last step demonstrates the essential absence of the side products and gradual full conversion of the initial dibenzochrysene to give the desired **7** in 80% yield (Figure 2c). Thus, the final product requires virtually no further purification. The obtained derivatives **6** and **7** were fully characterized by analytical methods including X-ray crystallography (Figure 2b). These findings make this approach superior over all existing alternative methods and allow us to consider the alumina-mediated HF elimination as a selective and efficient tool to obtain various geodesic polyarenes and their derivatives. Although the scheme described above allow for the synthesis of highly interesting derivatives in high yields exploiting conventional reactions, it still possesses some complications during the implementation and requires multistep synthesis of the precursors. One of the possibilities to improve the procedure is to postpone the maximal number of C–C bonds formation to the last step. Following this logic, we synthesized and investigated precursors **8**, **9** and **10**, which could be directly converted to **1** through consecutive triple domino-like aryl–aryl couplings (Figure 3). Indeed, the cyclization of **8** allowed us to obtain **1** through triple HF-zipping with quite moderate yields, which was connected to the unexpected side product **11** containing dibenzofuran fragment.

This observation indicates that the presence of fluorine in **8** within the phenanthrene core exacerbates the first electrophilic attack, redirecting the pathway of the reaction to the hydrolysis of C–F bond forming **11**. This viewpoint accounts for the absence of such a by-product in the case of **9**, where the reaction breaks off as soon as **12** is formed. According to our current knowledge on the mechanism of the alumina mediated HF elimination the reaction takes place via cation intermediates formed after S_EAr-like attack.[28] The relative positions of the fluorine atoms can be rationally altered to exclude/mini-

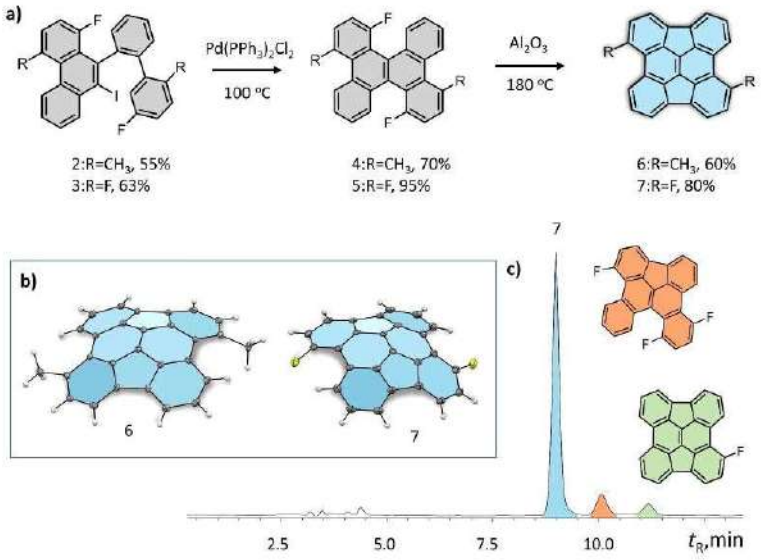

Figure 2. a) The synthesis of **6** and **7** through cove-region closures. b) ORTEP plot of **6** and **7** in the crystal. Thermal ellipsoids are drawn at the 50% probability level (only one orientation of **7** in the crystal is shown for clarity). c) HPLC profile of the reactionary mixture of **7** as obtained after reaction. Minor side products and the respective peaks on HPLC are coded by the same color.

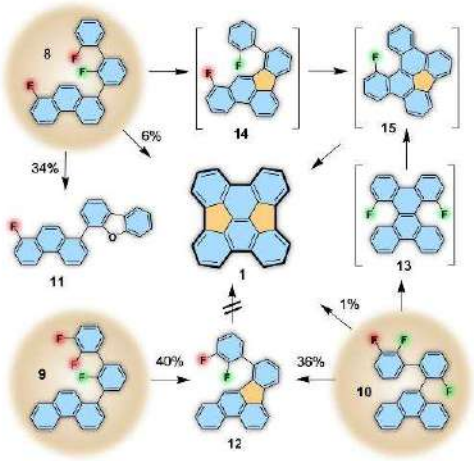

Figure 3. Implemented approaches to 1 through consecutive triple aryl–aryl coupling. "Active" and "inactive" fluorine atoms coded by green and red, respectively.

mize undesired electron withdrawing effect on the attacked π-system and thus to facilitate the reaction. Our current efforts show that it is important not only to take into a consideration the electron-withdrawing effects of the fluorine but also their mutual effect. Both **9** and **10** after HF elimination gave **12** as the major product, showing that such an *ortho*-position of the fluorine atoms does not allow for further coupling. Precursor **10** combines advantages of both **8** and **9**, having all electron-withdrawing groups out of the attacked π-system and no adjacent fluorine atoms in the bay-region, which could lead to the by-product analogous to **11**. Moreover, **10** has flexibility in terms of the choice of which cycle to form first. It might be either the five-membered ring to give **12** or the six-membered ring to give the corresponding dibenzochrysene derivative **13**. We found that the pentagon formation dominates, which leads to the abruption of further reactivity, whereas **1** forms as a minor product. Notably, no other products were observed according to HPLC analysis showing only two distinct peaks corresponding to **1** and **12**. These findings also reveal that transformation of **10** to **13** is considerably hindered supposedly due to appearance of two cove regions, leading to the substantial strain energy connected with the π-system twisting.

In the course of our attempts to obtain **1** through **8**, **9**, and **10** we have observed valuable results that shed a light on some idiosyncrasies of the alumina mediated HF elimination. First of all, we found out that, beside the necessity to facilitate the S_EAr-like step, there are some other factors affecting the eventual product formation. It remains unclear why **12** does not undergo the second HF elimination, whereas **14** readily reacts, considering that the latter is supposed to be less prone to undergo the electrophilic attacks. We tested several precursors that might lead to **1** through three consequent C–C bond formations and found that **8** indeed gives **1** on activated alumina, which makes the reaction attractive because only a few steps exploiting conventional methods are required to obtain **8**. Moreover, the experimental data provide us with some valuable insights into the design of the precursors for other related buckybowls.

Our further endeavors were aimed to manage the formation of the maximum number of C–C bonds at the last stage. According to this strategy, we have attempted to implement the synthetic scheme (Figure 4a) in which **1** was supposed to form from **16** after the sequence of four aryl–aryl couplings. Unfortunately, our efforts led neither to the desired product nor to any of the expected intermediate products, nevertheless the initial reagent was not observed in the extract after the reaction. The observed experimental data evidence that the attack of the formed cation-like species does not occur and some other side reactions proceed leading to the irreversible adsorption of the by-products on the solid phase. We assume that the reaction can be hindered by two possible factors. The unfavorable rigid geometry and, thus, the lack of the conformational flexibility, which plays the crucial role in the intramolecular interactions, serves as the first factor. Secondly, the reactive double C–C bond of **16** might be polarized on frustrated Lewis pairs formed on the surface of activated alumina, thus leading to undesired side reactions.

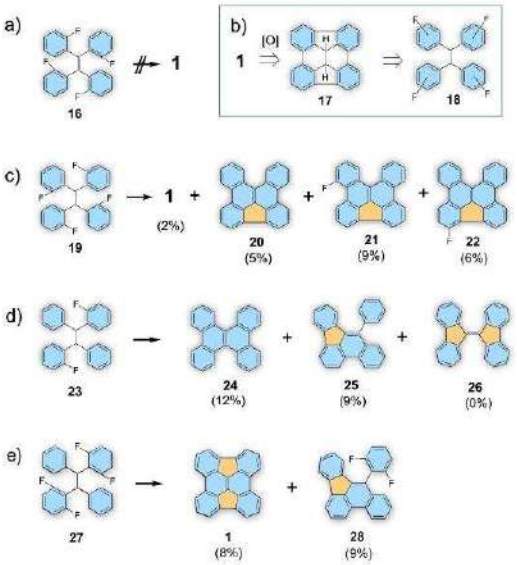

Figure 4. Multi-assemblies of fluorinated tetraphenyl ethanes.

To avoid the undesired reactions of the double bond and to increase the number of possible conformers, we modified our approach as shown in Figure 4b. The incorporation of sp^3-hybridized carbon atoms in **17** introduces additional flexibility into a system circumventing substantial strain energy arising during aryl–aryl coupling otherwise. The required precursor **18** can be obtained by standard McMurry coupling of the respective fluorinated benzophenone.[28] Thus, we have suggested a possible pathway enabling facile three-step synthesis of **1** from **19**. After subjecting **19** to the conditions of the alumina-mediated HF elimination we observed a rather complicated mixture, nevertheless we managed to isolate three major fractions by HPLC. Surprisingly, instead of the expected intermediate **17**, we observed the formation of the target molecule **1** along with several interesting side products, such as **20**, **21** and **22**. At this point, multiple fundamental questions arise, first of all the major question is how the formation of the middle double bond occurs. Therefore, we investigated whether dehydrogenation may occur under the conditions of HF elimination. For this purpose, we subjected *9H,9'H*-9,9'-bifluorene to activated alumina under vacuum and observed a significant conversion to 9,9'-bifluorenylidene, which was detected by HPLC analysis. This transformation shows that alumina can initiate the dehydrogenation. Moreover, in accordance with the previous experiment (Figure 4a), the dehydrogenation step must occur no sooner as at least one of C(aryl)–C(aryl) bond is formed. Otherwise, it leads to **16** and the abruption of the further reaction. One of the possible explanations for the presence of **20** is supported by the formation of the cation-like species, which can hardly undergo intramolecular S_EAr due to the presence of the electron-withdrawing groups. The system may undergo several alternative reactions, for example, a double bond formation through loss of HF (see Supporting Information); thus, three out of four fluorine atoms are responsible for the aryl–aryl coupling, whereas the elimination of the fourth HF leads to the double bond formation. The described above processes may serve as an account for the formation of both **1** and **20**, however the mechanism leading to the formation of **21** and **22** remains obscure. The *ipso*-substitution appears to be the only reasonable explanation of the observations, which accounts for the positions of the fluorine atoms in **21** and **22** (see Supporting Information). Given that we consider the S_EAr to be the direction-determining step, all three processes described above as side reactions might be suppressed upon the facilitation of S_EAr. It comes naturally to promote the electrophilic attack through disposal of fluorine atoms from the π-system. For this reason, we obtained **23**, which is supposed to undergo S_EAr easily, and could also shed a light on the sequence of couplings. The following experiment (Figure 4d) revealed two main products **24** and **25**, which correspond to double HF and H_2 elimination. In addition, by means of HPLC we found some phenanthrene derivatives, which were not isolated or characterized though; however, the collected data allow us to conclude that first the six-membered ring forms, leading to diphenylphenanthrene derivatives, after which multiple pathways are possible. Having these observations in hand, we tried to carry out the synthesis of **1** in the most efficient way. The precursor **27** possesses both flexibility of sp^3-hybridized atoms and non-substituted phenyl rings that may be readily attacked by electrophiles. As expected, **27** gave **1** after creation of five C–C bonds in quite reasonable yield along with the intermediate (**28**). Moreover, the attempt to obtain **1** from **28** revealed that **28** does not undergo aryl–aryl coupling on alumina, which allowed us to claim that **1** forms via another intermediate.

To establish the pathway that takes place during the transformation of **27** to **1**, we applied Bell–Evans–Polanyi principle to estimate relative rates of the competing reactions. For this purpose, we have calculated the differences between the enthalpies of formation of the precursors before HF elimination and corresponding σ-complexes formed during S_EAr-like process. The calculations were carried at the B3LYP/6-31G(d) level. Having in hand experimental results, such as the formation of **24** and **25** from **23** and the absence of **26**, one may reasonably infer the sequence of events, according to which the six-membered ring forms, whereas the two options for the second aryl–aryl coupling occur in equal shares considering that the eventual yields of **24** and **25** are comparable. These experimental observations are in line with the calculated data (Figure 5a), which predict the prevalence of **IM2**, leading to the phenanthrene derivative during the first step, and the equality between **IM4** and **IM5**, leading to **24** and **25**, respectively. In the case of **27**, the DFT data reveal a similar preference toward the formation of **IM7** over the **IM6**; this leads to the formation of **IM8**, which has three further pathways. Leaving aside **IM9** as an obviously unfavorable direction, we found out that the formation of **IM11** should prevail over **IM10**, in contrast to the analogous situation with **IM4** and **IM5** in which **24** and **25** are formed with almost the same yield. Taking into account the fact that **28** does not yield **1**, both experimental and DFT data prove that the formation of **1** occurs via **IM10** and the following closures of the cove regions. Both **23** and **27** are obtained as mixtures of diastereomers from the corresponding fluorinated benzophenones, thus, beside the variability in terms of the competition between formation of five- and six-membered ring at the first stage, there is also a competition between two diastereomers leading to either *syn*- or *anti*- dislocation of hydrogens adjacent to sp^3-carbon atoms. The calculations show that the *anti*-position generally prevails over *syn*-, not significantly though. Moreover, aromatization appears to occur after the first aryl–aryl coupling, thus, eliminating the issue in the following closures.

In summary, we contribute to the fundamental study of C–C bond formation in PAHs and report a comprehensive set of C–C coupling reactions, demonstrating the viability of the algorithm execution concept. We showed that the multiple C–C coupling can be performed in a truly domino-like fashion and the whole process can be rationally governed by managing the electronic effects. To our surprise and pleasure, we also discovered that alumina allows for effective one-pot multi C–C coupling/aromatization. In general, we demonstrate the unprecedentedly high flexibility in the design of precursors showing five new synthetic approaches to diindenochrysene core. Additionally, structurally related PAHs, such as chrysene derivatives

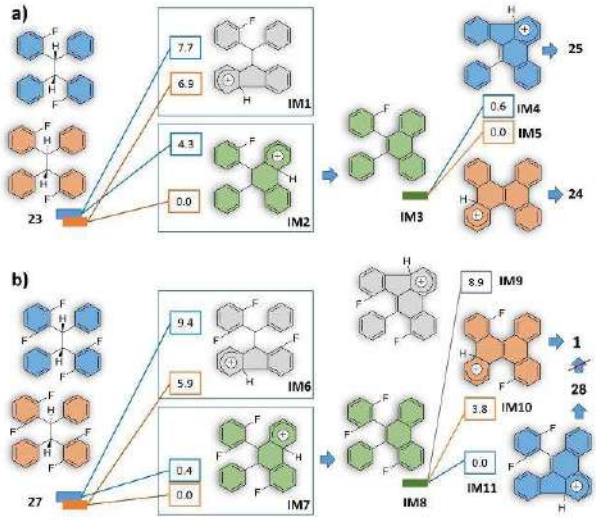

Figure 5. Graphical representation of the DFT-based thermochemical analysis. The ΔH values (kcal mol^{-1}) for the fluorinated precursors and corresponding σ-complexes are referenced to the lowest value in each separate step.

20, **24** and **25**, which are hardly available and require meticulous synthesis, might be easily obtained exploiting our approach. Moreover, the multi-assembly of **27** appears to be a very attractive approach for the preparative synthesis of **1** because it can be obtained just in one step. We also suppose that the multi-assembly approach through C–F bond activation on alumina will provide facile access to other interesting related bowl-shaped PAH systems.

Acknowledgements

Authors are thankful to Dr. Harald Maid for NMR measurements and spectra interpretations. Funded by the Deutsche Forschungsgemeinschaft (DFG; Projektnummer 182849149–SFB 953, AM407).

Conflict of interest

The authors declare no conflict of interest.

Keywords: aromatization · buckybowls · C–C coupling · C–F activation · multi-assembly

[1] L. T. Scott, H. E. Bronstein, D. V. Preda, R. B. M. Ansems, M. S. Bratcher, S. Hagen, *Pure Appl. Chem.* **1999**, *71*, 209–219.
[2] Y. T. Wu, J. S. Siegel, *Chem. Rev.* **2006**, *106*, 4843–4867.
[3] B. Trzaskowski, L. Adamowicz, W. Beck, K. Muralidharan, P. A. Deymier, *Chem. Phys. Lett.* **2014**, *595–596*, 6–12.
[4] W. E. Barth, R. G. Lawton, *J. Am. Chem. Soc.* **1966**, *88*, 380–381.
[5] R. G. Lawton, W. E. Barth, *J. Am. Chem. Soc.* **1971**, *93*, 1730–1745.
[6] V. M. Tsefrikas, L. T. Scott, *Chem. Rev.* **2006**, *106*, 4868–4884.
[7] H. A. Wegner, H. Reisch, K. Rauch, A. Demeter, K. A. Zachariasse, A. De Meijere, L. T. Scott, *J. Org. Chem.* **2006**, *71*, 9080–9087.
[8] E. Jackson, B. Steinberg, M. Bancu, A. Wakamiya, *J. Am. Chem. Soc.* **2007**, *129*, 484–485.
[9] S. Lampart, L. M. Roch, A. K. Dutta, Y. Wang, R. Warshamanage, A. D. Finke, A. Linden, K. K. Baldridge, J. S. Siegel, *Angew. Chem. Int. Ed.* **2016**, *55*, 14648–14652; *Angew. Chem.* **2016**, *128*, 14868–14872.
[10] S. Duttwyler, C. Douvris, N. L. P. Fackler, F. S. Tham, C. A. Reed, K. K. Baldridge, J. S. Siegel, *Angew. Chem. Int. Ed.* **2010**, *49*, 7519–7522; *Angew. Chem.* **2010**, *122*, 7681–7684.
[11] O. Allemann, S. Duttwyler, P. Romanato, K. K. Baldridge, J. S. Siegel, *Science* **2011**, *332*, 574–577.
[12] K. Y. Amsharov, M. A. Kabdulov, M. Jansen, *Angew. Chem. Int. Ed.* **2012**, *51*, 4594–4597; *Angew. Chem.* **2012**, *124*, 4672–4675.
[13] A. K. Steiner, K. Y. Amsharov, *Angew. Chem. Int. Ed.* **2017**, *56*, 14732–14736; *Angew. Chem.* **2017**, *129*, 14926–14931.
[14] T. Fujita, K. Fuchibe, J. Ichikawa, *Angew. Chem. Int. Ed.* **2019**, *58*, 390–402; *Angew. Chem.* **2019**, *131*, 396–413.
[15] N. Suzuki, T. Fujita, K. Y. Amsharov, J. Ichikawa, *Chem. Commun.* **2016**, *52*, 12948–12951.
[16] O. Papaianina, V. A. Akhmetov, A. A. Goryunkov, F. Hampel, F. W. Heinemann, K. Y. Amsharov, *Angew. Chem. Int. Ed.* **2017**, *56*, 4834–4838; *Angew. Chem.* **2017**, *129*, 4912–4916.
[17] H. E. Bronstein, L. T. Scott, *Tetrahedron* **2008**, *73*, 88–93.
[18] C. Kuo, M. Tsau, D. T. Weng, G. H. Lee, S. Peng, T. Luh, P. U. Biedermann, I. Agranat, *J. Org. Chem.* **1995**, *60*, 7380–7381.
[19] S. Pogodin, P. U. Biedermann, I. Agranat, *J. Org. Chem.* **1997**, *62*, 2285–2287.
[20] N. S. Mills, J. L. Malandra, A. Hensen, J. A. Lowery, *Polycyclic Aromat. Compd.* **1998**, *12*, 239–247.
[21] H. E. Bronstein, N. Choi, L. T. Scott, C. Hill, *Tetrahedron* **2002**, *58*, 8870–8875.
[22] H. I. Chang, H. T. Huang, C. H. Huang, M. Y. Kuo, Y. T. Wu, *Chem. Commun.* **2010**, *46*, 7241–7243.
[23] C. W. Li, C. I. Wang, H. Y. Liao, R. Chaudhuri, R. S. Liu, *J. Org. Chem.* **2007**, *72*, 9203–9207.

[24] K. Mochida, K. Kawasumi, Y. Segawa, K. Itami, *J. Am. Chem. Soc.* **2011**, *133*, 10716 – 10719.
[25] K. Kawai, K. Kato, L. Peng, Y. Segawa, L. T. Scott, K. Itami, *Org. Lett.* **2018**, *20*, 1932 – 1935.
[26] N. Suzuki, T. Fujita, J. Ichikawa, *Org. Lett.* **2015**, *17*, 4984 – 4987.
[27] T. S. Navale, K. Thakur, R. Rathore, *Org. Lett.* **2011**, *13*, 1634 – 1637.
[28] D. Sharapa, A.-K. Steiner, K. Amsharov, *Phys. Status Solidi* **2018**, *255*, 1800189.

Manuscript received: March 27, 2019
Accepted manuscript online: March 29, 2019
Version of record online: May 2, 2019

CHEMISTRY
A European Journal

Supporting Information

Tailoring Diindenochrysene through Intramolecular Multi-Assemblies by C–F Bond Activation on Aluminum Oxide

Vladimir Akhmetov,[a] Mikhail Feofanov,[a] Sergey Troyanov,[b] and Konstantin Amsharov*[a]

chem_201901450_sm_miscellaneous_information.pdf

Tailoring Diindenochrysene through Intramolecular Multi-Assemblies via C-F Bond Activation on Aluminum Oxide Supporting Information

Contents

1. General Information

All chemicals and solvents were purchased in reagent grade from commercial suppliers (Acros®, SigmaAldrich® or Fluka®, Fluorochem®, Merck®, chemPur®) and used as received unless otherwise specified. Microwav eassisted experiments were carried out using Discover SP Microwave Synthesizer, CEM. Solvents in HPLC grade were purchased from VWR® and SigmaAldrich®.Flash column chromatography was performed on Interchim PuriFlash 430 using flash grade silica gel from MacheryNagel 60 M (40-63 mm, deactivated). NMR spectra were recorded on a Bruker Avance Neo 300 operating at 300 MHz (^{1}H NMR), 75 MHz (^{13}C NMR) and 282 (^{19}F NMR), on a Bruker Avance Neo 400 operating at 400 MHz (^{1}H NMR), 100 MHz (^{13}C NMR) and 377 (^{19}F NMR), on a Bruker Avance Neo 500, operating at 500 MHz (^{1}H NMR), 125 MHz (^{13}C NMR) and 470 MHz (^{19}F NMR) and on a Bruker Avance Neo 600, operating at 600 MHz (^{1}H NMR), 150 MHz (^{13}C NMR) and 564(^{19}F NMR) at room temperature. The signals were referenced to residual solvent peaks (in parts per million (ppm) ^{1}H: $CDCl_3$, 7.27 ppm;

CD_2Cl_2, 5.32 ppm; $(CD_3)_2CO$, 2.05 ppm; ^{13}C: $CDCl_3$, 77.0 ppm; CD_2Cl_2, 53.84 ppm). Coupling constants were assigned as observed. The obtained spectra were evaluated with the program MestReNova. High resolution APPI MS spectra were recorded on a Bruker ESI TOF maXis4G instrument. The data was evaluated with the program Bruker Compass DataAnalysis 4.2. HPLC measurements were performed on a Shimadzu Prominence Liquid Chromatograph LC-20AT with communication bus module CBM-20A, diode array detector SPDM20A, the degassing unit DGU-20A5 R, column oven CTO-20AC or CTO-20A, respectively and with auto sampler SIL-20A HT. For separation a Cosmosil 5-PYE column (4.6 mm x 250mm) from Nacalai Tesque was used. As eluent a DCM/MeOH or toluene/MeOH mixture was used (UV-vis detection). The data was evaluated with the programs Shimadzu LCsolution and Shimadzu LabSolutions. TLC analyses were carried out with TLC sheets coated with silica gel with fluorescent indicator254 nm from Machery-Nagel (ALUGRAM® SIL G/UV254) and visualized via UV-light of 254nm or 366 nm.

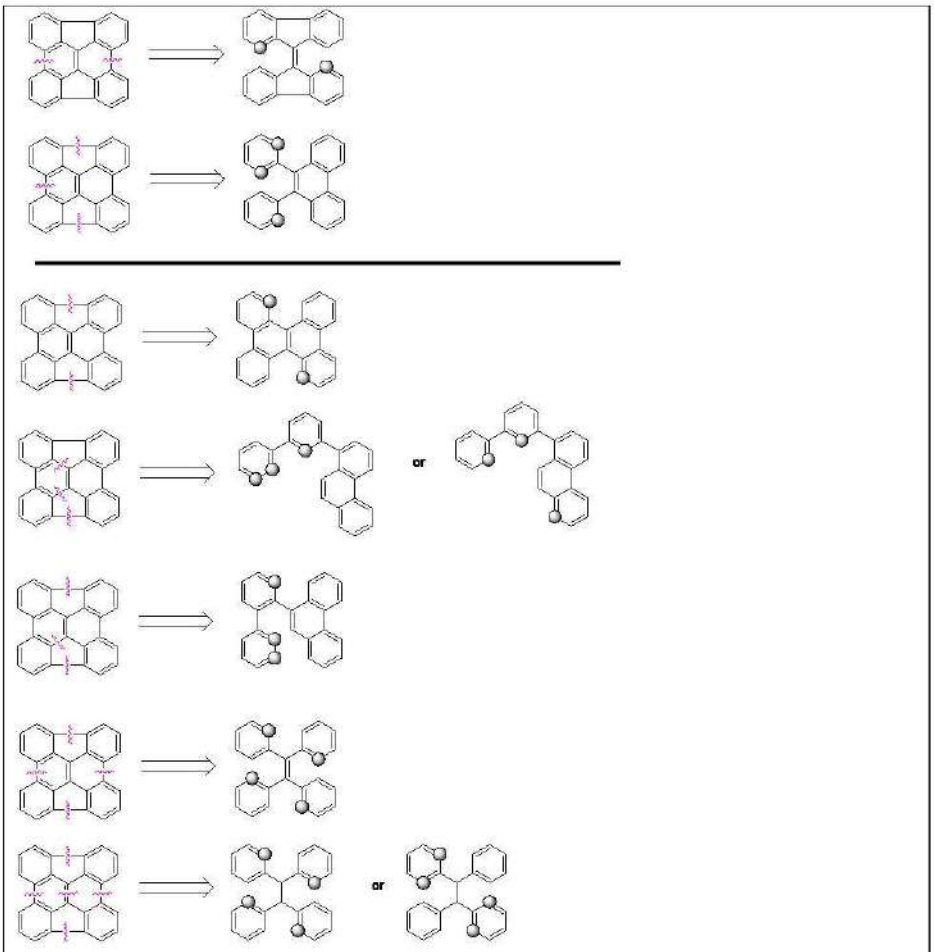

Figure S1. The retrosynthetic approaches to diindenochrysene implemented in this work (below the line) along with the approaches representing the published data (above the line).

2. Experimental Procedures

General Procedure A.

A glass tube was charged with 2-5 g of γ-Al_2O_3 (neutral, 50-200 micron) and preactivated at 450 ℃ for 3-4 hours. Then it was connected to a Schlenk line and heated at 590 ℃ under vacuum (10^{-3} mbar) for another 2 hours. The vessel was cooled down to r.t. and 1-10 mmol of fluoroarene was added under argon atmosphere. The tube containing the obtained mixture was sealed under vacuum and heated at 180-220°C for 2-72 h. After cooling to room temperature, products were extracted with toluene. Separation and final purification of the products were carried out by HPLC from the respective toluene extract.

General Procedure B.

1 g of γ-Al_2O_3 (neutral, 50-200 micron) were preactivated in glass ampule at 450°C under air conditions for 60 minutes and then activated at 590°C for another 30 minutes under vacuum (10^{-3} mbar). Activated aluminum oxide was added to the microwave glass vial containing 20 mg of fluoroarene dissolved in 3 mL of anhydrous o-dichlorobenzene. The glass vial was closed with the cap and placed into the microwave. All preparation steps were performed under argon atmosphere. Condensation was carried out typically at 150-220 °C for 2-72 h. After cooling to room temperature, products were extracted with toluene. Separation and final purification of the products were carried out by HPLC from the respective toluene extract.

General Procedure C.

The corresponding bromo- or iodoarene (5-20 mmol, 1eq) and boronic acid (1eq, unless specified otherwise) were dissolved in 50-100 ml of toluene:methanol (2:1) mixture containing potassium carbonate (6eq) and 2.5% mol of tetrakis(triphenylphosphine)palladium(0) as catalyst. The reaction mixture was stirred under reflux and argon atmosphere for 15 hours. Then the reaction mixture was extracted with dichloromethane and washed with water, organic layer was dried over Na_2SO_4, filtrated through a short silica plague. Solvent evaporation under reduced pressure was followed by flash chromatography purification of product (Hexane:Dichloromethane=10:1).

(1) Diindeno[1,2,3,4-*defg*:1',2',3',4'-*mnop*]chrysene

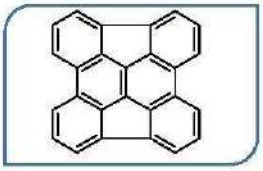

The compound was obtained according to the General Procedure A. The yield are given in the manuscript of the article and vary depending on the approach. ^{1}H NMR (600 MHz, CD_2Cl_2) δ 8.30 (d, J = 8.0 Hz, 4H), 7.94 (d, J = 7.1 Hz, 4H), 7.66 (dd, J = 8.0, 7.1 Hz, 4H). ^{13}C NMR (151 MHz, CD_2Cl_2) δ 141.69 (s), 139.06 (s), 137.58 (s), 133.67 (s), 129.26 (s), 124.90 (s), 122.97 (s).The NMR spectral data were consistent with that reported [1]. UV-vis (Dichloromethane/Methanol 1:1) λ_{max} (nm): 282, 344, 363, 401 (sh).

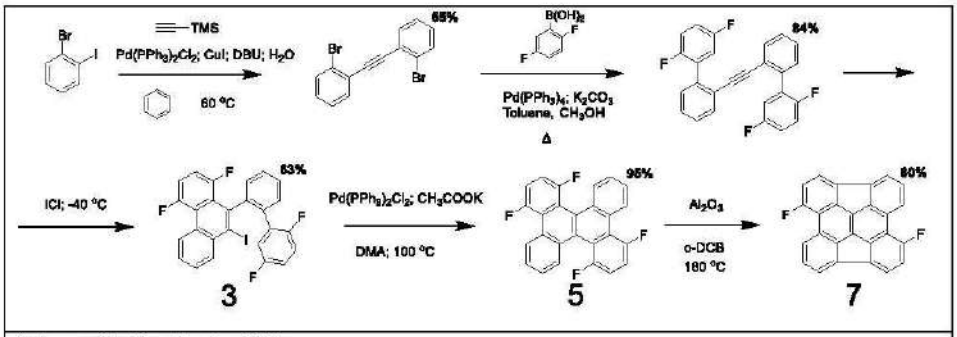

Scheme S1. Synthesis of (7).

1,2-bis(2-bromophenyl)ethyne

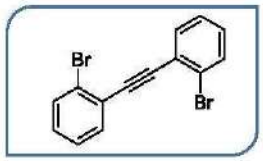

A two-neck flask equipped with a magnetic stirrer, a condenser was charged with 1-bromo-2-iodobenzene (2.83 g, 10.00 mmol), $Pd(PPh_3)Cl_2$ (0.42 g, 0.60 mmol) of and CuI (0.19 g, 1.00 mmol). The flask was degassed and filled with argon, then 50 ml of benzene, 1,8-Diazabicyclo[5.4.0]undec-7-ene (8.90 ml, 60.00 mmol), ice-cold trimethylsilylacetylene (0.70 ml, 5.00 mmol) and distilled water (0.70 ml, 40.00 mmol). The obtained mixture was stirred and heated at 60 ℃ for 16 hours under aluminium foil. The resulting black mixture was extracted with diethyl ether and washed with 10% HCl solution. The combined organic layers were dried over Na_2SO_4, and the product was purified by flash chromatography (Hexane:Ethylacetate=9:1). Yield 1.65 g (65%). ^{1}H NMR (400 MHz, CD_2Cl_2) δ

7.64 (dt, *J*=7.6, 1.6 Hz, 4H), 7.35 (dt, *J*=7.6, 1.6 Hz, 2H), 7.24 (dt, *J*=7.2, 2.0 Hz; 2H). ^{13}C NMR (101 MHz, CD_2Cl_2) δ 134.0, 133.0, 130.4, 127.6, 125.7, 125.4, 92.5.

1,2-bis(2',5'-difluoro-[1,1'-biphenyl]-2-yl)ethyne.

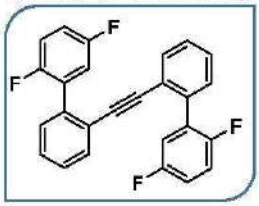

The compound was obtained according to the General Procedure C using 1,2-bis(2-bromophenyl)ethyne (1.4 g) and (2,5-difluorophenyl)boronic acid (0.7 g). Yield 1.5 g (84%). ^{1}H NMR (300 MHz, CD_2Cl_2) δ 7.41-7.33 (m, 8H), 7.20 – 6.82 (m, 6H). ^{19}F NMR (282 MHz, CD_2Cl_2) δ -119.85 – -121.50 (m, 2F), -121.38 – -121.50 (m; 2F). ^{13}C NMR (101 MHz, CD_2Cl_2) δ 161.1 (d, *J* = 251.7 Hz), 158.5 (d, *J* = 249.7 Hz), 137.1 (s), 133.2 (s), 132.9 (s), 130.4 (d, *J* = 1.9 Hz), 128.7 (d, *J* = 24.5 Hz), 123.0 (s), 118.4 (dd, *J* = 24.4, 3.6 Hz), 116.9 (dd, *J* = 25.6, 8.9 Hz), 116.3 (dd, *J* = 24.1, 8.5 Hz), 91.4 (s). One aromatic quaternary carbon atom was not unambiguously assigned. APPI HRMS calculated for $C_{26}H_{14}F_4$ [M^+] *m/z* 402.1026, found 402.1030.

(3) 10-(2',5'-difluoro-[1,1'-biphenyl]-2-yl)-1,4-difluoro-9-iodophenanthrene.

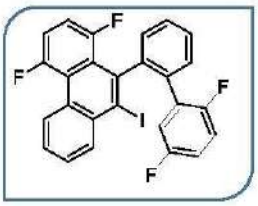

To a CH_2Cl_2 solution (60 mL) of 1,2-bis(2',5'-difluoro-[1,1'-biphenyl]-2-yl)ethyne (300 mg, 0.75 mmol) was added ICl (1.0 M in CH_2Cl_2, 1.65 mmol) at -78 ℃, and the mixture was kept on stirring at –40 ℃ for 0.5 h before it was quenched with sodium thiosulphate solution. The organic layer was extracted with CH_2Cl_2, dried over MgSO4, and purified by column chromatography (Hexane:Ethylacetate=98:2) to give (4) as yellowish solid. Yield 250 mg (63%). ^{1}H NMR (300 MHz, CD_2Cl_2) δ 9.09 – 9.04 (m, 1H), 8.49 – 8.46 (m, 1H), 7.74 – 7.67 (m, 2H), 7.60 – 7.46 (m, 3H), 7.41 – 7.32 (m, 2H), 7.15 (ddd, *J* = 11.9, 8.8, 4.1 Hz, 1H), 6.86 – 6.66 (m, 3H). ^{19}F NMR (282 MHz, CD_2Cl_2) δ -107.0 – -107.16 (m), -112.02 – -112.17 (m), -120.23 – -120.37 (m), -120.49 – -120.54 (m). ^{13}C NMR (75 MHz, CD_2Cl_2) δ 158.1 (d, *J* = 251.7 Hz), 158.0 (d, *J* = 251.2 Hz), 157.5 (d, *J* = 249.8 Hz), 147.1 (d, *J* = 4.4 Hz), 139.2 (t, *J* = 2.6 Hz), 135.5 (s), 133.8 (d, *J* = 4.5 Hz), 133.3 (s), 131.1 (s), 130.9 (d, *J* = 5.0 Hz), 129.4 (d, *J* = 2.4 Hz), 129.0 (d, *J* = 2.6 Hz), 128.5 (s), 128.2 (s), 128.0 – 127.9 (m), 127.5 (s), 118.1 (dd, *J* = 22.4, 5.5 Hz), 116.8 (dd, *J* = 24.9, 10.0 Hz), 115.8 (s), 115.4 (d, *J* = 9.6 Hz), 115.0 (d, *J* = 8.7 Hz), 114.7 (d, *J* = 9.6 Hz), 113.6 (dd, *J* = 28.4, 9.0 Hz). One aromatic

quaternary carbon atom was not unambiguously assigned. APPI HRMS calculated for $C_{26}H_{13}F_4I$ [M^+] *m/z* 527.9993, found 528.0000.

(5) 1,4,9,12-tetrafluorodibenzo[*g*,*p*]chrysene.

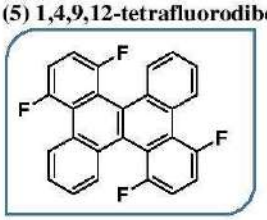

Compound (3) (250 mg, 0.47 mmol), $PdCl_2(PPh_3)_2$ (26.6 mg, 0.038 mmol) and CH_3COONa (249 mg, 3.03 mmol) were dissolved in DMA (40 ml), and heated to 100 ℃ for 2.5 h. The mixture was extracted with ethyl acetate, dried over anhydrous MgSO4, and evaporated under vacuum. The product was purified by flash chromatography (Hexane:Ethylacetate=98:2). Yield 185 mg (95%). ^{1}H NMR (300 MHz, CD_2Cl_2) δ 8.94 – 8.88 (m, 2H), 7.97 – 7.90 (m, 2H), 7.64 – 7.61 (m, 4H), 7.49-7.36 (m, 4H). ^{19}F NMR (282 MHz, CD_2Cl_2) δ -105.13 (dtd, *J* = 18.8, 11.3, 4.2 Hz), -116.53 – -116.80 (m). ^{13}C NMR (75 MHz, CD_2Cl_2) δ 156.8 (d, *J* =244.9 Hz), 154.4(d, *J* = 248.7 Hz), 129.4 (d, *J* = 12.4 Hz), 127.8 (d, *J* = 7.4 Hz), 127.3 (d, *J* = 19.7 Hz), 126.7, 121.3 (dd, *J*=11.9, *J*=3.4 Hz), 119.4 (d, *J*= 11.6 Hz), 115.3 (d, *J* = 12.5 Hz), 115.0 (d, *J* = 12.3 Hz), 114.6 (d, *J* = 23.2 Hz), 114.3 (d, *J* = 10.2 Hz). For crystal data see the section X-Ray crystallography. APPI HRMS calculated for $C_{26}H_{12}F_4$ [M^+] *m/z* 400.0881, found 400.0875. UV-vis (Dichloromethane/Methanol 1:1) λ_{max} (nm): 346, 355, 388 (sh).

(7) 1,7-difluorodiindeno[1,2,3,4-defg:1',2',3',4'-mnop]chrysene.

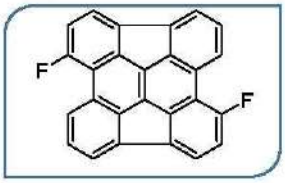

The compound was obtained according to the General Procedure A using compound (9) (50 mg). Yield 37 mg (80%). ^{1}H NMR (600 MHz, CD_2Cl_2) δ 8.47 (d, *J* = 8.1 Hz, 2H), 7.97 (d, *J* = 7.1 Hz, 2H), 7.94 (d, *J* = 7.7 Hz, 2H), 7.70 (dd, *J* = 8.1, 7.2 Hz, 2H), 7.31 (d, *J* = 7.7 Hz, 2H). ^{19}F NMR (471 MHz, CD_2Cl_2) δ -111.50 (s). ^{13}C NMR (151 MHz, CD_2Cl_2) δ 161.3 (d, *J* = 259.1 Hz), 141.3 (s), 140.3 (d, *J* = 8.2 Hz), 138.4 (s), 137.6 (s), 136.1 (s), 131.3 (s), 130.2 (s), 127.5 (d, *J* = 6.9 Hz), 125.5 (d, *J* = 8.5 Hz), 123.4 (s), 121.5 (d, *J* = 16.0 Hz), 115.7 (d, *J* = 24.2 Hz). For crystal data see the section X-Ray crystallography. APPI HRMS calculated for $C_{26}H_{10}F_2$ [M^+] *m/z* 360.0745, found 360.0748. UV-vis (Dichloromethane/Methanol 1:1) λ_{max} (nm): 283, 337, 357, 400.

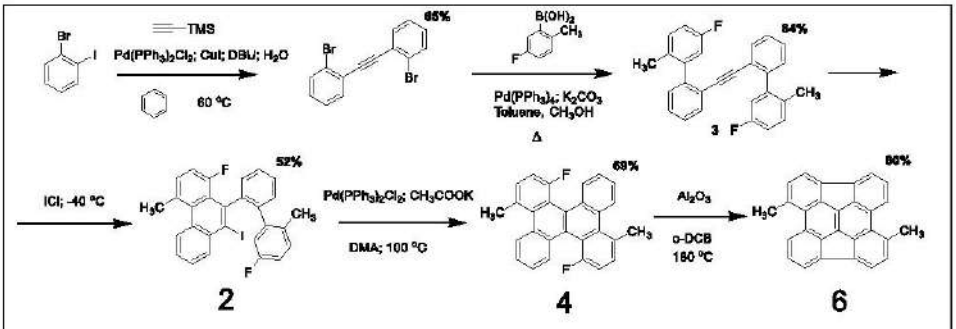

Scheme S2. Synthesis of (6).

1,2-bis(5'-fluoro-2'-methyl-[1,1'-biphenyl]-2-yl)ethyne

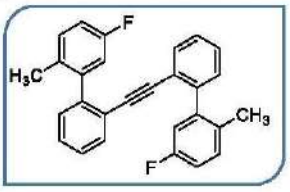

The compound was obtained according to the General Procedure C using compound (2) (1.3 g) and (5-fluoro-2-methylphenyl)boronic acid (0.6 g). Yield 1.2 g (84%). ^{1}H NMR (400 MHz, CD_2Cl_2) δ 7.35 (td, *J* = 7.4, 1.7 Hz, 2H), 7.28 (td, *J* = 7.5, 1.5 Hz, 2H), 7.25 – 7.15 (m, 6H), 6.99 (td, *J* = 8.5, 2.8 Hz, 2H), 6.84 (dd, *J* = 9.5, 2.8 Hz, 2H), 2.00 (s, 6H). ^{19}F NMR (377 MHz, CD_2Cl_2) δ -119.40 (m, 2F). ^{13}C NMR (101 MHz, CD_2Cl_2) δ 160.9 (d, *J* = 242.7 Hz), 143.3 (s), 142.6 (d, *J* = 7.9 Hz), 132.6 (s), 132.4 (d, *J* = 2.9 Hz), 131.4 (d, *J* = 8.0 Hz), 129.74 (s), 128.65 (s), 127.75 (s), 122.96 (s), 116.5 (d, *J* = 21.1 Hz), 114.5 (d, *J* = 21.1 Hz), 91.50 (s), 19.21 (s). APPI HRMS calculated for $C_{28}H_{20}F_2$ [M^+] *m/z* 394.1527, found 394.1532.

(4) 4,12-difluoro-1,9-dimethyldibenzo[*g,p*]chrysene.

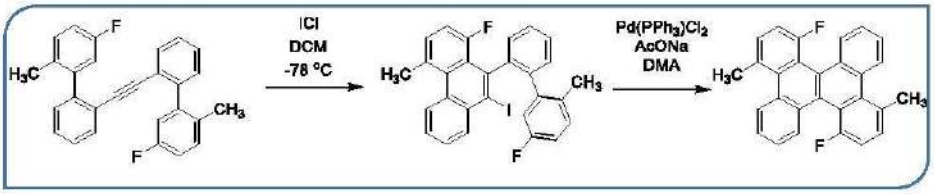

To a CH_2Cl_2 solution (60 mL) of 1,2-bis(5'-fluoro-2'-methyl-[1,1'-biphenyl]-2-yl)ethyne (0.50 g, 1.27 mmol) was added ICl (1.0 M in CH_2Cl_2, 2.79 mmol) at -78 °C, and the mixture was kept on stirring at −40 °C for 0.5 h before it was quenched with sodium thiosulphate solution. The

organic layer was extracted with CH_2Cl_2, dried over MgSO4, and filtered through a short silica plug to give (2) as yellowish solid, which was used in the following step without additional purification. Compound (2) (250 mg, 0.63 mmol), $PdCl_2(PPh_3)_2$ (26.6 mg, 0.038 mmol) and CH_3COONa (249 mg, 3.023 mmol) were dissolved in DMA (40 ml), and heated to 100 ℃ for 1.5 h. The mixture was extracted with ethyl acetate, dried over anhydrous $MgSO_4$, and evaporated under vacuum. The crude sample was recrystallized in hot acetone, this led to the isolation of a complicated mixture of isomers with of dibenzo[*g*,*p*]chrysene derivatives (see section 5) that could not be isolated. The obtained mixture (145 mg) was used for the next step.

(6) 1,7-dimethyldiindeno[1,2,3,4-defg:1',2',3',4'-mnop]chrysene.

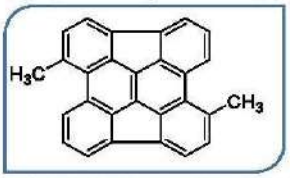

The compound was obtained according to the General Procedure A using mixture (4) (30 mg). Yield 15 mg (estimated to be 60%). ^{1}H NMR (600 MHz, CD_2Cl_2) δ 8.50 (d, *J* = 8.2 Hz, 2H), 7.97 (d, *J* = 7.0 Hz, 2H), 7.89 (d, *J* = 7.1 Hz, 2H), 7.69 (dd, *J* = 8.2, 7.0 Hz, 2H), 7.47 (dd, *J* = 7.1, 0.9 Hz, 2H), 3.14 (s, 6H). ^{13}C NMR (151 MHz, CD_2Cl_2) δ 141.6 (s), 139.7 (s), 138.9 (s), 138.1 (s), 137.7 (s), 135.0 (s), 133.4 (s), 131.9 (s), 131.6 (s), 129.23 (s), 127.3 (s), 123.4 (s), 122.57 (s), 23.2 (s). For crystal data see the section X-Ray crystallography. APPI HRMS calculated for $C_{28}H_{16}$ [M^+] *m/z* 352.1246, found 352.1242. UV-vis (Dichloromethane/Methanol 1:1) λ_{max} (nm): 287, 311 (sh), 344, 362, 401 (sh).

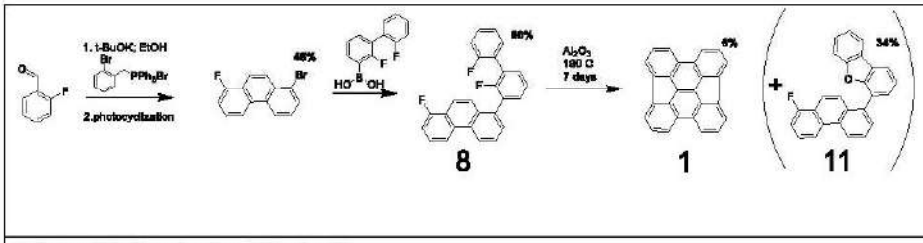

Scheme S3. Synthesis of (1) via (8).

1-bromo-8-fluorophenanthrene.

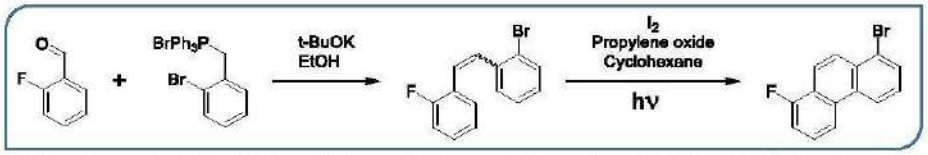

2-fluorobenzaldehyde (0.73 g, 5.83 mmol), bromo(2-bromobenzyl)triphenyl-λ^5-phosphane (3.00 g, 5.83 mmol) were dissolved in 75 ml of dry ethanol. The mixture was stirred at r.t. for 5 min and t-BuOK (0.74 g, 6.59 mmol) was added in portions: The obtained orange suspension was refluxed overnight, cooled down and quenched with 1M HCl to pH=5.5. The mixture was concentrated under reduced pressure, extracted with dichloromethane and organic layer was dried over anhydrous $MgSO_4$. Filtration through a short silica plug gave the mixture of (Z/E)-bromo-2-(2-fluorostyryl)benzene. Yield 1.50 g (93%) which was dissolved in 600 ml of cyclohexane. Iodine (1.65 g, 6.49 mmol), propylene oxide (3.75 ml, 54.00 mmol) were added to the solution before it was irradiated. Photocyclization reaction were carried out using the Katz improvement of the Mallory photocyclization procedure [2]. After full conversion the mixture was concentrated under reduced pressure, the product was precipitated with methanol, filtered and washed with cold methanol to give 1-bromo-8-fluorophenanthrene. Yield 0.825 g (55%). ^{1}H NMR (400 MHz, CD_2Cl_2) δ 8.68 (d, J = 8.4 Hz, 1H), 8.48 (d, J = 8.4 Hz, 1H), 8.28 (d, J = 9.4 Hz, 1H), 8.13 (d, J = 9.4 Hz, 1H), 7.95 (dd, J = 7.6, 0.9 Hz, 1H), 7.65 (td, J = 8.2, 5.9 Hz, 1H), 7.59 – 7.50 (m, 1H), 7.35 (ddd, J = 9.9, 7.8, 0.7 Hz, 1H). ^{19}F NMR (377 MHz, CD_2Cl_2) δ -122.62 (d, J = 15.3 Hz). ^{13}C NMR (101 MHz, CD_2Cl_2) δ 159.6 (d, J = 250.3 Hz), 132.2 (d, J = 4.2 Hz), 131.8 (s), 131.7 (s), 131.0 (s), 127.9 (s), 127.6 (d, J = 8.6 Hz), 126.1 (d, J = 1.9 Hz), 124.1 (s), 123.3 (s), 121.9 (d, J = 15.9 Hz), 120.4 (d, J = 7.0 Hz), 119.2 (d, J = 3.9 Hz), 112.1 (d, J = 20.1 Hz).

(8) 1-(2,2'-difluoro-[1,1'-biphenyl]-3-yl)-8-fluorophenanthrene.

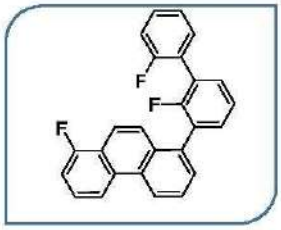

The compound was obtained according to the General Procedure C using 1-bromo-8-fluorophenanthrene (0.35 g) and (2,2'-difluoro-[1,1'-biphenyl]-3-yl)boronic acid [3] (0.33 g). Yield 0.40 g (80%). ^{1}H NMR (400 MHz, CD_2Cl_2) δ 8.80 (d, *J* = 8.5 Hz, 1H), 8.57 (d, *J* = 8.5 Hz, 1H), 8.00 (d, *J* = 9.4 Hz, 1H), 7.79 (dd, *J* = 8.4, 7.2 Hz, 1H), 7.73 (dd, *J* = 9.4, 2.5 Hz, 1H), 7.69 – 7.60 (m, 2H), 7.57 – 7.38 (m, 5H), 7.38 – 7.30 (m, 1H), 7.28 (td, *J* = 7.5, 1.2 Hz, 1H), 7.25 – 7.16 (m, *J* = 9.5, 6.9, 1.1 Hz, 1H). ^{19}F NMR (377 MHz, CD_2Cl_2) δ -114.98 – -115.57 (m), -116.17 – -116.58 (m), -123.08 (d, *J* = 15.6 Hz). ^{13}C NMR (101 MHz, CD_2Cl_2) δ 160.3 (d, *J* = 247.9 Hz), 158.5 (d, *J* = 248.5 Hz), 157.6 (d, *J* = 249.8 Hz), 135.1 (s), 132.7 (d, *J* = 3.5 Hz), 132.1 (dd, *J* = 3.4, 1.2 Hz), 132.0 (s), 131.9 – 131.7 (m), 130.7 (s), 130.4 (d, *J* = 1.8 Hz), 130.4 (s), 130.2 (d, *J* = 2.2 Hz), 129.56 (s), 128.8 (d, *J* = 17.3 Hz), 127.2 (d, *J* = 8.7 Hz), 126.9 (s), 125.2 (s), 124.6 (t, *J* = 3.9 Hz), 124.2 (s), 123.8 (s), 121.7 (d, *J* = 16.0 Hz), 119.2 (d, *J* = 3.9 Hz), 119.1 (d, *J* = 7.1 Hz), 117.5 (s), 116.1 (d, *J* = 22.4 Hz), 111.6 (d, *J* = 20.3 Hz). APPI HRMS calculated for $C_{26}H_{15}F_3$ [M^+] *m/z* 384.1120, found 384.1124.

(11) 4-(8-fluorophenanthren-1-yl)dibenzo[b,d]furan.

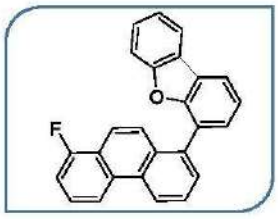

The compound (11) was isolated by means of HPLC as a major product during the synthesis of (1) from (8). Yield 12 mg (34%). ^{1}H NMR (400 MHz, Acetone) δ 9.02 (d, *J* = 8.4 Hz, 1H), 8.79 (d, *J* = 8.5 Hz, 1H), 8.27 (t, *J* = 4.5 Hz, 1H), 8.25 – 8.16 (m, 1H), 7.95 (d, *J* = 9.4 Hz, 2H), 7.93 (s, *J* = 8.3 Hz, 1H), 7.91 (d, *J* = 8.3 Hz, 1H), 7.68 (d, *J* = 9.4 Hz, 1H), 7.61 (dd, *J* = 4.6, 0.6 Hz, 2H), 7.54 – 7.39 (m, 4H). ^{19}F NMR (377 MHz, Acetone) δ -124.18 (d, *J* = 13.6 Hz). APPI HRMS calculated for $C_{26}H_{15}FO$ [M^+] *m/z* 362.1101, found 362.1106.

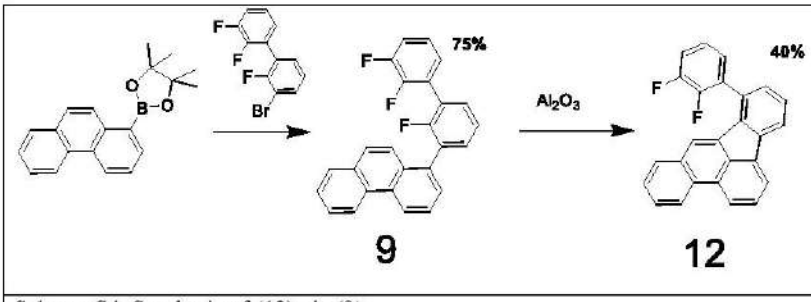

Scheme S4. Synthesis of (12) via (9).

4,4,5,5-tetramethyl-2-(phenanthren-1-yl)-1,3,2-dioxaborolane.

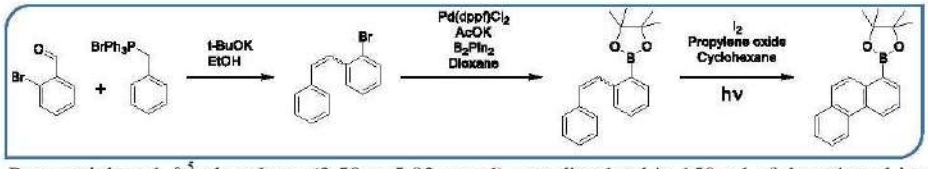

Bromotriphenyl- λ^5-phosphane (3.50 g, 5.83 mmol) was dissolved in 150 ml of dry ethanol in a two-neck flask. The mixture was degassed and the flask was filled with argon. After stirring at r.t. for 5 min t-BuOK (1.36 g, 12.15 mmol) was added in portions and a solution of 2-bromobenzaldehyde (1.50 g, 8.10 mmol) in 15 ml of ethanol was added dropwise. The obtained orange suspension was refluxed under argon atmosphere overnight, cooled down and quenched with 1M HCl to pH=5.5. The mixture was concentrated under reduced pressure, extracted with dichloromethane and organic layer was dried over anhydrous $MgSO_4$. Filtration through a short silica plug gave the mixture of (Z/E)-1-bromo-2-styrylbenzene. Yield 1.88 g (90%). The obtained stilbenes, potassium acetate (2.14 g, 21.87 mmol), bis(pinacolato)diboron (2.76 g, 10.93 mmol) and $Pd(dppf)Cl_2$ (0.21 g, 0.29 mmol) were dissolved in 75 ml of dioxane and refluxed under argon atmosphere for 10 hours. After full conversion the mixture was extracted with dichloromethane and washed with brine, organic layer was dried over anhydrous $MgSO_4$ and filtered through a short silica plug to give a mixture of (Z/E)- 4,4,5,5-tetramethyl-2-(2-styrylphenyl)-1,3,2-dioxaborolane: Yield (1.67, 75%). The obtained crude mixture was dissolved in 600 ml of cyclohexane. Iodine (1.60 g, 6.01 mmol), propylene oxide (3.45 ml, 50.00 mmol) were added to the solution before it was irradiated. Photocyclization reaction were carried out using the Katz

improvement of the Mallory photocyclization procedure [2]. After full conversion the mixture was concentrated under reduced pressure, quenched with $Na_2S_2O_3$ solution and extracted with dichloromethane. Combined organic layer was dried over anhydrous $MgSO_4$. The final product was isolated by flash chromatography (Hexane:Ethylacetate=90:10) to give (13) as yellowish solid. Yield 1.32 g (80%) Overall yield 55%. ^{1}H NMR (400 MHz, $CDCl_3$) δ 8.83 (d, *J* = 8.3 Hz, 1H), 8.71 (dd, *J* = 12.5, 8.7 Hz, 2H), 8.18 (d, *J* = 7.0 Hz, 1H), 7.89 (d, *J* = 7.8 Hz, 1H), 7.79 (d, *J* = 9.1 Hz, 1H), 7.63 (ddd, *J* = 13.6, 12.5, 7.6 Hz, 3H), 1.43 (d, *J* = 10.2 Hz, 12H). ^{13}C NMR (101 MHz, $CDCl_3$) δ 136.2 (s), 135.7 (s), 131.7 (s), 130.5 (s), 129.9 (s), 128.3 (s), 127.2 (s), 127.1 (s), 126.4 (s), 126.3 (s), 125.8 (s), 125.6 (s), 122.6 (s), 83.8 (s), 25.0 (s).

3-bromo-2,2',3'-trifluoro-1,1'-biphenyl.

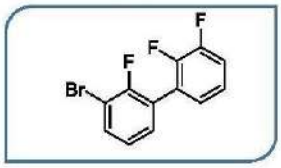

The compound was obtained according to the General Procedure C using 1-bromo-2-fluoro-3-iodobenzene (0.28 g) and (2,3-difluorophenyl)boronic acid (0.18 g). Yield 0.21 g (80%). ^{1}H NMR (400 MHz, CD_2Cl_2) δ 7.65 (ddd, *J* = 8.1, 6.5, 1.7 Hz, 1H), 7.39 – 7.33 (m, 1H), 7.29 – 7.13 (m, 4H). ^{19}F NMR (377 MHz, CD_2Cl_2) δ -108.00 – -108.94 (m), -138.46 (d, *J* = 17.1 Hz), -139.79 – -140.84 (m). ^{13}C NMR (101 MHz, CD_2Cl_2) δ 156.1 (d, *J* = 249.1 Hz), 150.8 (dd, *J* = 247.7, 13.0 Hz), 148.0 (dd, *J* = 250.2, 13.3 Hz), 133.8 (s), 130.7 (s), 126.4 – 125.8 (m), 125.3 (d, *J* = 4.7 Hz), 124.9 (d, *J* = 12.3 Hz), 124.3 (dd, *J* = 7.1, 4.7 Hz), 123.8 (dd, *J* = 16.9, 2.6 Hz), 117.4 (d, *J* = 17.3 Hz), 109.6 (d, *J* = 21.7 Hz). APPI HRMS calculated for $C_{12}H_6BrF_3$ [M^+] *m/z* 285.9599, found 285.9601.

(9) 1-(2,2',3'-trifluoro-[1,1'-biphenyl]-3-yl)phenanthrene.

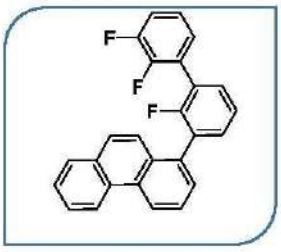

The compound was obtained according to the General Procedure C using 3-bromo-2,2',3'-trifluoro-1,1'-biphenyl (0.31 g) and 4,4,5,5-tetramethyl-2-(phenanthren-1-yl)-1,3,2-dioxaborolane (0.30 g). Yield 0.30 g (75%). ^{1}H NMR (400 MHz, CD_2Cl_2) δ 8.83 (d, *J* = 8.5 Hz, 1H), 8.79 (d, *J* = 8.2 Hz, 1H), 7.91 (dd, *J* = 7.8, 1.3 Hz, 1H), 7.80 – 7.68 (m, 3H), 7.68 – 7.61 (m, 3H), 7.53 (t, *J* = 8.1, 2H), 7.43 (dd, *J* = 8.1, 7.0 Hz, 1H), 7.31 – 7.19 (m, 3H). ^{19}F NMR (377 MHz, CD_2Cl_2) δ -115.47 – -117.39 (m), -138.10 – -139.56 (m), -139.71 – -140.87 (m). ^{13}C NMR (101

MHz, CD_2Cl_2) δ 157.4 (d, *J* = 248.9 Hz), 151.4 (d, *J* = 253.2 Hz), 134.6 (s), 133.3 (d, *J* = 3.6 Hz), 132.2 (s), 131.5 (s), 130.9 (s), 130.7 (d, *J* = 2.5 Hz), 129.2 (d, *J* = 17.5 Hz), 128.9 (d, *J* = 8.7 Hz), 127.7 (s), 127.3 (d, *J* = 3.1 Hz), 127.0 – 126.8 (m), 126.4 (s), 126.3 (s), 124.7 (d, *J* = 4.4 Hz), 124.6 – 124.5 (m), 123.5 (s), 123.3 (s), 117.5 (s, *J* = 17.3 Hz), 117.3 (s). Two aromatic quaternary carbon atoms were not unambiguously assigned. APPI HRMS calculated for $C_{26}H_{15}F_3$ [M^+] *m/z* 384.1120, found 384.1122.

(12) 9-(2,3-difluorophenyl)benzo[e]acephenanthrylene.

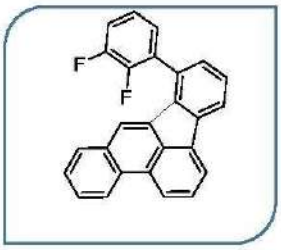

The compound was obtained according to the General Procedure A using compound (9) (25 mg). Yield 5 mg (40%). ^{1}H NMR (400 MHz, CD_2Cl_2) δ 8.67 (d, *J* = 8.0 Hz, 1H), 8.53 (d, *J* = 8.1 Hz, 1H), 8.10 (d, *J* = 7.0 Hz, 1H), 8.05 (dd, *J* = 7.6, 1.0 Hz, 1H), 7.83 (dd, *J* = 8.1, 7.2 Hz, 1H), 7.76 (dd, *J* = 8.0, 1.2 Hz, 1H), 7.69 (ddd, *J* = 8.3, 7.0, 1.4 Hz, 1H), 7.60 – 7.51 (m, 2H), 7.47 – 7.30 (m, 5H). ^{19}F NMR (377 MHz, CD_2Cl_2) δ -138.12 – -138.38 (m), -140.44 – -140.69 (m). APPI HRMS calculated for $C_{26}H_{14}F_2$ [M^+] *m/z* 364.1058, found 364.1052. UV-vis (Dichloromethane/Methanol 1:1) λ_{max} (nm): 296, 303, 352, 369 (sh).

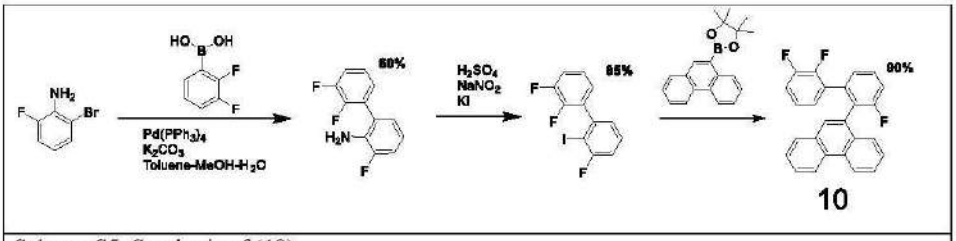

Scheme S5. Synthesis of (10)

2',3,3'-trifluoro-[1,1'-biphenyl]-2-amine.

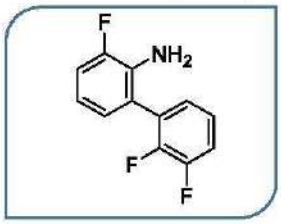

The compound was obtained according to the General Procedure C using 2-bromo-6-fluoroaniline (1.20 g) and (2,3-difluorophenyl)boronic acid (0.99 g). Yield 1.1 g (60%). ^{1}H NMR (400 MHz, CD_2Cl_2) δ 7.27 – 7.13 (m, 3H), 7.07 (ddd, *J* = 11.1, 8.1, 1.4 Hz, 1H), 6.93 (d, *J* = 7.3 Hz, 1H), 6.77 (td, *J* = 7.9, 5.3 Hz, 1H), 3.80 (s, 2H). ^{13}C NMR (101 MHz, CD_2Cl_2) δ 152.2 (d, *J* = 238.3 Hz), 151.5 (dd, *J* = 248.0, 13.2 Hz), 148.4 (dd, *J* = 247.8, 12.6 Hz), 133.6 (d, *J* = 13.1 Hz), 128.2 (dd, *J* = 12.9, 3.1 Hz), 126.9 (dd, *J* = 3.4, 2.2 Hz), 126.6 (d, *J* = 2.3 Hz), 125.1 (dd, *J* = 7.2, 4.9 Hz), 122.4 (dd, *J* = 3.5, 2.6 Hz), 117.9 (d, *J* = 7.6 Hz), 117.2 (d, *J* = 17.3 Hz), 115.3 (d, *J* = 18.9 Hz). APPI HRMS calculated for $C_{12}H_8F_3N$ [M^+] *m/z* 223.0603, found 223.0601.

2,3,3'-trifluoro-2'-iodo-1,1'-biphenyl.

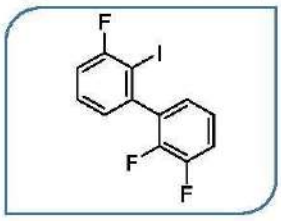

2',3,3'-trifluoro-[1,1'-biphenyl]-2-amine (0.80 g, 3.59 mmol) was dissolved in 15 ml of H_2SO_4 (conc) and obtained solution was cooled to 0 ℃. Then $NaNO_2$ (0.40 g, 5.76 mmol) was added in portions within 10 min. The resulting solution was stirred at 0 ℃ for 3 hours and poured on ice with KI (1.19 g, 7.16 mmol). Then the mixture was stirred for 45 minutes at r.t. Extraction with diethyl ether and wash with Na_2CO_3 were followed by flash chromatography (Hexane) to give (18) as yellowish solid. Yield 1.00 g (85%). ^{1}H NMR (400 MHz, CD_2Cl_2) δ 7.42 (ddd, *J* = 8.3, 7.6, 5.6 Hz, 1H), 7.32 – 7.24 (m, 1H), 7.23 – 7.16 (m, 1H), 7.16 – 7.09 (m, 2H), 7.01 (ddt, *J* = 7.7, 6.1, 1.7 Hz, 1H). ^{19}F NMR (377 MHz, CD_2Cl_2) δ -89.40 (d, *J* = 7.2 Hz), -138.12 – -138.94 (m), -139.58 (dd, *J* = 17.1, 7.4 Hz). ^{13}C NMR (101 MHz, CD_2Cl_2) δ 161.9 (d, *J* = 244.8 Hz),

150.7 (dd, J = 247.8, 12.7 Hz), 147.3 (dd, J = 247.8, 13.0 Hz), 142.4 (s), 132.8 (d, J = 15.0 Hz), 129.8 (d, J = 8.5 Hz), 126.2 (d, J = 1.8 Hz), 124.1 (dd, J = 7.1, 4.9 Hz), 117.2 (d, J = 17.2 Hz), 115.1 (d, J = 24.7 Hz), 87.0 (d, J = 25.6 Hz). APPI HRMS calculated for $C_{12}H_6F_3I$ [M^+] m/z 333.9460, found 333.9461.

(10) 9-(2',3,3'-trifluoro-[1,1'-biphenyl]-2-yl)phenanthrene.

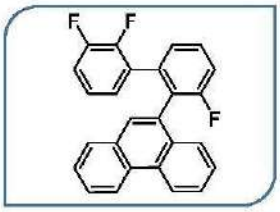

The compound was obtained according to the General Procedure C using 2,3,3'-trifluoro-2'-iodo-1,1'-biphenyl (0.10 g, 0.45 mmol) and phenanthren-9-ylboronic acid (0.15 g, 0.45 mmol). Yield 0.15 g (90%). ^{1}H NMR (400 MHz, CD_2Cl_2) δ 8.71 (d, J = 7.7 Hz, 1H), 8.67 (d, J = 8.2 Hz, 1H), 7.79 (dd, J = 7.9, 1.3 Hz, 1H), 7.69 – 7.63 (m, 3H), 7.63 – 7.53 (m, 4H), 7.41 – 7.31 (m, 2H), 6.89 – 6.77 (m, 2H), 6.69 (tdd, J = 8.1, 4.9, 1.5 Hz, 1H). ^{19}F NMR (377 MHz, CD_2Cl_2) δ -112.20 (s), -138.90 – -139.09 (m), -140.47 (dd, J = 27.0, 6.9 Hz). ^{13}C NMR (101 MHz, CD_2Cl_2) δ 161.1 (d, J = 245.4 Hz), 150.7 (dd, J = 247.2, 13.2 Hz), 148.1 (dd, J = 247.0, 13.0 Hz), 137.5 (t, J = 2.9 Hz), 131.6 (s), 131.5 (s), 130.8 (s), 130.5 (d, J = 8.2 Hz), 130.3 (dd, J = 12.5, 2.7 Hz), 129.8 (s), 129.7 (s), 129.1 (s), 128.0 (d, J = 17.9 Hz), 127.4 (s), 127.2 (s), 127.1 (s), 127.0 (s), 126.6 (s), 126.6 – 126.5 (m), 123.9 – 123.5 (m), 123.2 (s), 122.9 (s), 116.7 (s), 116.5 (s), 116.0 (s), 115.8 (s). APPI HRMS calculated for $C_{26}H_{15}F_3$ [M^+] m/z 384.1120, found 384.1123.

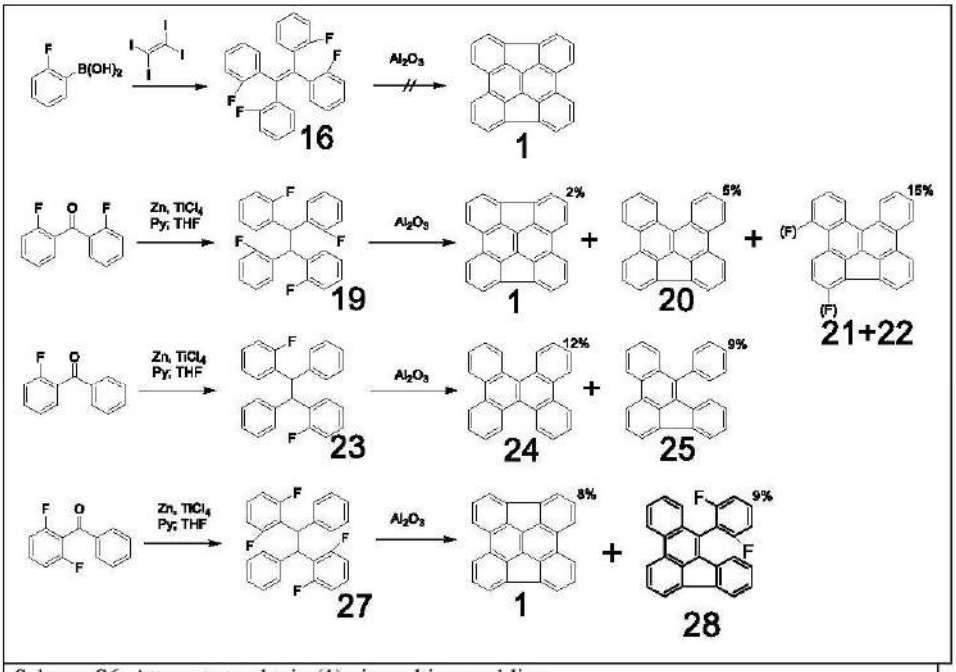

Scheme S6. Attempts to obtain (1) via multi assemblies.

(16) 1,1,2,2-tetrakis(2-fluorophenyl)ethene.

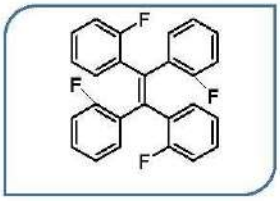

The compound was obtained according to the General Procedure C using periodoethene (0.20 g, 0.38 mmol) and (2-fluorophenyl)boronic acid (0.24 g, 1.73 mmol). Yield 0.10 g (65%). ^{1}H NMR (400 MHz, CD_2Cl_2) δ 7.56 (td, J = 7.4, 1.8 Hz, 1H), 7.41 – 7.35 (m, 1H), 7.20 – 7.12 (m, 2H). ^{19}F NMR (377 MHz, CD_2Cl_2) δ -110.44 – -110.53 (m). ^{13}C NMR (101 MHz, CD_2Cl_2) δ 162.99 (d, J = 251.4 Hz), 133.88 (s), 130.99 (d, J = 8.0 Hz), 124.58 (d, J = 3.7 Hz), 115.95 (d, J = 20.8 Hz), 111.74 (d, J = 15.6 Hz), 87.93 (s). APPI HRMS calculated for $C_{26}H_{16}F_4$ [M^+] m/z 404.1182, found 404.1181.

bis(2-fluorophenyl)methanone.

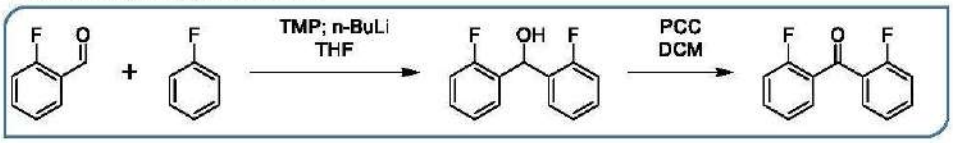

A three-necked round-bottom flask equipped with a magnetic stirring bar, a rubber septum and a condenser was charged with THF (75 mL) and was cooled to -78 °C. 2,2,6,6-Tetramethylpiperidine (3.18 mL, 18.75 mmol) was added, then *n*-BuLi 2.5 M in hexanes (7.00 mL, 17.5 mmol) was added dropwise via a syringe and the orange suspension stirred for 30 minutes at -78 °C. Fluorobenzene (1.20 g, 12.50 mmol) was added dropwise and the suspension stirred for further 30 minutes at -78 °C. Then 2-fluorobenzaldehyde (1.55 g, 12.50 mmol) was added and the mixture allowed to reach room temperature over a period of 3 h. A 1 M aqueous solution of HCl (5 mL) was added to quench the reaction and stirring at room temperature was continued for further 30 minutes. Water (10 mL) and CH_2Cl_2 (10 mL) were added, layers were separated and the aqueous phase extracted with CH_2Cl_2 (3 x 20 mL). The combined organic phases were dried over Na_2SO_4, filtered and the solvent evaporated to dryness. After short column chromatography over silica gel using Hexane:Ethylacetate=80:20 as eluent bis(2-fluorophenyl)methanol)1.20 g (70%) was obtained as yellow oil which was used in further step. The obtained alcohol was dissolved in 50 ml of dry dichloromethane and pyridinium chlorochromate (6.40 g, 29.63 mmol) was added. The obtained suspension was stirred at r.t. for 10 h and filtered through a short silica plug which was washed with extra 300 ml of dichloromethane. The obtained solution was concentrated and purified by flash chromatography (Hexane:Etylacetate=95:5) to give 1.10 g (85%) of bis(2-fluorophenyl)methanone. ^{1}H NMR (400 MHz, CD_2Cl_2) δ 7.69 (td, *J* = 7.5, 1.8 Hz, 1H), 7.61 – 7.54 (m, 1H), 7.29 (td, *J* = 7.6, 1.0 Hz, 1H), 7.15 (ddd, *J* = 10.7, 8.4, 0.9 Hz, 1H). ^{19}F NMR (377 MHz, CD_2Cl_2) δ -113.13 (d, *J* = 10.4 Hz). ^{19}F NMR (377 MHz, CD_2Cl_2) δ -113.13 (d, *J* = 10.4 Hz). ^{13}C NMR (101 MHz, CD_2Cl_2) δ 189.8 (s), 161.4 (d, *J* = 254.3 Hz), 134.7 (d, *J* = 9.4 Hz), 131.2 (s), 127.9 (d, *J* = 12.6 Hz), 125.2 – 124.3 (m), 116.6 (d, *J* = 22.5 Hz).

(19) 1,1,2,2-tetrakis(2-fluorophenyl)ethane.

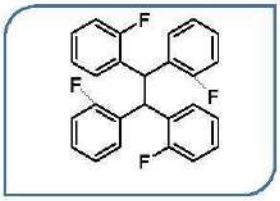

The compound (19) was obtained fully in accordance with the literature data [4].

(20) Benzo[p]indeno[1,2,3,4-defg]chrysene.

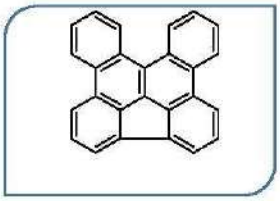

The compound was obtained according to the General Procedure A from (19). Yield 2 mg (~5%). ^{1}H NMR (400 MHz, Acetone) δ 9.53 (dd, *J* = 8.3, 1.2 Hz, 2H), 9.08 (dd, *J* = 8.0, 1.5 Hz, 2H), 8.67 (d, *J* = 8.1 Hz, 2H), 8.31 (d, *J* = 7.0 Hz, 2H), 8.00 – 7.85 (m, 6H). APPI HRMS calculated for $C_{26}H_{14}$ [M^+] *m/z* 326.1090, found 326.1094. UV-vis (Dichloromethane/Methanol 1:1) λ_{max} (nm): 276, 286 (sh), 306, 313, 327, 363, 375, 382.

(21+22) Mixture of 4-fluorobenzo[p]indeno[1,2,3,4-defg]chrysene and 7-fluorobenzo[p]indeno[1,2,3,4-defg]chrysene.

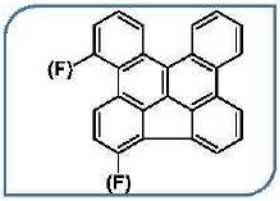

The mixture was obtained according to the General Procedure A from (19). Yield 6 mg (~15%). APPI HRMS calculated for $C_{26}H_{13}F$ [M^+] *m/z* 344.0995, found 344.0999. UV-vis (Dichloromethane/Methanol 1:1) λ_{max} (nm): 277, 312, 332, 362, 375. (see NMR data in section 6).

(23) 1,2-bis(2-fluorophenyl)-1,2-diphenylethane.

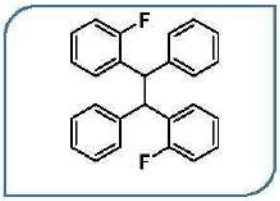

The compound (23) was obtained fully in accordance with the literature data [4].

(24) Dibenzo[g,p]chrysene.

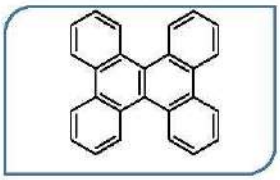

The compound was obtained according to the General Procedure A from (23). Yield 5 mg (20 %). ^{1}H NMR (600 MHz, CD_2Cl_2) δ 8.74 (dd, *J* = 8.1, 1.3 Hz, 4H), 8.71 (dd, *J* = 8.2, 1.1 Hz, 4H), 7.72 (ddd, *J* = 8.2, 7.0, 1.3 Hz, 4H), 7.66 (ddd, *J* = 8.2, 7.0, 1.4 Hz, 4H). ^{13}C NMR (151 MHz, CD_2Cl_2) δ 130.8 (s), 129.1 (s), 128.8 (s), 127.4 (s), 126.6 (s), 126.6 (s), 123.6 (s). APPI HRMS calculated for $C_{26}H_{16}$ [M^+] *m/z* 328.1246, found 328.1251. UV-vis (Dichloromethane/Methanol 1:1) λ_{max} (nm): 288, 300, 337, 350, 383 (sh).

(25) 9-phenylbenzo[e]acephenanthrylene.

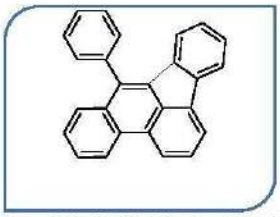

The compound was obtained according to the General Procedure A from (23). Yield 4 mg (15 %). ^{1}H NMR (600 MHz, CD_2Cl_2) δ 8.77 (dd, *J* = 8.4, 1.3 Hz, 1H), 8.55 (d, *J* = 8.1 Hz, 1H), 8.06 (dd, *J* = 7.1, 0.6 Hz, 1H), 7.95 – 7.91 (m, 1H), 7.82 (dd, *J* = 8.1, 7.1 Hz, 1H), 7.73 – 7.69 (m, 2H), 7.68 – 7.62 (m, 3H), 7.56 – 7.50 (m, 3H), 7.33 (td, *J* = 7.4, 1.1 Hz, 1H), 7.07 (td, *J* = 7.6, 1.1 Hz, 1H), 6.76 – 6.72 (m, 1H). ^{13}C NMR (151 MHz, CD_2Cl_2) δ 141.1 (s), 138.9 (s), 138.5 (s), 137.2 (s), 136.9 (s), 134.7 (s), 132.5 (s), 132.0 (s), 131.0 (s), 130.9 (s), 130.3 (s), 129.3 (s), 129.1 (s), 128.7 (s), 128.5 (s), 128.3 (s), 128.2 (s), 127.7 (s), 127.6 (s), 127.3 (s), 127.1 (s), 124.5 (s), 123.4 (s), 121.9 (s), 121.5 (s), 120.0 (s). APPI HRMS calculated for $C_{26}H_{16}$ [M^+] *m/z* 328.1246, found 328.1250. UV-vis (Dichloromethane/Methanol 1:1) λ_{max} (nm): 278, 294, 303, 339, 353, 372.

(27) 1,2-bis(2,6-difluorophenyl)-1,2-diphenylethane.

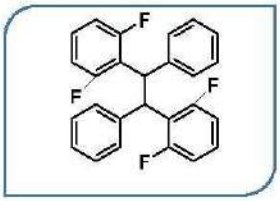

The compound (32) was obtained fully in accordance with the literature data [4].

(28) 8-(2,6-difluorophenyl)benzo[e]acephenanthrylene.

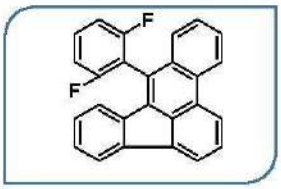

The compound was obtained according to the General Procedure A from (27). Yield 38 mg (9 %). ^{1}H NMR (400 MHz, CD_2Cl_2) δ 8.80 (d, *J* = 8.4 Hz, 1H), 8.01 (dd, *J* = 7.1, 0.5 Hz, 1H), 7.89 – 7.81 (m, 1H), 7.75 (ddd, *J* = 8.2, 7.1, 0.9 Hz, 1H), 7.61 – 7.52 (m, 3H), 7.48 – 7.33 (m, 5H), 7.26 (td, *J* = 7.5, 1.1 Hz, 1H), 6.99 (td, *J* = 7.6, 1.1 Hz, 1H), 6.59 (dt, *J* = 7.7, 0.8 Hz, 1H). ^{19}F NMR (377 MHz, CD_2Cl_2) δ -111.97 (d, *J* = 10.6 Hz). ^{13}C NMR (151 MHz, CD_2Cl_2) δ 162.03 (d, *J* = 251.2 Hz), 140.80 (s), 138.01 (s), 137.90 (s), 136.97 (d, *J* = 5.0 Hz), 136.61 (s), 135.89 (d, *J* = 3.1 Hz), 133.30 (s), 131.87 (s), 129.78 (s), 128.98 (s), 128.56 (d, *J* = 2.6 Hz), 128.24 (s), 128.10 (s), 127.23 (s), 126.68 (d, *J* = 1.7 Hz), 126.62 (s), 126.54 (s), 124.98 (d, *J* = 3.6 Hz), 124.47 (d, *J* = 3.2 Hz), 124.27 (s), 120.92 (s), 120.02 – 119.95 (m), 119.53 (d, *J* = 11.9 Hz), 113.58 (s), 113.42 (s). APPI HRMS calculated for $C_{26}H_{14}F_2$ [M^+] *m/z* 364.1058, found 364.1062. UV-vis (Dichloromethane/Methanol 1:1) λ_{max} (nm): 261, 290, 303, 339, 353, 373.

3. Spectroscopic Analysis and Characterization

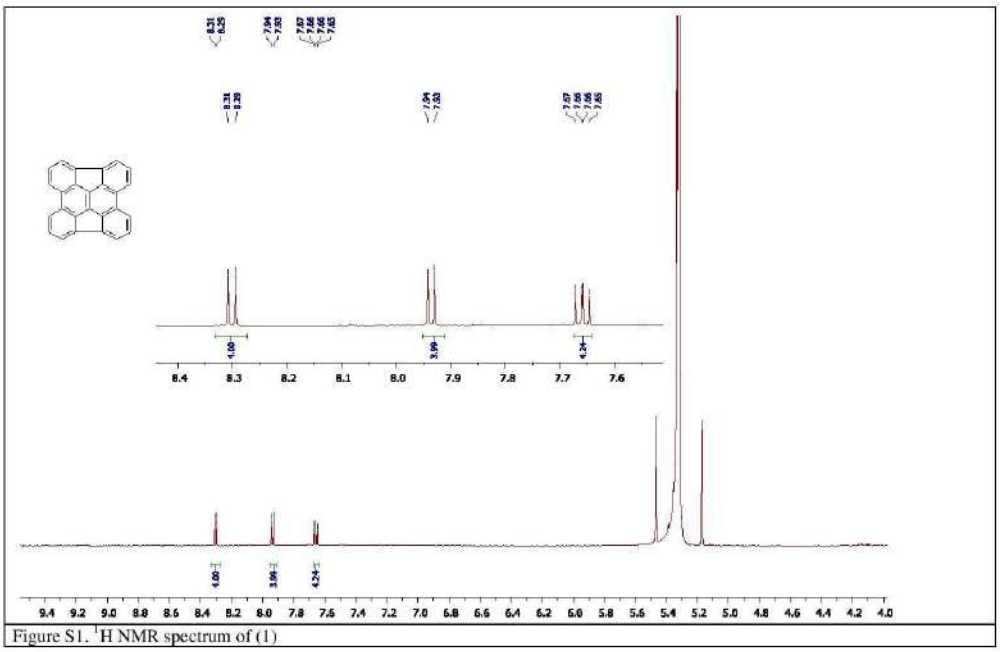

Figure S1. ^{1}H NMR spectrum of (1)

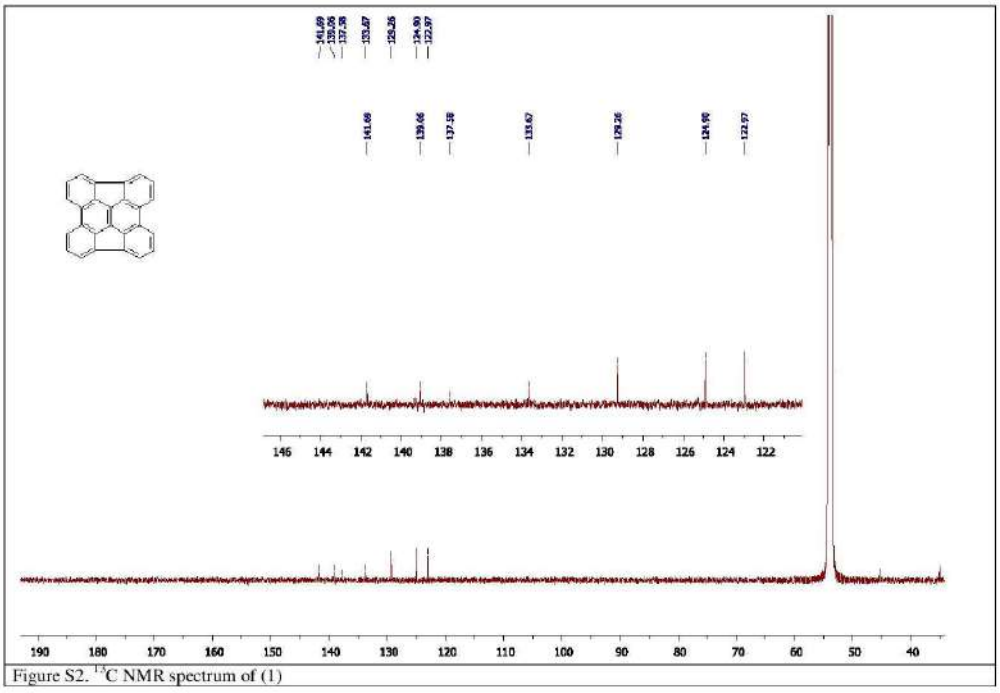

Figure S2. ^{13}C NMR spectrum of (1)

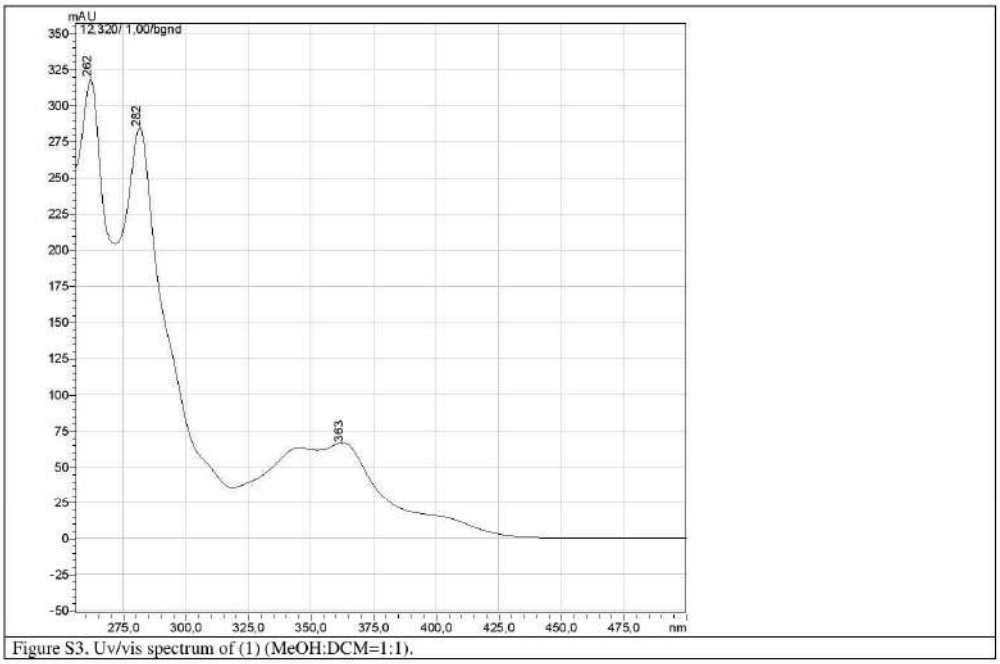

Figure S3. Uv/vis spectrum of (1) (MeOH:DCM=1:1).

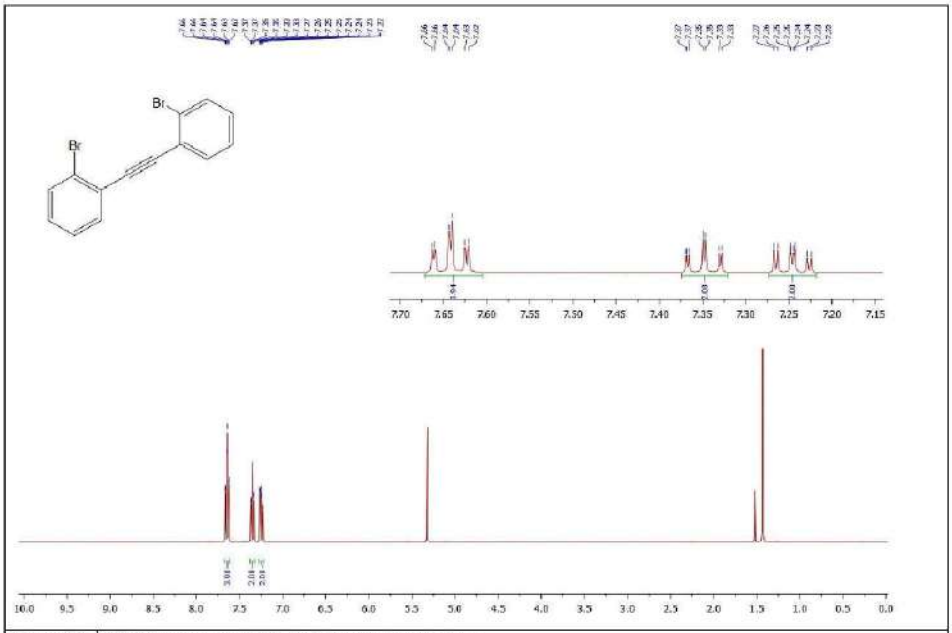

Figure S4. ^{1}H NMR spectrum of 1,2-bis(2-bromophenyl)ethyne

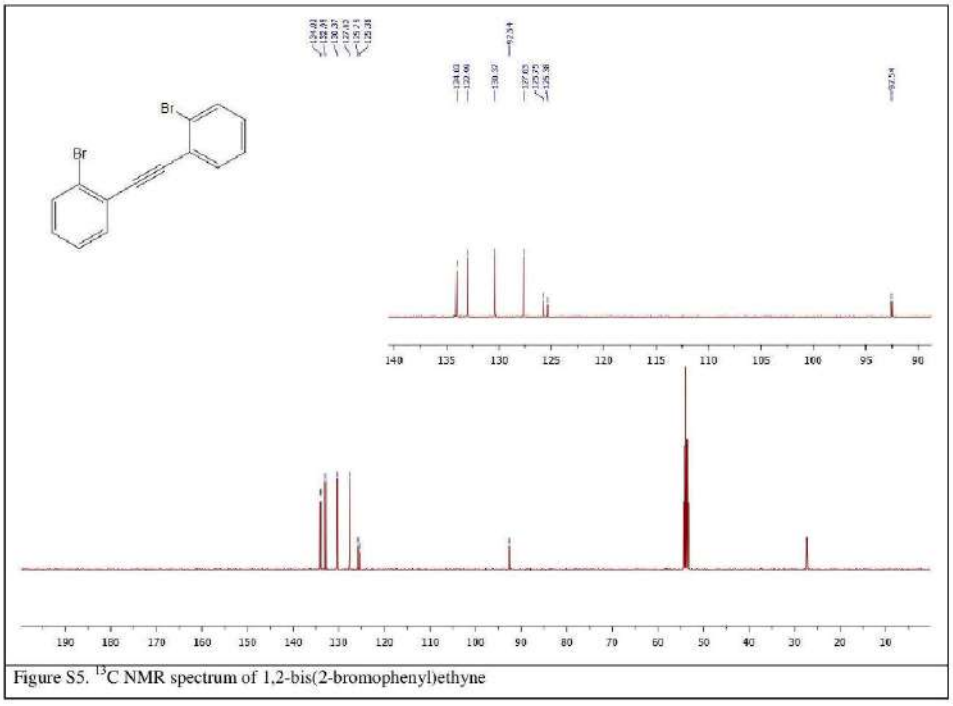

Figure S5. ^{13}C NMR spectrum of 1,2-bis(2-bromophenyl)ethyne

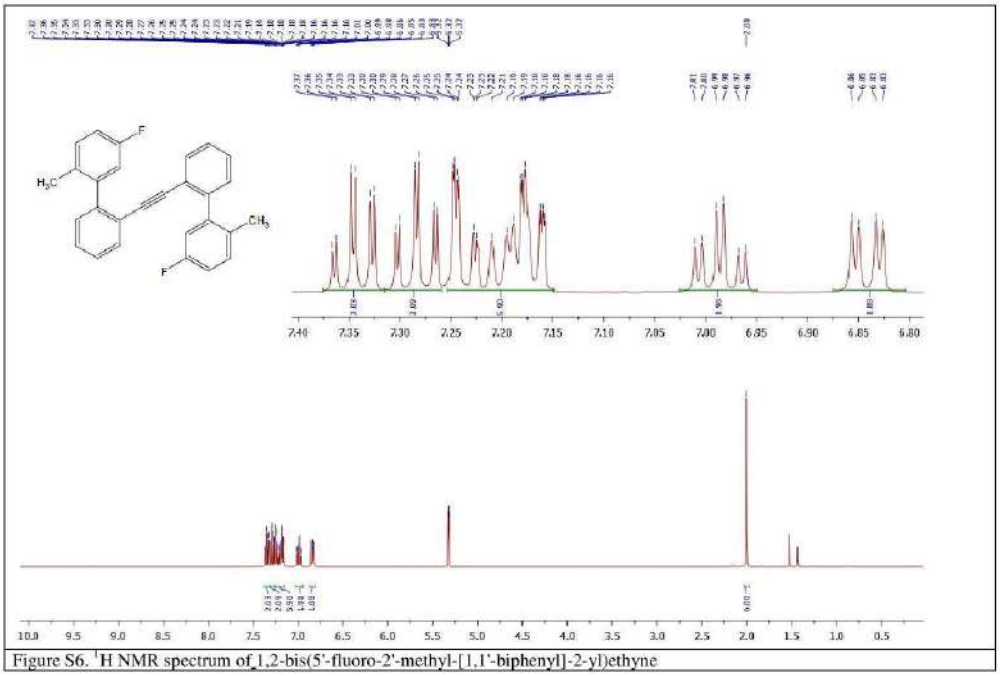

Figure S6. ^{1}H NMR spectrum of 1,2-bis(5'-fluoro-2'-methyl-[1,1'-biphenyl]-2-yl)ethyne

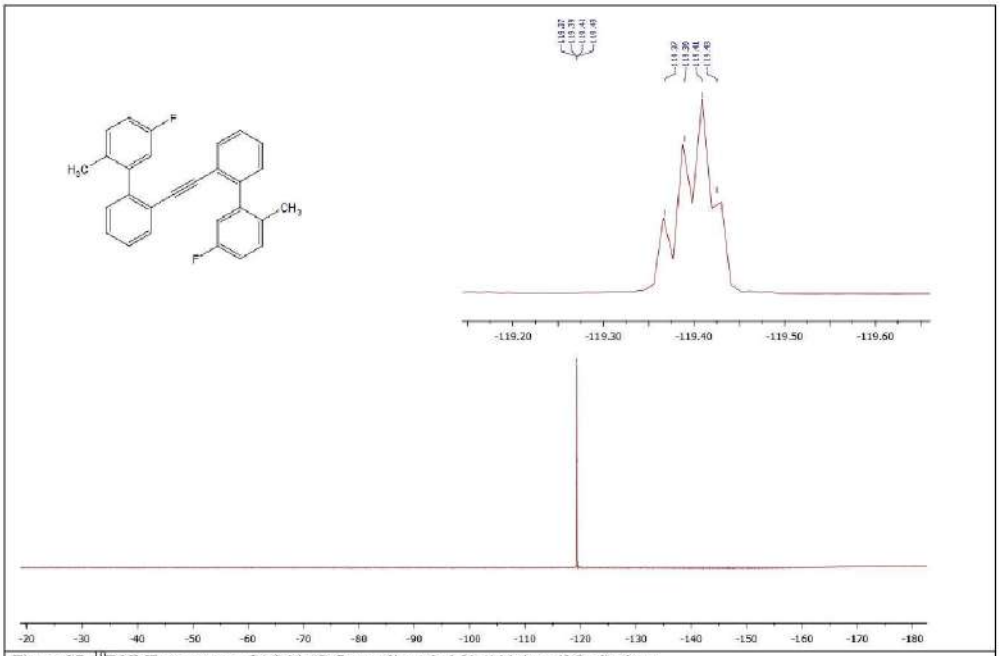

Figure S7. ^{19}F NMR spectrum of 1,2-bis(5'-fluoro-2'-methyl-[1,1'-biphenyl]-2-yl)ethyne

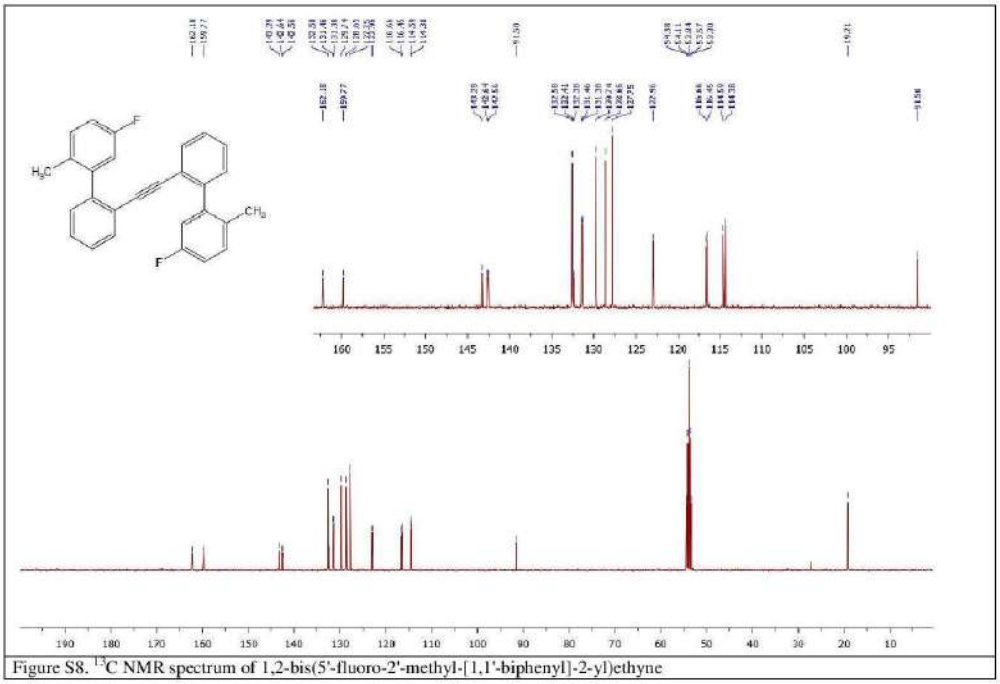

Figure S8. ^{13}C NMR spectrum of 1,2-bis(5'-fluoro-2'-methyl-[1,1'-biphenyl]-2-yl)ethyne

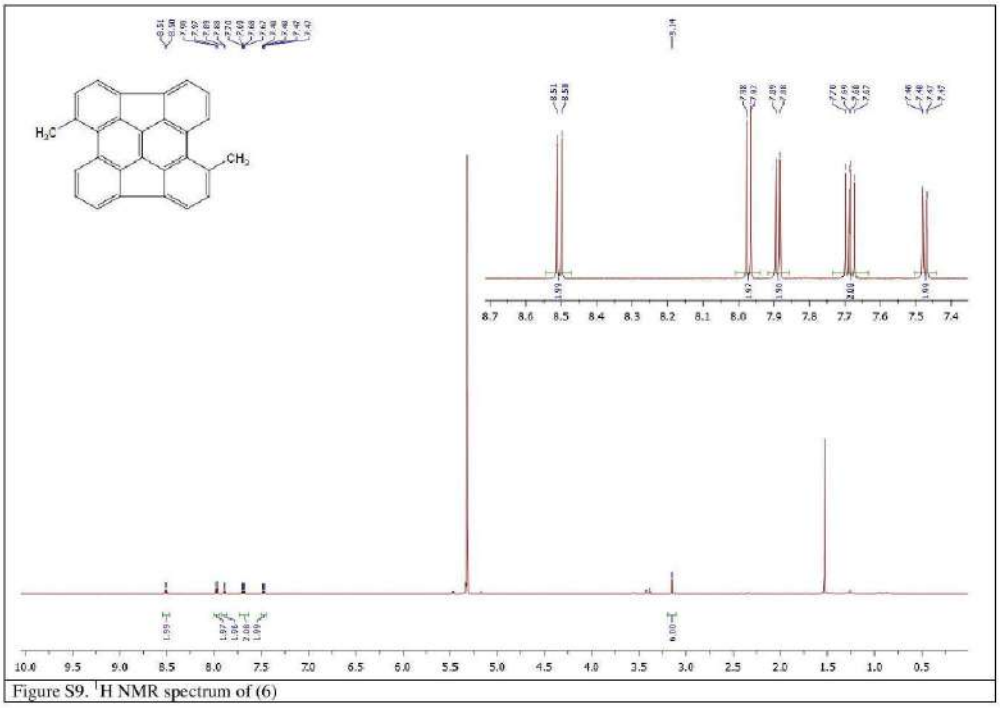

Figure S9. ^{1}H NMR spectrum of (6)

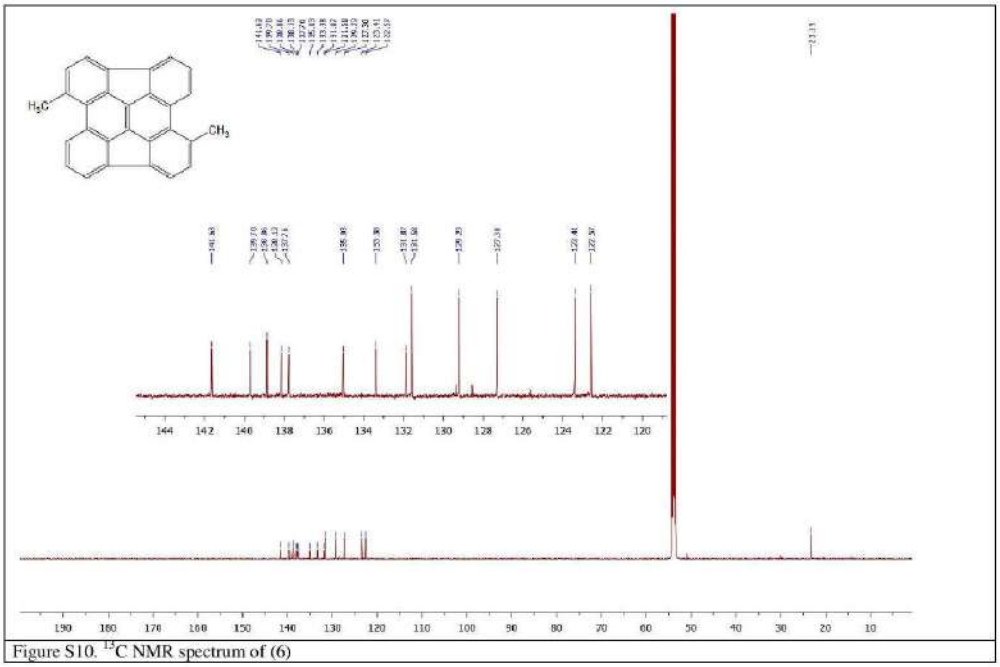

Figure S10. ^{13}C NMR spectrum of (6)

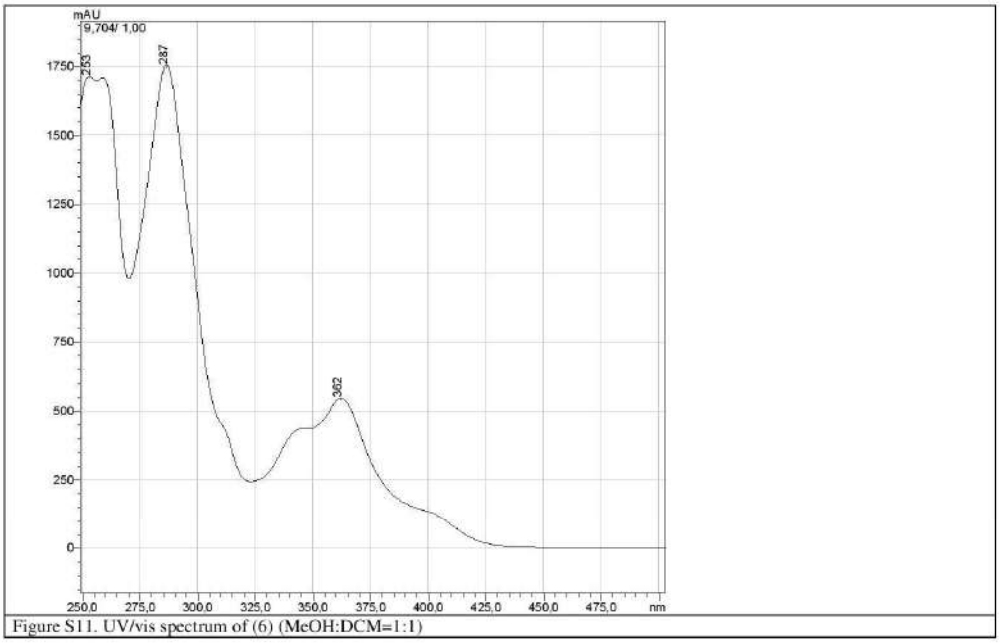

Figure S11. UV/vis spectrum of (6) (MeOH:DCM=1:1)

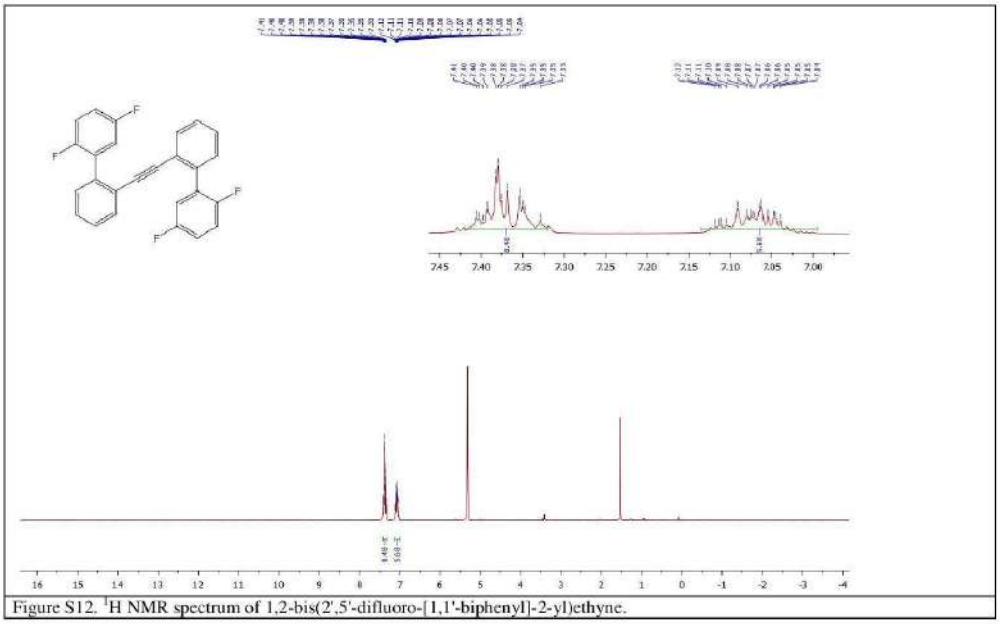

Figure S12. ^{1}H NMR spectrum of 1,2-bis(2',5'-difluoro-[1,1'-biphenyl]-2-yl)ethyne.

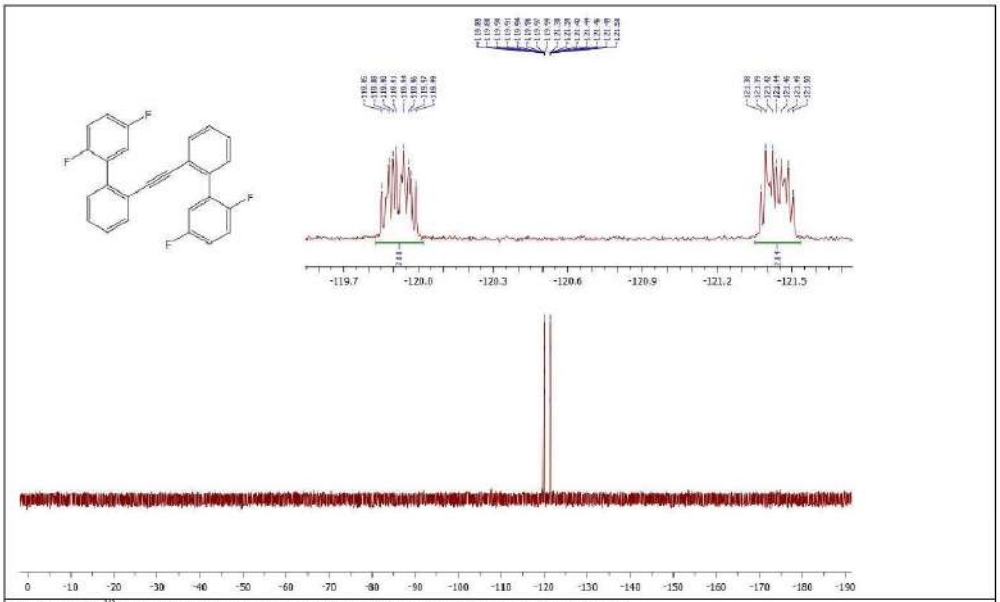

Figure S13. ^{19}F NMR spectrum of 1,2-bis(2',5'-difluoro-[1,1'-biphenyl]-2-yl)ethyne.

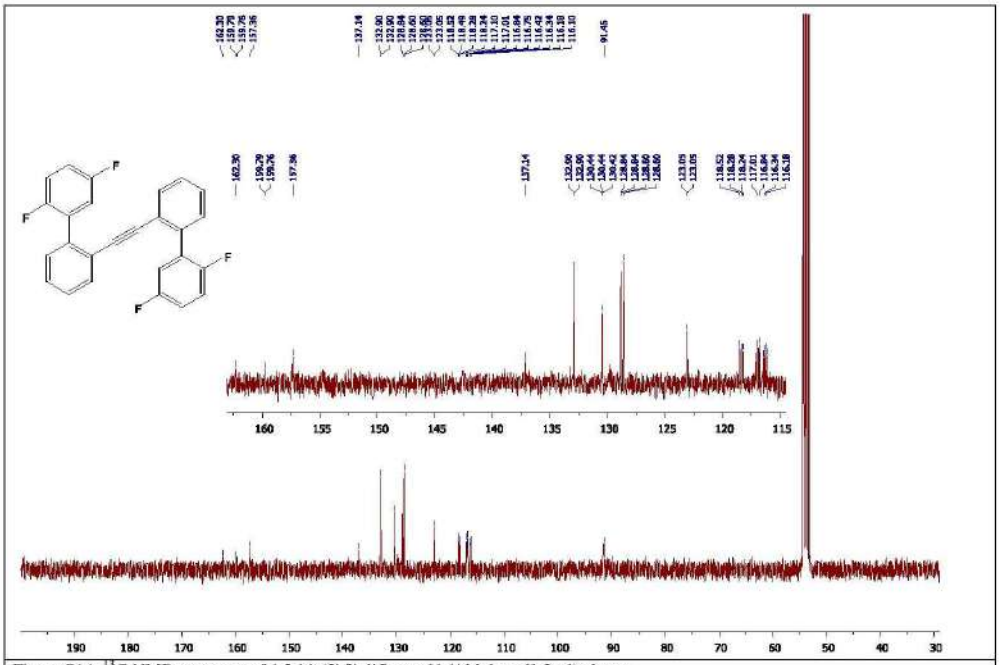

Figure S14. ^{13}C NMR spectrum of 1,2-bis(2',5'-difluoro-[1,1'-biphenyl]-2-yl)ethyne.

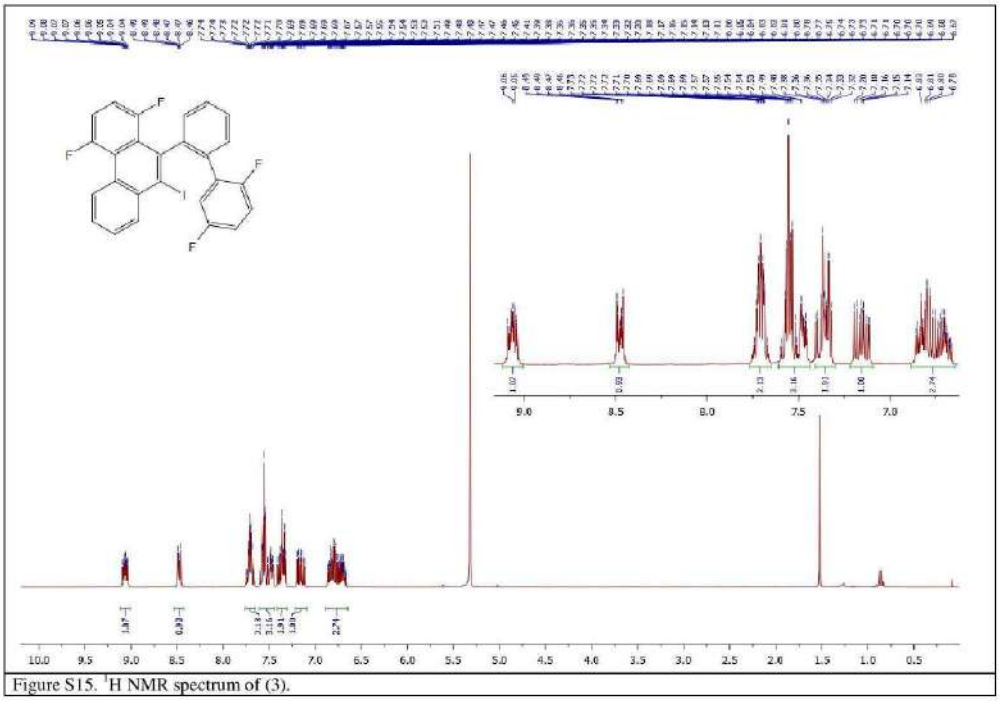

Figure S15. ^{1}H NMR spectrum of (3).

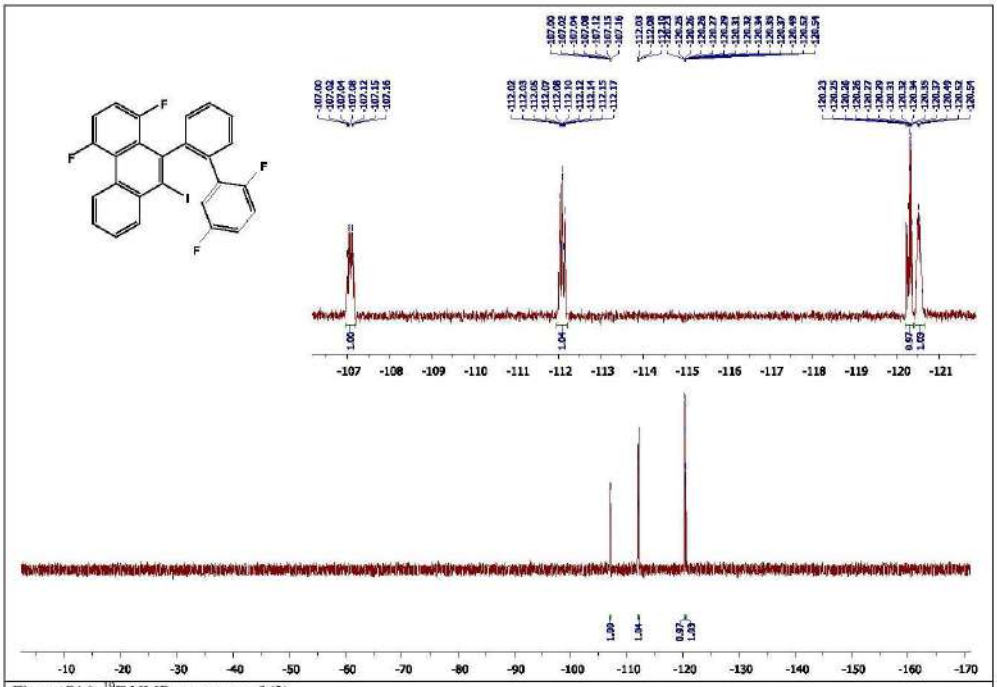

Figure S16. ^{19}F NMR spectrum of (3).

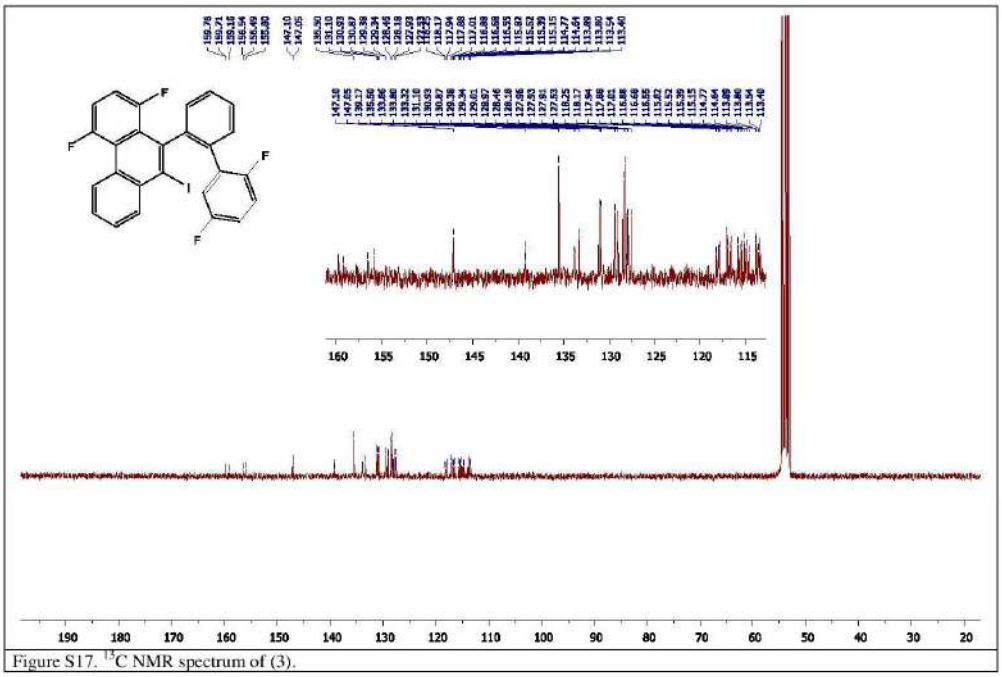

Figure S17. ^{13}C NMR spectrum of (3).

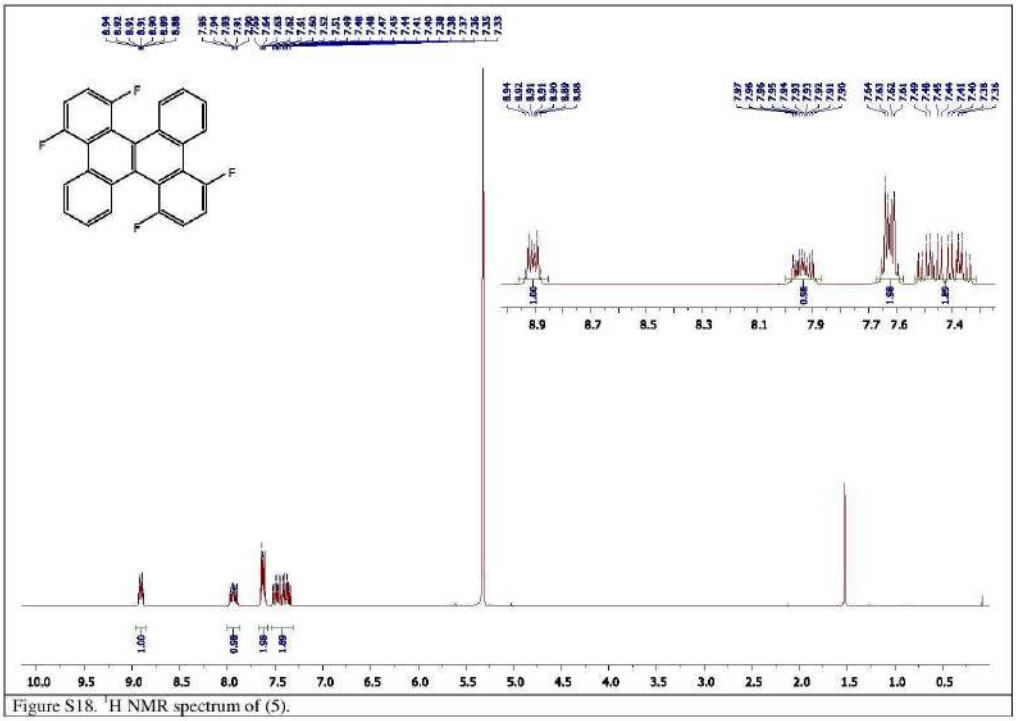

Figure S18. ^{1}H NMR spectrum of (5).

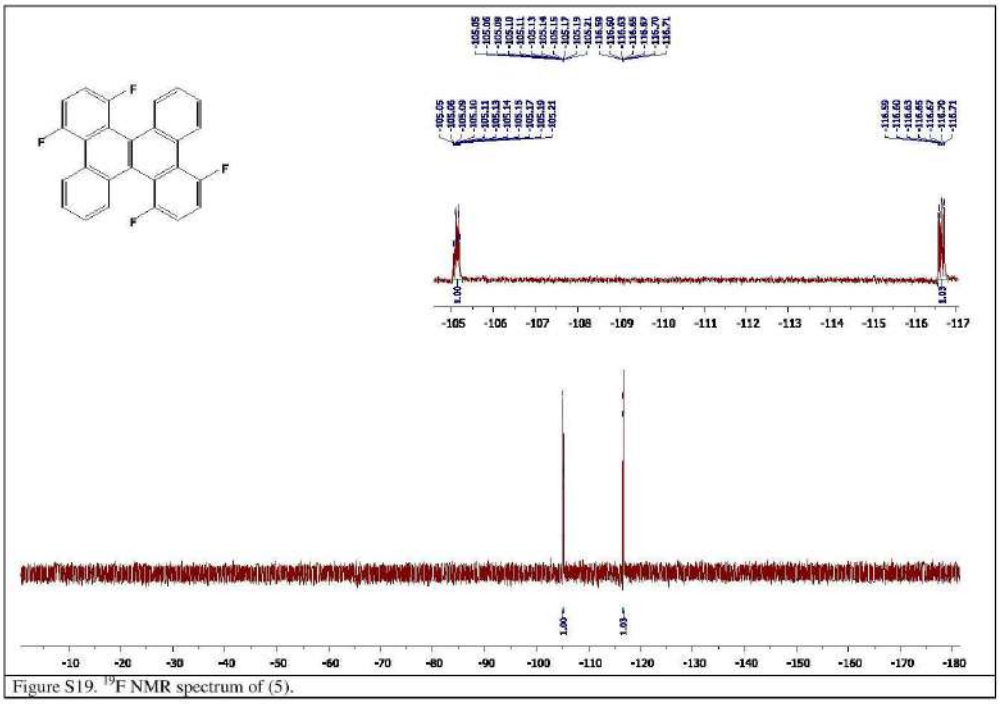

Figure S19. ^{19}F NMR spectrum of (5).

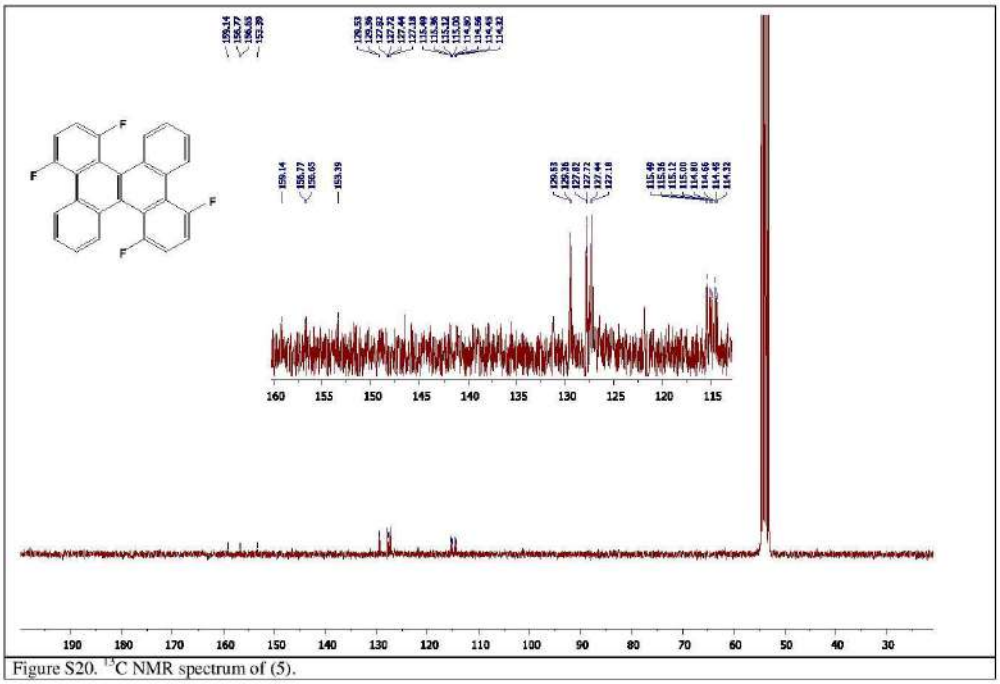

Figure S20. ^{13}C NMR spectrum of (5).

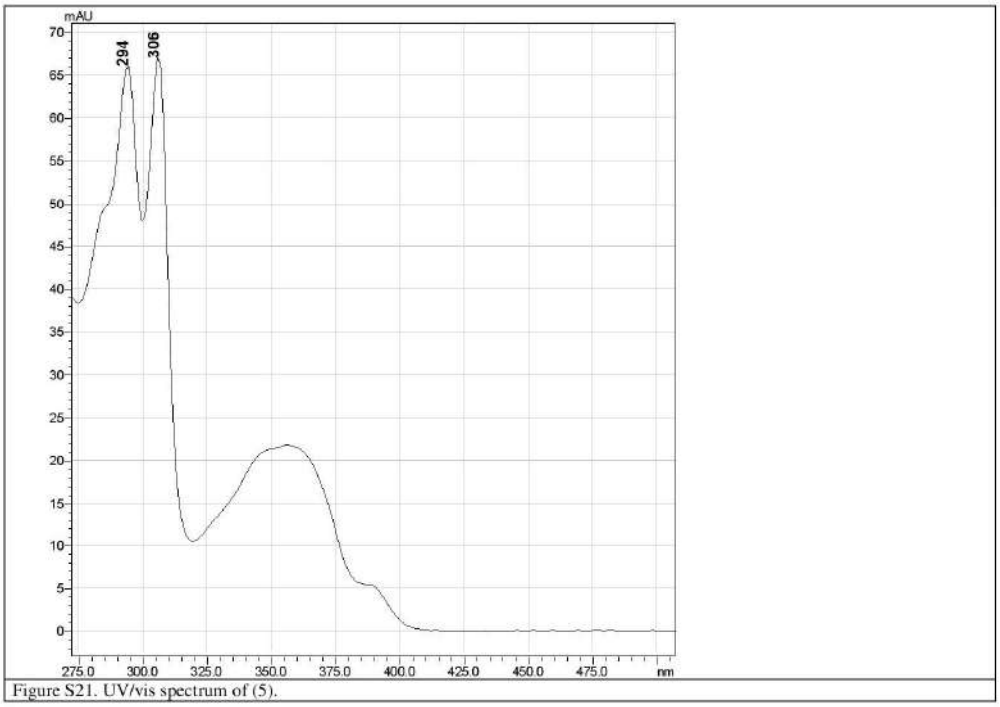

Figure S21. UV/vis spectrum of (5).

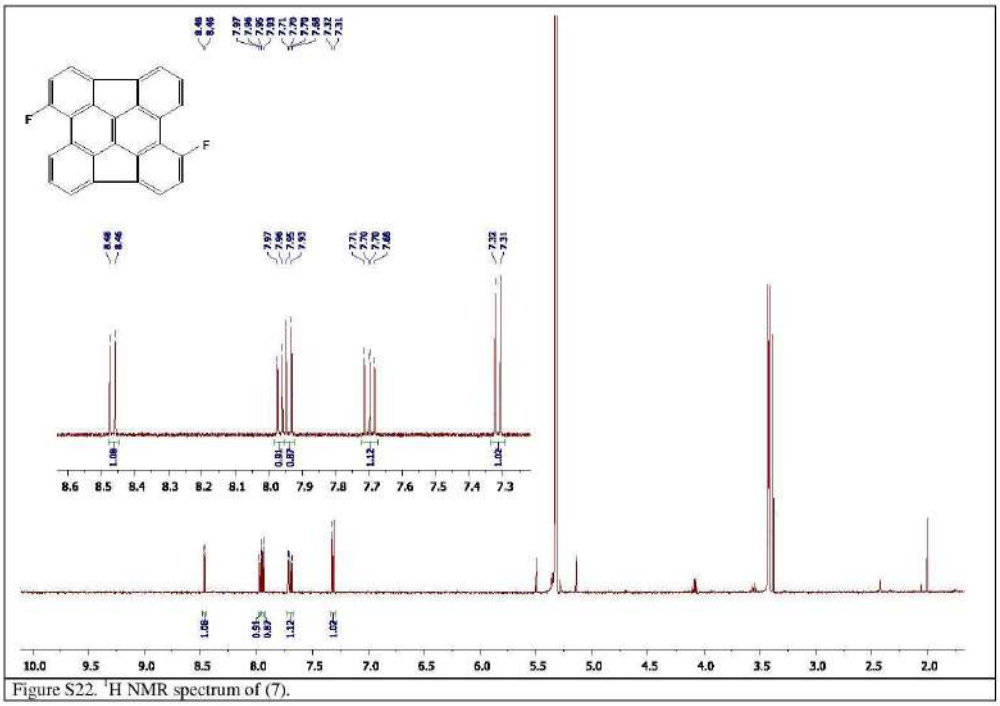

Figure S22. ^{1}H NMR spectrum of (7).

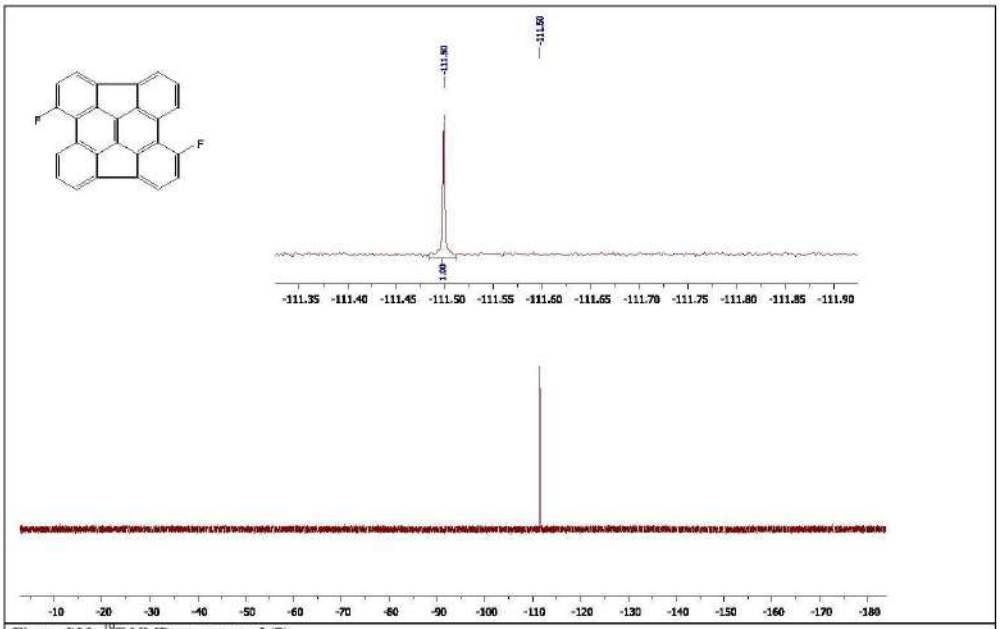

Figure S23. ^{19}F NMR spectrum of (7).

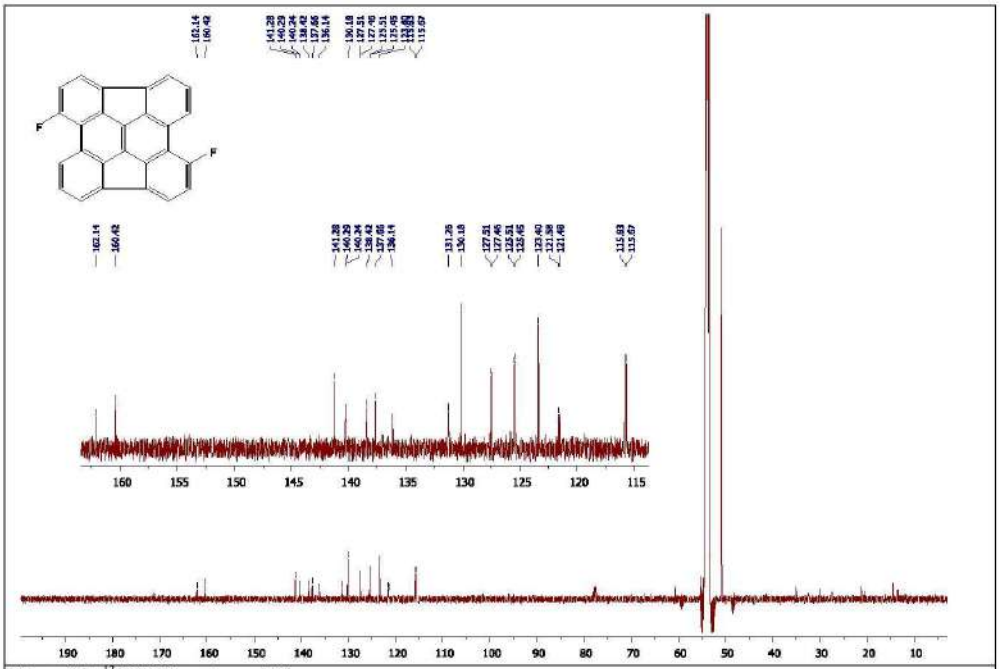

Figure S24. ^{13}C NMR spectrum of (7).

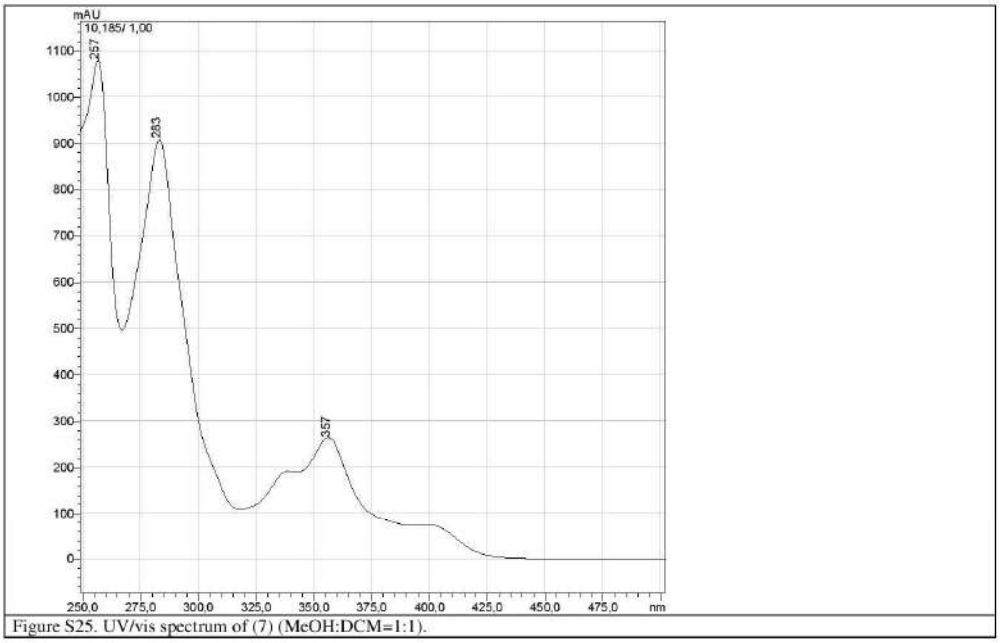

Figure S25. UV/vis spectrum of (7) (MeOH:DCM=1:1).

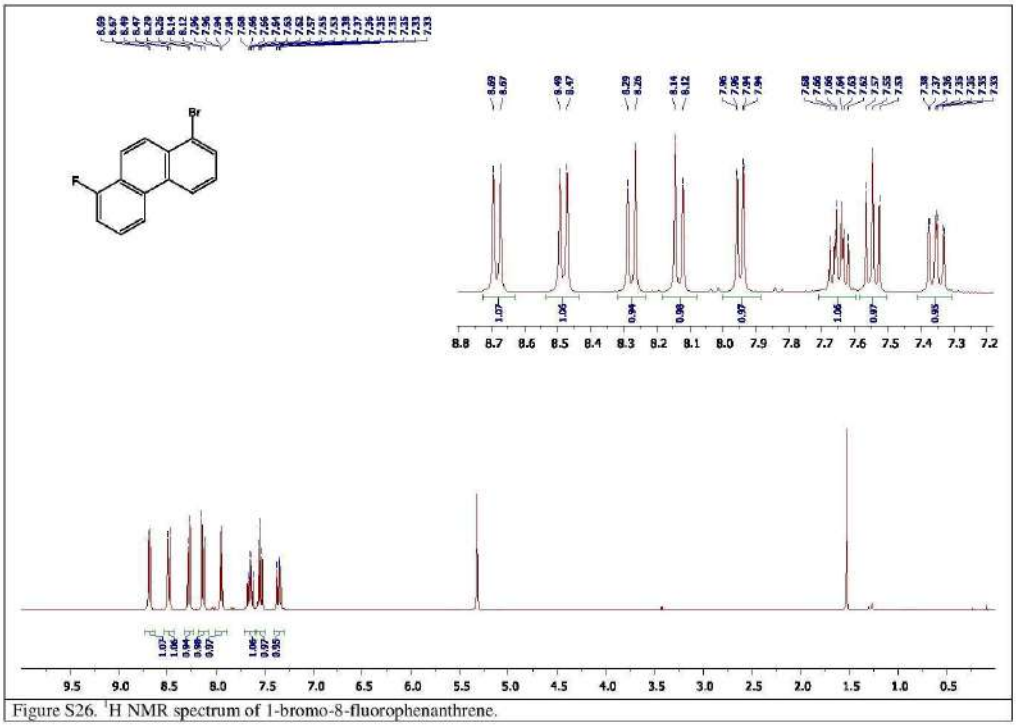

Figure S26. ^{1}H NMR spectrum of 1-bromo-8-fluorophenanthrene.

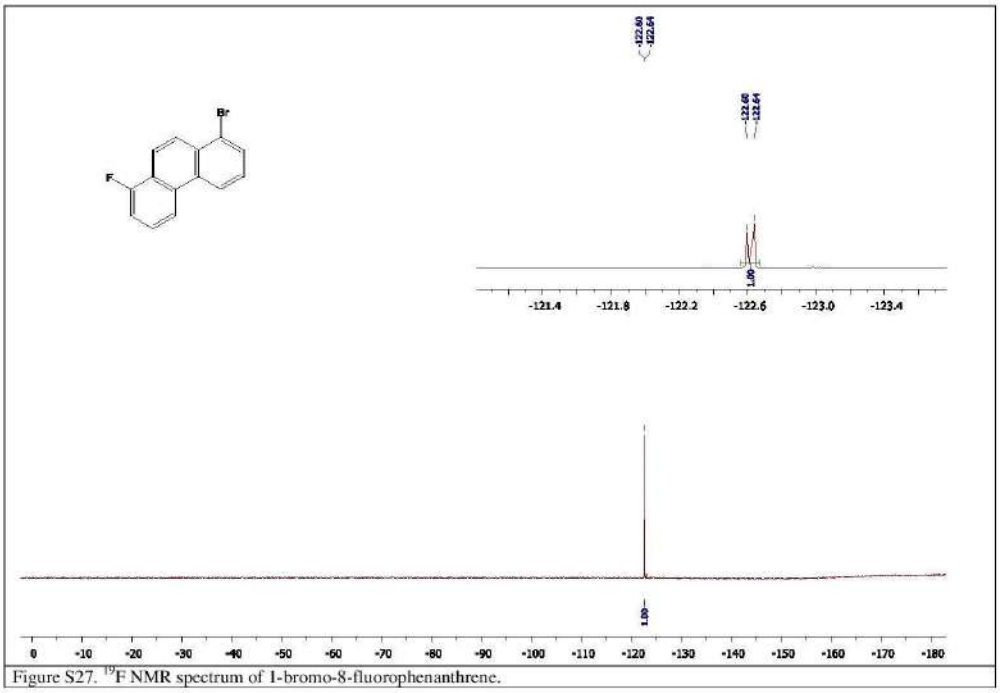

Figure S27. ^{19}F NMR spectrum of 1-bromo-8-fluorophenanthrene.

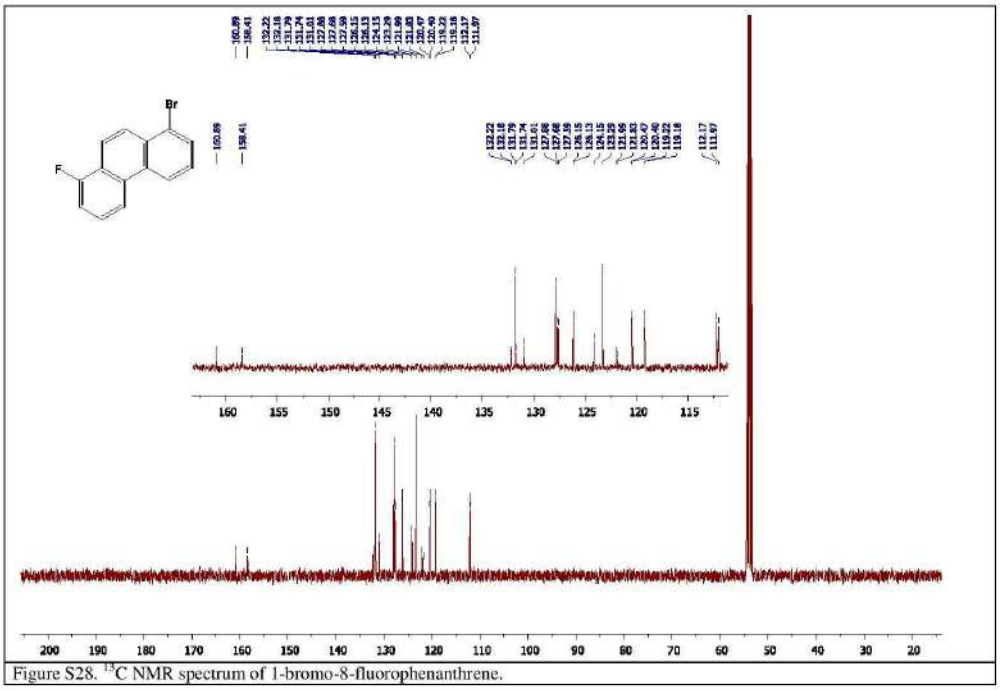

Figure S28. ^{13}C NMR spectrum of 1-bromo-8-fluorophenanthrene.

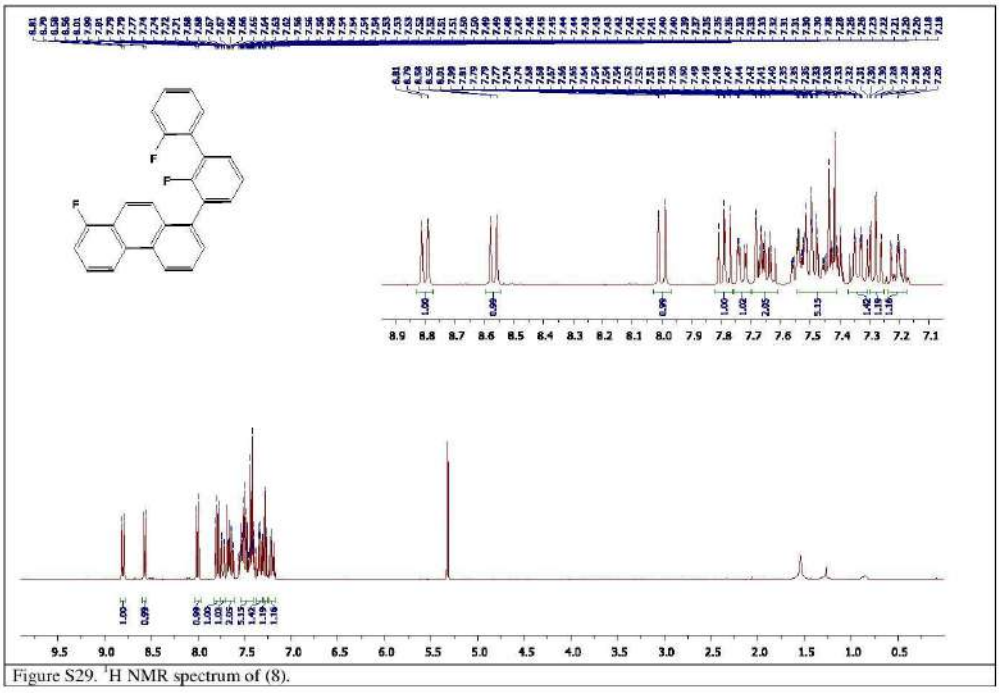

Figure S29. ^{1}H NMR spectrum of (8).

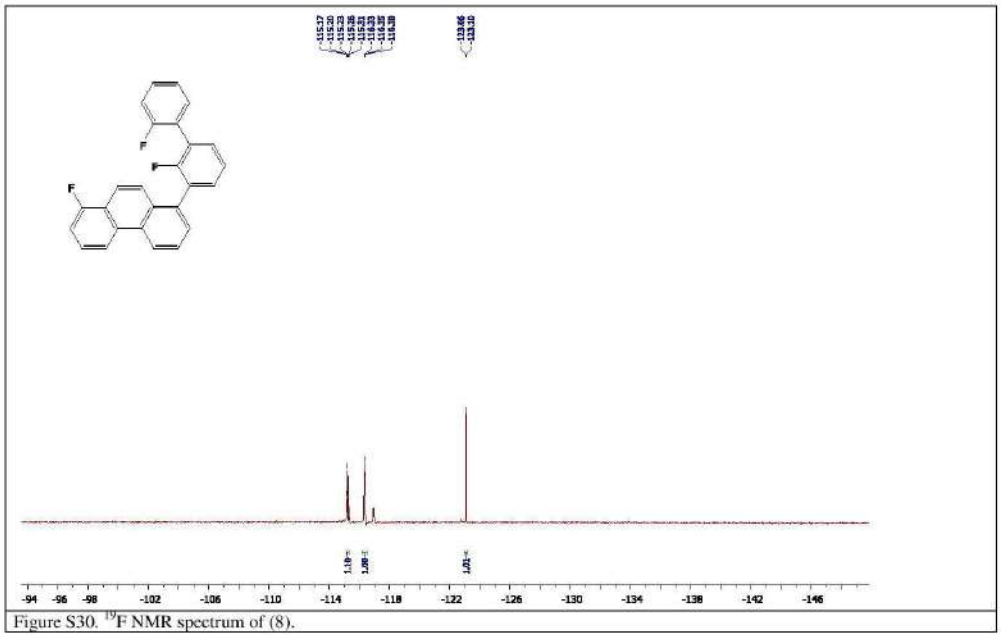

Figure S30. ^{19}F NMR spectrum of (8).

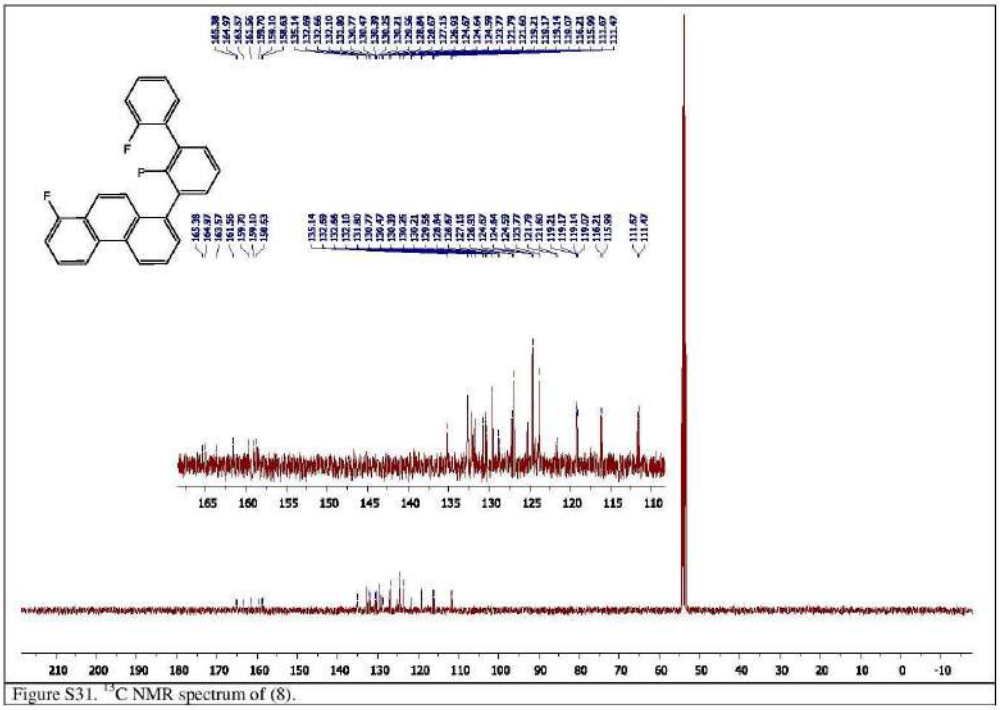

Figure S31. ^{13}C NMR spectrum of (8).

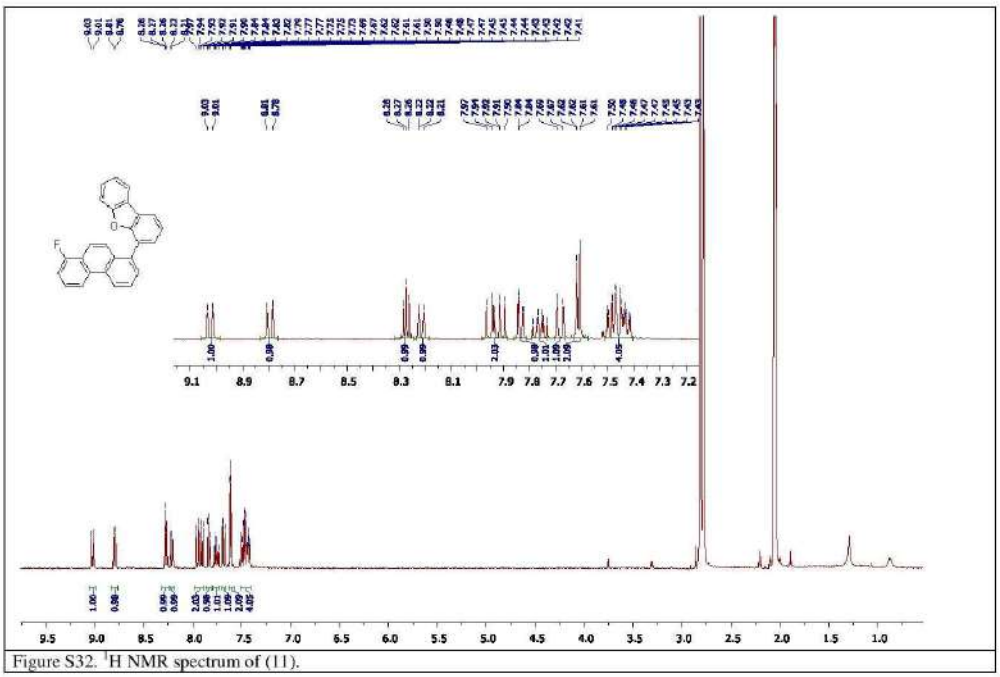

Figure S32. ^{1}H NMR spectrum of (11).

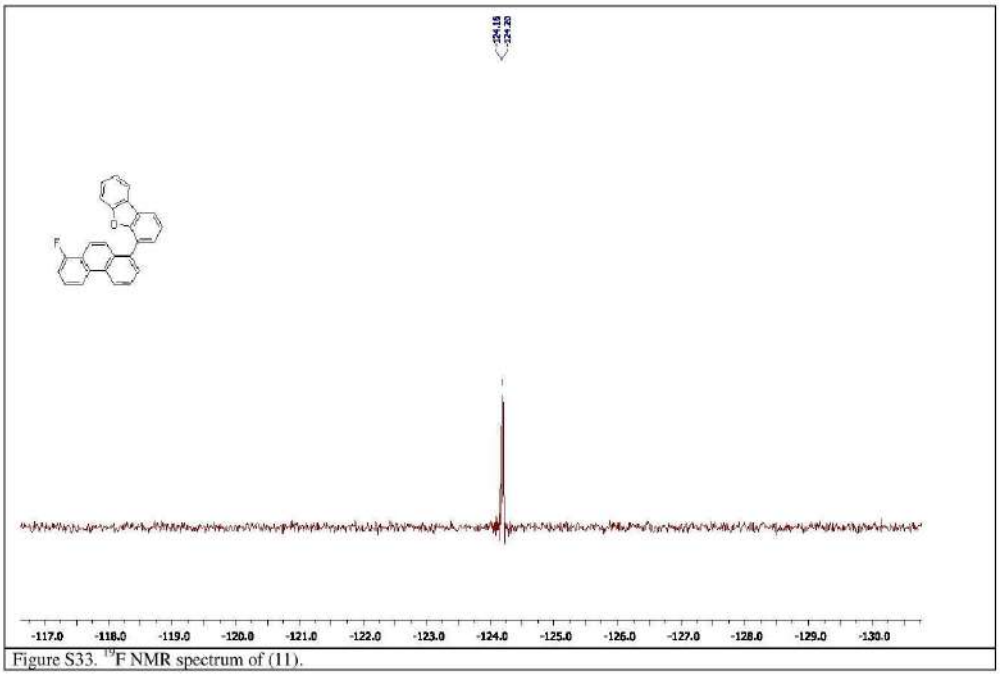

Figure S33. ^{19}F NMR spectrum of (11).

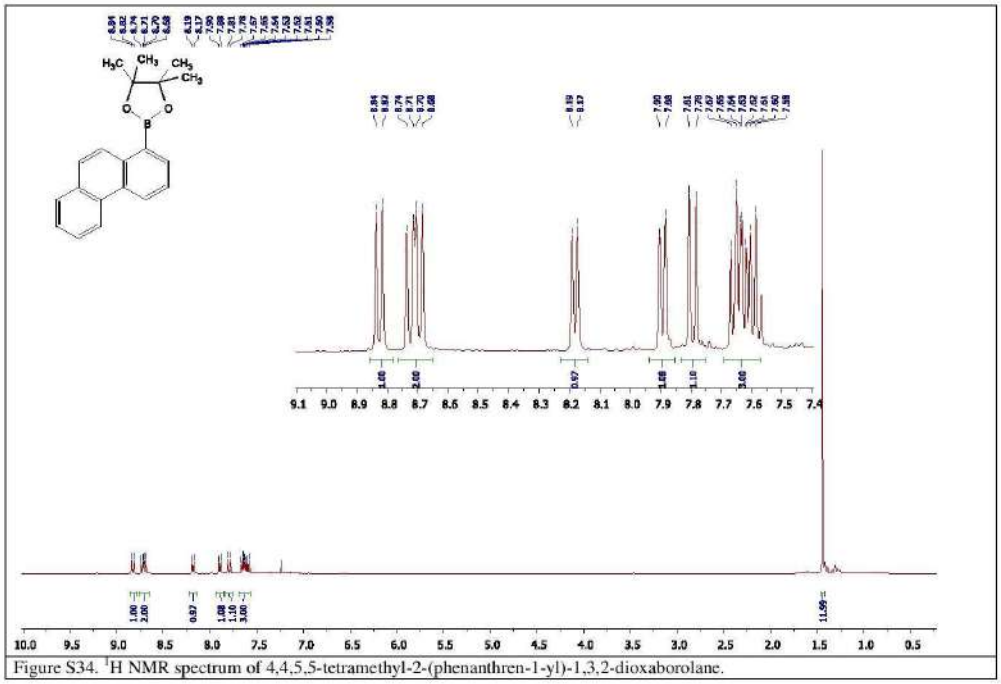

Figure S34. ^{1}H NMR spectrum of 4,4,5,5-tetramethyl-2-(phenanthren-1-yl)-1,3,2-dioxaborolane.

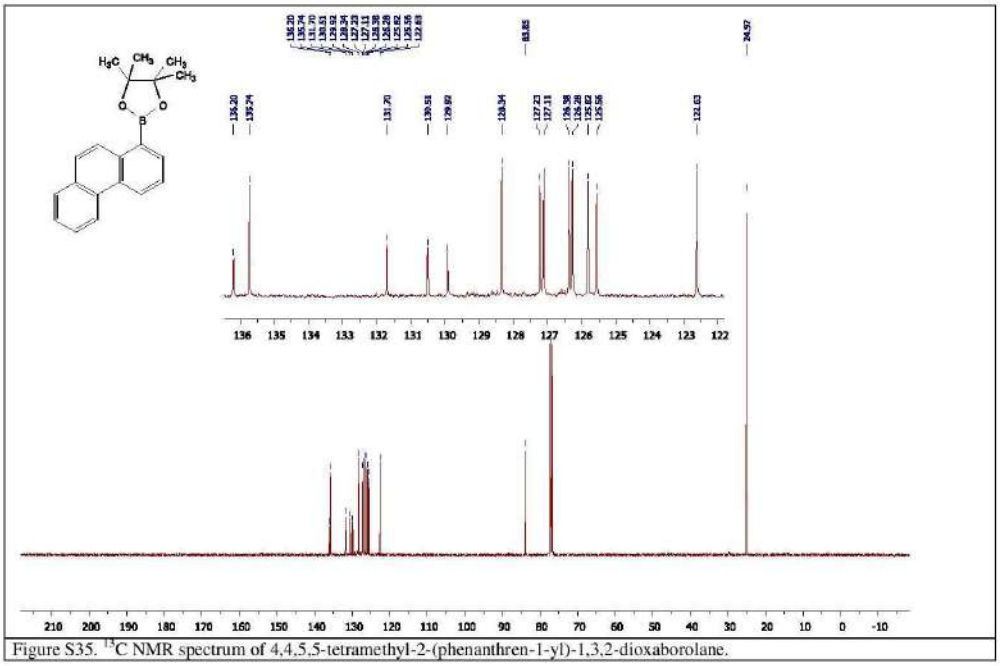

Figure S35. ^{13}C NMR spectrum of 4,4,5,5-tetramethyl-2-(phenanthren-1-yl)-1,3,2-dioxaborolane.

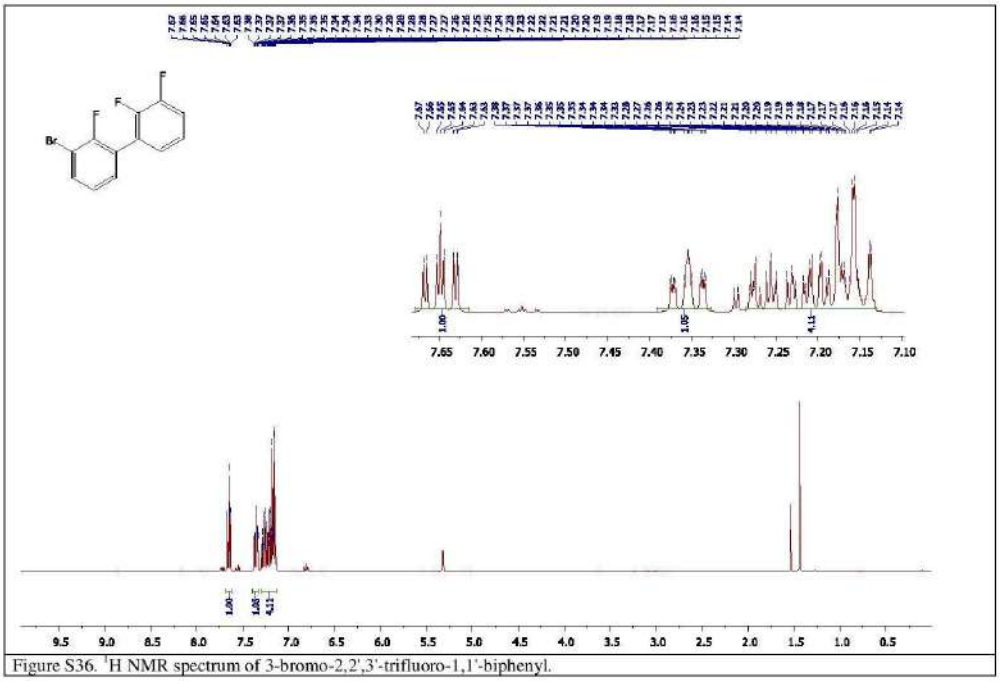

Figure S36. ^{1}H NMR spectrum of 3-bromo-2,2',3'-trifluoro-1,1'-biphenyl.

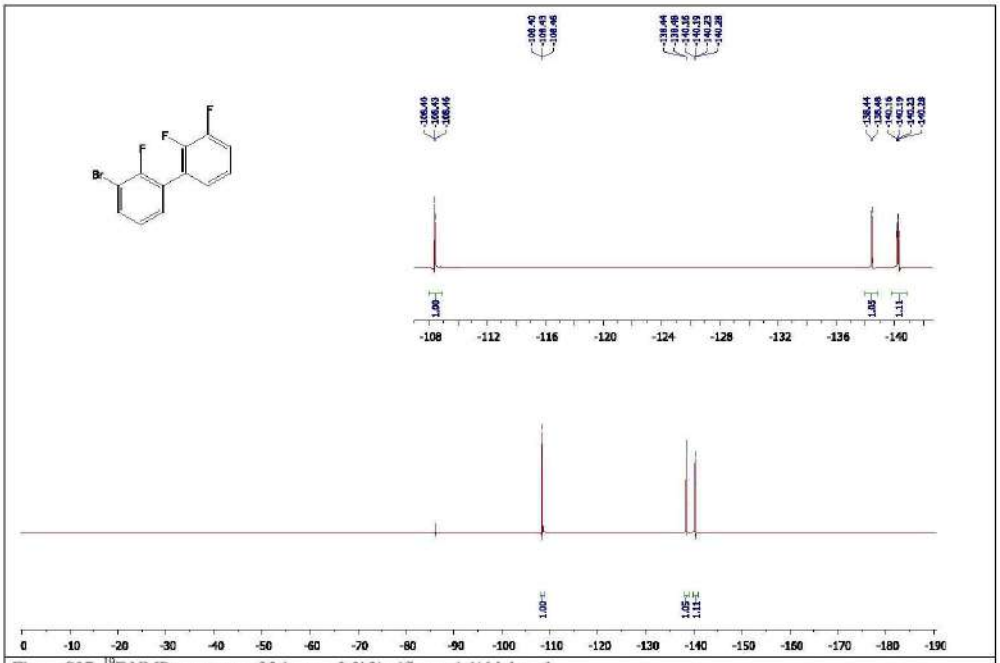

Figure S37. ^{19}F NMR spectrum of 3-bromo-2,2',3'-trifluoro-1,1'-biphenyl.

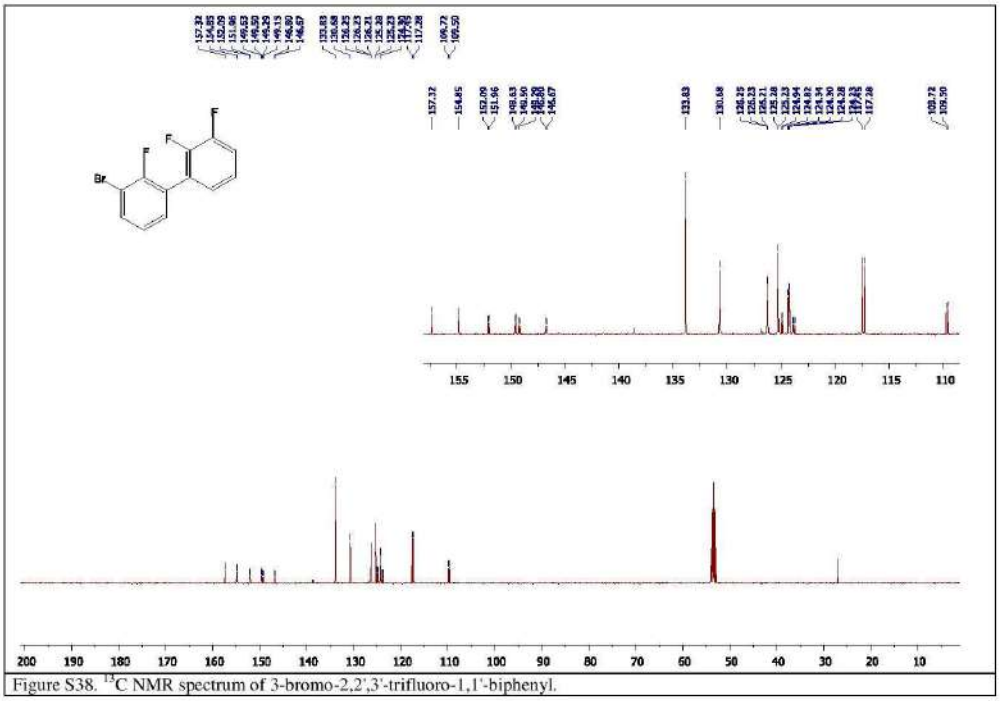

Figure S38. ^{13}C NMR spectrum of 3-bromo-2,2',3'-trifluoro-1,1'-biphenyl.

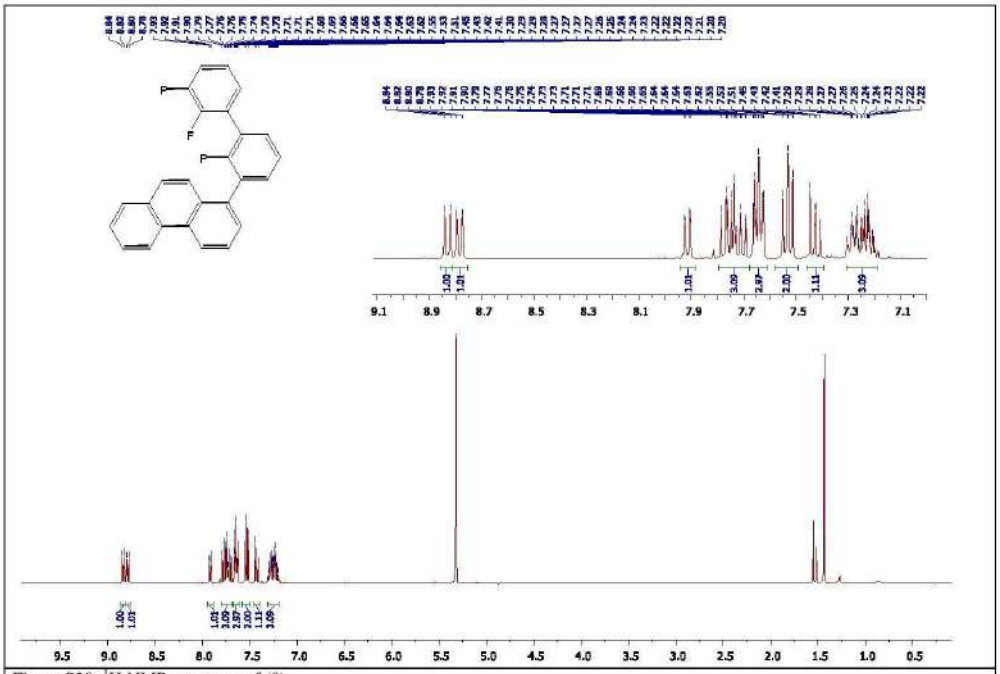

Figure S39. ^{1}H NMR spectrum of (9).

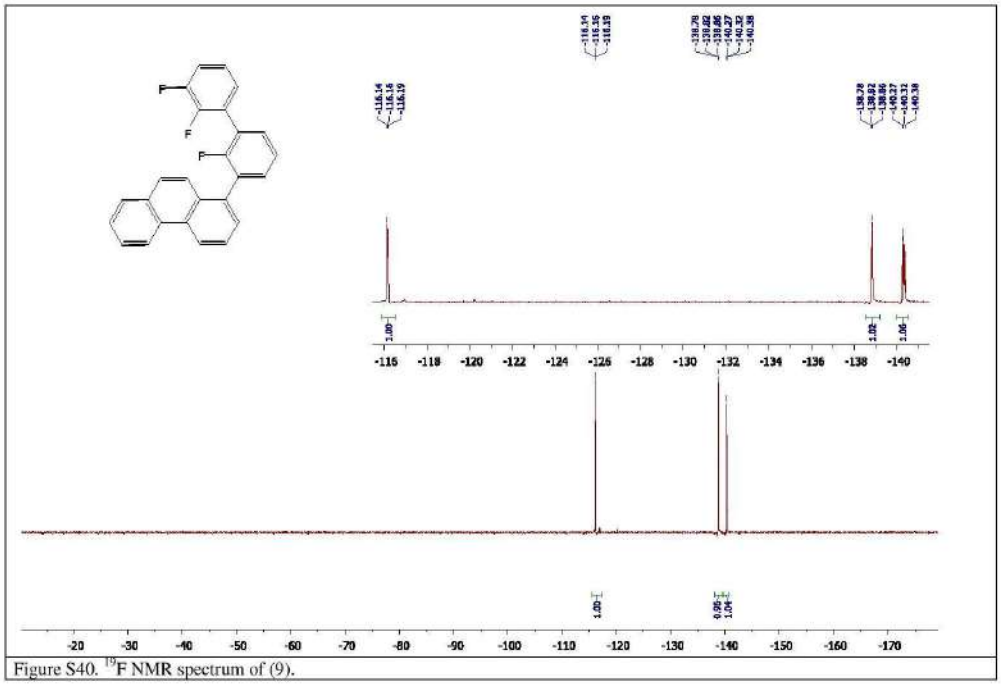

Figure S40. ^{19}F NMR spectrum of (9).

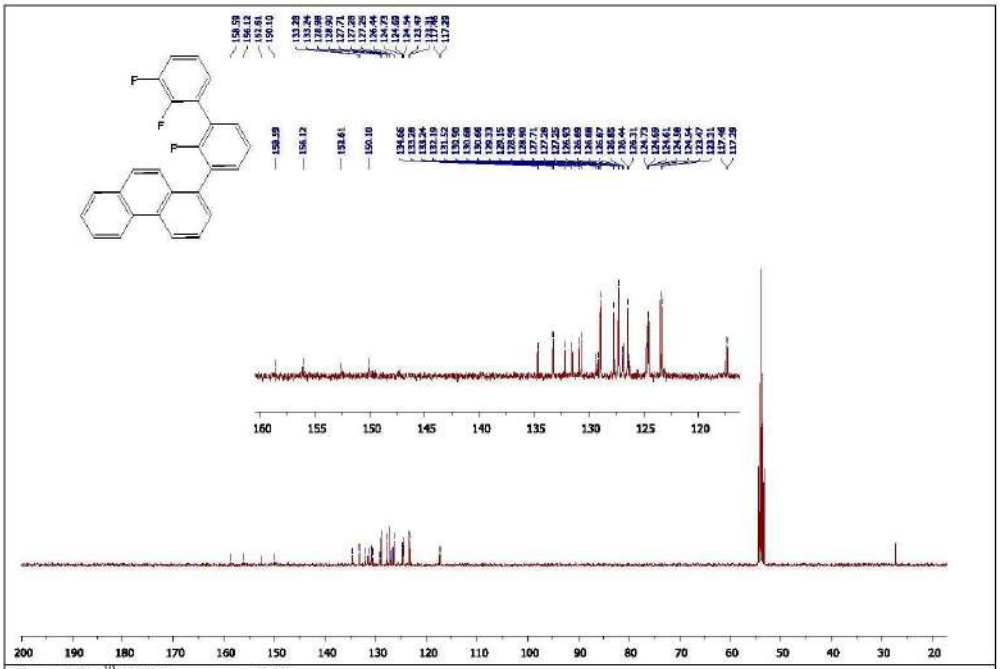

Figure S41. ^{19}F NMR spectrum of (9).

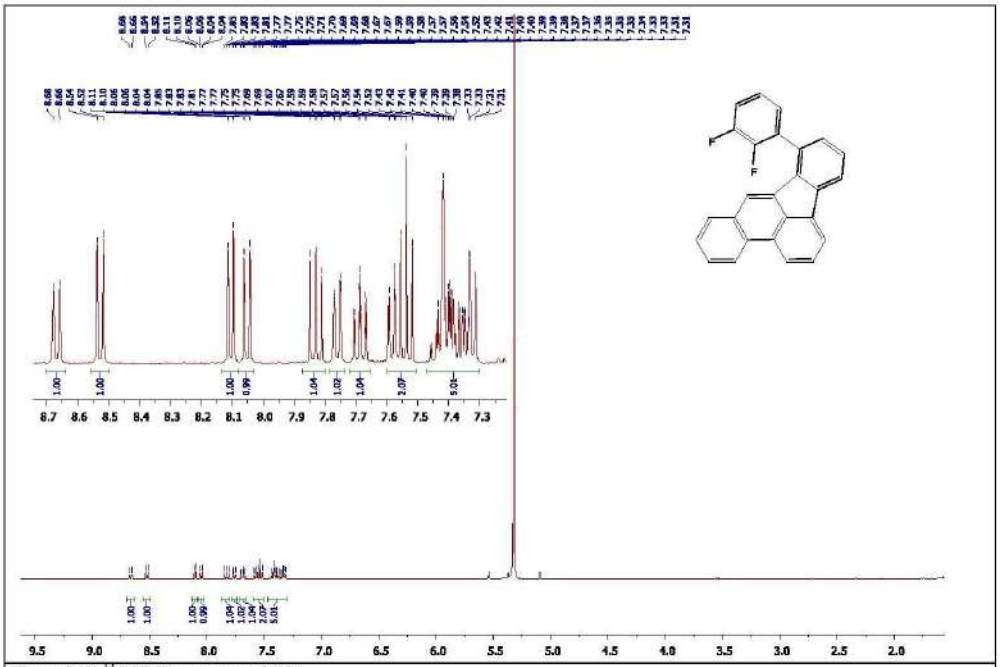

Figure S42. ^{13}C NMR spectrum of (12).

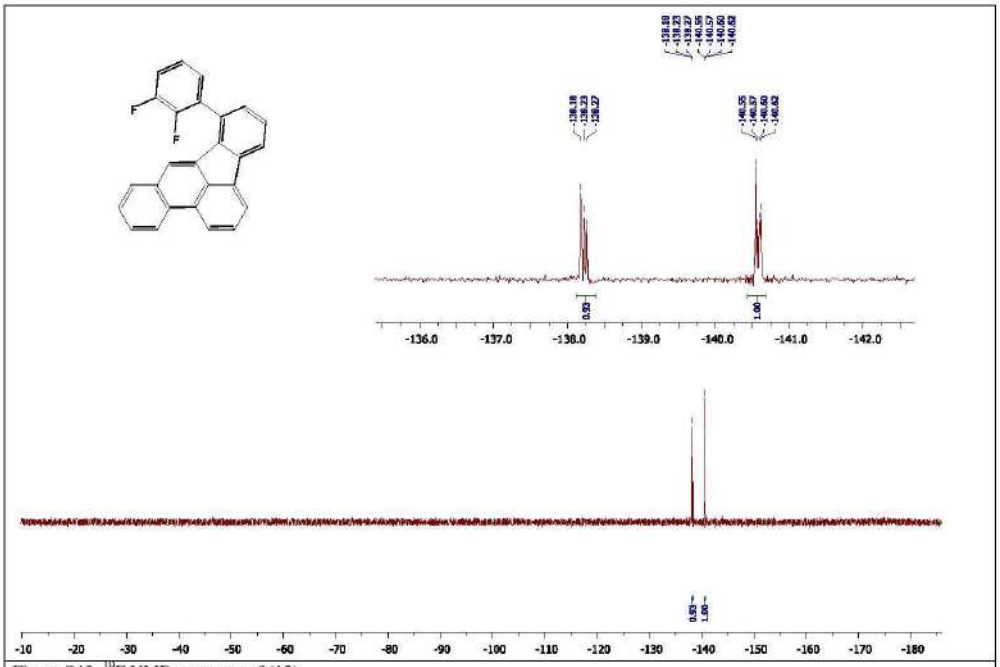

Figure S43. ^{19}F NMR spectrum of (12).

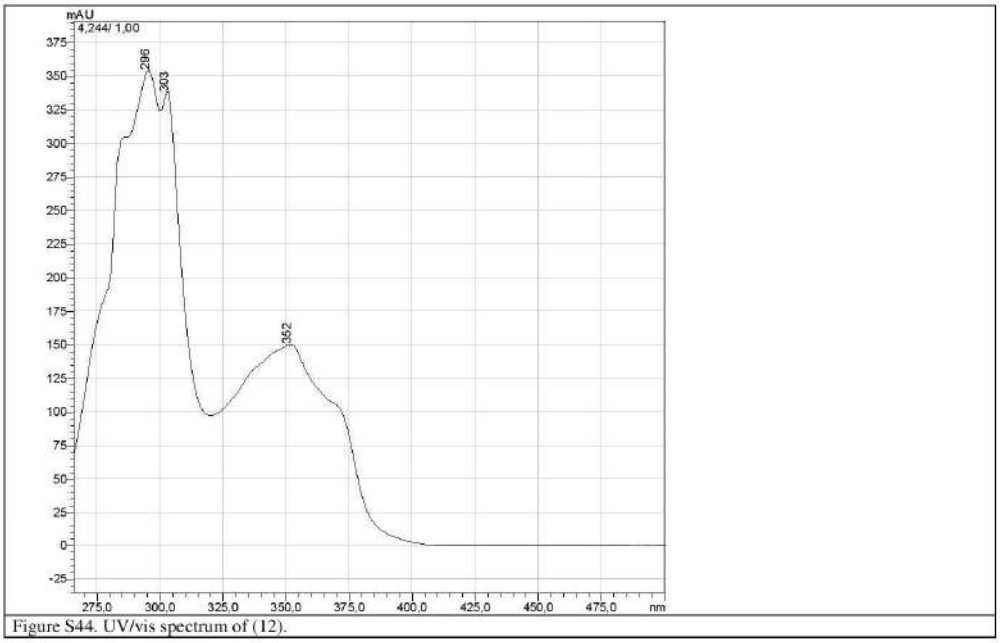

Figure S44. UV/vis spectrum of (12).

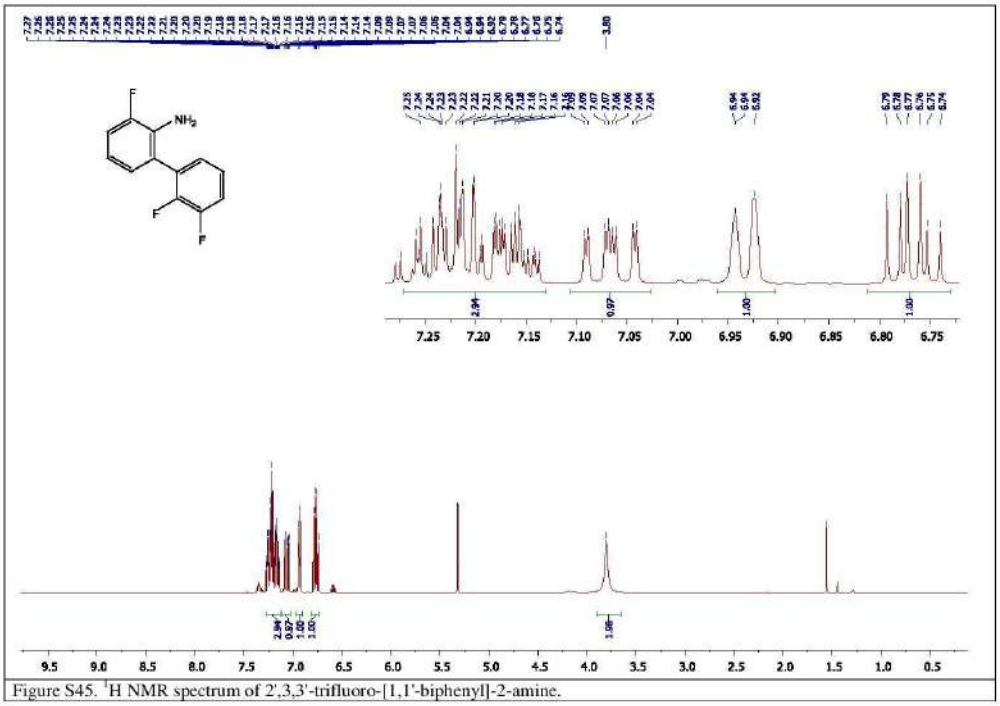

Figure S45. ^{1}H NMR spectrum of 2',3,3'-trifluoro-[1,1'-biphenyl]-2-amine.

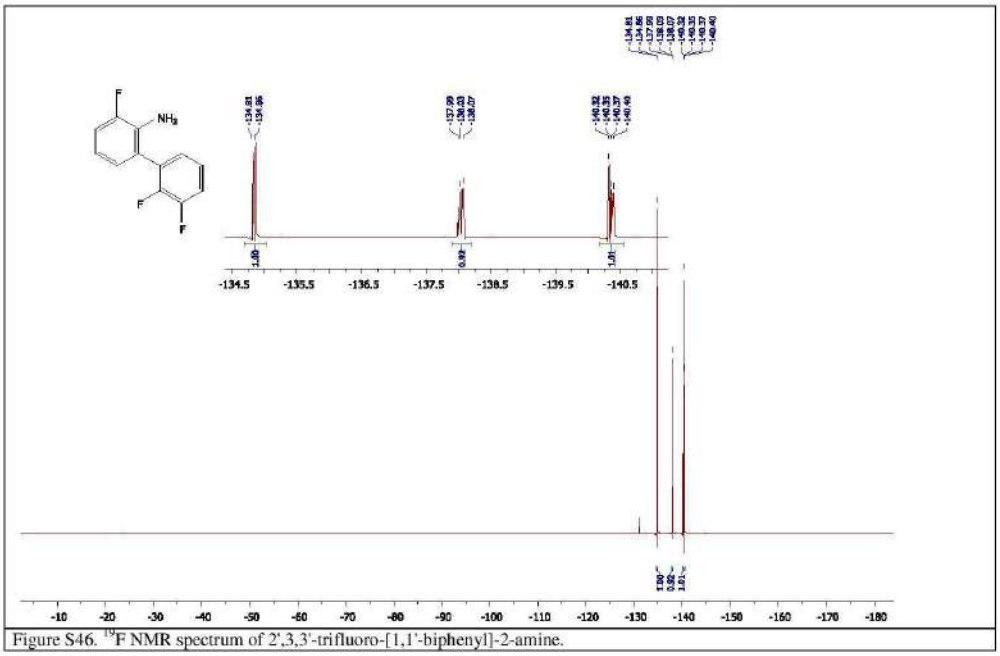

Figure S46. ^{19}F NMR spectrum of 2',3,3'-trifluoro-[1,1'-biphenyl]-2-amine.

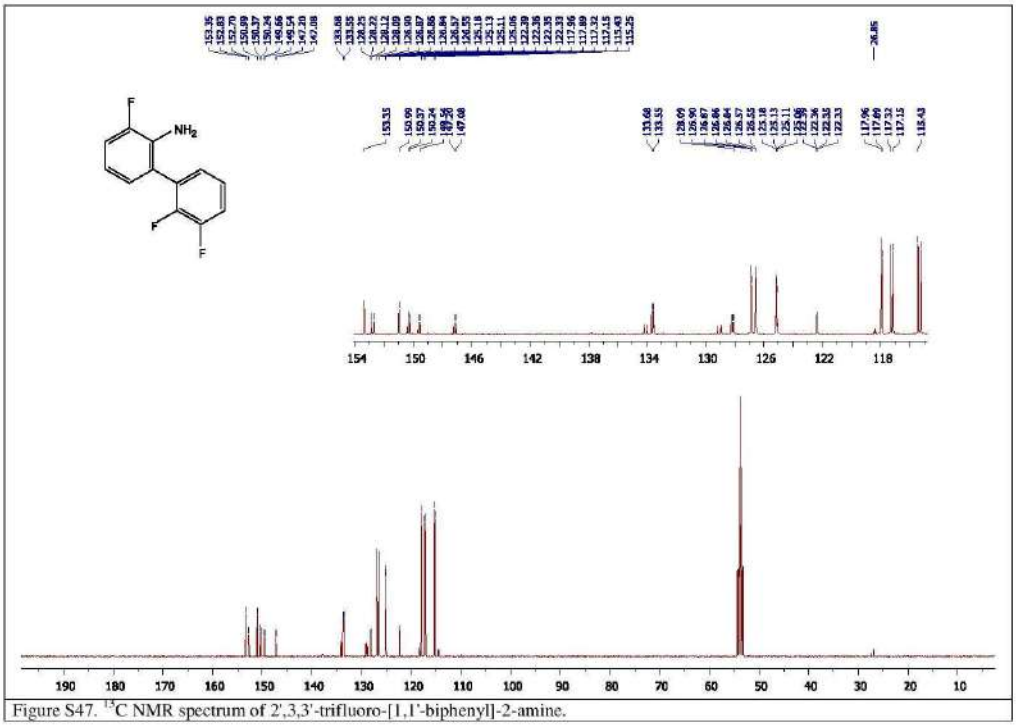

Figure S47. ^{13}C NMR spectrum of 2',3,3'-trifluoro-[1,1'-biphenyl]-2-amine.

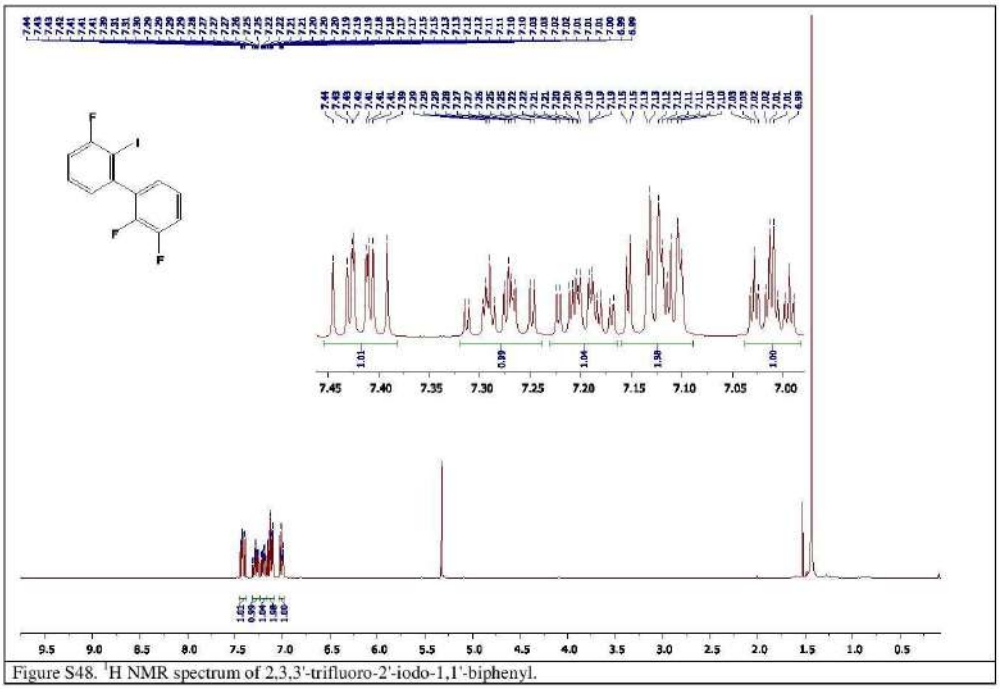

Figure S48. ^{1}H NMR spectrum of 2,3,3'-trifluoro-2'-iodo-1,1'-biphenyl.

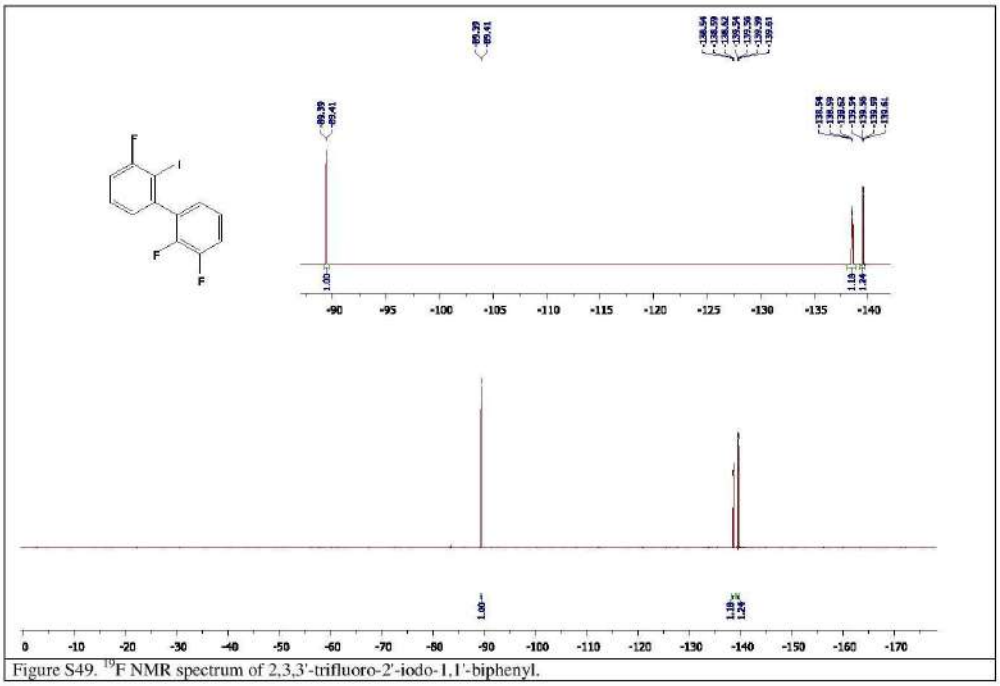

Figure S49. ^{19}F NMR spectrum of 2,3,3'-trifluoro-2'-iodo-1,1'-biphenyl.

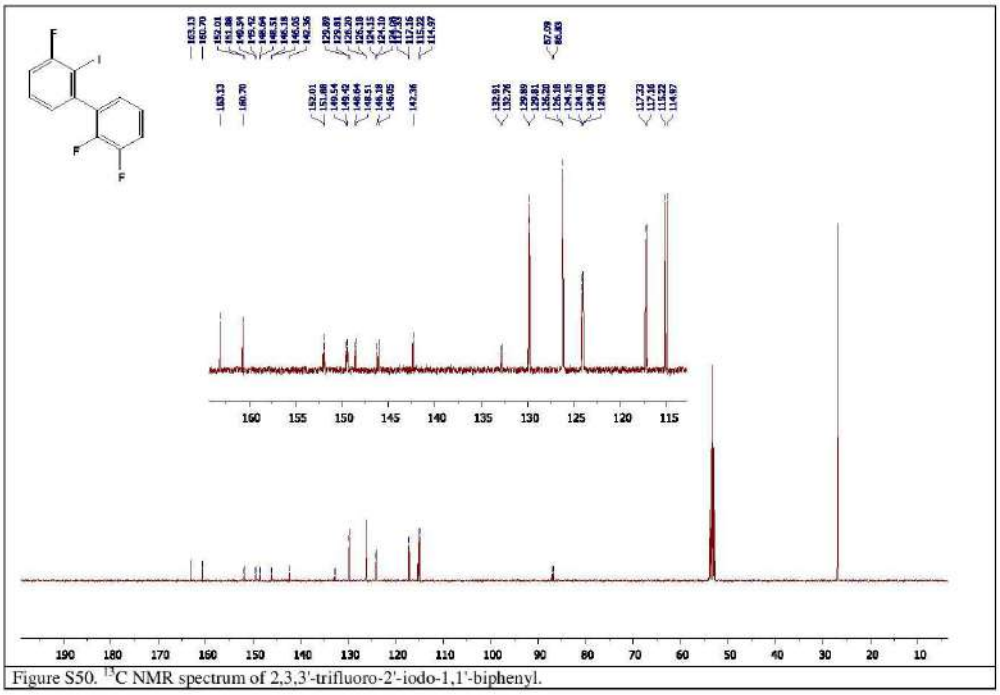

Figure S50. ^{13}C NMR spectrum of 2,3,3'-trifluoro-2'-iodo-1,1'-biphenyl.

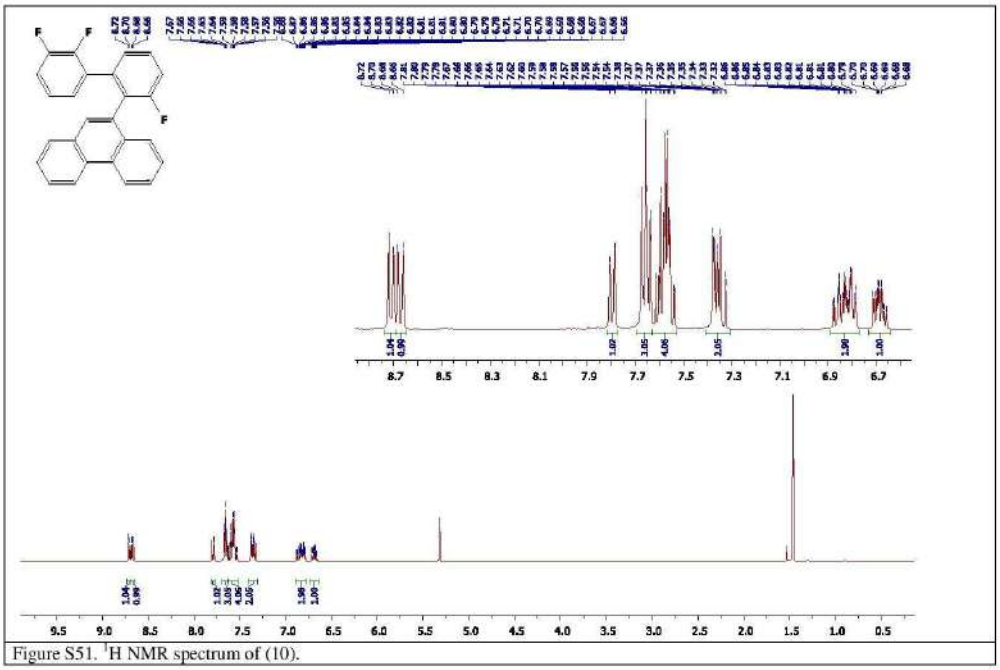

Figure S51. ^{1}H NMR spectrum of (10).

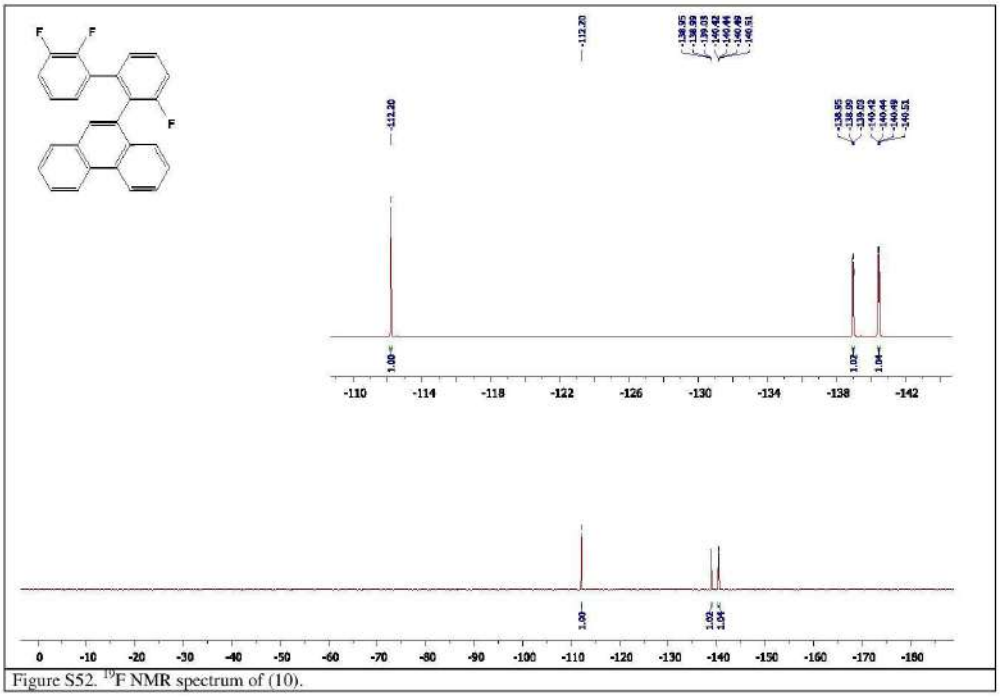

Figure S52. ^{19}F NMR spectrum of (10).

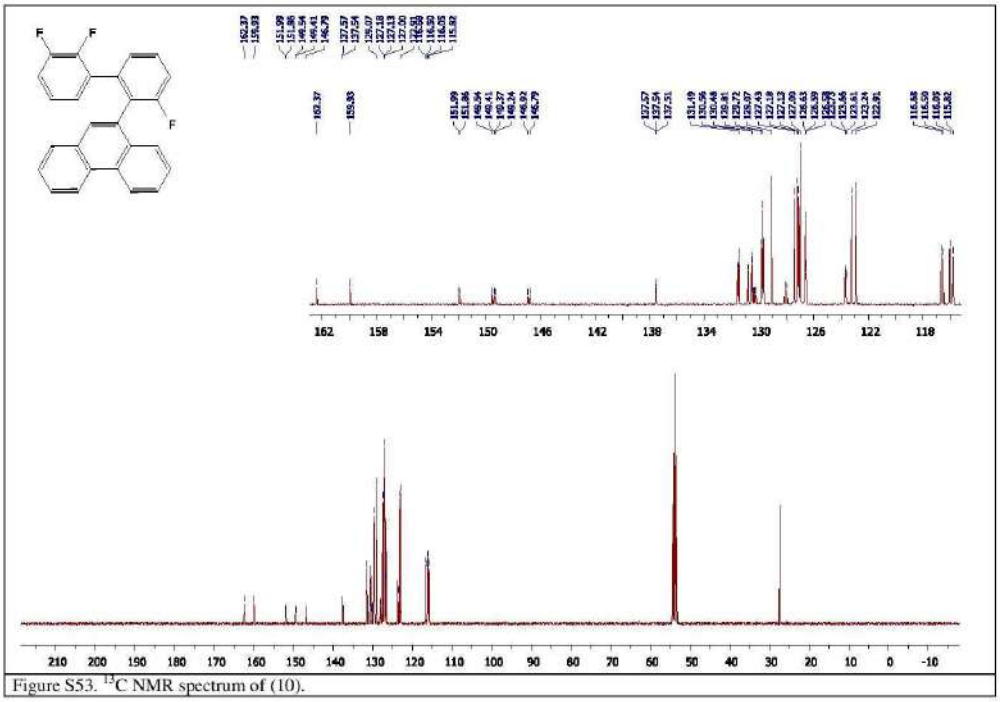

Figure S53. ^{13}C NMR spectrum of (10).

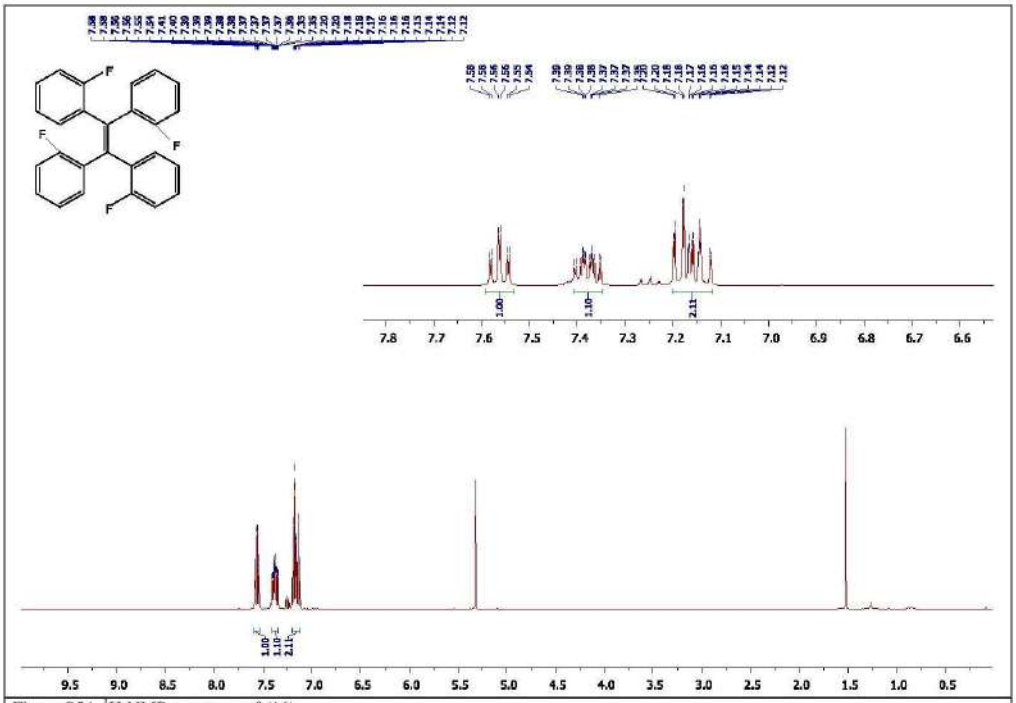

Figure S54. ^{1}H NMR spectrum of (16).

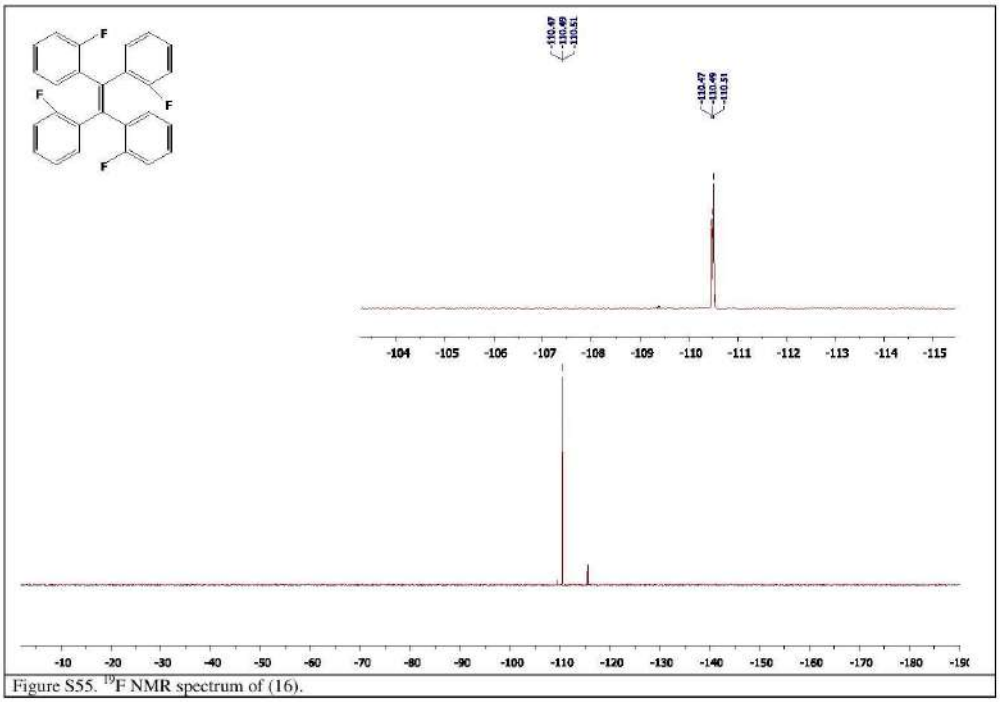

Figure S55. ^{19}F NMR spectrum of (16).

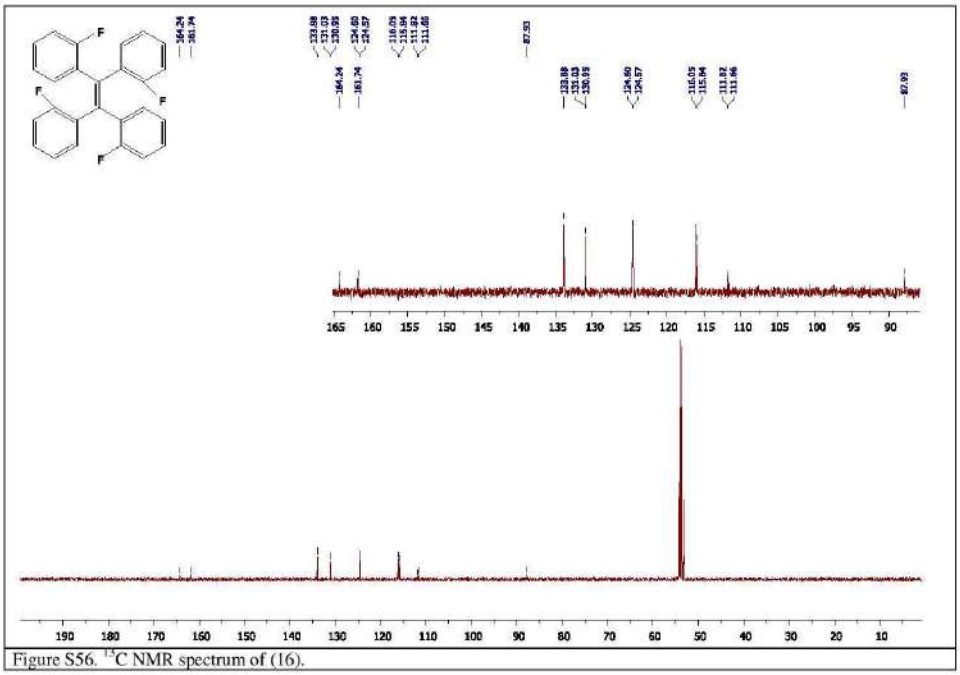

Figure S56. ^{13}C NMR spectrum of (16).

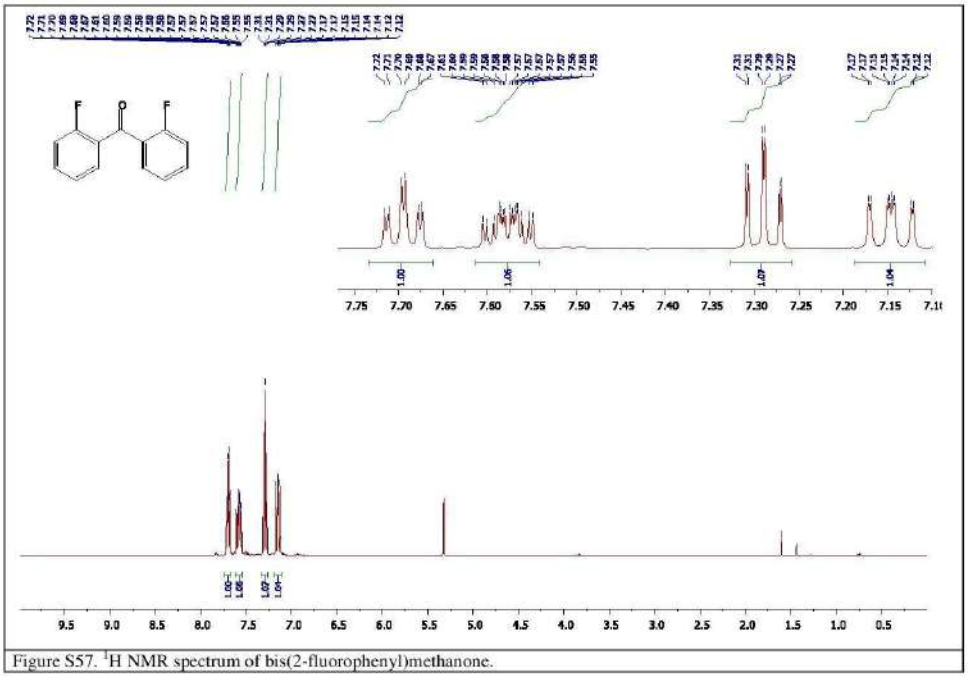

Figure S57. ^{1}H NMR spectrum of bis(2-fluorophenyl)methanone.

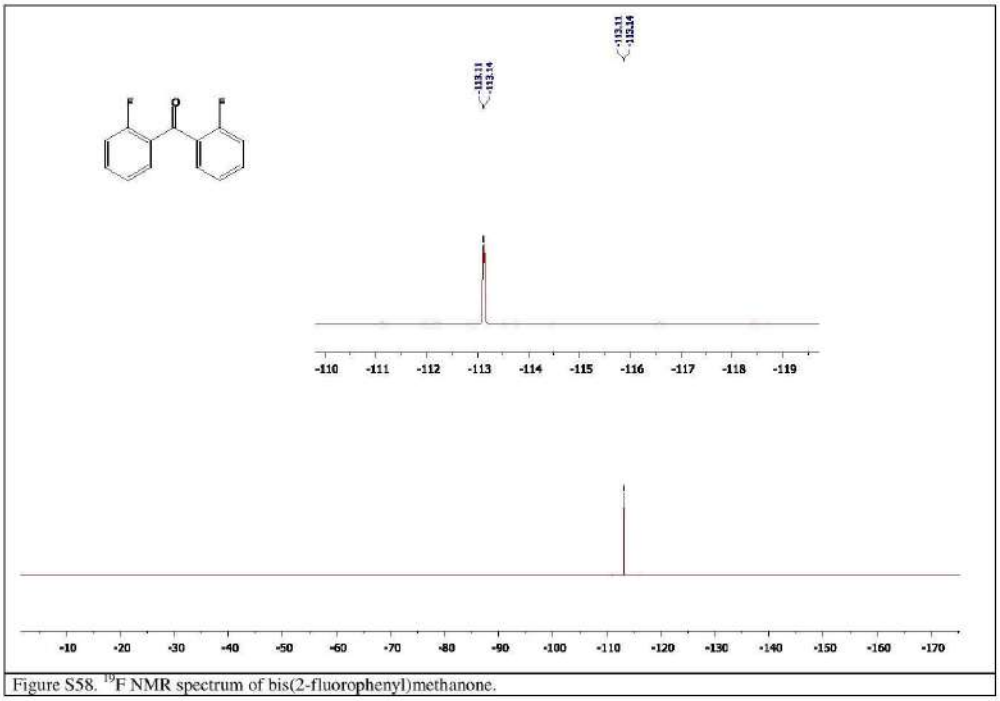

Figure S58. ^{19}F NMR spectrum of bis(2-fluorophenyl)methanone.

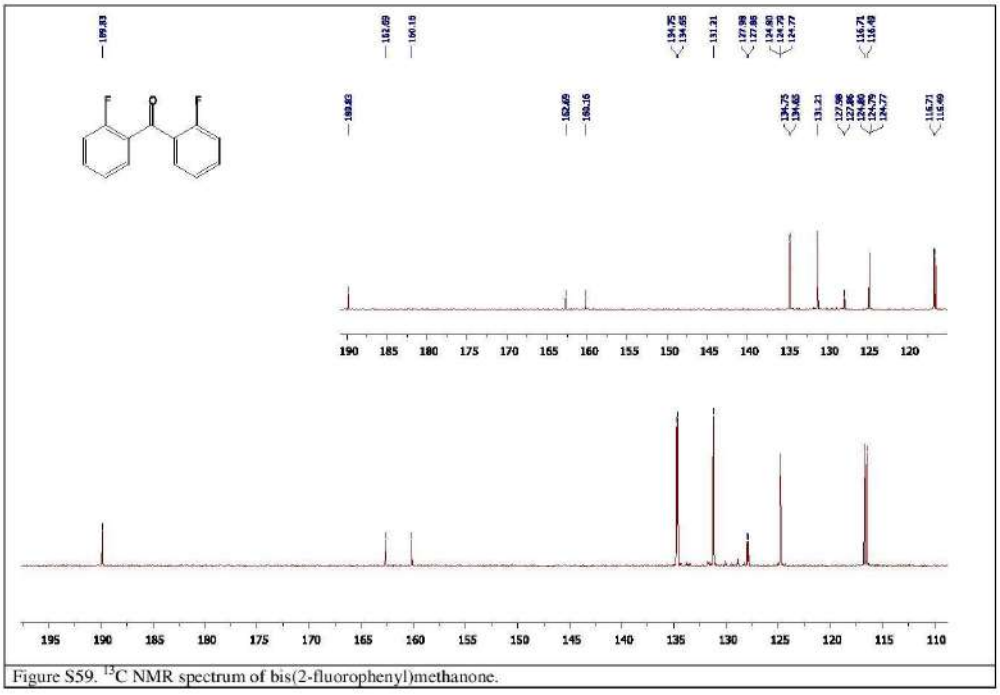

Figure S59. ^{13}C NMR spectrum of bis(2-fluorophenyl)methanone.

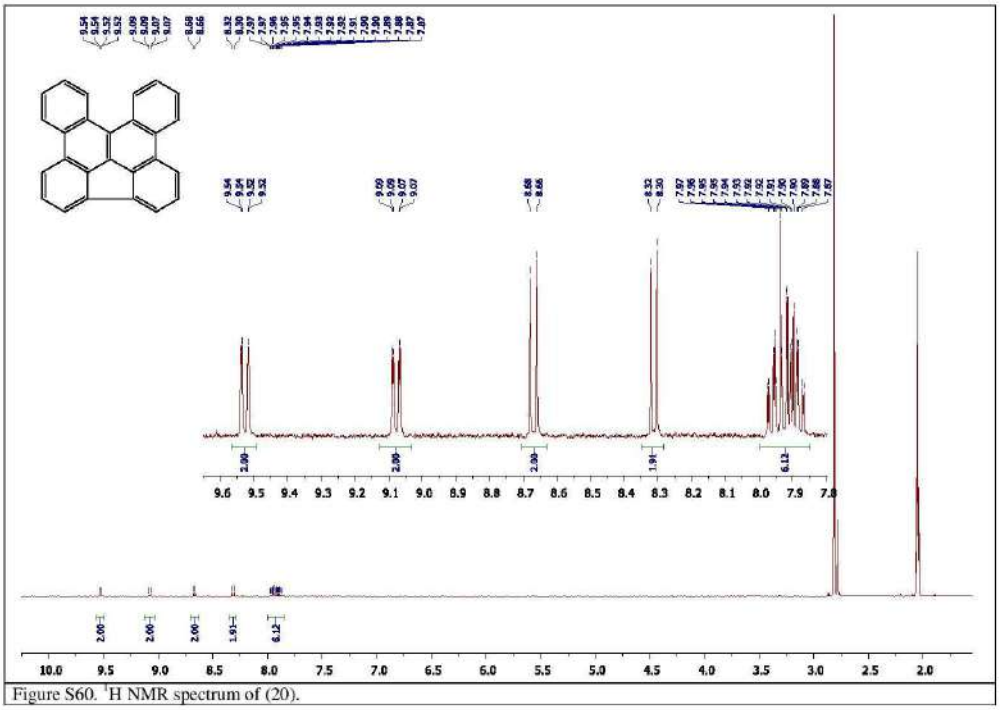

Figure S60. ^{1}H NMR spectrum of (20).

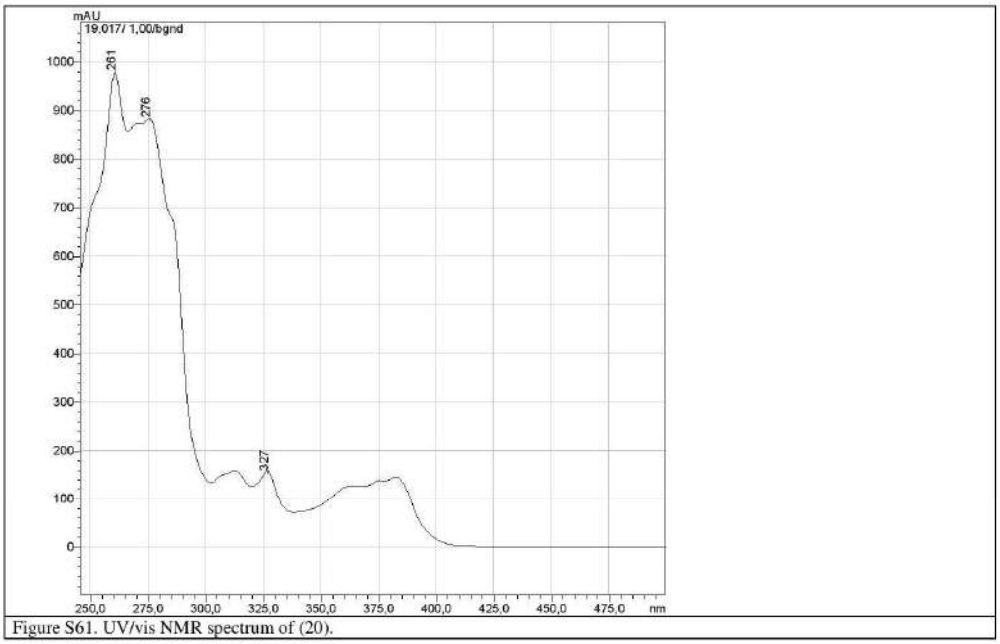

Figure S61. UV/vis NMR spectrum of (20).

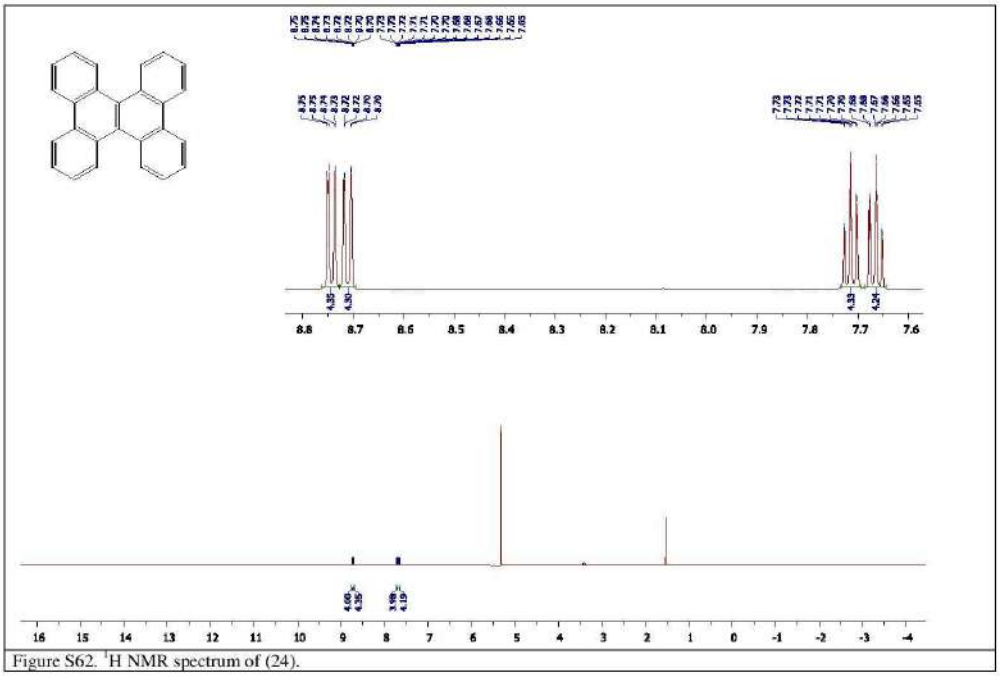

Figure S62. ^{1}H NMR spectrum of (24).

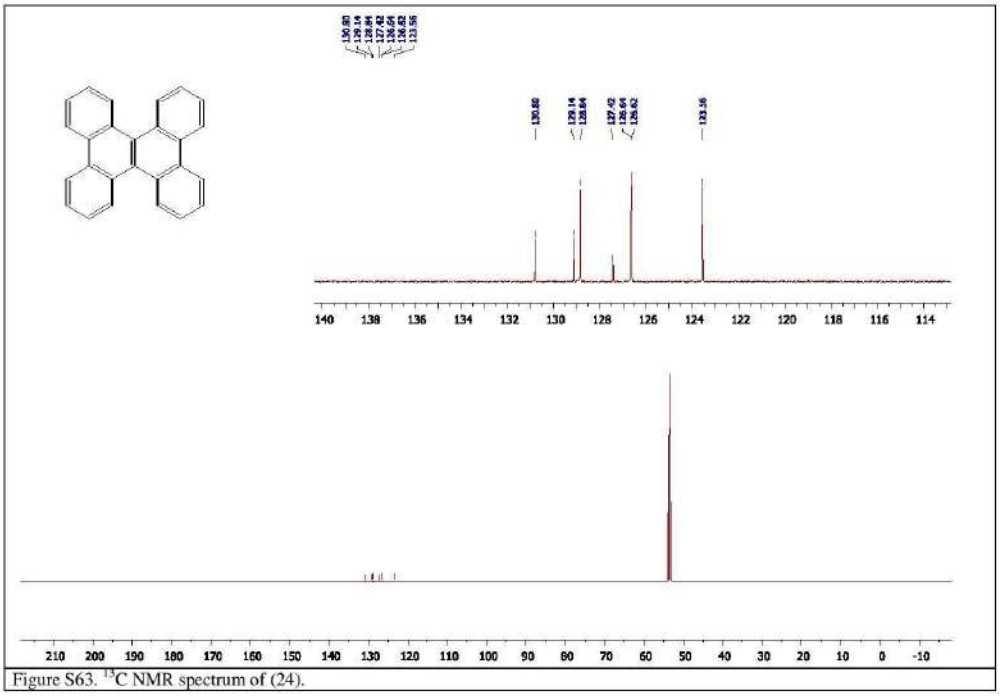

Figure S63. ^{13}C NMR spectrum of (24).

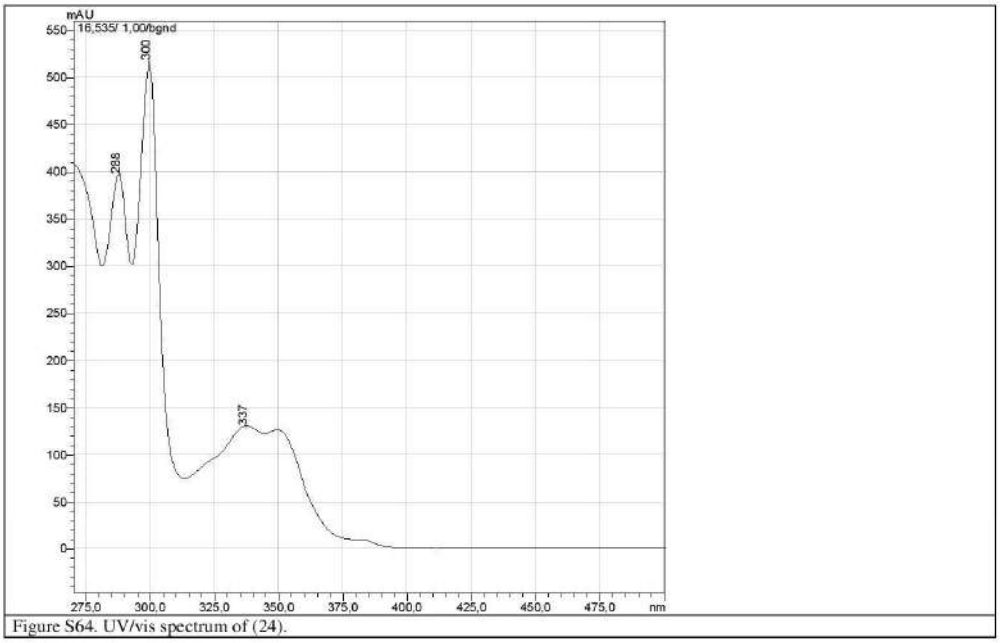

Figure S64. UV/vis spectrum of (24).

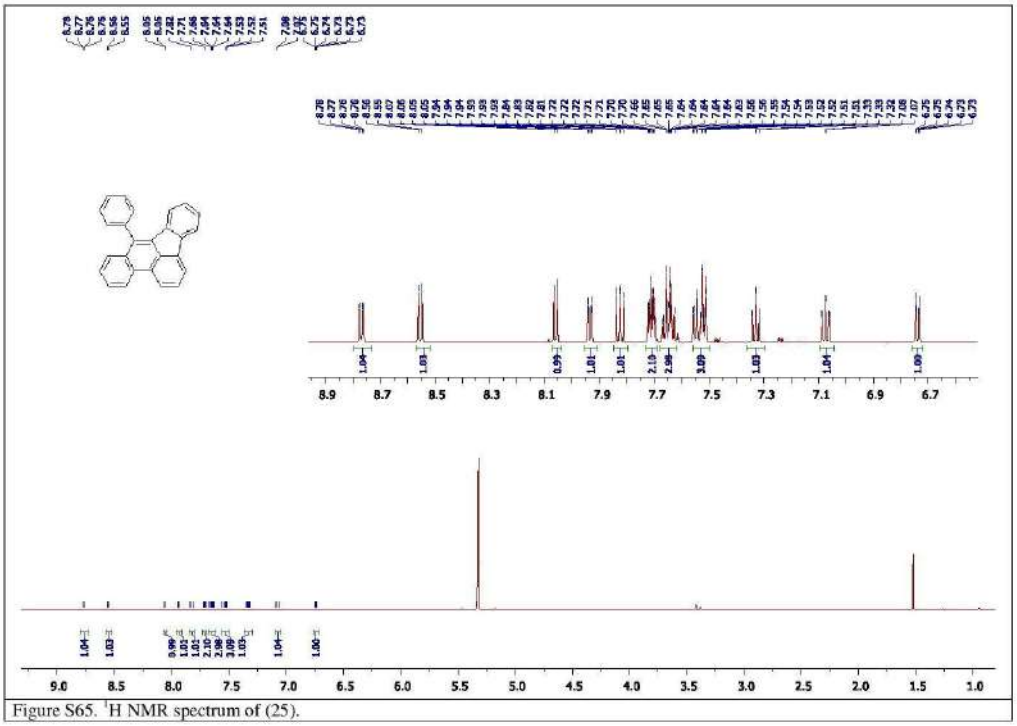

Figure S65. ^{1}H NMR spectrum of (25).

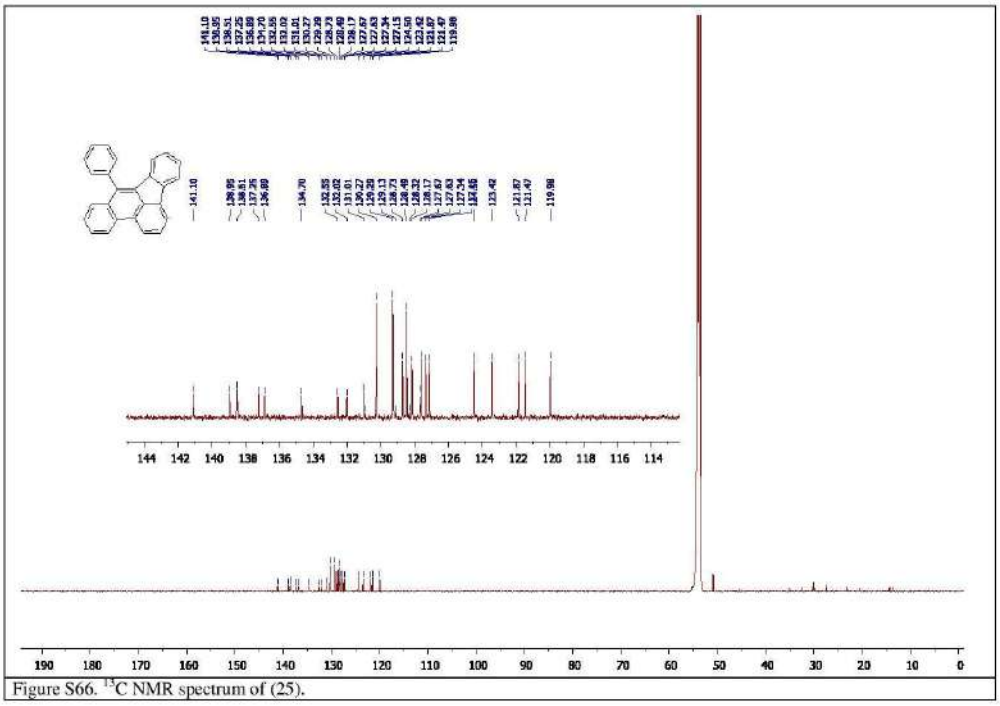

Figure S66. ^{13}C NMR spectrum of (25).

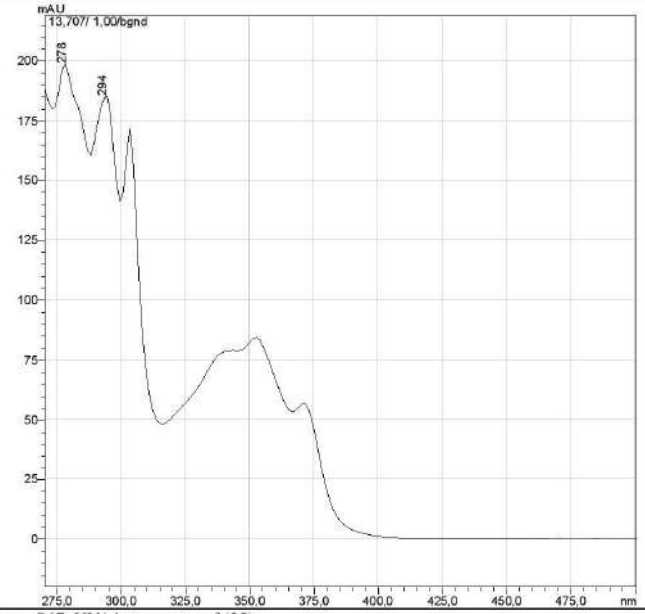

Figure S67. UV/vis spectrum of (25).

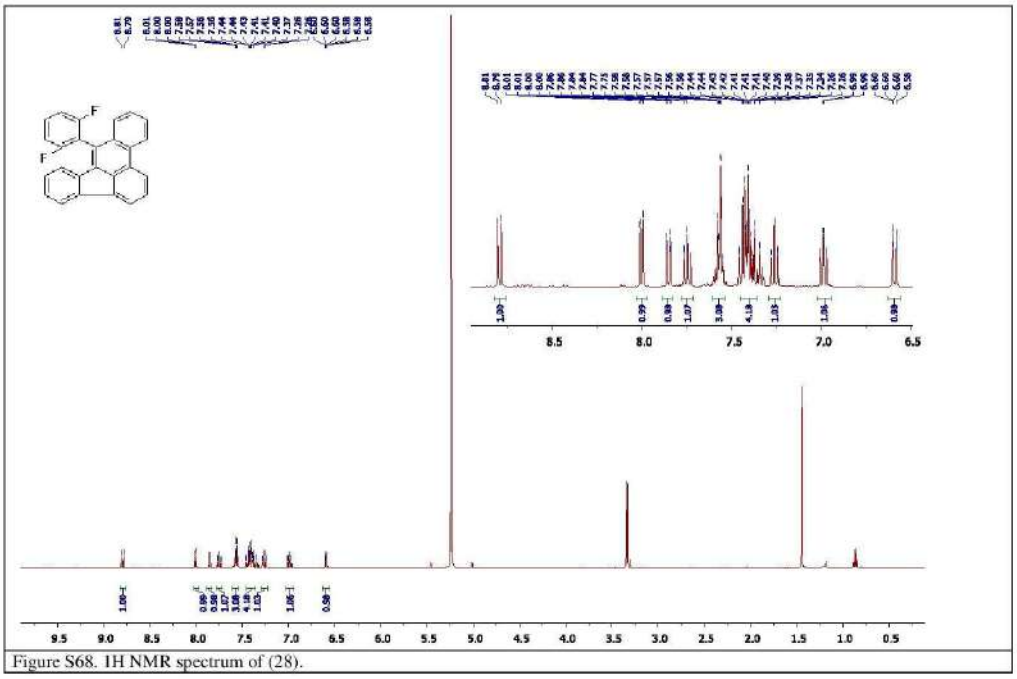

Figure S68. 1H NMR spectrum of (28).

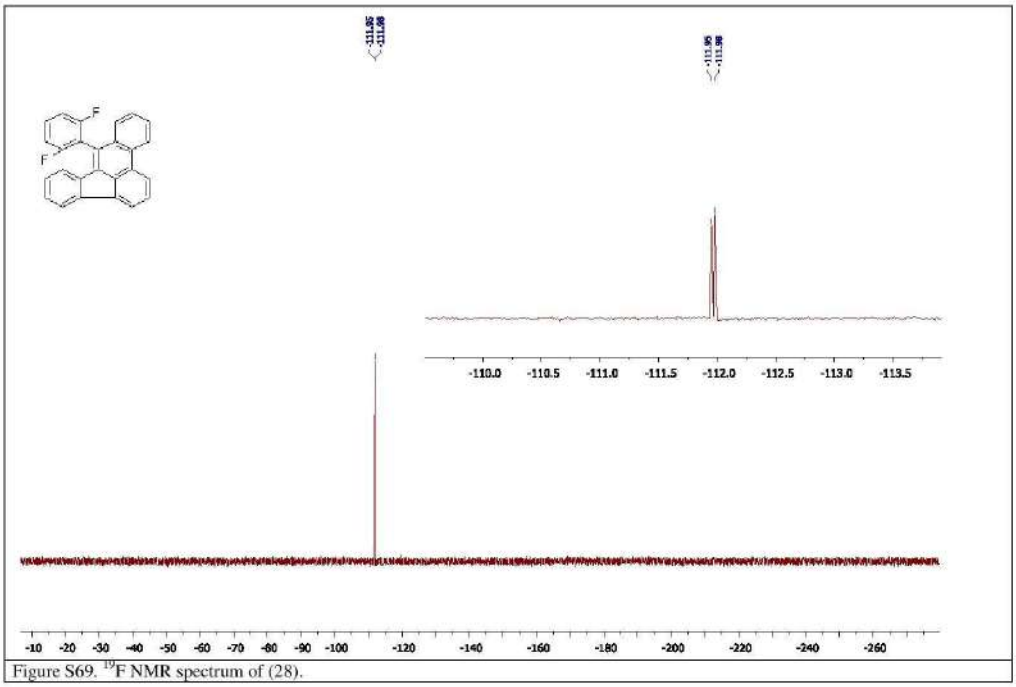

Figure S69. ^{19}F NMR spectrum of (28).

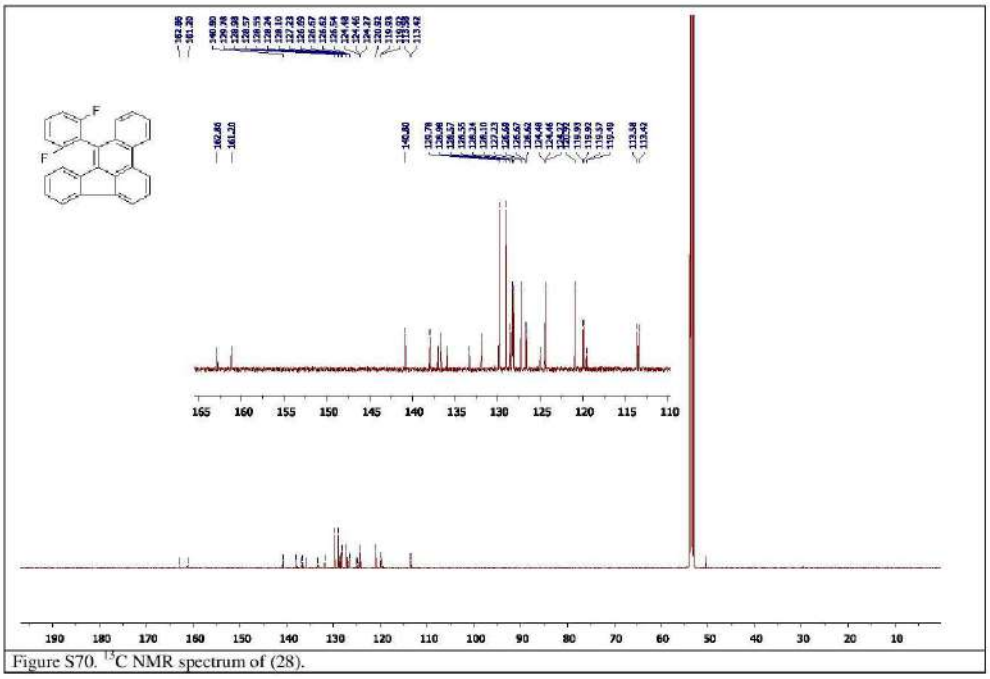

Figure S70. ^{13}C NMR spectrum of (28).

4. X-Ray crystallography

Synchrotron X-ray data for a crystal of **5** were collected at 100 K on BL14.3 at the BESSY storage ring (Berlin, Germany) using a MAR225 detector (λ = 0.8950 Å). X-ray data for crystals of **6** and **7** were collected at 100 K on an image plate diffractometer (IPDS-3) and Mo-Kα radiation (λ = 0.71073 Å). All structures were solved and anisotropically refined using the SHELX package. Hydrogen atoms in structure **5** were localized as strongest peaks of electron density in a difference Fourier map and refined isotropically. Hydrogen atoms in structures **6** and **7** were placed in calculated positions and refined in a riding mode. Selected crystallographic data and CCDC deposition numbers are given in Table S1.

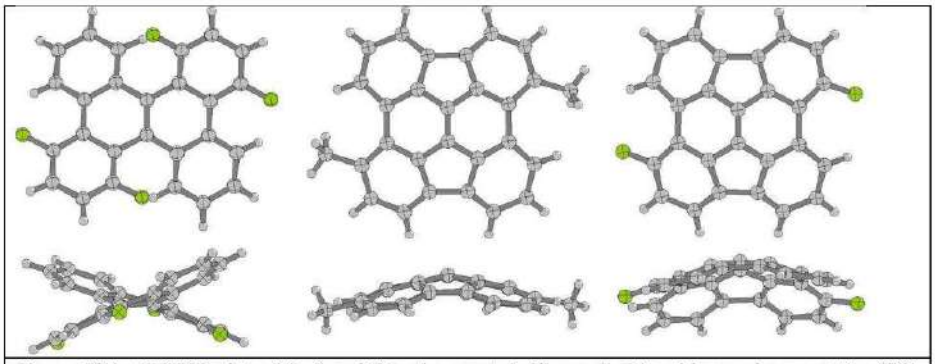

Figure S71. ORTEP plot of 5, 6 and 7 in the crystal. Thermal ellipsoids are drawn at the 50% probability level

Table S1. Selected crystallographic data and some details of data collection and refinement for three compounds.

Compound	**5**	**6**	**7**
Formula	$C_{26}H_{12}F_4$	$C_{28}H_{16}$	$C_{26}H_{10}F_2$
M_r	400.36	352.41	360.34
crystal system	monoclinic	Monoclinic	monoclinic
space group	*Cc*	$P2_1$	*C*2
a [Å]	8.501(1)	10.1680(4)	20.0175(9)
b [Å]	22.097(2)	7.3302(2)	3.8985(2)
c [Å]	9.911(1)	11.6266(5)	21.8709(10)
α [°]	90	90	90
β [°]	111.469(9)	109.249(3)	111.347(3)
γ [°]	90	90	90
V [Å^3]	1732.6(3)	818.12(5)	1508.12(13)
Z	4	2	4

D_c [g cm^{-3}]	1.535	1.431	1.587
refls collected/R_{int}	11539/0.057	12499/0.051	14520/0.139
data / parameters	3703 / 319	4378 / 255	4023 / 263
$R_1(I \geq 2\sigma(I)$	0.035/0.093	0.035/0.086	0.056/ 0.124
$\Delta\rho_{max / min}$ [e Å^{-3}]	0.31 /–0.20	0.36 / -0.20	0.61 / –0.28
CCDC	1895038	1895039	1895040

Structure **7** contains two independent molecule halves on two-fold axes. Whereas one molecule of $C_{26}H_{10}F_2$ is fully ordered, the second one is disordered due to an overlap of a chiral equivalent in the same crystallographic site with occupation factors 0.588/0.412(7), respectively.

5. Suggested mechanism for the formation of regioisomers of (2).

Several side products with low overall yield were detected such as X1 and X2. The mixture could not be properly separated, that is why we attempted to subject the mixture of (2), X1 and X2 to conditions of the Pd-catalyzed reaction expecting that (4), Y1 and Y2 can be separated which turned out also to be rather complicated mixture for a separation. Nevertheless, the final outcome after HF elimination allows to claim that this approach still allows to obtain the target molecule (6) with rather reasonable yields. The described complications did not appear in case of the synthesis of (7).

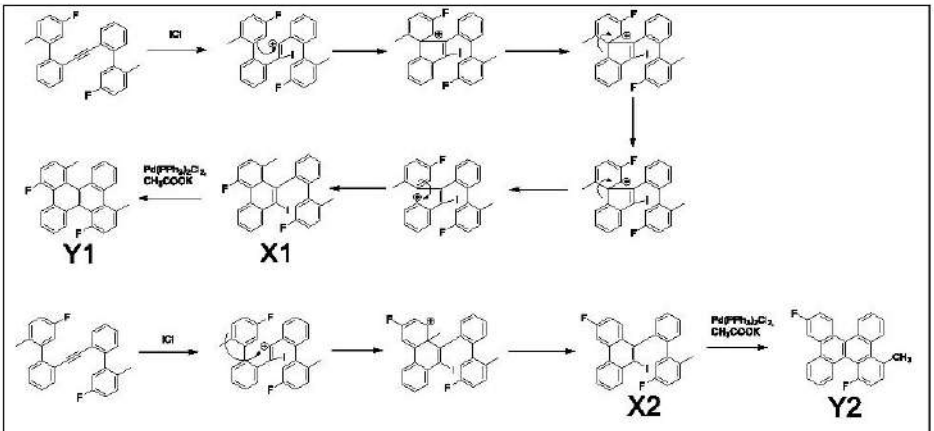

Scheme S7. Suggested mechanism of the formation of the side products during the synthesis of (2) [5].

6. Analysis of (21)+(22).

(21) and (22) were found as a mixture among the other products after HF elimination of (19). Since we assume that the reaction proceeds via formation of "cation-like" species, ipso-substitution appears as the only reasonable explanation for the eventual positions of fluorine atoms.

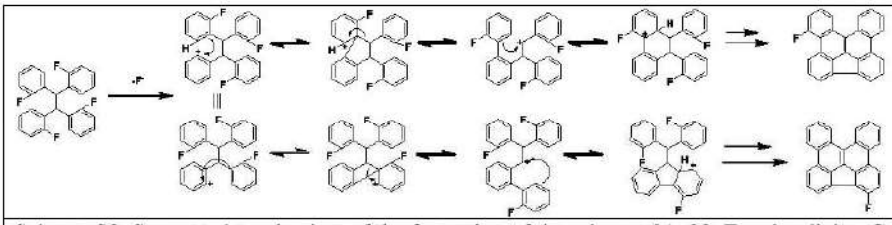

Scheme S8. Suggested mechanism of the formation of the mixture 21+22. For simplicity, C-F polarized bonds depicted as "+".

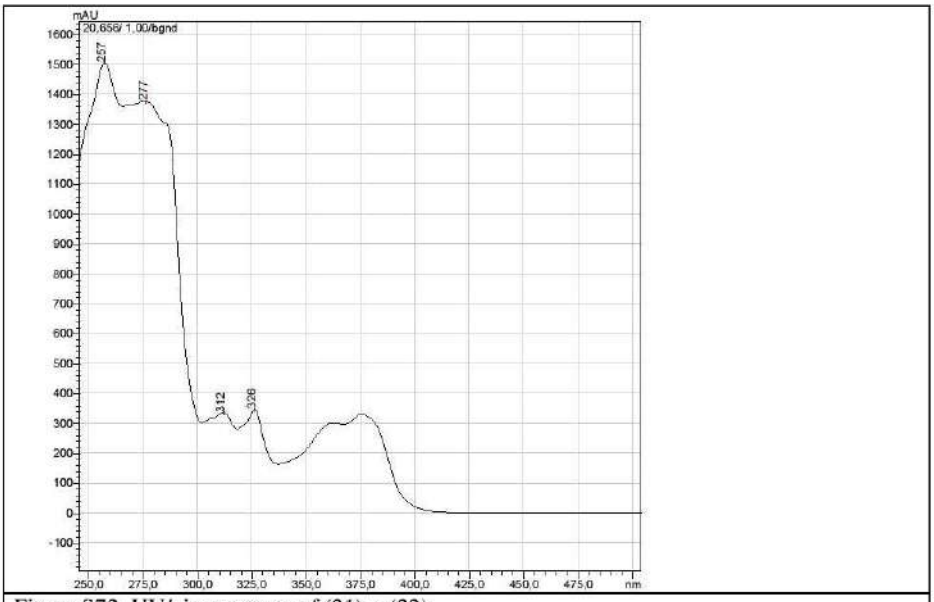

Figure S72. UV/vis spectrum of (21) + (22).

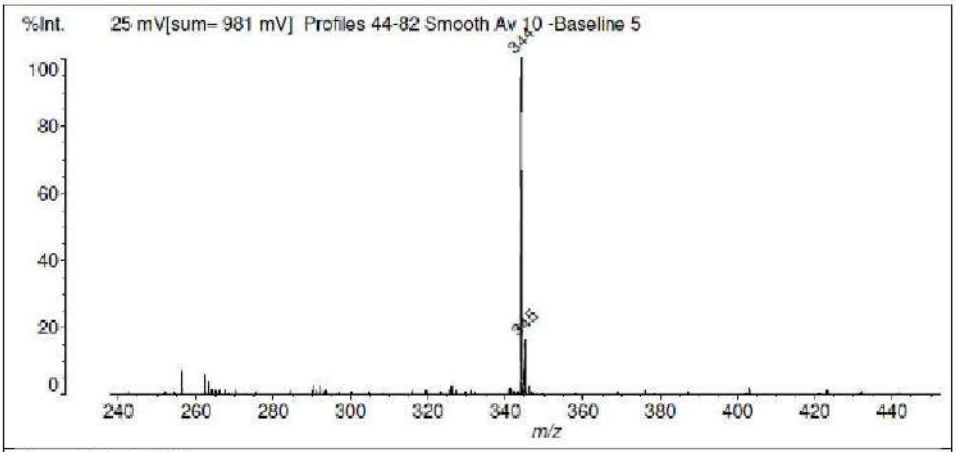

Figure S73. UV/vis spectrum

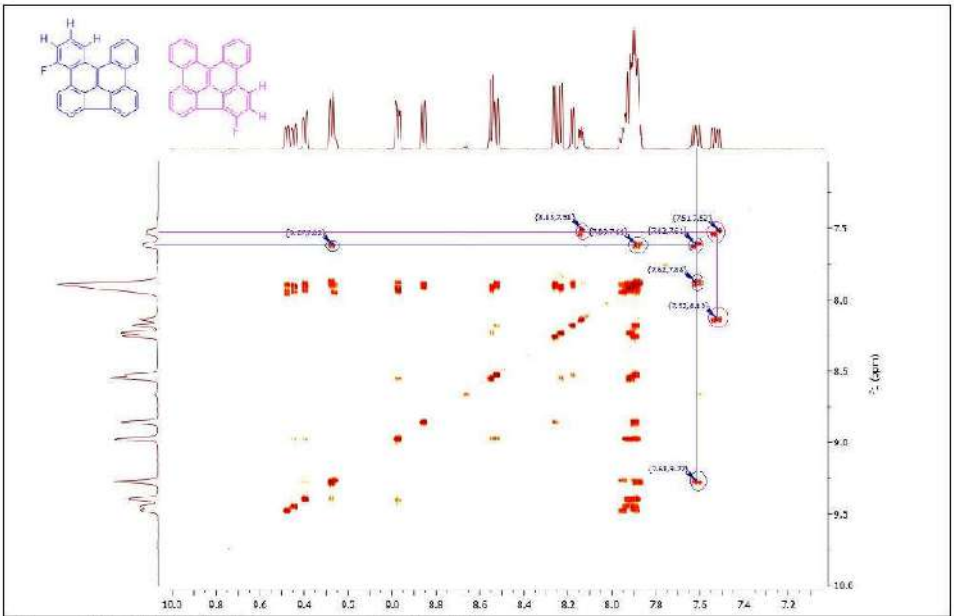

Figure S74. COSY ^{1}H-^{1}H spectrum of (21) + (22).

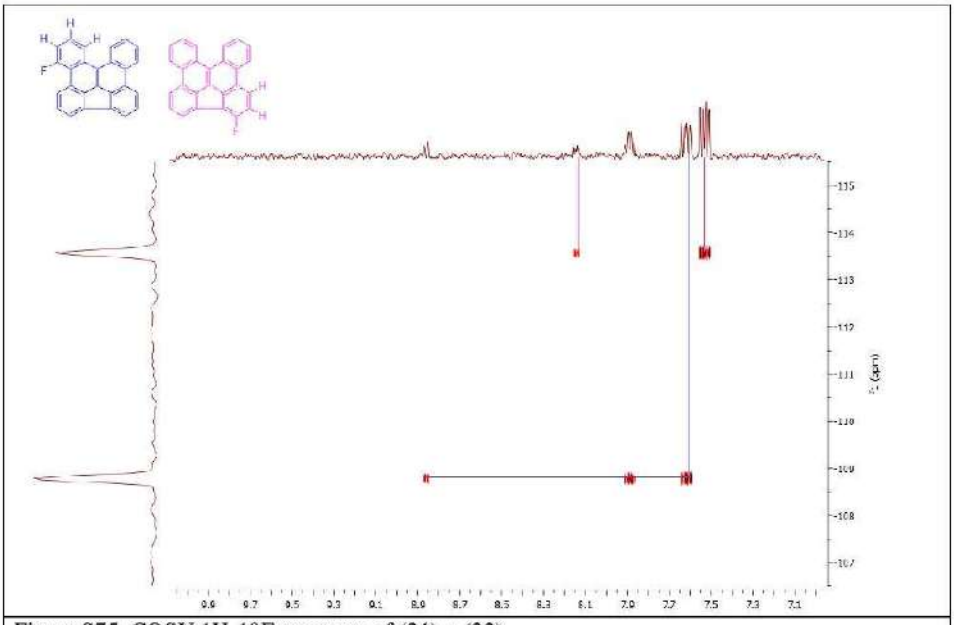

Figure S75. COSY 1H-19F spectrum of (21) + (22).

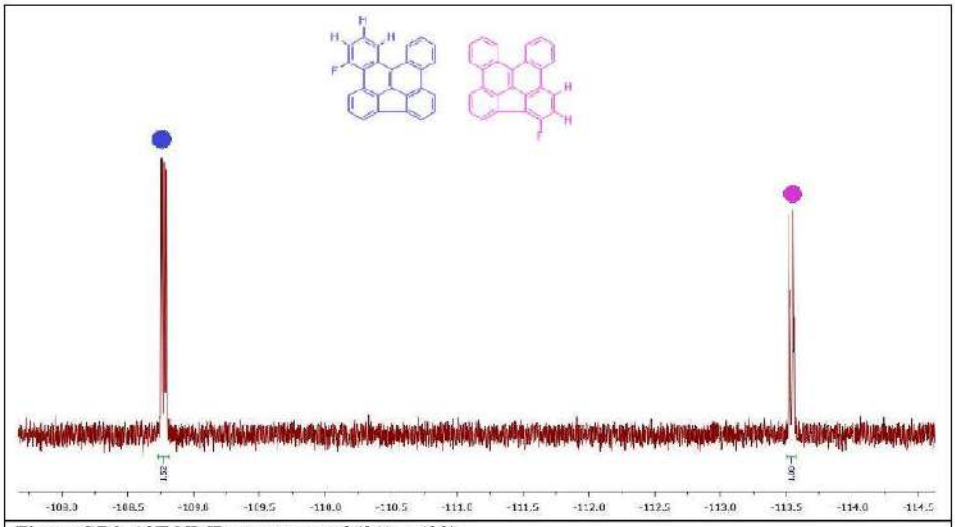

Figure S76. 19F NMR spectrum of (21) + (22).

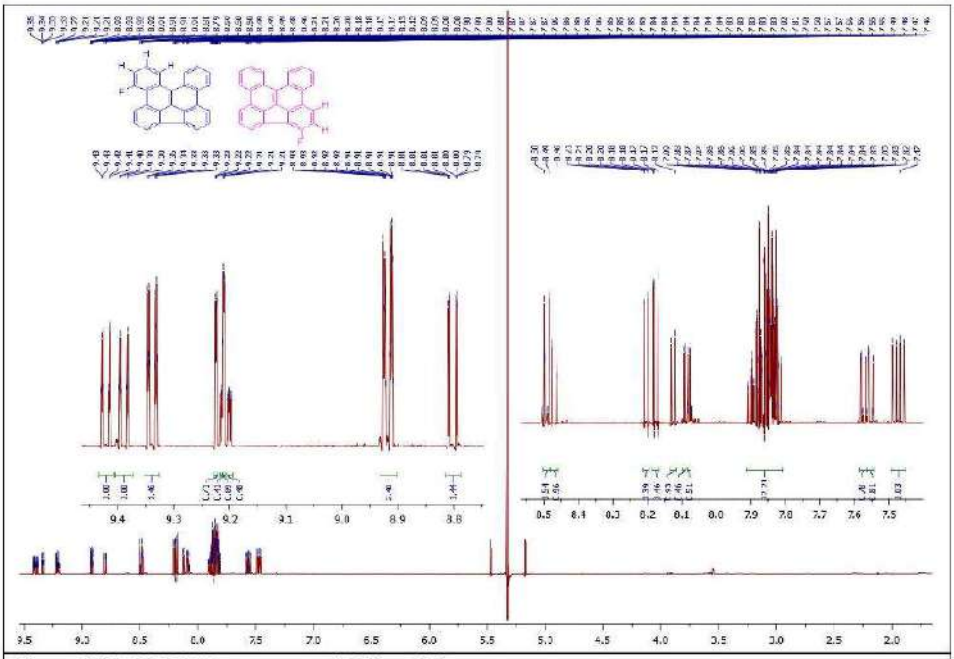

Figure S77. 1H NMR spectrum of (21) + (22).

7. Suggested mechanism for the formation of (20).

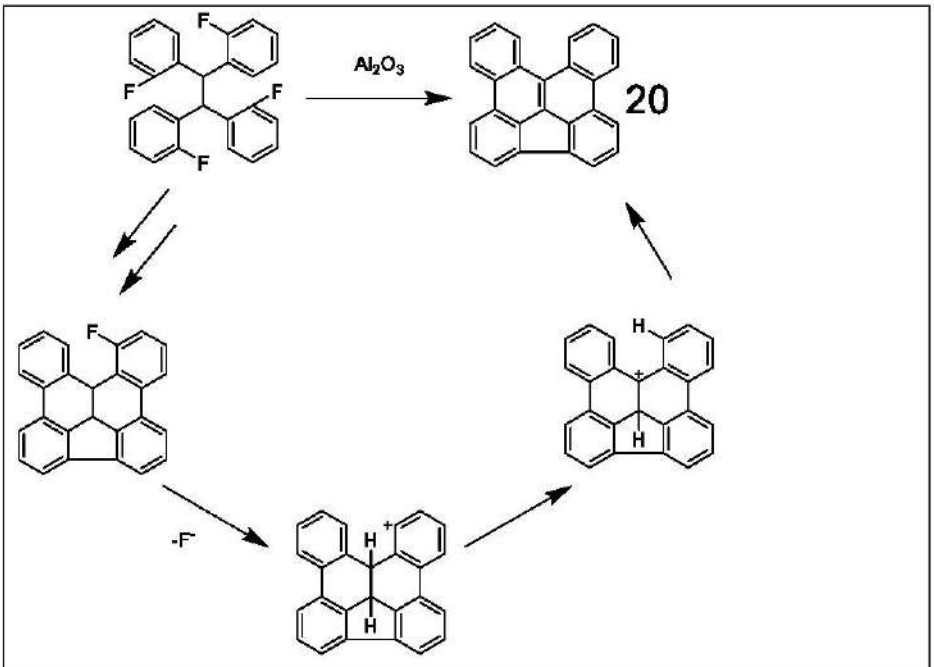

Scheme S9. Formation of (20). For simplicity, C-F polarized bonds depicted as "+".

8. Computational data.

The geometries and energies of the structures were calculated at DFT level (B3LYP/6-31G(d)) with the preoptimization at semi-empirical level of calculations (AM1). Gassuian09 software was exploited [6]. XYZ coordinates are listed below.

Table S2. Optimized geometry coordinates of (23).

6	3.024963000	-1.528675000	-1.031202000
6	1.828457000	-0.965577000	-0.588514000
6	1.713252000	0.419484000	-0.457251000
6	2.785923000	1.265482000	-0.763062000
6	3.984452000	0.687905000	-1.208009000
6	4.102406000	-0.695421000	-1.339444000
6	2.631930000	2.781600000	-0.611334000
6	2.843999000	3.496289000	-1.947674000
6	3.492200000	3.324169000	0.581452000
6	3.496316000	4.843614000	0.706400000
6	3.068093000	2.670570000	1.899987000
6	4.087831000	3.864319000	-2.466247000
6	4.251851000	4.488241000	-3.696335000
6	3.126728000	4.763901000	-4.471615000
6	1.862751000	4.408040000	-3.999619000
6	1.735153000	3.787256000	-2.757536000
6	4.636911000	5.478473000	1.208934000
6	4.729416000	6.850847000	1.396339000
6	3.630155000	7.647967000	1.075903000
6	2.470775000	7.057046000	0.573540000
6	2.411695000	5.673573000	0.392493000
6	1.846543000	2.980122000	2.514036000
6	1.467968000	2.364655000	3.706901000

1	7.927517000	-0.100683000	0.332333000
1	7.295015000	1.418954000	2.223912000
1	4.167922000	8.670077000	-0.361937000
1	6.592533000	8.434919000	0.115372000
1	7.647681000	6.200987000	0.131571000
1	6.358004000	4.134852000	-0.021244000

Table S19. Energies of intermediates calculated on B3LYP/6-31G(d) level of theory.

	Energy, hartri/mole	Energy, kcal/mole
23	-1202,487913	-754572,5887
IM1_anti	-1102,378257	-691752,8287
IM1_syn	-1102,377078	-691752,0887
IM2_anti	-1102,389377	-691759,8065
IM2_syn	-1102,382454	-691755,4624
IM3	-1100,872841	-690808,1658
IM4	-1000,779783	-627998,8212
IM5	-1000,780852	-627999,492
27	-1400,957051	-879113,8585
IM6_anti	-1300,830014	-816283,1918
IM6_syn	-1300,835608	-816286,7017
IM7_anti	-1300,845088	-816292,6506
IM7_syn	-1300,844421	-816292,2322
IM8	-1299,333139	-815343,8881
IM11	-1199,243755	-752536,8492
IM9	-1199,229575	-752527,9509
IM10	-1199,237672	-752533,0317

9. References.

[1]- H. E. Bronstein, N. Choi, and L. T. Scott, *J. Am. Chem. Soc.*, **2002**, 124, 8870-8875.

[2]-L. B. Liu, B. W. Yang, T. J. Katz, M. K. Poindexter, *J. Org. Chem.* **1991**, 56, 3769-3775.

[3]-A.-K. Steiner, K.Y. Amsharov, *Angew. Chem. Int. Ed.*, **2017**, 56, 14732 –14736.

[4]-V. Akhmetov, M. Feofanov, V. Ioutsi, F. Hampel and K. Amsharov, *Chem. Eur. J.*, 10.1002/chem.201805290.

[5]-C.-W. Li, C.-I Wang, H.-Y. Liao, R. Chaudhuri and R.-S. Liu, *J. Org. Chem.* **2007**, *72*, 9203-9207.

[6]-M. J. Frisch, G. W. Trucks, H. B. Schlegel, G. E. Scuseria, M. A. Robb, J. R. Cheeseman, G. Scalmani, V. Barone, B. Mennucci, G. A. Petersson, H. Nakatsuji, M. Caricato, X. Li, H. P. Hratchian, A. F. Izmaylov, J. Bloino, G. Zheng, J. L. Sonnenberg, M. Hada, M. Ehara, K. Toyota, R. Fukuda, J. Hasegawa, M. Ishida, T. Nakajima, Y. Honda, O. Kitao, H. Nakai, T. Vreven, J. A. Montgomery, Jr., J. E. Peralta, F. Ogliaro, M. Bearpark, J. J. Heyd, E. Brothers, K. N. Kudin, V. N. Staroverov, R. Kobayashi, J. Normand, K. Raghavachari, A. Rendell, J. C. Burant, S. S. Iyengar, J. Tomasi, M. Cossi, N. Rega, J. M. Millam, M. Klene, J. E. Knox, J. B. Cross, V. Bakken, C. Adamo, J. Jaramillo, R. Gomperts, R. E. Stratmann, O. Yazyev, A. J. Austin, R. Cammi, C. Pomelli, J. W. Ochterski, R. L. Martin, K. Morokuma, V. G. Zakrzewski, G. A. Voth, P. Salvador, J. J. Dannenberg, S. Dapprich, A. D. Daniels, Ö. Farkas, J. B. Foresman, J. V. Ortiz, J. Cioslowski, and D. J. Fox, *Gaussian 09* (Gaussian, Inc., Wallingford CT, 2009).

Publication 4.

Effect of the Cove Region Geometry in PAHs on Alumina Assisted Cyclodehydrofluorination.

V. Akhmetov, K. Y. Amsharov.

Phys. Status Solidi B DOI:10.1002/pssb.201900254. First Published on 11th of July, **2019**.

ABSTRACT:

Despite conventional opinion on high inertness of aluminum oxide and exceptional stability of the carbon fluorine bond, activated γ-alumina effectively polarizes C-F bond. This process is known to implement effective C-C coupling in the cove region leading to intramolecular annulation and formation of non-alternant polycyclic aromatic hydrocarbons (PAHs). This study shows the importance of the cove region geometry on annulation efficiency. This is demonstrated using precursor **1** as a model which allows investigation of the cove region's major feature, namely its helical geometry, and effect of its structure on the efficiency of intramolecular C-C bond formation. Herein, the synthesis of **1**, its behavior on activated alumina and reasoning for the observed outcomes are described.

Effect of the Cove Region Geometry in PAHs on Alumina Assisted Cyclodehydrofluorination

*Vladimir Akhmetov and Konstantin Amsharov**

Friedrich-Alexander University Erlangen-Nuernberg, Department of Chemistry and Pharmacy, Organic Chemistry II, Nikolaus-Fiebiger Str. 10, 91058 Erlangen, Germany.

E-mail: konstantin.amsharov@fau.de

Keywords: C-F bond activation, cyclodehydrofluorination, aluminum oxide, solid-state synthesis

Abstract. Despite conventional opinion on high inertness of aluminum oxide and exceptional stability of the carbon fluorine bond, activated γ-alumina effectively polarizes C-F bond. This process is known to implement effective C-C coupling in the cove region leading to intramolecular annulation and formation of non-alternant polycyclic aromatic hydrocarbons (PAHs). This study shows the importance of the cove region geometry on annulation efficiency. This is demonstrated using precursor **1** as a model which allows investigation of the cove region's major feature, namely its helical geometry, and effect of its structure on the efficiency of intramolecular C-C bond formation. Herein, the synthesis of **1**, its behavior on activated alumina and reasoning for the observed outcomes are described.

1. Introduction

In the past decade nanographenes or large PAHs have received a significant attention from synthetic chemists. This is mainly fueled by the demand from physicist chasing for the unique PAHs' properties such as charge carrier mobilities, singlet fission and many others.[1][2][3][4] Naturally, family of PAHs consists of numerous subclasses, among which non-planar PAHs bearing bowl-shaped geometry possess highly interesting features, which cannot be properly investigated due to drastic lack of the synthetic approaches towards the so-called buckybowls.[5][6][7][8] The explanation for such a scarcity of methodologies in the seemingly well-established field is mainly connected to the strain energies that originate from the valence angles' deviations resulting in non-planar structures resembling a bowl. Thus, the strain energy and the bowl-shape like geometry are inextricably interconnected raising the question of how the issue should be treated and tackled. One of the recent advances demonstrates that the solid-state alumina mediated C-F bond activation along with the rational planning and the design of the precursor allow to overcome the strain energy hindrance.[9][10] Aside from low costs, transition metal free conditions and accessible scale up the method bears specific to a solid-state technique advantages such as a possibility to operate with low soluble molecules together with the simplified purification ensued from the adsorption of polar side products which remain on the solid surface unless washed with a protic solvent. Even more outstanding advantage is the tolerance to the "dormant" fluorine atoms that remain intact on alumina (Fig. 1).[11] All these allow considering the alumina mediated reaction as an outstanding tool for the various intramolecular C-C couplings. The closure of the cove region

may serve as one of the most illustrative examples where the appropriate helical architecture of the precursors leads to selective and frequently quantitative C-C bond formations.

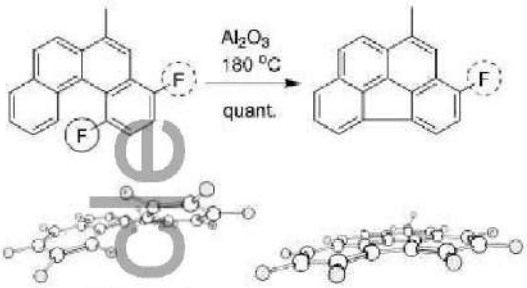

Figure 1. Alumina mediated cyclodehydrofluorination and its selectivity to "dormant" fluorine on periphery (depicted with dashed circle). The DFT-optimized (B3LYP/6-31G(d)) geometries showing the helical structure of fluorinated cove region and its loss after C-C bond formation.

The cove region, indeed, possesses a number of idiosyncrasies; first of all, it has already rather strained helical structure. From the viewpoint of thermodynamics it could be potentially used for the transfer of the "helical" strain to the "bowl-shape" strain in a facile manner. Furthermore, the structure of cove region forces the π-system to be above the generated electrophilic center, promoting the following S_EAr-like attack according our previous DFT study. [12] At this point a reasonable question arises, if the helix of the cove region is untangled, will it still undergo the C-C coupling in effective manner, or will it deactivate fluorine atom making it a mere peripheral substituent. In order to address the issue we have prepared **1** that serves as an extremely interesting model for the studies aimed to answer the question posed above.

2. Experimental

In order to obtain **1**, we have carried out Wittig reaction using 1-bromonaphthaldehyde and triphenylposphonium bromide obtained from 1-bromo-2-(bromomethyl)naphthalene followed by the bromination of the obtained E/Z alkenes mixture. Subsequent double dehydrobromination and standard Suzuki coupling with difluorophenylboronic acid gave derivative **1e**, which was transformed to tribenzopicene derivative **1** in accordance with the established procedure.[13] The single crystal X-Ray analysis of **1** confirms the highly twisted geometry which should facilitate the alumina mediated cyclodehydrofluorination (see Fig.2 and SI).

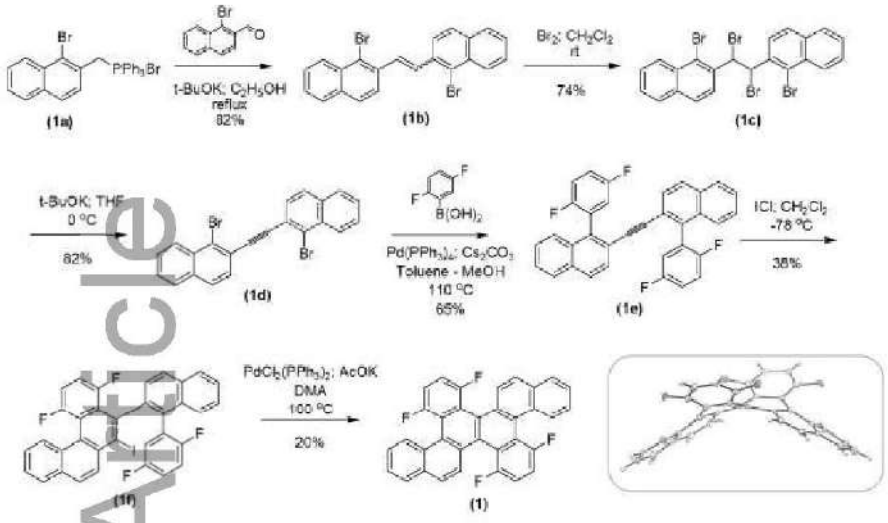

Figure 2. Synthetic route to **1**. ORTEP projection of **1** in the crystal showing twisted geometry is given in inset. (Thermal ellipsoids are set to 30% probability level)

At first sight, **1** has only two different cove regions, although eight intermediates in principle might be formed depending on the sequence of C-C coupling occurring during the reaction (see SI). Moreover, each cove closure affects the rest of the system since the atom crowding is eliminated together with HF molecule and PAH acquires more strained bowl-shaped geometry leading to widening of the remaining cove regions. Thus, **1** is rather interesting precursor that allows studies on various cove region closures, where our principle question was to investigate if the desired molecule **2** is formed during the reaction.

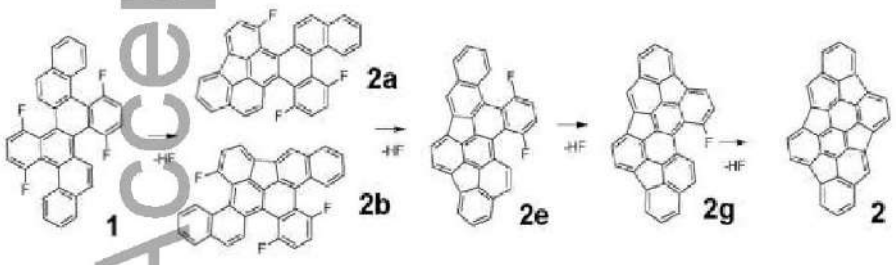

Figure 3. The expected sequence of HF eliminations in compound **1** leading to **2**.

Despite the numerous possible products (see SI, Fig. S19) the HPLC monitoring of the reactionary mixture revealed only few peaks showing that after 2 hours the initial reagent **1** was nearly fully consumed. Moreover, even trace amounts of single closure intermediates (**2a** and **2b**) could not be detected according LDI-mass spectrometry analysis indicating higher reactivity of **2a** and **2b** in comparison to **1**. Similar behavior was previously observed during double closure in fluorinated benzopicene.[11] At the same time NMR revealed the major products of the reaction to be **2e** and **2g**. HPLC separation of the mixture did not lead to the isolation of any other intermediates, indicating either their absence or high reactivity.

Additionally, both isolated **2e** and **2g** were attempted to undergo further alumina mediated HF elimination, these experiments revealed that **2e** is an intermediate yielding **2g**, while the last one is a terminal product that does not give detectable amounts of **2**. The traces of **2** were detected by means of LDI-MS of the reactionary mixture obtained after exposure of **1** to alumina and the following extraction of the solid Al_2O_3 with boiling toluene. However, the following HPLC treatment of the mixture did not allow us isolating the substance **2** (see SI). Thus, we can claim that **1** undergoes only three C-C couplings under the applied conditions yielding **2g** in 15%.

Having these experimental results in hand we demonstrate the importance of the helical geometry of the cove region in order to implement effective C-C coupling via alumina mediated C-F bond activation. The DFT optimized (B3LYP/6-31G(d)) geometry of **2g** clearly shows the loss of helical structure and reveals that the obtained fragment becomes similar to bay region, in which case the C-F bond is dormant . Note, that **2g** possesses rather large bowl depth (3.63 Å - DFT optimized geometry), which would have been increased even further, if **2** had been formed. Interestingly enough, rather similar precursor **3** obtained in our group earlier undergoes full four-fold HF elimination yielding **4** nearly quantitatively.[11]

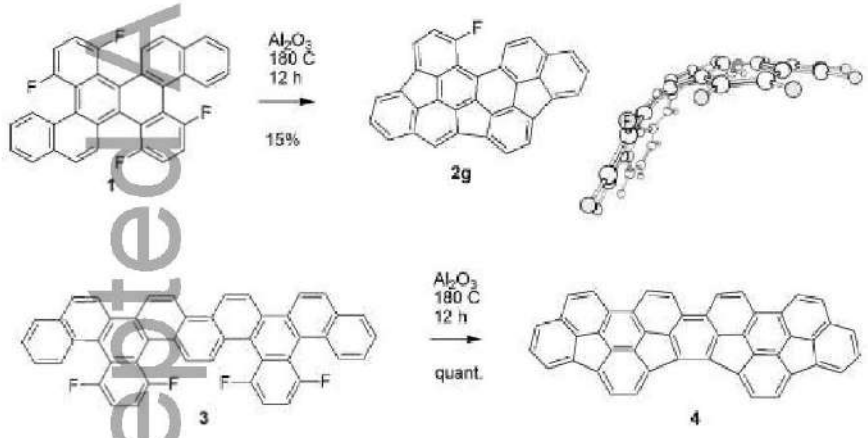

Figure 4. The comparison of two relevant large PAHs containing four cove regions each and the outcome of their exposure to activated alumina at 180 °C under vacuum. DFT optimized structure of **2g** is shown as ball-and-stick model.

This apparent inconsistency is easily unraveled, once the geometry of the cove regions is considered. In the case of **3** the initial three closures do not significantly affect the last remaining cove region, regardless of the sequence implemented during the C-C couplings. Thus, the desired product **4** is obtained in facile manner in contrast to **2**, where each formed C-C bond drastically alter the structure of the remaining cove regions. Eventually, after three closures the last cove region is so widened that it does not have any twisted like geometry anymore. Despite its inertness on alumina, the remaining cove region is an interesting candidate for the thermally triggered gas-phase closure, since under flash vacuum pyrolysis conditions HF elimination is known to occur in a concerted manner.[14]

3. Conclusion

Summing up, this study will help to approach the alumina mediated HF elimination in more precise and accurate manner during the design of the precursors. Once we know that the

widening of cove region, indeed, leads to drastic changes in its reactivity transforming fluorine atom from extremely reactive functionality to a mere peripheral substituent that does not trigger intramolecular C-C coupling we may use it in order to carry out regioselective HF elimination. Moreover, the obtained bowl shaped molecules **2e** and **2g** are already interesting molecules barely available otherwise. These molecule might be used for the further functionalization or transformed to target molecule **2** via other C-F bond activation approaches.

Supporting Information

Supporting Information including experimental procedures, characterization of compounds and X-ray crystallography data is available from the Wiley Online Library.

Acknowledgements

Authors are thankful to Dr. Harald Maid for NMR measurements and spectra interpretations, Dr. Juergen Nuss for single crystal measurements. Authors Funded by the Deutsche Forschungsgemeinschaft (DFG) – Projektnummer 182849149 – SFB 953 and AM407.

Received: ((will be filled in by the editorial staff))
Revised: ((will be filled in by the editorial staff))
Published online: ((will be filled in by the editorial staff))

References

[1] J. Li, K. Zhou, J. Liu, Y. Zhen, L. Liu, J. Zhang, H. Dong, X. Zhang, L. Jiang, W. Hu, *J. Am. Chem. Soc.* **2017**, *139*, 17261–17264.

[2] P. Ruffieux, S. Wang, B. Yang, C. Sanchez-Sanchez, J. Liu, T. Dienel, L. Talirz, P. Shinde, C. A. Pignedoli, D. Passerone, et al., *Nature* **2016**, *531*, 489–492.

[3] J. Liu, H. Zhang, H. Dong, L. Meng, L. Jiang, L. Jiang, Y. Wang, J. Yu, Y. Sun, W. Hu, et al., *Nat. Commun.* **2015**, *6*, 10032.

[4] C. Sutton, N. R. Tummala, D. Beljonne, J.-L. Brédas, *Chem. Mater.* **2017**, *29*, 2777–2787.

[5] V. M. Tsefrikas, L. T. Scott, *Chem. Rev.* **2006**, *106*, 4868–4884.

[6] M. Shimizu, I. Nagao, Y. Tomioka, T. Hiyama, *Angew. Chemie - Int. Ed.* **2008**, *47*, 8096–8099.

[7] W. Matsuoka, H. Ito, K. Itami, *Angew. Chemie - Int. Ed.* **2017**, *56*, 12224–12228.

[8] O. Papaianina, V. A. Akhmetov, A. A. Goryunkov, F. Hampel, F. W. Heinemann, K. Y.

Amsharov, *Angew. Chemie - Int. Ed.* **2017**, *56*, 4834–4838.

[9] A. K. Steiner, K. Y. Amsharov, *Angew. Chemie - Int. Ed.* **2017**, *56*, 14732–14736.

[10] V. Akhmetov, M. Feofanov, S. Troyanov, K. Y. Amsharov, *Chem. – A Eur. J.* **2019**, chem.201901450.

[11] K. Y. Amsharov, M. A. Kabdulov, M. Jansen, *Angew. Chemie - Int. Ed.* **2012**, *51*, 4594–4597.

[12] D. Sharapa, A.-K. Steiner, K. Amsharov, *Phys. Status Solidi* **2018**, *1800189*, 1800189.

[13] C. W. Li, C. I. Wang, H. Y. Liao, R. Chaudhuri, R. S. Liu, *J. Org. Chem.* **2007**, *72*, 9203–9207.

[14] K. Y. Amsharov, M. A. Kabdulov, M. Jansen, *Chem. - A Eur. J.* **2010**, *16*, 5868–5871.

Alumina mediated solid state cyclodehydrofluorination and its suitability for the synthesis of the elusive buckybowls were studied and investigated. An interesting molecule containing non-equivalent cove regions was exposed to activated alumina, revealing some new features of the reaction, namely, the effect of the cove region twist on the fluorine reactivity.

Keyword C-F activation, Aryl-Aryl coupling, Activated alumina, Solid state synthesis, Buckybowls, Geodesic polyarenes, Cyclodehydrofluorination

Vladimir Akhmetov and Konstantin Amsharov

Effect of the Cove Region Geometry in PAHs on Alumina Assisted Cyclodehydrofluorination

Supporting information

Contents

1. General Information

All chemicals and solvents were purchased in reagent grade from commercial suppliers (Acros®, SigmaAldrich® or Fluka®, Fluorochem®, Merck®, chemPur®) and used as received unless otherwise specified. Microwav eassisted experiments were carried out using Discover SP Microwave Synthesizer, CEM. Solvents in HPLC grade were purchased from VWR® and SigmaAldrich®.Flash column chromatography was performed on Interchim PuriFlash 430 using flash grade silica gel from MacheryNagel 60 M (40-63 mm, deactivated). NMR spectra were recorded on a Bruker Avance Neo 300 operating at 300 MHz (^{1}H NMR), 75 MHz (^{13}C NMR) and 282 (^{19}F NMR), on a Bruker Avance Neo 400 operating at 400 MHz (^{1}H NMR), 100 MHz (^{13}C NMR) and 377 (^{19}F NMR), on a Bruker Avance Neo 500, operating at 500 MHz (^{1}H NMR), 125 MHz (^{13}C NMR) and 470 MHz (^{19}F NMR) and on a Bruker Avance Neo 600, operating at 600 MHz (^{1}H NMR), 150 MHz (^{13}C NMR) and 564(^{19}F NMR) at room temperature. The signals were referenced to residual solvent peaks (in parts per million (ppm) ^{1}H: $CDCl_3$, 7.27 ppm; CD_2Cl_2, 5.32 ppm; $(CD_3)_2CO$, 2.05 ppm; ^{13}C: $CDCl_3$, 77.0 ppm; CD_2Cl_2, 53.84 ppm). Coupling constants were assigned as observed. The obtained spectra were evaluated with the program

MestReNova. High resolution APPI MS spectra were recorded on a Bruker ESI TOF maXis4G instrument. The data was evaluated with the program Bruker Compass DataAnalysis 4.2. HPLC measurements were performed on a Shimadzu Prominence Liquid Chromatograph LC-20AT with communication bus module CBM-20A, diode array detector SPDM20A, the degassing unit DGU-20A5 R, column oven CTO-20AC or CTO-20A, respectively and with auto sampler SIL-20A HT. For separation a Cosmosil 5-PYE column (4.6 mm x 250mm) from Nacalai Tesque was used. As eluent a DCM/MeOH or toluene/MeOH mixture was used (UV-vis detection). The data was evaluated with the programs Shimadzu LCsolution and Shimadzu LabSolutions. TLC analyses were carried out with TLC sheets coated with silica gel with fluorescent indicator254 nm from Machery-Nagel (ALUGRAM® SIL G/UV254) and visualized via UV-light of 254nm or 366 nm.

2. Experimental Procedures

Synthesis of 1b.

Dissolved 1a (1.75g, 3.11 mmol, 1 eq.) in 50 ml. of ethanol was added to the solution of 1-bromo-2-naphthaldehyde (0.73g, 3.11 mmol, 1 eq.) and t-BuOK (0.35g, 3.11 mmol, 1 eq.). The reaction mixture was refluxed for 4.5 hours. The mixure was evaporated under reduced pressure, extracted with dichloromethane (3 x 30 mL), washed with water (3 x 30 mL), dried over Na_2SO_4 and the solvent was evaporated. The mixture was purified by flash column chromatography using petroleum ether-CCl_4 (1:2, $R_f = 0.6$) and used as obtained in the following step. Yield of 1b (as a mixture of cis- and trans-adducts): 82 % (1.12g , yellow solid).

Synthesis of 1c.

Bromine (0.12 mL, 2.50 mmol, 1.1 eq.) was added to solution of 1b (1g, 2.28 mmol, 1 eqv) in 30 mL of dichloromethane and the obtained mixture was stirred at rt for 1 hour. After washing the mixture with water (100 ml) and saturated sodium thiosulfate solution (50 ml) the mixture was extracted with dichloromethane (3 x 25 mL),) washed with water (3 x 30 mL), dried over Na_2SO_4 and the solvent was evaporated. The mixture was purified by flash column chromatography using petroleum ether-CCl_4 (1:2, $R_f = 0.5$) Yield of 1c: 74 % (1.0 g , white solid). ^{1}H NMR (500 MHz, CD_2Cl_2) δ 8.09 (d, J = 8.5 Hz, 1H), 7.56 (s, 2H), 7.53 (d, J = 8.0 Hz, 1H), 7.43 – 7.37 (m, 1H), 7.36 – 7.27 (m, 1H), 6.60 (s, 1H). ^{13}C NMR (126 MHz, CD_2Cl_2) δ 136.25 (s), 134.42 (s), 132.27 (s), 128.98 (s), 128.50 (s), 128.46 (s), 128.41 (s), 127.92 (s), 124.92 (s), 123.51 (s), 58.43 (s).

Synthesis of 1d.

To a solution of 1c (500 mg, 0,836 mmol, 1eq.) in 25 ml of anhydrous THF cooled to 0 °C solution of t-BuOK (281 mg. 2.508 mmol, 3 eq.) in anhydrous THF (10 ml) was added under argon and stirred at rt for 2 hours. The reaction was quenched with 10 ml of water, diluted with 30mL of n-hexane-toluene (4:1), washed with brine solution (1 x 25 ml) and water (2x 25 mL.). The organic layer was dried over Na_2SO_4 and the solvent was evaporated. The mixture was purified by flash column chromatography using petroleum ether- CCl_4 (1:3, $R_f = 0.5$) Yield of

1d: 82 % (300 mg , white solid). ^{1}H NMR (300 MHz, $CDCl_3$) δ 8.35 (d, *J* = 8.4 Hz, 2H), 8.01 – 7.79 (m, 4H), 7.78 – 7.45 (m, 6H). ^{13}C NMR (75 MHz, $CDCl_3$) δ 134.35 (s), 132.67 (s), 129.49 (s), 128.72 (s), 128.52 (s), 128.14 (s), 128.12 (s), 127.93 (s), 126.92 (s), 123.61 (s), 94.77 (s).

Synthesis of 1e.

A solution of 1d (l.5 g, 3.43 mmol, 1 eq.), 2.5-dituorobenzeneboronic acid (1.19 g 7.54 mmol, 2.2 eq.), $Pd(PPh_3)_4$ (593 mg, 0.514 mmol, 0.15 eq) and cesium carbonate (6.7g, 20.58 mmol, 6 eq.) in 100 ml of toluene and 50 ml of methanol was degassed and refluxed under argon for 2 hours. The reaction mixture was extracted with CCl_4 (3x 40 mL), washed with water (3 x 30 ml.), dried over Na_2SO_4 and filtered through a short silica plug followed by flash column chromatography using petroleum ether- CCl_4 (1:3, R_f = 0.3) Yield of 1e: 65 % (1.13g , white solid). ^{1}H NMR (300 MHz, $CDCl_3$) δ 7.86 (dd, *J* = 8.3, 3.5 Hz, 2H), 7.62 (d, *J* = 8.8 Hz, 1H), 7.52 – 7.43 (m, 1H), 7.42 – 7.36 (m, 2H), 7.27 (tdd, *J* = 7.3, 2.6, 1.8 Hz, 1H), 7.11 – 7.00 (m, 2H). APPI HRMS calculated for $C_{34}H_{18}F_4$ [M^+] *m/z* 502.1339, found 502.1342.

Synthesis of 1f.

Dissolved 1e (0.5g, 0.995 mmol, 1 eq.) in 30 ml of dichloromethane was cooled to -78° C. Afterwards 1M solution of ICl (0.325g, 2.01 mmol, 1.9997 eqv) in dichloromethane was added at -78° C and the obtained mixture was stirred for 15 minutes. Then the mixture was stirred at -40 ° C for 30 minutes followed by quenching with saturated sodium thiosulfate solution (50 ml). The reaction mixture was extracted with dichloromethane (3 x 30 mL), washed with water (3 x 30 mL), dried over Na_2SO_4 and purified by flash column chromatography using petroleum ether-$CHCl_3$ (4:1, R_f = 0.35) Yield of 1f: 38 % (0.24g , white solid). The obtained product was used in the next step without additional purification and characterization.

Synthesis of 1.

Compound 1f (0.12g, 0.190 mmol, 1 eq.) was dissolved in 10 mL of dimethylacetamide followed by addition of $PdCl_2(PPh_3)_2$ (0.007g, 0.01 mmol, 0.05 eq.) and potassium acetate (0.075g, 0.76 mmol, 4 eq.). The reaction mixture was degassed and heated at 100° C for 1.5 hours under argon. The compound was extracted with dichloromethane (3 x 25 mL), washed with water (3 x 30

mL), dried over Na_2SO_4 and purified by flash column chromatography using CCl_4 (R_f = 0.6) Yield of 1: 25 % (24 mg , yellow solid). ^{1}H NMR (500 MHz, CD_2Cl_2) δ 7.52 (dd, *J* = 13.3, 8.4 Hz, 2H), 7.36 – 7.27 (m, 4H), 7.20 (d, *J* = 7.4 Hz, 2H), 6.92 – 6.81 (m, 4H), 6.77 – 6.67 (m, 4H). ^{13}C NMR (126 MHz, CD_2Cl_2) δ 158.76 (d, *J* = 198.2 Hz), 156.78 (d, *J* = 197.4 Hz), 135.24 (s), 132.79 (s), 132.42 (s), 132.29 (s), 132.18 (s), 132.15 (s), 132.13 (s), 130.88 (s), 130.74 (s), 129.72 (s), 129.05 (s), 128.49 (d, *J* = 12.7 Hz), 125.57 (s), 123.35 (d, *J* = 16.0 Hz), 122.45 (d, *J* = 14.4 Hz). APPI HRMS calculated for $C_{34}H_{16}F_4$ [M^+] *m/z* 500.1182, found 500.1182.

Synthesis of 2g.

A glass tube was charged with 3 g of γ-Al_2O_3 (neutral, 50-200 micron) and preactivated at 540 ℃ for 3-4 hours. Then it was connected to a Schlenk line and heated at 540 ℃ under vacuum (10^{-3} mbar) for another 2 hours. The vessel was cooled down to r.t. and 0,05 mmol of 1 was added under argon atmosphere. The tube containing the obtained mixture was sealed under vacuum and heated at 190-220°C for 2-72 h. After cooling to room temperature, products were extracted with toluene. Separation and final purification of the product were carried out by HPLC from the respective toluene extract. Under the following conditions: 190°C, 12h 2g was isolated by means of HPLC (Cosmosil PBr column, Tol:MeOH, 5 ml/min, t_r=11min) to yield 4 mg (18%) of yellowish solid.

^{1}H NMR (400 MHz, CD_2Cl_2) δ 8.94 (dd, *J* = 9.2, 4.1 Hz, 1H), 8.08 (s, 1H), 7.99 (dd, *J* = 7.6, 3.2 Hz, 1H), 7.94 (d, *J* = 8.6 Hz, 1H), 7.91 – 7.72 (m, 6H), 7.60 – 7.40 (m, 3H). ^{19}F NMR (377 MHz, CD_2Cl_2) δ -98.42 (d, *J* = 12.8 Hz). ^{1}H NMR (500 MHz, CD_2Cl_2) δ 8.94 (d, *J* = 9.1 Hz, 1H), 8.08 (s, 1H), 7.99 (d, *J* = 7.5 Hz, 1H), 7.94 (d, *J* = 9.2 Hz, 1H), 7.90 – 7.73 (m, 6H), 7.57 – 7.47 (m, 2H), 7.45 (d, *J* = 7.5 Hz, 1H). ^{19}F NMR (471 MHz, CD_2Cl_2) δ -98.43 (s). APPI HRMS calculated for $C_{34}H_{13}F$ [M^+] *m/z* 440.0995, found 440.0996.

Synthesis of 2e.

A glass tube was charged with 3 g of γ-Al_2O_3 (neutral, 50-200 micron) and preactivated at 540 ℃ for 3-4 hours. Then it was connected to a Schlenk line and heated at 540 ℃ under vacuum (10^{-3} mbar) for another 2 hours. The vessel was cooled down to r.t. and 0,05 mmol of 1 was added under argon atmosphere. The tube containing the obtained mixture was sealed under vacuum and

heated at 190-220°C for 2-72 h. After cooling to room temperature, products were extracted with toluene. Separation and final purification of the product were carried out by HPLC from the respective toluene extract. Under the following conditions: 190°C, 3h 2e was isolated by means of HPLC (Cosmosil PBr column, Tol:MeOH, 5 ml/min, t_r=7,5 min) to yield 7 mg (30%) of yellowish solid. ^{1}H NMR (400 MHz, CD_2Cl_2) δ 8.51 (dd, *J* = 9.1, 4.4 Hz, 1H), 8.36 – 8.29 (m, 1H), 8.28 (s, 1H), 8.00 (d, *J* = 6.6 Hz, 1H), 7.97 – 7.88 (m, 4H), 7.78 (d, *J* = 8.1 Hz, 1H), 7.69 – 7.50 (m, 5H). ^{19}F NMR (377 MHz, CD_2Cl_2) δ -101.99 – -102.32 (m), -109.50 – -109.94 (m). ^{1}H{^{19}F} NMR (500 MHz, CD_2Cl_2) δ 8.51 (d, *J* = 9.1 Hz, 1H), 8.32 (d, *J* = 8.4 Hz, 1H), 8.28 (s, 1H), 8.00 (dd, *J* = 7.9, 1.5 Hz, 1H), 7.97 – 7.88 (m, 4H), 7.78 (d, *J* = 8.1 Hz, 1H), 7.66 (d, *J* = 8.9 Hz, 1H), 7.61 – 7.50 (m, 4H). ^{19}F{^{1}H} NMR (471 MHz, CD_2Cl_2) δ -102.11 (d, *J* = 16.5 Hz), -109.73 (d, *J* = 16.2 Hz).

APPI HRMS calculated for $C_{34}H_{14}F_2$ [M^+] *m/z* 460.1058, found 460.1060.

3. Spectroscopic Analysis and Characterization

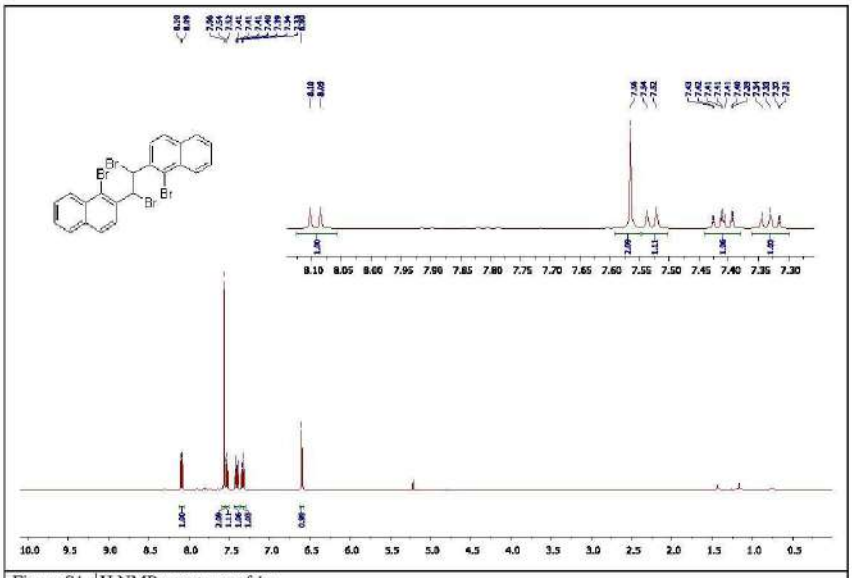

Figure S1. ^{1}H NMR spectrum of 1c.

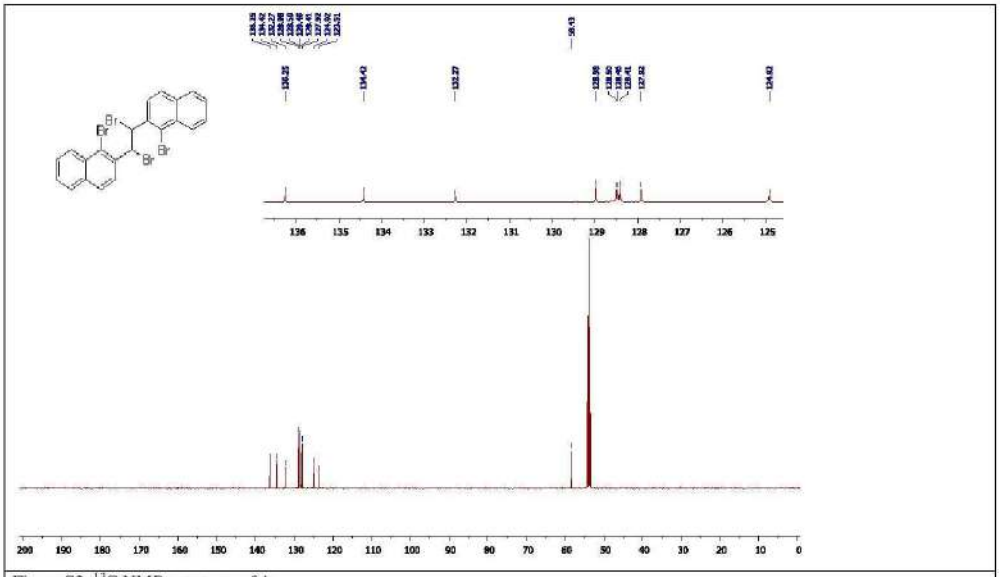

Figure S2. ^{13}C NMR spectrum of 1c.

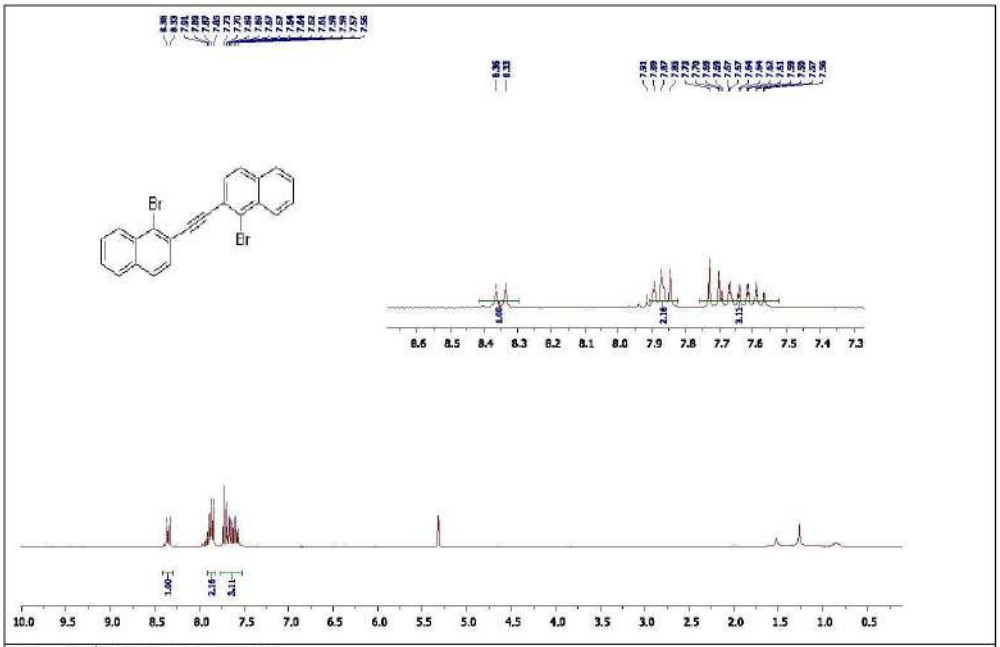

Figure S3. ^{1}H NMR spectrum of 1d.

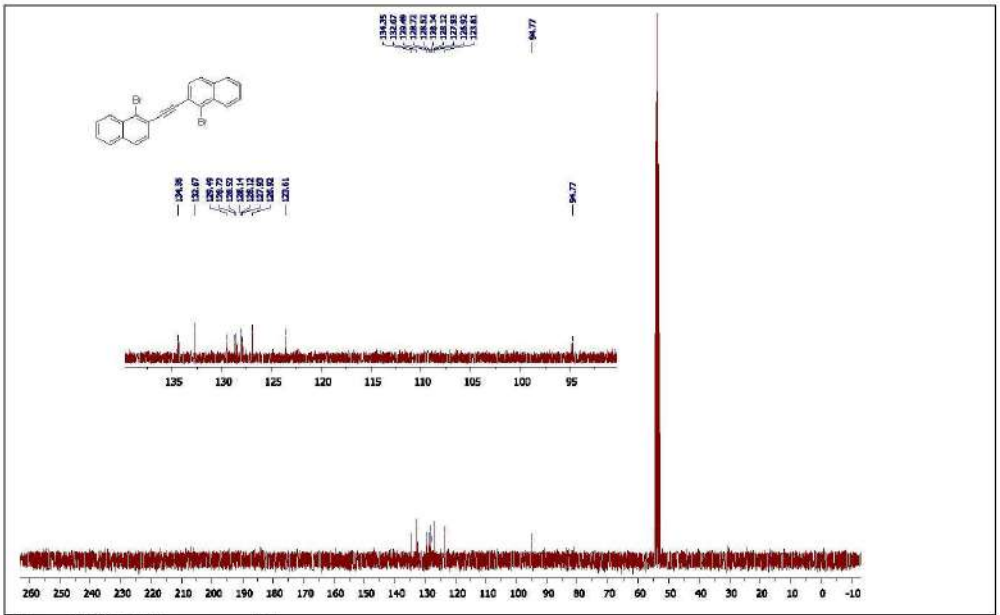

Figure S4. ^{13}C NMR spectrum of 1d.

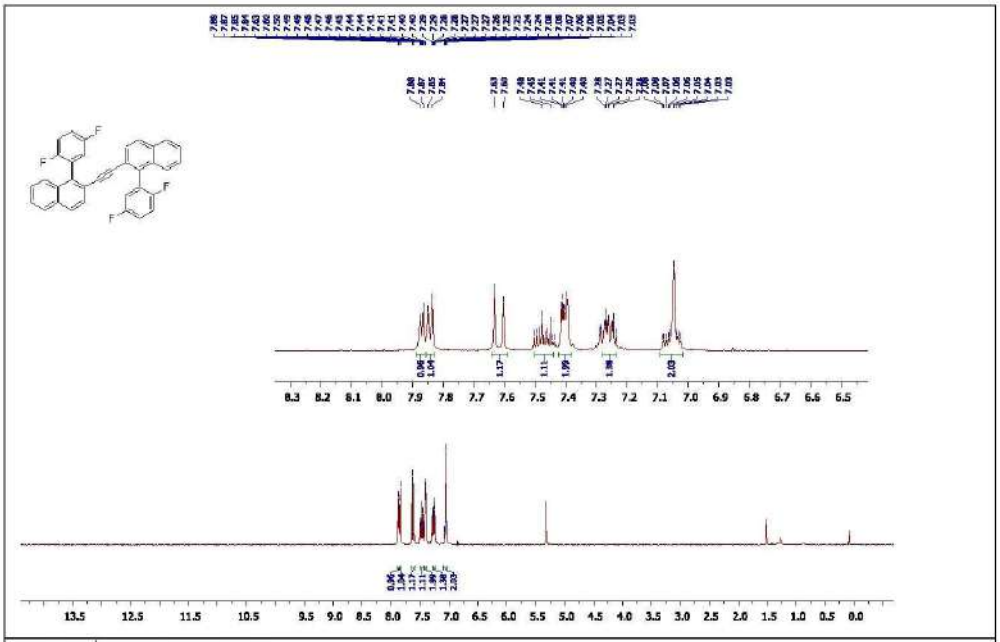

Figure S5. ^{1}H NMR spectrum of 1e.

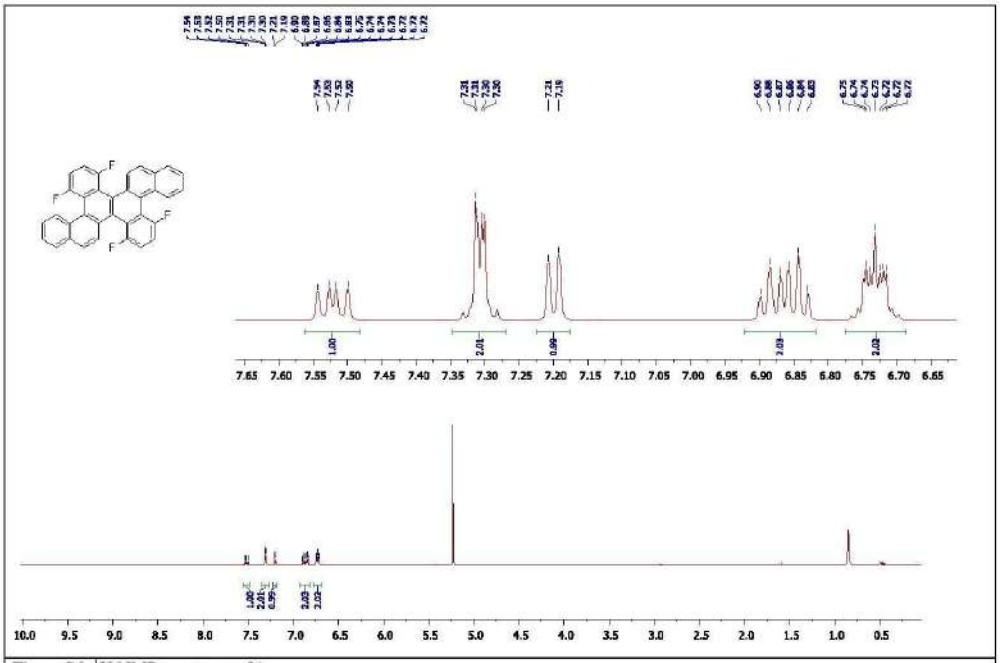

Figure S6. ^{1}H NMR spectrum of 1.

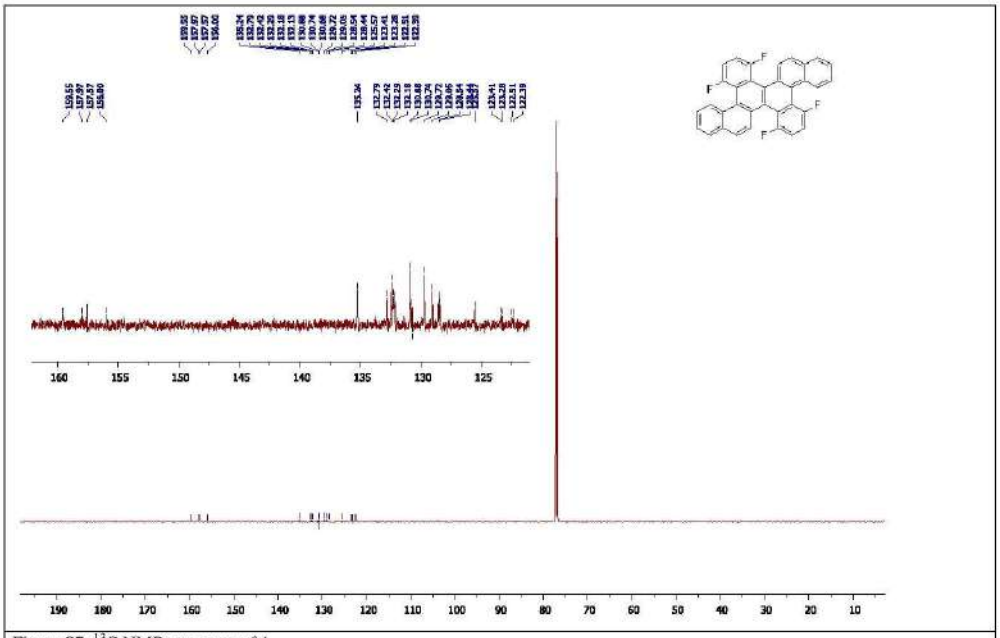

Figure S7. ^{13}C NMR spectrum of 1.

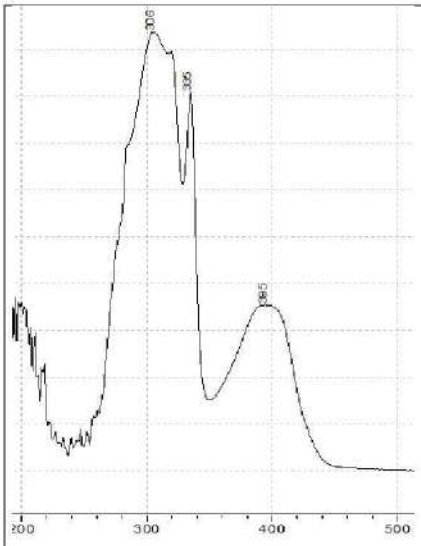

Figure S8. Uv/vis spectrum of 1 (MeOH:Tol=1:1).

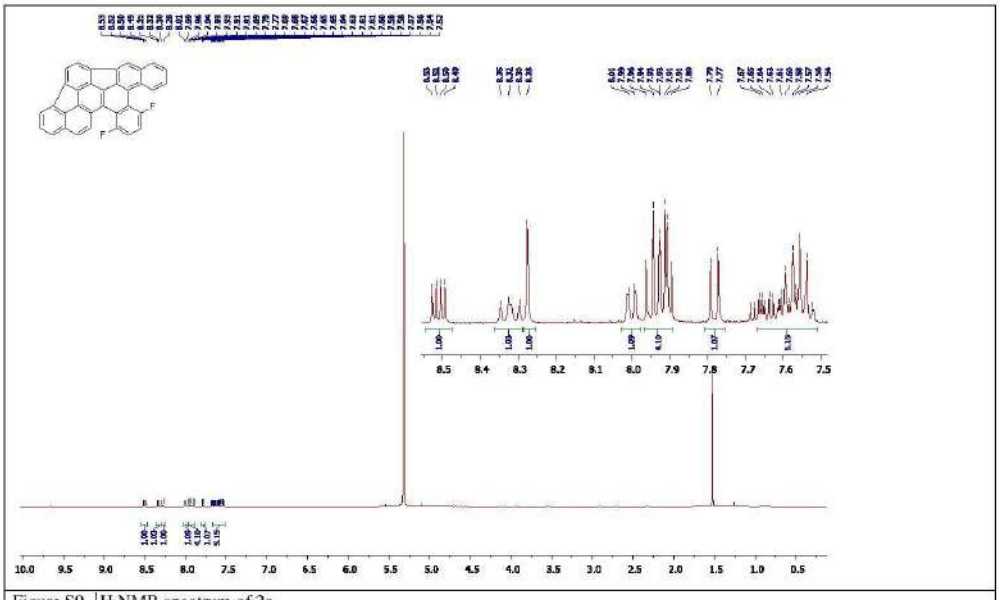

Figure S9. ^{1}H NMR spectrum of 2e.

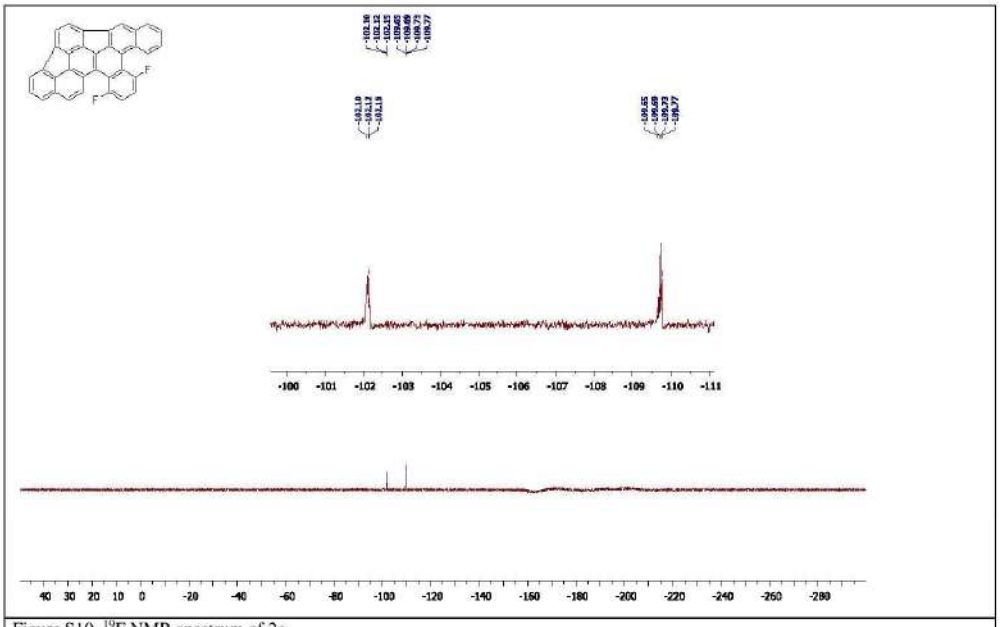

Figure S10. ^{19}F NMR spectrum of 2e

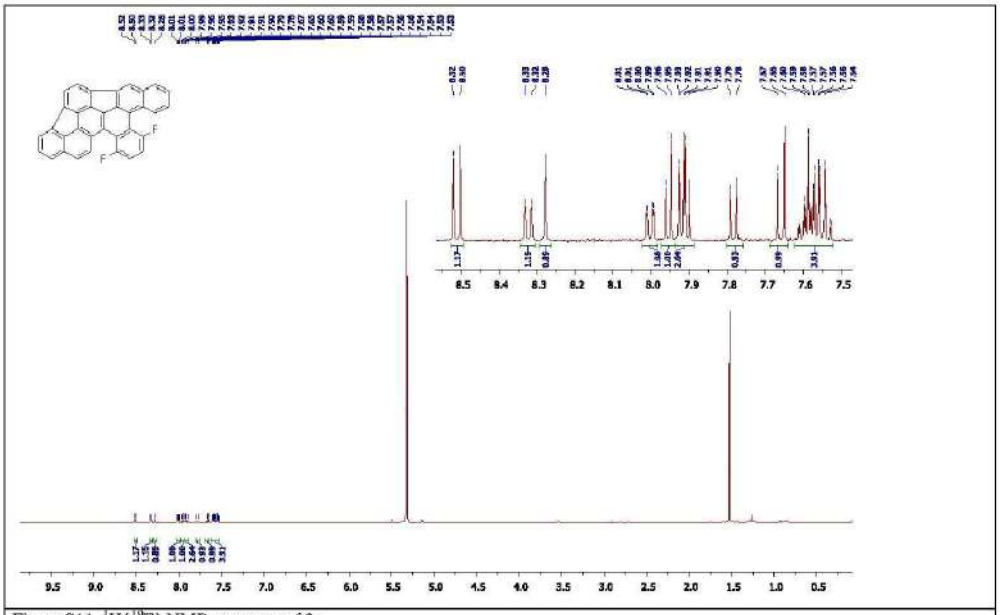

Figure S11. $^{1}H\{^{19}F\}$ NMR spectrum of 2e.

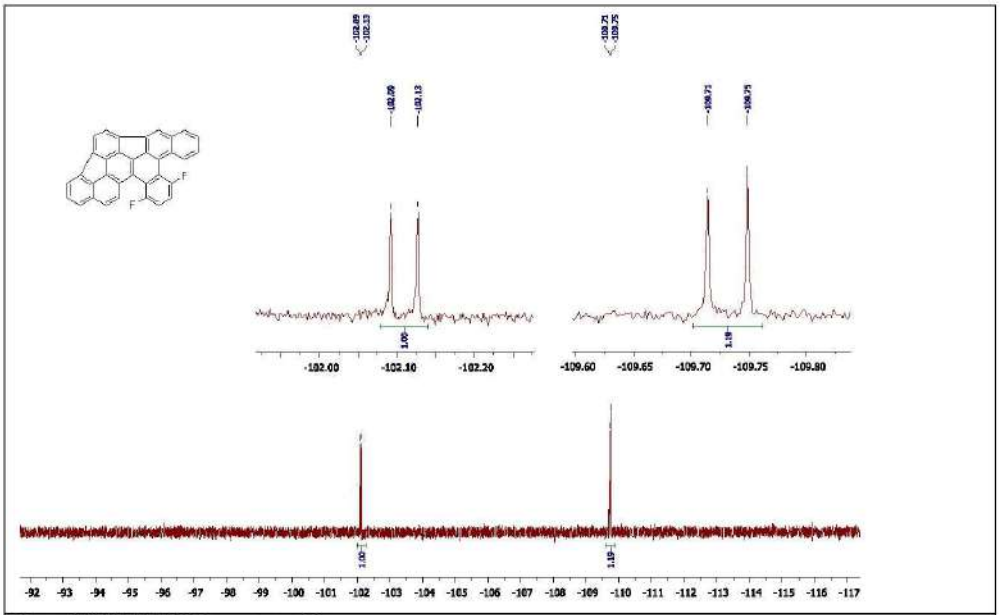

Figure S12. $^{19}F\{^{1}H\}$ NMR spectrum of 2e.

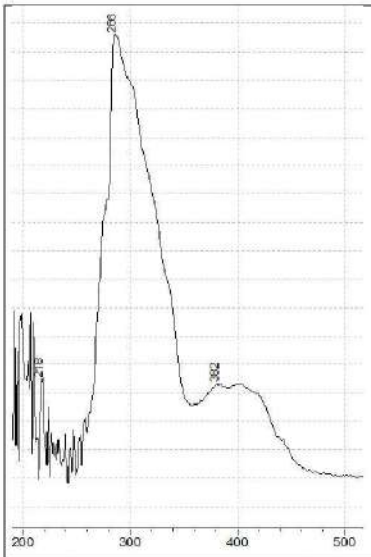

Figure S13. Uv/vis spectrum of 2e (MeOH:Tol=1:1).

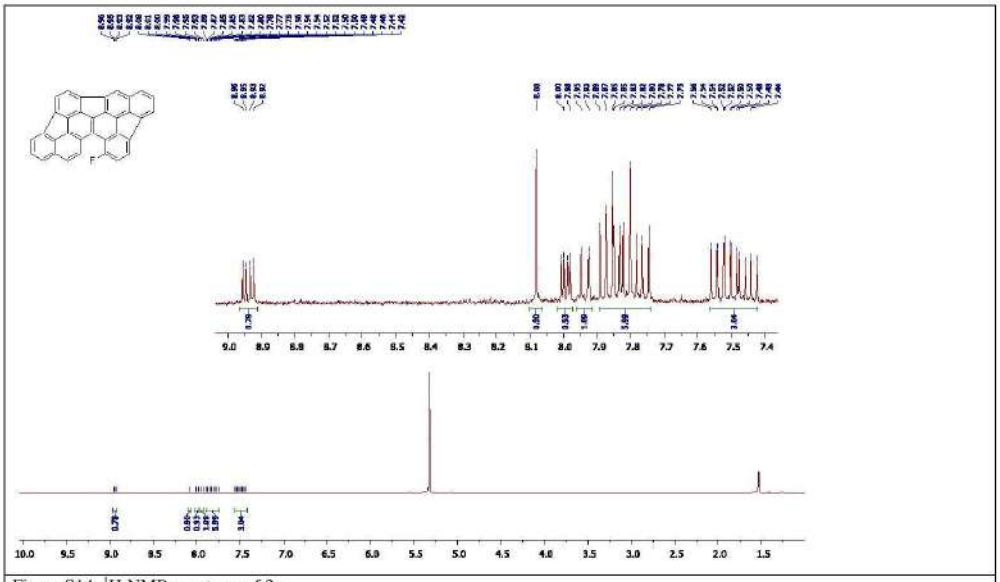

Figure S14. ^{1}H NMR spectrum of 2g.

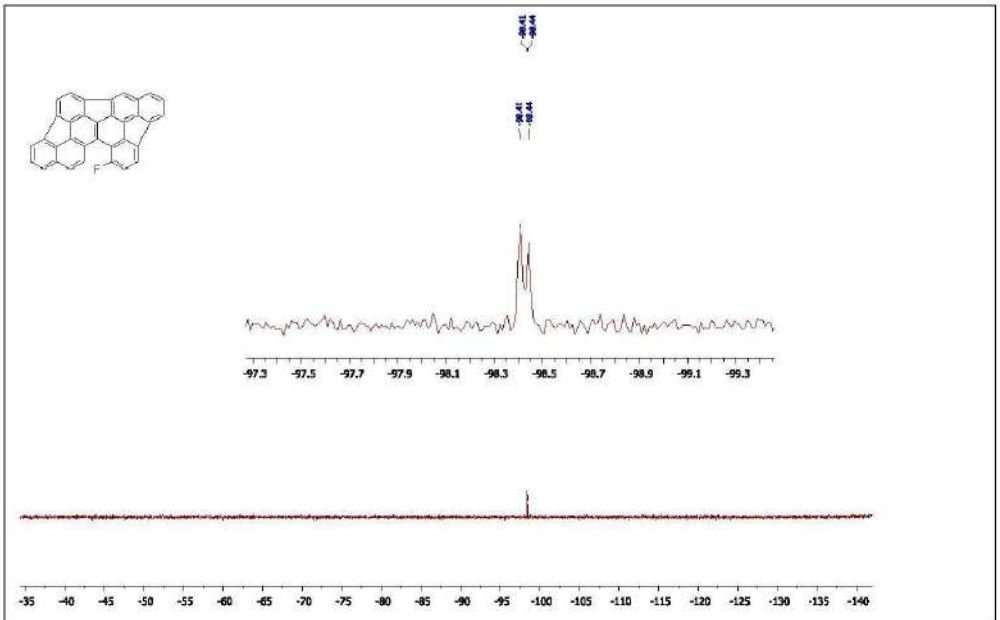

Figure S15. ^{19}F NMR spectrum of 2g.

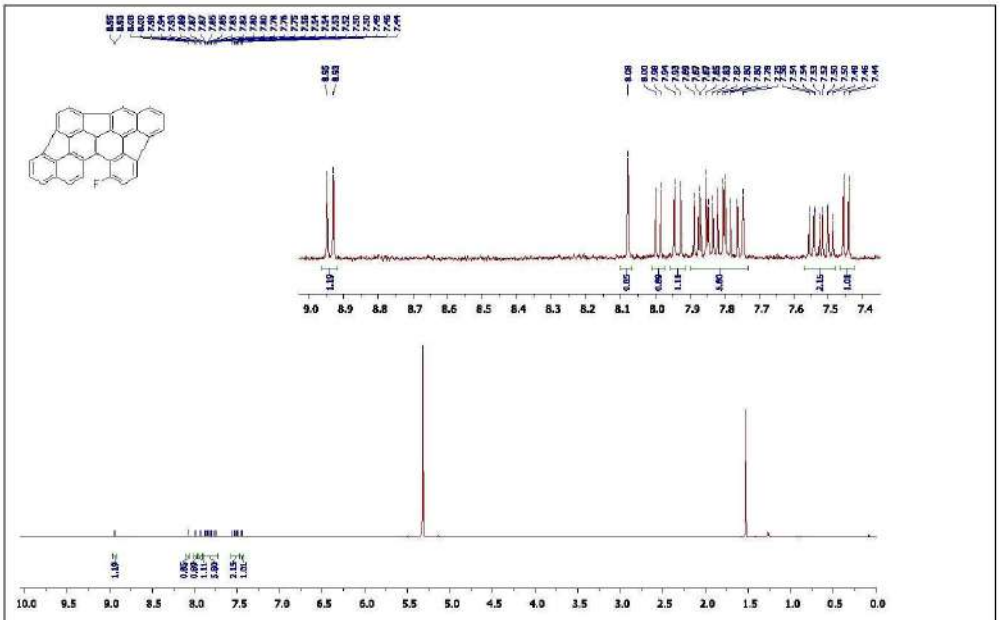

Figure S16. $^{1}H\{^{19}F\}$ NMR spectrum of 2g.

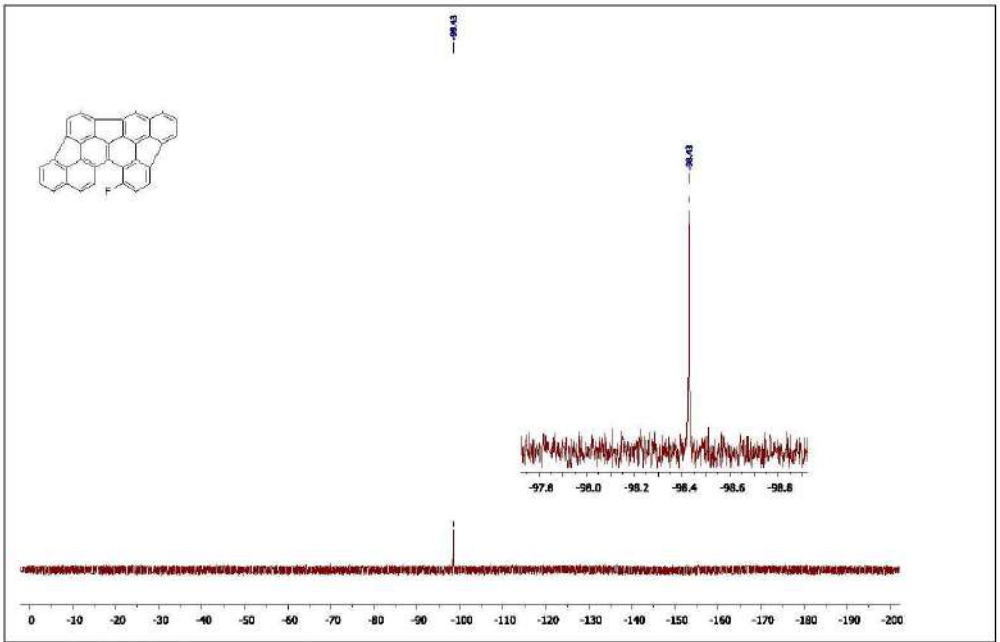

Figure S17. $^{19}F\{^{1}H\}$ NMR spectrum of 2g.

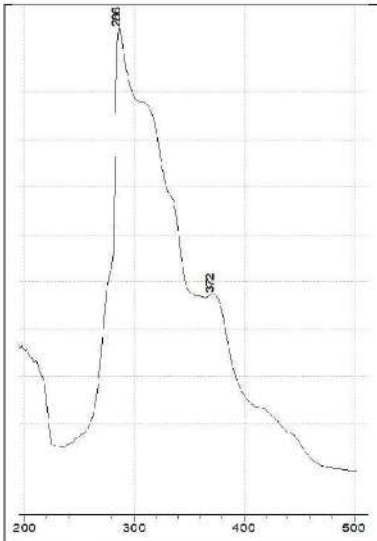

Figure S18. Uv/vis spectrum of 2e (MeOH:Tol=1:1).

a)

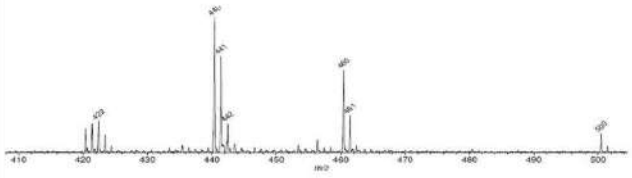

b)

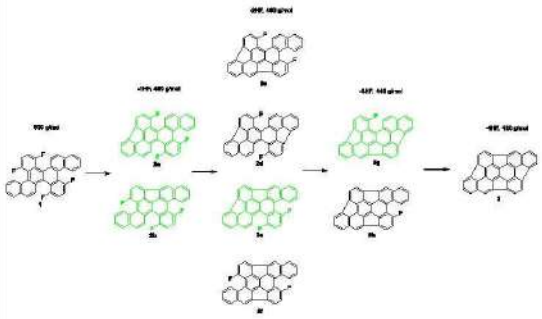

Figure S19. a) LDI-MS analysis of the toluene extract obtained after 5h exposure of 1 to activated alumina at 190 ºC under vacuum. b) The transformation of 1 to 2. The suggested pathway is labeled with green color.

4. X-Ray Crystallography.

Crystal data and structure refinement for compound 1.

Identification code	ams_93
Empirical formula	$C_{34}H_{16}F_4$
Formula weight	500.47
Temperature/K	100(10)
Crystal system	monoclinic
Space group	*C* 2/c
a/Å	29.14(5)
b/Å	14.36(2)
c/Å	10.828(17)
α/°	90
β/°	96.331(18)
γ/°	90
Volume/Å^3	4503(12)
Z	8
Crystal size/mm^3	0.1 × 0.05 × 0.05
Radiation	Mo Kα (λ = -0.71073)
2Θ max/°	10.4
Index ranges	-28 ≤ h ≤ 29, -14 ≤ k ≤ 14, -10 ≤ l ≤ 10
Reflections collected	2353
Independent reflections	1305 [R_{int} = 0.2132]
Final R indexes [I>=2σ (I)]	R_1 = 0.2132, wR_2 = 0.5348

Publication 5.

Towards Non-alternant Nanographenes by Self-Promoted Intramolecular Indenoannulation Cascade via C-F Bond Activation.

V. Akhmetov, M. Feofanov, O. Papaianina, S. Troyanov, K. Y. Amsharov.

Chem. – A Eur. J. DOI: 10.1002/chem.201902586. First Published on 13th of July, **2019**.

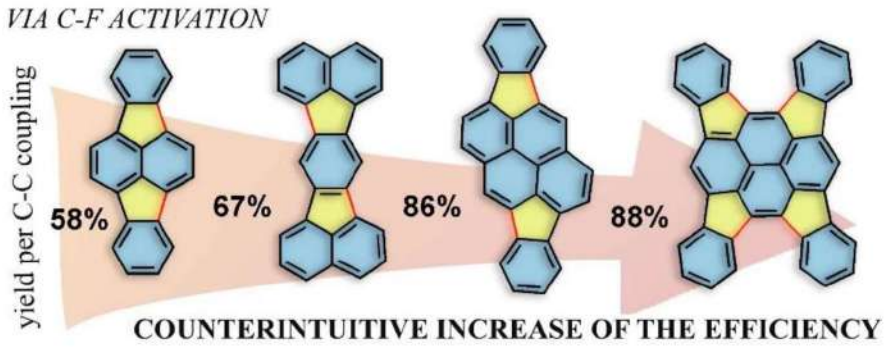

ABSTRACT:

The development of new synthetic approaches to large PAHs and NGs appears as a matter of great importance. Nevertheless, a serious downside of the bottom-up approach is the necessity of oftentimes meticulous multi-step synthesis demanding serious time and financial investments. One of the possibilities to avoid such an unpleasant obstacle is a design of the one-pot procedures, where multiple bonds are formed at once. However, in the general perception, the endeavours to perform several reactions at once lead to the notable drop of the yields with the increase of the number of bonds created. Moreover, the reactions which give an opportunity to form several bonds at once are rather scarce. Scholl reaction, enabling multiple Aryl-Aryl couplings, may serve as an illustrative example of such reactions. Despite its broad applicability, the method allows synthesis only honeycomb like structures and cannot be exploited to insert the pentagons into a PAH's core. Meanwhile, PAHs bearing pentagons within their structure possess an outstanding scope of properties and possible applications e.g. electronics and supramolecular chemistry. Here we report that alumina-mediated HF elimination may be used for the self-promoted multiple

indenoannulation yielding useful non-alternant NGs. We demonstrate that the unique nature of the reaction leads to a rather counter-intuitive outcome and allows considering each previous Aryl-Aryl coupling as a promoter of the following ones.

CHEMISTRY
A European Journal

A Journal of
ChemPubSoc Europe

Accepted Article

Title: Towards Nonalternant Nanographenes by Self-Promoted Intramolecular Indenoannulation Cascade via C-F bond Activation

Authors: Vladimir Akhmetov, Mikhail Feofanov, Olena Papaianina, Sergey Troyanov, and Konstantin Y Amsharov

To be cited as: *Chem. Eur. J.* 10.1002/chem.201902586

Link to VoR: http://dx.doi.org/10.1002/chem.201902586

Supported by
ACES

WILEY-VCH

10.1002/chem.201902586

WILEY-VCH

COMMUNICATION

Towards Non-alternant Nanographenes by Self-Promoted Intramolecular Indenoannulation Cascade via C-F Bond Activation

Vladimir Akhmetov[a], Mikhail Feofanov[a], Olena Papaianina[a], Sergey Troyanov[b] and Konstantin Amsharov*[a]

Abstract: Large polycyclic aromatic hydrocarbons (PAHs) containing pentagons represent an important class of compounds which are considered to be superior materials in future nano-electronic applications. From this perspective, the development of synthetic approaches to large PAHs and nanographenes (NGs) is a matter of great importance. In this context indenoannulation appears to be the most practical way to introduce pentagons into NGs. Here we report that alumina-mediated C-F bond activation is an attractive tool for the synthesis of non-alternant NGs bearing several pentagons. We demonstrate that the unique nature of the reaction leads to a rather counter-intuitive outcome and allows considering each previous Aryl-Aryl coupling as a promoter of the following ones, despite continuously increasing strain energy. Thus, the presented strategy combines both facile synthesis and significant yields for large nonalternant PAHs and NGs.

Among various PAHs non-alternant systems containing pentagons attract special interest which stems from their unusual physical properties including high electron affinities[1,2] and anomalous fluorescence.[3] Until recently the synthetic chemists were mainly concentrated on the synthesis of alternant NGs, resembling the honeycomb fragment i.e. composed exclusively of six-membered rings.[4–6] Meanwhile, the methods allowing the incorporation of pentagons into the large PAH structure still remain rather scarce.[9–11] The synthetic difficulties related to pentagons-bearing structures are mainly associated with the enhanced strain caused by distortion of π -system and deviation of valence angles from the optimal sp^2-hybridized carbon atoms geometry. Naturally, these obstacles tend to exacerbate the synthetic accessibility of PAHs' cores containing several pentagons even further. Nevertheless, physical and chemical properties acquired along with pentagons within aromatic core justify efforts to develop decent synthetic approaches toward such attractive structures.[12,13] The multiple indenoannulation appears to be an appealing strategy allowing facile construction of complex non-alternant PAHs, which in certain cases possess curved aromatic π-surface resembling fullerenes. For a rather long time such transformations were feasible only applying high-temperature flash vacuum pyrolysis (FVP),[14] which, however, faces some limitations such as substantial drop of efficiency during the attempts to obtain larger structures such as fullerenes[15]. This fact is accompanied by low tolerance to functional groups and rather mediocre yields.[16–18]

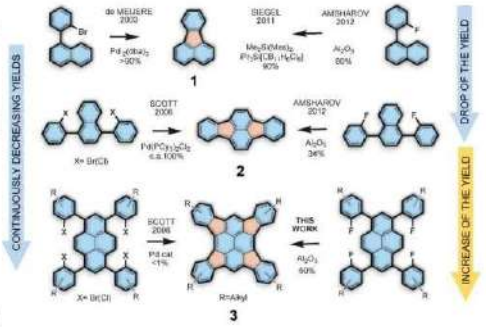

Figure 1. Indenoannulation implemented via different synthetic approaches showing the applicability of alumina C-F activation for the synthesis of large PAHs on example of **3**.

Among alternative liquid-phase techniques palladium(0)-catalyzed direct arylation exploiting aromatic C-Br and C-Cl bonds was found to be effective.[19–22] De Meijere et al. first demonstrated the efficiency of Pd-catalyzed indenoannulation on synthesis of fluoranthrene (Figure 1, compound **1**) and several related small PAHs.[23] The main drawback of this reaction is a high loading of the Pd catalyst that is required for the maintenance of the synthesis (typically 20% per C-Br bond), thus absolute mass of the catalyst frequently exceed the mass of the final product. In 2011 Siegel et al. have demonstrated alternative indenoannulation via C-F bond activation under transition-metal free conditions, preparing fluoranthrene **1**.[24,25] Even though this transformation yields **1** in nearly 95% yield, it requires even more expensive silylium carborane catalyst limiting its broad application. Soon after our group reported on highly effective cove-region closure via C-F bond activation using readily available γ-Al_2O_3,which allows synthesis of various pentagons bearing bowl shaped PAHs with close to quantitative yields.[26–28] This method

[a] Friedrich-Alexander University Erlangen-Nuernberg
Department of Chemistry and Pharmacy, Organic Chemistry II,
Nikolaus-Fiebiger Str. 10, 91058 Erlangen,
Germany.
E-mail: konstantin.amsharov@fau.de
[b] Moscow State University, Chemistry Department, Leninskie gory,
119991, Moscow Russia.

Supporting information for this article is given via a link at the end of the document.

has shown efficiency not only in case of pentagon formation via cove region (4-helicene motive) closure, where the predisposition of the eliminated hydrogen and fluorine may play a crucial role but it was also applied for indenoannulation allowing generation of fluoranthrene **1** with acceptable 80% yield (Figure 1). Regardless of the approach, the efficiency of coupling drops drastically as number of introduced indene's fragment increases. This comes as an anticipated result of continuously increased strain. Here, the Pd-catalyzed strategy appears to be the most powerful tool allowing rather effective introduction of several indeno fragments. Thus, Scott et al. have shown that double Pd-catalyzed indenoannulation of naphthalene (Figure 1, compound **2**) can be achieved with nearly quantitative yield, moreover, the applicability of the approach for multiple indenoannulation was demonstrated,[29] where indenoannulation of pyrene clearly illustrates the scope and limitation of the Pd-catalyzed approach, since target tetraindenopyrene **3** was obtained with less than 1% yield (Figure 1).[29] Silylium carborane catalyzed C-F bond activation appears to be less effective providing only moderate yields of about 50% in case of double indenoannulation of anthracene and corannulene.[30,31] In that respect, alumina mediated C-F activation strategy reveals even more remarkable decrease of the yield to 34% already for double indenoannulation of naphthaline (Figure 1, compound **2**).[26] These observations logically lead to assumption that the approach is more probably limited to synthesis of small nonalternant PAHs. Our current work is aimed to refute the fallacious conclusions prompting from the just mentioned observations on alumina mediated C-F activation. Here we show that the π-system involved into indenoannulation has a huge impact on alumina mediated HF elimination and could drastically influence the cyclization process. Namely, we demonstrate that the increase of π-system substantially improves the efficiency of the intramolecular arylation via C-F bond activation, and thus our research reveal how allegedly stable and inert aromatic C-F bond might be exploited for the highly effective synthesis of extended nonalternant PAHs and NGs systems via multiple indenoannulations on activated γ-Al_2O_3. The progressive expansion of π-system during indenoannulation, which continuously improves coupling efficiency, can be considered as an intramolecular "auto-catalysis" process continuously reducing the activation barrier for cyclization. The efficiency is demonstrated on several challenging indenoannulations, including the quadruple indenoannulation of pyrene with unprecedentedly high yield of 60% (Figure 1, compound **3**).

In the course of our studies on alumina-mediated HF elimination we have reinvestigated the model of single indenoannulation in more details. For this purpose, compound **4** was converted to 8-methylfluoranthrene (**5**) in five gram scale with 85% yield. Worth mentioning that side products were not detected in toluene extract of the reactionary mixture, which makes the reaction very attractive for preparative synthesis, since virtually no additional purification procedures are needed. However, in this particular case we were aiming to establish the fate of remaining 15% of the precursor. We found that treatment of the alumina after the reaction completion with methanol or other protic solvent allows extracting two additional side products, which appeared to be phenol **6** and ether **7** (Scheme 1a). According to our recent investigations of the reaction's mechanism,[32] the reaction should be considered as Friedel-Crafts-like arylation[33–35], where the rate-determining step includes electrophilic attack on neighboring aromatic system by fluorinated carbon bearing partial cationic character obtained after C-F bond polarization (Scheme 1). Moreover, we have previously observed that alumina provokes hydrolysis of C-F bond in trifluoromethylated arenes,[36] having in hand these data we have suggested a reasonable picture describing the events occurring to fluoroarenes on alumina. As a result of C-F bond polarization, electrophilic carbon can be attacked by the alumina oxygen leading to covalent bonding of substrate to alumina phase. This explains the fact that no side products can be extracted from the reactionary mixture using aprotic solvents such as toluene. On the other hand the O-Al bond can be easily hydrolyzed by weak acids or even protic solvents such as methanol yielding phenol **6**. The formation of ether **7** must take place no sooner than methanol treatment since **7** is not observed in the toluene extract. From these data it is reasonable to conclude that if the attack of aromatic system is hindered by either electronic or steric factors the competing hydrolysis process occurs, leading to the drop of the desired product's yield. On the other hand, the selectivity can be enhanced by providing electron rich π-system or more suitable geometry for the electrophilic attack. This explains the exceptionally effective cove region closure where the molecule has rigid and appropriately predefined geometry for the Aryl-Aryl coupling.

10.1002/chem.201902586

COMMUNICATION

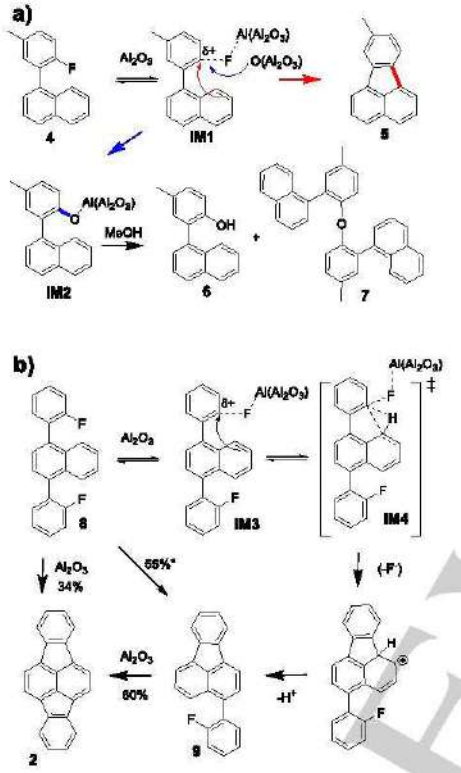

Scheme 1. a) Mechanistic consideration C-F bond polarization on activated alumina. Competition between C-F bond hydrolysis (blue arrow) and indenoannulation (red arrow). b) Effect of the electron-withdrawing group and the size of π-system on the efficiency of indenoannulation illustrated on the example of **2** obtained from **8** and **9**. *The yield of 55% corresponds to the estimated yield, provided that the yields of the transformations of **8** and **9** to **2** are known.

Therefore, the reasons for the relatively low conversion of 1,4-bis(2-fluorophenyl)naphthalene **8** to indeno[1,2,3-cd]fluoranthene **2** were reconsidered. Initially, it was assumed that the introduction of the second five-membered ring causes severe geometrical complications, and thus leads to moderate yields. However, since the reaction is believed to occur via cation-like mechanism the presence of fluorophenyl as an electron withdrawing substituent may impede the first attack of the aromatic system i.e. first indenoannulation (Scheme 1). This can be easily understood considering the stabilization/destabilization effects in the intermediate σ-complex (**IM4**), whose stability is expected to correlate with the activation energy in accordance with Hammond postulate and Bell-Evans-Polyany principle. Thus, it remained unclear whether the reason for the low yields of **2** was caused by the first or the second cyclization step. In order to resolve the issue we have prepared 3-(2-fluorophenyl)fluoranthene (**9**), which enabled the synthesis of **2** in 60% yield indicating that the efficiency of the first cyclization drops from 85% in case of **4** to 55% in case of **8** due to deactivation of the naphthalene core by fluorophenyl substituent (Scheme 1b). Thus, we can unambiguously claim that the drop of the yield was mainly connected to electronic effects rather than to strained geometry of the product **2**. These experimental observations reveal that the mechanism of the reaction can be, indeed, rationalized as S_EAr-like process, which is under these conditions is the rate determining step.

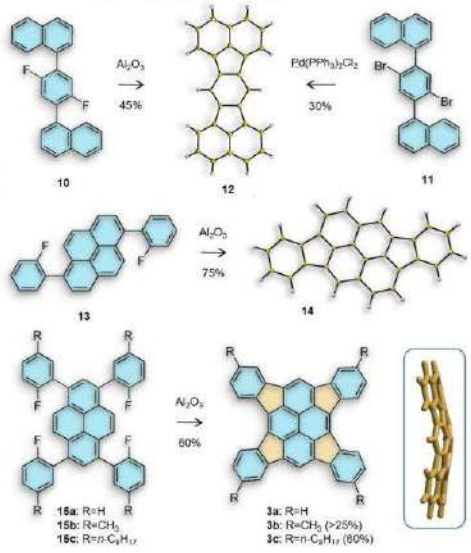

Figure 2. Scope of alumina promoted indenoannulation demonstrating continuously improved efficiency of the cyclization with the increase of π – system size. ORTEP projections of **12** and **14** are shown at 50% probability level. DFT optimized geometry of **3a** reveals its relation to bowl shaped PAHs.

In order to demonstrate the importance of fluorine atoms' negative inductive effect, we investigated the condensation of precursor **10** expecting slightly lower efficiency than observed for **4** (85%), but higher than observed for **8** (34%). Indeed, we managed to convert **10** to **12** with 45% yield, demonstrating the appropriateness of our assumption. Interestingly enough, the C-F activation protocol appears to be more effective for the synthesis of **12** in comparison with the standard Pd-catalyzed procedure (Figure 2). The alumina-mediated reaction shows not only higher yields, but also significantly simpler purification process (only trace amounts of mono- condensation product were detected in the reactionary mixture as a side product).

10.1002/chem.201902586

Moreover, the synthesis of respective fluorinated precursors utilizing Suzuki coupling appears to be much more practical than the synthesis of respective brominated analogues.

Consideration of the S_EAr-like nature of the reaction and extension of our concept further bring us to suggestion that each previous HF elimination increases the size of the π-system, generally increases the capability for S_EAr, and thus eventually may facilitate the following indenoannulations. In overall, reaction including more than one closure may be considered as tandem cyclization. However, fluorine atoms should be located preferably far enough from each other in order to avoid their commutative negative inductive effect. Thus, the combination of possibility to construct complex architectures along with the absence of any considerable amounts of by-products and "auto-activation" of the intramolecular arylation with the increase of the substrate's size makes γ-Al_2O_3 mediated HF elimination very attractive tool for the synthesis of large nonalternant PAHs and NGs. Fully in accordance with our suggestion we have obtained diindeno[1,2,3-cd:1',2',3'-jk]pyrene (**14**) in 75% yield, which significantly exceeds the yield of **2** obtained via double indenoannulation. These observations go in line with the mechanistic considerations mentioned above, since pyrene core is more active for the S_EAr than naphthalene and the inductive effect of the F atoms can be neglected due to their remoteness.

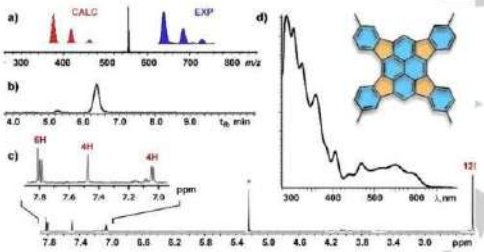

Figure 3. Characterization of **3b**. a) LDI-MS positive mode, with theoretical and observed isotopic distributions. b) HPLC of o-DCB extract obtained after the reaction without additional purification c) ^1H NMR in CD_2Cl_2. d) UV-Vis spectrum (Toluene-Methanol=9:1).

As one of the most illustrative and simplest models showing the further applicability of our approach we have chosen to test 1,3,6,8-tetrakis(2-fluorophenyl)pyrene (**15a**), which under HF elimination conditions gave tetraindenopyrene (**3a**) possessing bowl-shape like structure. The derivative of this compound was synthesized by Scott with the yield less than 1% enabling us to compare the known UV-Vis spectrum of the compound. Unfortunately, the solubility of the product was too low even in boiling 1,2-dichlorobenzene to extract it completely from alumina after the reaction completion, thus making it impossible neither to estimate the yield nor to measure the NMR spectra. Nevertheless, HPLC allows claiming the nearly full conversion after three days at 190 °C and UV-Vis spectrum accompanied by LDI-MS unambiguously supports the formation of the desired product (Figure 3). In order to increase solubility, we have introduced four methyl groups on periphery of the tetraindenopyrene core. As in the previous example according to HPLC, satisfactory conversion occurred after three days at 190 °C and following extraction with 1,2-dichlorobenzene allowed to estimate the yield to be at least 25%. The structure was confirmed by means of UV-Vis, LDI-MS and ^1H NMR. Even though the solubility was slightly improved in comparison to the non-substituted analogue, it was still not enough to estimate the yield properly and to measure ^{13}C NMR. In order to fulfill the yield estimation and to obtain a readily soluble derivative we introduced four n-octyl chains responsible for sufficient solubility to estimate yield as 60% and fully characterize the product.

The current work confirms our suggestions on the nature of the alumina-mediated HF elimination mechanism and extends our knowledge on the scope of the applicability. We compare Pd-catalyzed reaction with alumina-mediated to show the advantages of the latter. Among them are the simpler preparation of the precursors, absence of the meticulous purification and remarkably higher yields. We demonstrate that the efficiency of intramolecular aryl-aryl coupling via C-F activation on alumina strongly depends on size of π-system and in case of multiple-indenoannulation can be considered as self-promoted reaction yielding PAHs with pentagons in its structure. At first, the eventual result appears as a rather counter-intuitive conclusion since our approach turns out to work better with the increase of the size system, which is typically vice versa in case of other conventional methods. However, the mechanistic considerations give rather reasonable account for the observed phenomena. Considering this feature, the alumina mediated HF elimination becomes an extremely attractive tool enabling synthesis of large non-alternant PAHs and NGs.

Acknowledgements

Authors are thankful to Dr. Harald Maid for NMR measurements and spectra interpretations.

Funded by the Deutsche Forschungsgemeinschaft (DFG) – Projektnummer 182849149 – SFB 953, AM407

Keywords: C-F activation • Buckybowls • Indenoannulation • C-C coupling • Aromatization

[1] C. Koper, M. Sarobe, L. W. Jenneskens, *Phys. Chem. Chem. Phys.* **2004**, *6*, 319–327.

[2] W. B. Fellows, A. M. Rice, D. E. Williams, E. A. Dolgopolova, A. K. Vannucci, P. J. Pellechia, M. D. Smith, J. A. Krause, N. B. Shustova, *Angew. Chemie Int. Ed.* **2016**, *55*, 2195–2199.

[3] C. Gooijer, I. Kozin, N. H. Velthorst, M. Sarobe, L. W. Jenneskens, E. J. Vlietstra, *Spectrochim. Acta Part A Mol. Biomol. Spectrosc.* **1998**, *54*, 1443–1449.

[4] D. Wu, H. Ge, S. H. Liu, J. Yin, *RSC Adv.* **2013**, *3*, 22727.
[5] F. Dötz, J. D. Brand, S. Ito, L. Gherghel, K. Müllen, *J. Am. Chem. Soc.* **2000**, *122*, 7707–7717.
[6] X. Zhang, Z. Xu, W. Si, K. Oniwa, M. Bao, Y. Yamamoto, T. Jin, *Nat. Commun.* **2017**, *8*, 15073.
[7] X. Feng, W. Pisula, K. Müllen, *Pure Appl. Chem.* **2009**, *81*, 2203–2224.
[8] D. Lungerich, O. Papaianina, M. Feofanov, J. Liu, M. Devarajulu, S. I. Troyanov, S. Maier, K. Amsharov, *Nat. Commun.* **2018**, *9*, 4756.
[9] M.A. Petrukhina, L.T. Scott, in *Fragments of Fullerenes and Carbon Nanotubes*, *John Wiley & Sons, Inc.*, New Jersey, **2012**.
[10] K. Amsharov in *From Polyphenylenes to Nanographenes and Graphene Nanoribbons*, (Eds.: K. Müllen, X. Feng), Springer Verlag, Berlin/Heidelberg, **2017**, pp. 127–145.
[11] S. Higashibayashi, H. Sakurai in *Polycyclic Arenes and Heteroarenes*, (Ed.: Q. Miao), Wiley-VCH Verlag GmbH & Co, Weinheim, **2016**, pp.61-80.
[12] J. D. Wood, J. L. Jellison, A. D. Finke, L. Wang, K. N. Plunkett, *J. Am. Chem. Soc.* **2012**, *134*, 15783–15789.
[13] S. R. Bheemireddy, M. P. Hautzinger, T. Li, B. Lee, K. N. Plunkett, *J. Am. Chem. Soc.* **2017**, *139*, 5801–5807.
[14] V. M. Tsefrikas, L. T. Scott, *Chem. Rev.* **2006**, *106*, 4868–4884.
[15] L. T. Scott, *Science (80-.).* **2002**, *295*, 1500–1503.
[16] D. M. Forkey, S. Attar, B. C. Noll, R. Koerner, M. M. Olmstead, A. L. Balch, *J. Am. Chem. Soc.* **1997**, *119*, 5766–5767.
[17] L. T. Scott, M. S. Bratcher, S. Hagen, *J. Am. Chem. Soc.* **1996**, *118*, 8743–8744.
[18] R. B. M. Ansems, L. T. Scott, *J. Am. Chem. Soc.* **2000**, *122*, 2719–2724.
[19] D. Alberico, M. E. Scott, M. Lautens, *Chem. Rev.* **2007**, *107*, 174–238.
[20] A. M. Echavarren, B. Gómez-Lor, J. J. González, O. de Frutos, *Synlett* 2003, 0585–0597.
[21] B. D. Steinberg, E. A. Jackson, A. S. Filatov, A. Wakamiya, M. A. Petrukhina, L. T. Scott, *J. Am. Chem. Soc.* **2009**, *131*, 10537–10545.
[22] S. Pascual, P. de Mendoza, A. M. Echavarren, *Org. Biomol. Chem.* **2007**, *5*, 2727.
[23] H. A. Wegner, L. T. Scott, A. de Meijere, *J. Org. Chem.* **2003**, *68*, 883–887.
[24] S. Duttwyler, C. Douvris, N. L. P. Fackler, F. S. Tham, C. A. Reed, K. K. Baldridge, J. S. Siegel, *Angew. Chemie - Int. Ed.* **2010**, *49*, 7519–7522.
[25] O. Allemann, S. Duttwyler, P. Romanato, K. K. Baldridge, J. S. Siegel, *Science (80-.).* **2011**, *332*, 574–577.
[26] K. Y. Amsharov, P. Merz, *J. Org. Chem.* **2012**, *77*, 5445–5448.
[27] O. Papaianina, V. A. Akhmetov, A. A. Goryunkov, F. Hampel, F. W. Heinemann, K. Y. Amsharov, *Angew. Chemie - Int. Ed.* **2017**, *56*, 4834–4838.
[28] K. Y. Amsharov, M. A. Kabdulov, M. Jansen, *Angew. Chemie - Int. Ed.* **2012**, *51*, 4594–4597.
[29] H. A. Wegner, H. Reisch, K. Rauch, A. Demeter, K. A. Zachariasse, M. de Armin, L. T. Scott, *J. Org. Chem.* **2007**, *72*, 1870.
[30] X. Tian, L. M. Roch, K. K. Baldridge, J. S. Siegel, *European J. Org. Chem.* **2017**, *2017*, 2801–2805.
[31] O. Allemann, S. Duttwyler, P. Romanato, K. K. Baldridge, J. S. Siegel, *Science* **2011**, *332*, 574–577.
[32] D. Sharapa, A.-K. Steiner, K. Amsharov, *Phys. Status Solidi* **2018**, *1800189*, 1800189.
[33] R. Sunke, S. B. Nallapati, J. S. Kumar, K. Shiva Kumar, M. Pal, *Org. Biomol. Chem.* **2017**, *15*, 4042–4057.
[34] J. Zhou, W. Yang, B. Wang, H. Ren, *Angew. Chemie - Int. Ed.* **2012**, *51*, 12293–12297.
[35] M. Grzybowski, K. Skonieczny, H. Butenschön, D. T. Gryko, *Angew. Chemie - Int. Ed.* **2013**, *52*, 9900–9930.
[36] O. Papaianina, K. Y. Amsharov, *Chem. Commun.* **2016**, *52*, 1505–1508.

WILEY-VCH

COMMUNICATION

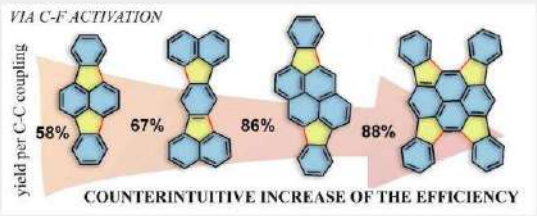

*Vladimir Akhmetov, Mikhail Feofanov, Olena Papaianina, Sergey Troyanov and Konstantin Amsharov**

Page No. – Page No.

Towards Nonalternant Nanographenes by Self-Promoted Intramolecular Indenoannulation Cascade via C-F bond activation

Towards Nonalternant Nanographenes by Self-Promoted Intramolecular Indenoannulation Cascade via C-F bond Activation

Vladimir Akhmetov, Mikhail Feofanov, Olena Papaianina, Sergey Troyanov and Konstantin Amsharov

Supporting Information

Table of contents

General Information

All chemicals and solvents were purchased in reagent grade from commercial suppliers (Acros®, SigmaAldrich® or Fluka®, Fluorochem®, Merck®, ChemPur®) and used as received unless otherwise specified. Microwave assisted experiments were carried out using Discover SP Microwave Synthesizer, CEM. Solvents in HPLC grade were purchased from VWR® and SigmaAldrich®.Flash column chromatography was performed on Interchim PuriFlash 430 using flash grade silica gel from MacheryNagel 60 M (40-63 mm, deactivated). NMR spectra were recorded on a Bruker Avance Neo 300 operating at 300 MHz (^{1}H NMR), 75 MHz (^{13}C NMR) and 282 (^{19}F NMR), on a Bruker Avance Neo 400 operating at 400 MHz (^{1}H NMR), 100 MHz (^{13}C NMR) and 377 (^{19}F NMR), on a Bruker Avance Neo 500, operating at 500 MHz (^{1}H NMR), 125 MHz (^{13}C NMR) and 470 MHz (^{19}F NMR) and on a Bruker Avance Neo 600, operating at 600 MHz (^{1}H NMR), 150 MHz (^{13}C NMR) and 564(^{19}F NMR) at room temperature. The signals were referenced to residual solvent peaks (in parts per million (ppm) ^{1}H: $CDCl_3$, 7.27 ppm, CD_2Cl_2, 5.32 ppm, $(CD_3)_2CO$, 2.05 ppm, ^{13}C: $CDCl_3$, 77.0 ppm, CD_2Cl_2, 53.84 ppm). Coupling constants were assigned as observed. The obtained spectra were evaluated with the program MestReNova. High resolution APPI MS spectra were recorded on a Bruker ESI TOF maXis4G instrument. The data was evaluated with the program Bruker Compass DataAnalysis 4.2. HPLC measurements were performed on a Shimadzu Prominence Liquid Chromatograph LC-20AT with communication bus module CBM-20A, diode array detector SPDM20A, the degassing unit DGU-20A5 R, column oven CTO-20AC or CTO-20A, respectively and with auto sampler SIL-20A HT. For separation a Cosmosil 5-PYE column (4.6 mm x 250mm) from Nacalai Tesque was used. As eluent a DCM/MeOH or toluene/MeOH mixture was used (UV-vis detection). The data was evaluated with the programs Shimadzu LCsolution and Shimadzu LabSolutions. TLC analyses were carried out with TLC sheets coated with silica gel with fluorescent indicator254 nm from Machery-Nagel (ALUGRAM® SIL G/UV254) and visualized via UV-light of 254nm or 366 nm.

Experimental Procedures

General Procedure A.

A glass tube was charged with 2-5 g of γ-Al_2O_3 (neutral, 50-200 micron) and preactivated at 450 ℃ for 3-4 hours. Then it was connected to a Schlenk line and heated at 590 ℃ under vacuum (10^{-3} mbar) for another 2 hours. The vessel was cooled down to r.t. and 1-10 mmol of fluoroarene was added under argon atmosphere. The tube containing the obtained mixture was sealed under vacuum and heated at 180-220°C for 2-96 h. After cooling to room temperature, products were extracted with toluene. Separation and final purification of the products were carried out by flash chromatography or HPLC of the respective toluene/*o*-DCB extract.

General Procedure B.

The corresponding bromo- or iodoarene (5-20 mmol, 1eq) and boronic acid (1eq, unless specified otherwise) were dissolved in 50-100 ml of toluene:methanol (2:1) mixture containing potassium carbonate (6eq) and 2.5% mol of tetrakis(triphenylphosphine)palladium(0) as catalyst. The reaction mixture was stirred under reflux and argon atmosphere for 15 hours. Then the reaction mixture was extracted with dichloromethane and washed with water, organic layer was dried over Na_2SO_4, filtrated through a short silica plague. Solvent evaporation under reduced pressure was followed by flash chromatography purification of product (Hexane:Dichloromethane=10:1).

(9) 3-(2-fluorophenyl)fluoranthene

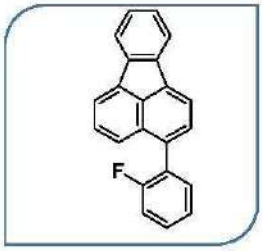

The compound was obtained according to the General Procedure B using 3-bromofluoranthene (200 mg) and 2-fluorophenylboronic acid (100 mg). Yield 160 mg (76%).

^{1}H NMR (400 MHz, CD_2Cl_2) δ 8.02 (d, J = 7.1 Hz, 1H), 8.00 – 7.93 (m, 3H), 7.76 – 7.70 (m, 1H), 7.67 – 7.61 (m, 2H), 7.55 – 7.46 (m, 2H), 7.46 – 7.40 (m, 2H), 7.37 – 7.27 (m, 2H). ^{19}F NMR (377 MHz, CD_2Cl_2) δ -115.00 (s). ^{13}C NMR (101 MHz, CD_2Cl_2) δ 160.40 (d, J = 246.2 Hz), 140.00 (s), 139.45 (s), 137.44 (d, J = 6.0 Hz), 134.22 (s), 133.09 (d, J = 3.2 Hz), 132.83 (s), 130.14 (s), 130.06 (s), 129.21 (s), 128.66 (s), 128.16 (s), 128.11 (s), 127.43 (d, J = 15.9 Hz), 125.87 (s), 124.63 (d, J = 3.6 Hz), 122.00 (s), 121.98 (s), 120.62 (s), 120.27 (s), 116.29 (s), 116.07 (s). APPI HRMS calculated for $C_{22}H_{13}F$ [M+] m/z 296.1001, found 296,1005.

(2) Indeno[1,2,3-cd]fluoranthene

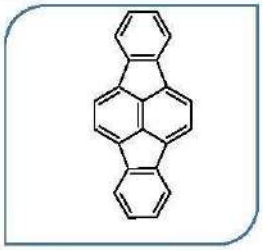

The compound was obtained according to the General Procedure A using either compound (9) (15 mg) or compound (8) (600mg). Yield 60% (8 mg) and 34% (180 mg) respectively. ^{1}H NMR (400 MHz, CD_2Cl_2) δ 7.61 (dd, J = 5.5, 3.1 Hz, 1H), 7.58 (s, 1H), 7.19 (dd, J = 5.5, 3.1 Hz, 1H). ^{13}C NMR (101 MHz, CD_2Cl_2) δ 142.4, 138.0, 133.1, 128.6, 123.2, 122.4. The NMR spectral data were consistent with that reported.[1]

(8) 1,4-bis(2-fluorophenyl)naphthalene

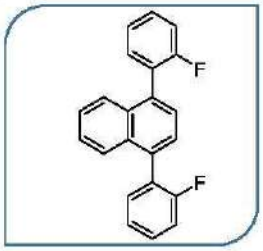

The compound was obtained according to the General Procedure B. using 1,4-dibromonaphtalene (880 mg) and 2-fluorophenylboronic acid (1g). Yield 950 mg (90%).

^{1}H NMR (400 MHz, Acetone-d_6) δ 7.55 (dt, J = 6.0, 2.5 Hz, 2H), 7.37 (m, 8H), 7.27 – 7.14 (m, 2H). ^{19}F NMR (377 MHz, Acetone-d_6) δ -114.95 (d, J = 84.3 Hz). ^{19}F NMR (377 MHz, Acetone-d_6) δ -114.84 (s, 1F), -115.06 (s, 1F). ^{13}C NMR (101 MHz, Acetone-d_6) δ 160.98 (d, J = 245.2 Hz), 135.25, 133.25, 132.83, 130.91 (d, J = 8.1 Hz), 128.64 (d, J = 16.3 Hz), 128.00, 127.20, 126.89, 125.42 (d, J = 3.6 Hz), 116.49 (d, J = 22.2 Hz). The NMR spectral data were consistent with that reported.[2]

(4) 1-(2-fluoro-5-methylphenyl)naphthalene

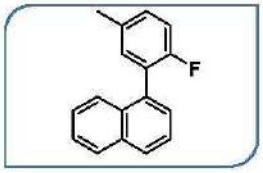

The compound was obtained according to the General Procedure B using compound 1-bromonaphtalene (10g) and (2-fluoro-4-methylphenyl)boronic acid (7.5g). Yield 10 g (87%).

^{1}H NMR (400 MHz, CD_2Cl_2) δ 7.92 (t, *J* = 6.8 Hz, 2H), 7.66 (d, *J* = 6.4 Hz, 1H), 7.60 – 7.48 (m, 2H), 7.45 (t, *J* = 7.4 Hz, 2H), 7.30 (t, *J* = 7.6 Hz, 1H), 7.12 (d, *J* = 7.7 Hz, 1H), 7.07 (d, *J* = 10.7 Hz, 3H), 2.47 (s, 2H). ^{19}F NMR (377 MHz, CD_2Cl_2) δ -115.87 (s, 1F). ^{13}C NMR (101 MHz, CD_2Cl_2) δ 160.31 (d, *J* = 245.2 Hz), 140.71 (d, *J* = 7.9 Hz), 134.46, 134.01, 132.37 (d, *J* = 4.1 Hz), 128.60 (d, *J* = 5.9 Hz), 128.11, 126.55, 126.24 (d, *J* = 6.8 Hz), 125.73, 116.46 (d, *J* = 22.1 Hz), 21.32. APPI HRMS calculated for $C_{17}H_{13}F$ [M+] *m/z* 236.1001, found 236,1005.

(5) 8-methylfluoranthene

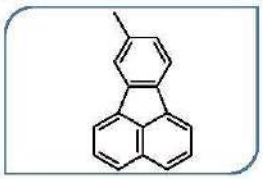

The compound was obtained according to the General Procedure B using compound (4) (5g). Yield 3.8 g (85%). The NMR spectral data were consistent with that reported[3].

(6) 4-methyl-2-(naphthalen-1-yl)phenol

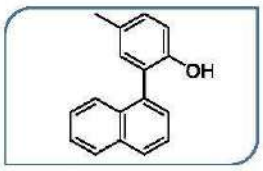

The compound was obtained according to the General Procedure A from (4) (5g) after additional methanol treatment and following flash chromatography. Yield 150 mg (3%) ^{1}H NMR (400 MHz, CD_2Cl_2) δ 7.95 (dd, *J* = 7.2, 6.2 Hz, 2H), 7.67 (d, *J* = 8.4 Hz, 1H), 7.63 – 7.51 (m, 2H), 7.51 – 7.44 (m, 2H), 7.19 (dd, *J* = 8.2, 2.1 Hz, 1H), 7.10 (d, *J* = 2.0 Hz, 1H), 6.95 (d, *J* = 8.2 Hz, 1H), 4.74 (s, 1H), 2.36 (s, 3H). ^{13}C NMR (101 MHz, CD_2Cl_2) δ 151.4, 135.0, 134.4, 132.3, 132.1, 130.4, 130.2, 129.0, 128.8, 128.5, 127.0, 126.7, 126.6, 126.2, 126.1, 115.7, 20.63. The NMR spectral data were consistent with that reported[4].

(7) 1,1'-(oxybis(4-methyl-2,1-phenylene))dinaphthalene

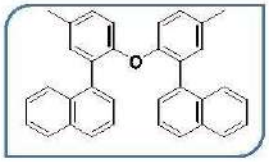

The compound was obtained according to the General Procedure A from (4) (5g) after additional methanol treatment and following flash chromatography. Yield 280 mg (6%) ^{1}H NMR (400 MHz, CD_2Cl_2) δ 7.97 (m, 4H), 7.93 – 7.88 (m, 4H), 7.65 – 7.59 (m, 2H), 7.58 – 7.51 (m, 4H), 7.19 (d, *J* = 2.1 Hz, 2H), 7.10 (dd, *J* = 8.1, 1.9 Hz, 2H), 6.90 (d, *J* = 8.2 Hz, 2H), 2.35 (s, 6H).^{13}C NMR (101 MHz, CD_2Cl_2) δ 150.3, 135.4, 134.0, 133.0, 131.38, 130.6, 130.0, 129.1, 128.4, 128.2, 128.1, 128.1, 127.7, 126.9, 126.7, 116.1, 27.34. APPI HRMS calculated for $C_{34}H_{26}O$ [M+] *m/z* 450.1984, found 450,1990.

(11) 1,1'-(2,5-dibromo-1,4-phenylene)dinaphthalene

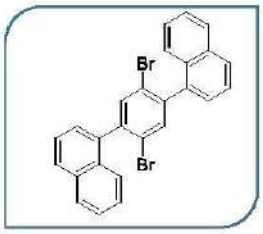

The compound was obtained according to the literature procedure[5].

(10) 1,1'-(2,5-difluoro-1,4-phenylene)dinaphthalene

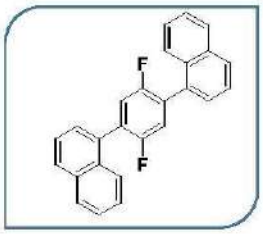

The compound was obtained according to the General Procedure B using 1,4-dibromo-2,5-difluorobenzene (880 mg) naphthalene-1-boronic acid (1.12 g). Yield 1.1g (84%).

^{1}H NMR (300 MHz, CD_2Cl_2) δ 7.35 – 7.27 (m, 4H), 7.17 (brs, 2H), 6.93 (m, 8H), 6.65 (t, *J* = 7.7 Hz, 2H). ^{19}F NMR (282 MHz, CD_2Cl_2) δ -119.67 (t, *J* = 7.1 Hz).^{13}C NMR (75 MHz, CD_2Cl_2) δ 156.38 (d, *J* = 244.5 Hz), 156.34 (d, 245.0 Hz), 134.13, 133.11, 132.02, 129.35, 128.84, 128.28, 126.99, 126.59, 125.99, 125.80, 119.46 (d, *J* = 12.2 Hz), 119.23 (d, *J* = 12.2 Hz). APPI HRMS calculated for $C_{26}H_{16}F_2$ [M+] *m/z* 366.1220, found 366.1215.

(12) acenaphtho[1,2-k]fluoranthene

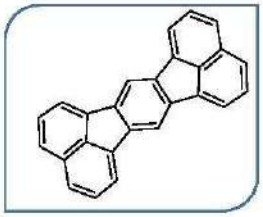

The compound was obtained according to the General Procedure A using compound (10) (100 mg). Yield 40 mg (45%).

^{1}H NMR (300 MHz, CD_2Cl_2) δ 8.50 (s, 1H), 8.09 (d, *J* = 6.9 Hz, 2H), 7.90 (d, *J* = 8.1 Hz, 2H), 7.71 (dd, *J* = 8.2, 6.9 Hz, 2H). ^{13}C NMR (151 MHz, CD_2Cl_2) δ 139.6, 137.3, 133.3, 130.4, 128.6, 127.1, 120.6, 115.4. UV/Vis (Toluene-MeOH, 1-1, 293 K): λ [nm]) = 315, 391, 415. APPI HRMS calculated for $C_{36}H_{14}$ [M+] *m/z* 326.1096, found 326.1098.

(13) 1,6-bis(2-fluorophenyl)pyrene

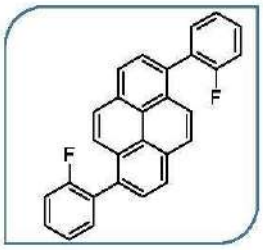

The compound was obtained according to the General Procedure B using 1,6-dibromopyrene (1g) and -2-fluorophenylboronic acid (400 mg). Yield 820 mg (80%).

^{1}H NMR (400 MHz, DMSO-d*6*) 8.40 (d, *J*=7.89 Hz, 2H), 8.25 (d, *J*=9.29 Hz, 2H), 8.06 (d, *J*=7.81 Hz, 2H), 7.87 (dd, *J*=2.42, 9.19 Hz, 2H), 7.66-7.58 (m, 4H), 7.52-7.43 (m, 4H). ^{19}F NMR (377 MHz, DMSO-d*6*) -114.4--114.6 (m, 4F).^{13}C NMR (101 MHz, DMSO-d*6*) 159.47 (d, *J*=244.56 Hz), 132.72, 131.06, 130.34, 130.31 (d, *J*=6.57 Hz), 128.59, 128.41, 127.96 , 127.50 (d, *J*=16.05 Hz), 125.08 , 124.92, 124.88 (d, *J*=3.48 Hz), 123.88 , 115.86 (d, *J*=22.12 Hz). APPI HRMS calculated for $C_{28}H_{16}F_2$ [M+] *m/z* 390.1220, found 390.1224.

(14) Diindeno[1,2,3-cd:1',2',3'-jk]pyrene

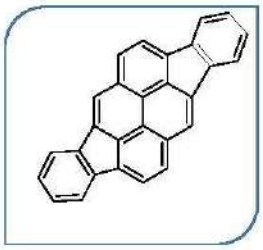

The compound was obtained according to the General Procedure A. using compound (13) (50 mg). Yield 33 mg (75%). The spectral data were consistent with previously reported[6].

(15a) 1,3,6,8-tetrakis(2-fluorophenyl)pyrene

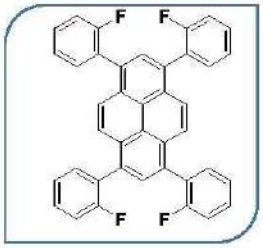

The compound was obtained according to the General Procedure B using 1,3,5,7-tetrabromopyrene (380mg) and (2-fluorophenyl) boronic acid (456 mg). Yield 365 mg (86%).

^{1}H NMR (400 MHz, $CDCL_3$) δ 8.03 – 7.91 (m, 6H), 7.63 – 7.51 (m, 4H), 7.47 – 7.39 (m, 4H), 7.35 – 7.20 (m, 8H). ^{19}F NMR (282 MHz, $CDCl_3$) δ -109.79 – -117.80 (m, 4H). ^{13}C NMR (101 MHz, $CDCL_3$) δ 160.27 (d, *J* = 246.9 Hz), 132.99 (dd, *J* = 6.4, 5.2 Hz), 131.18, 130.33, 129.74, 129.67, 129.17, 128.22, 128.06, 125.71, 116.31 – 115.34 (m). APPI HRMS calculated for $C_{40}H_{22}F_4$ [M+] *m/z* 578.1658, found 578.1660.

(3a) Tetraindeno[1,2,3-cd:1',2',3'-fg:1'',2'',3''-jk:1''',2''',3'''-mn]pyrene

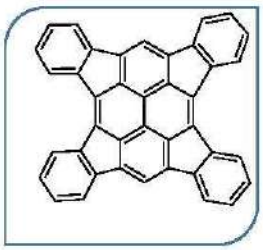

The compound was obtained according to the General Procedure A using compound (15a) (20 mg). Yield was not determined due to low solubility of (3a).

UV/Vis (Toluene-MeOH, 9-1, 293 K): λ [nm]) = 290, 307, 327, 360, 407, 442, 550, 595. APPI HRMS calculated for $C_{40}H_{18}$ [M+] *m/z* 498.1409, found 498.1420

(15b) 1,3,6,8-tetrakis(2-fluoro-5-methylphenyl)pyrene

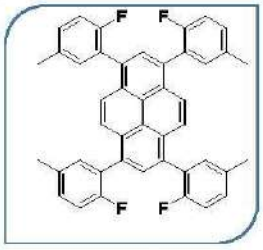

The compound was obtained according to the General Procedure B using 1,3,5,7-tetrabromopyrene (380mg) and (2-fluoro-5-methyphenyl)boronic acid (500 mg). Yield 365 mg (77%).

^{1}H NMR (400 MHz, CD_2Cl_2) δ 8.03 (s, 6H), 7.43 – 7.40 (m, 4H), 7.29 – 7.26 (m, 4H), 7.23 – 7.06 (m, 4H), 2.43 (s, 12H). ^{19}F NMR (377 MHz, CD_2Cl_2) δ -119.59 – -120.36 (m, 4F). ^{13}C NMR (101 MHz, CD_2Cl_2) δ 160.45 – 157.07 (m), 134.72 – 134.22 (m), 133.64 (d, *J* = 3.4 Hz), 132.32, 131.92, 131.55 (d, *J* = 11.8 Hz), 130.76, 130.63, 130.56, 129.48, 128.77, 127.98, 126.07, 125.86, 125.48, 116.47 – 115.10 (m), 20.84 (s). APPI HRMS calculated for $C_{44}H_{30}F_4$ [M+] *m/z* 634.2284, found 634.2286.

(3b)2,7,11,16-tetramethyltetraindeno[1,2,3-cd:1',2',3'-fg:1'',2'',3''-jk:1''',2''',3'''-mn]pyrene

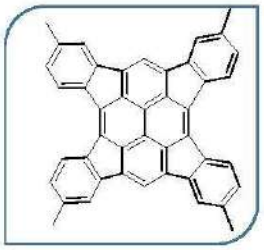

The compound was obtained according to the General Procedure A. using compound (15b) (15 mg). Yield was not determined due to low solubility of (16)

^{1}H NMR (601 MHz, CD_2Cl_2) δ 7.92 (s, 2H), 7.89 (d, *J* = 8.1 Hz, 4H), 7.57 (s, 4H), 7.14 (d, *J* = 8.0 Hz, 4H), 2.47 (s, 12H). APPI HRMS calculated for $C_{44}H_{26}$ [M+] *m/z* 554.2035, found 554.2040.

2-(2-fluoro-5-octylphenyl)-4,4,5,5-tetramethyl-1,3,2-dioxaborolane.

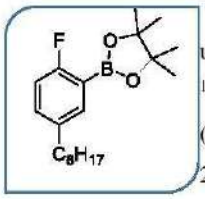

The compound was obtained according to known literature procedure[7] using 1-fluoro-4-octylbenzene (1g). Yield 0.96g (60%).

^{1}H NMR (300 MHz, CD_2Cl_2) δ 7.50 (dd, *J* = 5.8, 2.3 Hz, 1H), 7.31 – 7.20 (m, 1H), 6.99 – 6.86 (m, 1H), 2.58 (dd, *J* = 12.7, 5.3 Hz, 2H), 1.69 – 1.47 (m, 2H), 1.45 – 1.22 (m, 22H), 0.91 (dd, *J* = 13.7, 6.4 Hz, 3H). ^{19}F NMR (282 MHz, CD_2Cl_2) δ -106.46 – -110.26 (m, 1F). ^{13}C NMR (101 MHz, CD_2Cl_2) δ 165.9 (d, *J* = 247.7 Hz), 138.6 (d, *J* = 3.3 Hz), 138.6 (d, *J* = 3.4 Hz), 136.8 (d, *J* = 8.0 Hz), 133.5 (d, *J* = 8.6 Hz), 115.1 (d, *J* = 24.0 Hz), 84.2, 35.3, 35.1, 34.3 (d, *J* = 1.0 Hz), 32.3, 32.14 (d, *J* = 1.0 Hz), 29.9, 29.7, 29.65, 25.1, 23.1, 22.7, 14.3, 14.2. APPI HRMS calculated for $C_{20}H_{32}BFO_2$ [M+] *m/z* 334.2479, found 334.2482.

(15c) 1,3,6,8-tetrakis(2-fluoro-5-octylphenyl)pyrene

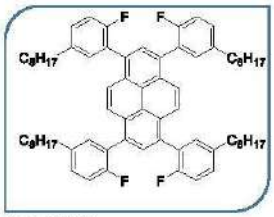

The compound was obtained according to the General Procedure B using 1,3,5,7-tetrabromopyrene (150 mg) and (2-fluoro-5-methyphenyl)boronic acid (490 mg). Yield 280 mg (93%).

^{1}H NMR (300 MHz, CD_2Cl_2) δ 8.01 (m, 4H), 7.50 – 7.10 (m,12H), 2.69 (m, 8H), 1.67 (m, 8H), 1.49 – 1.19 (m, 32H), 0.91 (m, 18H).

^{13}C NMR (75 MHz, CD_2Cl_2) δ 158.96 (d, *J* = 243.7 Hz), 139.53 (d, *J* = 11.9 Hz), 133.06, 132.01 (d, *J* = 3.3 Hz), 130.79, 129.99 (d, *J* = 7.8 Hz), 129.52, 128.01 (d, *J* = 16.4 Hz), 126.07, 125.59 (d, *J* = 6.6 Hz), 125.39 (d, *J* = 4.6 Hz), 116.23 – 115.75 (m), 115.84 – 115.42 (m), 35.63, 35.32, 34.28,

32.32, 32.11, 23.10, 22.81, 14.30, 14.14. APPI HRMS calculated for $C_{72}H_{86}F_4$ [M+] *m/z* 1026.6666, found 1026.6672.

(3c) 2,7,11,16-tetraoctyltetraindeno[1,2,3-cd:1',2',3'-fg:1'',2'',3''-jk:1''',2''',3'''-mn]pyrene

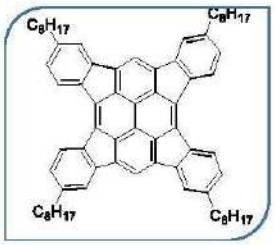

The compound was obtained according to the General Procedure B using compound (15c) (50 mg). Yield 28 mg (60%).

^{1}H NMR (300 MHz, Methylene Chloride-d_2) δ 7.28-7.25 (m, 4H), 7.16 (brs, 4H), 6.92-6.89 (m, 8H), 2.74-2.69 (m, 8H), 1.92 – 1.76 (m, 8H), 1.66 – 1.31 (m, 38H), 1.10 (t, J = 7.3 Hz, 4H), 1.01 – 0.86 (m, 10H).^{13}C NMR (75 MHz, CD_2Cl_2) δ 144.2, 143.7, 139.0, 138.4, 136.8, 133.2, 127.5, 126.4, 122.5, 113.2, 36.8, 36.4, 34.2, 32.5, 32.1, 30.2, 30.1, 29.9, 23.2, 23.1, 14.3. APPI HRMS calculated for $C_{72}H_{82}$ [M+] *m/z* 946.6417, found 946.6420.

References.

[1] L. M. Geary, T. Y. Chen, T. P. Montgomery, M. J. Krische, *J. Am. Chem. Soc.* **2014**, *136*, 5920–5922.
[2] K. Y. Amsharov, P. Merz, *J. Org. Chem.* **2012**, *77*, 5445–5448.
[3] M. Yamaguchi, M. Higuchi, K. Tazawa, K. Manabe, *J. Org. Chem.* **2016**, *81*, 3967–3974.
[4] S. K. Rastogi, D. C. Medellin, A. Kornienko, *Org. Biomol. Chem.* **2014**, *12*, 410–413.
[5] S. Kumar, D.-C. Huang, S. Venkateswarlu, Y.-T. Tao, *J. Org. Chem.* **2018**, *83*, 11614–11622.
[6] H. A. Wegner, H. Reisch, K. Rauch, A. Demeter, K. A. Zachariasse, A. de Meijere, L. T. Scott, *J. Org. Chem.* **2006**, *71*, 9080–9087.
[7] A.-K. Steiner, K. Y. Amsharov, *Angew. Chemie Int. Ed.* **2017**, *56*, 14732–14736.

Spectroscopic Analysis and Characterization

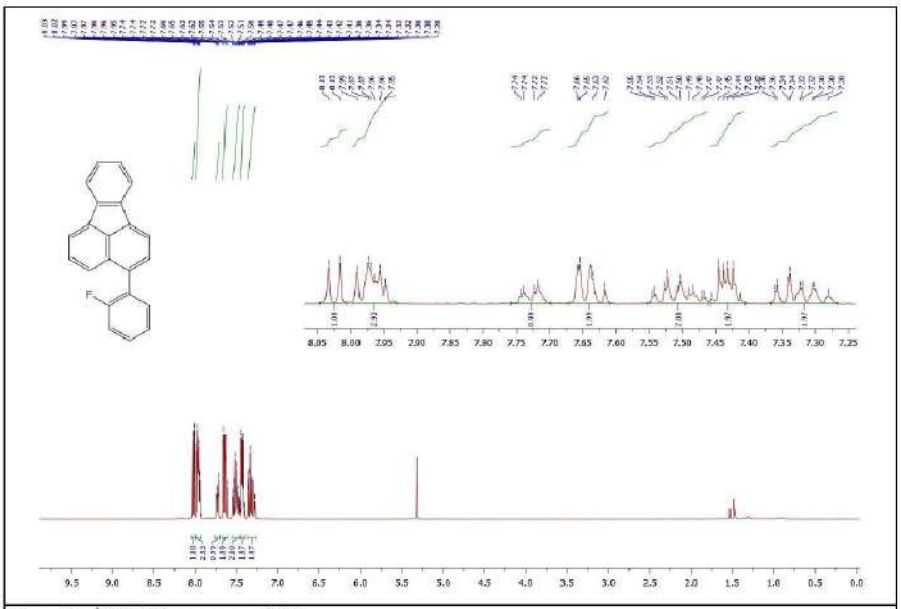

Figure S1. ^{1}H NMR spectrum of (9)

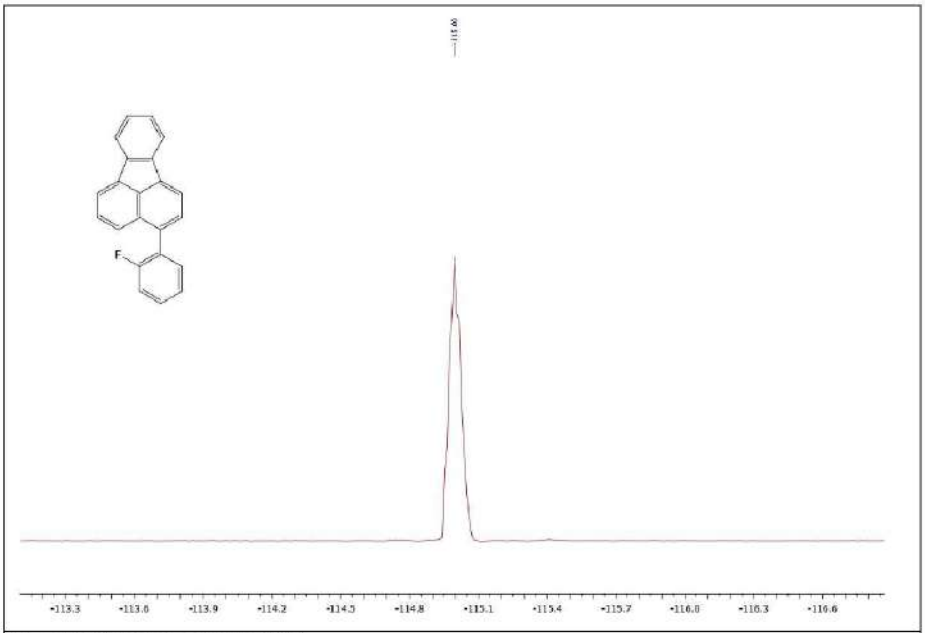

Figure S2. ^{19}F NMR spectrum of (9)

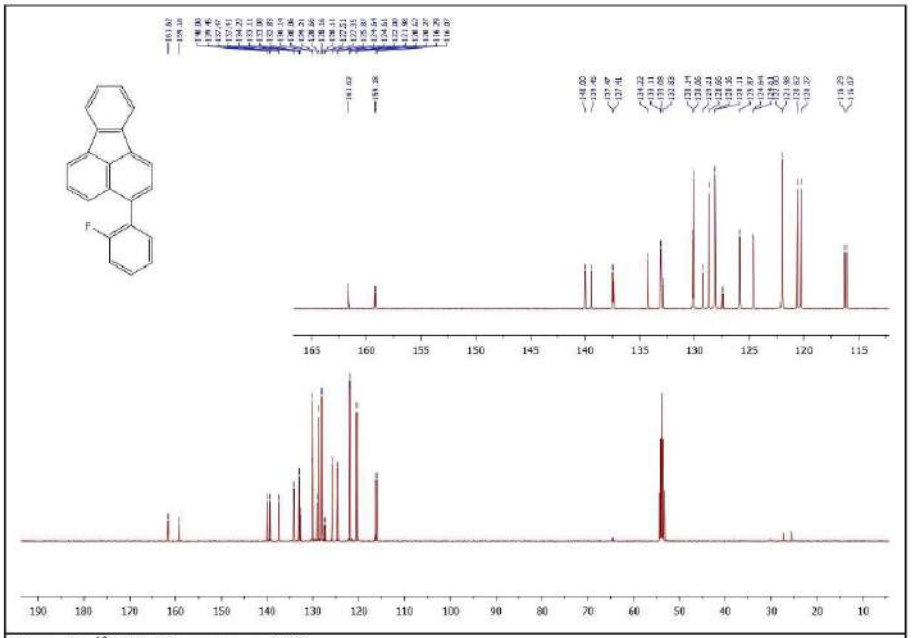

Figure S3. ^{13}C NMR spectrum of (9)

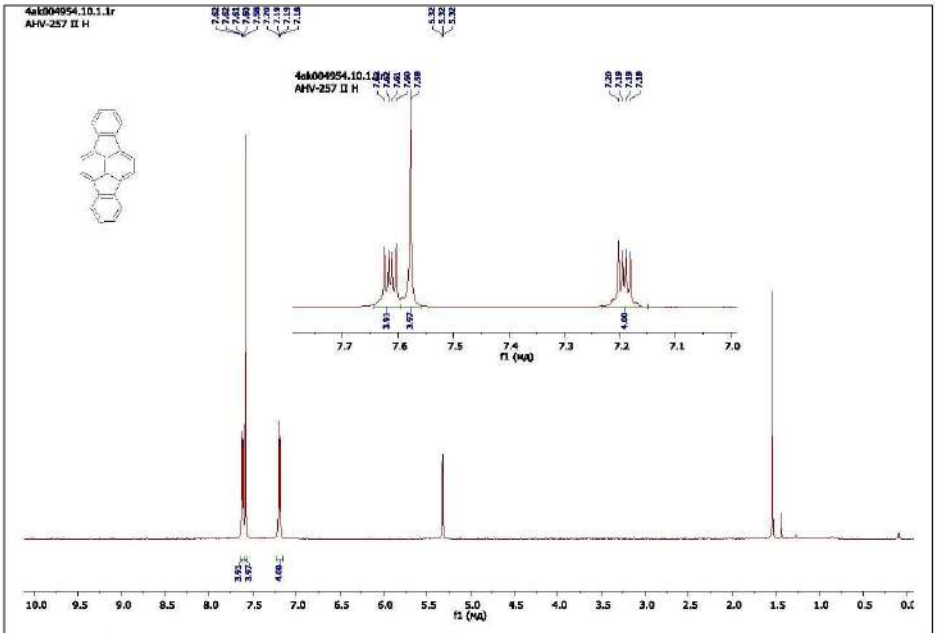

Figure S4. ^{1}H NMR spectrum of (2)

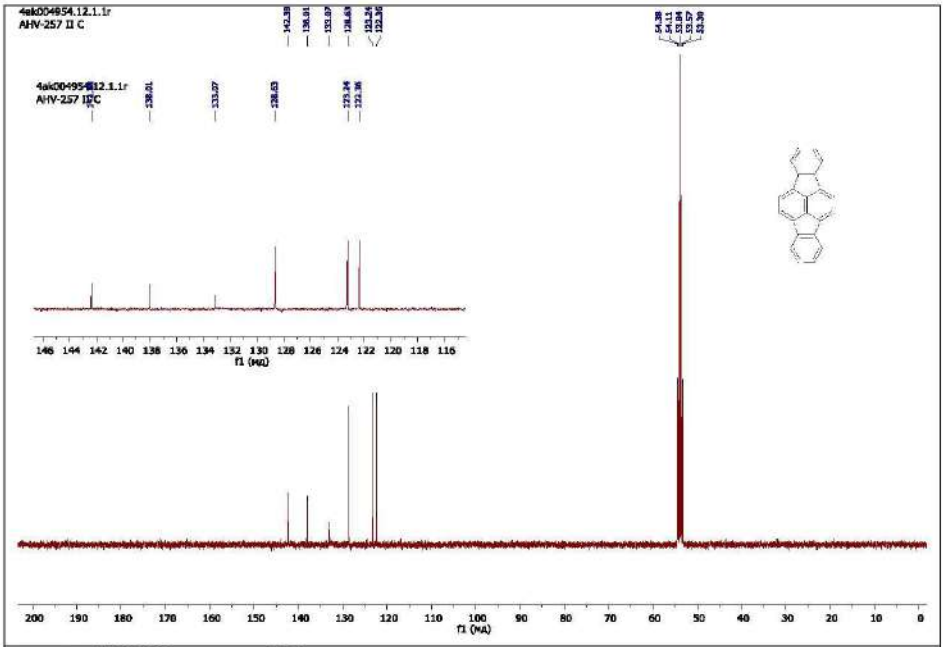

Figure S5. ^{13}C NMR spectrum of (2)

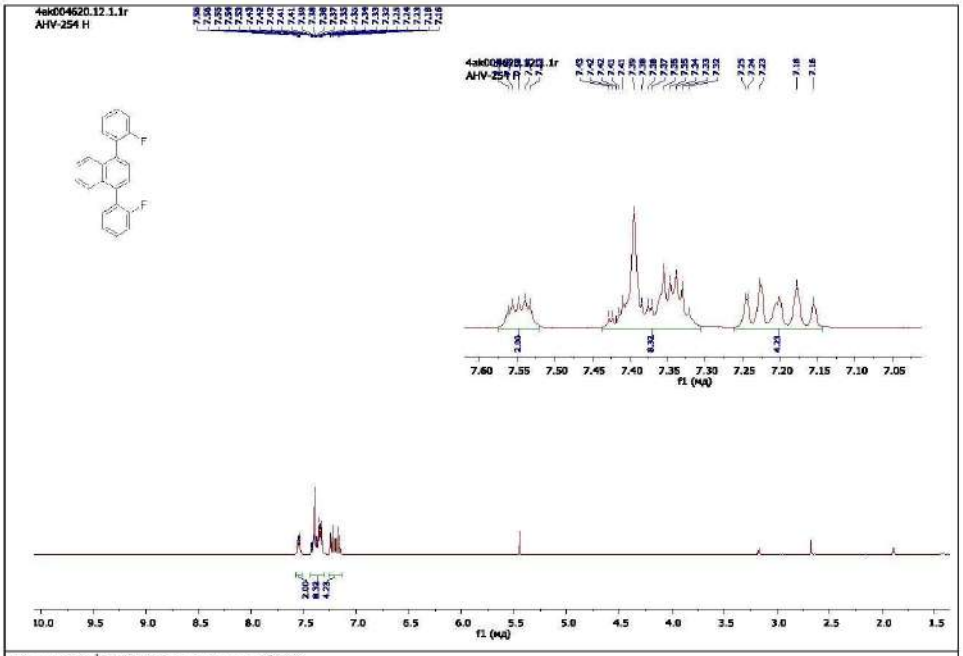

Figure S6. ^{1}H NMR spectrum of (8)

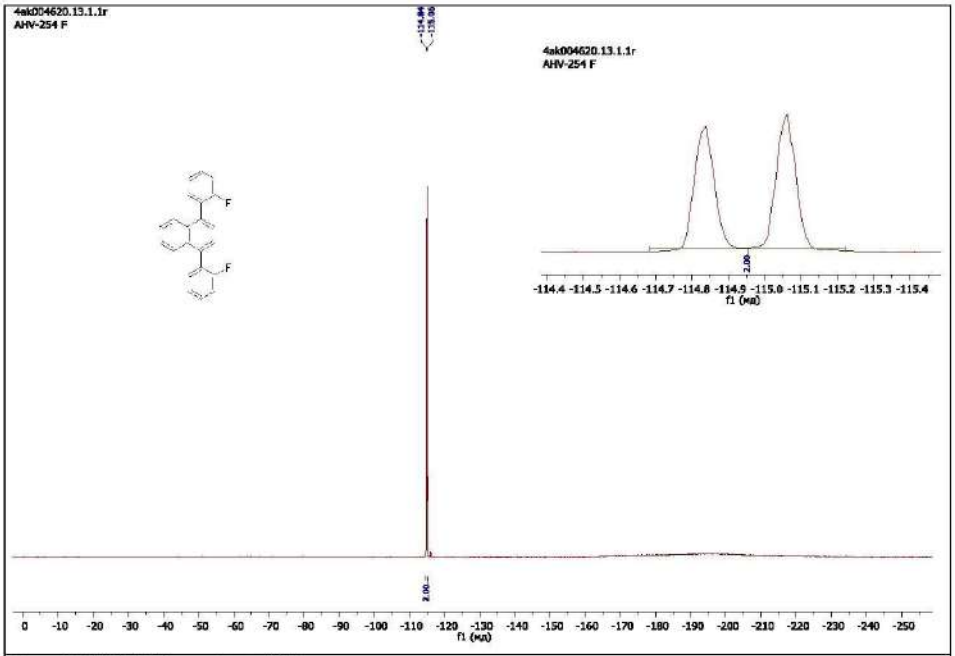

Figure S7. ^{19}F NMR spectrum of (8)

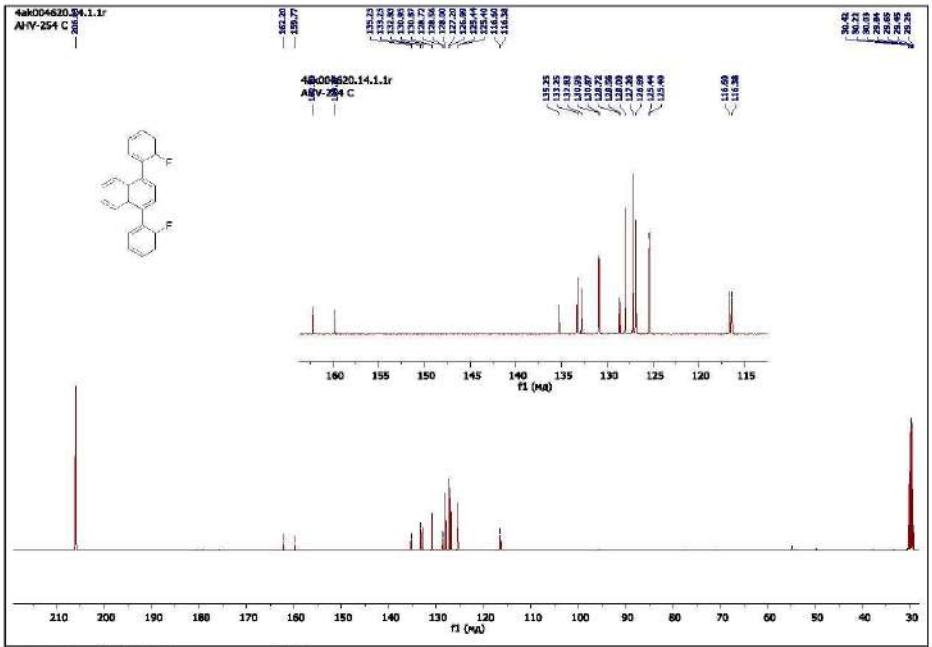

Figure S8. ^{13}C NMR spectrum of (8)

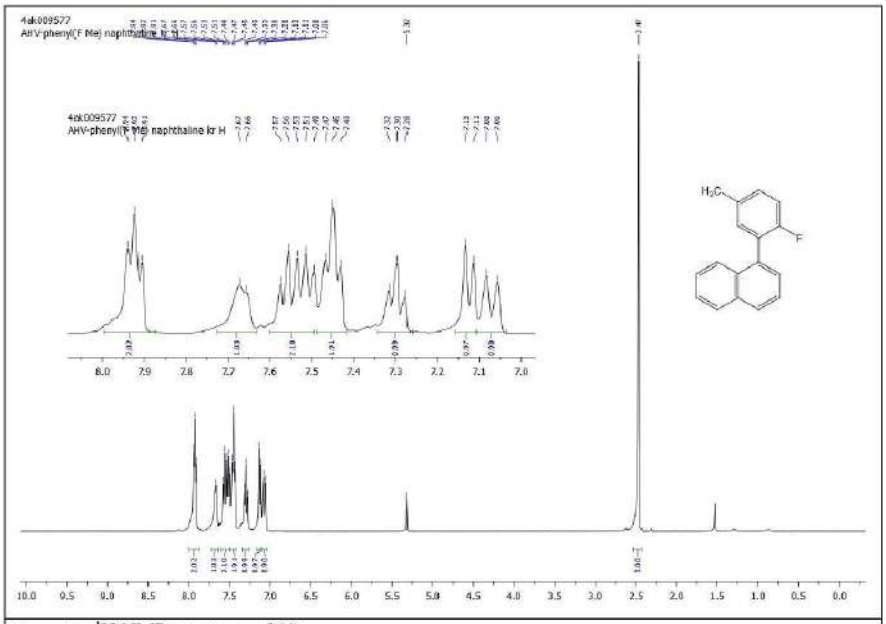

Figure S9. ^{1}H NMR spectrum of (4)

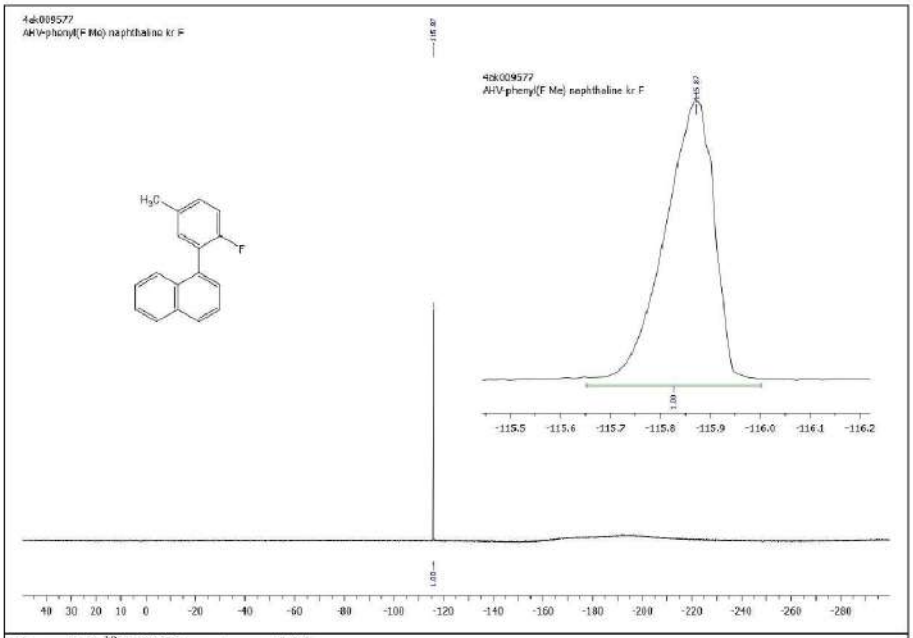

Figure S10. ^{19}F NMR spectrum of (4)

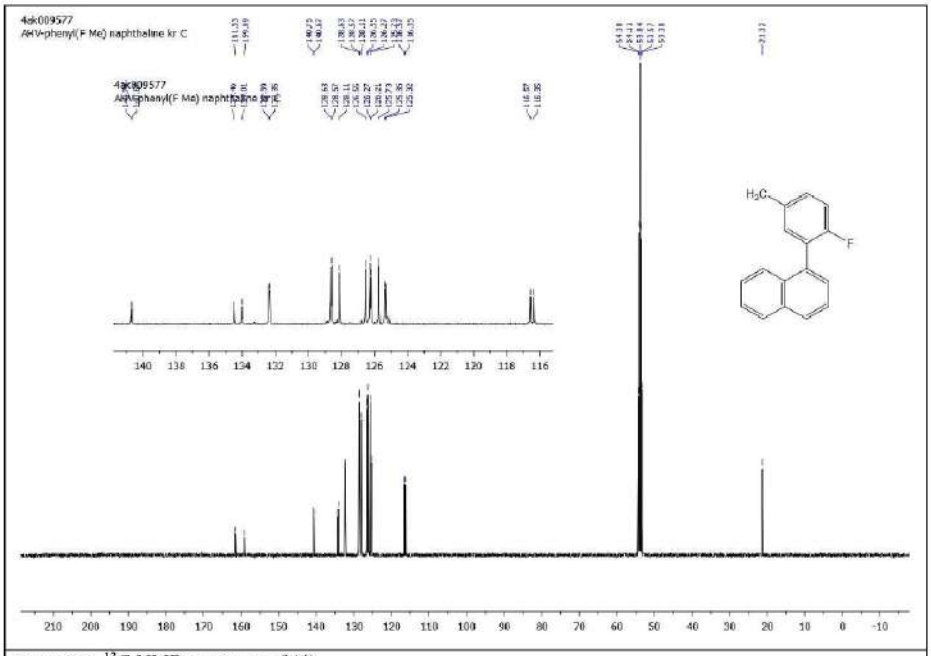

Figure S11. ^{13}C NMR spectrum of (4)

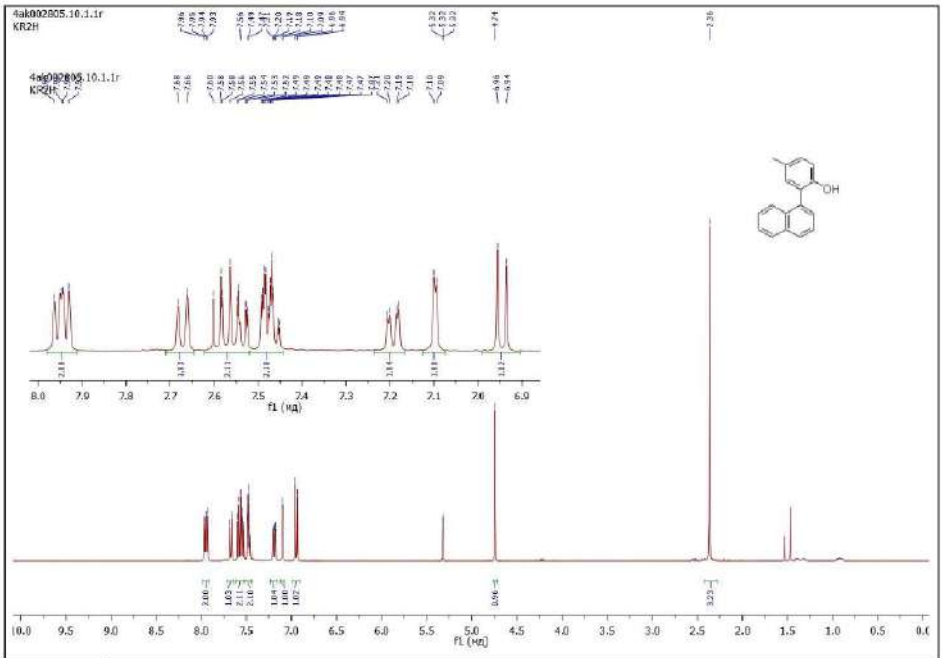

Figure S12. ^{1}H NMR spectrum of (6)

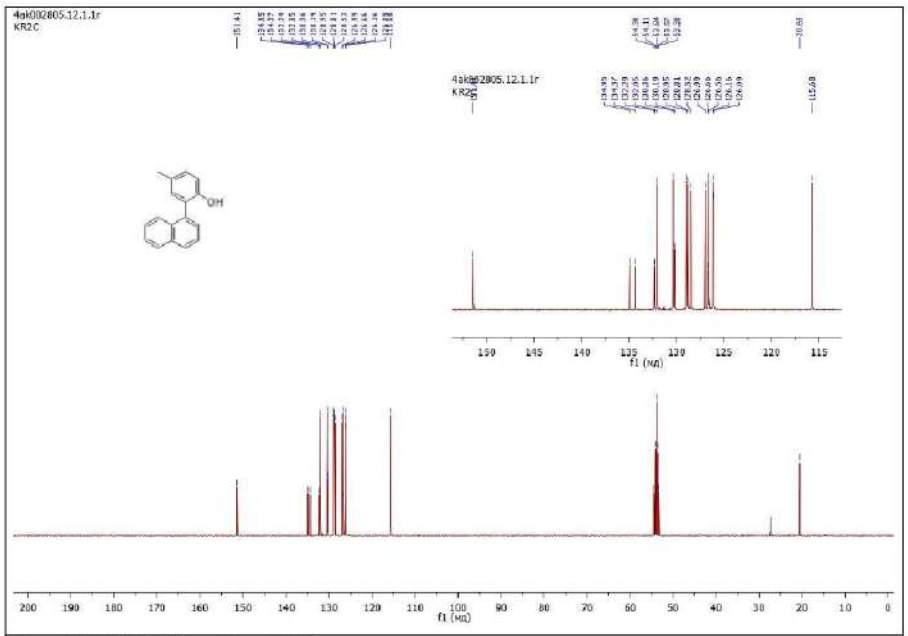

Figure S13. ^{13}C NMR spectrum of (6)

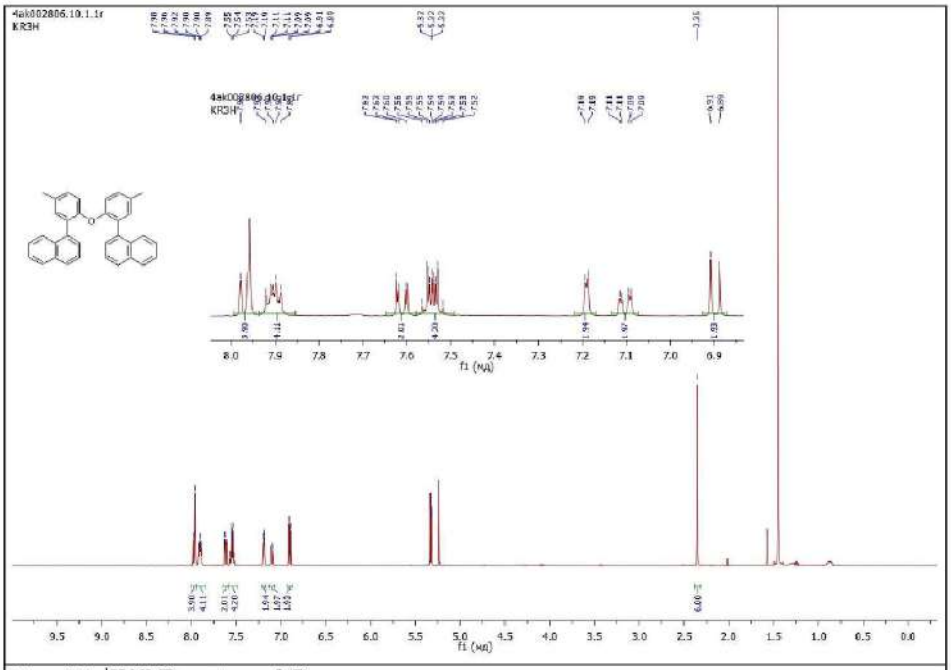

Figure S14. ^{1}H NMR spectrum of (7)

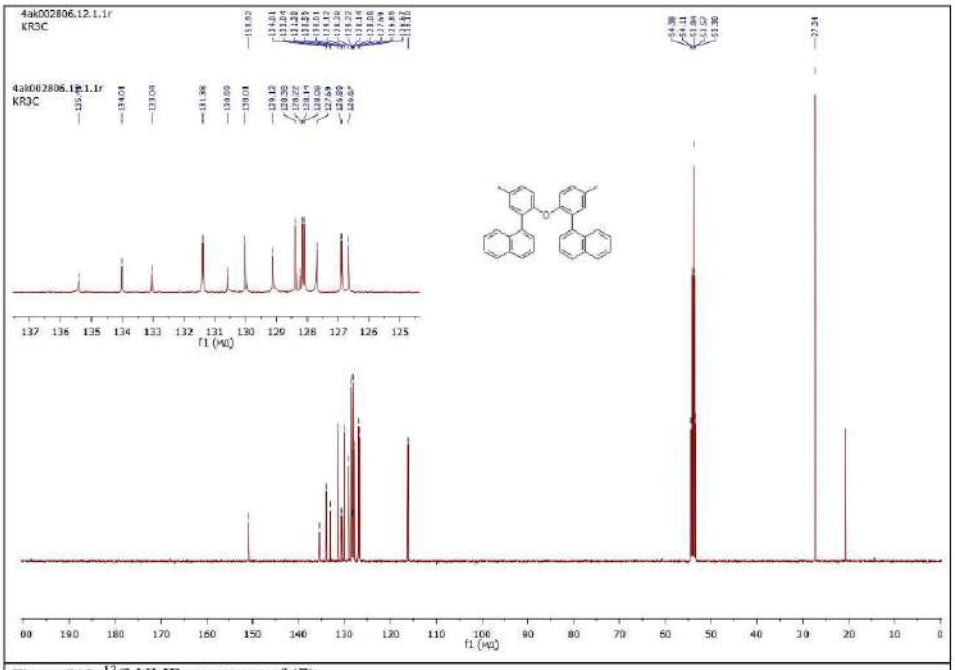

Figure S15. ^{13}C NMR spectrum of (7)

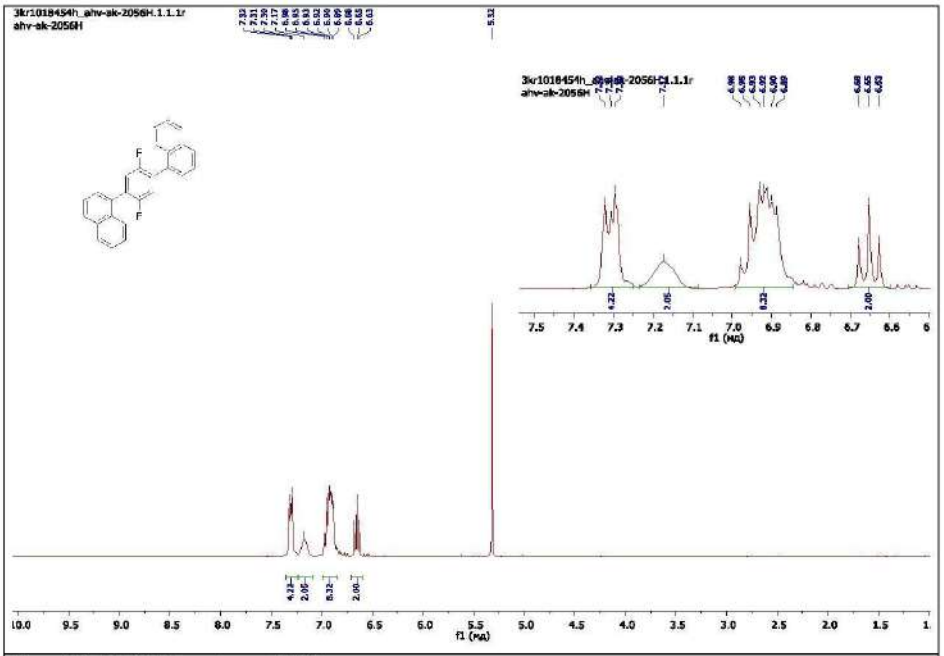

Figure S16. ^{1}H NMR spectrum of (10)

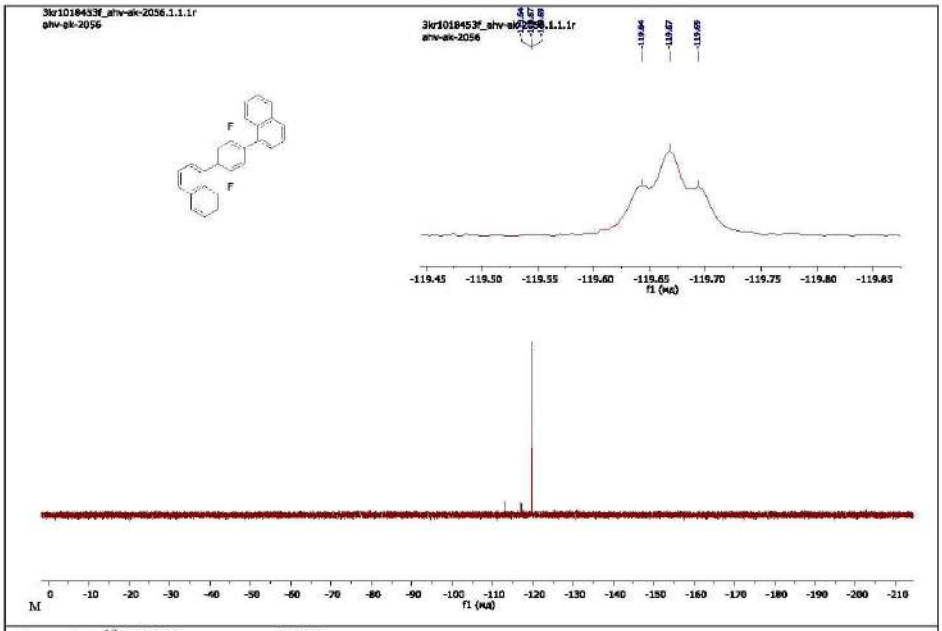

Figure S17. ^{19}F NMR spectrum of (10)

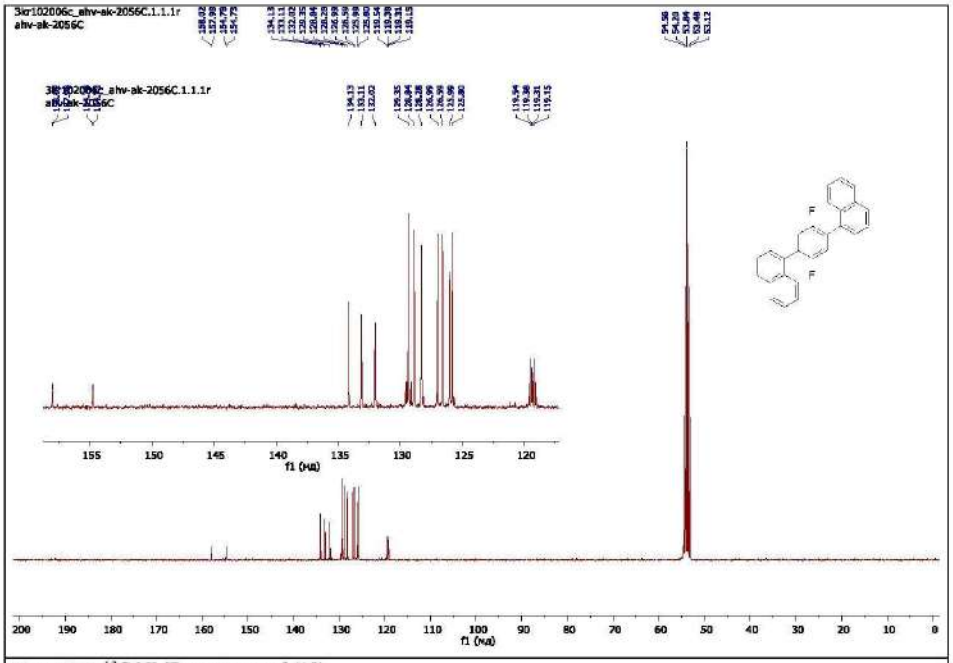

Figure S18. ^{13}C NMR spectrum of (10)

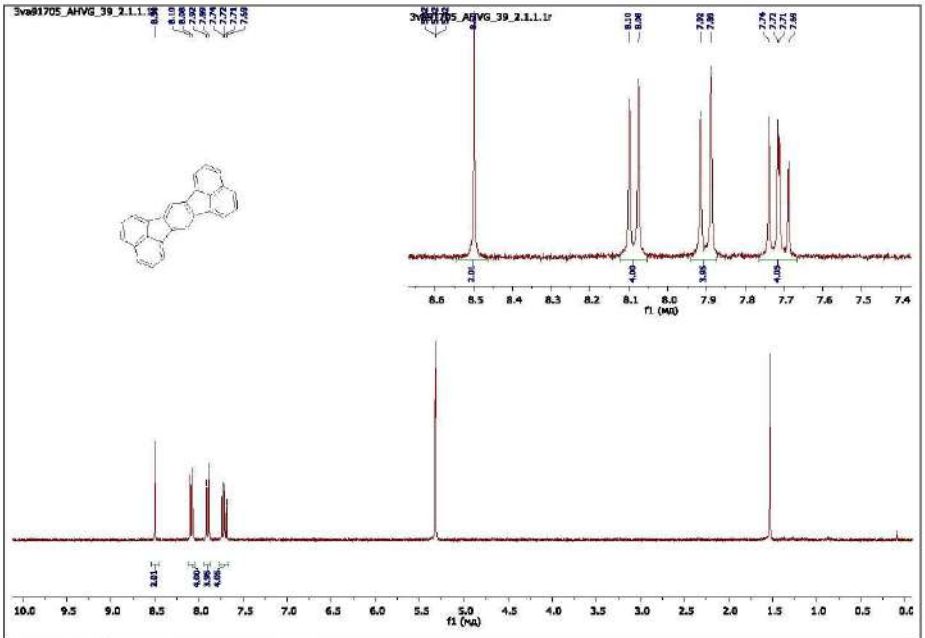

Figure S19. ^{1}H NMR spectrum of (12)

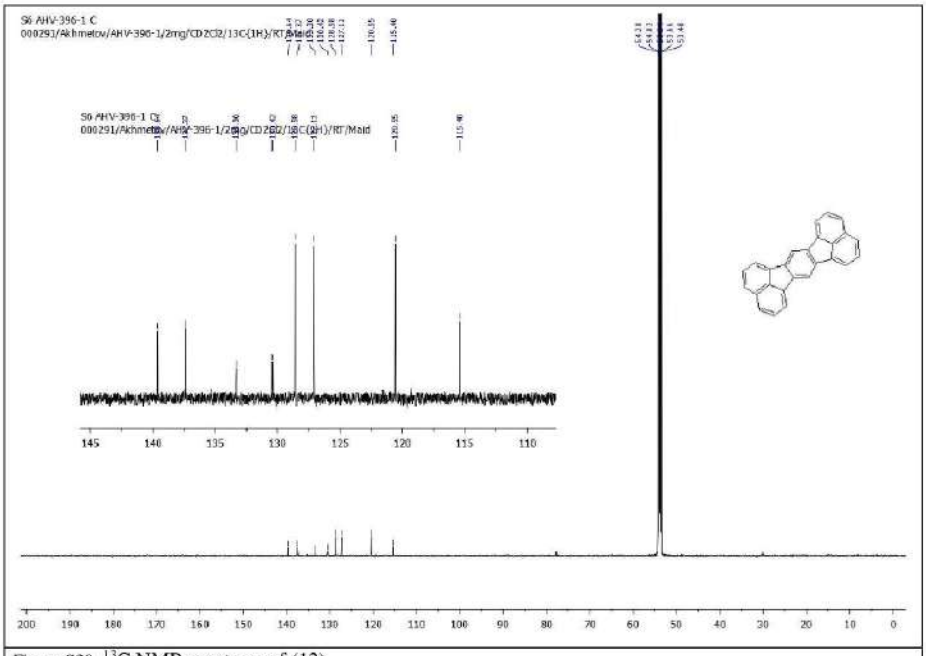

Figure S20. ^{13}C NMR spectrum of (12)

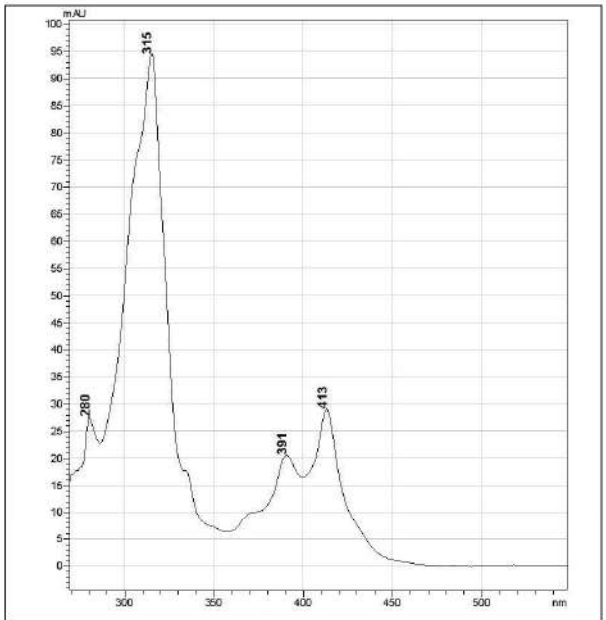

Figure S21. UV/Vis spectrum of (12)

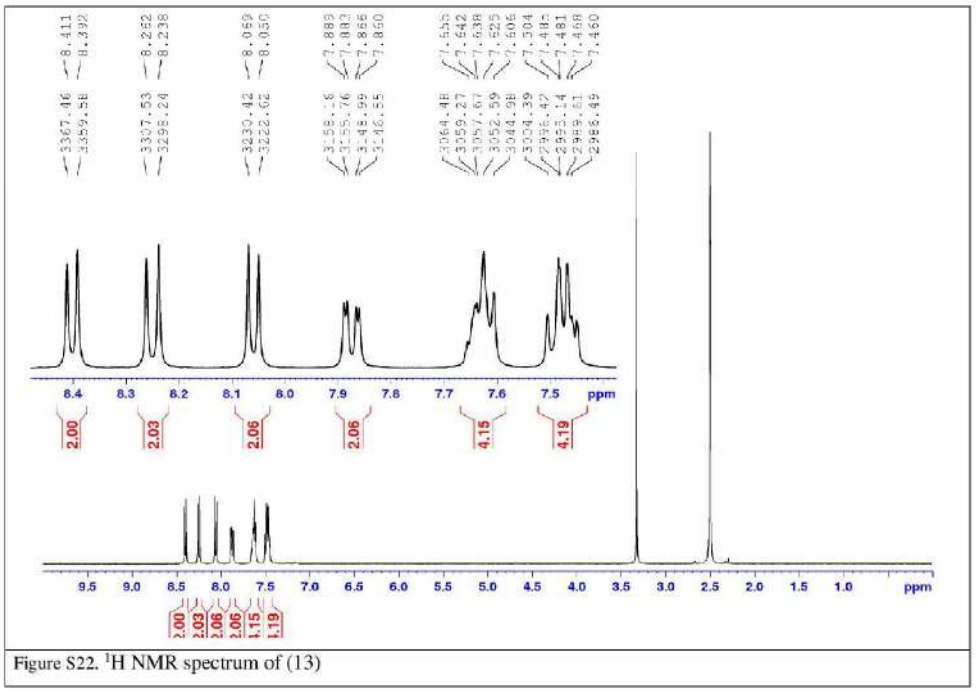

Figure S22. ^{1}H NMR spectrum of (13)

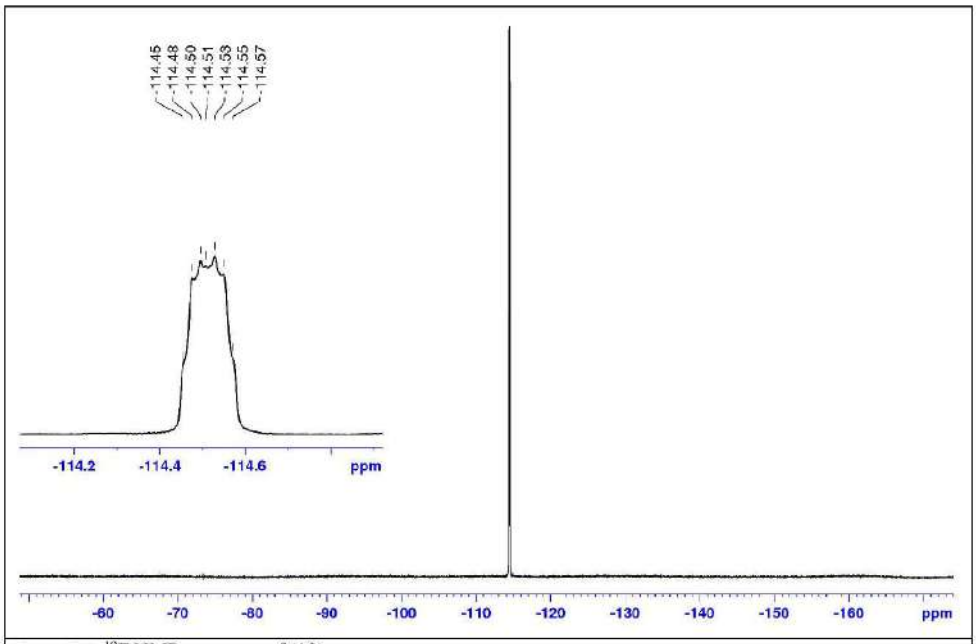

Figure S23. ^{19}F NMR spectrum of (13)

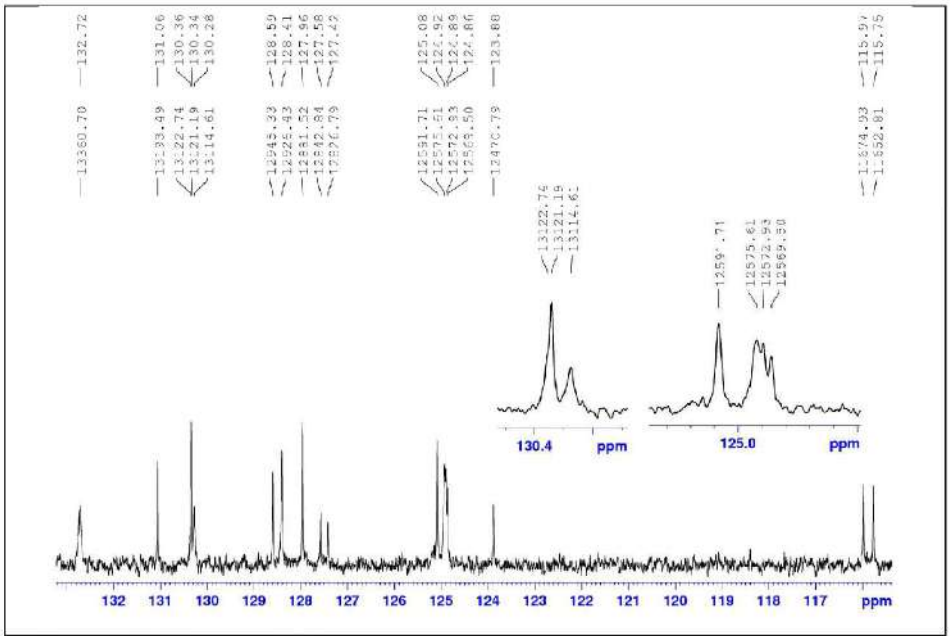

Figure S24. ^{13}C NMR spectrum of (13)

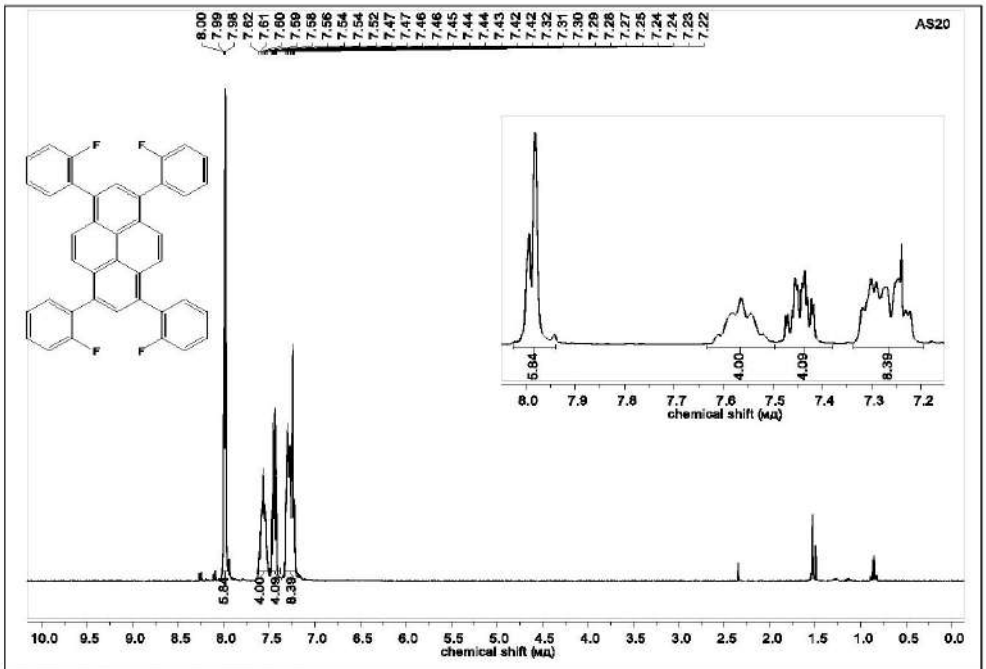

Figure S25. ^{1}H NMR spectrum of (15a)

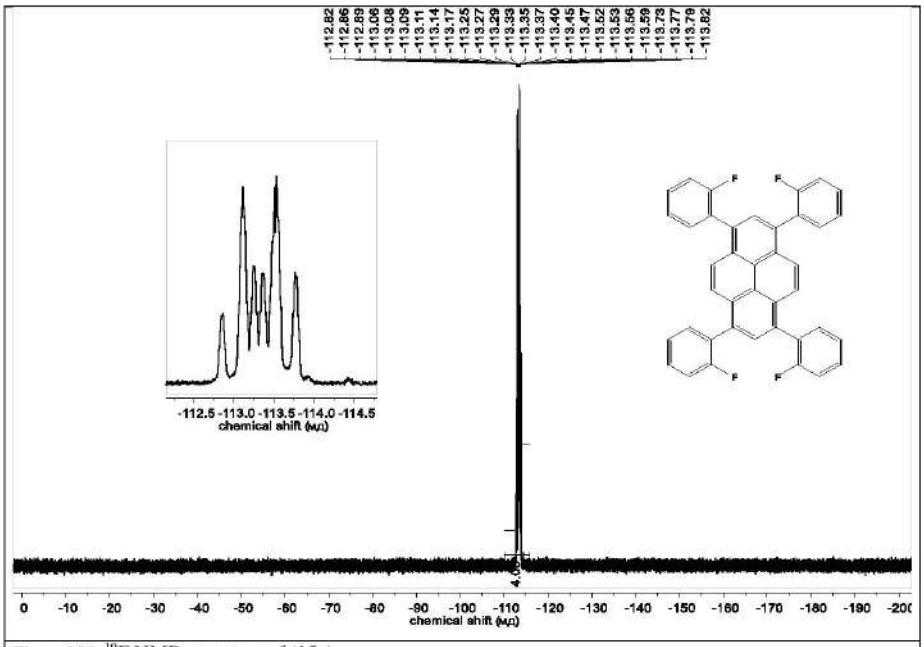

Figure S26. ^{19}F NMR spectrum of (15a)

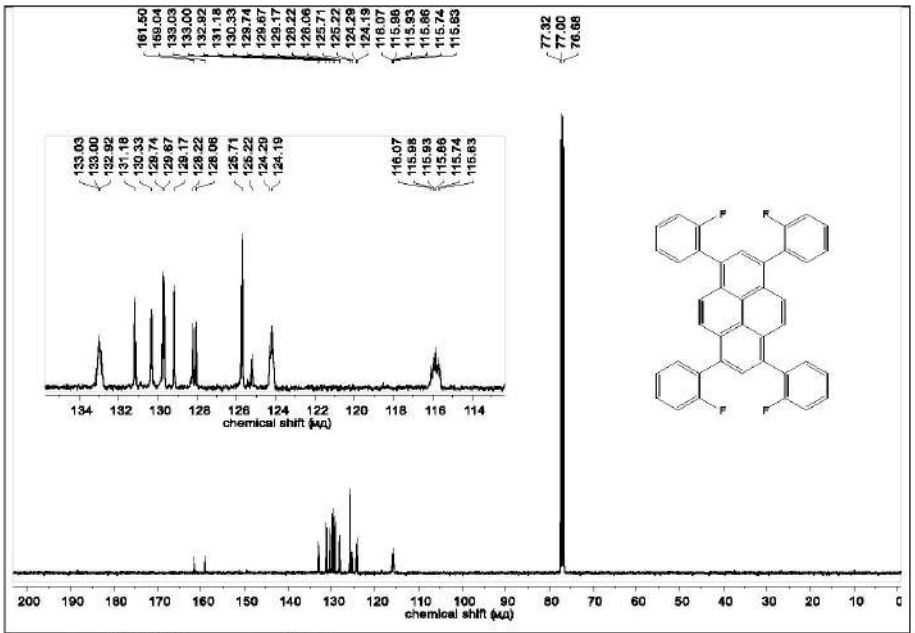

Figure S27. ^{13}C NMR spectrum of (15a)

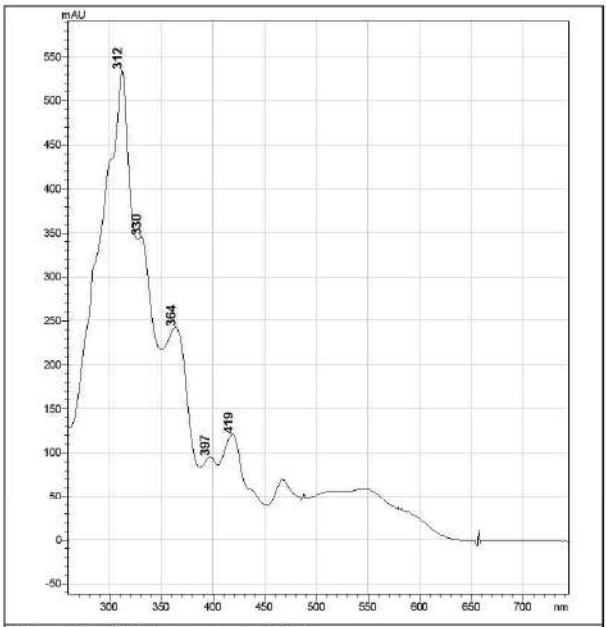

Figure S28. UV/Vis spectrum of (3a)

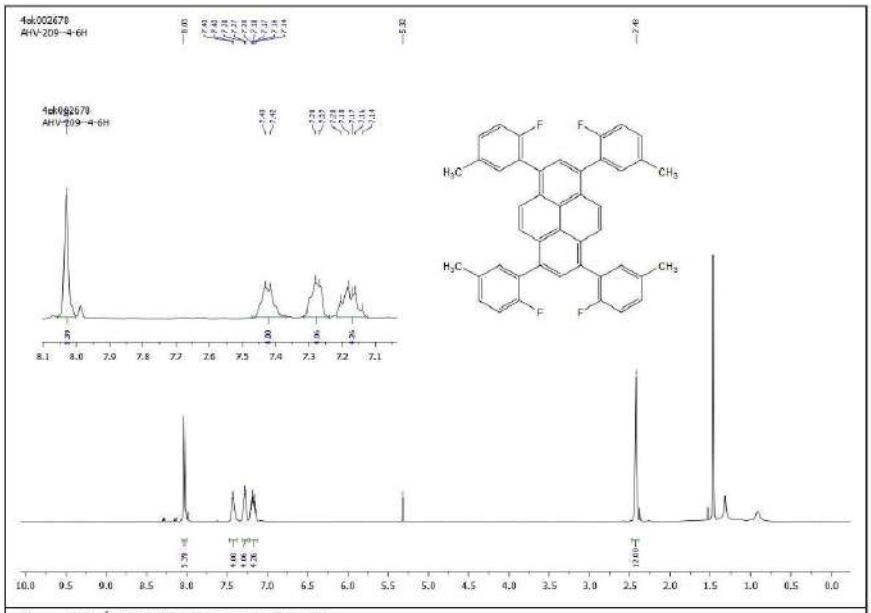

Figure S29. ^{1}H NMR spectrum of (15b)

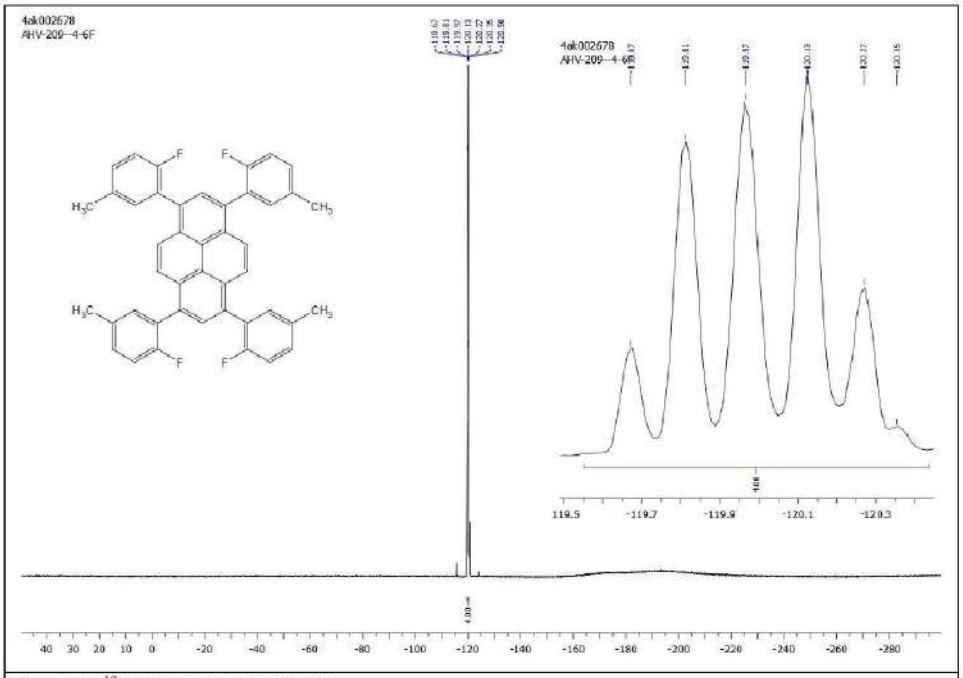

Figure S30. ^{19}F NMR spectrum of (15b)

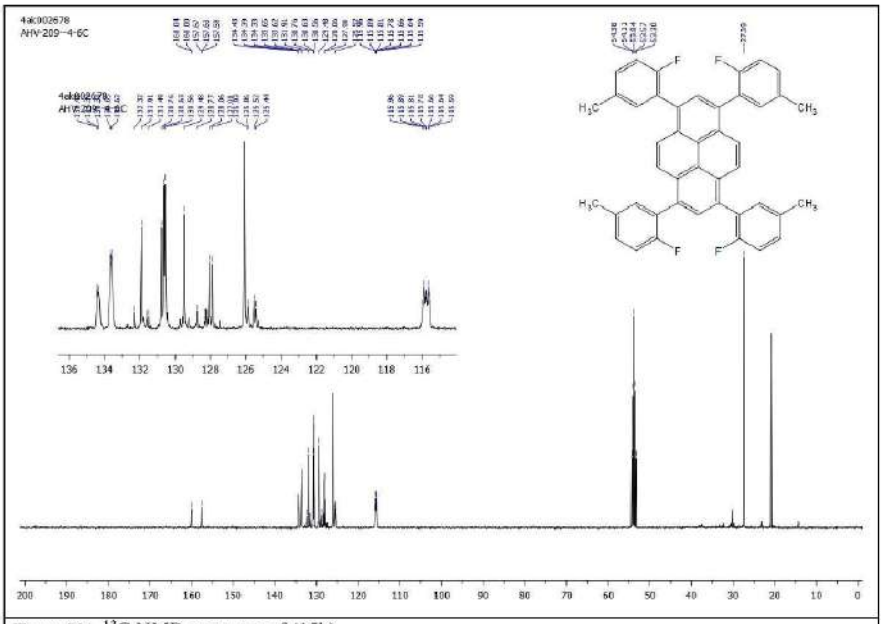

Figure S31. ^{13}C NMR spectrum of (15b)

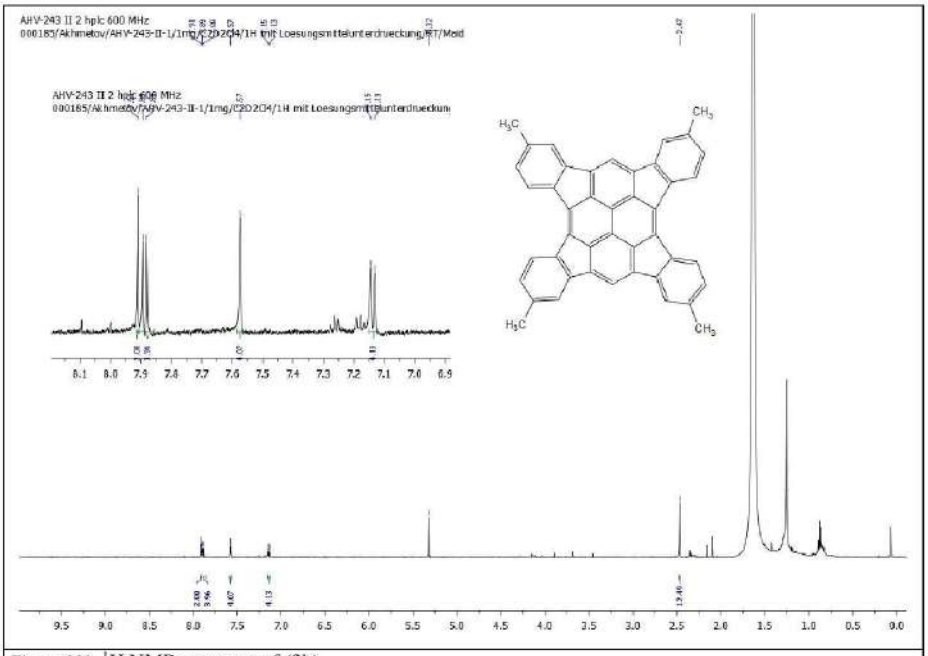

Figure S32. ^{1}H NMR spectrum of (3b)

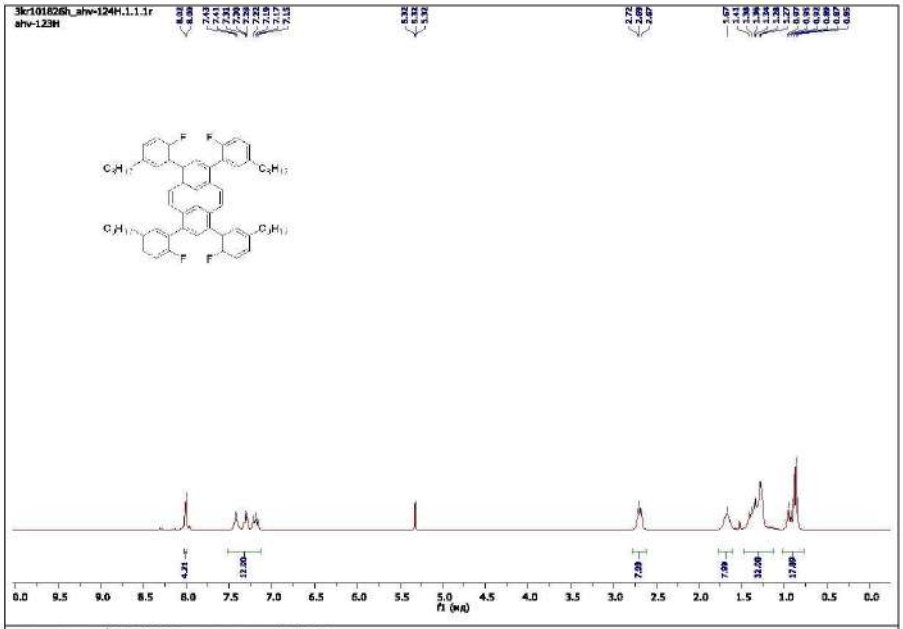

Figure S33. ^{1}H NMR spectrum of (15c)

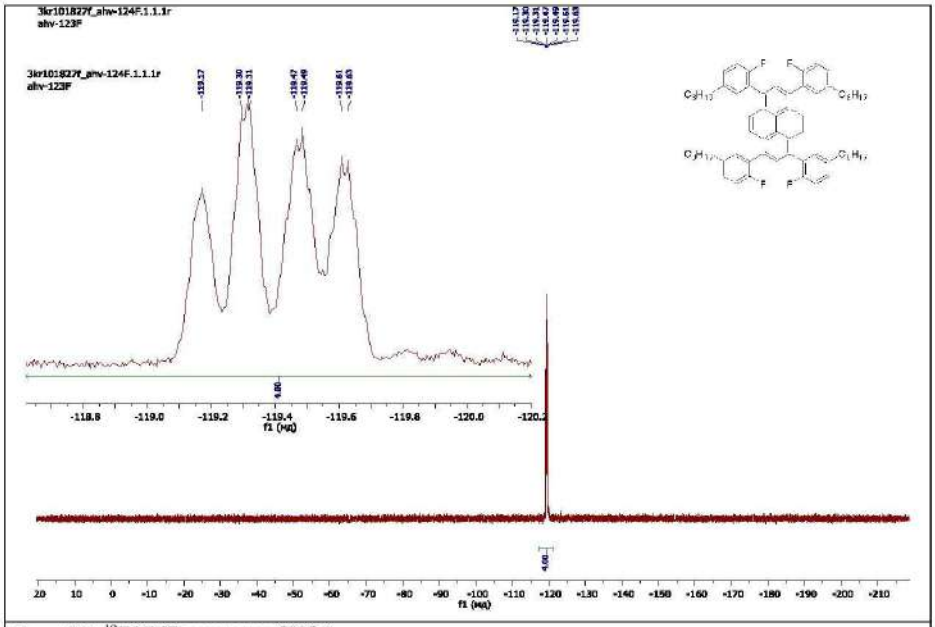

Figure S34. ^{19}F NMR spectrum of (15c)

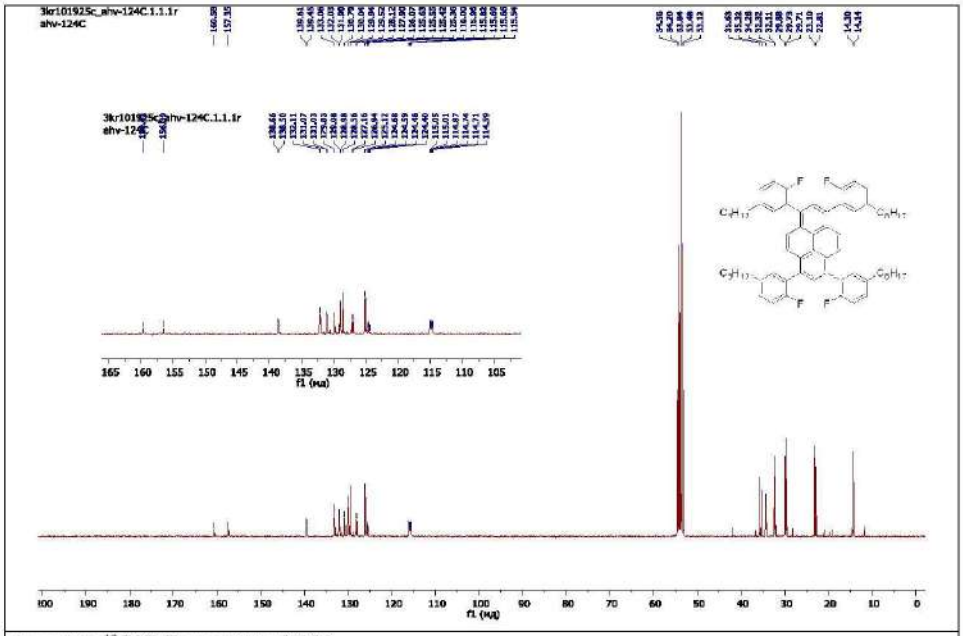

Figure S35. ^{19}C NMR spectrum of (15c)

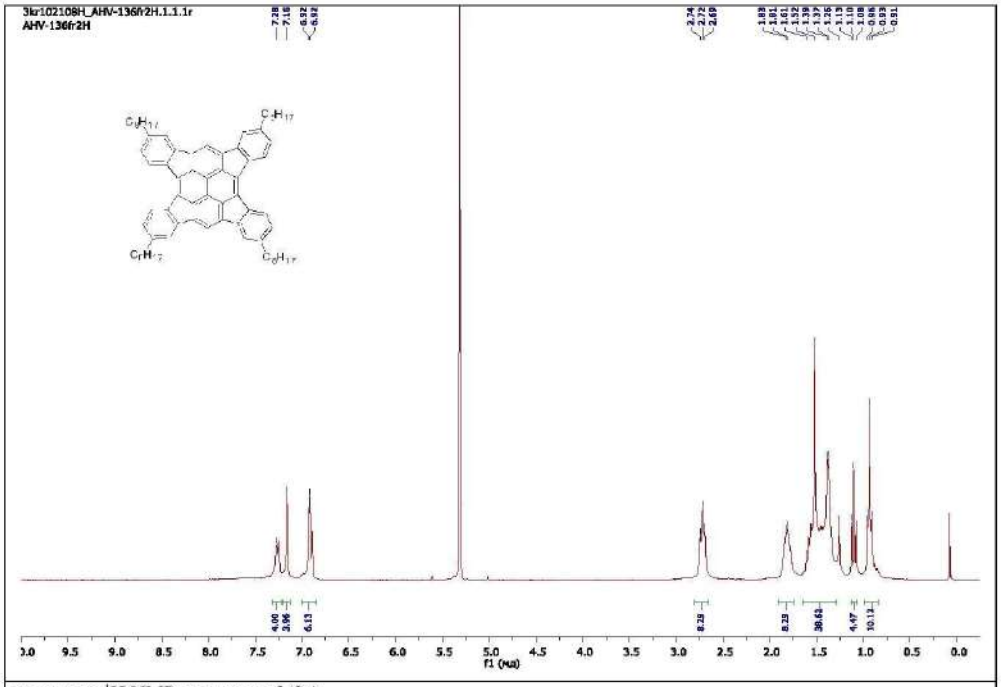

Figure S36. ^{1}H NMR spectrum of (3c)

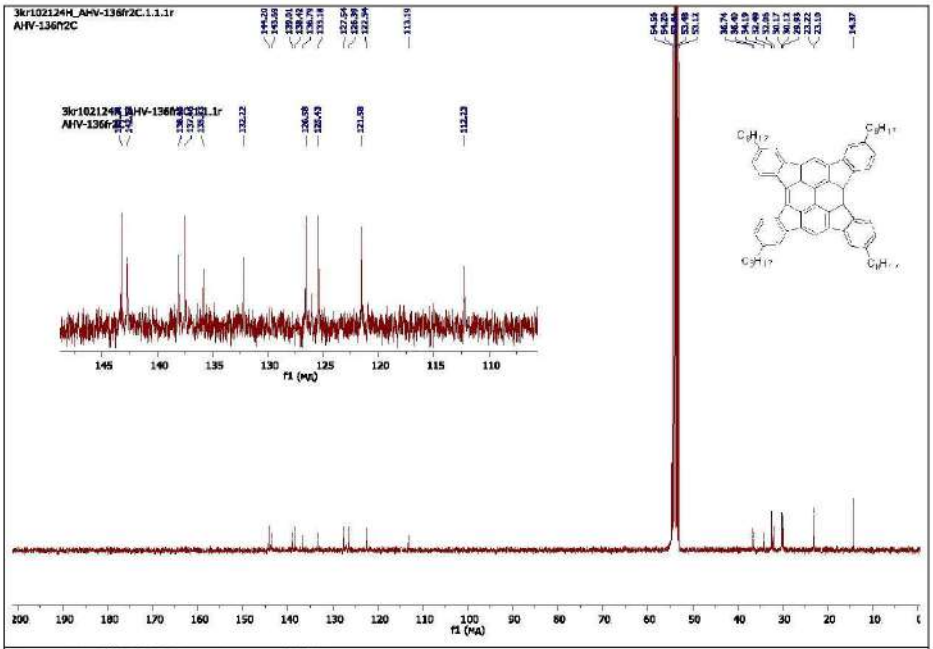

Figure S37. ^{13}C NMR spectrum of (3c)

X-ray crystallography

Synchrotron X-ray data for **12** were collected at 100 K on BL14.3 using a MAR225 detector (λ = 0.8950 Å) whereas the data for **14** were obtained at 100 K on BL14.2 with a pixel detector Pilatus2M (λ = 0.8266 Å) both at the BESSY storage ring (Berlin, Germany). All structures were solved and anisotropically refined using the SHELX package. Selected crystallographic data and CCDC deposition numbers are given in Table S1.

Table S1. Selected crystallographic data and some details of data collection and refinement for compounds **12** and **14**.

Compound	**12**	**14**
Formula	$C_{26}H_{14}$	$C_{56}H_{28}$
M_r	326.37	350.39
crystal system	monoclinic	monoclinic
space group	$P2_1/c$	$P2_1/c$
a [Å]	3.8210(8)	10.465(1)
b [Å]	25.372(2)	3.6371(4)
c [Å]	23.680(2)	20.208(2)
α [°]	90	90
β [°]	90.242(9)	102.609(3)
γ [°]	90	90
V [Å^3]	2295.7(5)	750.61(13)
Z	6	2
D_c [g cm^{-3}]	1.416	1.550
refls collected/R_{int}	33986/0.076	10317/0.035
data / parameters	5063 / 352	2199 / 155
$R_1(I \geq 2\sigma(I))$	0.060/0.159	0.049/0.128
$\Delta\rho_{max/min}$ [e Å^{-3}]	0.51 /–0.40	0.56 / -0.32
CCDC	1916300	1916301

5 Summary

The main objective of this thesis was to develop alumina-mediated C-F activation from infant state to established general method enabling the facile synthesis of pristine and functionalized buckybowls. By infant state here, we imply previously reported achievements in our group, namely, it was shown that activated alumina is capable of C-F bond polarization, which in its turn induces effective C-C coupling. Moreover, it has been shown that C-C coupling occurs even if significant strain energies are required to be overcome, as it is usually so in the case of buckybowls' synthesis. Single examples demonstrated perspectives to implement selective C-F activation and to preserve C-Br functionality. Even though these observations are already impressive, they do not make the method well studied, since no scope and limitation are investigated. Additionally, the selectivity to C-F bonds opens a new horizon of domino-like reactions and their application for synthesis of elusive non-planar PAHs. Besides bright perspectives, these phenomena also indicate the mechanism of the reaction to be far from trivial and tough for perception. Thus, among synthetic applicability of the method, we aimed to determine the mechanistic details of the process. The following chapter briefly describes our achievements and observations made during the thesis fulfillment.

First of all, buckybowls were and still remain to be molecules with a high scientific demand and unmet synthetic supply. Even brighter this contrast comes out in case of functionalized buckybowls, which can be used for the construction of yet subtler and more sophisticated materials, but the low availability of such buckybowls hampers this field from thriving. These issues served as the main motivation for the first work mentioned in the thesis. There we developed a facile synthesis of both pristine and halogenated buckybowls that will be used as valuable building blocks in future works.

Secondly, we investigated whether selective activation of C-F bonds can be used to perform consequent C-F bond activation generating several C-C bonds in one synthetic step. As a model compound, archetypal buckybowl- diindenochrysene, has been chosen. Despite multiple efforts, there are only two published works, where authors successfully obtained this fundamental buckybowl. This makes it not merely a model molecule, but actually hard-to-reach target molecule. Nevertheless, exploiting alumina-mediated technique we managed to obtain diindenochrysene via

several synthetic pathways, in which two, three and five! C-C bonds were created at the last stage. There we demonstrate both zipping and multi-assembly of fluorinated PAHs yielding diindenochrysene and its derivatives. Eventually, we offer two-step procedure enabling the synthesis of pristine diindenochrysene in 5% overall yield.

Additionally, in the course of preparation of some precursors, we discovered an unusual fusion of fluorinated benzophenones, which were expected to undergo McMurry coupling solely, but besides that we also observed fluorinated 9,10-diphenylantracenes formed in substantial yields. We have investigated the scope and limitations of the transformation and carried out DFT calculations that shed some light on the mechanism of the process.

As of mechanistic studies, we investigated the role of twisted structure of [4]-helicene in efficiency of cove-region closure. The strain energy is the major problem interfering with the synthesis of buckybowls. That is why structure (especially its distortion) plays a crucial role in C-C coupling. This thought comes as quite reasonable and rather intuitive, nevertheless, different methods tend to have different thresholds, which they are capable of overcoming. The question we were trying to answer was where is the limit/threshold of alumina-mediated C-F bond activation. We compared several fluorinated PAHs bearing multiple cove-regions and examined the efficiency of cyclodehydrofluorination. This comparison shows that structure and distortion of cove-region are, indeed, crucial for the process of HF elimination.

Moreover, we offer an alternative pathway to effective indennoannulation, which was previously done via either Pd-catalysis or silylium carboranes-mediated C-F activation. As a major advantage, we show that our approach tends to work better for larger systems. Thus, the more C-C bonds are generated during the process, the more effective each cyclization becomes. This trend has been clearly shown on the example of several indenonaphthalenes and pyrenes. Noteworthy, that other methods possess reversed dynamic (larger molecule-poorer efficiency). Besides demonstrating the power of the technique to generate non-alternant large PAHs, we also reveal the unusual nature of alumina-mediated cyclodehydrofluorination mechanism, where electronic effects turn out to be more important than steric.

Summing up our performance, we pushed the state of alumina-mediated C-F activation to a rather well-developed method, where currently accumulated knowledge shows major advantages and limitations of this method. The obtained information clarifies mechanistic details and allows

critical comparison of our approach with others described in the literature methods. As a major achievement, the development of attractive technique, which does not require any expensive catalyst or reagents should be mentioned. Moreover, this technique effectively overcomes strain energy and show tolerance to key functionalities such as halogens, opening facile access to buckybowls and their derivatives.

6 Zusammenfassung

Das Hauptziel dieser Arbeit war es, die durch Aluminiumoxid-vermittelte C-F Aktivierung von einem frühen Anfangsstadium zu einem etablierten allgemeinen Verfahren zu entwickeln, das eine einfache Synthese von reinen und funktionalisierten Buckybowls ermöglicht. Dabei bezieht hier das frühe Anfangsstadium bereits in unserer Gruppe gemeldete Erfolge ein: Es wurde gezeigt, dass aktiviertes Aluminiumoxid eine C-F Bindungspolarisation auslösen kann, die wiederum eine C-C Kupplung induziert. Darüber hinaus wurde gezeigt, dass eine C-C Kupplung auch dann auftritt, wenn erhebliche Spannungsenergien überwunden werden müssen, wie dies normalerweise bei der Buckybowl-Synthese der Fall ist. Einzelne Beispiele zeigten Perspektiven auf, um eine selektive C-F-Aktivierung zu implementieren und die C-Br-Funktionalität zu erhalten. Obwohl diese Beobachtungen bereits beeindruckend sind, bleibt die Methode jedoch nicht ausreichend untersucht, da kein Geltungsbereich und keine Einschränkung untersucht werden. Darüber hinaus eröffnet die Selektivität für C-F-Bindungen einen neuen Horizont für dominoartige Reaktionen und deren Anwendung für die Synthese schwer fassbarer nichtplanarer PAK Diese Phänomene weisen neben aussichtsreichen Perspektiven auch darauf hin, dass der Reaktionsmechanismus alles andere als trivial und schwer zu verstehen ist. Daher wollten wir neben der synthetischen Anwendbarkeit der Methode auch mechanistische Details des Prozesses bestimmen. Das folgende Kapitel beschreibt kurz unsere Errungenschaften und Beobachtungen, die während der Erfüllung der Dissertation gemacht wurden.

Erstens waren und sind Buckybowls immer noch Moleküle mit hohem wissenschaftlichen Anspruch und unbefriedigendem Syntheseangebot. Noch stärker ist dieser Kontrast bei funktionalisierten Buckybowls, die für den Bau von noch feineren und anspruchsvolleren Materialien verwendet werden können. Die geringe Verfügbarkeit solcher Buckybowls beeinträchtigt jedoch das Florieren dieses Bereichs. Diese Fragen dienten als Hauptmotivation für die erste in der Dissertation erwähnte Tätigkeit. Dort haben wir eine einfache Synthese von sowohl unfunktionalisierten als auch halogenierten Buckybowls entwickelt, die in zukünftigen Arbeiten als wertvolle Bausteine verwendet werden.

Zweitens haben wir untersucht, ob die selektive Aktivierung von C-F-Bindungen verwendet werden kann, um eine aufeinanderfolgende C-F-Aktivierung durchzuführen, die mehrere C-C-

Bindungen in einem Syntheseschritt erzeugt. Als Modellverbindung wurde der archetypische Buckybowl Diindenochrysen gewählt. Trotz mehrfacher Bemühungen gibt es nur zwei veröffentlichte Werke, bei denen Autoren erfolgreich Diindenochrysen erhielten. Damit ist es nicht nur ein Modellmolekül, sondern auch ein schwer zugängliches Zielmolekül. Dennoch ist es uns mit Hilfe des Aluminiumoxid-vermittelten Verfahrens gelungen Diindenochrysen über mehrere Synthesewege herzustellen denen im letzten Schritt zwei, drei und fünf! C-C-Bindungen gebildet wurden. Dort zeigen wir sowohl das Zippen als auch die Mehrfachanordnung von fluorierten PAK zu Diindenochrysen und seinen Derivaten. Schließlich bieten wir ein zweistufiges Verfahren an, das die Synthese von reinem Diindenochrysen in einer Gesamtausbeute von 5% ermöglicht.

Zusätzlich entdeckten wir im Laufe der Herstellung einiger Vorläufer eine ungewöhnliche Fusion von fluorierten Benzophenonen, von denen erwartet wurde, dass sie ausschließlich eine McMurry-Kupplung eingehen. Daneben beobachteten wir jedoch auch fluorierte 9,10-Diphenylantracen, die in erheblichen Ausbeuten gebildet wurden. Wir haben Umfang und Grenzen der Transformation untersucht und DFT-Berechnungen durchgeführt, die Aufschluss über den Mechanismus des Prozesses geben.

Im Rahmen mechanistischer Studien untersuchten wir die Rolle der verdrillten Struktur von [4]-Helicen hinsichtlich/bezüglich der Effizienz bei Ringschlüssen in Cove- Regionen. Die Spannungsenergie ist das Hauptproblem bei der Synthese von Buckybowls. Aus diesem Grund spielt die Struktur (insbesondere ihre Verzerrung) bei der C-C-Kupplung eine entscheidende Rolle. Dieser Gedanke ist durchaus vernünftig und eher intuitiv, doch neigen verschiedene Methoden dazu, unterschiedliche Schwellenwerte zu haben, die sie zu überwinden vermögen. Die Frage, die wir zu beantworten versuchten, war, wo die Grenze / Schwelle der durch Aluminiumoxid-vermittelten C-F Aktivierung liegt. Wir verglichen mehrere fluorierte PAK mit mehreren Cove-Regionen miteinander und untersuchten die Effizienz der HF-Eliminierung. Dieser Vergleich zeigt, dass Struktur und Verzerrung der Cove-Region tatsächlich eine entscheidende Rolle bei der HF-Eliminierung spielen.

Darüber hinaus bieten wir einen alternativen Weg zur effektiven Indennoannulierung, die zuvor entweder über Pd-Katalyse oder durch Silyliumcarborane-vermittelte C-F-Aktivierung durchgeführt wurde. Als großen Vorteil zeigen wir, dass unser Ansatz tendenziell besser bei größeren Systemen funktioniert. Je mehr C-C-Bindungen während des Prozesses erzeugt werden,

desto effektiver wird somit jede Zyklisierung. Dieser Trend wurde am Beispiel mehrerer Indenonaphthalins und Pyrens deutlich. Bemerkenswert ist, dass andere Methoden eine umgekehrte Dynamik aufweisen (größere Moleküle - schlechtere Effizienz). Neben dem leistungsstarken Verfahren zur Erzeugung nicht alternierender großer PAK zeigen wir auch die ungewöhnliche Natur des Aluminiumoxid-vermittelten Mechanismus, bei dem elektronische Effekte wichtiger sind als sterische.

Zusammenfassend lässt sich sagen, dass wir den Stand der Aluminiumoxid-vermittelten C-F-Aktivierung auf eine recht gut entwickelte Methode gebracht haben, bei der die derzeit gesammelten Erkenntnisse wesentliche Vorteile und Grenzen dieser Methode aufzeigen. Die gewonnenen Informationen verdeutlichen mechanistische Details und ermöglichen einen kritischen Vergleich unseres Ansatzes mit anderen in der Literatur beschriebenen. Als wesentliche erzielte Vorteile haben wir eine recht attraktive Technik entwickelt, die ohne teure Katalysatoren oder Reagenzien auskommt. Darüber hinaus überwindet dieses Verfahren effektiv die Spannungsenergie, zeigt Toleranz gegenüber Schlüsselfunktionalitäten wie Halogenen und eröffnet damit den einfachen Zugang zu Buckybowls und deren Derivaten.

7 Literature

[1] H. W. Kroto, J. R. Heath, S. C. O'Brien, R. F. Curl, R. E. Smalley, *Nature* **1985**, *318*, 162–163.

[2] K. S. Novoselov, *Science (80-.).* **2004**, *306*, 666–669.

[3] L. T. Scott, H. E. Bronstein, D. V. Preda, R. B. M. Ansems, M. S. Bratcher, S. Hagen, *Pure Appl. Chem.* **1999**, *71*, 209–219.

[4] E. Hückel, *Zeitschrift für Phys.* **1931**, *70*, 204–286.

[5] E. Clar, in *Polycycl. Hydrocarb.*, Springer Berlin Heidelberg, Berlin, Heidelberg, **1964**, pp. 32–39.

[6] A. Hirsch, Z. Chen, H. Jiao, *Angew. Chemie* **2000**, *39*, 3915–3917.

[7] P. R. von Schleyer, H. Jiao, *Pure Appl. Chem.* **1996**, *68*, 209–218.

[8] † Zhongfang Chen *, † Chaitanya S. Wannere, † Clémence Corminboeuf, ‡ Ralph Puchta, † and Paul von Ragué Schleyer*, *Chem. Rev.* **2005**, *105*, 3842–3888.

[9] H. Hopf, *Classics in Hydrocarbon Chemistry*, **2000**.

[10] T. P. Radhakrishnan, I. Agranat, *Struct. Chem.* **1991**, *2*, 107–115.

[11] W. V. Volland, E. R. Davidson, W. T. Borden, *J. Am. Chem. Soc.* **1979**, *101*, 533–537.

[12] S. Vázquez, P. Camps, *Tetrahedron* **2005**, *61*, 5147–5208.

[13] R. C. Haddon, *J. Am. Chem. Soc.* **1986**, *108*, 2837–2842.

[14] R. C. Haddon, *J. Am. Chem. Soc.* **1987**, *109*, 1676–1685.

[15] R. C. Haddon, L. T. Scott, *Pure Appl. Chem.* **1986**, *58*, 137–142.

[16] H. C. Bai, Y. Zhu, N. N. Yuan, Y. Q. Ji, W. Y. Qiao, Y. H. Huang, *Jiegou Huaxue* **2013**, *32*, 695–703.

[17] W. E. Barth, R. G. Lawton, *J. Am. Chem. Soc.* **1971**, *93*, 1730–1745.

[18] W. E. Barth, R. G. Lawton, *J. Am. Chem. Soc.* **1966**, *88*, 380–381.

[19] L. T. Scott, P.-C. Cheng, M. M. Hashemi, M. S. Bratcher, D. T. Meyer, H. B. Warren, *J. Am. Chem. Soc.* **1997**, *119*, 10963–10968.

[20] A. M. Butterfield, B. Gilomen, J. S. Siegel, *Org. Process Res. Dev.* **2012**, *16*, 664–676.

[21] H. I. Chang, H. T. Huang, C. H. Huang, M. Y. Kuo, Y. T. Wu, *Chem. Commun.* **2010**, *46*, 7241–7243.

[22] H. E. Bronstein, N. Choi, L. T. Scott, C. Hill, *Tetrahedron* **2002**, 8870–8875.

[23] H. Sakurai, *Science (80-.).* **2003**, *301*, 1878–1878.

[24] M. Maggini, G. Scorrano, M. Prato, *J. Am. Chem. Soc.* **1993**, *115*, 9798–9799.

[25] O. Tsuge, S. Kanemasa, **1989**, pp. 231–349.

[26] C. Bingel, *Chem. Ber.* **1993**, *126*, 1957–1959.

[27] M. Yamada, T. Akasaka, S. Nagase, *Chem. Rev.* **2013**, *113*, 7209–7264.

[28] P. A. Troshin, R. N. Lyubovskaya, *Russ. Chem. Rev.* **2008**, *77*, 323–369.

[29] T. J. Seiders, E. L. Elliott, G. H. Grube, J. S. Siegel, *J. Am. Chem. Soc.* **1999**, *121*, 7804–7813.

[30] H. E. Bronstein, L. T. Scott, *J. Org. Chem.* **2008**, *73*, 88–93.

[31] M. M. Haley, R. R. Tykwinski, Eds. , *Carbon-Rich Compounds*, Wiley, **2006**.

[32] D. Eisenberg, R. Shenhar, M. Rabinovitz, in *Fragm. Fullerenes Carbon Nanotub.*, John Wiley & Sons, Inc., Hoboken, NJ, USA, **2011**, pp. 63–93.

[33] A. Sygula, P. W. Rabideau, *J. Mol. Struct. THEOCHEM* **1995**, *333*, 215–226.

[34] A. Ayalon, A. Sygula, P.-C. Cheng, M. Rabinovitz, P. W. Rabideau, L. T. Scott, *Science (80-.).* **1994**, *265*, 1065–1067.

[35] A. Ayalon, M. Rabinovitz, P.-C. Cheng, L. T. Scott, *Angew. Chemie Int. Ed. English* **1992**, *31*, 1636–1637.

[36] M. Baumgarten, L. Gherghel, M. Wagner, A. Weitz, M. Rabinovitz, P.-C. Cheng, L. T. Scott, *J. Am. Chem. Soc.* **1995**, *117*, 6254–6257.

[37] L. Zoppi, L. Martin-Samos, K. K. Baldridge, *J. Am. Chem. Soc.* **2011**, *133*, 14002–14009.

[38] G. Valenti, C. Bruno, S. Rapino, A. Fiorani, E. A. Jackson, L. T. Scott, F. Paolucci, M. Marcaccio, *J. Phys. Chem. C* **2010**, *114*, 19467–19472.

[39] A. M. Rice, W. B. Fellows, E. A. Dolgopolova, A. B. Greytak, A. K. Vannucci, M. D. Smith, S. G. Karakalos, J. A. Krause, S. M. Avdoshenko, A. A. Popov, et al., *Angew. Chemie Int. Ed.* **2017**, *56*, 4525–4529.

[40] R. Chen, R.-Q. Lu, P.-C. Shi, X.-Y. Cao, *Chinese Chem. Lett.* **2016**, *27*, 1175–1183.

[41] R.-Q. Lu, Y.-Q. Zheng, Y.-N. Zhou, X.-Y. Yan, T. Lei, K. Shi, Y. Zhou, J. Pei, L. Zoppi, K. K. Baldridge, et al., *J. Mater. Chem. A* **2014**, *2*, 20515–20519.

[42] C.-Z. Li, H.-L. Yip, A. K.-Y. Jen, *J. Mater. Chem.* **2012**, *22*, 4161.

[43] F. Biedermann, H.-J. Schneider, *Chem. Rev.* **2016**, *116*, 5216–5300.

[44] J. Lehn, *Science (80-.).* **1993**, *260*, 1762–1763.

[45] J. W. Steed, J. L. Atwood, *Supramolecular Chemistry*, John Wiley & Sons, Ltd, Chichester, UK, **2009**.

[46] E. P. Kyba, R. C. Helgeson, K. Madan, G. W. Gokel, T. L. Tarnowski, S. S. Moore, D. J. Cram, *J. Am. Chem. Soc.* **1977**, *99*, 2564–2571.

[47] T. Kawase, H. Kurata, *Chem. Rev.* **2006**, *106*, 5250–5273.

[48] A. Sygula, F. R. Fronczek, R. Sygula, P. W. Rabideau, M. M. Olmstead, *J. Am. Chem. Soc.* **2007**, *129*, 3842–3843.

[49] W. Xiao, D. Passerone, P. Ruffieux, K. Aït−Mansour, O. Gröning, E. Tosatti, J. S. Siegel, R. Fasel, *J. Am. Chem. Soc.* **2008**, *130*, 4767–4771.

[50] C. Mück-Lichtenfeld, S. Grimme, L. Kobryn, A. Sygula, *Phys. Chem. Chem. Phys.* **2010**, *12*, 7091.

[51] Y.-M. Liu, D. Xia, B.-W. Li, Q.-Y. Zhang, T. Sakurai, Y.-Z. Tan, S. Seki, S.-Y. Xie, L.-S. Zheng, *Angew. Chemie Int. Ed.* **2016**, *55*, 13047–13051.

[52] L. Kobryn, W. P. Henry, F. R. Fronczek, R. Sygula, A. Sygula, *Tetrahedron Lett.* **2009**, *50*, 7124–7127.

[53] J. Leblond, A. Petitjean, *ChemPhysChem* **2011**, *12*, 1043–1051.

[54] D.-C. Yang, M. Li, C.-F. Chen, *Chem. Commun.* **2017**, *53*, 9336–9339.

[55] A. Sygula, W. E. Collier, in *Fragm. Fullerenes Carbon Nanotub.*, John Wiley & Sons, Inc., Hoboken, NJ, USA, **2011**, pp. 1–40.

[56] A. A. Voityuk, M. Duran, *J. Phys. Chem. C* **2008**, *112*, 1672–1678.

[57] K. Kanagaraj, K. Lin, W. Wu, G. Gao, Z. Zhong, D. Su, C. Yang, *Symmetry (Basel).* **2017**, *9*, 174.

[58] S. Higashibayashi, H. Sakurai, *J. Am. Chem. Soc.* **2008**, *130*, 8592–8593.

[59] Q. Tan, S. Higashibayashi, S. Karanjit, H. Sakurai, *Nat. Commun.* **2012**, *3*, 891.

[60] C. Thilgen, F. Diederich, *Chem. Rev.* **2006**, *106*, 5049–5135.

[61] R. S. Cahn, C. Ingold, V. Prelog, *Angew. Chemie Int. Ed. English* **1966**, *5*, 385–415.

[62] M. A. Petrukhina, K. W. Andreini, L. Peng, L. T. Scott, *Angew. Chemie Int. Ed.* **2004**, *43*, 5477–5481.

[63] T. J. Seiders, K. K. Baldridge, G. H. Grube, J. S. Siegel, *J. Am. Chem. Soc.* **2001**, *123*, 517–525.

[64] L. T. Scott, M. M. Hashemi, M. S. Bratcher, *J. Am. Chem. Soc.* **1992**, *114*, 1920–1921.

[65] D. Bandera, K. K. Baldridge, A. Linden, R. Dorta, J. S. Siegel, *Angew. Chemie Int. Ed.* **2011**, *50*, 865–867.

[66] G. A. Hembury, V. V. Borovkov, Y. Inoue, *Chem. Rev.* **2008**, *108*, 1–73.

[67] L. Zhang, L. Qin, X. Wang, H. Cao, M. Liu, *Adv. Mater.* **2014**, *26*, 6959–6964.

[68] R. C. Dunbar, *J. Phys. Chem. A* **2002**, *106*, 9809–9819.

[69] M. A. Petrukhina, K. W. Andreini, J. Mack, L. T. Scott, *Angew. Chemie Int. Ed.* **2003**, *42*, 3375–3379.

[70] M. A. Petrukhina, L. T. Scott, *Dalt. Trans.* **2005**, 2969.

[71] M. A. Petrukhina, Y. Sevryugina, A. Y. Rogachev, E. A. Jackson, L. T. Scott, *Organometallics* **2006**, *25*, 5492–5495.

[72] A. Y. Rogachev, Y. Sevryugina, A. S. Filatov, M. A. Petrukhina, *Dalt. Trans.* **2007**, 3871.

[73] M. A. Petrukhina, *Angew. Chemie Int. Ed.* **2008**, *47*, 1550–1552.

[74] P. A. Vecchi, C. M. Alvarez, A. Ellern, R. J. Angelici, A. Sygula, R. Sygula, P. W. Rabideau, *Angew. Chemie Int. Ed.* **2004**, *43*, 4497–4500.

[75] D. Eisenberg, A. S. Filatov, E. A. Jackson, M. Rabinovitz, M. A. Petrukhina, L. T. Scott, R. Shenhar, *J. Org. Chem.* **2008**, *73*, 6073–6078.

[76] J. S. Siegel, K. K. Baldridge, A. Linden, R. Dorta, *J. Am. Chem. Soc.* **2006**, *128*, 10644–10645.

[77] E. D. Jemmis, P. Parameswaran, A. Anoop, *Int. J. Quantum Chem.* **2003**, *95*, 810–815.

[78] A. S. Filatov, M. A. Petrukhina, *Coord. Chem. Rev.* **2010**, *254*, 2234–2246.

[79] M. Kabdulov, M. Jansen, K. Y. Amsharov, *Chem. - A Eur. J.* **2013**, *19*, 17262–17266.

[80] L. T. Scott, *Science (80-.).* **2002**, *295*, 1500–1503.

[81] J. R. Sanchez-Valencia, T. Dienel, O. Gröning, I. Shorubalko, A. Mueller, M. Jansen, K. Amsharov, P. Ruffieux, R. Fasel, *Nature* **2014**, *512*, 61–64.

[82] E. H. Fort, P. M. Donovan, L. T. Scott, *J. Am. Chem. Soc.* **2009**, *131*, 16006–16007.

[83] E. H. Fort, L. T. Scott, *Angew. Chemie Int. Ed.* **2010**, *49*, 6626–6628.

[84] L. T. Scott, E. A. Jackson, Q. Zhang, B. D. Steinberg, M. Bancu, B. Li, *J. Am. Chem. Soc.* **2012**, *134*, 107–110.

[85] K. Y. Amsharov, *Phys. status solidi* **2015**, *252*, 2466–2471.

[86] A. Mueller, K. Y. Amsharov, M. Jansen, *Fullerenes, Nanotub. Carbon Nanostructures* **2012**, *20*, 401–404.

[87] K. Amsharov, N. Abdurakhmanova, S. Stepanow, S. Rauschenbach, M. Jansen, K. Kern,

Angew. Chemie Int. Ed. **2010**, *49*, 9392–9396.

[88] A. Sygula, *European J. Org. Chem.* **2011**, *2011*, 1611–1625.

[89] C.-H. Kuo, M.-H. Tsau, D. T.-C. Weng, G. H. Lee, S.-M. Peng, T.-Y. Luh, P. U. Biedermann, I. Agranat, *J. Org. Chem.* **1995**, *60*, 7380–7381.

[90] J. Craig, M. Robins, *Aust. J. Chem.* **1968**, *21*, 2237.

[91] J. Davy, M. Iskander, J. Reiss, *Aust. J. Chem.* **1979**, *32*, 1067.

[92] N. S. Mills, J. L. Malandra, A. Hensen, J. A. Lowery, *Polycycl. Aromat. Compd.* **1998**, *12*, 239–247.

[93] A. Sygula, G. Xu, Z. Marcinow, P. W. Rabideau, *Tetrahedron* **2001**, *57*, 3637–3644.

[94] E. M. Muzammil, D. Halilovic, M. C. Stuparu, *Commun. Chem.* **2019**, *2*, 58.

[95] X. Li, F. Kang, M. Inagaki, *Small* **2016**, *12*, 3206–3223.

[96] R. G. Lawton, W. E. Barth, *J. Am. Chem. Soc.* **1971**, *93*, 1730–1745.

[97] W. E. Barth, R. G. Lawton, *J. Am. Chem. Soc.* **1966**, *88*, 380–381.

[98] A. Borchardt, A. Fuchicello, K. V. Kilway, K. K. Baldridge, J. S. Siegel, *J. Am. Chem. Soc.* **1992**, *114*, 1921–1923.

[99] G. Zimmermann, U. Nuechter, S. Hagen, M. Nuechter, *Tetrahedron Lett.* **1994**, *35*, 4747–4750.

[100] L. T. Scott, M. M. Hashemi, D. T. Meyer, H. B. Warren, *J. Am. Chem. Soc.* **1991**, *113*, 7082–7084.

[101] V. M. Tsefrikas, L. T. Scott, *Chem. Rev.* **2006**, *106*, 4868–4884.

[102] Z. Marcinow, D. I. Grove, P. W. Rabideau, *J. Org. Chem.* **2002**, *67*, 3537–3539.

[103] H. A. Reisch, M. S. Bratcher, L. T. Scott, *Org. Lett.* **2000**, *2*, 1427–1430.

[104] G. Mehta, P. V. V. Srirama Sarma, *Chem. Commun.* **2000**, 19–20.

[105] L. T. Scott, *Pure Appl. Chem.* **1996**, *68*, 291–300.

[106] H. E. Bronstein, N. Choi, L. T. Scott, *J. Am. Chem. Soc.* **2002**, *124*, 8870–8875.

[107] P. W. Rabideau, A. H. Abdourazak, H. E. Folsom, Z. Marcinow, A. Sygula, R. Sygula, *J. Am. Chem. Soc.* **1994**, *116*, 7891–7892.

[108] L. T. Scott, M. S. Bratcher, S. Hagen, *J. Am. Chem. Soc.* **1996**, *118*, 8743–8744.

[109] K. K. Wang, H. Cui, B. Wen, in *Fragm. Fullerenes Carbon Nanotub.*, John Wiley & Sons, Inc., Hoboken, NJ, USA, **2011**, pp. 41–61.

[110] T. J. Seiders, K. K. Baldridge, J. S. Siegel, *J. Am. Chem. Soc.* **1996**, *118*, 2754–2755.

[111] A. Sygula, P. W. Rabideau, *J. Am. Chem. Soc.* **1998**, *120*, 12666–12667.

[112] A. Borchard, K. Hardcastle, P. Gantzel, J. S. Siegella, *Tetrahedron Lett.* **1993**, *34*, 273–276.

[113] A. Sygula, P. W. Rabideau, *J. Am. Chem. Soc.* **1999**, *121*, 7800–7803.

[114] A. Sygula, S. D. Karlen, R. Sygula, P. W. Rabideau, *Org. Lett.* **2002**, *4*, 3135–3137.

[115] A. Sygula, P. W. Rabideau, *J. Am. Chem. Soc.* **2000**, *122*, 6323–6324.

[116] Z. Marcinow, A. Sygula, A. Ellern, P. W. Rabideau, *Org. Lett.* **2001**, *3*, 3527–3529.

[117] L. Wang, P. B. Shevlin, *Tetrahedron Lett.* **2000**, *41*, 285–288.

[118] D. Alberico, M. E. Scott, M. Lautens, *Chem. Rev.* **2007**, *107*, 174–238.

[119] S. Pascual, P. de Mendoza, A. M. Echavarren, *Org. Biomol. Chem.* **2007**, *5*, 2727.

[120] Y.-T. Wu, J. S. Siegel, *Chem. Rev.* **2006**, *106*, 4843–4867.

[121] H. A. Wegner, L. T. Scott, A. de Meijere, *J. Org. Chem.* **2003**, *68*, 883–887.

[122] H. A. Wegner, H. Reisch, K. Rauch, A. Demeter, K. A. Zachariasse, A. de Meijere, L. T. Scott, *J. Org. Chem.* **2006**, *71*, 9080–9087.

[123] X. Tian, L. M. Roch, K. K. Baldridge, J. S. Siegel, *European J. Org. Chem.* **2017**, *2017*, 2801–2805.

[124] S. Lampart, L. M. Roch, A. K. Dutta, Y. Wang, R. Warshamanage, A. D. Finke, A.

Linden, K. K. Baldridge, J. S. Siegel, *Angew. Chemie Int. Ed.* **2016**, *55*, 14648–14652.

[125] L. M. Roch, L. Zoppi, J. S. Siegel, K. K. Baldridge, *J. Phys. Chem. C* **2017**, *121*, 1220–1234.

[126] E. A. Jackson, B. D. Steinberg, M. Bancu, A. Wakamiya, L. T. Scott, *J. Am. Chem. Soc.* **2007**, *129*, 484–485.

[127] L. Wang, P. B. Shevlin, *Org. Lett.* **2000**, *2*, 3703–3705.

[128] H.-I. Chang, H.-T. Huang, C.-H. Huang, M.-Y. Kuo, Y.-T. Wu, *Chem. Commun.* **2010**, *46*, 7241.

[129] D. Kim, J. L. Petersen, K. K. Wang, *Org. Lett.* **2006**, *8*, 2313–2316.

[130] S. Pogodin, P. U. Biedermann, I. Agranat, *J. Org. Chem.* **1997**, *62*, 2285–2287.

[131] T. Ahrens, J. Kohlmann, M. Ahrens, T. Braun, *Chem. Rev.* **2015**, *115*, 931–972.

[132] C. Liu, B. Zhang, *Chem. Rec.* **2016**, *16*, 667–687.

[133] M. Tobisu, T. Xu, T. Shimasaki, N. Chatani, *J. Am. Chem. Soc.* **2011**, *133*, 19505–19511.

[134] X.-W. Liu, J. Echavarren, C. Zarate, R. Martin, *J. Am. Chem. Soc.* **2015**, *137*, 12470–12473.

[135] T. Niwa, H. Ochiai, Y. Watanabe, T. Hosoya, *J. Am. Chem. Soc.* **2015**, *137*, 14313–14318.

[136] Y. Nakamura, N. Yoshikai, L. Ilies, E. Nakamura, *Org. Lett.* **2012**, *14*, 3316–3319.

[137] N. Suzuki, T. Fujita, J. Ichikawa, *Org. Lett.* **2015**, *17*, 4984–4987.

[138] N. Suzuki, T. Fujita, K. Y. Amsharov, J. Ichikawa, *Chem. Commun.* **2016**, *52*, 12948–12951.

[139] J. Ichikawa, H. Jyono, T. Kudo, M. Fujiwara, M. Yokota, *Synthesis (Stuttg).* **2004**, *2005*, 39–46.

[140] J. Ichikawa, M. Kaneko, M. Yokota, M. Itonaga, T. Yokoyama, *Org. Lett.* **2006**, *8*, 3167–3170.

[141] J. Ichikawa, M. Yokota, T. Kudo, S. Umezaki, *Angew. Chemie Int. Ed.* **2008**, *47*, 4870–4873.

[142] W. Nakanishi, T. Matsuno, J. Ichikawa, H. Isobe, *Angew. Chemie Int. Ed.* **2011**, *50*, 6048–6051.

[143] K. Fuchibe, Y. Mayumi, N. Zhao, S. Watanabe, M. Yokota, J. Ichikawa, *Angew. Chemie Int. Ed.* **2013**, *52*, 7825–7828.

[144] K. Fuchibe, T. Morikawa, K. Shigeno, T. Fujita, J. Ichikawa, *Org. Lett.* **2015**, *17*, 1126–1129.

[145] S. Duttwyler, C. Douvris, N. L. P. Fackler, F. S. Tham, C. A. Reed, K. K. Baldridge, J. S. Siegel, *Angew. Chemie Int. Ed.* **2010**, *49*, 7519–7522.

[146] O. Allemann, K. K. Baldridge, J. S. Siegel, *Org. Chem. Front.* **2015**, *2*, 1018–1021.

[147] O. Allemann, S. Duttwyler, P. Romanato, K. K. Baldridge, J. S. Siegel, *Science (80-.).* **2011**, *332*, 574–577.

[148] K. Y. Amsharov, M. A. Kabdulov, M. Jansen, *Chem. - A Eur. J.* **2010**, *16*, 5868–5871.

[149] M. A. Kabdulov, K. Y. Amsharov, M. Jansen, *Tetrahedron* **2010**, *66*, 8587–8593.

[150] Z. Li, R. J. Twieg, *Chem. - A Eur. J.* **2015**, *21*, 15534–15539.

[151] F. B. Mallory, C. S. Wood, J. T. Gordon, L. C. Lindquist, M. L. Savitz, *J. Am. Chem. Soc.* **1962**, *84*, 4361–4362.

[152] K. B. Jørgensen, *Molecules* **2010**, *15*, 4334–4358.

[153] K. Amsharov, *Phys. status solidi* **2016**, *253*, 2473–2477.

[154] O. Papaianina, K. Y. Amsharov, *Chem. Commun.* **2016**, *52*, 1505–1508.

[155] K. Y. Amsharov, P. Merz, *J. Org. Chem.* **2012**, *77*, 5445–5448.

[156] A.-K. Steiner, K. Y. Amsharov, *Angew. Chemie Int. Ed.* **2017**, *56*, 14732–14736.

[157] K. Y. Amsharov, M. A. Kabdulov, M. Jansen, *Angew. Chemie Int. Ed.* **2012**, *51*, 4594–4597.

[158] D. Sharapa, A. K. Steiner, K. Amsharov, *Phys. Status Solidi Basic Res.* **2018**, *255*, 1–6.

8 Acknowledgments

For making this work possible many people applied their efforts, among them I appreciate the most contribution of my supervisor, Konstantin Amsharov, whose proper ratio of guidance and support facilitated and improved the work manyfold. I also thank my colleagues Mikhail Feofanov, Ann-Kristin Steiner and Elena Papaianina for their work and eventual contribution to my thesis. I am grateful to other both past and present colleagues from our group and beyond, i.e. AK Hirsch, Jux and Mokhir. Particular words of gratitude should be addressed to NMR department co-workers, Dr. Harald Maid and Christian Placht, who facilitated the most technical part of the thesis, carrying out multiple meticulous, time- and effort-demanding measurements. Thanks to all colleagues from Chemistry Department Organic Chair 2. I would also like to thank Prof.Dr. Sergey Troyanov for X-ray measurements and Olga Mazaleva for help with DFT calculations.

As of non-technical side, I am grateful to my family, especially to my grandmother who has incepted my interest in chemistry. I am endlessly thankful to my wife Iana for her patience and support; for preventing me from working too much, and fully supporting even if I sometimes did.